

Applying environmental DNA metabarcoding to investigate patterns of Arctic marine biodiversity with a focus on gelatinous zooplankton

Ayla Rosina Cherrington Sealey Murray



PS131 - FRAMSTRASSE (81°11'5.89" N 7°37'52.57" E) © CHRISTIAN R. ROHLEDER 14.07.22 14:46:49 UTC (CC BY-SA)



Universität
Bremen

Applying environmental DNA metabarcoding to investigate patterns of Arctic marine biodiversity with a focus on gelatinous zooplankton

Ayla Rosina Cherrington Sealey Murray

Dissertation zur Erlangung des akademischen Grades einer

Doktorin der Naturwissenschaften

Dr. rer. nat.

Fachbereich 2

Universität Bremen

Submitted: 29th November 2024

Colloquium date: 5th February 2025

Room NW2 C0300

This thesis was undertaken in the Helmholtz Young Investigator Group Arctic Jellies – ARJEL at the Alfred Wegener Institute Helmholtz Centre for Polar and Marine Research (AWI), Bremerhaven, Germany and the Faculty 2 - Biology and Chemistry at the University of Bremen, Bremen, Germany. This thesis was supervised by Prof. Dr. Charlotte Havermans.



Thesis Reviewers

First Reviewer:

Dr. Véronique Helfer

Mangrove Ecology, Leibniz Centre for Tropical Marine Ecology, Bremen, Germany

Second Reviewer:

Dr. Astrid Cornils

Polar Biological Oceanography, Alfred Wegener Institute Helmholtz Centre for Polar and Marine Research, Bremerhaven, Germany

Third Reviewer:

Dr. Agnes Weiner

Molecular Ecology and Paleogenomics (MEP), NORCE Climate and Environment, Bjerknes Centre for Climate Research, Bergen, Norway

Examination Board

- Commission Chair: **Prof. Dr. Martin Diekmann**
Vegetation Ecology & Conservation Biology, Faculty 2
– Biology and Chemistry, University of Bremen,
Bremen, Germany
- Examiner 1: **Prof. Dr. Charlotte Havermans**
BreMarE – Bremen Ecology Centre for Research &
Education Marine Zoology, Faculty 2 - Biology and
Chemistry, University of Bremen, Bremen, Germany
- Examiner 2: **Dr. Véronique Helfer**
Mangrove Ecology, Leibniz Centre for Tropical Marine
Ecology, Bremen, German
- Examiner 3: **Dr. Astrid Cornils**
Polar Biological Oceanography, Alfred Wegener
Institute Helmholtz Centre for Polar and Marine
Research, Bremerhaven, Germany
- Student Member: **M. Sc. Lilian Böhringer**
PhD candidate, University of Bremen, Faculty 2 –
Biology and Chemistry, Bremen, Germany.
Deep-Sea Ecology and Technology, Alfred Wegener
Institute Helmholtz Centre for Polar and Marine
Research, Bremerhaven, Germany
- Student Member: **B. Sc. Liova Idahl**
Master Student, Faculty 2 – Biology and Chemistry,
University of Bremen, Bremen, Germany

Table of Contents

Summary	9
Zusammenfassung	11
List of Abbreviations	13
Chapter 1: General Introduction	15
1.1 What is biodiversity?	15
1.2 Marine biodiversity: understudied and threatened	15
1.3 Arctic marine biodiversity	16
1.4 Threats to Arctic marine biodiversity	17
1.5 Current methods for Arctic marine surveys	19
1.6 A novel method for biodiversity surveys: Environmental DNA metabarcoding	21
1.6.1 What is environmental DNA?	21
1.6.2 General eDNA metabarcoding workflow	23
1.7 Gelatinous zooplankton and their role in Arctic marine ecosystems	24
1.7.1 What are gelatinous zooplankton?	24
1.7.2 Roles of gelatinous zooplankton in marine ecosystems	25
1.7.3 Gelatinous zooplankton in the Arctic	26
1.8 Motivation and research objectives	27
1.9 References	29
Chapter 2: Investigating pelagic biodiversity and gelatinous zooplankton communities in the rapidly changing European Arctic: An eDNA metabarcoding survey	39
Chapter 3: Eukaryotic biodiversity of sub-ice water in the Marginal Ice Zone of the European Arctic: A multi-marker eDNA metabarcoding survey	69
Chapter 4: Surveying marine biodiversity using eDNA metabarcoding of seawater and sediment in a high Arctic fjord during the polar night (Kongsfjorden, Svalbard)	149
Chapter 5: On the effectiveness of two universal metabarcoding primer pairs in amplifying gelatinous zooplankton DNA from tissue and environmental samples	197
Chapter 6: Overview	233
6.1 Overview	233

Chapter 7: Synthesis	235
7.1 Synthesis.....	235
7.2. Environmental DNA for detecting drivers of pelagic diversity in Fram Strait	235
7.2.1 Spatial patterns of diversity.....	236
7.2.2 Further abiotic drivers	236
7.3 Environmental DNA for investigating biodiversity across different habitats, spatial scales and seasons in the Atlantic Arctic	237
7.4 Environmental DNA and gelatinous zooplankton in the Arctic	239
7.5 Marker and primer choice and Arctic gelatinous zooplankton DNA	241
7.6 Perspectives for eDNA-based research in the Arctic Ocean.....	243
7.6.1 Open questions and limitations	243
7.6.2 Future opportunities	244
7.6.3 Conclusions	246
7.7 References	247
8.Appendix	257
8.1 Acknowledgements.....	257
8.2 Curriculum vitae	259
8.3 Own contribution to manuscripts.....	263
8.4 Eidesstattliche Erklärung	265

Summary

The Arctic is warming at least four times faster than the global average, as a result of anthropogenic climate change. Sea and air temperatures are rising, and perennial sea ice coverage has declined over the last four decades, with ice-free summers predicted to occur before 2050. Furthermore, in the Arctic gateway, Fram Strait, an increasing influence of warm Atlantic water is driving the 'Atlantification' of both environmental and biological processes. These changes affect habitat and resource availability for marine species in the region, causing shifts in species distributions and assemblages. There has been an intensification in research targeting the impacts of these changes over the last decades, however, important gaps in baseline knowledge of the current state of Arctic marine biodiversity still remain. The development of environmental DNA (eDNA) metabarcoding techniques has given rise to cost-effective and non-invasive methods for biodiversity assessments. One major advantage of eDNA is that it has the potential to detect delicate or elusive taxa that are typically overlooked or damaged by traditional net sampling, such as gelatinous zooplankton (GZP). This highly diverse group plays major roles across Arctic marine ecosystems. However, gaps in basic ecological data persist, including information on species assemblages and distribution. Thus, the overarching aim of this thesis was to apply eDNA metabarcoding to increase our knowledge of Arctic marine biodiversity, with a focus on GZP ecology.

Environmental DNA signals elucidated well-known vertical structuring of pelagic diversity and community composition in the open ocean (Chapter Two) and in the marginal ice zone (Chapter Three) of Fram Strait. Distinct community assemblages were linked to environmental conditions, which represented different water masses (Chapter Two) and different sea ice and meltwater dynamics (Chapter Three). Finally, significant structuring in community composition was revealed across the inner section of a Svalbard fjord (Chapter Four), based on seawater- and sediment-derived eDNA. These findings demonstrate that eDNA metabarcoding is a valuable tool for investigating the spatial patterns and abiotic drivers of marine biodiversity in the Arctic. It also proved to be a sensitive and accurate method for investigating biodiversity across different spatial scales, habitats, seasons and environmental conditions. It was applied across a large area of the open ocean in Fram Strait during summer, in a sampling scheme that encompassed depths from surface waters down to the bathypelagic (Chapter Two). It was also used to detect fine-scale patterns in the upper meters of the sub-ice water column in the marginal ice zone, during the late summer (Chapter Three). Lastly, it was implemented during the polar night period, in the central section of a semi-enclosed fjord system with high levels of glacier input and water turbidity (Chapter Four).

Additionally, this thesis was able to demonstrate that eDNA metabarcoding is a valuable method for investigating the diversity of GZP in the Arctic Ocean. Comparisons between eDNA and non-DNA-based survey methods (Chapters Two and Four) showed that eDNA recovered the highest numbers of species. It was also evident that each technique had inherent biases, with different GZP communities detected depending on the survey method used. Thus, we were able to confirm that eDNA greatly improves our repertoire for sampling GZP in the Arctic, but a combination of sampling methods should be employed to gain a more accurate picture of the diversity present. Finally, multi-marker analyses were applied (Chapters Three and Five) to further investigate the accuracy of two commonly used universal metabarcoding markers and their associated primers for amplifying common Arctic GZP taxa. The COI gene showed higher taxonomic resolution (e.g., species-level) but was affected by primer mismatches for some groups. The 18S gene was able to amplify more GZP groups, but genus and species-level assignments were not accurate. Therefore, it was evident that both are useful for investigating GZP diversity, but which one to prioritize should be determined by the research question at hand. Finally, it was evident that gaps in reference databases persist for both genes and that filling these with GZP samples from the Arctic should be a priority for future research.

Overall, the research presented in this thesis supports the use of eDNA metabarcoding as a non-invasive and sensitive method for improving our understanding of Arctic marine biodiversity. It shows the utility of eDNA metabarcoding to go beyond presence data and to investigate abiotic drivers of eukaryotic biodiversity in different marine habitats and conditions. Moreover, it highlights the benefits of incorporating eDNA methods into GZP research to better understand how this important, yet understudied group will be affected by ongoing climate change in the Arctic. Finally, this thesis contributes valuable baseline data to our current understanding of marine eukaryotic biodiversity in the Atlantic sector of the Arctic.

Zusammenfassung

Die Arktis erwärmt sich infolge des anthropogenen Klimawandels mindestens viermal so schnell wie der globale Durchschnitt. Die Meeres- und Lufttemperaturen steigen, die ganzjährige Meereisbedeckung ist in den letzten vier Jahrzehnten zurückgegangen und bis 2050 werden eisfreie Sommer vorhergesagt. Darüber hinaus führt der zunehmende Einfluss des warmen Atlantikwassers, der Framstraße, zu einer „Atlantifizierung“ sowohl der Umwelt als auch der biologischen Prozesse. Diese Veränderungen wirken sich auf den Lebensraum und die Verfügbarkeit von Ressourcen für die marinen Arten in der Region aus und führen zu Verschiebungen in der Verteilung und Zusammensetzung der Arten. Die Forschung zu den Auswirkungen dieser Veränderungen hat sich in den letzten Jahrzehnten intensiviert, aber es gibt immer noch große Wissenslücken in Bezug auf den aktuellen Zustand der arktischen Meeresbiodiversität. Die Entwicklung von Metabarcoding-Techniken für Umwelt-DNA (eDNA) hat kosteneffektive und nicht-invasive Methoden zur Bewertung der biologischen Vielfalt hervorgebracht. Ein großer Vorteil der eDNA ist, dass sie das Potenzial hat, empfindliche oder schwer erfassbare Taxa aufzuspüren, die bei herkömmlichen Netzprobenahmen typischerweise übersehen oder beschädigt werden, wie z. B. gelatinöses Zooplankton (GZP). Diese äußerst vielfältige Gruppe spielt in den arktischen Meeresökosystemen eine wichtige Rolle. Es gibt jedoch nach wie vor Lücken in den grundlegenden ökologischen Daten, einschließlich Informationen über die Artenzusammensetzung und -verteilung. Daher war das übergreifende Ziel dieser Arbeit die Anwendung von eDNA-Metabarcoding, um unser Wissen über die biologische Vielfalt der arktischen Meere zu erweitern, wobei der Schwerpunkt auf der Ökologie des GZP lag.

DNA-Signale aus der Umwelt brachten Aufschluss über die bekannte vertikale Strukturierung der pelagischen Vielfalt und der Zusammensetzung der Lebensgemeinschaften im offenen Ozean (Kapitel zwei) und in der Eisrandzone (Kapitel drei) der Framstraße. Unterschiedliche Lebensgemeinschaften wurden mit Umweltbedingungen assoziiert, die unterschiedliche Wassermassen (Kapitel zwei) und unterschiedliche Meereis- und Schmelzwasserdynamiken (Kapitel drei) repräsentieren. Schließlich wurde anhand der aus Meerwasser und Sediment gewonnenen eDNA eine signifikante Strukturierung der Lebensgemeinschaften im inneren Teil eines Svalbard-Fjords festgestellt (Kapitel vier). Diese Ergebnisse zeigen, dass eDNA-Metabarcoding ein wertvolles Instrument zur Untersuchung der räumlichen Muster und abiotischen Einflussfaktoren der marinen Biodiversität in der Arktis ist. Sie erwies sich auch als eine empfindliche und genaue Methode zur Untersuchung der biologischen Vielfalt in verschiedenen räumlichen Maßstäben, Lebensräumen, Jahreszeiten und Umweltbedingungen. Sie wurde in einem großen Gebiet des offenen Ozeans in der

Framstraße während des Sommers in einem Probenahme-Schema angewandt, das Tiefen vom Oberflächenwasser bis hinunter zum Bathypelagial umfasste (Kapitel zwei). Sie wurde ebenfalls eingesetzt, um im Spätsommer feinskalige Muster in den oberen Metern der Untereis-Wassersäule in der Randeiszone zu erkennen (Kapitel drei). Schließlich wurde sie während der Polarnacht im zentralen Abschnitt eines halbgeschlossenen Fjordsystems mit hohem Gletschereintrag und hoher Wassertrübung eingesetzt (Kapitel vier).

Darüber hinaus konnte in dieser Arbeit gezeigt werden, dass eDNA-Metabarcoding eine wertvolle Methode zur Untersuchung der Vielfalt der GZP im Arktischen Ozean ist. Vergleiche zwischen eDNA- und nicht-DNA-basierten Erhebungsmethoden (Kapitel zwei und vier) zeigten, dass mit eDNA die höchste Anzahl an Arten gefunden wurde. Es wurde auch deutlich, dass jede Technik inhärente Verzerrungen aufweist und dass je nach Erhebungsmethode unterschiedliche GZP-Gemeinschaften entdeckt wurden. So konnten wir bestätigen, dass eDNA unser Repertoire für die Beprobung von GZP in der Arktis erheblich verbessert, dass aber eine Kombination von Beprobungsmethoden eingesetzt werden sollte, um ein genaueres Bild der vorhandenen Vielfalt zu erhalten. Schließlich wurden Multi-Marker-Analysen durchgeführt (Kapitel drei und fünf), um die Genauigkeit von zwei häufig verwendeten universellen Metabarcoding-Markern und den dazugehörigen Primern für die Amplifikation häufiger arktischer GZP-Taxa weiter zu untersuchen. Das COI-Gen zeigte eine höhere taxonomische Auflösung (z. B. auf Artniveau), war aber in einigen Gruppen von Primer-Fehlpaarungen betroffen. Das 18S-Gen war in der Lage, mehr GZP-Gruppen zu amplifizieren, aber die Zuordnungen auf Gattungs- und Artniveau waren nicht präzise. Es wurde also deutlich, dass beide Methoden für die Untersuchung der GZP-Vielfalt nützlich sind, aber die Entscheidung, welcher Methode der Vorzug zu geben ist, von der jeweiligen Forschungsfrage abhängig gemacht werden sollte. Schließlich wurde deutlich, dass für beide Gene noch Lücken in den Referenzdatenbanken bestehen und dass die Schließung dieser Lücken mit GZP-Proben aus der Arktis eine Priorität für die zukünftige Forschung darstellen sollte.

Insgesamt unterstützt die in dieser Arbeit vorgestellte Forschung den Einsatz von eDNA-Metabarcoding als nicht-invasive und empfindliche Methode zur Verbesserung unseres Verständnisses der arktischen Meeresbiodiversität. Sie zeigt den Nutzen von eDNA-Metabarcoding, um über Präsenzdaten hinauszugehen und abiotische Einflüsse auf eukaryotische Biodiversität in verschiedenen marinen Lebensräumen und Bedingungen zu untersuchen. Darüber hinaus werden die Vorteile der Einbeziehung von eDNA-Methoden in die GZP-Forschung hervorgehoben, um besser zu verstehen, wie diese wichtige, aber noch nicht ausreichend untersuchte Gruppe vom Klimawandel in der Arktis betroffen sein wird. Schließlich leistet diese Arbeit einen wertvollen Beitrag zu unserem derzeitigen Verständnis der marinen eukaryotischen Biodiversität im atlantischen Sektor der Arktis.

List of Abbreviations

GZP	Gelatinous zooplankton
DNA	Deoxyribonucleic acid
eDNA	Environmental DNA
ASV	Amplicon sequence variant
MOTU	Molecular operational taxonomic unit
RRA	Relative read abundance
COI	Cytochrome c oxidase subunit I
18S	Small subunit ribosomal RNA
Bp	Base pairs
CTD	Conductivity, temperature and depth
WSC	West Spitsbergen current
EGC	East Greenland current
MIZ	Marginal ice zone
NMDS	Non-metric multidimensional scaling
PERMANOVA	Non-parametric multivariate statistical permutation
ANOVA	Analysis of variance
DF	Degrees of freedom
sPLS	Sparse partial least squares

Chapter 1: General Introduction

1.1 What is biodiversity?

The term “biodiversity” was coined from the longer “biological diversity”. One of the most inclusive and widely used definitions used today was given in the United Nations Convention on Biological Diversity in June 1992:

‘The variability among living organisms from all sources including, inter alia, terrestrial, marine and other aquatic ecosystems and the ecological complexes of which they are part; this includes diversity within species, between species and of ecosystems.’

In this definition, variability is emphasised as the major factor of biodiversity and it goes beyond a basic species richness focus (i.e., how many are there). It encompasses intra-specific (e.g., genetic) and ecosystem (e.g., across local or regional levels) diversity as important sources of said variability. This definition is employed in the present thesis, as it is inclusive, relevant in policy-making and integral to international conservation decision-making (e.g., at the United Nations level) (Mace et al., 2012).

Assessing and understanding patterns of biodiversity is foundational in detecting and interpreting the biological and ecological processes of our natural world. Biodiversity is in a constant state of flux, but the global trend over the last century is one of rapid decline (Díaz et al., 2019; Pörtner et al., 2023) and it has been argued that we are approaching a sixth mass extinction (Barnosky et al., 2011). Present biodiversity loss has many drivers including pollution, increased natural resource exploitation, urbanization, intensified agriculture and over-fishing. It is also tightly intertwined with anthropogenic climate change (Calvin et al., 2023; Pörtner et al., 2023). There are many consequences and adverse impacts of biodiversity loss on societies, the economy and the natural world. These include but are not limited to: species and local extinctions; reductions in ecosystem function and productivity; the increased spread of pathogens; reduction in carbon sequestration and storage as well as ecosystem resilience; and the loss of traditional knowledge and cultural heritage of indigenous people (Calvin et al., 2023; Pearson et al., 2023; Pörtner et al., 2023; Weiskopf et al., 2024).

1.2 Marine biodiversity: understudied and threatened

Oceans cover 70% of the earth’s surface area and host a huge spectrum of unique ecosystems and habitats including sea ice, rocky shores, estuaries, fjords, the deep sea, and tropical reefs. An enormous diversity of life forms and species inhabit the world’s oceans, yet they remain largely unexplored, resulting in vast arrays of unknown diversity and ecological relationships. It is estimated that only 26% of the ocean floor has been mapped (GEBCO Compilation Group, 2024) and up to 90% of marine eukaryotic species are yet to be identified

(Mora et al., 2011). Ocean ecosystems are crucial for sustaining life on earth but are highly threatened by anthropogenic climate change. They absorb up to 90% of the heat resulting from human activity (Li et al., 2023) and have absorbed approximately 25% of carbon emissions since the 1960's (Gruber et al., 2023; Hoegh-Guldberg and Bruno, 2010). These effects have led to rapid environmental changes, including increasing temperatures, sea ice loss and ocean acidification. These changes have fundamentally affected global marine biodiversity and will continue to do so, all the way from the individual level through to community and ecosystem levels (Hoegh-Guldberg and Bruno, 2010). Indeed, human activity has directly affected more than 80% of the world's oceans, with only an estimated 13% of global marine wilderness remaining (Jones et al., 2018; Watson et al., 2018). Much of this remaining wilderness is located in the deep sea as well as polar high latitude oceans such as the Arctic (Jones et al., 2018).

1.3 Arctic marine biodiversity

The Arctic Ocean, the world's smallest, has historically been believed to be an area of low biodiversity compared to lower latitude oceans and the Antarctic (Hardy et al., 2011; Piepenburg, 2005; Vinogradov and Melnikov, 1980). However, research over the last few decades has shown that the Arctic Ocean hosts at least 8,000 known extant eukaryotic species. It is now considered to be a region of intermediate biodiversity (CAFF, 2017; H. CAFF, 2013). New and cryptic species are continuously being described and it is predicted that there are many more species yet to be detected (Bluhm et al., 2011; Hardy et al., 2011). Levels of endemism are lower in the Arctic compared to Antarctica for example, due to more recent colonization events and connection to adjacent oceans through the Pacific (Bering Strait) and Atlantic (Fram Strait) gateways (Piepenburg, 2005). Present-day Arctic marine diversity (especially pelagic diversity) is composed of species with a mixture of biogeographic origins (arctic, arctic-boreal and boreal) (CAFF, 2013). Arctic marine taxa can be largely grouped into three categories: sea ice-associated, pelagic and benthic (Bluhm et al., 2011). Sea ice biota (sympagic) include eukaryotes that inhabit the sea ice and its brine channels, as well as those that exist in the ice-ocean interface. This category is the least diverse of the three, although species inventory lists are still incomplete (Bluhm et al., 2011, 2010). Sympagic biota are not regularly monitored anywhere in the Arctic and existing efforts are particularly affected by the loss of taxonomic expertise (CAFF, 2017). The pelagic is more diverse than the sea ice realm and sampling coverage is better than for both sea ice and benthos, although large regional gaps in data still remain (Bluhm et al., 2011). The benthos has the highest species richness of the three categories (e.g., 90% of marine invertebrates are benthic), and also remains the least covered in terms of sampling, especially in the deep sea (CAFF, 2017; Ramirez-Llodra et al., 2024). In summary, while our understanding of Arctic

marine biodiversity is increasing, our view is incomplete across all three marine realms. This represents a major challenge to measuring the current status of biodiversity in the Arctic Ocean, as well as to tracking changes and implementing comprehensive and robust monitoring and management strategies.

1.4 Threats to Arctic marine biodiversity

The Arctic Ocean is one of the most susceptible areas to climate warming, despite relatively low levels of human activity (IPCC, 2022). In a process referred to “Arctic Amplification”, the Arctic has warmed up to four times faster than any other region over the last 40 years (Rantanen et al., 2022). Year-round surface air and sea temperatures have continued to increase, while sea ice extent and thickness, snow cover, and the mass of the Greenland ice sheet have decreased. Every year since 2007 has exhibited the lowest September sea ice extent since satellite measurements began in 1979 and the summer of 2023 was the warmest Arctic summer on record (Thoman et al., 2023). Additionally, winter warming (**Figure 1**) can delay sea ice formation and is leading to reductions in winter sea ice coverage and retreats in the winter ice edge (Ingvaldsen et al., 2021). As a result of this accelerated warming, the Arctic Ocean is transitioning from an ice/cryosphere dominated ecosystem into a warmer, open water system with increased levels of precipitation and more extreme weather events (IPCC, 2022). Arctic marine ecosystems are directly affected by these environmental changes and unprecedented shifts in habitat availability, species distributions, community composition and food web structure are already underway (Csapó et al., 2021; Wassmann et al., 2011).

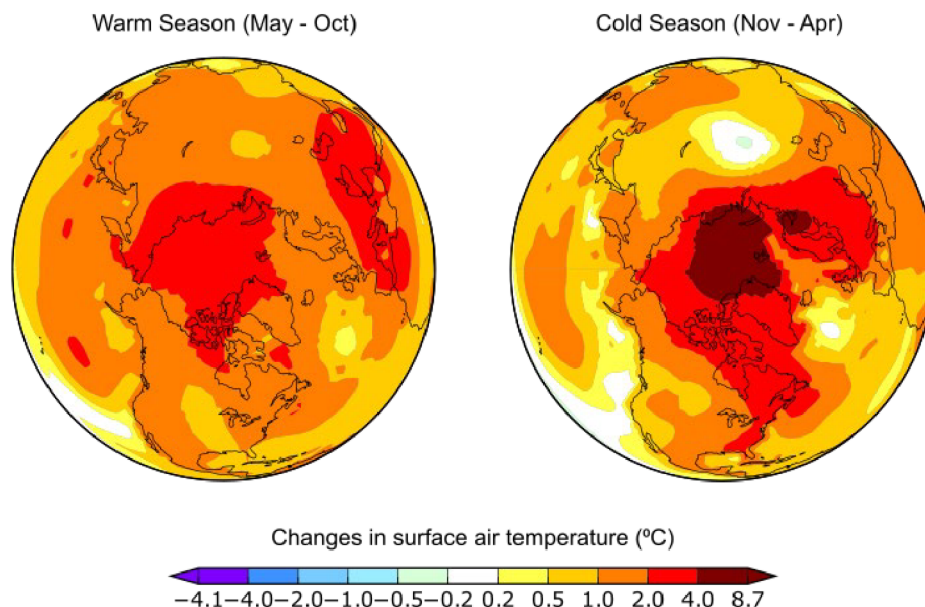


Figure 1. Historical trends in surface air temperature in the Arctic. Graphic shows the spatial pattern of Arctic warming for the period 1980–2023 in the cold season and warm season. Colour indicates change in temperature since 1980 in degrees Celsius. Maps were produced using GISTEMP v4 data by NASA: data.giss.nasa.gov/gistemp/ (accessed on 2024-10-08).

Fram Strait, the Atlantic gateway between the Arctic Ocean and the Atlantic, is the only deep-water connection between the Arctic basin and is the largest source of oceanic heat into the central Arctic (Beszczynska-Moeller et al., 2011). This area is a hotspot for Arctic warming and is experiencing a growing influence of Atlantic conditions which are driving a phenomenon known as “Atlantification” or “Borealization” (Polyakov et al., 2020, 2017). In terms of physical oceanography, the biggest driver of this process is the increased advection of warmer and saltier water masses of Atlantic origin. From a biological perspective, these water masses not only carry species of sub-arctic and Atlantic-origin, but also provide more temperate-like environmental conditions that are optimal to the newcomers’ survival and ability to establish reproducing populations (Csapó et al., 2021). True “polar” species are exhibiting poleward range-contractions, while sub-arctic and boreal species are expanding their ranges northward (Andrews et al., 2019; Basedow et al., 2018; Dalpadado et al., 2016). At the base of Arctic food webs, spatial and temporal shifts of phytoplankton blooms have been reported as a result declining sea ice and changing light and nutrient availability (Lannuzel et al., 2020; Leu et al., 2011). In addition, the establishment of sub-arctic and boreal phytoplankton taxa is shifting the species composition of spring and summer blooms (Barton et al., 2016). This affects food availability and quality for key grazers such as *Calanus* copepods, which make up the majority of pelagic biomass in the Arctic and whose life cycles are closely adapted to these phytoplankton blooms. These copepods are vital sources of lipids to consumers at higher trophic levels, and reduction in lipid content can have wide reaching impacts across food webs as a result (reviewed in Barber et al., 2015).

There are a myriad of other threats affecting the both the Fram Strait region as well as the wider Arctic and its adjacent seas. Many relate to the increased potential for resource exploitation, which is largely driven by reductions in sea ice extent opening up access to areas previously untouched by human activity (CAFF, 2017). For example, summer shipping activity has increased in the last two decades and ice-free summers are predicted to occur by the middle of this century. This is expected to increase the commercial viability of regular shipping routes through the Arctic Ocean (PAME, 2020). Overall fishery output and harvest in Arctic waters is also predicted to increase with climate change (Meredith et al., 2022). Many commercially exploited species of fish in sub-Arctic and temperate seas, such as Atlantic cod, have been expanding their distributions into Arctic waters (Fossheim et al., 2015). This opens up new opportunities for expanding existing fishery activities in the area, as well as exploitation of hitherto unharvested species. Simultaneously, tourism opportunities have increased in the Arctic. Commercial cruise liners now regularly visiting Svalbard and Greenland, and tourism is the fastest growing industry in some Arctic regions (Dawson et al., 2017; Stephen, 2018). Historically, the Arctic Ocean has been considered to be less susceptible to invasions by non-

indigenous species (NIS) than other regions due to extremely cold conditions, extreme light regimes, lack of accessibility and low shipping activity. However, with the aforementioned increases in vessel activity comes the increased chance of establishment of invasive species which can be transported in ballast water or biofouling (Goldsmit et al., 2020; Qi et al., 2024). There are a variety of other risks associated with higher levels of human activity, including pollution (e.g., mercury and persistent organic pollutants), increased risk of catastrophic events such as oil spills and potential for the spread of pathogens and parasites (CAFF, 2017; Mueter et al., 2021).

1.5 Current methods for Arctic marine surveys

There are a multitude of techniques used to survey marine biodiversity in the Arctic. As with any biological survey method, there are benefits and disadvantages associated with each that can result in biases and overlooked components of marine ecosystems (**Table 1**). Many of these methods are invasive (i.e., require the capture of the organism) and can potentially harm the species they aim to protect or non-target species (i.e., bycatch). Invasive techniques include plankton nets, fishing nets and trawls of varying sizes, as well as grabs and corers for benthic taxa (Eleftheriou, 2013; Sameoto et al., 2000; Whitmore et al., 2019). However, non-invasive methods are also common. Some examples include optical surveys with both stationary (e.g., Balazy et al., 2021) and towed cameras (e.g., Golikov et al., 2023), as well as sediment traps for collecting carcasses and marine snow (e.g., Schröter et al., 2019). Many of these established methods require either expensive equipment and components or vessel-time. They can also be time- and expertise-intensive, especially in areas of the Arctic that are logistically challenging to access. Moreover, they typically have a heavy reliance on morphological identification, which comes with inherent limitations (Hebert et al., 2003). For example, it requires specialist taxonomic knowledge, which is declining worldwide (Engel et al., 2021). Additionally, the reliance on morphological features alone can lead to both cryptic species being overlooked and to misidentifications due phenotypic plasticity. All of these factors can create time and financial bottlenecks, or incorrect species lists, which can prevent these methods from being as widely employed as researchers would like (spatially and temporally). As a result, our understanding of the current status of and trends in biodiversity in the Arctic Ocean remains limited. The rapid development and implementation of molecular methods in marine surveys over the last two decades has provided solutions to circumvent the challenges and biases of traditional methods, and represent less destructive approaches to monitoring biodiversity (Hebert et al., 2003; Taberlet et al., 2012). One of the most revolutionary methods that has emerged is the use of environmental DNA (eDNA) metabarcoding, which is non-invasive, cost-effective and can produce information on ecosystem-wide biodiversity as well as group or species-specific data.

Table 1. Examples and descriptions of benefits and disadvantages of methods commonly employed to survey Arctic marine biodiversity.

	Examples	Spatial coverage	Example target taxa	Benefits	Disadvantages
Water sampling	→ Water bottle samplers → Pumps	→ Discrete depths → Integrated	→ Phytoplankton → Small zooplankton	→ Abundance data → Large volumes possible (for pumps) → Whole organisms captured	→ Small volumes (for water bottles) → Can be depth limited (for pumps) → Taxonomic expertise required
Net sampling	→ Bongo-Nets → Multi-Nets → Continuous Plankton Recorder → Bottom trawls → Purse-seine nets → Beam trawl	→ Vertically integrating → Stratified depths (closing nets only) → Horizontally integrating	→ Phytoplankton → Zooplankton → Nekton → Fish (Fish trawls)	→ Cover thousands of litres of water → Abundance data → Tissue available for molecular identification → Whole organisms captured	→ Can damage delicate specimens → Net avoidance behaviour → Size class biases depending on net measurements → Can be expensive → Vessel normally required for deployment → Bycatch common (fish trawls) → Relies on taxonomic expertise
Optical surveys	→ Towed camera systems → Stationary cameras → Underwater Vision Profiler (UVP)	→ Horizontally integrating → Discrete points → Vertical integrating	→ Zooplankton, large invertebrates → Fish, gelatinous zooplankton → Picoplankton	→ Can cover many thousands of litres of water → Abundance data → Non-invasive → Many images produced	→ Expensive → Highly specialised → Does not capture larger species (UVP) → Taxonomic expertise required → No tissue for molecular identification → Identification dependent on image quality
Acoustic surveys	→ Ship-based scanners (EK80) → Mooring hydrophones	→ Integrating → Discrete point (mooring)	→ Fish → Whales → Zooplankton	→ Non-invasive → Long term (moorings) → Wide spatial coverage possible	→ No visual species identification → No tissue for molecular species identification → Can miss organisms with low reflectivity (side-scanners)
Sediment sampling	→ Multi-corer → Van-Veen grab → Box-corer	→ Discrete points	→ Infauna	→ Whole organisms captured	→ Small spatial coverage → Not effective on hard substrates → Taxonomic expertise required
eDNA metabarcoding	→ Water → Sediment → Passive sampling	→ Discrete depths/points → Integrating (passive sampling)	→ Whole communities → Specific groups (e.g., zooplankton)	→ Little taxonomic expertise necessary → Can target specific species or many eukaryotic groups in same samples → Vessel not always needed (e.g., shallow and coastal samples) → Non-invasive	→ Limited by quality and coverage of reference databases → Sensitive to contamination → Primer and/or PCR biases can skew results → Semi-quantitative

Notes: Information taken from Eleftheriou, 2013; Sameoto et al., 2000; Whitmore et al., 2019 and personal observations

1.6 A novel method for biodiversity surveys: Environmental DNA metabarcoding

1.6.1 What is environmental DNA?

Environmental DNA (eDNA) can be simply defined as DNA which is isolated from environmental samples. The specifics of what actually constitutes eDNA can be broad and at times conflicting, due to the broad nature of studies employing the technique. Environmental DNA exists in a variety of forms, including mucus, excreted metabolic waste products (e.g., faeces and urine), gametes, or degradation products of dead organisms (Thomsen and Willerslev, 2015). It can be mix of both cellular and extra-cellular DNA, depending on the target taxa, the state of degradation of the cell membranes and the sample type. For multicellular eukaryotes, eDNA usually refers to extra-organismal DNA. But small and microscopic organisms (e.g., meiofauna) and single cellular organisms (e.g., phytoplankton) can easily be captured whole and are impossible to distinguish from extra-organismal DNA (Figure 2). The definition of eDNA used for the purpose of this thesis is that given by Taberlet and colleagues:

“...a complex mixture of genomic DNA from many different organisms found in an environmental sample.” (Taberlet et al., 2012).

Environmental DNA can be isolated from a range of different substrates including water (e.g., Ficetola et al., 2008), ice (e.g., Doyle and Christner, 2022; Varotto et al., 2021), sediment and permafrost (e.g., Willerslev et al., 2003) and air (e.g., Johnson et al., 2019). The vast majority of marine studies however, involve water and sediment-derived eDNA (reviewed in Havermans et al., 2022). Other sample types that can be considered environmental include

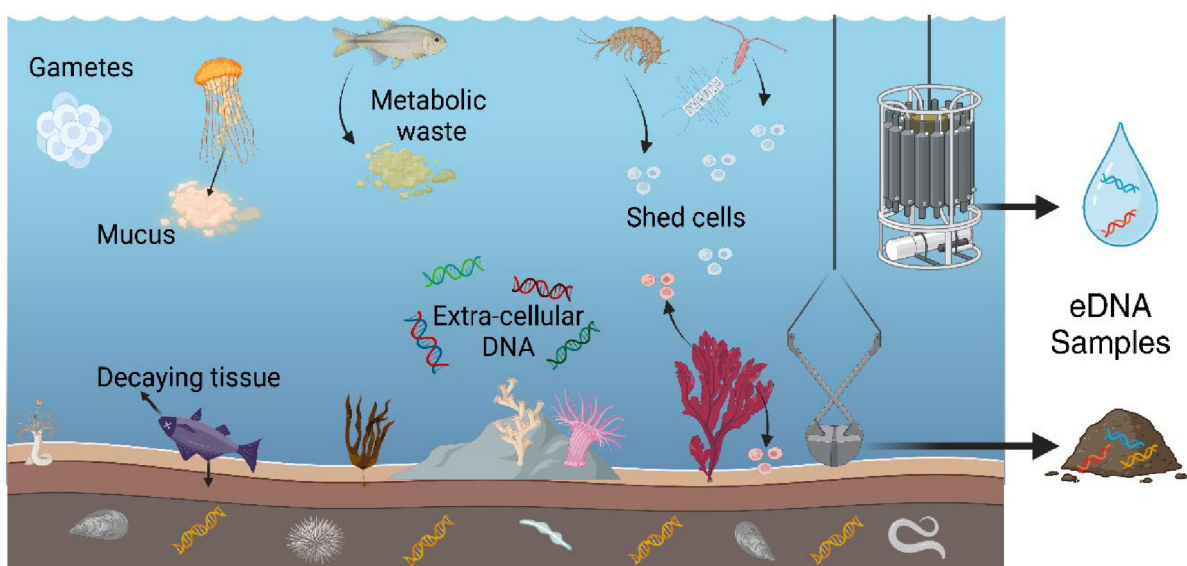


Figure 2. Representative sources of environmental DNA in marine ecosystems. Figure produced with BioRender.

faeces (e.g., Staley et al., 2018) sediment traps (e.g., Wietz et al., 2024), settlement plates (e.g., Leray and Knowlton, 2015) and even filter organisms considered as “natural samplers” (e.g., Turon et al., 2020). However, these largely target sampling bulk organismal DNA (with the exception of natural samplers) and are not considered as eDNA for the purpose of this thesis.

The roots of eDNA methodology originate in microbial research (Taberlet et al., 2018). The first study to focus on metabarcoding of macroorganisms was reported in 2003 by Willersev and colleagues, who successfully amplified mammoth DNA from ancient permafrost and DNA of an extinct giant flightless bird from cave sediments in New Zealand. A seminal paper by Ficetola et al., (2008) demonstrated the effectiveness of eDNA for detecting current species presence, by targeting DNA traces left by an invasive frog species in a freshwater system. In marine systems, it was used in a study published in 2012 to detect marine mammals (Foote et al., 2012). Since then, the use of eDNA as a tool to characterize marine species presence and distribution has expanded exponentially (Deiner et al., 2017; Havermans et al., 2022; Shea et al., 2023).

Environmental DNA studies generally fall into two categories: single-species detection and metabarcoding (i.e., the simultaneous detection of multiple species or taxonomic groups from a mixed sample) (Taberlet et al., 2018; Thomsen and Willerslev, 2015). The former relies on the development of primers designed to be specific enough to amplify only the target species and not its conspecifics. These studies typically rely on conventional Polymerase Chain Reaction (PCR), quantitative PCRs and/or Sanger-sequencing technology. They are often employed for the rapid detection of species that are rare or endangered (e.g., sawfish; Bonfil et al., 2021), elusive (e.g., coelacanths; Oliver et al., 2024), dangerous (e.g., box jellyfish; Morrissey et al., 2022) or invasive species (e.g frogs; Ficetola et al., 2008). They were the most abundant eDNA studies until approximately 2015, when the use of Next Generation Sequencing (NGS) technology began to be widely used and allowed the amplification of the DNA of multiple species or metabarcoding (Riaz et al., 2011; Taberlet et al., 2018). Metabarcoding typically targets short DNA fragments (approximately 100 - 500 base pairs), allowing for the amplification of degraded DNA. Furthermore, universal gene fragments and primer pairs are generally used as opposed to species specific ones (Riaz et al., 2011). As with eDNA, metabarcoding originated in microbial research and was first implemented in larger organisms to analyse faeces and stomach contents (Deagle et al., 2010; Pompanon et al., 2012) and then for environmental samples like sediment (Sønstebø et al., 2010) and seawater (Foote et al., 2012; Thomsen et al., 2012).

1.6.2 General eDNA metabarcoding workflow

The eDNA metabarcoding workflow employed in this thesis is described in **Figure 3**. Briefly, water samples were filtered across membranes in enclosed filter capsules optimised for DNA capture (Sterivex 0.22 μ m). Technical triplicates of two litres were filtered at each sampling point for a total of six litres. Sediment was preserved immediately after collection. The eDNA was then preserved by freezing at -20°C (sediment) or -80°C (filters) to prevent further degradation. Next, the DNA was isolated (from filter or sediment sample) using commercially produced extraction kits optimized for the different sample mediums. Once the DNA was isolated and cleaned, it was amplified with universal primers and PCR and tagged with specific indices (library preparation). Bovine albumin serum (BSA) was included in the PCR product as a precaution against the presence of PCR inhibitors. The PCR-product was then sequenced with the NGS platform Illumina NovaSeq 6000. The resulting sequencing output was processed using gene-specific bioinformatics pipelines. Raw sequences were demultiplexed, quality filtered and taxonomically assigned to produce a “species” list which was curated and then used for downstream data analyses. Metabarcoding of the ‘Leray’ fragment within the mitochondrial cytochrome c oxidase I (COI) gene is the foundation of this thesis, however the potential of increasing taxonomic coverage with the nuclear small-subunit ribosomal RNA gene (18S) is also explored.

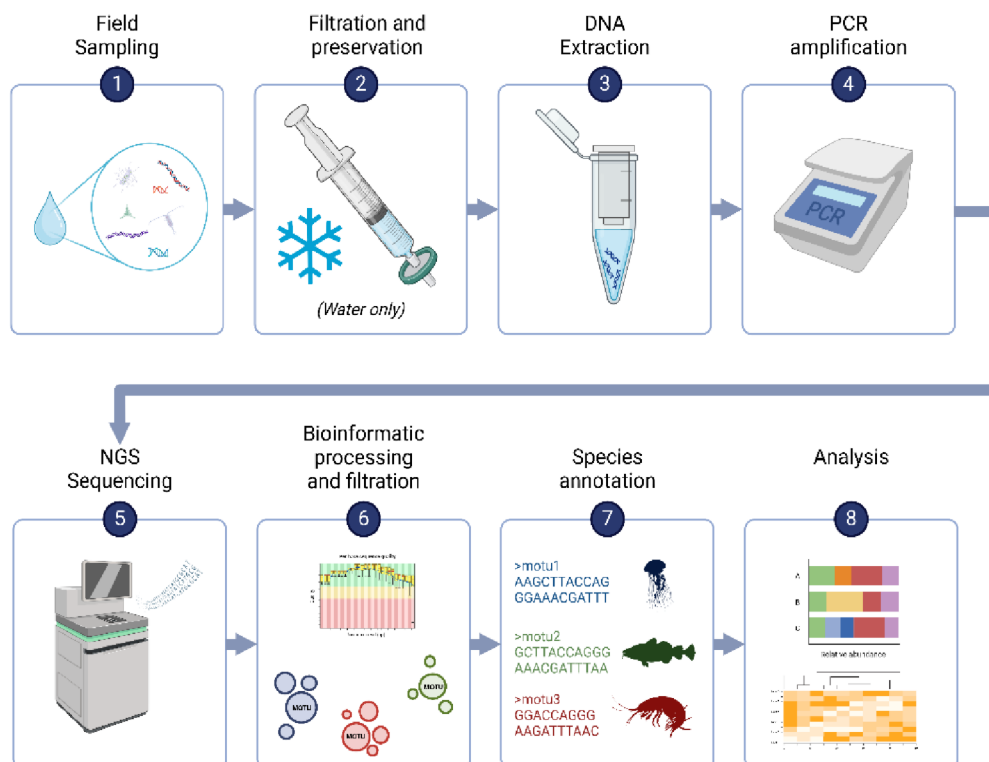


Figure 3. General overview of the eDNA metabarcoding sampling and processing workflow employed in this thesis. Figure produced using BioRender.

1.7 Gelatinous zooplankton and their role in Arctic marine ecosystems

1.7.1 What are gelatinous zooplankton?

Gelatinous zooplankton (GZP) is an umbrella term given to a highly diverse group of paraphyletic taxa that share some physical and life-history similarities. The definition of GZP used in this thesis is limited to ctenophores (class: Nuda and Tentaculata), cnidarians (class: Hydrozoa and Scyphozoa) and tunicates (class: Appendicularia and Salpa) with pelagic life stages. Individuals and species fall within a broad size spectrum, from millimetres to meters in diameters or length and they exist in a huge variety of shapes and morphotypes (**Figure 4**). GZP taxa also exhibit a wide range of life cycles, including those that remain in the water

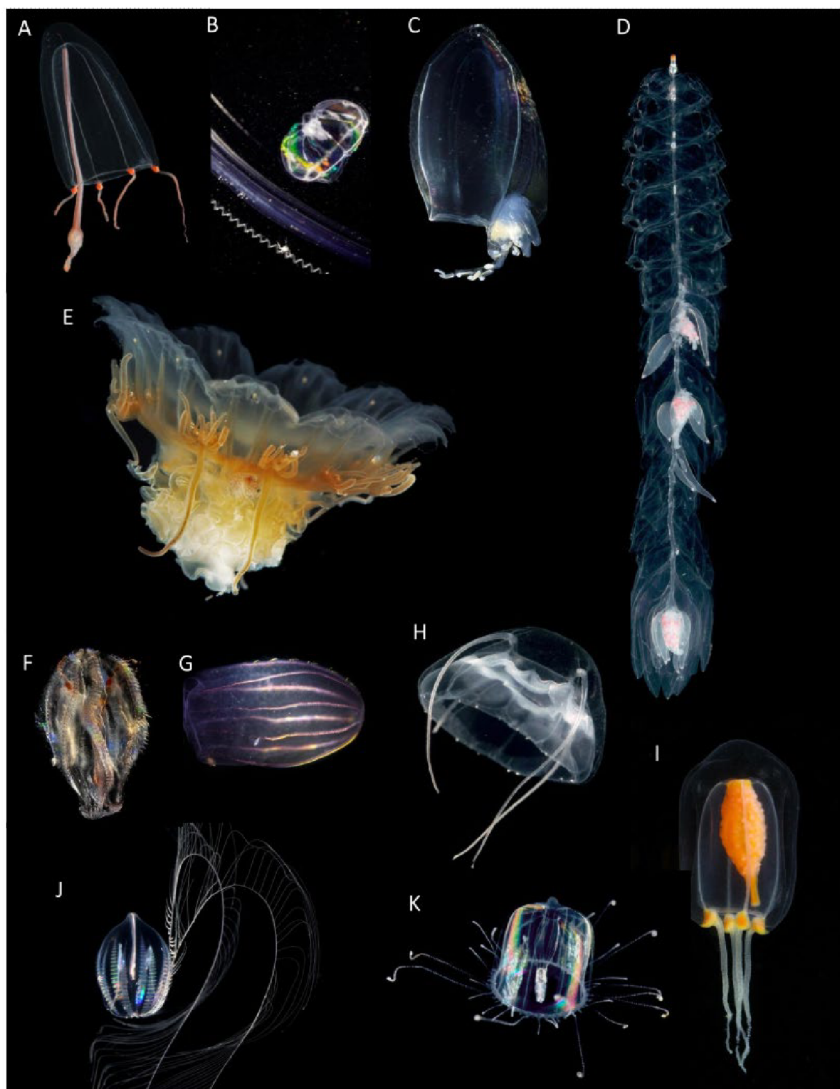


Figure 4. Representatives of the gelatinous zooplankton community found in the Arctic. (A) *Sarsia princeps* (B) *Sminthea arctica* (C) *Dimophyes arctica* (D) *Aglana elegans* (E) *Cyanea capitata* (F) Cydippid ctenophore (G) *Beroe* spp. (H) *Aeginopsis laurentii* (I) *Euphysa flammea* (J) *Pleurobrachia pileus* (K) *Aglantha digitale*. Photos B, F, and G are courtesy of Mario Hopman and all others are courtesy of Joan-J. Soto Angel. Images are not to scale.

column their whole life cycle (holoplanktonic) and those with benthic and pelagic life stages (meroplanktonic). The major unifying characteristics of this group are their fragile, transparent and gelatinous bodies as well as the existence of at least one planktonic life stage (Haddock, 2004).

1.7.2 Roles of gelatinous zooplankton in marine ecosystems

Gelatinous zooplankton play major roles throughout marine food webs, both globally and in the Arctic Ocean. Until recently, they were considered to be a trophic dead-end in marine food-webs and regularly overlooked in zooplankton surveys (reviewed in Hays et al., 2018). However, this assumption is changing as research investigating their trophic roles has increased over the last two decades. Many GZP species have been revealed as important prey items to a range of predators globally, including fish (Günther et al., 2021; Ruiz et al., 2024b, 2024a) and penguins (Thiebot et al., 2017). A number of species are phytoplankton grazers (e.g., appendicularians), while others are predatory, feeding on both zooplankton and nekton and at times representing substantial competition to fish (Boero et al., 2008; Haddock, 2007; Purcell et al., 2010; Schroeder et al., 2023). Additionally, scyphozoans and ctenophores are known to feed on ichthyoplankton and fish juveniles (Purcell, 1985; Purcell et al., 2010). Moreover, GZP can contribute significantly to benthic-pelagic coupling and carbon export through shedding of mucus and appendicularian “houses” (Jaspers et al., 2023; Taucher et al., 2024), as well as through the sinking of significant biomass of their carcasses (Lebrato et al., 2013).

Many GZP species have the capability to proliferate, or “bloom”, in favourable conditions due to the ability to switch from sexual to asexual reproduction which allows for rapid increases in population size. These blooms are driven by a wide range of factors including food availability, nutrient concentrations, and removal of top predators from an ecosystem (Condon et al., 2013; Duarte et al., 2013; Fernández-Alfás et al., 2024; Richardson et al., 2009). Aggregations, on the other hand, can be caused by environmental drivers such as wind and currents causing re-distribution and increased concentrations of otherwise spread-out populations. These aggregations and blooms can be centimetres to tens of meters thick and horizontally distributed from meters to hundreds of kilometres (Graham et al., 2001). Such large concentrations of GZP can have significant impacts on the commercial exploitation of marine resources as well as tourism. For example, severe negative impacts on the growing aquaculture industry have been documented, particularly for finfish aquaculture. High abundances in GZP around fish farms can lead to blockages in water flow, cause hypoxia in the captive fish, wound and kill fish with their stinging cells (nematocysts) and enhance the spread of harmful pathogens (reviewed in Pitt et al., 2024). Those GZP with stinging abilities

(cnidarians only) that can harm humans can lead to beach closures and negative impacts on coastal tourism industries in warmer regions such as the Mediterranean (Ruiz-Frau, 2023).

Despite the increased interest in GZP across multiple disciplines and marine ecosystems, there remain many gaps in baseline ecological knowledge of this group in the world's oceans. One of the major contributing factors is their tendency to be easily destroyed by the nets and trawls (**Table 1**) employed to sample and preserve other pelagic organisms (Haddock, 2007; Licandro et al., 2015; Raskoff et al., 2010; Ronowicz et al., 2015). Furthermore, accurate and high-resolution morphologically identification can be hindered by damage caused in sampling, a lack of detectible distinguishing features, complicated taxonomy or the presence of species complexes. Their tendency to be patchily dispersed also adds to complexities of surveying them with more traditional methods such as towed nets and cameras (Purcell, 2009).

1.7.3 Gelatinous zooplankton in the Arctic

Gelatinous zooplankton play significant roles in Arctic marine ecosystems. As grazers, appendicularians have been shown to consume substantial amounts of phytoplankton in polynyas (Deibel et al., 2005). As prey, multiple GZP groups have been found to be substantial components in the diets of crustaceans (Dischereit et al., 2022, 2024a; Urban et al., 2022) and of multiple fish species in the region (Dischereit et al., 2024b). As predators, the abundant ctenophores *Bolinopsis infundibulum* and *Mertensia ovum* are voracious feeders of copepods, amphipods and pteropods (Purcell et al., 2010), while the genus *Beroe* and narcomedusae species such as *Aeginopsis laurentii* specialize in feeding on other GZP species (Purcell et al., 2010; Raskoff, 2002). In terms of biodiversity, it is difficult to formulate a precise estimate of how many GZP species are in the Arctic due to limited baseline data. However, the class Hydrozoa is by far the richest with species numbers estimated between 176 and 268, followed by scyphozoan with seven and then the phylum Ctenophora with six species (reviewed in Majaneva et al., 2024). Although the true number of species is likely higher as uncertainties in phylogeny and taxonomy, as well as the presence of cryptic species remain unresolved (Majaneva et al., 2024; Majaneva and Majaneva, 2013; Ronowicz et al., 2015). These factors, combined with limited spatio-temporal sampling in the Arctic in general, means they are likely underestimated in richness, abundance and distribution in Arctic marine ecosystems. Nevertheless, a small number of recent studies targeting Arctic GZP have predicted that a number of GZP species commonly found in the Arctic are susceptible to range shifts with the ongoing climate change in the region (Maňko et al., 2020; Pantiukhin et al., 2024). Furthermore, Pantiukhin et al., (2023) predicted an overall increase in the abundance of GZP, and a concurrent decline in species richness under current climate change scenarios. These findings highlight a pressing need to fill existing knowledge gaps in order to better track and understand such changes on GZP in the Arctic Ocean.

1.8 Motivation and research objectives

Understanding current patterns and shifts in biodiversity in the Arctic Ocean is fundamental to quantifying how its ecosystems have and will continue to alter to in response to climate change. Biodiversity data plays a crucial role in formulating monitoring programs as well as mitigation and protection strategies and identifying potential future risks. The central aim of this thesis is to expand our current knowledge of Arctic eukaryotic marine biodiversity through the implementation of eDNA metabarcoding techniques. It has a particular focus on characterising the ecology of GZP communities in Fram Strait and Western Svalbard, which are hotspots for climate change in the region. To achieve this aim, this thesis sets out to accomplish the following objectives:

1. **To elucidate the environmental drivers of diversity and community composition of marine eukaryotes in Fram Strait.** Chapter Two investigates spatial patterns of metazoan diversity in Fram Strait. It also explores the effects of further abiotic variables (e.g., temperature, salinity and depth) on the composition of pelagic metazoan communities. Chapter Three investigates meltwater dynamics and sea ice conditions as drivers of eukaryotic community composition in the marginal ice zone. Chapter Four investigates spatial patterns of eukaryotic community composition in a semi-enclosed fjord system.
2. **To use eDNA metabarcoding to characterise eukaryotic communities and diversity across multiple Arctic marine ecosystems, spatial scales, and seasons.** Chapter Two investigates patterns of metazoan diversity on a regional scale in the open ocean Fram Strait. This study was conducted in early summer and samples were collected from the epipelagic, mesopelagic and bathypelagic ocean zones. Chapter Three investigates eukaryotic diversity in the sub-ice water column across different ice regimes of the marginal ice zone in summer. Sampling was conducted on a vertical scale of five meters and a horizontal scale of tens of kilometres. Chapter Four focuses on eukaryotic diversity at a local scale, with sampling stations all within the central part of the Kongsfjorden (Svalbard) during the polar night.
3. **To investigate the effectiveness of eDNA metabarcoding compared to traditional morphology-based sampling methods for characterising GZP biodiversity in the Arctic.** In Chapter Two, both optical and net-based sampling methods were conducted alongside the eDNA metabarcoding of water samples in Fram Strait. In Chapter Four, net catches and eDNA metabarcoding of water and sediment samples were collected and compared in Kongsfjorden, Svalbard.

- 4. To evaluate the effectiveness of two commonly used universal metabarcoding gene fragments for detecting Arctic GZP species.** In Chapter Five a multi-marker approach was employed *in silico* and on a mock community to investigate the effectiveness of two common metabarcoding markers and their associated primers to amplify a number of GZP taxa regularly found in the Arctic Ocean. In Chapter Three, a multi marker approach was employed *in situ* with the aim of increasing the chances of detecting GZP under sea ice.

1.9 References

- Andrews, A.J., Christiansen, J.S., Bhat, S., Lynghammar, A., Westgaard, J.I., Pampoulie, C., Præbel, K., 2019. Boreal marine fauna from the Barents Sea disperse to Arctic Northeast Greenland. *Scientific reports* 9, 1–8.
- Balazy, P., Anderson, M.J., Chelchowski, M., Włodarska-Kowalczyk, M., Kuklinski, P., Berge, J., 2021. Shallow-Water Scavengers of Polar Night and Day – An Arctic Time-Lapse Photography Study. *Front. Mar. Sci.* 8. <https://doi.org/10.3389/fmars.2021.656772>
- Barber, D.G., Hop, H., Mundy, C.J., Else, B., Dmitrenko, I.A., Tremblay, J.-E., Ehn, J.K., Assmy, P., Daase, M., Candlish, L.M., Rysgaard, S., 2015. Selected physical, biological and biogeochemical implications of a rapidly changing Arctic Marginal Ice Zone. *Progress in Oceanography, Overarching perspectives of contemporary and future ecosystems in the Arctic Ocean* 139, 122–150. <https://doi.org/10.1016/j.pocean.2015.09.003>
- Barnosky, A.D., Matzke, N., Tomiya, S., Wogan, G.O.U., Swartz, B., Quental, T.B., Marshall, C., McGuire, J.L., Lindsey, E.L., Maguire, K.C., Mersey, B., Ferrer, E.A., 2011. Has the Earth's sixth mass extinction already arrived? *Nature* 471, 51–57. <https://doi.org/10.1038/nature09678>
- Barton, A.D., Irwin, A.J., Finkel, Z.V., Stock, C.A., 2016. Anthropogenic climate change drives shift and shuffle in North Atlantic phytoplankton communities. *Proceedings of the National Academy of Sciences* 113, 2964–2969. <https://doi.org/10.1073/pnas.1519080113>
- Basedow, S.L., Sundfjord, A., Appen, W.-J., Halvorsen, E., Kwasniewski, S., Reigstad, M., 2018. Seasonal variation in transport of zooplankton into the Arctic basin through the Atlantic gateway, Fram Strait. *Frontiers in Marine Science* 5, 194.
- Beszczyńska-Moeller, A., Woodgate, R.A., Lee, C., Melling, H., Karcher, M., 2011. A synthesis of exchanges through the main oceanic gateways to the Arctic Ocean. *Oceanography* 24, 82–99.
- Bluhm, B., Gebruk, A., Gradinger, R., Hopcroft, R., Huettmann, F., Kosobokova, K., Sirenko, B., Weslawski, M., 2011. Arctic Marine Biodiversity: An Update of Species Richness and Examples of Biodiversity Change. *Oceanog.* 24, 232–248. <https://doi.org/10.5670/oceanog.2011.75>
- Bluhm, B.A., Gradinger, R., Schnack-Schiel, S., 2010. Sea Ice Meio- and Macrofauna, in: *Sea Ice*. Wiley, pp. 357–393.
- Boero, F., Bouillon, J., Gravili, C., Miglietta, M., Parsons, T., Piraino, S., 2008. Gelatinous plankton: irregularities rule the world (sometimes). *Mar. Ecol. Prog. Ser.* 356, 299–310. <https://doi.org/10.3354/meps07368>
- Bonfil, R., Palacios-Barreto, P., Vargas, O.U.M., Ricaño-Soriano, M., Díaz-Jaimes, P., 2021. Detection of critically endangered marine species with dwindling populations in the wild using eDNA gives hope for sawfishes. *Mar Biol* 168, 60. <https://doi.org/10.1007/s00227-021-03862-7>
- CAFF, 2017. State of the Arctic Marine Biodiversity: Key Findings and Advice for Monitoring. Conservation of Arctic Flora and Fauna International Secretariat, Akureyri, Iceland.
- CAFF, 2013. Arctic Biodiversity Assessment 2013: Status and trends in Arctic biodiversity. Conservation of Arctic Flora and Fauna, Akureyri, Iceland.
- Calvin, K., Dasgupta, D., Krinner, G., Mukherji, A., Thorne, P.W., Trisos, C., Romero, J., Aldunce, P., Barrett, K., Blanco, G., Cheung, W.W.L., Connors, S., Denton, F., Diongue-Niang, A., Dodman, D., Garschagen, M., Geden, O., Hayward, B., Jones, C., Jotzo, F., Krug, T., Lasco, R., Lee, Y.-Y., Masson-Delmotte, V., Meinshausen, M., Mintenbeck, K., Mokssit, A., Otto, F.E.L., Pathak, M., Pirani, A., Poloczanska, E., Pörtner, H.-O., Revi, A., Roberts, D.C., Roy, J., Ruane, A.C., Skea, J., Shukla, P.R., Slade, R., Slangen, A., Sokona, Y., Sörensson, A.A., Tignor, M., Van Vuuren, D., Wei, Y.-M., Winkler, H., Zhai, P., Zommers, Z., Hourcade, J.-C., Johnson, F.X.,

- Pachauri, S., Simpson, N.P., Singh, C., Thomas, A., Totin, E., Arias, P., Bustamante, M., Elgizouli, I., Flato, G., Howden, M., Méndez-Vallejo, C., Pereira, J.J., Pichs-Madruga, R., Rose, S.K., Saheb, Y., Sánchez Rodríguez, R., Ürge-Vorsatz, D., Xiao, C., Yassaa, N., Alegría, A., Armour, K., Bednar-Friedl, B., Blok, K., Cissé, G., Dentener, F., Eriksen, S., Fischer, E., Garner, G., Guivarch, C., Haasnoot, M., Hansen, G., Hauser, M., Hawkins, E., Hermans, T., Kopp, R., Leprince-Ringuet, N., Lewis, J., Ley, D., Ludden, C., Niamir, L., Nicholls, Z., Some, S., Szopa, S., Trewin, B., Van Der Wijst, K.-I., Winter, G., Witting, M., Birt, A., Ha, M., Romero, J., Kim, J., Haites, E.F., Jung, Y., Stavins, R., Birt, A., Ha, M., Orendain, D.J.A., Ignon, L., Park, S., Park, Y., Reisinger, A., Cammaramo, D., Fischlin, A., Fuglestvedt, J.S., Hansen, G., Ludden, C., Masson-Delmotte, V., Matthews, J.B.R., Mintenbeck, K., Pirani, A., Poloczanska, E., Leprince-Ringuet, N., Péan, C., 2023. IPCC, 2023: Climate Change 2023: Synthesis Report. Contribution of Working Groups I, II and III to the Sixth Assessment Report of the Intergovernmental Panel on Climate Change [Core Writing Team, H. Lee and J. Romero (eds.)]. IPCC, Geneva, Switzerland. Intergovernmental Panel on Climate Change (IPCC). <https://doi.org/10.59327/IPCC/AR6-9789291691647>
- Condon, R.H., Duarte, C.M., Pitt, K.A., Robinson, K.L., Lucas, C.H., Sutherland, K.R., Mianzan, H.W., Bogeberg, M., Purcell, J.E., Decker, M.B., Uye, S., Madin, L.P., Brodeur, R.D., Haddock, S.H.D., Malej, A., Parry, G.D., Eriksen, E., Quiñones, J., Acha, M., Harvey, M., Arthur, J.M., Graham, W.M., 2013. Recurrent jellyfish blooms are a consequence of global oscillations. *Proceedings of the National Academy of Sciences* 110, 1000–1005. <https://doi.org/10.1073/pnas.1210920110>
- Csapó, H.K., Grabowski, M., Węśławski, J.M., 2021. Coming home - Boreal ecosystem claims Atlantic sector of the Arctic. *Science of The Total Environment* 771, 144817. <https://doi.org/10.1016/j.scitotenv.2020.144817>
- Dalpadado, P., Hop, H., Rønning, J., Pavlov, V., Sperfeld, E., Buchholz, F., Rey, A., Wold, A., 2016. Distribution and abundance of euphausiids and pelagic amphipods in Kongsfjorden, Isfjorden and Rijpfjorden (Svalbard) and changes in their relative importance as key prey in a warming marine ecosystem. *Polar Biol* 39, 1765–1784. <https://doi.org/10.1007/s00300-015-1874-x>
- Dawson, J., Johnston, M., Stewart, E., 2017. The unintended consequences of regulatory complexity: The case of cruise tourism in Arctic Canada. *Marine Policy* 76, 71–78. <https://doi.org/10.1016/j.marpol.2016.11.002>
- Deagle, B.E., Chiaradia, A., McInnes, J., Jarman, S.N., 2010. Pyrosequencing faecal DNA to determine diet of little penguins: is what goes in what comes out? *Conserv Genet* 11, 2039–2048. <https://doi.org/10.1007/s10592-010-0096-6>
- Deibel, D., Saunders, P., Acuna, J., Bochdansky, A., Shiga, N., Rivkin, R., 2005. The role of appendicularian tunicates in the biogenic carbon cycle of three Arctic polynyas, in: *Response of Marine Ecosystems to Global Change: Ecological Impact of Appendicularians*. pp. 327–358.
- Deiner, K., Bik, H.M., Mächler, E., Seymour, M., Lacoursière-Roussel, A., Altermatt, F., Creer, S., Bista, I., Lodge, D.M., de Vere, N., Pfrender, M.E., Bernatchez, L., 2017. Environmental DNA metabarcoding: Transforming how we survey animal and plant communities. *Molecular Ecology* 26, 5872–5895. <https://doi.org/10.1111/mec.14350>
- Díaz, S., Settele, J., Brondízio, E.S., Ngo, H.T., Agard, J., Arneth, A., Balvanera, P., Brauman, K.A., Butchart, S.H.M., Chan, K.M.A., Garibaldi, L.A., Ichii, K., Liu, J., Subramanian, S.M., Midgley, G.F., Miloslavich, P., Molnár, Z., Obura, D., Pfaff, A., Polasky, S., Purvis, A., Razaque, J., Reyers, B., Chowdhury, R.R., Shin, Y.-J., Visseren-Hamakers, I., Willis, K.J., Zayas, C.N., 2019. Pervasive human-driven decline of life on Earth points to the need for transformative change. *Science* 366, eaax3100. <https://doi.org/10.1126/science.aax3100>
- Dischereit, A., Beermann, J., Lebreton, B., Wangensteen, O.S., Neuhaus, S., Havermans, C., 2024a. DNA metabarcoding reveals a diverse, omnivorous diet of Arctic

- amphipods during the polar night, with jellyfish and fish as major prey. *Front. Mar. Sci.* 11. <https://doi.org/10.3389/fmars.2024.1327650>
- Dischereit, A., Throm, J.K., Werner, K.-M., Neuhaus, S., Havermans, C., 2024b. A belly full of jelly? DNA metabarcoding shows evidence for gelatinous zooplankton predation by several fish species in Greenland waters. *Royal Society Open Science*. <https://doi.org/10.1098/rsos.240797>
- Dischereit, A., Wangensteen, O.S., Præbel, K., Auel, H., Havermans, C., 2022. Using DNA Metabarcoding to Characterize the Prey Spectrum of Two Co-Occurring Themisto Amphipods in the Rapidly Changing Atlantic-Arctic Gateway Fram Strait. *Genes* 13, 2035. <https://doi.org/10.3390/genes13112035>
- Doyle, S.M., Christner, B.C., 2022. Variation in bacterial composition, diversity, and activity across different subglacial basal ice types. *The Cryosphere* 16, 4033–4051. <https://doi.org/10.5194/tc-16-4033-2022>
- Duarte, C.M., Pitt, K.A., Lucas, C.H., Purcell, J.E., Uye, S., Robinson, K., Brotz, L., Decker, M.B., Sutherland, K.R., Malej, A., Madin, L., Mianzan, H., Gili, J.-M., Fuentes, V., Atienza, D., Pagés, F., Breitbart, D., Malek, J., Graham, W.M., Condon, R.H., 2013. Is global ocean sprawl a cause of jellyfish blooms? *Frontiers in Ecology and the Environment* 11, 91–97. <https://doi.org/10.1890/110246>
- Eleftheriou, A., 2013. *Methods for the Study of Marine Benthos*. John Wiley & Sons.
- Engel, M.S., Ceriaco, L.M.P., Daniel, G.M., Dellapé, P.M., Löbl, I., Marinov, M., Reis, R.E., Young, M.T., Dubois, A., Agarwal, I., Lehmann A., P., Alvarado, M., Alvarez, N., Andreone, F., Araujo-Vieira, K., Ascher, J.S., Baêta, D., Baldo, D., Bandeira, S.A., Barden, P., Barrasso, D.A., Bendifallah, L., Bockmann, F.A., Böhme, W., Borkent, A., Brandão, C.R.F., Busack, S.D., Bybee, S.M., Channing, A., Chatzimanolis, S., Christenhusz, M.J.M., Crisci, J.V., D'elía, G., Da Costa, L.M., Davis, S.R., De Lucena, C.A.S., Deuve, T., Fernandes Elizalde, S., Faivovich, J., Farooq, H., Ferguson, A.W., Gippoliti, S., Gonçalves, F.M.P., Gonzalez, V.H., Greenbaum, E., Hinojosa-Díaz, I.A., Ineich, I., Jiang, J., Kahono, S., Kury, A.B., Lucinda, P.H.F., Lynch, J.D., Malécot, V., Marques, M.P., Marris, J.W.M., Mckellar, R.C., Mendes, L.F., Nihei, S.S., Nishikawa, K., Ohler, A., Orrico, V.G.D., Ota, H., Paiva, J., Parrinha, D., Pauwels, O.S.G., Pereyra, M.O., Pestana, L.B., Pinheiro, P.D.P., Prendini, L., Prokop, J., Rasmussen, C., Rödel, M.-O., Rodrigues, M.T., Rodríguez, S.M., Salatnaya, H., Sampaio, Í., Sánchez-García, A., Shebl, M.A., Santos, B.S., Solórzano-Kraemer, M.M., Sousa, A.C.A., Stoev, P., Teta, P., Trape, J.-F., Dos Santos, C.V.-D., Vasudevan, K., Vink, C.J., Vogel, G., Wagner, P., Wappler, T., Ware, J.L., Wedmann, S., Zacharie, C.K., 2021. The taxonomic impediment: a shortage of taxonomists, not the lack of technical approaches. *Zoological Journal of the Linnean Society* 193, 381–387. <https://doi.org/10.1093/zoolinlean/zlab072>
- Fernández-Alías, A., Marcos, C., Pérez-Ruzafa, A., 2024. The unpredictability of scyphozoan jellyfish blooms. *Front. Mar. Sci.* 11. <https://doi.org/10.3389/fmars.2024.1349956>
- Ficetola, G.F., Miaud, C., Pompanon, F., Taberlet, P., 2008. Species detection using environmental DNA from water samples. *Biology Letters* 4, 423–425. <https://doi.org/10.1098/rsbl.2008.0118>
- Foote, A.D., Thomsen, P.F., Sveegaard, S., Wahlberg, M., Kielgast, J., Kyhn, L.A., Salling, A.B., Galatius, A., Orlando, L., Gilbert, M.T.P., 2012. Investigating the Potential Use of Environmental DNA (eDNA) for Genetic Monitoring of Marine Mammals. *PLOS ONE* 7, e41781. <https://doi.org/10.1371/journal.pone.0041781>
- Fossheim, M., Primicerio, R., Johannesen, E., Ingvaldsen, R.B., Aschan, M.M., Dolgov, A.V., 2015. Recent warming leads to a rapid borealization of fish communities in the Arctic. *Nature Clim Change* 5, 673–677. <https://doi.org/10.1038/nclimate2647>
- GEBCO Compilation Group, 2024. GEBCO 2024 Grid. <https://doi.org/0.5285/1c44ce99-0a0d-5f4f-e063-7086abc0ea0f>

- Goldsmith, J., McKindsey, C.W., Schlegel, R.W., Stewart, D.B., Archambault, P., Howland, K.L., 2020. What and where? Predicting invasion hotspots in the Arctic marine realm. *Global Change Biology* 26, 4752–4771. <https://doi.org/10.1111/gcb.15159>
- Golikov, A.V., Stauffer, J.B., Schindler, S.V., Taylor, J., Boehringer, L., Purser, A., Sabirov, R.M., Hoving, H.-J., 2023. Miles down for lunch: deep-sea in situ observations of Arctic finned octopods *Cirroteuthis muelleri* suggest pelagic–benthic feeding migration. *Proceedings of the Royal Society B: Biological Sciences* 290, 20230640. <https://doi.org/10.1098/rspb.2023.0640>
- Graham, W.M., Pagès, F., Hamner, W.M., 2001. A physical context for gelatinous zooplankton aggregations: a review, in: Purcell, J.E., Graham, W. M., Dumont, H.J. (Eds.), *Jellyfish Blooms: Ecological and Societal Importance*. Springer Netherlands, Dordrecht, pp. 199–212. https://doi.org/10.1007/978-94-010-0722-1_16
- Gruber, N., Bakker, D.C.E., DeVries, T., Gregor, L., Hauck, J., Landschützer, P., McKinley, G.A., Müller, J.D., 2023. Trends and variability in the ocean carbon sink. *Nat Rev Earth Environ* 4, 119–134. <https://doi.org/10.1038/s43017-022-00381-x>
- Günther, B., Fromentin, J.-M., Metral, L., Arnaud-Haond, S., 2021. Metabarcoding confirms the opportunistic foraging behaviour of Atlantic bluefin tuna and reveals the importance of gelatinous prey. *PeerJ* 9, e11757. <https://doi.org/10.7717/peerj.11757>
- Haddock, S.H.D., 2007. Comparative feeding behavior of planktonic ctenophores. *Integrative and Comparative Biology* 47, 847–853. <https://doi.org/10.1093/icb/icm088>
- Haddock, S.H.D., 2004. A golden age of gelata: past and future research on planktonic ctenophores and cnidarians. *Hydrobiologia* 530, 549–556. <https://doi.org/10.1007/s10750-004-2653-9>
- Hardy, S.M., Carr, C.M., Hardman, M., Steinke, D., Corstorphine, E., Mah, C., 2011. Biodiversity and phylogeography of Arctic marine fauna: insights from molecular tools. *Mar Biodiv* 41, 195–210. <https://doi.org/10.1007/s12526-010-0056-x>
- Havermans, C., Dischereit, A., Pantiukhin, D., Friedrich, M., Murray, A., 2022. Environmental DNA in an ocean of change: Status, challenges and prospects. *Archivos de Ciencias Do Mar* 55, 298–337. <https://doi.org/10.32360/acmar.v55iEspecial.78188>
- Hays, G.C., Doyle, T.K., Houghton, J.D.R., 2018. A Paradigm Shift in the Trophic Importance of Jellyfish? *Trends in Ecology & Evolution* 33, 874–884. <https://doi.org/10.1016/j.tree.2018.09.001>
- Hebert, P.D., Ratnasingham, S., Waard, J.R., 2003. Barcoding animal life: cytochrome c oxidase subunit 1 divergences among closely related species, in: *Proceedings of the Royal Society of London*. <https://doi.org/10.1098/rsbl.2003.0025>
- Hoegh-Guldberg, O., Bruno, J.F., 2010. The Impact of Climate Change on the World's Marine Ecosystems. *Science* 328, 1523–1528. <https://doi.org/10.1126/science.1189930>
- Ingvaldsen, R.B., Assmann, K.M., Primicerio, R., Fossheim, M., Polyakov, I.V., Dolgov, A.V., 2021. Physical manifestations and ecological implications of Arctic Atlantification. *Nat Rev Earth Environ* 2, 874–889. <https://doi.org/10.1038/s43017-021-00228-x>
- Intergovernmental Panel On Climate Change (IPCC), 2022. *The Ocean and Cryosphere in a Changing Climate: Special Report of the Intergovernmental Panel on Climate Change*, 1st ed. Cambridge University Press. <https://doi.org/10.1017/9781009157964>
- Jaspers, C., Hopcroft, R.R., Kjørboe, T., Lombard, F., López-Urrutia, Á., Everett, J.D., Richardson, A.J., 2023. Gelatinous larvacean zooplankton can enhance trophic transfer and carbon sequestration. *Trends in Ecology & Evolution* 0. <https://doi.org/10.1016/j.tree.2023.05.005>
- Johnson, M.D., Cox, R.D., Barnes, M.A., 2019. Analyzing airborne environmental DNA: A comparison of extraction methods, primer type, and trap type on the ability to detect airborne eDNA from terrestrial plant communities. *Environmental DNA* 1, 176–185. <https://doi.org/10.1002/edn3.19>
- Jones, K.R., Klein, C.J., Halpern, B.S., Venter, O., Grantham, H., Kuempel, C.D., Shumway, N., Friedlander, A.M., Possingham, H.P., Watson, J.E.M., 2018. The Location and

- Protection Status of Earth's Diminishing Marine Wilderness. *Current Biology* 28, 2506-2512.e3. <https://doi.org/10.1016/j.cub.2018.06.010>
- Lannuzel, D., Tedesco, L., van Leeuwe, M., Campbell, K., Flores, H., Delille, B., Miller, L., Stefels, J., Assmy, P., Bowman, J., Brown, K., Castellani, G., Chierici, M., Crabeck, O., Damm, E., Else, B., Fransson, A., Fripiat, F., Geilfus, N.-X., Jacques, C., Jones, E., Kaartokallio, H., Kotovitch, M., Meiners, K., Moreau, S., Nomura, D., Peeken, I., Rintala, J.-M., Steiner, N., Tison, J.-L., Vancoppenolle, M., Van der Linden, F., Vichi, M., Wongpan, P., 2020. The future of Arctic sea-ice biogeochemistry and ice-associated ecosystems. *Nat. Clim. Chang.* 10, 983–992. <https://doi.org/10.1038/s41558-020-00940-4>
- Lebrato, M., Mendes, P. de J., Steinberg, D.K., Cartes, J.E., Jones, B.M., Birsá, L.M., Benavides, R., Oschlies, A., 2013. Jelly biomass sinking speed reveals a fast carbon export mechanism. *Limnology and Oceanography* 58, 1113–1122. <https://doi.org/10.4319/lo.2013.58.3.1113>
- Leray, M., Knowlton, N., 2015. DNA barcoding and metabarcoding of standardized samples reveal patterns of marine benthic diversity. *Proceedings of the National Academy of Sciences* 112, 2076–2081. <https://doi.org/10.1073/pnas.1424997112>
- Leu, E., Søreide, J.E., Hessen, D.O., Falk-Petersen, S., Berge, J., 2011. Consequences of changing sea-ice cover for primary and secondary producers in the European Arctic shelf seas: Timing, quantity, and quality. *Progress in Oceanography, Arctic Marine Ecosystems in an Era of Rapid Climate Change* 90, 18–32. <https://doi.org/10.1016/j.pocean.2011.02.004>
- Li, Z., England, M.H., Groeskamp, S., 2023. Recent acceleration in global ocean heat accumulation by mode and intermediate waters. *Nat Commun* 14, 6888. <https://doi.org/10.1038/s41467-023-42468-z>
- Licandro, P., Blackett, M., Fischer, A., Hosia, A., Kennedy, J., Kirby, R.R., Raab, K., Stern, R., Tranter, P., 2015. Biogeography of jellyfish in the North Atlantic, by traditional and genomic methods. *Earth System Science Data* 7, 173–191. <https://doi.org/10.5194/essd-7-173-2015>
- Mace, G.M., Norris, K., Fitter, A.H., 2012. Biodiversity and ecosystem services: a multilayered relationship. *Trends in Ecology & Evolution* 27, 19–26. <https://doi.org/10.1016/j.tree.2011.08.006>
- Majaneva, S., Havermans, C., Hopcroft, R., Kosobokova, K., Verhaegen, G., Hosia, A., 2024. Gelatinous zooplankton - delicate drifters of the Arctic Ocean, in: *Elements of a Pan-Arctic Ocean Ecology*. Orkana Forlag, pp. 234–247.
- Majaneva, S., Majaneva, M., 2013. Cydippid ctenophores in the coastal waters of Svalbard: is it only *Mertensia ovum*? *Polar Biol* 36, 1681–1686. <https://doi.org/10.1007/s00300-013-1377-6>
- Mańko, M.K., Gluchowska, M., Weydmann-Zwolicka, A., 2020. Footprints of Atlantification in the vertical distribution and diversity of gelatinous zooplankton in the Fram Strait (Arctic Ocean). *Progress in Oceanography* 189, 102414. <https://doi.org/10.1016/j.pocean.2020.102414>
- Meredith, M., Sommerkorn, M., Cassotta, S., Derksen, C., Ekaykin, A., Hollowed, A., Kofinas, G., Mackintosh, A., Melbourne-Thoma, J., Muelber, M.M.C., Ottersen, G., Pritchard, H., Schuur, E.A.G., 2022. *The Ocean and Cryosphere in a Changing Climate: Special Report of the Intergovernmental Panel on Climate Change*, 1st ed. Cambridge University Press. <https://doi.org/10.1017/9781009157964>
- Mora, C., Tittensor, D.P., Adl, S., Simpson, A.G.B., Worm, B., 2011. How Many Species Are There on Earth and in the Ocean? *PLoS Biology* 9, e1001127. <https://doi.org/10.1371/journal.pbio.1001127>
- Morrissey, S.J., Jerry, D.R., Kingsford, M.J., 2022. Genetic Detection and a Method to Study the Ecology of Deadly Cubozoan Jellyfish. *Diversity* 14, 1139. <https://doi.org/10.3390/d14121139>
- Mueter, F.J., Planque, B., Hunt, G.L., Alabia, I.D., Hirawake, T., Eisner, L., Dalpadado, P., Chierici, M., Drinkwater, K.F., Harada, N., Arneberg, P., Saitoh, S.-I., 2021. Possible

- future scenarios in the gateways to the Arctic for Subarctic and Arctic marine systems: II. prey resources, food webs, fish, and fisheries. *ICES Journal of Marine Science* 78, 3017–3045. <https://doi.org/10.1093/icesjms/fsab122>
- Oliver, J.-C., Shum, P., Mariani, S., Sink, K.J., Palmer, R., Matcher, G.F., 2024. Enhancing African coelacanth monitoring using environmental DNA. *Biology Letters* 20, 20240415. <https://doi.org/10.1098/rsbl.2024.0415>
- PAME, P. of the A.M.E., 2020. The increase in Arctic shipping—Arctic shipping status report. (No. 1). Protection of the Arctic Marine Environment working group, Akureyri, Iceland.
- Pantiukhin, D., Verhaegen, G., Havermans, C., 2024. Pan-Arctic distribution modeling reveals climate-change-driven poleward shifts of major gelatinous zooplankton species. *Limnology and Oceanography* 69, 1316–1334. <https://doi.org/10.1002/lno.12568>
- Pantiukhin, D., Verhaegen, G., Kraan, C., Jerosch, K., Neitzel, P., Hoving, H.-J.T., Havermans, C., 2023. Optical observations and spatio-temporal projections of gelatinous zooplankton in the Fram Strait, a gateway to a changing Arctic Ocean. *Frontiers in Marine Science* 10.
- Pearson, J., Jackson, G., McNamara, K.E., 2023. Climate-driven losses to knowledge systems and cultural heritage: A literature review exploring the impacts on Indigenous and local cultures. *The Anthropocene Review* 10, 343–366. <https://doi.org/10.1177/20530196211005482>
- Piepenburg, D., 2005. Recent research on Arctic benthos: common notions need to be revised. *Polar Biol* 28, 733–755. <https://doi.org/10.1007/s00300-005-0013-5>
- Pitt, K.A., Haberlin, D., Stantic, B., Doyle, T.K., 2024. Mitigating and managing the impacts of gelatinous zooplankton on finfish aquaculture. *Aquaculture* 581, 740403. <https://doi.org/10.1016/j.aquaculture.2023.740403>
- Polyakov, I.V., Alkire, M.B., Bluhm, B.A., Brown, K.A., Carmack, E.C., Chierici, M., Danielson, S.L., Ellingsen, I., Ershova, E.A., Gårdfeldt, K., Ingvaldsen, R.B., Pnyushkov, A.V., Slagstad, D., Wassmann, P., 2020. Borealization of the Arctic Ocean in Response to Anomalous Advection From Sub-Arctic Seas. *Frontiers in Marine Science* 7.
- Polyakov, I.V., Pnyushkov, A.V., Alkire, M.B., Ashik, I.M., Baumann, T.M., Carmack, E.C., Goszczko, I., Guthrie, J., Ivanov, V.V., Kanzow, T., Kirshfield, R., 2017. Greater role for Atlantic inflows on sea-ice loss in the Eurasian Basin of the Arctic Ocean. *Science* 356, 285–291.
- Pompanon, F., Deagle, B.E., Symondson, W.O.C., Brown, D.S., Jarman, S.N., Taberlet, P., 2012. Who is eating what: diet assessment using next generation sequencing. *Molecular Ecology* 21, 1931–1950. <https://doi.org/10.1111/j.1365-294X.2011.05403.x>
- Pörtner, H.-O., Scholes, R.J., Arneeth, A., Barnes, D.K.A., Burrows, M.T., Diamond, S.E., Duarte, C.M., Kiessling, W., Leadley, P., Managi, S., McElwee, P., Midgley, G., Ngo, H.T., Obura, D., Pascual, U., Sankaran, M., Shin, Y.J., Val, A.L., 2023. Overcoming the coupled climate and biodiversity crises and their societal impacts. *Science* 380, eabl4881. <https://doi.org/10.1126/science.abl4881>
- Purcell, J., 2009. Extension of methods for jellyfish and ctenophore trophic ecology to large-scale research. *Hydrobiologia* 616, 23–50. <https://doi.org/10.1007/s10750-008-9585-8>
- Purcell, J.E., 1985. Predation on fish eggs and larvae by pelagic cnidarians and ctenophores. *Bulletin of Marine Science* 37, 739–755.
- Purcell, J.E., Hopcroft, R.R., Kosobokova, K.N., Whitley, T.E., 2010. Distribution, abundance, and predation effects of epipelagic ctenophores and jellyfish in the western Arctic Ocean. *Deep Sea Research Part II: Topical Studies in Oceanography, Observations and Exploration of the Arctic's Canada Basin and the Chukchi Sea: the Hidden Ocean and RUSALCA Expeditions* 57, 127–135. <https://doi.org/10.1016/j.dsr2.2009.08.011>

- Qi, X., Li, Z., Zhao, C., Zhang, Q., Zhou, Y., 2024. Environmental impacts of Arctic shipping activities: A review. *Ocean & Coastal Management* 247, 106936. <https://doi.org/10.1016/j.ocecoaman.2023.106936>
- Ramirez-Llodra, E., Meyer, H.K., Bluhm, B.A., Brix, S., Brandt, A., Dannheim, J., Downey, R.V., Egilsdóttir, H., Eilertsen, M.H., Gaudron, S.M., Gebruk, A., Golikov, A., Hasemann, C., Hilario, A., Jørgensen, L.L., Kaiser, S., Korfhage, S.A., Kürzel, K., Lörz, A.-N., Buhl-Mortensen, P., Olafsdóttir, S.H., Piepenburg, D., Purser, A., Ribeiro, P.A., Sen, A., Soltwedel, T., Stratmann, T., Steger, J., Svavarsson, J., Tandberg, A.H.S., Taylor, J., Theising, F.I., Uhlir, C., Waller, R.G., Xavier, J.R., Zhulay, I., Saaedi, H., 2024. The emerging picture of a diverse deep Arctic Ocean seafloor: From habitats to ecosystems. *Elementa: Science of the Anthropocene* 12, 00140. <https://doi.org/10.1525/elementa.2023.00140>
- Rantanen, M., Karpechko, A.Y., Lipponen, A., Nordling, K., Hyvärinen, O., Ruosteenoja, K., K, V., Laaksonen, A., 2022. The Arctic has warmed nearly four times faster than the globe since 1979. *Communications Earth & Environment* 3, 1–10.
- Raskoff, K., 2002. Foraging, prey capture, and gut contents of the mesopelagic narcomedusa *Solmissus* spp. (Cnidaria: Hydrozoa). *Marine Biology* 141, 1099–1107. <https://doi.org/10.1007/s00227-002-0912-8>
- Raskoff, K.A., Hopcroft, R.R., Kosobokova, K.N., Purcell, J.E., Youngbluth, M., 2010. Jellies under ice: ROV observations from the Arctic 2005 hidden ocean expedition. *Deep Sea Research Part II: Topical Studies in Oceanography, Observations and Exploration of the Arctic's Canada Basin and the Chukchi Sea: the Hidden Ocean and RUSALCA Expeditions* 57, 111–126. <https://doi.org/10.1016/j.dsr2.2009.08.010>
- Riaz, T., Shehzad, W., Viari, A., Pompanon, F., Taberlet, P., Coissac, E., 2011. ecoPrimers: inference of new DNA barcode markers from whole genome sequence analysis. *Nucleic Acids Research* 39, e145–e145. <https://doi.org/10.1093/nar/gkr732>
- Richardson, A.J., Bakun, A., Hays, G.C., Gibbons, M.J., 2009. The jellyfish joyride: causes, consequences and management responses to a more gelatinous future. *Trends in Ecology & Evolution* 24, 312–322. <https://doi.org/10.1016/j.tree.2009.01.010>
- Ronowicz, M., Kukliński, P., Mapstone, G.M., 2015. Trends in the Diversity, Distribution and Life History Strategy of Arctic Hydrozoa (Cnidaria). *PLOS ONE* 10, e0120204. <https://doi.org/10.1371/journal.pone.0120204>
- Ruiz, M.B., Moreira, E., Novillo, M., Neuhaus, S., Leese, F., Havermans, C., 2024a. Detecting the invisible through DNA metabarcoding: The role of gelatinous taxa in the diet of two demersal Antarctic key stone fish species (Notothenioidei). *Environmental DNA* 6, e561. <https://doi.org/10.1002/edn3.561>
- Ruiz, M.B., Saunders, R.A., Tarling, G.A., Murray, A., Leese, F., Havermans, C., 2024b. The secret meal of Antarctic mesopelagic fish (Myctophidae: *Electrona*) revealed by multimarker metabarcoding The secret meal of Antarctic myctophids. *Front. Mar. Sci.* 11. <https://doi.org/10.3389/fmars.2024.1474424>
- Ruiz-Frau, A., 2023. Impacts of jellyfish presence on tourists' holiday destination choices and their willingness to pay for mitigation measures. *Journal of Environmental Planning and Management* 66, 2107–2125. <https://doi.org/10.1080/09640568.2022.2061926>
- Sameoto, D., Wiebe, P., Runge, J., Postel, L., Dunn, J., Miller, C., Coombs, S., 2000. 3 - Collecting zooplankton, in: Harris, R., Wiebe, Peter, Lenz, J., Skjoldal, H.R., Huntley, M. (Eds.), *ICES Zooplankton Methodology Manual*. Academic Press, London, pp. 55–81. <https://doi.org/10.1016/B978-012327645-2/50004-9>
- Schroeder, A., Camatti, E., Pansera, M., Pallavicini, A., 2023. Feeding pressure on meroplankton by the invasive ctenophore *Mnemiopsis leidyi*. *Biol Invasions* 25, 2007–2021. <https://doi.org/10.1007/s10530-023-03023-5>
- Schröter, F., Havermans, C., Kraft, A., Knüppel, N., Beszczynska-Möller, A., Bauerfeind, E., Nöthig, E.-M., 2019. Pelagic Amphipods in the Eastern Fram Strait With Continuing Presence of *Themisto compressa* Based on Sediment Trap Time Series. *Frontiers in Marine Science* 6.

- Shea, M.M., Kuppermann, J., Rogers, M.P., Smith, D.S., Edwards, P., Boehm, A.B., 2023. Systematic review of marine environmental DNA metabarcoding studies: toward best practices for data usability and accessibility. *PeerJ* 11, e14993. <https://doi.org/10.7717/peerj.14993>
- Sønstebo, J.H., Gielly, L., Brysting, A.K., Elven, R., Edwards, M., Haile, J., Willerslev, E., Coissac, E., Rioux, D., Sannier, J., Taberlet, P., Brochmann, C., 2010. Using next-generation sequencing for molecular reconstruction of past Arctic vegetation and climate. *Molecular Ecology Resources* 10, 1009–1018. <https://doi.org/10.1111/j.1755-0998.2010.02855.x>
- Staley, Z.R., Chuong, J.D., Hill, S.J., Grabuski, J., Shokralla, S., Hajibabaei, M., Edge, T.A., 2018. Fecal source tracking and eDNA profiling in an urban creek following an extreme rain event. *Sci Rep* 8, 14390. <https://doi.org/10.1038/s41598-018-32680-z>
- Stephen, K., 2018. Societal Impacts of a Rapidly Changing Arctic. *Curr Clim Change Rep* 4, 223–237. <https://doi.org/10.1007/s40641-018-0106-1>
- Taberlet, P., Bonin, A., Zinger, L., Coissac, E., 2018. *Environmental DNA: For Biodiversity Research and Monitoring*. Oxford University Press.
- Taberlet, P., Coissac, E., Hajibabaei, M., Rieseberg, L.H., 2012. Environmental DNA. *Molecular Ecology* 21, 1789–1793. <https://doi.org/10.1111/j.1365-294X.2012.05542.x>
- Taucher, J., Lechtenböcker, A.K., Bouquet, J.-M., Spisla, C., Boxhammer, T., Minutolo, F., Bach, L.T., Lohbeck, K.T., Sswat, M., Dörner, I., Ismar-Rebitz, S.M.H., Thompson, E.M., Riebesell, U., 2024. The appendicularian *Oikopleura dioica* can enhance carbon export in a high CO₂ ocean. *Glob Chang Biol* 30, e17020. <https://doi.org/10.1111/gcb.17020>
- Thiebot, J.-B., Arnould, J.P., Gómez-Laich, A., Ito, K., Kato, A., Mattern, T., Mitamura, H., Noda, T., Poupert, T., Quintana, F., Raclot, T., Ropert-Coudert, Y., Sala, J.E., Seddon, P.J., Sutton, G.J., Yoda, K., Takahashi, A., 2017. Jellyfish and other gelata as food for four penguin species – insights from predator-borne videos. *Frontiers in Ecology and the Environment* 15, 437–441. <https://doi.org/10.1002/fee.1529>
- Thoman, R.L., Moon, T.A., Druckenmiller, M.L., 2023. NOAA Arctic Report Card 2023 : Executive Summary. <https://doi.org/10.25923/5VFA-K694>
- Thomsen, P.F., Kielgast, J., Iversen, L.L., Møller, P.R., Rasmussen, M., Willerslev, E., 2012. Detection of a Diverse Marine Fish Fauna Using Environmental DNA from Seawater Samples. *PLOS ONE* 7, e41732. <https://doi.org/10.1371/journal.pone.0041732>
- Thomsen, P.F., Willerslev, E., 2015. Environmental DNA – An emerging tool in conservation for monitoring past and present biodiversity. *Biological Conservation, Special Issue: Environmental DNA: A powerful new tool for biological conservation* 183, 4–18. <https://doi.org/10.1016/j.biocon.2014.11.019>
- Turon, M., Angulo-Preckler, C., Antich, A., Præbel, K., Wangensteen, O.S., 2020. More Than Expected From Old Sponge Samples: A Natural Sampler DNA Metabarcoding Assessment of Marine Fish Diversity in Nha Trang Bay (Vietnam). *Front. Mar. Sci.* 7. <https://doi.org/10.3389/fmars.2020.605148>
- Urban, P., Præbel, K., Bhat, S., Dierking, J., Wangensteen, O.S., 2022. DNA metabarcoding reveals the importance of gelatinous zooplankton in the diet of *Pandalus borealis*, a keystone species in the Arctic. *Molecular Ecology* 31, 1562–1576. <https://doi.org/10.1111/mec.16332>
- Varotto, C., Pindo, M., Bertoni, E., Casarotto, C., Camin, F., Girardi, M., Maggi, V., Cristofori, A., 2021. A pilot study of eDNA metabarcoding to estimate plant biodiversity by an alpine glacier core (Adamello glacier, North Italy). *Sci Rep* 11, 1208. <https://doi.org/10.1038/s41598-020-79738-5>
- Vinogradov, M.E., Melnikov, I.A., 1980. The study of the pelagic ecosystem of the central Arctic Basin. *Biology of the central Arctic Basin* 5–14.
- Wassmann, P., Duarte, C.M., Agustí, S., Sej, M.K., 2011. Footprints of climate change in the Arctic marine ecosystem. *Global Change Biology* 17, 1235–1249. <https://doi.org/10.1111/j.1365-2486.2010.02311.x>

- Watson, J.E.M., Venter, O., Lee, J., Jones, K.R., Robinson, J.G., Possingham, H.P., Allan, J.R., 2018. Protect the last of the wild. *Nature* 563, 27–30.
<https://doi.org/10.1038/d41586-018-07183-6>
- Weiskopf, S.R., Isbell, F., Arce-Plata, M.I., Di Marco, M., Harfoot, M., Johnson, J., Lerman, S.B., Miller, B.W., Morelli, T.L., Mori, A.S., Weng, E., Ferrier, S., 2024. Biodiversity loss reduces global terrestrial carbon storage. *Nat Commun* 15, 4354.
<https://doi.org/10.1038/s41467-024-47872-7>
- Whitmore, B.M., Nickels, C.F., Ohman, M.D., 2019. A comparison between Zooglider and shipboard net and acoustic mesozooplankton sensing systems. *Journal of Plankton Research* 41, 521–533. <https://doi.org/10.1093/plankt/fbz033>
- Wietz, M., Engel, A., Ramondenc, S., Niwano, M., Von Appen, W., Priest, T., Von Jackowski, A., Metfies, K., Bienhold, C., Boetius, A., 2024. The Arctic summer microbiome across Fram Strait: Depth, longitude, and substrate concentrations structure microbial diversity in the euphotic zone. *Environmental Microbiology* 26, e16568. <https://doi.org/10.1111/1462-2920.16568>
- Willerslev, E., Hansen, A.J., Binladen, J., Brand, T.B., Gilbert, M.T.P., Shapiro, B., Bunce, M., Wiuf, C., Gilichinsky, D.A., Cooper, A., 2003. Diverse Plant and Animal Genetic Records from Holocene and Pleistocene Sediments. *Science* 300, 791–795.
<https://doi.org/10.1126/science.1084114>

Chapter 2

Investigating pelagic biodiversity and gelatinous zooplankton communities in the rapidly changing European Arctic: An eDNA metabarcoding survey

Ayla Murray^{1,2}, Taylor Priest³, Adria Antich⁴, Wilken-Jon von-Appen¹, Stefan Neuhaus¹, Charlotte Havermans^{1,2}

1. Alfred Wegener Institute Helmholtz Centre for Polar and Marine Research, Bremerhaven, Germany
2. University of Bremen, Bremen, Germany
3. ETH Zurich, Zurich, Switzerland
4. NORCE Climate and Environment, NORCE Norwegian Research Centre AS and Bjerknes Centre for Climate Research, Bergen, Norway

Manuscript published in Environmental DNA (May 2024)

Investigating pelagic biodiversity and gelatinous zooplankton communities in the rapidly changing European Arctic: An eDNA metabarcoding survey

Ayla Murray^{1,2}  | Taylor Priest³ | Adria Antich⁴ | Wilken-Jon von Appen¹ | Stefan Neuhaus¹ | Charlotte Havermans^{1,2} 

¹Alfred Wegener Institute Helmholtz Centre for Polar and Marine Research, Bremerhaven, Germany

²University of Bremen, Bremen, Germany

³ETH Zurich, Zürich, Switzerland

⁴NORCE Climate and Environment, NORCE Norwegian Research Centre AS and Bjerknes Centre for Climate Research, Bergen, Norway

Correspondence

Ayla Murray, Alfred Wegener Institute Helmholtz Centre for Polar and Marine Research, Bremerhaven, Germany.
Email: ayla.murray@awi.de

Funding information

Alfred-Wegener-Institut, Helmholtz-Zentrum für Polar- und Meeresforschung, Grant/Award Number: AWI_PS126_09 and VH-NG-1400

Abstract

Fram Strait, the gateway between the Arctic and Atlantic Oceans, is undergoing major climate change-induced physical and biological transformations. In particular, rapid warming and ongoing “Atlantification” are driving species range shifts and altering food web structures in the Arctic. Understanding and predicting the consequences of these processes on future ecosystems requires detailed assessments of local and pelagic biodiversity. Gelatinous zooplankton (GZP) is an important component of pelagic communities, and recent evidence indicates that such communities are undergoing major changes in the Fram Strait. However, as sampling GZP is challenging, they are regularly underestimated in biodiversity, distribution, and abundance. To overcome this and address existing ecological knowledge gaps, we investigated patterns of pelagic metazoan diversity in Fram Strait using environmental DNA (eDNA) metabarcoding of the cytochrome c oxidase I (COI) gene. We successfully detected a broad range of taxa from the marine metazoan and GZP communities across sampling locations and ocean depth zones. We demonstrate the vertical structuring of diversity and elucidate relationships between taxa and water mass indicators, such as salinity and temperature. Furthermore, when comparing eDNA data with net and video transect data for GZP at the same period and location, we found that eDNA uncovered a higher number of taxa, including several that were not detected by the other methods. This study is a contribution to the formation of baseline Arctic GZP biodiversity datasets, as well as future research on changing marine metazoan biodiversity and community composition.

KEYWORDS

Arctic Ocean, deep sea, environmental DNA, Fram Strait, jellyfish, open ocean

This is an open access article under the terms of the [Creative Commons Attribution](https://creativecommons.org/licenses/by/4.0/) License, which permits use, distribution and reproduction in any medium, provided the original work is properly cited.

© 2024 The Author(s). *Environmental DNA* published by John Wiley & Sons Ltd.

1 | INTRODUCTION

The Arctic is undergoing rapid and unprecedented transformations because of anthropogenic climate change. It is warming four times faster than the global mean (Rantanen et al., 2022), which is evidenced by the rising sea surface temperatures and declining perennial sea-ice cover observed in recent decades (Huang et al., 2017; Rantanen et al., 2022). The largest source of oceanic heat into the central Arctic is the Fram Strait (Beszczynska-Moeller et al., 2011), which is known as the Atlantic gateway to the Arctic. This hydrographically dynamic strait is the only deepwater inflow into the Arctic Basin, acting as the transition between Atlantic-boreal and high-Arctic biogeographic zones (Hop et al., 2019). The “Atlantification” of the Arctic, underpinned by increasing volumes and temperature of northward flowing Atlantic water, is having growing influences on both physical and biological processes in the region, and its impacts are predicted to increase drastically in the coming years (Ingvaldsen et al., 2021; Polyakov et al., 2017, 2020). Biodiversity-linked consequences of this Atlantification, such as shrinking habitat ranges of Arctic- and northward encroachment of Atlantic species have been observed in phytoplankton (Neukermans et al., 2018; Oziel et al., 2020), zooplankton (Csapó et al., 2021; Ingvaldsen et al., 2021) and fish (Polyakov et al., 2017). Changes in species' distribution ranges and the subsequent increases in the number of boreal-Atlantic species and biomass are leading to the restructuring of Arctic ecosystems (Basedow et al., 2018; Csapó et al., 2021). The collection of baseline datasets with biodiversity surveys is crucial in the establishment of long-term monitoring for understanding climate-change impacts on marine ecosystems. These will allow us to document and track species distribution shifts in the Arctic Ocean, particularly in the major gateways connecting it with temperate regions.

Zooplankton are a crucial link between primary producers and higher trophic levels, and they play a pivotal role in the biological carbon pump. The zooplankton community in Fram Strait typically consists of a mix of “true” Arctic, Arctic-boreal, and boreal-Atlantic expatriates (Weydmann et al., 2014). The distribution, composition, and food-web structure of these communities is heavily influenced by environmental factors such as sea-ice cover, temperature, salinity, and nutrient supply (Gluchowska, Dalpadado et al., 2017; Wassmann et al., 2015). For instance, the abundant Arctic copepod *Calanus glacialis* is typically associated with colder temperatures and higher sea-ice coverage, whereas its boreal congener *C. finmarchicus* is an indicator of warmer temperatures and Atlantic water masses (Hatlebakk et al., 2022). An important component of the pelagic community is the gelatinous zooplankton (GZP), or jellyfish, a polyphyletic and highly diverse group including cnidarian medusae, ctenophores, and pelagic tunicates. They serve major ecosystem roles as predators and are important in pelagic-benthic coupling and vertical carbon export (Jaspers et al., 2023; Lebrato et al., 2012, 2013), particularly when occurring in high numbers (aggregations or blooms). Recent studies have shown poleward expansions of the distribution ranges of boreal species, e.g., for the large scyphozoan *Periphylla periphylla* around Svalbard and in the Nansen

Basin (Geoffroy et al., 2018; Ingvaldsen et al., 2023). Additionally, increased abundances of the arcto-boreal hydrozoan *Aglantha digitale* have been found in warmer water masses in the North Atlantic (Haberlin et al., 2019) and in Atlantic water masses in Fram Strait (Maňko et al., 2020), where it is predicted to become a dominant species as the Arctic warms (Maňko et al., 2020; Pantiukhin et al., 2023a). In contrast, “true” Arctic species are predicted to experience significant decreases in abundance in coming decades, as shown for the midwater hydrozoan *Sminthea arctica* (Pantiukhin et al., 2023a). Overall, an increase in GZP abundances but a decrease in GZP richness has been projected under future climate-change scenarios (Pantiukhin et al., 2023a), which makes this group an important candidate for zooplankton monitoring efforts.

Despite an increase in studies with a focus on GZP diversity and distribution in the Arctic, sampling limitations to typical survey methods remain. Successful detection of different taxa varies among the type of trawl or net used (Hosia et al., 2017; Nogueira Júnior et al., 2015), as they can destroy more delicate specimens or capture only a limited size range. While optical methods can detect individuals without damaging them and hence provide more reliable abundance estimates for some taxa (Pantiukhin et al., 2023a), they also have known biases (Hosia et al., 2017; Raskoff et al., 2010) and can be resource-intensive and deployed only in limited spatial areas. To fill in the knowledge gaps on GZP diversity in the Arctic and improve monitoring efforts to document ongoing species shifts, there is an urgent need for time- and cost-effective methods that can yield a high taxonomic resolution and be implemented at various spatial and temporal scales.

Metabarcoding of environmental DNA (eDNA) has become an efficient and non-invasive approach increasingly used in impact assessments, biodiversity and community structure surveys, species-specific detection, and biosecurity applications in the last decade (Bunholi et al., 2023). It is highly sensitive, allows for non-invasive detection, and can provide high resolution of taxonomic identification without the necessity of expert taxonomic knowledge. The efficacy of eDNA metabarcoding as a tool to monitor metazoan biodiversity has been validated against traditional methods in various marine habitats (Djurhuus et al., 2018; Feng et al., 2022; Govindarajan et al., 2021; Lacoursière-Roussel et al., 2018; Suter et al., 2021). While there has been an increasing number of studies using eDNA to detect GZP in recent years, they have largely been focused on single-species detection rather than metabarcoding (Bolte et al., 2021; Minamoto et al., 2017; Morrissey et al., 2022; Ogata et al., 2021; Takasu et al., 2019) and GZP community studies with eDNA are so far missing. Furthermore, the application of eDNA metabarcoding to specifically assess GZP biodiversity in polar regions is yet to be implemented.

In this study, we provide the first assessment of the pelagic marine metazoan community in the rapidly changing Fram Strait using metabarcoding of the mitochondrial COI fragment. The aim of this research was to (i) survey marine metazoan biodiversity across the Fram Strait, (ii) investigate GZP alpha and beta diversity and the environmental drivers of community composition across polar- and

temperate-derived water masses, and finally (iii) compare the efficacy of eDNA metabarcoding as a survey method for GZP to other sampling and observational approaches, including net caught specimens and in situ camera transects.

2 | MATERIALS AND METHODS

2.1 | Study area and sample collection

Samples were collected in May and June of 2021 during the oceanographic cruise PS126 (Soltwedel, 2021) of the R/V Polarstern (Knust, 2017). Seven locations were sampled in the HAUSGARTEN observatory, with two in the East Greenland Current (EG1 and EG4), three in central Fram Strait (HG4, N4, and S3), and two on the West Spitsbergen Shelf (SV2 and SV4) (Figure 1a). At each location, seawater samples for metabarcoding were collected at specific depths throughout the water column (all stations: 0, 20, 50, 100m; deep stations additionally: 200, 400, 500, 750, 1000, 1300, 1600, 2000, 2250, and 2500m), using 12L Niskin bottles mounted on a conductivity-temperature-depth (CTD) Rosette. Sterilized canisters were filled with 6L of water from a single Niskin per depth, from which triplicate 2L samples were taken, resulting in a total of 194 samples (Table S1). The 2L samples were filtered through 0.22 μ m Sterivex-GP filters (Merck Millipore) using a Masterflex peristaltic pump. Field blanks were taken by filtering MilliQ water across one filter per CTD cast. New tubing was used for each depth when collecting water from the Niskin bottles and during filtering. All work benches and other necessary lab equipment were sterilized with a

10% bleach solution, followed by MilliQ water in between stations and the plastic canisters between samples. Filters were stored at -80°C until laboratory processing.

Hydrographic data was obtained simultaneously with water collection at each station using an SBE911+ CTD sensor mounted on the rosette water sampler. Water masses were determined based on temperature and salinity measurements modified from Rudels et al. (2013) (Table S2). Depth zones were classified as upper-epipelagic (0–99m), lower-epipelagic (100–200m), mesopelagic (201–1000m), and bathypelagic (>1001m).

Samples for morphological identification were collected using a Maxi-Multinet (Hydrobios) and Bongo plankton nets (Hydrobios). Depth-stratified Multinet hauls, with 330 μ m mesh size, were carried out vertically between 2500m and the surface at a wire speed of 0.5m/s. At most stations, we carried out oblique Bongo net tows, with mesh sizes of 335 and 500 μ m, equipped with a large non-filtering cod-end and a V-Fin depressor, deployed between 100 and 740m depths, at a speed of 2 knots. At station N4, vertical Bongo net hauls were carried out due to heavy ice cover. Specimens were identified to the lowest possible taxonomic level on board using taxonomy keys (Bouillon et al., 2006; Licandro et al., 2017; Licandro & Lindsay, 2017). Damaged or ambiguous specimens were only identified at higher taxonomic levels to avoid misidentification (e.g., order Trachymedusae).

Video data were obtained by deploying the Pelagic In Situ Observation System (PELAGIOS) (Hoving et al., 2019), during horizontal transects at three of the stations. All data for video observations were taken from the publicly available dataset on PANGAEA (Pantiukhin et al., 2023b). We used GZP presence data from all

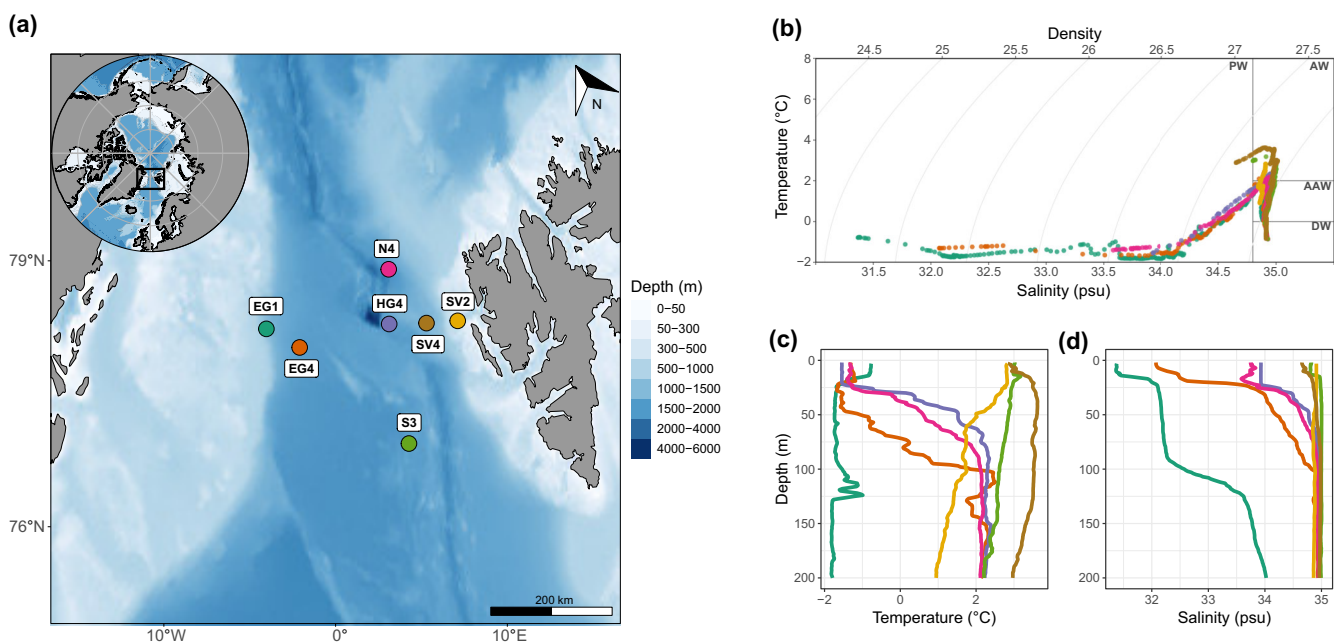


FIGURE 1 Study sites and oceanographic profiles. (a) Map of the seven sampling locations in Fram Strait. (b) Temperature-Salinity plot of the entire water column at each station, with indicated water masses defined as Polar Water (PW), Atlantic Water (AW), Arctic Atlantic Water (AAW), and Deep Water (DW). (c) Temperature ($^{\circ}\text{C}$) and (d) salinity (psu) of upper 200m of all stations. Colors of profiles and points correspond to station colors on the map.

depths combined at each station for comparison with the eDNA data from the present study and the available net data (Havermans et al., 2021).

2.2 | eDNA extraction, library preparation, and sequencing

Environmental DNA was extracted using the DNeasy Blood and Tissue kit (QIAGEN) according to the manufacturer's protocol, with small modifications as described in Visser et al. (2021). DNA was diluted in 2 × 50 µL AE Buffer, and extraction blanks were taken during every extraction. All equipment and benches were cleaned in between extractions using a 1:10 Bleach and MilliQ solution, followed by a MilliQ rinse, 70% ethanol, and finally treated with UV light for a minimum of 1 h. Immediately before and during the extractions, DNA/RNA-ExitusPlus (AppliChem) was used for sterilizing equipment. The DNA extracts were stored at -20°C for further processing.

The DNA metabarcoding library preparation and sequencing were carried out by AllGenetics & Biology SL, Spain (www.allgenetics.eu). In order to amplify DNA of as many marine metazoans as possible, we used the common universal metazoan 313bp mitochondrial cytochrome oxidase c subunit 1 (COI) barcode, known as the "Leray" fragment. This barcode has been successfully implemented to detect a broad array of marine taxa, including GZP (Antich et al., 2022; Dischereit et al., 2022; Urban et al., 2022). The forward primer is mICOIintF-XT: (5'GGWACWRGWTGRACWITITAYCCYCC3') (Wangensteen et al., 2018) and the reverse primer jgHCO2198: (5'TAIACYTCIGGRTGICCRARAAYCA3') (Leray et al., 2013). The PCR master mix for the first PCR step consisted of 2.5 µL of template DNA, 0.5 µM of the primers, 6.25 µL of Supreme NZYTaq 2x Green Master Mix (NZYTech), and ultrapure water with a final volume of 12.5 µL. The PCR cycle included an initial denaturation step at 95°C for 5 min, followed by 35 cycles of 95°C for 30s, 54.7°C for 45s, 72°C for 45s, and a final extension step at 72°C for 7 mins. In the second PCR step, oligonucleotide indices were attached with the same conditions as the first but with five cycles and an annealing temperature of 60°C. PCR controls were included in each PCR to check for contamination during library preparation. Library size was verified on 2% agarose gels stained with GreenSafe (NZYTech) and purified using ag-Bind RXNPurePlus magnetic beads (Omega Biotek), according to the manufacturer's protocol. The concentration of the final libraries was checked on a Qubit dsDNA with the HS Assay (Thermo Fisher Scientific) before pooling at equimolar amounts. The final pool was sequenced on a PE250 flow cell (Illumina) on a NovaSeq platform (Illumina), aiming for a total output of 27 gigabases and a high target sequencing depth per sample (500,000bp). In order to increase the chances of detecting rare taxa, we chose to use the NovaSeq platform for greater sequencing depth and improved performance of the flow cell compared to the MiSeq platform (Singer et al., 2019).

2.3 | Bioinformatics

We applied a metabarcoding pipeline based on OBITOOLS version 1.01.22 (Boyer et al., 2016), following Antich et al. (2021) to process the raw sequences. Pair-end reads were assembled using *illumina-pairedend*, and those with median phred quality scores <40 were discarded. Demultiplexing and primer removal were done using *ngs-filter*. Length filtering (299–320bp) and the removal of sequences containing erroneous bases were done with *obigrep*, and sequence dereplication with *obiuniq*. We used the *Uchime-denovo* algorithm in VSEARCH (Rognes et al., 2016) to remove chimeric sequences. SWARM 3.0 (Mahé et al., 2015) was used to cluster the remaining sequences into molecular operational taxonomic units (MOTUs) with a *d* value of 13. Taxonomic assignment was done with the *eco-tag*, using a local reference database consisting of 174,544 COI sequences from Genbank, BOLD, and in-house sequences (available at: <https://github.com/uit-metabarcoding/DUFA/>). We used the LULU algorithm (Frøslev et al., 2017) as a post-clustering filter to remove any remaining erroneous MOTUs. Blank correction followed with the removal of MOTUs that were present in blank or control samples at more than 10% of their total read abundance (Table S3). To reduce the impact of tag-jumping but still allow the possibility to detect rare MOTUs, we applied a minimum threshold abundance of 0.0005% to each sample before removing any remaining MOTUs with less than 5 reads. One sample failed in sequencing and was removed from the dataset. The assignments of the remaining sequence annotations were further improved where possible by using BOLDigger (Buchner & Leese, 2020) and the BOLD database (<http://www.barcodinglife.com>) (Ratnasingham & Hebert, 2007). For this, we modified the sequence similarity thresholds and adjusted the taxonomic assignment accordingly. The thresholds used were species (97%), genus (95%), family (90%), order (85%), class (80%), and phylum (<80%). Finally, MOTUs assigned as prokaryotes, terrestrial taxa (e.g., insects), fungi, and phytoplankton were removed, so only marine metazoans with a taxonomic assignment threshold higher than 80% remained.

2.4 | Data analysis

All statistical analyses and data visualizations were conducted in R 4.1.0 (R Core Team, 2021). We pooled triplicates from the same station and depth by summing read counts. Read counts were then normalized to the lowest number observed in the dataset using the scaling with ranked subsampling (SRS) method (Beule & Karlovsky, 2020), with the *srs()* function in the SRS package in R (Heidrich et al., 2021). In order to avoid the impact of sampling biases between stations with different sampling intensities (shallow stations: surface—max. 100m; deep stations: surface—max. 2500m), we split the metazoan MOTU dataset for alpha diversity analyses into (1) the upper 100m of all seven stations, and (2) all ocean zones at deep stations only (EG4, HG4, N4, and S3). The alpha diversity analyses for the GZP dataset were only calculated on the four deep stations due to low or no GZP detections at

the other stations. To analyze differences in diversity across the sampling locations and depth zones, we calculated the Shannon-Wiener index and species richness based on normalized MOTU data using the *vegan* package v.2.5-6 (Oksanen et al., 2019). We compared alpha diversity between depth zones and locations using ANOVA, followed by pairwise comparisons with Tukey's HSD. We calculated species richness on non-rarefied data for the GZP dataset only, for which assumptions of parametric data were not met. In this case, we used Welch's one-way tests and Game-Howell pairwise comparisons.

To investigate differences in community composition across locations and depth zones, beta-diversity analyses were performed for both the metazoan and GZP datasets. We calculated Jaccard distances based on presence-absence data and visualized them with non-metric multidimensional scaling ordination (nMDS) using the *metaMDS()* function in *vegan*. Permutational multivariate analysis of variance (perMANOVA) tests with 999 permutations was conducted to check for significant differences between locations and ocean zones, using the *adonis2()* function. Subsequent pairwise comparisons with Bonferroni adjusted *p*-values were done using *pairwise.adonis()* from the *pairwiseAdonis* package (Martinez Arbizu, 2020) in R. Data dispersion was performed to check for multivariate homogeneity using the *betadisper()* function.

Correlations between the relative abundances of individual MOTUs and environmental parameters, including water mass indicators, were identified using sparse partial least squares (sPLS) regression analysis. The sPLS was conducted using raw MOTU count data. We removed MOTUs with near zero variance using the *nearZeroVar()* function in the *mixOmics* package (Rohart et al., 2017) and replaced zeros with pseudo counts of 1. Environmental variables were standardized using the *decostand()* function with the method *standardize* in *vegan*. The sPLS was done using the *spls()* function from *mixOmics*, with canonical mode and a centered-log ratio transformation. We used the output from the sPLS model to compute pairwise similarity matrices, and the significant correlations were visualized in a heatmap using the *cim()* function.

We compared the efficacy of eDNA with net and optical sampling methods based on taxon richness. To account for divergences in sampling procedures, only presence data recorded from nets and video tows was used rather than abundance data. To investigate the efficiency of eDNA and nets to detect GZP diversity, we compared the taxon richness at each taxonomic level for all stations combined. Furthermore, we compared all three methods (eDNA analysis, net catches, and camera tows) at three stations (EG4, HG4, and S3), where all methods were deployed. To investigate how the detection efficiency of each of the three methods compares at a finer taxonomic level, we used only the MOTUs identified to genus and/or species level for cnidaria but to class level for cydippid ctenophores. This was done to account for known taxonomic uncertainties related to morphological identifications, which was the case for the scyphozoan genus *Atolla* (Matsumoto et al., 2022), the hydrozoan *Botrynema* genus (Montenegro et al., 2023) and the ctenophores belonging to the *Beroe* genus (Shiganova & Abyzova, 2022) and the

class Cydippidia (Majaneva & Majaneva, 2013). The validity of these taxa was further checked against the World Register of Marine Species (WoRMS) available from (<https://www.marinespecies.org>).

3 | RESULTS

3.1 | Oceanographic properties

The oceanographic properties varied across sampling stations (Figure 1b–d), reflecting the different water masses of the Fram Strait. Temperature values ranged from the highest at 3.6°C at SV4 to the lowest at -1.7°C at EG1 (Figure 1c and Table S1). Salinity values ranged from 31.2psu at EG1 to 34.9psu at S3 (Figure 1d and Table S1). Details of all water parameters measured are available in Table S1. In addition to longitudinal shifts in conditions, depth-stratified water bodies were observed (Figure 1b). At stations SV4 and S3, a small layer of Polar Water (PW) occurred in the upper tens of meters, with Atlantic Water (AW), Arctic Atlantic Water (AAW), and Deep Water (DW) below. The deepwater stations HG4 and N4 both had PW close to the freezing point in the top 25 m, as well as AW, AAW, and DW in the lower water column. The top 100 m of EG4 consisted of PW with very low salinities, an AW layer, and AAW and DW formed at depth. EG1 was largely dominated by low salinity PW and some AAW and DW at lower depths.

3.2 | Pelagic metazoan alpha diversity

Sequencing of the COI fragment resulted in a total of 105.5 million sequence reads. After quality control and refinement, 700,000 reads assigned to marine metazoans were kept, representing 239 MOTUs. Rarefaction curves showed that most samples reached a plateau with the obtained sequencing depth (Figure S1). A large diversity of marine metazoans was captured, with the majority of the metazoan sequences assigned to ten phyla (Figure 2a). Arthropoda was the most dominant phyla, making up 84.6% of the metazoan reads in the dataset, followed by Cnidaria (7.56%) and Porifera (1.9%). The remaining phyla consisted of less than 1%, along with unassigned metazoans. We successfully detected most of the marine metazoan groups known to exist in high abundance in the Arctic Ocean, including Annelida (Polychaeta, Sipuncula), Arthropoda (Copepoda, Malacostraca, Ostrocooda), Chordata (Actinopterygii, Ascidiacea, Mammalia), Cnidaria (Anthozoa, Hydrozoa, Scyphozoa), Ctenophora (Nuda, Tentaculata), Echinodermata (Crinoidea, Echinoidea, Holothuroidea), Mollusca (Bivalvia, Cephalopoda, Gastropoda, Scapopoda), and Porifera (Demospongiae, Hexactinellida). The groups with the highest number of reads detected were copepods and cnidarians (Table 1). The highest number of MOTUs were detected in Cnidaria (58), followed by Arthropoda (49), Porifera (35), Annelida (27), and the remaining phyla.

The analysis of alpha diversity indices showed that location did not have a significant effect on the Shannon index [*anova*,

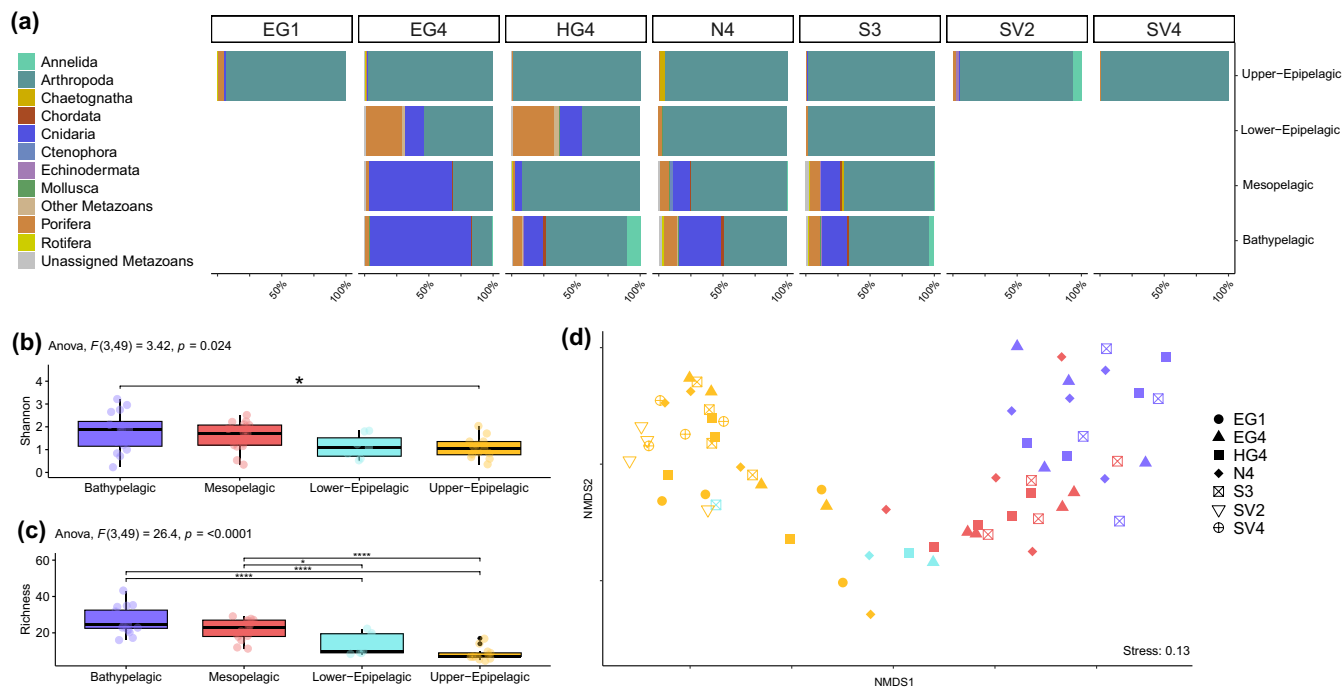


FIGURE 2 Pelagic metazoan alpha and beta-diversity patterns. (a) Relative read abundances of marine metazoan MOTUs phyla at each depth zone and sampling location. (b) Shannon diversity index (H') and (c) species richness of SRS normalized metazoan MOTU data at each depth zone for all four deep stations combined. Tukey's HSD pairwise comparison with Tukey adjusted p -values was used. * indicates a significant difference of <0.05 and **** indicates a significant difference of <0.0001 . (d) Nonlinear multidimensional scaling for community structuring of MOTUs ($K=2$) based on Jaccard distance. Colors indicate ocean zones, and point shape indicates station, stress value displayed on plot. Depth zones are defined as upper-epipelagic (0–99 m), lower-epipelagic (100–200 m), mesopelagic (201–1000 m), and bathypelagic (>1000 m).

DF=(6, 49), $F=2.536, p=0.053$], nor on MOTU richness in the upper 100 m of the seven stations analyzed [anova, DF=(6,49), $F=2.005, p=0.11$]. When comparing the four deep stations, location also did not have a significant effect on Shannon index [anova, DF=(3,49), $F=1.273, p=0.294$], nor MOTU richness [anova, DF=(3, 49), $F=0.083, p=0.969$]. However, the depth zone was found to be significantly different on both the Shannon index [anova, DF=(3,49), $F=3.417, p=0.024$] and MOTU richness [anova, DF=(3,49), $F=26.402, p \leq 0.01$]. Subsequent pairwise comparisons showed that the bathypelagic zone had a significantly higher Shannon index than the upper-epipelagic zone (Figure 2b). The bathypelagic and mesopelagic zones were found to be significantly higher in MOTU richness than each of the epipelagic layers (Figure 2c).

3.3 | GZP alpha diversity

A total of 53 GZP MOTUs were recovered with more than 80% similarity, of which 51 were cnidarians and two ctenophores. In total, 12 GZP MOTUs were assigned to species level, 14 to genus, 16 to family, 18 to order, and all to class level. Both Ctenophora classes, Nuda and Tentaculata, were detected, five hydrozoan orders (Anthoathecata, Leptothecata, Narcomedusae, Siphonophorae, and Trachymedusae),

and three scyphozoan orders (Coronatae, Rhizostomeae, and Semaestomeae) (Table S4). The most abundant GZP MOTU by read abundance was the mid-water hydrozoan *Botrynuma brucei* (39.0% of GZP reads), followed by the siphonophore *Marrus orthocanna* (31.1%), the 33 unassigned hydrozoans (19.5% combined), the deepwater scyphozoan *Atolla tenella* (2.68%) and unassigned Anthoathecata (2.39%). The remaining GZP taxa each made up less than 2% of the detected reads.

When analyzing alpha diversity indices based on rarefied data at the four deep stations, we found no significant effect of location on GZP Shannon index [anova, DF=(3, 33), $F=1.745, p=0.137$] nor MOTU richness [anova, DF=(3, 33), $F=1.904, p=0.148$]. Likewise, no significant effect of depth zone on GZP Shannon index [anova, DF=(3, 33), $F=1.62, p=0.213$] nor MOTU richness [anova, DF=(3, 33), $F=2.277, p=0.118$] was found. However, given the focus on the smaller GZP component of the dataset (7.56% of total MOTUs), we also analyzed MOTU richness based on non-rarefied data with the goal of retaining rarer taxa. Here, we found that depth zone had a significant effect on GZP MOTU richness (Figure 3b). The subsequent pairwise comparison found that the bathypelagic and the mesopelagic layers had significantly higher richness than the lower- and upper-epipelagic layers, respectively (Figure 3b). Nevertheless, non-rarefied data must be treated with caution as differences in sequencing depth cannot be ruled out as a significant driver behind significant differences.

TABLE 1 Molecular operational taxonomic units (MOTUs) detected in the eDNA dataset had the highest number of reads per phylum.

Phylum (total no. MOTUs)	Family	MOTU name	Depth zone	Location	Biogeographical distribution
Annelida (28)	Pholoidae	<i>Pholoe assimilis</i>	U-E	SV2	Arctic-boreal (Degen & Faulwetter, 2019)
	Spionidae	<i>Laonice</i> sp.	B	EG4, S3, N4, HG4	
	Trichobranchidae	<i>Terebellides</i> sp.	B	HG4	
		Polychaeta_2	B	HG4, S3	
	Golfingiidae	<i>Nephasoma</i> spp.	B	HG4	
Arthropoda (49)	Calanidae	<i>Calanus hyperboreus</i>	U-E, M, B	EG1, HG4, N4, S3, SV2, SV4	Arctic (Ingvaldsen et al., 2023a)
	Oithonidae	<i>Oithona similis_2</i>	All	All	Ubiquitous (Weydmann et al., 2014)
	Calanidae	<i>Calanus finmarchicus</i>	All	All	Boreal (Weydmann et al., 2014)
	Clausocalanidae	<i>Pseudocalanus minutus</i>	U-E	SV2, SV4	Arctic-boreal (Weydmann et al., 2014)
	Metridinidae	<i>Metridia longa</i>	All	EG1, EG4, HG4, N4, S3, SV2	Arctic-boreal (Weydmann et al., 2014)
	Clausocalanidae	<i>Microcalanus pusillus</i>	U-E, L-E, M	All	Arctic-boreal (Weydmann et al., 2014)
		Copepoda_5	M, B	EG4, HG4, N4, S3	
	Oithonidae	<i>Oithona similis_1</i>	U-E, L-E	All	Ubiquitous (Weydmann et al., 2014)
	Clausocalanidae	<i>Microcalanus pygmaeus_2</i>	M, B	EG4, HG4, N4, S3	Arctic-boreal (Weydmann et al., 2014)
	Euchaetidae	<i>Paraeuchaeta glacialis</i>	U-E, B	EG1, EG4, HG4	Arctic-boreal (Kosobokova et al., 2011)
	Oncaeidae	<i>Triconia borealis</i>	All	All	Arctic-boreal (Weydmann et al., 2014)
	Oithonidae	<i>Oithona atlantica</i>	U-E, L-E	EG4, HG4, N4, S3, SV2	Boreal (Wassmann et al., 2015)
		Cyclopoida_2	B	EG4, HG4, N4, S3	
	Calanidae	<i>Calanus glacialis</i>	U-E, M, B	All	Arctic (Weydmann et al., 2014)
	Arthropoda_4	All	EG1, EG4, N4, S3, SV4		
Chaetognatha (3)	Eukrohniidae	<i>Eukrohnia bathyantartica</i>	U-E, M, B	EG4, HG4, N4, S3	Ubiquitous (Miyamoto et al., 2012)
	Sagittidae	<i>Sagitta</i> sp.	U-E, L-E	EG1, EG4	
	Sagittidae	<i>Pseudosagitta maxima</i>	M	EG4	Ubiquitous (Kulagin & Neretina, 2017)
Chordata (12)	Zoarcidae	<i>Lycodes esmarkii</i>	B	HG4, S3	
	Clupeidae	<i>Sardinella maderensis</i>	M	S3	
	Gadidae	<i>Boreogadus saida</i>	U-E, M, B	EG1, HG4, S3	Arctic (Ingvaldsen et al., 2023a)
	Balaenidae	<i>Balaena mysticetus</i>	M, B	EG4, N4	
	Gadidae	<i>Micromesistius poutassou</i>	B	S3	
Cnidaria (58)	Halicreatidae	<i>Botrynema brucei</i>	M, B	EG4, HG4, N4, S3	Ubiquitous (Montenegro et al., 2023)
	Agalmatidae	<i>Marrus orthocanna</i>	M, B	EG4, HG4, N4, S3	Arctic-boreal (Stepanjants, 1989)

(Continues)

TABLE 1 (Continued)

Phylum (total no. MOTUs)	Family	MOTU name	Depth zone	Location	Biogeographical distribution
		Hydrozoa_28	All	EG1, EG4, HG4, N4, S3	
	Atollidae	<i>Atolla tenella</i>	M, B	EG4, HG4, N4, S3	Arctic (Raskoff et al., 2010)
		Anthoathecata_1	M, B	EG4, HG4, N4, S3	
		Hydrozoa_27	All	EG1, EG4, HG4, N4, S3	
		Mitrocomidae	M, B	HG4, N4, S3	
		Scyphozoa	U-E, L-E, M	EG1, EG4, HG4, N4, S3, SV2	
		Anthozoa_3	U-E, M, B	EG1, EG4, HG4, N4, S3	
		Hydrozoa_26	B	EG4, HG4, N4, S3	
		Hydrozoa_25	M	N4	
		Hydrozoa_24	M, B	EG4, HG4, N4, S3	
		Hydrozoa_22	U-E, L-E, M	EG1, EG4, HG4, N4, S3	
Ctenophora (2)	Bolinopsidae	<i>Bolinopsis</i> sp.	L-E, M	HG4, N4, S3	
		<i>Nuda</i>	M	N4	
Echinodermata (9)	Ophiuridae	<i>Ophiocten gracilis</i>	U-E, M, B	S3	Arctic-boreal (Degen & Faulwetter, 2019)
	Ophiuridae	<i>Ophiura robusta</i>	U-E	SV2	Arctic-boreal (Degen & Faulwetter, 2019)
	Ophiactidae	<i>Ophiopholis aculeata</i>	U-E	N4, SV2	Arctic-boreal (Degen & Faulwetter, 2019)
	Pourtalesiididae	<i>Pourtalesia jeffreysi</i>	B	HG4	Arctic (Degen & Faulwetter, 2019)
	Echinodermata		All	EG4, HG4, N4, S3	
Mollusca (13)	Hiatellidae	<i>Hiatella</i> sp.	M, B	N4	
	Cirroteuthidae	<i>Cirroteuthis muelleri</i>	B	EG4, HG4, S3	Arctic-boreal (Xavier et al., 2018)
	Gonatidae	<i>Gonatus</i> sp.	M, B	N4, S3	Arctic-boreal (Xavier et al., 2018)
	Gadilidae	<i>Siphonodentalium lobatum</i>	M, B	HG4, N4	Arctic-boreal (Degen & Faulwetter, 2019)
		Gastropoda_7	B	EG4, N4, S3	
Porifera (33)		Demospongiae_21	All	EG1, EG4, HG4, N4, S3, SV2	
		Demospongiae_20	All	EG1, EG4, HG4, N4, S3	
		Demospongiae_19	M, B	EG4, HG4, N4, S3	
		Demospongiae_18	U-E, M, B	EG4, HG4, N4, S3, SV2	

TABLE 1 (Continued)

Phylum (total no. MOTUs)	Family	MOTU name	Depth zone	Location	Biogeographical distribution
Rotifera (10)		Demospongiae_17	U-E, L-E	All	
		Monogononta_2	U-E	EG4	
	Euchlanidae	<i>Euchlanis dilatata</i>	M, B	EG4, HG4, N4, S3	
		Ploima_6	U-E	EG1, EG4	
		Monogononta_1	B	N4, S3	
		Ploima_5	B	S3	

Note: 15 MOTUs are displayed each for Arthropoda and Cnidaria, five each for the remaining phyla. Details on which sampling location and depth zone each MOTU was detected in are also shown. Depth zones are defined as B, bathypelagic; L-E, lower-epipelagic; M, mesopelagic; U-E, upper-epipelagic. When assigned to species level, the biogeographic origin was listed where possible, with references therein.

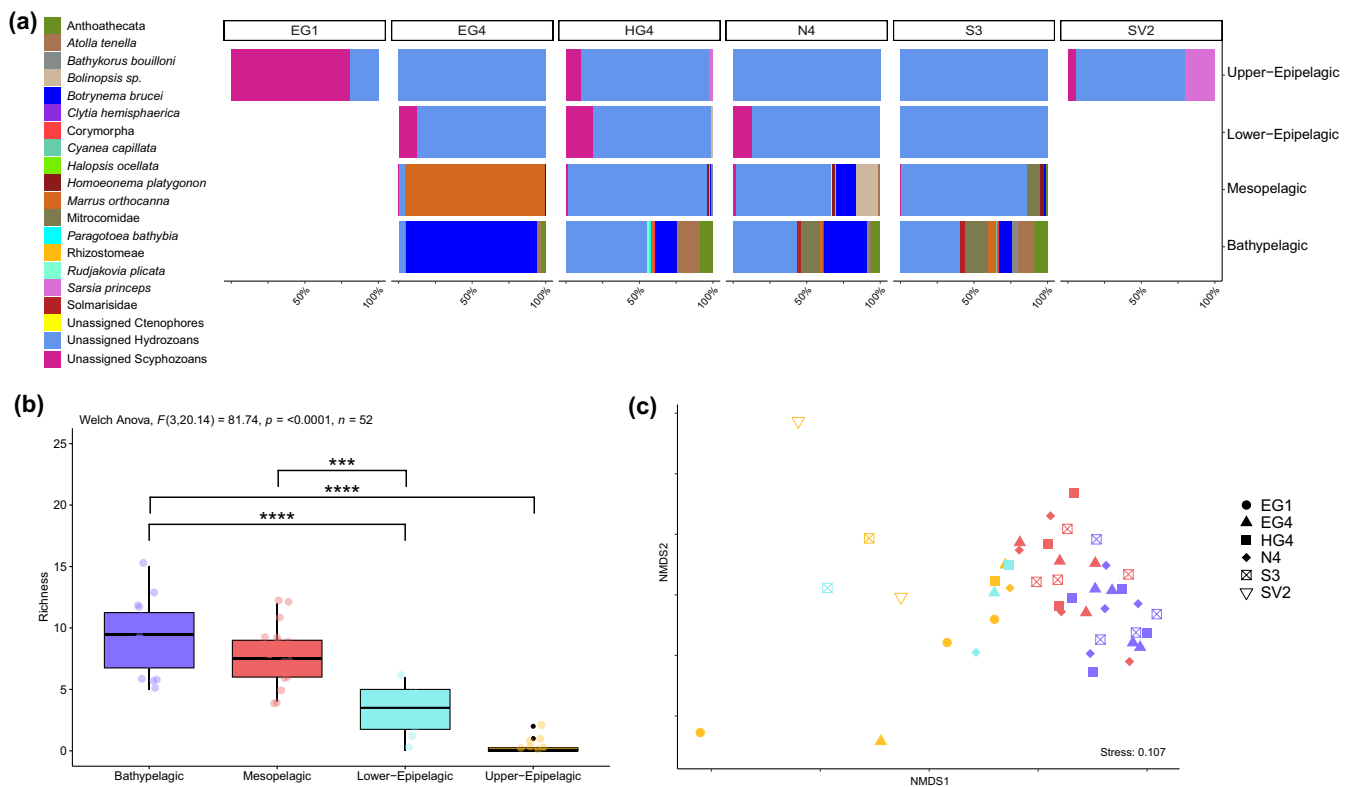


FIGURE 3 Gelatinous zooplankton (GZP) alpha and beta-diversity patterns. (a) Relative read abundances of GZP MOTUs were assigned to >80% for each of the surveyed stations except SV4, where no GZP MOTUs were detected. MOTUs have been pooled by the lowest taxonomic level identified. (b) Species richness was tested with Welch ANOVA on non-rarefied data at the four deep stations. Pairwise comparison with Games-Howell. (c) Nonlinear multidimensional scaling for community structuring of GZP MOTUs ($K=2$). Stress value displayed on plot. Ordination is based on presence-absence data with Jaccard distance. Colors indicate ocean zones, and point shape indicates station, stress value displayed on plot. Depth zones are defined as upper-epipelagic (0–99 m), lower-epipelagic (100–200 m), mesopelagic (201–1000 m), and bathypelagic (>1000 m).

3.4 | Beta diversity and environmental drivers of community composition

We used beta-diversity analysis to test for significant effects of location and depth zone on community composition. For marine metazoans, we identified a significant difference between samples based on depth zone (Figure 2d) (PERMANOVA; $F=7.7276$,

$p=0.001$). Further pairwise comparisons indicated that all depth layers were significantly different from each other (pairwise.adonis, $p<0.05$; Table S4). Similarly, depth zone was identified as a significant driver of beta diversity in the GZP dataset (Figure 3d) (PERMANOVA; $F=3.9143$, $p=0.001$), with differences between all zones (pairwise.adonis, $p<0.05$) except for the upper-epipelagic and lower-epipelagic layers (Table S4). However, this

PERMANOVA result could be affected by the non-homogeneous dispersion detected in the upper-epipelagic zone (*betadisper*, $F=3.9767$, $p=0.01413$).

We conducted an sPLS regression analysis to investigate the correlation between MOTUs and environmental conditions (Figure 4). We identified 40 marine metazoan MOTUs that exhibited significant correlations to at least one measured environmental parameter (Pearson's coefficient >0.4 , $p<0.05$), 11 of which were GZP. The hierarchical clustering suggested that these MOTUs make up three main clusters. The MOTUs in cluster 1 showed strong positive correlations with oxygen saturation, fluorescence, temperature, and longitude, as well as a correlation with shallow sampling depths. These conditions are indicative of surface waters of Atlantic origin near Svalbard. This cluster was largely dominated by copepod MOTUs, including species of the *Oithona*, *Pseudocalanus*, and *Calanus* genera. In contrast, cluster 2 MOTUs exhibited negative

correlations with salinity, longitude, and depth, and positive correlations with oxygen saturation, all of which are characteristic of upper ocean polar water masses (PW). This cluster contained hydrozoan and scyphozoan MOTUs as well as the cold-water associated copepod *Microcalanus pygmaeus*. The MOTUs in cluster 3 represented deepwater (DW) residing organisms, indicated by strong positive correlations with depth. This cluster contained the most MOTUs, including the deepwater GZP *Bathylorus bouilloni* and *A.tenella*, as well as the glass sponge *Caulophacus arcticus*.

3.5 | eDNA versus net and optical sampling methods

We set out to compare our metabarcoding results with those obtained from net tows and video surveys for the detection GZP. Both

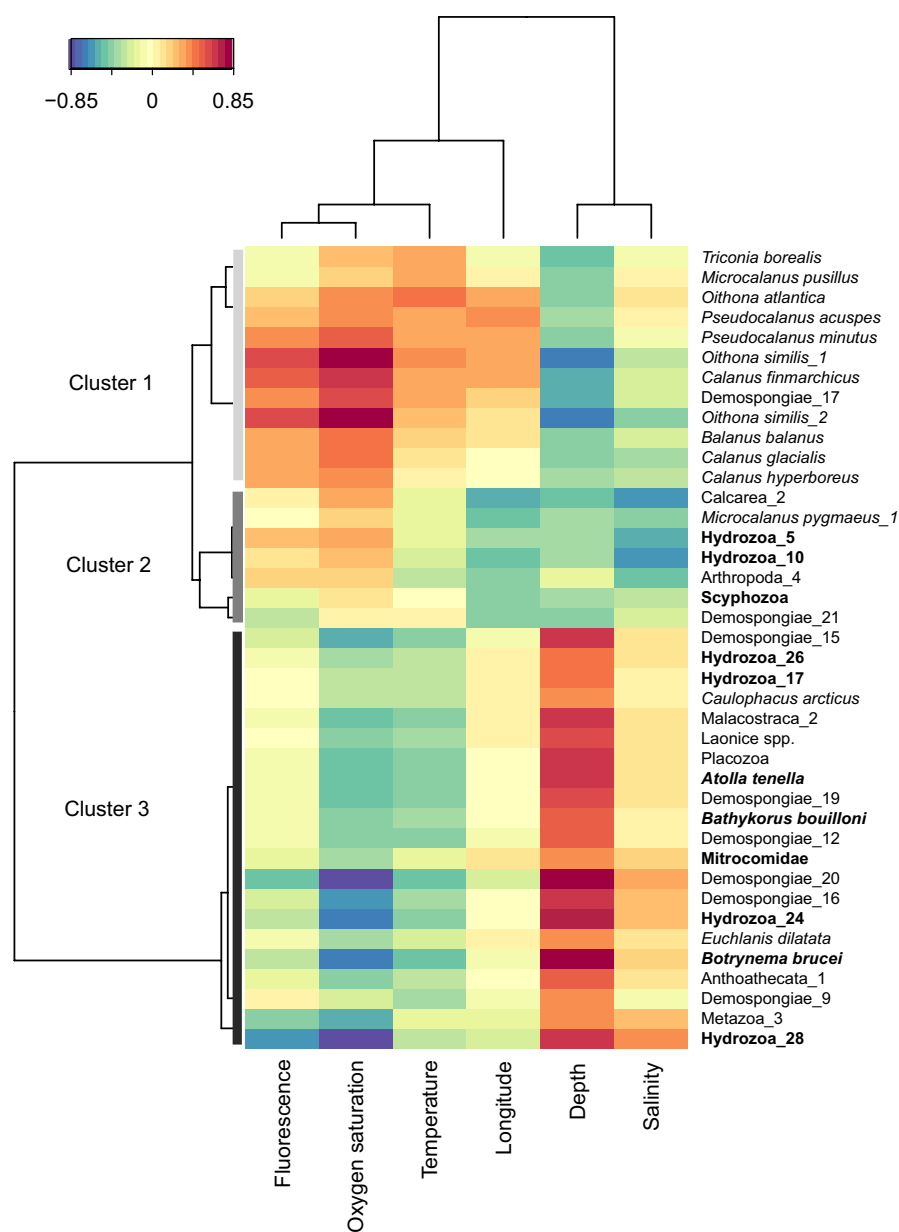


FIGURE 4 A clustered image map (CIM) of three sPLS components with significant pairwise correlations of metazoan MOTU abundance with environmental variables. sPLS clusters on the Y-axis. Correlation cut-off = 0.4. Fluorescence was measured in (mg/m^3), Oxygen saturation in (%), Temperature in degrees Celsius, Longitude in decimal degrees, sample depth in meters, and salinity in (psu). Color indicates correlation type (red = positive and blue = negative) and strength of environmental parameter with a relative abundance of MOTU. Gelatinous zooplankton MOTUs are indicated in bold text.

eDNA and net sampling were undertaken at all seven locations. A total of 22 GZP taxa were detected with eDNA metabarcoding (with MOTUs collapsed into the closest taxonomic match), while net tows detected 19 taxa (Figure 5a). The only overlapping taxon was the hydrozoan species *Sarsia princeps*, which was found at one station (SV2) with nets and at two with eDNA (SV2 and HG4). Although both eDNA and nets detected specimens of the *Botrynema* and *Atolla* genera, species-level identification of net specimens was not possible without further confirmation by molecular barcoding. When comparing the recovery of GZP taxa between the methods at each of the seven stations, eDNA detected an equal or higher number of taxa than nets at each taxonomic level (Figure 5b). The largest differences were at the order level (eDNA $n=13$ vs. nets $n=8$) and the species level (eDNA $n=11$ vs. nets $n=7$). At three stations (EG4, HG4, and S3), three methods were deployed: video transects (PELAGIOS), net, and eDNA sampling. Here, we detected 11 taxa at the genus and species levels (class for ctenophores) with both eDNA and video analyses, while eight taxa were detected in the nets. Three ctenophore taxa (*Beroe* spp., *Bolinopsis* sp., and *Cydippida*) were detected with the video transects compared to one ctenophore taxon (*Bolinopsis* sp.) detected with eDNA and nets. A higher number of taxa were shared between the nets and video transects ($n=5$) compared to eDNA and video transects ($n=2$). The only taxa detected by all three methods were the *Atolla* and *Botrynema* genera (Figure 5c).

4 | DISCUSSION

As a gateway between the Atlantic Ocean and the Arctic Basin, Fram Strait is a region particularly affected by rapid ecosystem changes. Zooplankton communities, long considered sentinels for biotic and abiotic changes, have already exhibited alterations in species composition, range-shifts, and food web structure in the region, driven by Atlantification (Berry et al., 2019; Csapó et al., 2021). To monitor such changes and their consequences on the wider ecosystem, an increase in biodiversity surveillance is necessary. Metabarcoding of eDNA in water samples is a cost-efficient biodiversity monitoring tool, which is increasingly utilized in marine ecosystems and can help fill knowledge gaps left by traditional monitoring methods. Many studies investigating marine metazoan biodiversity with eDNA have focused on coastal areas and the epipelagic zone, with few targeting mesopelagic and bathypelagic zones or the open ocean (Feng et al., 2022; Govindarajan et al., 2021; Suter et al., 2021). This leaves the vast, deep ocean zones and difficult-to-access areas, such as the Arctic, understudied, particularly with respect to metazoan and GZP diversity (Havermans et al., 2022). In the Arctic, there have been studies using the COI marker to target metazoan biodiversity in coastal areas (Lacoursière-Roussel et al., 2018; Leduc et al., 2019; Nguyen et al., 2023; Sevellec et al., 2021), as well as in the open Chukchi Sea (Questel et al., 2021) and the Pacific Arctic (Ershova et al., 2019). A previous eDNA study has investigated metazoan diversity in Fram Strait, albeit with taxon-specific markers including fish 12S rDNA primers and a primer set targeting cephalopods

(Merten et al., 2023). Our study is the first to investigate pelagic metazoan diversity, and specifically GZP diversity, in Fram Strait using the universal metazoan COI metabarcoding marker. Here, we show that eDNA successfully detected a high proportion of the zooplankton community in the area. Furthermore, we characterized marine metazoan and GZP communities by depth zone and revealed significant relationships between taxa and water masses. Lastly, we show that eDNA is an effective and resource-efficient method for increasing GZP detections and enriching traditional biodiversity surveys.

4.1 | Taxonomic composition

Consistent with previous studies in the region, the pelagic community detected by eDNA metabarcoding in our study was made up of a combination of species with different biogeographical distributions. We successfully detected “true” Arctic species (e.g., *C. glacialis*, *Boreogadus saida*, and *B. bouilloni*), as well as arctic-boreal (e.g., *Microcalanus* spp., *Gonatus* sp., and *Pholoe assimilis*) and boreal species (*C. finmarchicus* and *Oithona* spp.) (Table 1). Species known to be highly abundant in Fram Strait were indeed represented by a large number of reads in the eDNA dataset, including the copepods *Calanus hyperboreus*, *C. finmarchicus*, and *Oithona* spp. This is in line with morphological studies in the same area (Darnis & Fortier, 2014; Gluchowska, Dalpadado et al., 2017; Ingvaldsen et al., 2023; Kosobokova et al., 2011), as well as findings in the Chukchi Sea (Questel et al., 2021). We recovered sequences from holoplanktonic (e.g., physonect siphonophores and calanoid copepods) and benthic taxa (e.g., bryozoans and polychaete worms), including many with meroplankton life stages (e.g., echinoderms and poriferans). Benthic taxa are often missed by pelagic sampling techniques, while the pelagic stages of meroplanktonic taxa are commonly sampled with nets but often are difficult to identify based on morphology due to their small size and their lack of easily identifiable features (Descôteaux et al., 2021; Ershova et al., 2019). Furthermore, we detected larger invertebrates (*Cirroteuthis muelleri*) and vertebrates such as the narwhal (*Monodon monoceros*), the bowhead whale (*Balaena mysticetus*), and Brünnich's guillemot (*Uria lomvia*). The ability of COI metabarcoding to detect a wide range of marine metazoans at the community and species level has been well-documented in recent years (e.g., Antich et al., 2022; Ershova et al., 2019; Wangensteen et al., 2018). The large taxonomic and size spectrum of organisms detected in the present study further highlights the efficacy of the COI fragment as a marker for detecting the presence of highly mobile, less abundant, and elusive taxa in the Arctic, as well as a range of life strategies that typically require distinct sampling strategies.

Both the marine metazoan sequence reads, and species richness values were dominated by copepods (Calanoida and Cyclopoida) and Hydromedusae taxa (*B. brucei* and *M. orthocanna*). While the reads showed expected relationships between read abundances of highly abundant taxa (i.e., in *Calanus* copepods), further quantitative interpretations related to abundance or biomass must be made with



FIGURE 5 Comparisons between eDNA metabarcoding results and net and video sampling methods. (a) The number of taxa detected by eDNA and nets across all of the seven sampling locations combined. MOTUs are collapsed into the closest taxonomic level. (b) The number of taxa detected at each taxonomic level from presence data detected by nets and eDNA from all of the seven sampling locations combined. (c) Shows the class (ctenophores only), genus, and species-level detections at the three stations where eDNA, nets, and video surveys were conducted (EG4, HG4, and S3). Gray squares indicate the presence of a taxa.

caution. Positive relationships between sequence reads and biomass have been found for a number of zooplankton taxa (Ershova et al., 2023), and specifically copepods (Ershova et al., 2021) when metabarcoding bulk samples. However, factors including the different nature of extra-cellular DNA versus bulk samples, PCR biases (Lacoursière-Roussel et al., 2018; Wangensteen et al., 2018) and taxon-specific knowledge gaps (Bucklin et al., 2010) still limit the use of eDNA metabarcoding to draw these conclusions on a community-wide scale. It is noteworthy that we had low read abundances or failed to detect zooplankton taxa that are commonly caught in net and optical surveys in the Arctic. For example, we obtained low read numbers and MOTU richness for Malacostraca (e.g., *Thysanoessa inermis*, *T. longicaudata*, and *Themisto libellula*), which are typically characterized by high biomass in the Arctic seas (Eriksen et al., 2017; Kosobokova et al., 2011). These false negatives could have multiple explanations, where primer and PCR biases as well as underrepresentation on public databases (e.g., appendicularians and the ctenophore *Mertensia ovum*), appear most likely. Furthermore, the COI Leray fragment may be an unsuitable barcode region for certain zooplankton taxa (Bucklin et al., 2021), although here we applied the modified Leray-XT primer, which has improved coverage of some marine taxa than the original (Wangensteen et al., 2018). Nevertheless, the inclusion of additional markers such as 18S regions or group-specific primers could help to resolve these omissions. Moreover, reasons such as taxon-specific eDNA shedding rates, higher degradation rates (Andruszkiewicz Allan et al., 2021), or the limited sampling volume of seawater cannot be excluded.

4.2 | Vertical patterns of diversity

Epipelagic waters in the Arctic are typically dominated by a low number of zooplankton species, mainly *Calanus* copepods, which exhibit high biomass and abundance (Gluchowska, Trudnowska et al., 2017; Hop et al., 2019). This was reflected in our eDNA results, wherein epipelagic layers were characterized by a low diversity and dominated by Arthropoda. Alpha diversity increased in the mesopelagic and bathypelagic layers, where the contributions of other phyla such as cnidarians and poriferans increased both in reads and taxa richness. Multivariate analysis of community composition showed the greatest differences between the epipelagic and the bathypelagic assemblages in both datasets. These vertical patterns are consistent with findings of net-based zooplankton studies in the Arctic, which have shown similar results of diversity peaking in the mesopelagic or deeper, despite a decrease in overall biomass (Gluchowska, Trudnowska et al., 2017; Kosobokova et al., 2011). It also corroborates previous eDNA results on fish in Fram Strait, showing a maximum species richness in the bathypelagic zone (Merten et al., 2023).

We detected clear vertical gradients in diversity and relative read abundances for GZP. Both diversity and relative abundances increased from epi- to meso- and bathypelagic layers, where, at one station, GZP were present in higher proportions than Arthropoda (Figure 2a). These vertical patterns reflect previous

findings from Fram Strait (Gluchowska, Trudnowska et al., 2017; Mańko et al., 2020; Pantiukhin et al., 2023a) and other Arctic regions (Kosobokova et al., 2011; Raskoff et al., 2010). For instance, Raskoff et al. (2010) reported higher species richness in the meso- and bathypelagic layers, dominated by medusae, in the Canada Basin and Chukchi Plateau, with reduced diversity but increased numbers of ctenophores and siphonophores in shallower layers. An optical survey with the PELAGIOS video system, conducted during the same expedition as the present study, also resulted in depth being identified as a significant driver of GZP diversity and distribution (Pantiukhin et al., 2023a), with peak diversity detected at 1200m. Furthermore, eDNA zooplankton surveys in the open ocean have also found the diversity of GZP to increase with depth (Feng et al., 2022; Govindarajan et al., 2021), indicating that eDNA metabarcoding of the COI gene enables the accurate detection of vertical diversity gradients. Although the overall patterns of vertical diversity observed in this study are in line with those previously reported from Fram Strait, it is important to acknowledge that factors, including sampling time and filter choice, as well as a degree of uncertainty regarding the source of eDNA signals, can impact the results. For instance, high levels of biological activity in Arctic surface waters during summer due to phytoplankton blooms and seasonal vertical migration of zooplankton (Norrbin et al., 2009) result in elevated levels of particles suspended in the water column. Under such conditions, the use of small pore-size membrane filters, as was the case here, increases the susceptibility of clogging compared to large pore-size membrane filters (Kumar et al., 2022; Singer et al., 2019), resulting in potentially lower observed diversity in the epipelagic layer. The persistence of eDNA may also affect patterns observed, with eDNA signals being potentially advected or remaining detectable for extended periods. However, Suter et al., 2021 were able to detect diel migration patterns in copepods, indicating that the eDNA was detected when the organisms were present. This and other recent findings suggest that eDNA is potentially diluted or degraded more rapidly in marine environments than in experimental conditions (e.g., Jeunen et al., 2019). The significantly higher alpha diversity observed in the bathypelagic may in part be explained by the fact that eDNA is typically preserved in higher quality and concentrations in sediment than water (Holman et al., 2019; Ogata et al., 2021; Sakata et al., 2020). Disturbances in sediment may lead to eDNA being resuspended in the demersal layer. We cannot exclude that these factors may have impacted the patterns of metazoan diversity observed in the present study. Although eDNA metabarcoding has known limitations relating to the identification of sequences, with the common issue of unassigned MOTUs (Berry et al., 2019), alpha and beta-diversity analyses are independent of taxon information and therefore prove valuable insights into biodiversity and community composition. Taxa with lower matches in databases still provide valuable information pertaining to patterns of diversity. We highlight the need for more eDNA surveys in deeper areas, increasing water volume filtered and the number of sampling points throughout the water column to allow for higher taxonomic and depth resolution.

4.3 | Water mass indicators as drivers of community composition

The role of water masses as drivers of Arctic zooplankton distribution and community composition is well documented for Fram Strait based on net-based surveys (e.g., Basedow et al., 2018; Gluchowska, Dalpadado et al., 2017; Hop et al., 2019) and sediment traps (e.g., Ramondenc et al., 2023; Schröter et al., 2019). Similar patterns have also been shown for GZP, based both on net and optical surveys (Mańko et al., 2020, 2022; Pantiukhin et al., 2023a). In an eDNA study based on sediment samples, the influence of AW masses was found to be a significant driver of foraminifera community composition in Svalbard fjords (Nguyen et al., 2023). Through sparse partial least squares regression analysis (sPLS), our dataset revealed well-documented relationships between marine Metazoa and environmental variables, as well as associations that may point to previously unknown indicator taxa. These associations were most numerous in the copepod fraction of the zooplankton community. For example, the highly abundant and herbivorous Atlantic expatriate, *C. finmarchicus*, showed strong correlations with shallow depths, high oxygen and fluorescence values, indicating associations with phytoplankton bloom conditions. It also correlated with warmer temperatures and higher salinity, which are characteristics of AW masses. *Oithona atlantica* also showed significant correlations with AW mass characteristics as well as eastern longitudes, indicating a positive relationship with the Atlantic-influenced central Fram Strait and Svalbard stations. The increase of Atlantic *C. finmarchicus* and *Oithona* species is considered a signal of the progressing Atlantification in Fram Strait (Gluchowska, Dalpadado et al., 2017). In contrast, *M. pygmaeus*, a cold-water associated species (Sørreide et al., 2022), was significantly correlated with PW conditions of the East Greenland slope (low salinity, high oxygen), where it was found in high read numbers in the upper-epipelagic layer. Similar correlations were also observed for *Calanus glacialis* and *C. hyperboreus*, which have both been previously recognized as indicator species of PW masses (Gluchowska, Trudnowska et al., 2017; Svensen et al., 2011). Neither species showed strong correlations with temperature; however, higher sampling resolution across wider environmental gradients would likely improve the analysis.

Within the GZP community, we found correlations between eDNA read counts and environmental parameters that are in line with existing ecological knowledge of the species. *B. bouilloni*, *B. brucei*, and *A. tenella* were correlated with conditions of deepwater masses. This is in agreement with their detection in deep waters in Fram Strait using video surveys (Pantiukhin et al., 2023a) as well as findings from other Arctic regions (Raskoff, 2010; Raskoff et al., 2010). However, while Pantiukhin et al. (2023a) did not find a major effect of salinity on GZP community composition in Fram Strait, we found significant associations with higher salinity in the deepwater cluster and lower salinity in cluster 2 (the MOTUs named Hydrozoa_5, Hydrozoa_10 and Scyphozoa). Interestingly, we found significant negative correlations of the same three MOTUs with longitude despite finding no significant influence of sampling location

on community composition, suggesting an affinity to PW and the western side of Fram Strait.

The fact that we were able to detect well-known water mass associations of highly abundant copepod species and less abundant deepwater species such as *B. bouilloni*, highlights the strength of our approach for capturing zooplankton and, more specifically, GZP dynamics. Although conclusions from our sPLS analysis are somewhat hindered by the ability to taxonomically resolve MOTUs and the lack of knowledge about the ecology of detected taxa, it serves as a valuable approach for identifying potential indicator species associated with distinct conditions and as a means to generate hypotheses. Such hypotheses can be tested through increased resolution of eDNA sampling, especially in the understudied mesopelagic layers of the Arctic, in connection with net- and camera-based investigations. Therefore, this study shows the potential of eDNA as a cost- and time-effective tool for not only detecting pelagic Arctic diversity but also for monitoring shifts in Arctic zooplankton communities in the context of climate change-induced perturbations.

4.4 | eDNA as a tool to improve gelatinous zooplankton surveys

Gelatinous zooplankton are elusive and are notoriously difficult to catch in good condition. They are easily destroyed in typical zooplankton nets and other trawling gear. There are known sampling biases between types of trawls and nets (Nogueira Júnior et al., 2015), and while optical methods can detect individuals without destroying them, they also have known biases that can affect species composition results (Hosia et al., 2017). Even when detected or caught in good condition, GZP can also be difficult to identify morphologically without expert knowledge. Due to these challenges, GZP is regularly underestimated in terms of diversity, distribution, and abundance (Govindarajan et al., 2021; Hosia et al., 2017; Long et al., 2021). The implementation of eDNA for surveying GZP biodiversity has been integrated within broader assessments of marine biodiversity, including zooplankton in coral reefs in Florida (Djurhuus et al., 2018), as a part of a mesozooplankton survey in the Western Pacific (Feng et al., 2022) and in the mesopelagic zone in the North-Atlantic (Govindarajan et al., 2021). Studies with a focus on single-species GZP detection have been increasing in number in temperate and tropical areas including scyphozoan species in the Sea of Japan (Minamoto et al., 2017; Ogata et al., 2021; Takasu et al., 2019), and cubozoans (Bolte et al., 2021; Morrissey et al., 2022). However, the use of eDNA metabarcoding studies truly focused on jellyfish biodiversity and at the community level are limited. Jellyfish blooms can have major top-down ecosystem impacts on local and regional scales (Zagorodnyaya et al., 2023), on fisheries stocks and tourism (Bosch-Belmar et al., 2020; Ruiz-Frau, 2022). An increase in GZP abundances with further climate change has been projected for Fram Strait, concomitant with a decrease in diversity (Pantiukhin et al., 2023a). There is a need for cost-efficient monitoring tools

to track and further understand their community composition and abundance and implement mitigation strategies where necessary or make accurate future predictions.

Our results demonstrated that the GZP community composition detected is strongly influenced by the sampling methodology used. When comparing methods at the genus and species level, all three methods detected similar numbers of taxa, albeit with pronounced differences in composition (Figure 5a). When comparing eDNA with net catches, eDNA recovered more taxa overall, with nearly double the taxa at the order level (Figure 5b). Our results are consistent with several other studies that targeted open-ocean zooplankton communities and compared eDNA metabarcoding and net sampling. For example, Feng et al. (2022) and Govindarajan et al. (2021) both found two to four times as many medusae taxa with eDNA sampling compared to net tows. Given that all three sampling methods were conducted within hours of each other, it is unlikely that temporal shifts in the community composition of GZP are the reason for these differences. Thus, the differences are likely a consequence of varying sampling strategies, identification expertise, and underrepresentation of taxa on public barcode databases. The coverage and deployment of the three sampling strategies in this study are distinct in both the amount of water covered and their spatial dimensions. Water for eDNA sampling was taken at discrete depths on vertical CTD haul with a maximum sampling volume of 6 L at each sampling event. In contrast, nets were either hauled vertically or with oblique tows behind the ship, covering large sections of the water column. The video transects were carried out as horizontal transects at specific depths, also surveying thousands of liters of water (Pantiukhin et al., 2023a). Despite this, the eDNA study recovered the highest number of species-level detections.

An advantage of eDNA is that it can circumvent the likelihood of delicate and small specimens being destroyed or remaining undetected in net sampling, as well as the escape reactions of larger taxa (Andruszkiewicz Allan et al., 2021; Minamoto et al., 2017). Moreover, GZP has seemingly high DNA-shedding rates, increasing the likelihood of detection with eDNA (Andruszkiewicz Allan et al., 2021). Video surveys have the advantage of being able to detect different life stages, allow for abundance estimates and avoid damaging specimens like nets do. However, identifications to a lower taxonomic level may be hampered by image quality and the lack of molecular samples to reliably differentiate closely related or cryptic species (Montenegro et al., 2023). Issues with accurate morphological identifications have been highlighted for several GZP taxa recovered by nets and videos in Fram Strait. These include the distinction between species in the *Atolla* genus (Matsumoto et al., 2022), the narcomedusae *Aeginopsis laurentii* which is thought to have been historically confused with the recently described *B. bouilloni* (Raskoff, 2010), and the distinct bell shape used as the main identifier between *B. brucei* and *B. ellinorae* (Montenegro et al., 2023). Based on the eDNA results, we detected *A. tenella*, *B. bouilloni*, and *B. brucei* with 100% sequence identity matches. Furthermore, the species diversity of ctenophores is particularly poorly resolved in the Arctic (Majaneva & Majaneva, 2013).

Despite the many advantages, remaining limitations to eDNA metabarcoding prevent it from being a stand-alone survey method for capturing the entire GZP community. For example, we did not detect the hydrozoan species *A. digitale*, *S. arctica* and *Dimophyes arctica*, all of which are highly abundant in the area, as demonstrated by both the net and video surveys (Havermans et al., 2021; Pantiukhin et al., 2023a). All three of these GZP species are posited to be heavily influenced in the future by warming in the Arctic (Maňko et al., 2020, 2022; Pantiukhin et al., 2023a). Further omissions include reads assigned to the ctenophore *M. ovum* and appendicularians, both of which are particularly abundant components of the GZP community in Arctic surface waters (Gluchowska, Dalpadado et al., 2017; Raskoff et al., 2010), including Fram Strait (Havermans et al., 2021; Maňko et al., 2020). A number of GZP taxa known to occur in Fram Strait are poorly represented on public databases, severely hindering the ability of eDNA to detect them, with some having few available sequences (e.g., *Crystallophytes* sp.) and others with sequences only from other oceans (e.g., *D. arctica*). The highly abundant hydrozoan *S. arctica* has no publicly available COI barcodes on NCBI nor BOLD and has been categorized as “taxon inquirendum” in the WoRMs database (WoRMS Editorial Board, 2023). There are also no verified species-level barcode records of the Narcomedusae family Solmarisidae (detected here with eDNA). Additionally, taxa in the highly abundant Diphyidae family, known as bullet-shaped siphonophores, are difficult to identify morphologically due to their tendency to be damaged in nets and fixation by ethanol (Park et al., 2021). For example, *D. arctica* is often confused with *Muggiaea bargmannae* (Maňko et al., 2020) yet there are no publicly available COI sequences on BOLD for *M. bargmannae*, limiting our ability to further distinguish them with (meta)barcoding. With more than half of GZP MOTUs herein being identified only to class level, an increase in barcoding effort for GZP, and particularly hydrozoans, would no doubt increase our eDNA species list as well as improve the accuracy and taxonomic resolution of net detections. Furthermore, future research should include in silico PCRs to identify potential primer mismatches in GZP taxa, the impact of which on the current study cannot be ruled out.

5 | CONCLUSIONS

We demonstrated the use of eDNA metabarcoding as a successful and efficient method to complement the current biodiversity monitoring of pelagic metazoans in the Arctic Ocean and hereby provide the first GZP-focused eDNA metabarcoding biodiversity assessment in the Arctic. Our survey showed that it is possible to recover diversity patterns at a broad scale for the metazoan community as well as at a higher resolution with a targeted group of taxa using the COI barcode. Furthermore, we demonstrated that with only a single marker, a higher number of unique GZP taxa could be recovered from only a small amount of water compared to long net tows and video transects at the same locations. We propose eDNA as a supplementary tool to current biodiversity methods, both for metazoans and GZP,

rather than a replacement. As standardization improves and current limitations are overcome, for example, increased barcoding efforts to improve reference databases, the opportunity to use eDNA to detect and track changes in biodiversity across marine ecosystems will expand. Further analysis of community patterns, as well as crucial species-level information such as indicator species and rare and invasive taxa, will increase understanding of known shifts in marine communities, as well as validate predicted future scenarios in the Arctic.

AUTHOR CONTRIBUTIONS

CH conceived the study and, together with AM, developed the study design. CH planned the field work and collected the samples. AM conducted the laboratory work. AM analyzed the data, with contributions from TP, AA, WVA, and SN. AM wrote the manuscript with revisions by CH. CH acquired the funding resources. All authors contributed by revising the manuscript and approving the submitted version.

ACKNOWLEDGMENTS

We thank all the members of the FramJelly project on PS126 for their assistance with work on board. We are grateful to the ARJEL team members for their help during fieldwork, including water filtrations, sorting of the net catches, and analyses of the video data. We also thank the captain and crew on board Polarstern for their skillful support. We would like to thank Véronique Merten for her advice on eDNA sample processing. Lastly, we would like to thank the reviewers for their input. Open Access funding enabled and organized by Projekt DEAL.

FUNDING INFORMATION

This research was carried out in the Helmholtz Young Investigator Group “ARJEL—Arctic Jellies,” which has the project number VH-NG-1400 and is funded by the Helmholtz Society and the Alfred Wegener Institute Helmholtz Centre for Polar and Marine Research. Samples for this study were collected under the Polarstern project ID: AWI_PS126_09 (FramJelly, PI Charlotte Havermans). We acknowledge support by the Open Access Publication funds of Alfred Wegener Institute Helmholtz Centre for Polar and Marine Research.

CONFLICT OF INTEREST STATEMENT

The authors declare no conflict of interest.

DATA AVAILABILITY STATEMENT

The raw metabarcoding sequencing data from this project are publicly available at NCBI on the SRA database under the BioProject ID: [PRJNA1044054](https://doi.org/10.1044/PRJNA1044054). The oceanographic data is publicly available on the Pangea repository <https://doi.pangaea.de/10.1594/PANGAEA.940754>.

ORCID

Ayla Murray  <https://orcid.org/0000-0002-9134-7768>

Charlotte Havermans  <https://orcid.org/0000-0002-1126-4074>

REFERENCES

- Andruszkiewicz Allan, E., Zhang, W. G., Lavery, C., & Govindarajan, A. (2021). Environmental DNA shedding and decay rates from diverse animal forms and thermal regimes. *Environmental DNA*, 3(2), 492–514. <https://doi.org/10.1002/edn3.141>
- Antich, A., Palacín, C., Zarcero, J., Wangensteen, O. S., & Turon, X. (2022). Metabarcoding reveals high-resolution biogeographical and metaphylogeographical patterns through marine barriers. *Journal of Biogeography*, 5(3), 515–527.
- Antich, A., Palacín, C., Wangensteen, O. S., & Turon, X. (2021). To de-noise or to cluster, that is not the question: optimizing pipelines for COI metabarcoding and metaphylogeography. *BMC Bioinformatics*, 22(1). <https://doi.org/10.1186/s12859-021-04115-6>
- Basedow, S. L., Sundfjord, A., Appen, W.-J., Halvorsen, E., Kwasniewski, S., & Reigstad, M. (2018). Seasonal variation in transport of zooplankton into the Arctic basin through the Atlantic gateway, Fram Strait. *Frontiers in Marine Science*, 5, 194.
- Berry, T. E., Saunders, B. J., Coghlan, M. L., Stat, M., Jarman, S., Richardson, A. J., Davies, C. H., Berry, O., Harvey, E. S., & Bunce, M. (2019). Marine environmental DNA biomonitoring reveals seasonal patterns in biodiversity and identifies ecosystem responses to anomalous climatic events. *PLoS Genetics*, 15(2), e1007943. <https://doi.org/10.1371/journal.pgen.1007943>
- Beszczynska-Moeller, A., Woodgate, R. A., Lee, C., Melling, H., & Karcher, M. (2011). A synthesis of exchanges through the main oceanic gateways to the Arctic Ocean. *Oceanography*, 24(3), 82–99.
- Beule, L., & Karlovsky, P. (2020). Improved normalization of species count data in ecology by scaling with ranked subsampling (SRS): Application to microbial communities. *PeerJ*, 8, e9593. <https://doi.org/10.7717/peerj.9593>
- Bolte, B., Goldsbury, J., Huerlimann, R., Jerry, D., & Kingsford, M. (2021). Validation of eDNA as a viable method of detection for dangerous cubozoan jellyfish. *Environmental DNA*, 3(4), 769–779. <https://doi.org/10.1002/edn3.181>
- Bosch-Belmar, M., Milisenda, G., Basso, L., Doyle, T. K., Leone, A., & Piraino, S. (2020). Jellyfish impacts on marine aquaculture and fisheries. *Reviews in Fisheries Science & Aquaculture*, 29(2), 242–259. <https://doi.org/10.1080/23308249.2020.1806201>
- Bouillon, J., Gravili, C., Pagès, F., Gili, J.-M., & Boero, F. (2006). *An introduction to Hydrozoa* (p. 194). Mémoires du Muséum National d'Histoire Naturelle.
- Boyer, F., Mercier, C., Bonin, A., Le Bras, Y., Taberlet, P., & Coissac, E. (2016). Obitools: A unix-inspired software package for DNA metabarcoding. *Molecular Ecology Resources*, 16(1), 176–182. <https://doi.org/10.1111/1755-0998.12428>
- Buchner, D., & Leese, F. (2020). BOLDigger – A python package to identify and organise sequences with the barcode of life data systems. *Metabarcoding and Metagenomics*, 4, e53535. <https://doi.org/10.3897/mbmg.4.53535>
- Bucklin, A., Hopcroft, R. R., Kosobokova, K. N., Nigro, L. M., Ortman, B. D., Jennings, R. M., & Sweetman, C. J. (2010). DNA barcoding of Arctic Ocean holozooplankton for species identification and recognition. *Deep Sea Research Part II: Topical Studies in Oceanography*, 57(1), 40–48. <https://doi.org/10.1016/j.dsr2.2009.08.005>
- Bucklin, A., Peijnenburg, K. T. C. A., Kosobokova, K. N., O'Brien, T. D., Blanco-Bercial, L., Cornils, A., Falkenhaus, T., Hopcroft, R. R., Hosia, A., Laakmann, S., Li, C., Martell, L., Questel, J. M., Wall-Palmer, D., Wang, M., Wiebe, P. H., & Weydmann-Zwolicka, A. (2021). Toward a global reference database of COI barcodes for marine zooplankton. *Marine Biology*, 168(6). <https://doi.org/10.1007/s00227-021-03887-y>

- Bunholi, I. V., Foster, N. R., & Casey, J. M. (2023). Environmental DNA and RNA in aquatic community ecology: Toward methodological standardization. *Environmental DNA*, 5(6), 1133–1147. <https://doi.org/10.1002/edn3.476>
- Csapó, H. K., Grabowski, M., & Węstawski, J. M. (2021). Coming home-boreal ecosystem claims Atlantic sector of the Arctic. *Science of the Total Environment*, 771, 144817.
- Darnis, G., & Fortier, L. (2014). Temperature, food and the seasonal vertical migration of key arctic copepods in the thermally stratified Amundsen Gulf (Beaufort Sea, Arctic Ocean). *Journal of Plankton Research*, 36(4), 1092–1108. <https://doi.org/10.1093/plankt/fbu035>
- Degen, R., & Faulwetter, S. (2019). The Arctic traits database – A repository of Arctic benthic invertebrate traits. *Earth System Science Data*, 11(1), 301–322. <https://doi.org/10.5194/essd-11-301-2019>
- Descôteaux, R., Ershova, E., Wangensteen, O. S., Præbel, K., Renaud, P. E., Cottier, F., & Bluhm, B. A. (2021). Meroplankton diversity, seasonality and life-history traits across the Barents Sea polar front revealed by high-throughput DNA barcoding. *Frontiers in Marine Science*, 8, 677732. <https://doi.org/10.3389/fmars.2021.677732>
- Dischereit, A., Wangensteen, O. S., Præbel, K., Auel, H., & Havermans, C. (2022). Using DNA metabarcoding to characterize the prey spectrum of two co-occurring themisto amphipods in the rapidly changing Atlantic–Arctic gateway Fram Strait. *Genes*, 13(11), 2035. <https://doi.org/10.3390/genes13112035>
- Djurhuus, A., Pitz, K., Sawaya, N. A., Rojas-Márquez, J., Michaud, B., Montes, E., Muller-Karger, F., & Breitbart, M. (2018). Evaluation of marine zooplankton community structure through environmental DNA metabarcoding. *Limnology and Oceanography: Methods*, 16(4), 209–221. <https://doi.org/10.1002/lom3.10237>
- Eriksen, E., Skjoldal, H. R., Gjøsaeter, H., & Primicerio, R. (2017). Spatial and temporal changes in the Barents Sea pelagic compartment during the recent warming. *Progress in Oceanography*, 151, 206–226. <https://doi.org/10.1016/j.pocean.2016.12.009>
- Ershova, E. A., Descoteaux, R., Wangensteen, O. S., Iken, K., Hopcroft, R. R., Smoot, C., Grebmeier, J. M., & Bluhm, B. A. (2019). Diversity and distribution of meroplanktonic larvae in the Pacific Arctic and connectivity with adult benthic invertebrate communities. *Frontiers in Marine Science*, 6, 490. <https://doi.org/10.3389/fmars.2019.00490>
- Ershova, E. A., Wangensteen, O. S., Descoteaux, R., Barth-Jensen, C., & Præbel, K. (2021). Metabarcoding as a quantitative tool for estimating biodiversity and relative biomass of marine zooplankton. *ICES Journal of Marine Science*, 78(9), 3342–3355. <https://doi.org/10.1093/icesjms/fsab171>
- Ershova, E. A., Wangensteen, O. S., & Falkenhaus, T. (2023). Mock samples resolve biases in diversity estimates and quantitative interpretation of zooplankton metabarcoding data. *Marine Biodiversity*, 53(5). <https://doi.org/10.1007/s12526-023-01372-x>
- Feng, Y., Sun, D., Shao, Q., Fang, C., & Wang, C. (2022). Mesozooplankton biodiversity, vertical assemblages, and diel migration in the western tropical Pacific Ocean revealed by eDNA metabarcoding and morphological methods. *Frontiers in Marine Science*, 9, 1004410. <https://doi.org/10.3389/fmars.2022.1004410>
- Frøslev, T. G., Kjølner, R., Bruun, H. H., Ejrnæs, R., Brunbjerg, A. K., Pietroni, C., & Hansen, A. J. (2017). Algorithm for post-clustering curation of DNA amplicon data yields reliable biodiversity estimates. *Nature Communications*, 8(1), 1188. <https://doi.org/10.1038/s41467-017-01312-x>
- Geoffroy, M., Berge, J., Majaneva, S., Johnsen, G., Langbehn, T. J., Cottier, F., Mogstad, A. A., Zolich, A., & Last, K. (2018). Increased occurrence of the jellyfish *Periphylla periphylla* in the European high Arctic. *Polar Biology*, 41(12), 2615–2619. <https://doi.org/10.1007/s00300-018-2368-4>
- Gluchowska, M., Dalpadado, P., Beszczynska-Möller, A., Olszewska, A., Ingvaldsen, R. B., & Kwasniewski, S. (2017). Interannual zooplankton variability in the main pathways of the Atlantic water flow into the Arctic Ocean (Fram Strait and Barents Sea branches). *ICES Journal of Marine Science*, 74(7), 1921–1936. <https://doi.org/10.1093/icesjms/fsx033>
- Gluchowska, M., Trudnowska, E., Goszczko, I., Kubiszyn, A. M., Blachowiak-Samolyk, K., Walczowski, W., & Kwasniewski, S. (2017). Variations in the structural and functional diversity of zooplankton over vertical and horizontal environmental gradients en route to the Arctic Ocean through the Fram Strait. *PLoS One*, 12(2), e0171715.
- Govindarajan, A. F., Francolini, R. D., Jech, J. M., Lavery, A. C., Llopiz, J. K., Wiebe, P. H., & Zhang, W. (2021). Exploring the use of environmental DNA (eDNA) to detect animal taxa in the mesopelagic zone. *Frontiers in Ecology and Evolution*, 9, 574877. <https://doi.org/10.3389/fevo.2021.574877>
- Haberlin, D., Raine, R., McAllen, R., & Doyle, T. K. (2019). Distinct gelatinous zooplankton communities across a dynamic shelf sea. *Limnology and Oceanography*, 64(4), 1802–1818. <https://doi.org/10.1002/lno.11152>
- Hatlebakk, M., Kosobokova, K., Daase, M., & Søreide, J. E. (2022). Contrasting life traits of sympatric *Calanus glacialis* and *C. Finmarchicus* in a warming Arctic revealed by a year-round study in Isfjorden, Svalbard. *Frontiers in Marine Science*, 9, 877910. <https://doi.org/10.3389/fmars.2022.877910>
- Havermans, C., Dischereit, A., Hampe, H., Merten, V. J., Pantiukhin, D., Verhaegen, G., & Hoving, H. J. T. (2021). FRAMJELLY: Gelatinous zooplankton in the gateway to the Arctic: Advanced methods to study their diversity, distribution and role in the fram strait food web. In T. Soltwedel (Ed.), *The expedition PS126 of the research vessel POLARSTERN to the fram strait in 2021* (Vol. 757, pp. 96–109).
- Havermans, C., Dischereit, A., Pantiukhin, D., Friedrich, M., & Murray, A. (2022). Environmental DNA in an ocean of change: Status, challenges and prospects. *Arquivos de Ciências Do Mar*, 55, 298–337. <https://doi.org/10.32360/acmar.v55iEspecial.78188>
- Heidrich, V., Karlovsky, P., & Beule, L. (2021). 'SRS' R package and 'q2-SRS' QIIME 2 plugin: Normalization of microbiome data using scaling with ranked subsampling (SRS). *Applied Sciences*, 11(23), 11473. <https://doi.org/10.3390/app112311473>
- Holman, L. E., de Bruyn, M., Creer, S., Carvalho, G., Robidart, J., & Rius, M. (2019). Detection of introduced and resident marine species using environmental DNA metabarcoding of sediment and water. *Scientific Reports*, 9(1), 11559. <https://doi.org/10.1038/s41598-019-47899-7>
- Hop, H., Assmy, P., Wold, A., Sundfjord, A., Daase, M., Duarte, P., Kwasniewski, S., Gluchowska, M., Wiktor, J. M., Tatarek, A., Wiktor, J., Kristiansen, S., Fransson, A., Chierici, M., & Vihtakari, M. (2019). Pelagic ecosystem characteristics across the Atlantic water boundary current from Rippfjorden, Svalbard, to the Arctic Ocean during summer (2010–2014). *Frontiers in Marine Science*, 6, 181. <https://doi.org/10.3389/fmars.2019.00181>
- Hosia, A., Falkenhaus, T., Baxter, E. J., & Pagès, F. (2017). Abundance, distribution and diversity of gelatinous predators along the northern mid-Atlantic ridge: A comparison of different sampling methodologies. *PLoS One*, 12(11), e0187491. <https://doi.org/10.1371/journal.pone.0187491>
- Hoving, H.-J., Christiansen, S., Fabrizio, E., Hauss, H., Kiko, R., Linke, P., Neitzel, P., Piatkowski, U., & Körtzinger, A. (2019). The pelagic in situ observation system (PELAGIOS) to reveal biodiversity, behavior, and ecology of elusive oceanic fauna. *Ocean Science*, 15(5), 1327–1340. <https://doi.org/10.5194/os-15-1327-2019>
- Huang, J., Zhang, X., Zhang, Q., Lin, Y., Hao, M., Luo, Y., Zhao, Z., Yao, Y., Chen, X., Wang, L., Nie, S., Yin, Y., Xu, Y., & Zhang, J. (2017). Recently amplified arctic warming has contributed to a continual global warming trend. *Nature Climate Change*, 7(12), 875–879. <https://doi.org/10.1038/s41558-017-0009-5>
- Ingvaldsen, R. B., Assmann, K. M., Primicerio, R., Fosheim, M., Polyakov, I. V., & Dolgov, A. V. (2021). Physical manifestations and ecological implications of Arctic Atlantification. *Nature Reviews Earth and*

- Environment*, 2(12), 874–889. <https://doi.org/10.1038/s43017-021-00228-x>
- Ingvaldsen, R. B., Eriksen, E., Gjørseter, H., Engås, A., Schuppe, B. K., Assmann, K. M., Cannaby, H., Dalpadado, P., & Bluhm, B. A. (2023). Under-ice observations by trawls and multi-frequency acoustics in the Central Arctic Ocean reveals abundance and composition of pelagic fauna. *Scientific Reports*, 13(1), 1000. <https://doi.org/10.1038/s41598-023-27957-x>
- Jaspers, C., Hopcroft, R. R., Kiørboe, T., Lombard, F., López-Urrutia, Á., Everett, J. D., & Richardson, A. J. (2023). Gelatinous larvacean zooplankton can enhance trophic transfer and carbon sequestration. *Trends in Ecology & Evolution*, 38, 980–993. <https://doi.org/10.1016/j.tree.2023.05.005>
- Jeunen, G., Knapp, M., Spencer, H. G., Lamare, M. D., Taylor, H. R., Stat, M., Bunce, M., & Gemmell, N. J. (2019). Environmental DNA (eDNA) metabarcoding reveals strong discrimination among diverse marine habitats connected by water movement. *Molecular Ecology Resources*, 19(2), 426–438. <https://doi.org/10.1111/1755-0998.12982>
- Knust, R. (2017). Polar research and supply vessel POLARSTERN operated by the Alfred-Wegener-Institute. *Journal of Large-Scale Research Facilities*, 3, A119. <https://doi.org/10.17815/jlsrf-3-163>
- Kosobokova, K. N., Hopcroft, R. R., & Hirche, H.-J. (2011). Patterns of zooplankton diversity through the depths of the Arctic's central basins. *Marine Biodiversity*, 41(1), 29–50. <https://doi.org/10.1007/s12526-010-0057-9>
- Kulagin, D. N., & Neretina, T. V. (2017). Genetic and morphological diversity of the cosmopolitan chaetognath *Pseudosagitta maxima* (Conant, 1896) in the Atlantic Ocean and its relationship with the congeneric species. *ICES Journal of Marine Science*, 74(7), 1875–1884. <https://doi.org/10.1093/icesjms/fsw255>
- Kumar, G., Farrell, E., Reaume, A. M., Eble, J. A., & Gaither, M. R. (2022). One size does not fit all: Tuning eDNA protocols for high- and low-turbidity water sampling. *Environmental DNA*, 4(1), 167–180. <https://doi.org/10.1002/edn3.235>
- Lacoursière-Roussel, A., Howland, K., Normandeau, E., Grey, E. K., Archambault, P., Deiner, K., Lodge, D. M., Hernandez, C., Leduc, N., & Bernatchez, L. (2018). eDNA metabarcoding as a new surveillance approach for coastal Arctic biodiversity. *Ecology and Evolution*, 8(16), 7763–7777. <https://doi.org/10.1002/ece3.4213>
- Lebrato, M., Mendes, P., Steinberg, D. K., Cartes, J. E., Jones, B. M., Birsá, L. M., Benavides, R., & Oschlies, A. (2013). Jelly biomass sinking speed reveals a fast carbon export mechanism. *Limnology and Oceanography*, 58(3), 1113–1122. <https://doi.org/10.4319/lo.2013.58.3.1113>
- Lebrato, M., Pitt, K. A., Sweetman, A. K., Jones, D. O. B., Cartes, J. E., Oschlies, A., Condon, R. H., Molinero, J. C., Adler, L., Gaillard, C., Lloris, D., & Billett, D. S. M. (2012). Jelly-falls historic and recent observations: A review to drive future research directions. *Hydrobiologia*, 690(1), 227–245. <https://doi.org/10.1007/s10750-012-1046-8>
- Leduc, N., Lacoursière-Roussel, A., Howland, K. L., Archambault, P., Sevellec, M., Normandeau, E., Dispas, A., Winkler, G., McKindsey, C. W., Simard, N., & Bernatchez, L. (2019). Comparing eDNA metabarcoding and species collection for documenting Arctic metazoan biodiversity. *Environmental DNA*, 1(4), 342–358. <https://doi.org/10.1002/edn3.35>
- Leray, M., Yang, J. Y., Meyer, C. P., Mills, S. C., Agudelo, N., Ranwez, V., Boehm, J. T., & Machida, R. J. (2013). A new versatile primer set targeting a short fragment of the mitochondrial COI region for metabarcoding metazoan diversity: Application for characterizing coral reef fish gut contents. *Frontiers in Zoology*, 10(1), 34. <https://doi.org/10.1186/1742-9994-10-34>
- Licandro, P., Carré, C., & Lindsay, D. J. (2017). Cnidaria: Colonial Hydrozoa (Siphonophorae). In C. Castellani & M. Edwards (Eds.), *Marine Plankton: A Practical Guide to Ecology, Methodology, and Taxonomy* (pp. 232–250). Oxford University Press.
- Licandro, P., & Lindsay, D. J. (2017). Ctenophora. In C. Castellani & M. Edwards (Eds.), *Marine plankton: A practical guide to ecology, methodology, and taxonomy*. Oxford University Press.
- Long, A. P., Haberlin, D., Lyashevskaya, O., Brophy, D., O'Hea, B., O'Donnell, C., Scarrott, R. G., Lawton, C., & Doyle, T. K. (2021). Interannual variability of gelatinous mesozooplankton in a temperate shelf sea: Greater abundance coincides with cooler sea surface temperatures. *ICES Journal of Marine Science*, 78(4), 1372–1385. <https://doi.org/10.1093/icesjms/fsab030>
- Mańko, M. K., Gluchowska, M., & Weydmann-Zwolicka, A. (2020). Footprints of Atlantification in the vertical distribution and diversity of gelatinous zooplankton in the Fram Strait (Arctic Ocean). *Progress in Oceanography*, 189, 102414. <https://doi.org/10.1016/j.pocean.2020.102414>
- Mańko, M. K., Merchel, M., Kwasniewski, S., & Weydmann-Zwolicka, A. (2022). Oceanic fronts shape biodiversity of gelatinous zooplankton in the European Arctic. *Frontiers in Marine Science*, 9, 941025. <https://doi.org/10.3389/fmars.2022.941025>
- Mahé, F., Rognes, T., Quince, C., Vargas, C. d., & Dunthorn, M. (2015). Swarm v2: Highly-scalable and high-resolution amplicon clustering. *PeerJ*, 3, e1420. <https://doi.org/10.7717/peerj.1420>
- Majaneva, S., & Majaneva, M. (2013). Cydippid ctenophores in the coastal waters of Svalbard: Is it only *Mertensia ovum*? *Polar Biology*, 36(11), 1681–1686. <https://doi.org/10.1007/s00300-013-1377-6>
- Martinez Arbizu, P. (2020). *pairwiseAdonis: Pairwise multilevel comparison using adonis (0.4)* [R package].
- Matsumoto, G. I., Christianson, L. M., Robison, B. H., Haddock, S. H. D., & Johnson, S. B. (2022). *Atolla reynoldsi* sp. nov. (Cnidaria, Scyphozoa, Coronatae, Atollidae): A new species of coronate scyphozoan found in the eastern North Pacific Ocean. *Animals*, 12(6), 742. <https://doi.org/10.3390/ani12060742>
- Merten, V., Puebla, O., Bayer, T., Reusch, T. B. H., Fuss, J., Stefanschitz, J., Metfies, K., Stauffer, J. B., & Hoving, H.-J. (2023). Arctic nekton uncovered by eDNA metabarcoding: Diversity, potential range expansions, and pelagic-benthic coupling. *Environmental DNA*, 5(3), 503. <https://doi.org/10.1002/edn3.403>
- Minamoto, T., Fukuda, M., Katsuhara, K. R., Fujiwara, A., Hidaka, S., Yamamoto, S., Takahashi, K., & Masuda, R. (2017). Environmental DNA reflects spatial and temporal jellyfish distribution. *PLoS One*, 12(2), e0173073. <https://doi.org/10.1371/journal.pone.0173073>
- Miyamoto, H., Machida, R. J., & Nishida, S. (2012). Global phylogeography of the deep-sea pelagic chaetognath *Eukrohnia hamata*. *Progress in Oceanography*, 104, 99–109. <https://doi.org/10.1016/j.pocean.2012.06.003>
- Montenegro, J., Collins, A. G., Hopcroft, R. R., Questel, J. M., Thuesen, E. V., Bachtel, T. S., Bergman, L. A., Sangekar, M. N., Drazen, J. C., & Lindsay, D. J. (2023). Heterogeneity in diagnostic characters across ecoregions: A case study with *Botrynum* (Hydrozoa: Trachylina: Halicreatidae). *Frontiers in Marine Science*, 9, 1101699. <https://doi.org/10.3389/fmars.2022.1101699>
- Morrissey, S. J., Jerry, D. R., & Kingsford, M. J. (2022). Genetic detection and a method to study the ecology of deadly Cubozoan jellyfish. *Diversity*, 14(12), 1139. <https://doi.org/10.3390/d14121139>
- Neukermans, G., Oziel, L., & Babin, M. (2018). Increased intrusion of warming Atlantic water leads to rapid expansion of temperate phytoplankton in the Arctic. *Global Change Biology*, 24(6), 2545–2553. <https://doi.org/10.1111/gcb.14075>
- Nguyen, N.-L., Pawłowska, J., Angeles, I. B., Zajaczkowski, M., & Pawłowski, J. (2023). Metabarcoding reveals high diversity of benthic foraminifera linked to water masses circulation at coastal Svalbard. *Geobiology*, 21(1), 133–150. <https://doi.org/10.1111/gbi.12530>

- Nogueira Júnior, M., Pukanski, L. E., & Souza-Conceição, J. M. (2015). Mesh size effects on assessments of planktonic hydrozoan abundance and assemblage structure. *Journal of Marine Systems*, 144, 117–126. <https://doi.org/10.1016/j.jmarsys.2014.11.014>
- Norrbin, F., Eilertsen, H., & Degerlund, M. (2009). Vertical distribution of primary producers and zooplankton grazers during different phases of the Arctic spring bloom. *Deep Sea Research Part II: Topical Studies in Oceanography*, 56(21), 1945–1958. <https://doi.org/10.1016/j.dsr2.2008.11.006>
- Ogata, M., Masuda, R., Harino, H., Sakata, M. K., Hatakeyama, M., Yokoyama, K., Yamashita, Y., & Minamoto, T. (2021). Environmental DNA preserved in marine sediment for detecting jellyfish blooms after a tsunami. *Scientific Reports*, 11(1), 16830. <https://doi.org/10.1038/s41598-021-94286-2>
- Oksanen, J., Blanchet, G., Friendly, M., Kindt, R., Legendre, P., McGlenn, D., Minchin, P. R., O'hara, R. B., Simpson, G. L., Solymos, P., & Stevens, M. H. H. (2019). Vegan: Community ecology package (version 2.5-6). *The Comprehensive R Archive Network*.
- Oziel, L., Baudena, A., Ardyna, M., Massicotte, P., Randelhoff, A., Sallée, J.-B., Ingvaldsen, R. B., Devred, E., & Babin, M. (2020). Faster Atlantic currents drive poleward expansion of temperate phytoplankton in the Arctic Ocean. *Nature Communications*, 11(1), 1705. <https://doi.org/10.1038/s41467-020-15485-5>
- Pantiukhin, D., Verhaegen, G., Kraan, C., Jerosch, K., Neitzel, P., Hoving, H.-J. T., & Havermans, C. (2023a). Optical observations and spatio-temporal projections of gelatinous zooplankton in the Fram Strait, a gateway to a changing Arctic Ocean. *Frontiers in Marine Science*, 10, 987700. <https://doi.org/10.3389/fmars.2023.987700>
- Pantiukhin, D., Verhaegen, G., Kraan, C., Jerosch, K., Neitzel, P., Hoving, H.-J. T., & Havermans, C. (2023b). *Gelatinous zooplankton annotations of pelagic video transects in the Fram Strait during the R/V Polarstern expedition PS126* [dataset]. PANGAEA <https://doi.org/10.1594/PANGAEA.953888>
- Park, N., Yeom, J., Jeong, R., & Lee, W. (2021). Novel attempt at discrimination of a bullet-shaped siphonophore (Family Diphyidae) using matrix-assisted laser desorption/ionization time of flight mass spectrometry (MALDI-ToF MS). *Scientific Reports*, 11(1), 19077. <https://doi.org/10.1038/s41598-021-98724-z>
- Polyakov, I. V., Alkire, M. B., Bluhm, B. A., Brown, K. A., Carmack, E. C., Chierici, M., Danielson, S. L., Ellingsen, I., Ershova, E. A., Gårdfeldt, K., Ingvaldsen, R. B., Pnyushkov, A. V., Slagstad, D., & Wassmann, P. (2020). Borealization of the Arctic Ocean in response to anomalous advection from sub-Arctic seas. *Frontiers in Marine Science*, 7, 491. <https://doi.org/10.3389/fmars.2020.00491>
- Polyakov, I. V., Pnyushkov, A. V., Alkire, M. B., Ashik, I. M., Baumann, T. M., Carmack, E. C., Goszczko, I., Guthrie, J., Ivanov, V. V., Kanzow, T., & Kirshfield, R. (2017). Greater role for Atlantic inflows on sea-ice loss in the Eurasian Basin of the Arctic Ocean. *Science*, 356(6335), 285–291.
- Questel, J. M., Hopcroft, R. R., DeHart, H. M., Smoot, C. A., Kosobokova, K. N., & Bucklin, A. (2021). Metabarcoding of zooplankton diversity within the Chukchi Borderland, Arctic Ocean: Improved resolution from multi-gene markers and region-specific DNA databases. *Marine Biodiversity*, 51(1), 4. <https://doi.org/10.1007/s12526-020-01136-x>
- R Core Team. (2021). *R: A language and environment for statistical computing*. R Foundation for Statistical Computing.
- Ramondenc, S., Nöthig, E.-M., Hufnagel, L., Bauerfeind, E., Busch, K., Knüppel, N., Kraft, A., Schröter, F., Seifert, M., & Iversen, M. H. (2023). Effects of Atlantification and changing sea-ice dynamics on zooplankton community structure and carbon flux between 2000 and 2016 in the eastern Fram Strait. *Limnology and Oceanography*, 68(S1), S39–S53. <https://doi.org/10.1002/lno.12192>
- Rantanen, M., Karpechko, A. Y., Lipponen, A., Nordling, K., Hyvärinen, O., Ruosteenoja, K., & Laaksonen, A. (2022). The Arctic has warmed nearly four times faster than the globe since 1979. *Communications Earth & Environment*, 3(1), 1–10.
- Raskoff, K. A. (2010). *Bathykorus bouilloni*: A new genus and species of deep-sea jellyfish from the Arctic Ocean (Hydrozoa, Narcomedusae, Aeginidae). *Zootaxa*, 2361(1), 57. <https://doi.org/10.11646/zootaxa.2361.1.5>
- Raskoff, K. A., Hopcroft, R. R., Kosobokova, K. N., Purcell, J. E., & Youngbluth, M. (2010). Jellies under ice: ROV observations from the Arctic 2005 hidden ocean expedition. *Deep Sea Research Part II: Topical Studies in Oceanography*, 57(1), 111–126. <https://doi.org/10.1016/j.dsr2.2009.08.010>
- Ratnasingham, S., & Hebert, P. D. N. (2007). Bold: The barcode of life data system. *Molecular Ecology Notes*, 7(3), 355–364. <https://doi.org/10.1111/j.1471-8286.2007.01678.x>
- Rognes, T., Flouri, T., Nichols, B., Quince, C., & Mahé, F. (2016). VSEARCH: A versatile open source tool for metagenomics. *PeerJ*, 4, e2584. <https://doi.org/10.7717/peerj.2584>
- Rohart, F., Gautier, B., Singh, A., & Lê Cao, K.-A. (2017). mixOmics: An R package for 'omics feature selection and multiple data integration. *PLoS Computational Biology*, 13(11), e1005752. <https://doi.org/10.1371/journal.pcbi.1005752>
- Rudels, B., Schauer, U., Björk, G., Korhonen, M., Pisarev, S., Rabe, B., & Wisotzki, A. (2013). Observations of water masses and circulation with focus on the Eurasian Basin of the Arctic Ocean from the 1990s to the late 2000s. *Ocean Science*, 9(1), 147–169. <https://doi.org/10.5194/os-9-147-2013>
- Ruiz-Frau, A. (2022). Impacts of jellyfish presence on tourists' holiday destination choices and their willingness to pay for mitigation measures. *Journal of Environmental Planning and Management*, 66(10), 2107–2125. <https://doi.org/10.1080/09640568.2022.2061926>
- Sakata, M. K., Yamamoto, S., Gotoh, R. O., Miya, M., Yamanaka, H., & Minamoto, T. (2020). Sedimentary eDNA provides different information on timescale and fish species composition compared with aqueous eDNA. *Environmental DNA*, 2(4), 505–518. <https://doi.org/10.1002/edn3.75>
- Schröter, F., Havermans, C., Kraft, A., Knüppel, N., Beszczynska-Möller, A., Bauerfeind, E., & Nöthig, E.-M. (2019). Pelagic amphipods in the Eastern Fram Strait with continuing presence of *Themisto compressa* based on sediment trap time series. *Frontiers in Marine Science*, 6, 311.
- Sevellec, M., Lacoursière-Roussel, A., Bernatchez, L., Normandeau, E., Solomon, E., Arreak, A., Fishback, L., & Howland, K. (2021). Detecting community change in Arctic marine ecosystems using the temporal dynamics of environmental DNA. *Environmental DNA*, 3(3), 573–590. <https://doi.org/10.1002/edn3.155>
- Shiganova, T. A., & Abyzova, G. A. (2022). Revision of Beroidae (Ctenophora) in the southern seas of Europe: Systematics and distribution based on genetics and morphology. *Zoological Journal of the Linnean Society*, 194(1), 297–322. <https://doi.org/10.1093/zoolinnean/zlab021>
- Singer, G. A. C., Fahner, N. A., Barnes, J. G., McCarthy, A., & Hajibabaei, M. (2019). Comprehensive biodiversity analysis via ultra-deep patterned flow cell technology: A case study of eDNA metabarcoding seawater. *Scientific Reports*, 9(1), 5991. <https://doi.org/10.1038/s41598-019-42455-9>
- Soltwedel, T. (2021). *The Expedition PS126 of the Research Vessel POLARSTERN to the Fram Strait in 2021*. Berichte Zur Polar- Und Meeresforschung=Reports on Polar and Marine Research; Alfred Wegener Institute for Polar and Marine Research. https://doi.org/10.48433/BzPM_0757_2021
- Sørdeide, J. E., Dmoch, K., Blachowiak-Samolyk, K., Trudnowska, E., & Daase, M. (2022). Seasonal mesozooplankton patterns and timing of life history events in high-arctic fjord environments. *Frontiers in Marine Science*, 9, 933461. <https://doi.org/10.3389/fmars.2022.933461>

- Stepanjants, S. D. (1989). Hydrozoa of the Eurasian Arctic seas. In *The Arctic seas: Climatology, oceanography, geology, and biology* (pp. 397–430). Springer.
- Suter, L., Polanowski, A. M., Clarke, L. J., Kitchener, J. A., & Deagle, B. E. (2021). Capturing open ocean biodiversity: Comparing environmental DNA metabarcoding to the continuous plankton recorder. *Molecular Ecology*, 30(13), 3140–3157. <https://doi.org/10.1111/mec.15587>
- Svensen, C., Seuthe, L., Vasilyeva, Y., Pasternak, A., & Hansen, E. (2011). Zooplankton distribution across Fram Strait in autumn: Are small copepods and protozooplankton important? *Progress in Oceanography*, 91(4), 534–544. <https://doi.org/10.1016/j.pocean.2011.08.001>
- Takasu, H., Inomata, H., Uchino, K., Tahara, S., Mori, K., Hirano, Y., Harada, K., Yamaguchi, M., Nozoe, Y., & Akiyama, H. (2019). Spatio-temporal distribution of environmental DNA derived from Japanese sea nettle jellyfish *Chrysaora pacifica* in Omura Bay, Kyushu, Japan. *Plankton and Benthos Research*, 14(4), 320–323. <https://doi.org/10.3800/pbr.14.320>
- Urban, P., Præbel, K., Bhat, S., Dierking, J., & Wangensteen, O. S. (2022). DNA metabarcoding reveals the importance of gelatinous zooplankton in the diet of *Pandalus borealis*, a keystone species in the Arctic. *Molecular Ecology*, 31(5), 1562–1576. <https://doi.org/10.1111/mec.16332>
- Visser, F., Merten, V. J., Till Bayer, M. G., Oudejans, D. S. W., de Jonge, D. S. W., Puebla, O., Reusch, T. B. H., Fuss, J., & Hoving, H. J. T. (2021). Deep-sea predator niche segregation revealed by combined cetacean biologging and eDNA analysis of cephalopod prey. *Science Advances*, 7(14), eabf5908.
- Wangensteen, O. S., Palacín, C., Guardiola, M., & Turon, X. (2018). DNA metabarcoding of littoral hard-bottom communities: High diversity and database gaps revealed by two molecular markers. *PeerJ*, 6, e4705. <https://doi.org/10.7717/peerj.4705>
- Wassmann, P., Kosobokova, K. N., Slagstad, D., Drinkwater, K. F., Hopcroft, R. R., Moore, S. E., Ellingsen, I., Nelson, R. J., Carmack, E., Popova, E., & Berge, J. (2015). The contiguous domains of Arctic Ocean advection: Trails of life and death. *Progress in Oceanography*, 139, 42–65. <https://doi.org/10.1016/j.pocean.2015.06.011>
- Weydmann, A., Carstensen, J., Goszczko, I., Dmoch, K., Olszewska, A., & Kwasniewski, S. (2014). Shift towards the dominance of boreal species in the Arctic: Inter-annual and spatial zooplankton variability in the West Spitsbergen current. *Marine Ecology Progress Series*, 501, 41–52.
- WoRMS Editorial Board. (2023). *World Register of Marine Species* [dataset]. <https://doi.org/10.14284/170>
- Xavier, J. C., Cherel, Y., Allcock, L., Rosa, R., Sabirov, R. M., Blicher, M. E., & Golikov, A. V. (2018). A review on the biodiversity, distribution and trophic role of cephalopods in the Arctic and Antarctic marine ecosystems under a changing ocean. *Marine Biology*, 165(5), 1–26. <https://doi.org/10.1007/s00227-018-3352-9>
- Zagorodnyaya, Y. A., Piontkovski, S. A., & Gubanov, V. V. (2023). The pelagic ecosystem of the Black Sea goes gelatinous. *Marine Biology Research*, 19(6–7), 317–326. <https://doi.org/10.1080/17451000.2023.2235571>

SUPPORTING INFORMATION

Additional supporting information can be found online in the Supporting Information section at the end of this article.

How to cite this article: Murray, A., Priest, T., Antich, A., von Appen, W.-J., Neuhaus, S., & Havermans, C. (2024). Investigating pelagic biodiversity and gelatinous zooplankton communities in the rapidly changing European Arctic: An eDNA metabarcoding survey. *Environmental DNA*, 6, e569. <https://doi.org/10.1002/edn3.569>

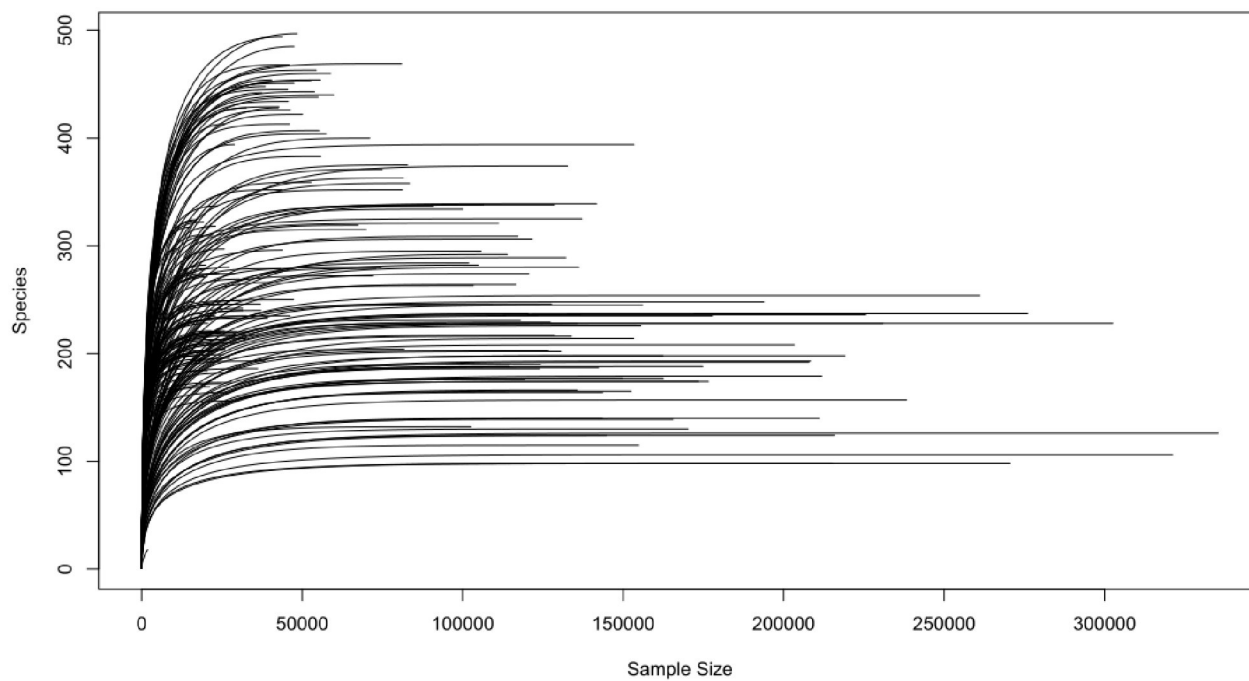


Figure S1. Rarefaction curves of MOTUs. Based on raw sequencing data.

Table S1. Sample details and environmental variables

Sample	Location	Depth		Station type	Fluorescence			Temp_C	Salinity_P	Density (kg/m3)	Oxygen saturation	Optical transmiss	Chl-a fluorescer
		Depth	Zone		(mg/m3)	Latitude	Longitude						
FIL0222	EG1	0	Upper-Epipelagic	Shallow	0.45603	78.986	-5.3813	-0.8922	31.2436	25.1064	108.69	91.9	0.49
FIL0223	EG1	0	Upper-Epipelagic	Shallow	0.45603	78.986	-5.3813	-0.8922	31.2436	25.1064	108.69	91.9	0.49
FIL0224	EG1	0	Upper-Epipelagic	Shallow	0.45603	78.986	-5.3813	-0.8922	31.2436	25.1064	108.69	91.9	0.49
FIL0219	EG1	20	Upper-Epipelagic	Shallow	0.45234	78.986	-5.3813	-1.6109	32.0561	25.7837	102.66	99.31	0.22
FIL0220	EG1	20	Upper-Epipelagic	Shallow	0.45234	78.986	-5.3813	-1.6109	32.0561	25.7837	102.66	99.31	0.22
FIL0221	EG1	20	Upper-Epipelagic	Shallow	0.45234	78.986	-5.3813	-1.6109	32.0561	25.7837	102.66	99.31	0.22
FIL0216	EG1	50	Upper-Epipelagic	Shallow	0.02285	78.986	-5.3813	-1.7359	32.1657	25.8753	100.77	101.26	-0.01
FIL0217	EG1	50	Upper-Epipelagic	Shallow	0.02285	78.986	-5.3813	-1.7359	32.1657	25.8753	100.77	101.26	-0.01
FIL0218	EG1	50	Upper-Epipelagic	Shallow	0.02285	78.986	-5.3813	-1.7359	32.1657	25.8753	100.77	101.26	-0.01
FIL0213	EG1	100	Upper-Epipelagic	Shallow	0.00222	78.986	-5.3813	-1.5087	32.7362	26.3336	95.89	101.07	0
FIL0214	EG1	100	Upper-Epipelagic	Shallow	0.00222	78.986	-5.3813	-1.5087	32.7362	26.3336	95.89	101.07	0
FIL0215	EG1	100	Upper-Epipelagic	Shallow	0.00222	78.986	-5.3813	-1.5087	32.7362	26.3336	95.89	101.07	0
FIL0199	EG4	0	Upper-Epipelagic	Deep	0.02864	78.7982	-2.7432	-0.8793	32.8901	26.4393	105.86	93.81	0.29
FIL0300	EG4	0	Upper-Epipelagic	Deep	0.02864	78.7982	-2.7432	-0.8793	32.8901	26.4393	105.86	93.81	0.29
FIL0301	EG4	0	Upper-Epipelagic	Deep	0.02864	78.7982	-2.7432	-0.8793	32.8901	26.4393	105.86	93.81	0.29
FIL0196	EG4	20	Upper-Epipelagic	Deep	0.08645	78.7982	-2.7432	-0.7488	33.0377	26.5541	108.04	93.96	0.69
FIL0197	EG4	20	Upper-Epipelagic	Deep	0.08645	78.7982	-2.7432	-0.7488	33.0377	26.5541	108.04	93.96	0.69
FIL0198	EG4	20	Upper-Epipelagic	Deep	0.08645	78.7982	-2.7432	-0.7488	33.0377	26.5541	108.04	93.96	0.69
FIL0193	EG4	50	Upper-Epipelagic	Deep	0.56237	78.7982	-2.7432	-1.1374	34.2704	27.5671	91.84	100.62	0.06
FIL0194	EG4	50	Upper-Epipelagic	Deep	0.56237	78.7982	-2.7432	-1.1374	34.2704	27.5671	91.84	100.62	0.06
FIL0195	EG4	50	Upper-Epipelagic	Deep	0.56237	78.7982	-2.7432	-1.1374	34.2704	27.5671	91.84	100.62	0.06
FIL0190	EG4	100	Upper-Epipelagic	Deep	0.01291	78.7982	-2.7432	1.9601	34.8741	27.8745	94.28	101.28	-0.01
FIL0191	EG4	100	Upper-Epipelagic	Deep	0.01291	78.7982	-2.7432	1.9601	34.8741	27.8745	94.28	101.28	-0.01
FIL0192	EG4	100	Upper-Epipelagic	Deep	0.01291	78.7982	-2.7432	1.9601	34.8741	27.8745	94.28	101.28	-0.01
FIL0187	EG4	200	Lower-Epipelagic	Deep	-0.0394	78.7982	-2.7432	2.1342	34.9311	27.9066	95.46	101.3	-0.02
FIL0188	EG4	200	Lower-Epipelagic	Deep	-0.0394	78.7982	-2.7432	2.1342	34.9311	27.9066	95.46	101.3	-0.02
FIL0189	EG4	200	Lower-Epipelagic	Deep	-0.0394	78.7982	-2.7432	2.1342	34.9311	27.9066	95.46	101.3	-0.02
FIL0178	EG4	400	Mesopelagic	Deep	-0.0246	78.7982	-2.7432	1.568	34.9152	27.9387	92	101.45	-0.02
FIL0179	EG4	400	Mesopelagic	Deep	-0.0246	78.7982	-2.7432	1.568	34.9152	27.9387	92	101.45	-0.02
FIL0180	EG4	400	Mesopelagic	Deep	-0.0246	78.7982	-2.7432	1.568	34.9152	27.9387	92	101.45	-0.02
FIL0181	EG4	500	Mesopelagic	Deep	-0.0225	78.7982	-2.7432	1.307	34.9274	27.9678	91.62	101.46	-0.02
FIL0182	EG4	500	Mesopelagic	Deep	-0.0225	78.7982	-2.7432	1.307	34.9274	27.9678	91.62	101.46	-0.02
FIL0183	EG4	500	Mesopelagic	Deep	-0.0225	78.7982	-2.7432	1.307	34.9274	27.9678	91.62	101.46	-0.02
FIL0184	EG4	750	Mesopelagic	Deep	-0.0239	78.7982	-2.7432	0.2541	34.8955	28.0098	87.13	101.73	-0.02
FIL0185	EG4	750	Mesopelagic	Deep	-0.0239	78.7982	-2.7432	0.2541	34.8955	28.0098	87.13	101.73	-0.02
FIL0186	EG4	750	Mesopelagic	Deep	-0.0239	78.7982	-2.7432	0.2541	34.8955	28.0098	87.13	101.73	-0.02
FIL0175	EG4	1000	Mesopelagic	Deep	-0.0232	78.7982	-2.7432	-0.1834	34.9042	28.0408	85.64	101.71	-0.02
FIL0176	EG4	1000	Mesopelagic	Deep	-0.0232	78.7982	-2.7432	-0.1834	34.9042	28.0408	85.64	101.71	-0.02
FIL0177	EG4	1000	Mesopelagic	Deep	-0.0232	78.7982	-2.7432	-0.1834	34.9042	28.0408	85.64	101.71	-0.02
FIL0172	EG4	1300	Bathypelagic	Deep	-0.0235	78.7982	-2.7432	-0.3768	34.9132	28.0583	86.9	101.68	-0.02
FIL0173	EG4	1300	Bathypelagic	Deep	-0.0235	78.7982	-2.7432	-0.3768	34.9132	28.0583	86.9	101.68	-0.02
FIL0174	EG4	1300	Bathypelagic	Deep	-0.0235	78.7982	-2.7432	-0.3768	34.9132	28.0583	86.9	101.68	-0.02
FIL0169	EG4	1600	Bathypelagic	Deep	-0.0233	78.7982	-2.7432	-0.5582	34.9144	28.0685	84.21	101.7	-0.02
FIL0170	EG4	1600	Bathypelagic	Deep	-0.0233	78.7982	-2.7432	-0.5582	34.9144	28.0685	84.21	101.7	-0.02
FIL0171	EG4	1600	Bathypelagic	Deep	-0.0233	78.7982	-2.7432	-0.5582	34.9144	28.0685	84.21	101.7	-0.02
FIL0166	EG4	2250	Bathypelagic	Deep	-0.0229	78.7982	-2.7432	-0.6898	34.9212	28.0815	82.01	101.66	-0.02
FIL0167	EG4	2250	Bathypelagic	Deep	-0.0229	78.7982	-2.7432	-0.6898	34.9212	28.0815	82.01	101.66	-0.02
FIL0168	EG4	2250	Bathypelagic	Deep	-0.0229	78.7982	-2.7432	-0.6898	34.9212	28.0815	82.01	101.66	-0.02
FIL0163	EG4	2500	Bathypelagic	Deep	-0.0231	78.7982	-2.7432	-0.7175	34.9254	28.0869	81.76	101.55	-0.02
FIL0164	EG4	2500	Bathypelagic	Deep	-0.0231	78.7982	-2.7432	-0.7175	34.9254	28.0869	81.76	101.55	-0.02
FIL0165	EG4	2500	Bathypelagic	Deep	-0.0231	78.7982	-2.7432	-0.7175	34.9254	28.0869	81.76	101.55	-0.02
FIL0082	HG4	0	Upper-Epipelagic	Deep	1.6002	79.064	4.19083	-0.9602	33.8595	27.2276	111.11	85.7	2.86
FIL0083	HG4	0	Upper-Epipelagic	Deep	1.6002	79.064	4.19083	-0.9602	33.8595	27.2276	111.11	85.7	2.86
FIL0084	HG4	0	Upper-Epipelagic	Deep	1.6002	79.064	4.19083	-0.9602	33.8595	27.2276	111.11	85.7	2.86
FIL0079	HG4	17	Upper-Epipelagic	Deep	2.0012	79.064	4.19083	-0.9062	34.2918	27.5758	99.26	93.99	0.81
FIL0080	HG4	17	Upper-Epipelagic	Deep	2.0012	79.064	4.19083	-0.9062	34.2918	27.5758	99.26	93.99	0.81
FIL0081	HG4	17	Upper-Epipelagic	Deep	2.0012	79.064	4.19083	-0.9062	34.2918	27.5758	99.26	93.99	0.81
FIL0076	HG4	50	Upper-Epipelagic	Deep	0.653	79.064	4.19083	1.208	34.7455	27.8269	94.14	100.91	0.04
FIL0077	HG4	50	Upper-Epipelagic	Deep	0.653	79.064	4.19083	1.208	34.7455	27.8269	94.14	100.91	0.04
FIL0078	HG4	50	Upper-Epipelagic	Deep	0.653	79.064	4.19083	1.208	34.7455	27.8269	94.14	100.91	0.04
FIL0073	HG4	100	Upper-Epipelagic	Deep	-0.0206	79.064	4.19083	2.4795	34.9524	27.8942	97.52	101.41	-0.03
FIL0074	HG4	100	Upper-Epipelagic	Deep	-0.0206	79.064	4.19083	2.4795	34.9524	27.8942	97.52	101.41	-0.03
FIL0075	HG4	100	Upper-Epipelagic	Deep	-0.0206	79.064	4.19083	2.4795	34.9524	27.8942	97.52	101.41	-0.03
FIL0070	HG4	200	Lower-Epipelagic	Deep	-0.0348	79.064	4.19083	2.5034	34.9685	27.9055	97.56	101.47	-0.02
FIL0071	HG4	200	Lower-Epipelagic	Deep	-0.0348	79.064	4.19083	2.5034	34.9685	27.9055	97.56	101.47	-0.02
FIL0072	HG4	200	Lower-Epipelagic	Deep	-0.0348	79.064	4.19083	2.5034	34.9685	27.9055	97.56	101.47	-0.02
FIL0055	HG4	400	Mesopelagic	Deep	-0.0229	79.064	4.19083	1.3407	34.9293	27.9665	92.32	101.71	-0.02
FIL0056	HG4	400	Mesopelagic	Deep	-0.0229	79.064	4.19083	1.3407	34.9293	27.9665	92.32	101.71	-0.02
FIL0069	HG4	400	Mesopelagic	Deep	-0.0229	79.064	4.19083	1.3407	34.9293	27.9665	92.32	101.71	-0.02
FIL0052	HG4	500	Mesopelagic	Deep	-0.0229	79.064	4.19083	1.1845	34.9408	27.9871	93.19	101.75	-0.02
FIL0053	HG4	500	Mesopelagic	Deep	-0.0229	79.064	4.19083	1.1845	34.9408	27.9871	93.19	101.75	-0.02
FIL0049	HG4	750	Mesopelagic	Deep	-0.0244	79.064	4.19083	0.0959	34.9059	28.0269	88.19	101.94	-0.02
FIL0050	HG4	750	Mesopelagic	Deep	-0.0244	79.064	4.19083	0.0959	34.9059	28.0269	88.19	101.94	-0.02
FIL0051	HG4	750	Mesopelagic	Deep	-0.0244	79.064	4.19083	0.0959	34.9059	28.0269	88.19	101.94	-0.02

FIL0057	HG4	1000 Mesopelagic	Deep	-0.0231	79.064	4.19083	-0.1958	34.9108	28.0468	87.94	101.93	-0.02
FIL0058	HG4	1000 Mesopelagic	Deep	-0.0231	79.064	4.19083	-0.1958	34.9108	28.0468	87.94	101.93	-0.02
FIL0059	HG4	1000 Mesopelagic	Deep	-0.0231	79.064	4.19083	-0.1958	34.9108	28.0468	87.94	101.93	-0.02
FIL0066	HG4	1300 Bathypelagic	Deep	-0.0236	79.064	4.19083	-0.4251	34.9143	28.0615	85.42	101.99	-0.03
FIL0067	HG4	1300 Bathypelagic	Deep	-0.0236	79.064	4.19083	-0.4251	34.9143	28.0615	85.42	101.99	-0.03
FIL0068	HG4	1300 Bathypelagic	Deep	-0.0236	79.064	4.19083	-0.4251	34.9143	28.0615	85.42	101.99	-0.03
FIL0063	HG4	1600 Bathypelagic	Deep	-0.0222	79.064	4.19083	-0.618	34.9128	28.0698	83.56	101.83	-0.03
FIL0064	HG4	1600 Bathypelagic	Deep	-0.0222	79.064	4.19083	-0.618	34.9128	28.0698	83.56	101.83	-0.03
FIL0065	HG4	1600 Bathypelagic	Deep	-0.0222	79.064	4.19083	-0.618	34.9128	28.0698	83.56	101.83	-0.03
FIL0060	HG4	2000 Bathypelagic	Deep	-0.0252	79.064	4.19083	-0.7242	34.9143	28.0767	81.85	101.66	-0.02
FIL0062	HG4	2000 Bathypelagic	Deep	-0.0252	79.064	4.19083	-0.7242	34.9143	28.0767	81.85	101.66	-0.02
FIL0046	HG4	2250 Bathypelagic	Deep	-0.0234	79.064	4.19083	-0.7294	34.9212	28.0832	81.76	101.61	-0.02
FIL0047	HG4	2250 Bathypelagic	Deep	-0.0234	79.064	4.19083	-0.7294	34.9212	28.0832	81.76	101.61	-0.02
FIL0048	HG4	2250 Bathypelagic	Deep	-0.0234	79.064	4.19083	-0.7294	34.9212	28.0832	81.76	101.61	-0.02
FIL00432	HG4	2250 Bathypelagic	Deep	-0.0235	79.064	4.19083	-0.729	34.9213	28.0832	81.75	101.61	-0.02
FIL0044	HG4	2250 Bathypelagic	Deep	-0.0235	79.064	4.19083	-0.729	34.9213	28.0832	81.75	101.61	-0.02
FIL0045	HG4	2250 Bathypelagic	Deep	-0.0235	79.064	4.19083	-0.729	34.9213	28.0832	81.75	101.61	-0.02
FIL0121	N4	0 Upper-Epipelagic	Deep	1.4711	79.7212	4.42117	-1.407	33.4096	26.8775	114.45	87.4	0.54
FIL0122	N4	0 Upper-Epipelagic	Deep	1.4711	79.7212	4.42117	-1.407	33.4096	26.8775	114.45	87.4	0.54
FIL0123	N4	0 Upper-Epipelagic	Deep	1.4711	79.7212	4.42117	-1.407	33.4096	26.8775	114.45	87.4	0.54
FIL0118	N4	20 Upper-Epipelagic	Deep	1.5376	79.7212	4.42117	-0.7084	34.1042	27.4159	106.49	81.06	3.89
FIL0119	N4	20 Upper-Epipelagic	Deep	1.5376	79.7212	4.42117	-0.7084	34.1042	27.4159	106.49	81.06	3.89
FIL0120	N4	20 Upper-Epipelagic	Deep	1.5376	79.7212	4.42117	-0.7084	34.1042	27.4159	106.49	81.06	3.89
FIL0115	N4	50 Upper-Epipelagic	Deep	0.05744	79.7212	4.42117	2.1602	34.888	27.8692	98.12	100.2	0.06
FIL0116	N4	50 Upper-Epipelagic	Deep	0.05744	79.7212	4.42117	2.1602	34.888	27.8692	98.12	100.2	0.06
FIL0117	N4	50 Upper-Epipelagic	Deep	0.05744	79.7212	4.42117	2.1602	34.888	27.8692	98.12	100.2	0.06
FIL0112	N4	100 Upper-Epipelagic	Deep	-0.0245	79.7212	4.42117	2.5768	34.9693	27.8993	98.15	100.74	-0.02
FIL0113	N4	100 Upper-Epipelagic	Deep	-0.0245	79.7212	4.42117	2.5768	34.9693	27.8993	98.15	100.74	-0.02
FIL0114	N4	100 Upper-Epipelagic	Deep	-0.0245	79.7212	4.42117	2.5768	34.9693	27.8993	98.15	100.74	-0.02
FIL0109	N4	200 Lower-Epipelagic	Deep	-0.0231	79.7212	4.42117	2.3253	34.9635	27.9167	96.99	101.06	-0.02
FIL0110	N4	200 Lower-Epipelagic	Deep	-0.0231	79.7212	4.42117	2.3253	34.9635	27.9167	96.99	101.06	-0.02
FIL0111	N4	200 Lower-Epipelagic	Deep	-0.0231	79.7212	4.42117	2.3253	34.9635	27.9167	96.99	101.06	-0.02
FIL0148	N4	400 Mesopelagic	Deep	-0.026	79.7212	4.42117	1.4557	34.9211	27.9517	91.54	101.53	-0.02
FIL0149	N4	400 Mesopelagic	Deep	-0.026	79.7212	4.42117	1.4557	34.9211	27.9517	91.54	101.53	-0.02
FIL0150	N4	400 Mesopelagic	Deep	-0.026	79.7212	4.42117	1.4557	34.9211	27.9517	91.54	101.53	-0.02
FIL0145	N4	500 Mesopelagic	Deep	-0.0258	79.7212	4.42117	1.103	34.9199	27.9759	90.92	101.54	-0.02
FIL0146	N4	500 Mesopelagic	Deep	-0.0258	79.7212	4.42117	1.103	34.9199	27.9759	90.92	101.54	-0.02
FIL0147	N4	500 Mesopelagic	Deep	-0.0258	79.7212	4.42117	1.103	34.9199	27.9759	90.92	101.54	-0.02
FIL0142	N4	750 Mesopelagic	Deep	-0.0284	79.7212	4.42117	0.1404	34.9051	28.0238	87.77	101.69	-0.02
FIL0143	N4	750 Mesopelagic	Deep	-0.0284	79.7212	4.42117	0.1404	34.9051	28.0238	87.77	101.69	-0.02
FIL0144	N4	750 Mesopelagic	Deep	-0.0284	79.7212	4.42117	0.1404	34.9051	28.0238	87.77	101.69	-0.02
N410001	N4	1000 Mesopelagic	Deep	-0.0242	79.7212	4.42117	-0.2243	34.9107	28.0481	87.13	101.69	-0.02
N410002	N4	1000 Mesopelagic	Deep	-0.0242	79.7212	4.42117	-0.2243	34.9107	28.0481	87.13	101.69	-0.02
N410003	N4	1000 Mesopelagic	Deep	-0.0242	79.7212	4.42117	-0.2243	34.9107	28.0481	87.13	101.69	-0.02
FIL0136	N4	1300 Bathypelagic	Deep	-0.0264	79.7212	4.42117	-0.4613	34.9146	28.0634	84.71	101.74	-0.03
FIL0137	N4	1300 Bathypelagic	Deep	-0.0264	79.7212	4.42117	-0.4613	34.9146	28.0634	84.71	101.74	-0.03
FIL0138	N4	1300 Bathypelagic	Deep	-0.0264	79.7212	4.42117	-0.4613	34.9146	28.0634	84.71	101.74	-0.03
FIL0133	N4	1600 Bathypelagic	Deep	-0.0243	79.7212	4.42117	-0.5873	34.9178	28.0725	83.26	101.73	-0.02
FIL0134	N4	1600 Bathypelagic	Deep	-0.0243	79.7212	4.42117	-0.5873	34.9178	28.0725	83.26	101.73	-0.02
FIL0135	N4	1600 Bathypelagic	Deep	-0.0243	79.7212	4.42117	-0.5873	34.9178	28.0725	83.26	101.73	-0.02
FIL0130	N4	2000 Bathypelagic	Deep	-0.0249	79.7212	4.42117	-0.6882	34.9179	28.0781	82.25	101.64	-0.02
FIL0131	N4	2000 Bathypelagic	Deep	-0.0249	79.7212	4.42117	-0.6882	34.9179	28.0781	82.25	101.64	-0.02
FIL0132	N4	2000 Bathypelagic	Deep	-0.0249	79.7212	4.42117	-0.6882	34.9179	28.0781	82.25	101.64	-0.02
FIL0127	N4	2250 Bathypelagic	Deep	-0.0244	79.7212	4.42117	-0.7109	34.9211	28.0823	82.01	101.62	-0.02
FIL0128	N4	2250 Bathypelagic	Deep	-0.0244	79.7212	4.42117	-0.7109	34.9211	28.0823	82.01	101.62	-0.02
FIL0129	N4	2250 Bathypelagic	Deep	-0.0244	79.7212	4.42117	-0.7109	34.9211	28.0823	82.01	101.62	-0.02
FIL0040	S3	0 Upper-Epipelagic	Deep	0.0788	77.6083	5.06283	3.1849	34.9213	27.805	104.23	97.6	0.15
FIL0041	S3	0 Upper-Epipelagic	Deep	0.0788	77.6083	5.06283	3.1849	34.9213	27.805	104.23	97.6	0.15
FIL0042	S3	0 Upper-Epipelagic	Deep	0.0788	77.6083	5.06283	3.1849	34.9213	27.805	104.23	97.6	0.15
FIL0037	S3	14 Upper-Epipelagic	Deep	0.1067	77.6083	5.06283	3.1474	34.9548	27.8354	104.12	97.89	0.13
FIL0038	S3	14 Upper-Epipelagic	Deep	0.1067	77.6083	5.06283	3.1474	34.9548	27.8354	104.12	97.89	0.13
FIL0039	S3	14 Upper-Epipelagic	Deep	0.1067	77.6083	5.06283	3.1474	34.9548	27.8354	104.12	97.89	0.13
FIL0034	S3	50 Upper-Epipelagic	Deep	0.02641	77.6083	5.06283	2.7054	34.9972	27.9102	99.9	100.57	0.06
FIL0035	S3	50 Upper-Epipelagic	Deep	0.02641	77.6083	5.06283	2.7054	34.9972	27.9102	99.9	100.57	0.06
FIL0036	S3	50 Upper-Epipelagic	Deep	0.02641	77.6083	5.06283	2.7054	34.9972	27.9102	99.9	100.57	0.06
FIL0031	S3	100 Upper-Epipelagic	Deep	0.02492	77.6083	5.06283	2.6153	34.9936	27.9153	99.82	100.27	0.06
FIL0032	S3	100 Upper-Epipelagic	Deep	0.02492	77.6083	5.06283	2.6153	34.9936	27.9153	99.82	100.27	0.06
FIL0033	S3	100 Upper-Epipelagic	Deep	0.02492	77.6083	5.06283	2.6153	34.9936	27.9153	99.82	100.27	0.06
FIL0028	S3	200 Lower-Epipelagic	Deep	-0.0051	77.6083	5.06283	2.2835	34.9921	27.9431	97.28	101.25	0.05
FIL0029	S3	200 Lower-Epipelagic	Deep	-0.0051	77.6083	5.06283	2.2835	34.9921	27.9431	97.28	101.25	0.05
FIL0030	S3	200 Lower-Epipelagic	Deep	-0.0051	77.6083	5.06283	2.2835	34.9921	27.9431	97.28	101.25	0.05
FIL0043	S3	200 Lower-Epipelagic	Deep	-0.0051	77.6083	5.06283	2.2835	34.9921	27.9431	97.28	101.25	0.05
FIL0025	S3	400 Mesopelagic	Deep	-0.0085	77.6083	5.06283	0.87	34.9368	28.0046	92.06	101.79	-0.02
FIL0026	S3	400 Mesopelagic	Deep	-0.0085	77.6083	5.06283	0.87	34.9368	28.0046	92.06	101.79	-0.02
FIL0027	S3	400 Mesopelagic	Deep	-0.0085	77.6083	5.06283	0.87	34.9368	28.0046	92.06	101.79	-0.02
FIL0022	S3	500 Mesopelagic	Deep	-0.0231	77.6083	5.06283	0.1191	34.9021	28.022	87.95	101.93	-0.01
FIL0023	S3	500 Mesopelagic	Deep	-0.0231	77.6083	5.06283	0.1191	34.9021	28.022	87.95	101.93	-0.01

FIL0024	S3	500 Mesopelagic	Deep	-0.0231	77.6083	5.06283	0.1191	34.9021	28.022	87.95	101.93	-0.01
FIL0019	S3	750 Mesopelagic	Deep	-0.0255	77.6083	5.06283	-0.1859	34.911	28.0458	88.18	102	-0.02
FIL0020	S3	750 Mesopelagic	Deep	-0.0255	77.6083	5.06283	-0.1859	34.911	28.0458	88.18	102	-0.02
FIL0021	S3	750 Mesopelagic	Deep	-0.0255	77.6083	5.06283	-0.1859	34.911	28.0458	88.18	102	-0.02
FIL0016	S3	1000 Mesopelagic	Deep	-0.0289	77.6083	5.06283	-0.3897	34.9133	28.0582	86.58	102.04	-0.02
FIL0017	S3	1000 Mesopelagic	Deep	-0.0289	77.6083	5.06283	-0.3897	34.9133	28.0582	86.58	102.04	-0.02
FIL0018	S3	1000 Mesopelagic	Deep	-0.0289	77.6083	5.06283	-0.3897	34.9133	28.0582	86.58	102.04	-0.02
FIL0013	S3	1300 Bathypelagic	Deep	-0.0182	77.6083	5.06283	-0.6011	34.9117	28.0674	84.27	101.98	-0.02
FIL0014	S3	1300 Bathypelagic	Deep	-0.0182	77.6083	5.06283	-0.6011	34.9117	28.0674	84.27	101.98	-0.02
FIL0015	S3	1300 Bathypelagic	Deep	-0.0182	77.6083	5.06283	-0.6011	34.9117	28.0674	84.27	101.98	-0.02
FIL0010	S3	1600 Bathypelagic	Deep	-0.0205	77.6083	5.06283	-0.6843	34.9127	28.0726	82.89	101.95	-0.02
FIL0011	S3	1600 Bathypelagic	Deep	-0.0205	77.6083	5.06283	-0.6843	34.9127	28.0726	82.89	101.95	-0.02
FIL0012	S3	1600 Bathypelagic	Deep	-0.0205	77.6083	5.06283	-0.6843	34.9127	28.0726	82.89	101.95	-0.02
FIL0007	S3	2000 Bathypelagic	Deep	-0.0239	77.6083	5.06283	-0.7321	34.9156	28.0781	81.75	101.72	-0.02
FIL0008	S3	2000 Bathypelagic	Deep	-0.0239	77.6083	5.06283	-0.7321	34.9156	28.0781	81.75	101.72	-0.02
FIL0009	S3	2000 Bathypelagic	Deep	-0.0239	77.6083	5.06283	-0.7321	34.9156	28.0781	81.75	101.72	-0.02
FIL0004	S3	2250 Bathypelagic	Deep	-0.0222	77.6083	5.06283	-0.7363	34.9255	28.087	82.06	101.78	-0.02
FIL0005	S3	2250 Bathypelagic	Deep	-0.0222	77.6083	5.06283	-0.7363	34.9255	28.087	82.06	101.78	-0.02
FIL0006	S3	2250 Bathypelagic	Deep	-0.0222	77.6083	5.06283	-0.7363	34.9255	28.087	82.06	101.78	-0.02
FIL0210	SV2	0 Upper-Epipelagic	Shallow	0.44048	78.9803	9.516	2.806	34.9078	27.8293	105.75	96.58	0.77
FIL0211	SV2	0 Upper-Epipelagic	Shallow	0.44048	78.9803	9.516	2.806	34.9078	27.8293	105.75	96.58	0.77
FIL0212	SV2	0 Upper-Epipelagic	Shallow	0.44048	78.9803	9.516	2.806	34.9078	27.8293	105.75	96.58	0.77
FIL0207	SV2	25 Upper-Epipelagic	Shallow	0.4202	78.9803	9.516	2.8754	34.9033	27.8195	105.98	97.65	0.38
FIL0208	SV2	25 Upper-Epipelagic	Shallow	0.4202	78.9803	9.516	2.8754	34.9033	27.8195	105.98	97.65	0.38
FIL0209	SV2	25 Upper-Epipelagic	Shallow	0.4202	78.9803	9.516	2.8754	34.9033	27.8195	105.98	97.65	0.38
FIL0204	SV2	50 Upper-Epipelagic	Shallow	0.14308	78.9803	9.516	1.8388	34.8524	27.8663	101.64	100.12	0.02
FIL0205	SV2	50 Upper-Epipelagic	Shallow	0.14308	78.9803	9.516	1.8388	34.8524	27.8663	101.64	100.12	0.02
FIL0206	SV2	50 Upper-Epipelagic	Shallow	0.14308	78.9803	9.516	1.8388	34.8524	27.8663	101.64	100.12	0.02
FIL0201	SV2	100 Upper-Epipelagic	Shallow	0.01701	78.9803	9.516	1.7071	34.8746	27.8945	104.64	99.94	0.02
FIL0202	SV2	100 Upper-Epipelagic	Shallow	0.01701	78.9803	9.516	1.7071	34.8746	27.8945	104.64	99.94	0.02
FIL0203	SV2	100 Upper-Epipelagic	Shallow	0.01701	78.9803	9.516	1.7071	34.8746	27.8945	104.64	99.94	0.02
FIL0106	SV4	0 Upper-Epipelagic	Shallow	0.56095	79.0202	7.09467	3.6482	34.7886	27.6541	112.39	94.11	0.52
FIL0107	SV4	0 Upper-Epipelagic	Shallow	0.56095	79.0202	7.09467	3.6482	34.7886	27.6541	112.39	94.11	0.52
FIL0108	SV4	0 Upper-Epipelagic	Shallow	0.56095	79.0202	7.09467	3.6482	34.7886	27.6541	112.39	94.11	0.52
FIL0103	SV4	25 Upper-Epipelagic	Shallow	0.57955	79.0202	7.09467	3.8788	34.8774	27.7014	110.82	89.68	0.85
FIL0104	SV4	25 Upper-Epipelagic	Shallow	0.57955	79.0202	7.09467	3.8788	34.8774	27.7014	110.82	89.68	0.85
FIL0105	SV4	25 Upper-Epipelagic	Shallow	0.57955	79.0202	7.09467	3.8788	34.8774	27.7014	110.82	89.68	0.85
FIL0100	SV4	50 Upper-Epipelagic	Shallow	0.38514	79.0202	7.09467	4.1473	34.9826	27.7572	102.66	99.44	0.48
FIL0101	SV4	50 Upper-Epipelagic	Shallow	0.38514	79.0202	7.09467	4.1473	34.9826	27.7572	102.66	99.44	0.48
FIL0102	SV4	50 Upper-Epipelagic	Shallow	0.38514	79.0202	7.09467	4.1473	34.9826	27.7572	102.66	99.44	0.48
FIL0097	SV4	100 Upper-Epipelagic	Shallow	0.01535	79.0202	7.09467	3.6979	34.9767	27.7995	101.28	100.13	0.1
FIL0098	SV4	100 Upper-Epipelagic	Shallow	0.01535	79.0202	7.09467	3.6979	34.9767	27.7995	101.28	100.13	0.1
FIL0099	SV4	100 Upper-Epipelagic	Shallow	0.01535	79.0202	7.09467	3.6979	34.9767	27.7995	101.28	100.13	0.1

Table S2. Water mass definitions

Water Mass	Abbreviation	Salinity.minimum	Salinity.maximum	Temperature.minimum	Temperature.maximum	
Polar Water	PW	<34.8		34.8 < 0		0
Atlantic Water	AW		34.8 Infinity		2 > 2	
Arctic Atlantic Water	AAW		34.8 Infinity		0	2
Deep Water	DW		34.8	< 0		0

Table S3. List of metazoan MOTUs removed during the blank correction process.

Kingdom	Phylum	Class	Order	Family	Genus	Species	Total reads
Metazoa	Arthropoda	Insecta	Diptera	Psychodidae	Psychoda	Psychoda phalaenoides	11
Metazoa	Arthropoda	Maxillopoda	Cyclopoida	NA	NA	NA	5
Metazoa	Arthropoda	NA	NA	NA	NA	NA	87
Metazoa	Chordata	Mammalia	Primates	Hominidae	Homo	Homo sapiens	371
Metazoa	Chordata	Mammalia	Primates	Hominidae	Homo	Homo sapiens	42
Metazoa	Rotifera	Monogononta	Ploima	Asplanchnidae	Asplanchna	Asplanchna sieboldii	14
Metazoa	Rotifera	Monogononta	Ploima	Trichotriidae	Trichotria	Trichotria tetractis	24
Metazoa	Rotifera	Monogononta	Ploima	NA	NA	NA	927
Metazoa	Rotifera	Monogononta	Ploima	NA	NA	NA	251
Metazoa	NA	NA	NA	NA	NA	NA	4953
Metazoa	NA	NA	NA	NA	NA	NA	54
Metazoa	NA	NA	NA	NA	NA	NA	15

Table S4. Statistic results from ANOVA analyses and subsequent Tukeys HSD tests.

Metazoans							
ANOVA (type II) testing for the effect of Location on Metazoan shannon diversity in the Upper-Epipelagic layer at all stations							
Effect	DFn	DFd	F	p	Generalised effect size		
Location		6	21	2.005	0.11	0.364	

Tukey's pairwise comparison of Metazoan shannon diversity in the Upper-Epipelagic layer at all stations

term	group1	group2	null.value	estimate	conf.low	conf.high	p.adj	p.adj.signif
Location	EG1	EG4	0	-0.3997	-1.35714	0.55775	0.817	ns
Location	EG1	HG4	0	-0.05174	-1.00918	0.9057	1	ns
Location	EG1	N4	0	0.04692	-0.91053	1.00436	1	ns
Location	EG1	S3	0	-0.05728	-1.01473	0.90016	1	ns
Location	EG1	SV2	0	0.52656	-0.43089	1.484	0.57	ns
Location	EG1	SV4	0	-0.28954	-1.24698	0.66791	0.952	ns
Location	EG4	HG4	0	0.34796	-0.60949	1.3054	0.893	ns
Location	EG4	N4	0	0.44661	-0.51083	1.40406	0.733	ns
Location	EG4	S3	0	0.34241	-0.61503	1.29986	0.9	ns
Location	EG4	SV2	0	0.92625	-0.03119	1.8837	0.0622	ns
Location	EG4	SV4	0	0.11016	-0.84728	1.0676	1	ns
Location	HG4	N4	0	0.09866	-0.85878	1.0561	1	ns
Location	HG4	S3	0	-0.00554	-0.96299	0.9519	1	ns
Location	HG4	SV2	0	0.5783	-0.37914	1.53574	0.464	ns
Location	HG4	SV4	0	-0.23779	-1.19524	0.71965	0.982	ns
Location	N4	S3	0	-0.1042	-1.06165	0.85324	1	ns
Location	N4	SV2	0	0.47964	-0.4778	1.43708	0.667	ns
Location	N4	SV4	0	-0.33645	-1.2939	0.62099	0.907	ns
Location	S3	SV2	0	0.58384	-0.3736	1.54129	0.453	ns
Location	S3	SV4	0	-0.23225	-1.1897	0.72519	0.984	ns
Location	SV2	SV4	0	-0.81609	-1.77354	0.14135	0.129	ns

ANOVA (type II) testing for the effect of Location on Metazoan OUT Richness in the Upper-Epipelagic layer at all stations

Effect	DFn	DFd	F	p	Generalised effect size		
Location		6	21	2.536	0.053	0.42	

Tukey's pairwise comparison of Metazoan OTU Richness in the Upper-Epipelagic layer at all stations

term	group1	group2	null.value	estimate	conf.low	conf.high	p.adj	p.adj.signif
Location	EG1	EG4	0	-1.75	-10.8379	7.33795	0.995	ns
Location	EG1	HG4	0	-3	-12.0879	6.08795	0.929	ns
Location	EG1	N4	0	-4.75	-13.8379	4.33795	0.624	ns
Location	EG1	S3	0	-3.25	-12.3379	5.83795	0.9	ns
Location	EG1	SV2	0	3.75	-5.33795	12.8379	0.825	ns
Location	EG1	SV4	0	-5.5	-14.5879	3.58795	0.462	ns
Location	EG4	HG4	0	-1.25	-10.3379	7.83795	0.999	ns
Location	EG4	N4	0	-3	-12.0879	6.08795	0.929	ns
Location	EG4	S3	0	-1.5	-10.5879	7.58795	0.998	ns
Location	EG4	SV2	0	5.5	-3.58795	14.5879	0.462	ns
Location	EG4	SV4	0	-3.75	-12.8379	5.33795	0.825	ns
Location	HG4	N4	0	-1.75	-10.8379	7.33795	0.995	ns
Location	HG4	S3	0	-0.25	-9.33795	8.83795	1	ns
Location	HG4	SV2	0	6.75	-2.33795	15.8379	0.241	ns
Location	HG4	SV4	0	-2.5	-11.5879	6.58795	0.969	ns
Location	N4	S3	0	1.5	-7.58795	10.5879	0.998	ns
Location	N4	SV2	0	8.5	-0.58795	17.5879	0.0767	ns
Location	N4	SV4	0	-0.75	-9.83795	8.33795	1	ns
Location	S3	SV2	0	7	-2.08795	16.0879	0.208	ns
Location	S3	SV4	0	-2.25	-11.3379	6.83795	0.982	ns
Location	SV2	SV4	0	-9.25	-18.3379	-0.16205	0.0443	*

ANOVA (type II) testing for the effect of Location on Metazoan Shannon Diversity at the four deep stations (HG4, N4, S3, EG4)

Effect	DFn	DFd	F	p	Generalised effect size		
Location		3	49	1.273	0.294	0.072	

Tukey's pairwise comparison of Metazoan shannon diversity at the four deep stations (HG4, N4, S3, EG4)

term	group1	group2	null.value	estimate	conf.low	conf.high	p.adj	p.adj.signif
Location	EG4	HG4	0	0.41886	-0.29615	1.13387	0.412	ns
Location	EG4	N4	0	0.4875	-0.24063	1.21563	0.295	ns
Location	EG4	S3	0	0.36588	-0.36225	1.09401	0.545	ns
Location	HG4	N4	0	0.06864	-0.64637	0.78365	0.994	ns
Location	HG4	S3	0	-0.05298	-0.76799	0.66203	0.997	ns
Location	N4	S3	0	-0.12162	-0.84975	0.60651	0.97	ns

ANOVA (type II) testing for the effect of Location on Metazoan MOTU Richness at the four deep stations (HG4, N4, S3, EG4)

Effect	DFn	DFd	F	p	Generalised effect size	
Location		3	49	0.083	0.969	0.005

Tukey's pairwise comparison of Metazoan MOTU Richness at the four deep stations (HG4, N4, S3, EG4)

term	group1	group2	null.value	estimate	conf.low	conf.high	p.adj	p.adj.signif
Location	EG4	HG4	0	0.95604	-8.78629	10.6984	0.994	ns
Location	EG4	N4	0	-0.53846	-10.4596	9.38264	0.999	ns
Location	EG4	S3	0	1	-8.92111	10.9211	0.993	ns
Location	HG4	N4	0	-1.49451	-11.2368	8.24783	0.977	ns
Location	HG4	S3	0	0.04396	-9.69838	9.78629	1	ns
Location	N4	S3	0	1.53846	-8.38264	11.4596	0.976	ns

ANOVA (type II) testing for the effect of Depth Zone on Metazoan Shannon Diversity at the four deep stations (HG4, N4, S3, EG4)

Location	DFn	DFd	F	p	Generalised effect size	
		3	49	3.417	0.024	0.173

Tukey's pairwise comparison of Metazoan MOTU Shannon Diversity in the different depth zones at the four deep stations (HG4, N4, S3, EG4)

term	group1	group2	null.value	estimate	conf.low	conf.high	p.adj	p.adj.signif
Depth_zo	Bathypelagic	Mesopelagic	0	-0.15778	-0.76827	0.45271	0.901	ns
Depth_zo	Bathypelagic	Lower-Epipelagic	0	-0.62701	-1.42127	0.16725	0.168	ns
Depth_zo	Bathypelagic	Upper-Epipelagic	0	-0.68433	-1.33878	-0.02988	0.0372	*
Depth_zo	Mesopelagic	Lower-Epipelagic	0	-0.46923	-1.25635	0.31789	0.396	ns
Depth_zo	Mesopelagic	Upper-Epipelagic	0	-0.52655	-1.17231	0.11922	0.146	ns
Depth_zo	Lower-Epipelagic	Upper-Epipelagic	0	-0.05732	-0.879	0.76436	0.998	ns

ANOVA (type II) testing for the effect of Depth Zone on Metazoan Species Richness at the four deep stations (HG4, N4, S3, EG4)

Location	DFn	DFd	F	p	Generalised effect size	
		3	49	0.083	0.969	0.005

Tukey's pairwise comparison of Metazoan MOTU Richness in the different depth zones at the four deep stations (HG4, N4, S3, EG4)

term	group1	group2	null.value	estimate	conf.low	conf.high	p.adj	p.adj.signif
Depth_zo	Bathypelagic	Mesopelagic	0	-4.86765	-10.3282	0.59287	9.64E-02	ns
Depth_zo	Bathypelagic	Lower-Epipelagic	0	-12.8929	-19.9971	-5.78864	8.07E-05	****
Depth_zo	Bathypelagic	Upper-Epipelagic	0	-18.3654	-24.2191	-12.5117	3.38E-10	****
Depth_zo	Mesopelagic	Lower-Epipelagic	0	-8.02521	-15.0655	-0.98488	1.96E-02	*
Depth_zo	Mesopelagic	Upper-Epipelagic	0	-13.4977	-19.2737	-7.72176	6.45E-07	****
Depth_zo	Lower-Epipelagic	Upper-Epipelagic	0	-5.47253	-12.822	1.87693	2.09E-01	ns

Gelatinous Zooplankton

ANOVA (type II) testing for the effect of Location on GZP Shannon Diversity at the four deep stations (HG4, N4, S3, EG4)

Location	DFn	DFd	F	p	Generalised effect size	
		3	33	1.745	0.177	0.137

Tukey's pairwise comparison of GZP Shannon Diversity at the four deep stations (HG4, N4, S3, EG4)

term	group1	group2	null.value	estimate	conf.low	conf.high	p.adj	p.adj.signif
Location	EG4	HG4	0	0.29857	-0.23645	0.83358	0.443	ns
Location	EG4	N4	0	0.30172	-0.24795	0.8514	0.458	ns
Location	EG4	S3	0	0.45971	-0.10776	1.02718	0.147	ns
Location	HG4	N4	0	0.00315	-0.54652	0.55283	1	ns
Location	HG4	S3	0	0.16115	-0.40632	0.72862	0.868	ns
Location	N4	S3	0	0.15799	-0.42332	0.73931	0.882	ns

ANOVA (type II) testing for the effect of Location on GZP MOTU Richness at the four deep stations (HG4, N4, S3, EG4)

Location	DFn	DFd	F	p	Generalised effect size	
		3	33	1.745	0.177	0.137

Tukey's pairwise comparison of GZP OTU Richness at the four deep stations (HG4, N4, S3, EG4)

term	group1	group2	null.value	estimate	conf.low	conf.high	p.adj	p.adj.signif
Location	EG4	HG4	0	0.9	-1.72487	3.52487	0.79	ns
Location	EG4	N4	0	1.3	-1.3968	3.9968	0.567	ns
Location	EG4	S3	0	2.425	-0.35909	5.20909	0.106	ns
Location	HG4	N4	0	0.4	-2.2968	3.0968	0.978	ns
Location	HG4	S3	0	1.525	-1.25909	4.30909	0.46	ns
Location	N4	S3	0	1.125	-1.72701	3.97701	0.712	ns

ANOVA (type II) testing for the effect of Depth Zone on GZP Shannon Diversity at the four deep stations (HG4, N4, S3, EG4)

Location	DFn	DFd	F	p	Generalised effect size	
		2	34	1.745	0.177	0.137

 Tukey's pairwise comparison of GZP Shannon Diversity in the depth zones at the four deep stations (HG4, N4, S3, EG4)

term	group1	group2	null.value	estimate	conf.low	conf.high	p.adj	p.adj.signif
Depth_zo	Bathypelagic	Lower-Epipelagic	0	-0.28454	-0.84718	0.2781	0.439	ns
Depth_zo	Bathypelagic	Mesopelagic	0	-0.26188	-0.65013	0.12638	0.238	ns
Depth_zo	Lower-Epipelagic	Mesopelagic	0	0.02266	-0.53998	0.5853	0.995	ns

ANOVA (type II) testing for the effect of Depth Zone on GZP MOTU Richness at the four deep stations (HG4, N4, S3, EG4)

	DFn	DFd	F	p	Generalised effect size
Location		2	34	2.277	0.118
					0.118

Chapter 3

Eukaryotic biodiversity of sub-ice water in the Marginal Ice Zone of the European Arctic: A multi-marker eDNA metabarcoding survey

Ayla Murray^{1,2}, Simon Ramondenc^{1,3}, Simon F. Reifenberg¹, Meret Jucker^{1,4}, Mara Neudert¹, Rebecca McPherson¹, Wilken-Jon von Appen¹, Charlotte Havermans^{1,2}

1. Alfred Wegener Institute Helmholtz Centre for Polar and Marine Research, Am Handelshafen 12, 27570 Bremerhaven, Germany

2. Marine Zoologie, Fachbereich 2, University of Bremen, Bremen, Germany

3. Sorbonne Université, CNRS, Laboratoire d'Océanographie de Villefranche (LOV), Villefranche-sur-Mer, France

4. Institute of Terrestrial Ecosystems, ETH Zurich, Universitätstrasse 16, 8092 Zurich, Switzerland

Manuscript under review in Science of the Total Environment (submitted August 2024)

Abstract

Across the Arctic Ocean, warming waters, loss of sea ice habitat, and the consequential changes in primary production are inducing shifts in the community composition and distributions of marine species. The marginal ice zone (MIZ) is a highly dynamic ecosystem and transition zone between pack ice and the open ocean. It is habitat to a wide range of organisms including sympagic and pelagic taxa (e.g., algae, phytoplankton, meiofauna and zooplankton), all of which are affected by the changing physical dynamics of the understudied MIZ. Here we use a multi-marker (18S rRNA V1-2 and COI Leray-XT fragments) approach to sequence environmental DNA extracted from seawater samples collected immediately under the sea ice and at 5 m at different locations in the MIZ. To investigate the abiotic drivers of under-ice communities uncovered by eDNA metabarcoding, environmental data were collected from satellite databases, as well as simultaneous *in situ* hydrographic measurements. We detected a range of sympagic and pelagic metazoans and primary producers typical to the region. Richness, evenness and levels of hidden diversity were higher immediately below the ice compared to 5 m depth and we found the different ice floes and depths to harbour different communities. We show that the properties of the meltwater stratification in the upper ocean, as well as sea ice concentration and distance to the ice edge, have significant impacts on eukaryotic diversity and community composition. Our findings demonstrate the effectiveness of eDNA metabarcoding for monitoring sub-ice communities and contribute to our current knowledge on MIZ eukaryotic biodiversity.

Key words

Environmental DNA, community composition, COI, 18S, sea ice, meltwater dynamics

1. Introduction

Marine environments are experiencing anthropogenic climate change at unprecedented rates. In the Arctic, warming is occurring up to four times faster than the rest of the world, and up to seven times faster in parts of the European Arctic (Rantanen et al., 2022). Sea surface and air temperatures are increasing, while sea ice thickness and extent are decreasing with ice-free periods predicted to occur in the Arctic as early as 2035 (Reviewed in: Jahn et al., 2024). This loss of sea ice habitat, as well as the consequential changes in primary production, is inducing shifts in the community composition and distributions of marine species across the Arctic Ocean (Meredith et al., 2022). These alterations in the distribution and availability of suitable habitat for marine species often result in detrimental consequences on biodiversity and ecosystem functions (Hodapp et al., 2023; Meredith et al., 2022). Temperate taxa, including zooplankton and commercially important fish species, are expanding their ranges northward, while true Arctic and ice-associated taxa are exhibiting range contractions (Mueter et al., 2021). Overall increases in species richness have been observed in multiple parts of the food web (Alabia et al., 2023). As Arctic marine ecosystems continue to change, the need to monitor shifts in biodiversity is increasing (Bernatchez et al., 2024; Lannuzel et al., 2020).

The marginal ice zone (MIZ) is a highly dynamic ecosystem that can span from tens to hundreds of kilometres in width (Strong, 2012). It is a transition zone between pack ice and the open ocean, and is categorised here by ice concentrations between 15 - 80% (Dumont, 2022; Strong and Rigor, 2013). Rapid warming is inducing major changes to the MIZ with multi-year ice being replaced with thinner, first-year ice. Its interior edge has shown a significant poleward expansion (Aksenov et al., 2017; Strong and Rigor, 2013) and more open water expanses are occurring at its southern edge (Rolph et al., 2020). Due to the low salinity of sea ice compared to the underlying ocean, the resultant meltwater is highly buoyant and accumulates at the ice-ocean interface, or at the surface in open water fractions around ice floes (leads), leading to strong near-surface stratification. The meltwater can form thin layers (lenses) at the ice-ocean boundary (centimetres to meters in depth) or, by mixing with the ambient water, can form the seasonal halocline (up to tens of meters in depth). As a result the upper ocean can be dynamically decoupled from the interior ocean during the melt season, while also restricting the atmosphere-ocean exchange of heat, momentum and nutrients, and thus playing a crucial role in many physical and biological processes (Smith et al., 2023).

The MIZ is habitat to a wide range of organisms including ice-associated (sympagic), sub-ice and pelagic taxa (e.g., algae, phytoplankton, meroplankton and zooplankton). In spring, when day length and light intensity increases, the ice begins to melt and sympagic algae grow in the bottom of the ice, marking the beginning of the spring bloom (Leu et al., 2015). Ice algae are

a crucial high quality food source for sympagic taxa such as copepods, amphipods, appendicularians, and meiofauna (Falk-Petersen et al., 2009; Leu et al., 2011; Søreide et al., 2010). During the melting season, ice algae may detach from the sea ice and are consumed by pelagic grazers or sink to the seafloor, acting as a food source to detritus feeders (Boetius et al., 2013). The pelagic bloom starts as the ice begins to break up to form the MIZ and enough light penetrates the water column (Galí et al., 2021). Increased near-surface stratification and light availability drive rapid growth and lead to highly concentrated patches of phytoplankton in the surface layers (Joy-Warren et al., 2023). These are an important source of energy and nutrients for zooplankton grazers, which have their life cycles finely tuned to the timing and duration of these blooms (Falk-Petersen et al., 2009; Søreide et al., 2010). The phenology and community composition of primary production blooms are shifting as ice conditions change in the MIZ. Sea ice algae and phytoplankton are predicted to be increasingly replaced by species adapted to higher light conditions (Lannuzel et al., 2020). Overall primary production is increasing with sea ice loss and more light availability, which is driving cascading changes throughout Arctic marine food webs (Castro de la Guardia et al., 2019; Lannuzel et al., 2020). Furthermore, the decline in the age and thickness of multi-year sea ice which typically hosts higher levels of biodiversity and distinct community assemblages compared to first-year ice (Barber et al., 2015; Bluhm et al., 2017), could result in the loss of these communities.

Due to the challenging environment and instrument limitations, few studies across the Arctic have investigated biodiversity of the water column directly beneath the sea ice. Most of these studies relied on morphological surveys (e.g., David et al., 2015; Ehrlich et al., 2020; Hop et al., 2011), which may have missed key components of under-ice communities due to gear-related collection biases or low-resolution morphological identifications. For example, plankton nets and trawls can destroy delicate individuals like gelatinous zooplankton (GZP), leading to underestimates in both abundance and diversity (Hosia et al., 2017). Within the MIZ, investigations have surveyed eukaryotic diversity, but with a focus on in-ice taxa (Kiko et al., 2017) or across large depth scales (Ribeiro et al., 2024; Vipindas et al., 2023; Xu et al., 2020). In the present study, we focused on the water directly under the sea ice (0 - 5 m) in the MIZ, where melting and high levels of biological activity occur, including primary production, grazing by zooplankton such as copepods and predation by macrozooplankton and other large predators. Environmental DNA (eDNA) enables the identification of organisms based on the DNA they release into the environment through gametes, faeces and other excretion products, as well as shed cells. It is a cost-efficient and non-invasive technique for monitoring biodiversity in marine ecosystems (Adams et al., 2023; Bernatchez et al., 2024), including the Arctic (Geraldini et al., 2024; Lacoursière-Roussel et al., 2018; Merten et al., 2023; Murray et

al., 2024; Weydmann-Zwolicka et al., 2024). It can be used to detect individual species as well as community composition and it can be combined with abiotic data to investigate the environmental drivers of biodiversity. For example, previous investigations have shown the ability of eDNA to uncover regional and depth-related patterns of zooplankton diversity and distribution (Murray et al., 2024; Suter et al., 2021).

In this study, we use multi-marker metabarcoding of under-ice seawater samples to investigate the eukaryotic biodiversity and community composition during the summer in the MIZ of the northern Fram Strait. Using high-throughput sequencing (HTS) of COI and 18S genes fragments, we aimed to (A) investigate under-ice marine eukaryotic diversity and (B) identify the drivers of diversity and community composition, as well as signature communities associated with varying environmental conditions in the MIZ.

2. Methods

2.1 Sampling Area

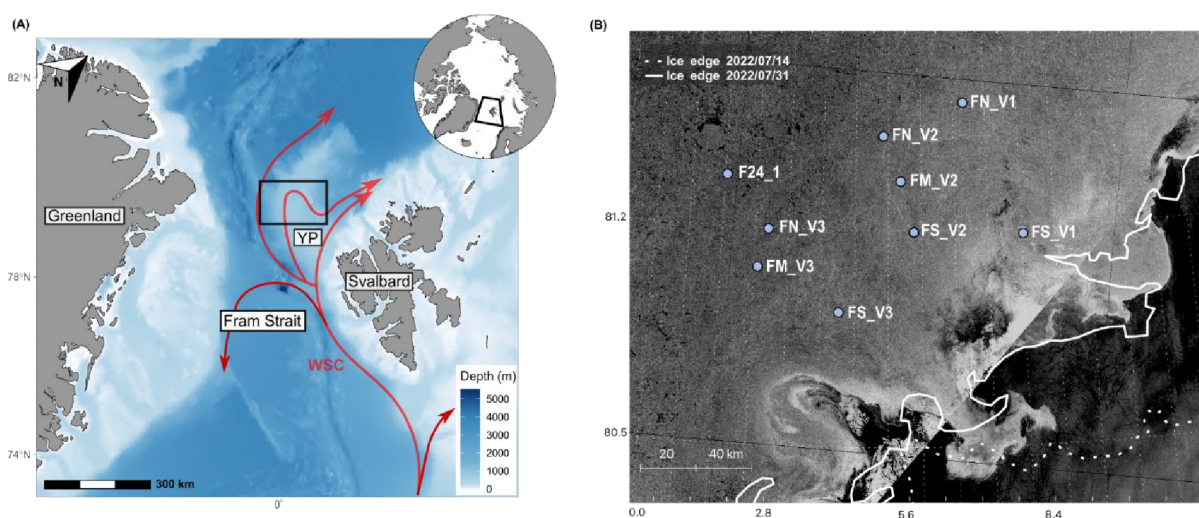


Figure 1. Location of the sampling area and the ice floe stations in the MIZ. (A) Map of the Fram Strait area, with approximate sampling area indicated by black polygons. Red arrows represent the approximate flow of warm Atlantic Water on branches of the West Spitzbergen Current (WSC). The WSC is one of the currents that transports the Atlantic Water before half of it recirculates towards Greenland and the rest continues northwards into the Central Arctic. YP = Yermak Plateau. (B) Sentinel-1 Synthetic Aperture Radar (SAR) image of the ice floe stations in the marginal ice zone. The dotted white line is a visual estimate of the ice edge at the beginning of the sampling period and the hard-white line the end of the sampling period. Maps produced using the R package ggOceanMaps. SAR scenes are available from ESA, Copernicus Open Access Hub, <https://scihub.copernicus.eu/dhus/#/home>, last access: 30 August 2022.

Fram Strait is the only deepwater inlet into the Arctic Basin and is a transition zone between the Arctic Ocean and the North Atlantic Ocean. The area is affected by the phenomenon known as the ‘Atlantification’ of the Arctic, which is largely driven by the increased transport of warm and saline Atlantic waters into the Arctic Ocean via the West Spitzbergen Current (WSC). This, along with the Atlantic water inflow through the Barents Sea opening, constitute the main sources of oceanic heat and salt to the Arctic Ocean (Tsubouchi et al., 2023).

Furthermore, less sea ice is being transported to Fram Strait via the transpolar drift due to accelerated melting rates (Krumpfen et al., 2019). The Yermak Plateau, where the sampling that forms the basis of this study took place, is a hydrographically dynamic region in Fram Strait where strong tides over the shallow bathymetry drive intense mixing of the Atlantic Water (Fer et al., 2010).

Sampling was undertaken during the PS131 expedition (Kanzow, 2023) on the *R/V Polarstern* in July 2022. Seawater samples were collected from the upper water column directly underneath selected ice floes in the MIZ, situated in northern Fram Strait. Three individual ice floes were visited repeatedly while they drifted across the Yermak Plateau. A fourth, floe F24_1, was situated over the eastern slope of the Yermak Plateau and visited only once. The ice floes were selected to be representative of different ice regimes typical of the MIZ, and the sample sites cover a range of different sea ice concentrations, and differ with respect to ice thickness, floe size, and distances to the ice edge. It must be noted that logistic and safety considerations such as ice stability played a role in the selection of these stations. Hence, the most outer floe being approximately 30 km from the open ocean and therefore not representative of the true outer edge of MIZ. We use the ice floe identifiers FN, FM, FS to reference the north, middle and south stations respectively, and F24_1 to identify the floe on which a 24-hour sampling regime was conducted. The respective visit numbers are thus denoted as V1 to V3, i.e., FN_V2 is the second visit to the north floe FN (**Figure 1**). We treated the ice floe visits as nine separate ice floe stations, as it is the water underneath the ice that was sampled, which is continuously exchanged by the ice-relative ocean current.

2.2 Sample Collection

2.2.1 Environmental data

To investigate the abiotic drivers of community composition, we analysed various environmental variables collected from instruments deployed on and under the ice, as well as satellite data (full details in **Table S7**). Salinity and temperature data were collected from directly under the ice to a depth of 10 m, using a RBR*concerto*³ conductivity, temperature, and depth (CTD) sensor. The CTD was deployed in the same ice hole from which the eDNA was sampled or within 10s of meters. For two sampling holes, we did not obtain CTD data (hole 1 on F24_1 and FM_V3), thus, we excluded these from analyses based on CTD data.

To describe the vertical density structure of the meltwater layer, data was taken from under-ice microstructure (MSS) measurements at each floe using a MSS90L profiler (Sea & Sun technology). Based on these profiles, we aimed to quantify the meltwater distribution in the upper ocean by calculating the buoyancy deficit (BD) and the equivalent depth of this meltwater layer (hBD) following Randelhoff et al. (2017). BD is a proxy for the amount of

meltwater accumulated in the upper ocean, while hBD describes how the meltwater is distributed vertically within the upper 50 m of the water column. For example, a larger (smaller) BD indicates that there is more (less) meltwater present. A high hBD indicates that this meltwater is more evenly distributed (mixed) while a low hBD indicates that it is accumulated in the upper layers (stratification). For a fixed BD, lower hBD values indicate that meltwater is accumulating closer to the surface. We calculated BD by vertically integrating the density deviation from a reference density, for which we chose the value at 50 m depth (**Figure S1**). We obtained hBD by dividing BD by the difference between the shallowest density observation from the MSS (taken at 3 m depth) and the reference density.

Sea ice concentration (SIC) and distance from the ice edge were calculated from Advanced Microwave Scanning Radiometer-2 (AMSR-2) sensor data. The SIC for each sample location was obtained by nearest-neighbour interpolation of the sample position to the gridded AMSR-2 data (10 km resolution). The distance to the ice edge (DIST_SIC) was determined as the shortest distance of the sample position to the ice edge, with the ice edge defined as the 15% SIC contour line.

2.2 Seawater for eDNA metabarcoding

Seawater samples were collected at two sampling depths through 1 - 3 drilled holes on each ice floe. The sampling point immediately underneath the ice was taken from 0 – 60 cm below the ice, and the second at 5 – 5.6 m below the ice. These sampling depths are henceforth referred to as “0 m” and “5 m” respectively. A total of 6L of water was collected per sampling point using a 4 L Niskin (Hydrobios, Kiel) bottle. The water was dispensed into pre-sterilized Kautex cannisters and kept on ice until filtration. Each sample was split across three filter triplicates of approximately 2 L of seawater. The water was filtered with a peristaltic pump across 0.22 μm Sterivex-GP filters (Merck Millipore). A field blank was taken at each ice floe station by filtering MilliQ water instead of seawater. All tubes and Kautex cannisters used in sample collection were sterilized using a 1:10 Bleach/MilliQ water solution and then flushed with MilliQ water in between sampling events. New tubing for filtration was used for every sample depth at each ice floe. After filtration, filters were sealed and stored at -80°C for processing.

2.2 DNA extraction, library preparation and sequencing

Environmental DNA was extracted using the DNeasy Blood and Tissue kit (QIAGEN, Germany) and contamination prevention measures were observed following Murray et al. (2024). An extraction control was included with each extraction. The DNA extracts were stored at -20°C until further processing. DNA metabarcoding library preparation and sequencing were carried out by AllGenetics & Biology SL. In the present study we took a multi-marker

approach to minimise the impacts of marker-specific limitations on biodiversity estimates (Clarke et al., 2017; Wangensteen et al., 2018b). The following two markers were amplified: (a) the 313bp COI region with the forward primer mICOLintF-XT (5'GGWACWRGWTGRACWITITAYCCYCC 3'; Wangensteen, Palacín, et al., 2018) and the reverse jgHCO2198 (5'TAIACYTCIGGRTGICCRAARAAYCA 3'; Geller et al., 2013); and (b) the ~400bp 18S V1-2 region with the forward primer SSU_F04 (5' GCTTGTCTCAAAGATTAAGCC 3'; Blaxter et al., 1998) and the reverse SSURmod (5' CCTGCTGCCTTCCTTRGA 3'; Sinniger et al., 2016). These primers have been successfully employed to detect a wide range of marine eukaryotes in eDNA studies (e.g., COI: Antich et al., 2022; Ershova et al., 2019; Murray et al., 2024 and 18S: Feng et al., 2022; He et al., 2021; Hestetun et al., 2021) and have comprehensive and curated reference databases publicly available. PCR master mix and conditions for COI were as described in Murray et al. (2024) and for 18S rDNA as in Dischereit et al. (2024). The final pool was sequenced on a PE250 flowcell of a NovaSeq platform (Illumina). Demultiplexing and removal of Illumina adaptors was completed by the sequencing company.

2.4 Bioinformatic analyses

Given the differing natures of the two genes (COI is mitochondrial and 18S is nuclear), we used separate pipelines and optimised metabarcoding units to process the sequencing reads accordingly. While denoising and amplicon sequence variants (ASVs) output have been employed for COI-based studies, there is the risk of overlooking intraspecific variation if clustering into molecular operational taxonomic units (MOTUs) is not used (Antich González et al., 2021). In contrast, applying clustering to 18S ASVs can underestimate biodiversity in a dataset (Giebner et al., 2020). Hence, we used denoising and then clustering with MOTUs as a unit for the COI data (Antich González et al., 2021) and denoising with ASVs for the 18S data.

The COI sequence reads were processed using a bioinformatics pipeline based 'OBITools 3' (Boyer et al., 2016) following Antich et al. (2022). Taxonomic assignment to the lowest common ancestor was done by *ecotag*, which is a phylogenetic tree-based method. We used a curated reference database with a focus on marine metazoans, containing 148,932 sequences from BOLD, NCBI and inhouse (available at: <https://github.com/adriantich/NJORDR-MJOLNIR3>). Taxonomic assignment was improved where possible using BOLDigger (Buchner and Leese, 2020) to query on BOLD (Ratnasingham and Hebert, 2007). This allows for the utilization of the latest COI barcodes that may not be included in the database used in the bioinformatics pipeline. When improved matches and extra taxonomic information were available, they were adjusted in the dataset. The following identity match thresholds were applied: > 97% for species, 95% for genus, 90%

for family, 85% for order and 75% for class (following Ershova et al., 2023). Identity matches <70% were marked as unassigned. The remaining MOTUs were named according to the highest taxonomic level possible, and with a unique number in cases where more than one MOTU had the same assignment.

The 18S raw sequence reads were processed using DADA2 v1.18 (Callahan et al., 2016) in Rstudio v 4.0.4. Forward reads were trimmed at 220 bp and reverse reads at 210 bp and filtered with a maximum expected error threshold of 2.2 and 2.1, for forward and reverse reads respectively. Sequences were denoised and paired ends were merged using a minimum overlap of 25bp and zero mismatches when aligning. Singletons were discarded and chimeras filtered out. We chose to use a zooplankton-focused database for taxonomic assignment in order to avoid known classification issues of other popular databases such as SILVA, where zooplankton are underrepresented (Questel et al., 2021). Taxonomic assignment of the resulting ASVs was done using the MetaZooGene database (Bucklin et al., 2021). The version “MZGdb 3.0” containing 68,484 18S rRNA sequences containing genus and species data from any ocean was used (Mode C). A minimum identification bootstrap value of 75% was set for taxonomic assignment, and lower values were set as unassigned. Assignments to higher taxonomic levels (genus and species) were not considered for metazoans in the 18S due to its conservative nature, which increases the chance of incorrect assignments at such high resolution (Giebner et al., 2020; Tang et al., 2012; Wangensteen et al., 2018a). This is especially true for copepods (Wu et al., 2015), which were the most dominant taxa in the dataset. However, taxonomic matches to genus level were acknowledged in the Chromista and Plantae kingdoms.

After taxonomic assignment was completed, we removed reads assigned to (i) bacteria, non-eukaryotes, fungi (18S only) and obvious contaminants (e.g., insects and terrestrial taxa). Blank corrections and further data curation steps were done for both datasets, following Murray et al., 2024.

2.5 Statistical analysis

All statistical analyses were conducted using R version 4.3.0 (R Core Team, 2023), and the majority of the visualizations were generated using the *ggplot2* (Wickham, 2016) and *phyloseq* packages (McMurdie and Holmes, 2013). Rarefaction curves, which assess the effectiveness of sequencing depth in capturing biodiversity within the samples, were performed on the raw MOTU and ASV data using the *vegan* package (Oksanen et al., 2019). To account for uneven sequencing depth in the alpha diversity analyses, samples were normalized to the lowest individual sample read count for both datasets (COI and 18S). This was done using the scaling with ranked subsampling method (SRS: Beule & Karlovsky, 2020) from the *SRS* package (Heidrich et al., 2021). Rarefied MOTUs/ASV richness (S) and Shannon-Wiener Index (H')

were calculated and we tested whether alpha diversity was significantly different between sampling depths and ice floes. This was done using Kruskal-Wallis rank tests and post-hoc Dunn pairwise comparisons using the *rstatx* package (Kassambara, 2023).

To explore the relationship between community composition and environmental variables, we conducted multivariate analyses. Ordination with non-metric multidimensional scaling (NMDS) was used to investigate broad patterns of community composition across different sampling depths and ice floes in the MIZ. Aitchison's distances, which consider the compositional nature of metabarcoding data (Quinn et al., 2018), were calculated by transforming raw read count data with centre log ratio (CLR, with pseudo count =1) and using Euclidean distance matrices. Then, we conducted Permutation Analysis of Variance (PERMANOVA) tests to assess significant differences in community compositions for the groupings.

The effects of environmental drivers on the community composition were further investigated through a sparse partial least squares (sPLS) regression analysis using the *mixOmics* package (Rohart et al., 2017). Prior to the analysis, MOTUs/ASVs were filtered for zero variance and the environmental variables were standardized to enhance normality and homoscedasticity. The sPLS analyses were performed in canonical mode with a cut off of 0.4 on the CLR-transformed MOTUs/ASVs datasets and 'average' clustering method.

3. Results

3.1 Variability of oceanographic and sea ice conditions

The origin of the sampled ice floes was determined by calculating back-trajectories based on daily ice velocity data (Krumpfen et al., 2020). All ice floes in the present study were second-year ice, originating from the Laptev Sea and transported towards Fram Strait via the Transpolar Drift (**Figure S2**).

The ice floe stations exhibited SIC ranging from 58% to 81%, with the highest concentration at floe F24_1 (81%) and the lowest at floe FS_V3 (58%) (**Table 1**). Station FN_V1 was located furthest from the ice edge (130 km), while FS_V2 was the closest to the ice edge (39 km). The water temperatures throughout the upper 5 m at all stations were generally below -1.4°C, with low salinities (< 33 psu) near the ice-ocean interface dominating the upper-ocean density structure (**Figure S3**). The profiles indicate that the upper water column was determined by sea ice melt at all stations and maintained by relatively low levels of mixing. The BD ranged between 11.6 – 29.1 kg/m² and the meltwater layer depth (hBD) was between 11.1 m and a maximum of 25.4 m at station F24_1, indicating that the melt water was mixed. The hBD values decreased towards the ice edge, indicating stronger stratification with a surface-intensified melt water layer (**Table 1**).

Table 1. Location, ice and meltwater conditions at each ice floe station. SIC = sea ice concentration, BD = buoyancy deficiency and hBD = depth of meltwater layer.

Ice Floe Station	Longitude (decimal)	Latitude (decimal)	SIC (%)	Distance to ice edge (km)	BD (kg/m ²)	hBD (m)
F24_1	1.286	81.325	81	100	24.4	25.4
FN_V1	6.813	81.596	68	130	14.6	21.5
FN_V2	4.779	81.501	75	81	17.2	17.5
FN_V3	2.36	81.179	68	87	17.7	16.5
FM_V2	5.127	81.351	71	67	14.5	11.2
FM_V3	2.123	81.069	63	80	21.0	15.0
FS_V1	7.728	81.183	72	84	11.6	15.3
FS_V2	5.425	81.189	70	39	14.1	12.1
FS_V3	3.784	80.927	58	51	29.1	14.5

3.2. Sequencing summary

We sequenced a total of 90 samples and 20 controls (field blanks, extraction controls and PCR controls). After bioinformatic processing and filtration steps, we obtained 5,776,833 reads assigned to 522 MOTUs with COI, and 18,191,862 reads assigned to 1,428 ASVs with 18S (**Table S1**). Rarefaction curves based on reads plateaued for all samples for both markers, indicating that the sequencing depth was sufficient to capture the full biodiversity of each sample (**Figure S4**). In COI, 95% of MOTUs were assigned to Kingdom level, 94% to Phylum, 73% to Class, 18% to Order, 13% to Family, 11% to genus and 5% to species. For 18S, 98% were assigned to Kingdom level, 95% to Phylum, 89% to Class, 75% to Order and 69% to Family.

3.3 Taxonomic composition

3.3.1 Overall composition

Common detections by both markers were highest at Kingdom level and decreased with taxonomic resolution (**Figure 2 and Table S3**). Fungi were recovered only by COI and only Protozoa by 18S, while Plantae, Chromista and Metazoa were in both datasets. Overlapping detections were the lowest at family level, where only 22 out of 122 taxa were recovered by both markers. All major marine metazoan phyla were detected by COI, but 18S failed to detect Annelida, Mollusca, Nemertea and Porifera. In contrast, 18S detected more Chromista phyla than COI, including Cercozoa, Ciliophora, Heliozoa and Radiozoa.

The overall read assemblage of the COI dataset was dominated by Chromista (52% of reads)

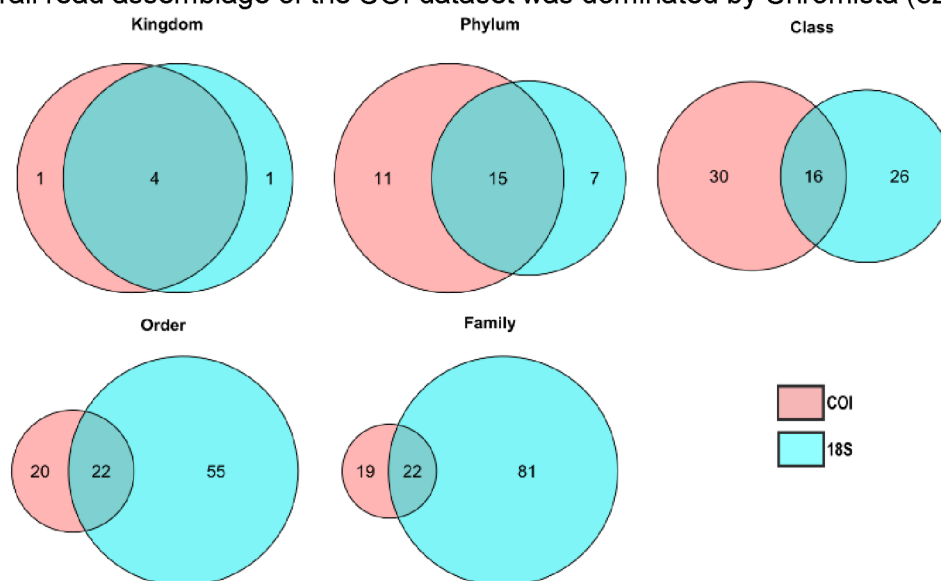


Figure 2. Taxa detected by the two markers at different taxonomic levels. Venn diagrams show the number of distinct taxa recovered by COI (pink) and 18s (blue) at different taxonomic ranks. Results are presented at Kingdom, Phylum, Class and Order levels by each marker. Genus and species not included here.

followed by Metazoa (41%), Plantae (7%), Fungi (0.04%) and reads unassigned at Kingdom level (0.05%) (**Figure S5A**). In the 18S dataset, Metazoa were the most dominant (79% of reads), followed by Chromista (18%), Plantae (3%), Protozoa (0.2%) and unassigned ASVs to Kingdom level (0.01%) (**Figure S5B**). We identified the top 15 MOTUs and ASVs by read abundance in each dataset to gain insights into the dominant taxa overall, as well as across different ice floe stations and depths (**Figure 3A and D**). The 15 most abundant MOTUs comprised 78% of the COI reads and the most abundant ASVs 91% of the 18S reads (**Table S4**). The complete taxonomic information of all MOTUs and ASVs in the eDNA datasets can be found in **Tables S5 and S6**.

3.3.2 Primary producers

Proportions of Chromista were higher under the ice than at 5 m in both datasets, except at the floe F24_1. Plantae abundances were the highest at 0 m in the COI dataset. The Plantae proportion of the 18S dataset was largely at F24_1, where it was also higher at 0 m than at 5 m. The most abundant Chromista phylum in the COI dataset was Heterokontophyta, making up 42.0% of the reads. The second was Ochrophyta (22.3%), then Haptophyta (17.7%), Myzozoa (11.8%) and the remaining phyla (<1% each). The highest MOTU richness was found in Ochrophyta (103 MOTUs), followed by Heterokontophyta (72), Oomycota (55), Myzozoa (48), and Haptophyta (25) (**Table S7**). The MOTU richness was <10 for each of the other three Chromista phyla. In the 18S dataset the phyla Myzozoa had the most reads (63.5%) and highest ASV richness (382), then Heterokontophyta (20.4 % and 81 ASVs), and Ochrophyta (25.6% and 150 ASVs). The remaining nine phyla had <5% relative read abundance each (**Table S4**). We detected Chromista genera typically found the region including the diatom genera *Thalassiosira*, *Chaetoceros*, *Pseudo-nitzschia*, *Nitzschia* and the haptophyte genera *Phaeocystis* and *Chrysochromulina*.

Three Plantae phyla were recovered with COI, with Chlorophyta being the most dominant (83% of Plantae reads), followed by Rhodophyta (11.7%) and Streptophyta (5.3 %). Rhodophyta had the highest MOTU richness with 27 MOTUs, followed by Chlorophyta (15). Chlorophyta was the only Plantae phylum in the 18S dataset and had 31 ASVs. In the COI dataset, we found the picoplankton genera *Bathycoccus* and *Micromonas* (order: Mamiellales) to be the most dominant Plantae MOTUs, which were present at every ice floe. The most abundant Plantae ASVs in the 18S dataset also belonged to the genus *Micromonas* and was also present at all ice floes.

In the top 15 MOTUs, a MOTU in the diatom family of Chaetocerotaceae (11.4% of reads from all kingdoms) was the most dominant non-metazoan, followed by a haptophyte MOTU in the Phaeocystales order (5.2%). In the 18S dataset, two dinoflagellate ASVs of the *Gyrodinium* genus were the most abundant Chromista (2.9% and 2.5%) and an ASV from the Plantae genus of *Micromonas* (2.5%) (**Figure 3**).

3.3.3 Metazoans

The proportion of metazoan reads in the overall dataset were larger at 5 m than right beneath the ice at all ice floe stations, for both markers, except at FS_V3 (outer) in the COI dataset (**Figure S5**). However, some individual taxa (e.g., Annelida, Anthozoa, and Rotifera) were more abundant at 0 m (**Figure S6**). Reads from the Arthropoda phylum made up 62.1% of the metazoan component of the COI dataset, followed by Annelida (12.2%), Cnidaria (12.1%), and Chordata (12.1%). Each of the remaining phyla accounted for less than 1.1 % of the total

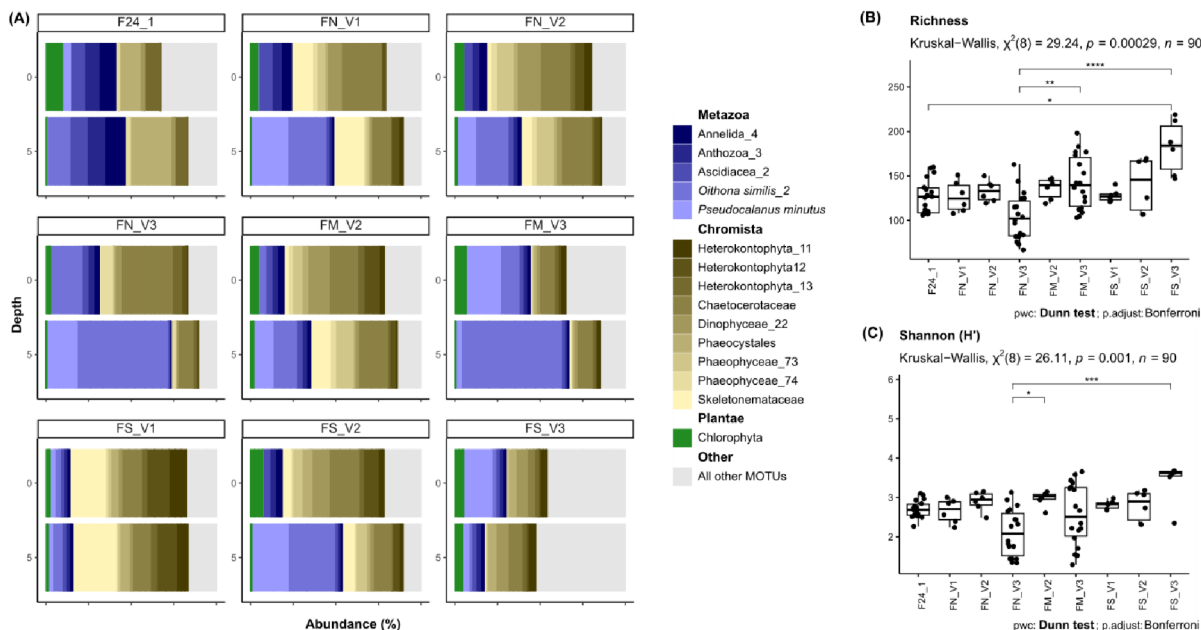
reads. The phyla with the highest MOTU richness were Arthropoda and Cnidaria (27 MOTUs each) and the remaining metazoan phyla had less than 10 MOTUs each. In the 18S dataset, Arthropoda (99.9%) was by far the most dominant metazoan phylum, comprising 99.9% of the reads and exhibiting the highest ASV richness with 474 ASVs. The remaining metazoan phyla made up <0.1 % of the reads and all had an ASV richness lower than 5 (**Table S7 and Figure S7**).

Metazoan MOTUs accounted for five of the top 15 most abundant MOTUs in the COI dataset (all kingdoms combined). These included the MOTU assigned to the cyclopoid copepod *Oithona similis* (18.7% of the total COI reads), followed by the calanoid copepod *Pseudocalanus minutus* (7.5%). The top 15 ASVs in the 18S dataset contained four metazoan ASVs and were strongly dominated by a single ASV from the Calanidae family (71.5% of all 18S reads), followed by another Calanidae ASV (3.0%) (**Table S4 and Figure 3**).

We detected MOTUs from the major gelatinous zooplankton (GZP) classes; Scyphozoa (6), Hydrozoa (17) and the phylum Ctenophora (4). The highest GZP richness was recovered by COI while only a single hydrozoan ASV (family: Rhopalonematidae) and three ctenophore ASVs (family: Bolinopsidae, Mertensiidae and Euplokamididae) were in the 18S dataset. The ctenophore family Bolinopsidae was detected by both markers. Finally, a single appendicularian ASV (family: Oikopleuridae) was recovered in the 18S dataset (**Tables S5 and S6**).

3.4 Alpha diversity

COI



18S

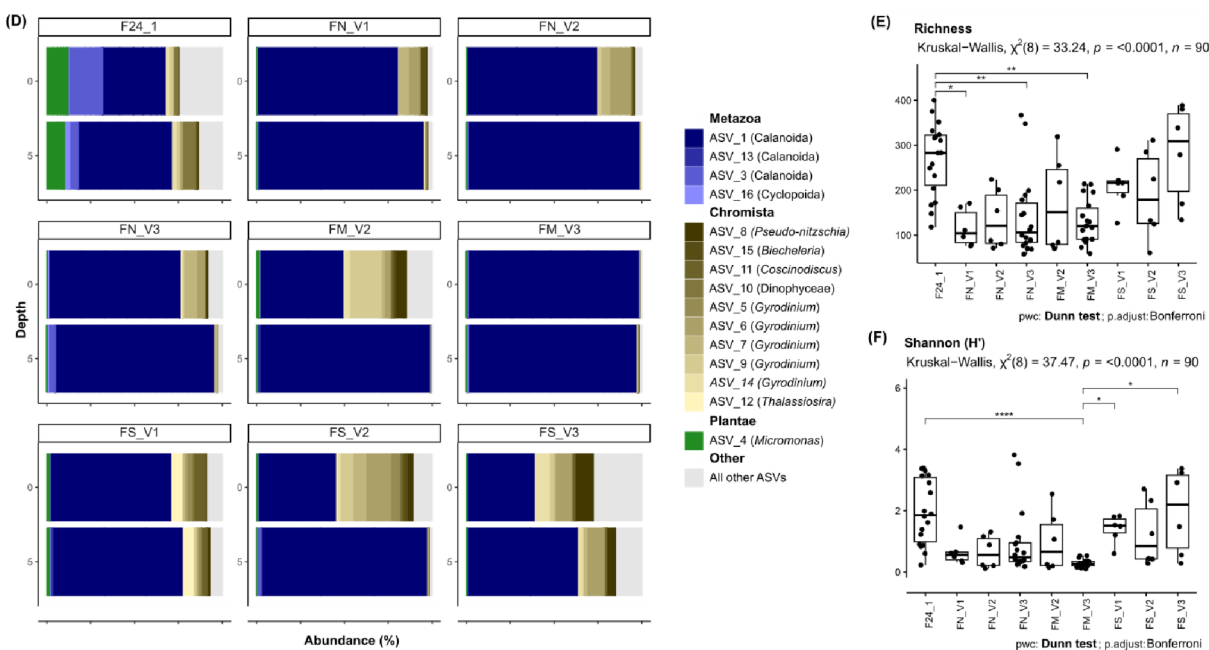


Figure 3. The 15 most dominant MOTUs/ASVs and alpha diversity indices at each ice floe station. (A) Relative read abundance of the 15 most abundant MOTUs in the COI dataset. MOTUs are labelled to the highest taxonomic resolution possible (up to species level). All remaining MOTUs are grouped together as “Other”. (B) MOTU richness and (C) Shannon (H') diversity as well as results of Kruskal-Wallis tests (non-parametric ANOVA) and significant subsequent pairwise comparisons (Dunn tests). (D) The 15 most abundant ASVs in the 18s dataset. Metazoan ASVs are labelled to the order level and Chromista and Plantae to genus level where possible. All remaining ASVs are grouped together as “Other”. (E) ASV richness and (C) Shannon (H') diversity as well as results of Kruskal-Wallis tests (non-parametric ANOVA) and significant subsequent pairwise comparisons (Dunn tests). Richness and Shannon indices are calculated based on SRS normalised data.

Alpha diversity analyses revealed that both species richness (COI: $\chi^2= 34.9$, $p= <0.01$ and 18S: $\chi^2=11.6$, $p= <0.01$) and the Shannon index (COI: $\chi^2= 29.36$, $p= <0.01$ and 18S: $\chi^2= 7.29$, $p= <0.01$) were significantly higher at 0 m than 5 m in both datasets (**Figure S7**). We found that the individual ice floe station had a significant effect on alpha diversity for both datasets (**Figure 3**). Pairwise comparisons showed that MOTU richness was significantly higher at FS_V3 than FN_V3 and F24_1 (**Figure 3B**). The FM_V3 station had significantly higher richness than FN_V3. Shannon index was also significantly higher in FS_V3 than FN_V3 (**Figure 3C**). In the 18S dataset, ASV richness was higher at the F24_1 station than at FN_1, FN_V2 and FM_V3 (**Figure 3E**). The F24_1 station also had significantly higher Shannon index than FM_V3. Two of the outer stations (FS_V2 and FS_V1) had higher Shannon index than the middle station FM_V3 (**Figure 3F**). A higher Shannon index indicates greater evenness, reflecting a wider spread of dominant taxa, whereas a lower Shannon index suggests that a smaller number of taxa dominated, resulting in reduced evenness. This can be clearly seen at FS_V3 in the COI dataset (high Shannon index), where there is a high proportion of 'Other' MOTUs (**Figure 3A**) and a correspondingly high Shannon index value (**Figure 3C**). In contrast, FM_V3 is dominated by a single ASV (**Figure 3D**) and has a significantly low Shannon index (**Figure 3F**).

3.5 Beta diversity

Non-metric Multidimensional Scaling with Aitchison's distances of community composition showed congruent results for both datasets, with significant clustering by both ice floe station and depth (**Figure 4**). Ice floe F24_1 showed the most obvious separation from all the other stations for the COI and 18S datasets (**Figure 4**). Differences in community composition by depth was most apparent in the COI dataset (**Figures 4A and B**). Subsequent PERMANOVA analysis supported these ordination results, indicating that both station and depth, as well as an interaction, were significant variables influencing community composition (**Table S8**).

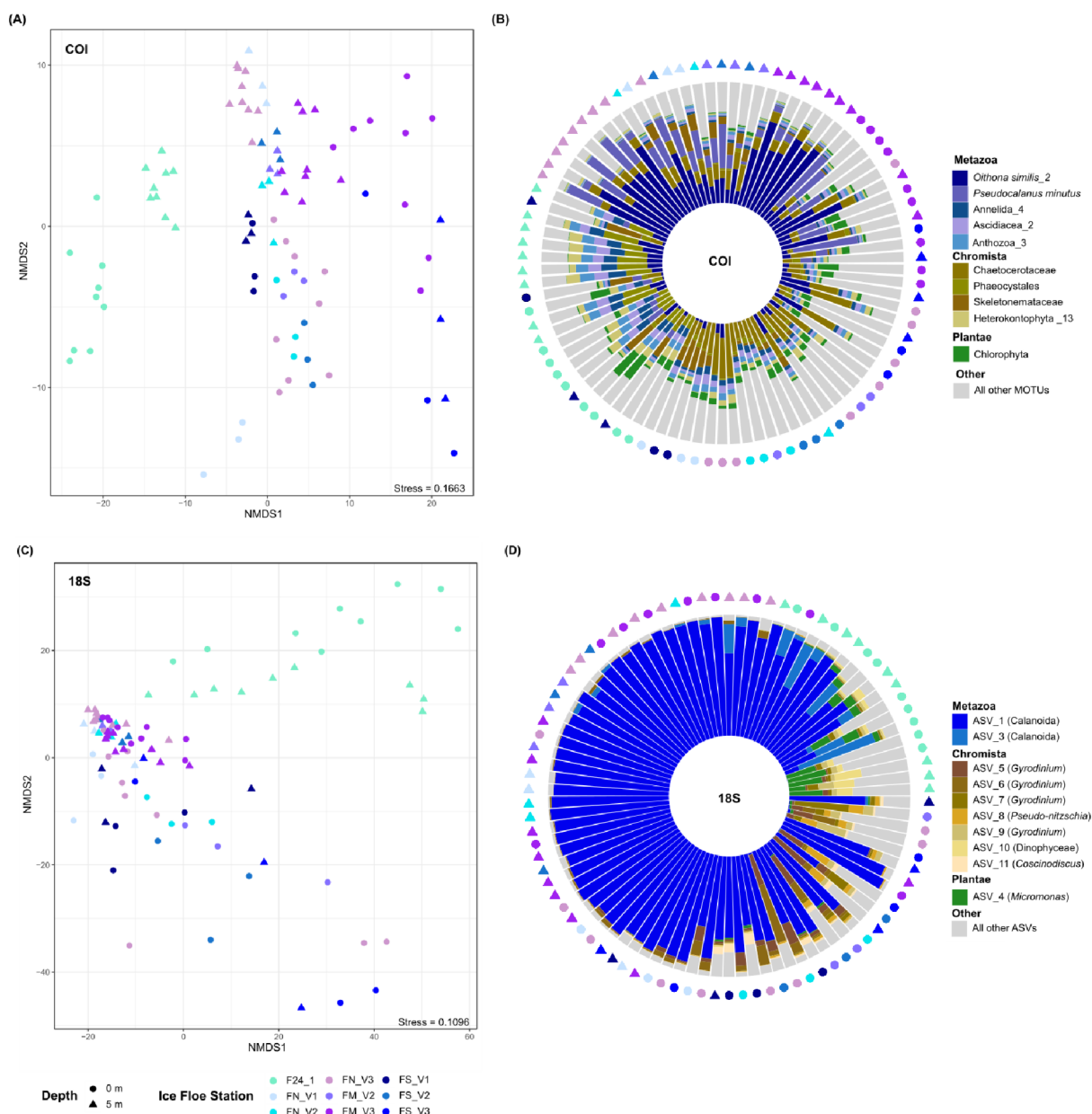


Figure 4. Non-metric Multi-dimensional scaling (NMDS) ordination plots and Iris plots of eukaryotic community composition. (A) COI NMDS plot and (B) iris plot of relative abundance of the 10 most abundant MOTUs. (C) 18S NMDS plot and (D) iris plot of relative abundance of the 10 most abundant ASVs. NMDS were performed on CLR transformed data and Euclidean distance matrices (Aitchison's distance). Shapes indicate depth, colours indicate ice floes. Order of bars on Iris plots are arranged according to the NMDS ordination axes.

3.6 Signature communities in the MIZ

In the sPLS analyses, 34% of the COI MOTUs, and 31% of the 18S ASVs were significantly linked to environmental variables (Figure 5). Among these MOTUs and ASVs, Chromista were predominant in both the COI (66.0%) and 18S (75.1%) datasets, while Metazoa comprised 13.3% and 12.9%, respectively. Two independent hierarchical clustering analyses (one for each marker) grouped these MOTUs and ASVs into four clusters, each representing distinct

communities associated with varying environmental conditions within the MIZ (**Figure 5**). Details taxonomic information on the significant MOTUs and ASVs from the sPLS analyses, including their correlations with environmental variables, clusters assignments, and abundances at each ice floe station, is provided in **Tables S9** and **S10**.

3.6.1 sPLS analysis of the COI dataset

COI

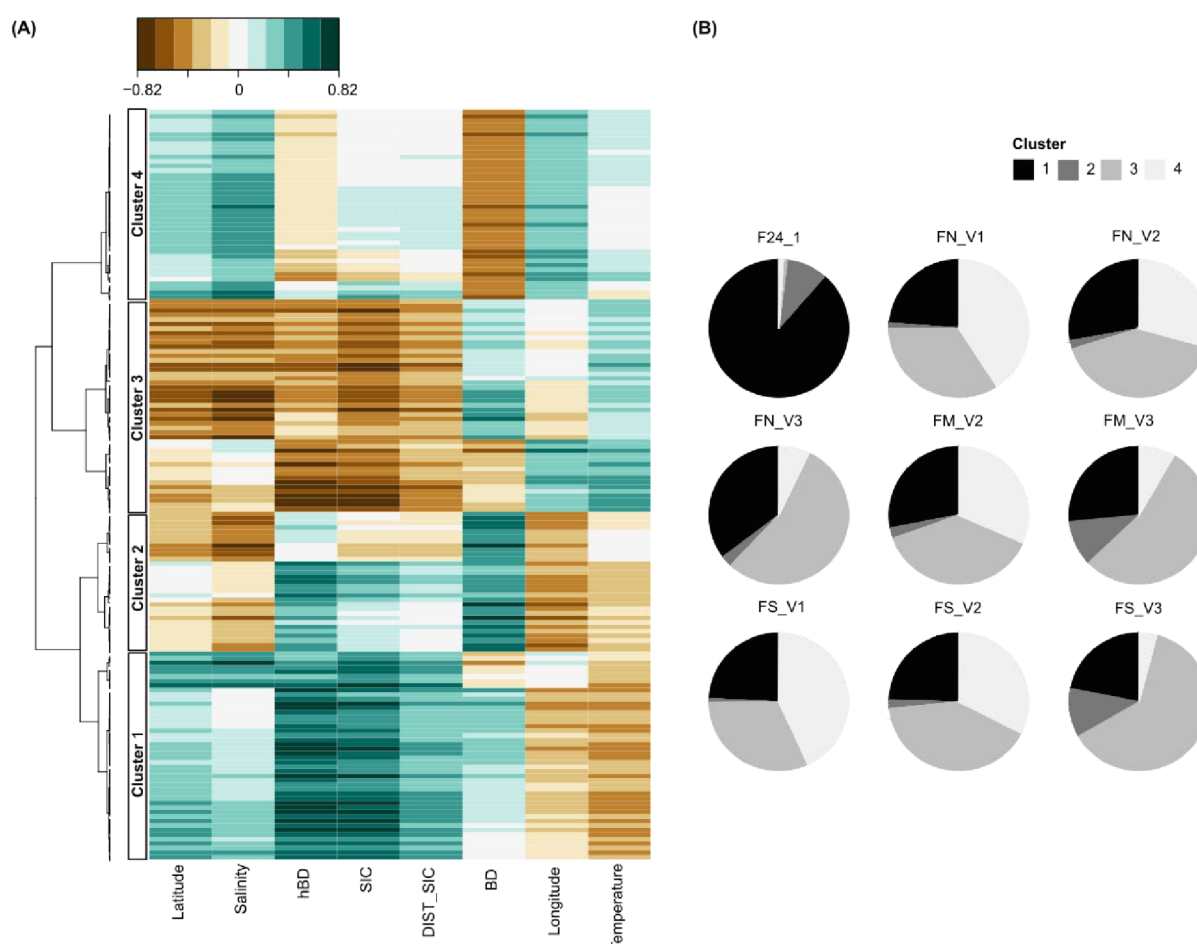


Figure 5. Sparse least square analyses (sPLS) indicating relationships between community composition and environmental variables in the COI dataset. (A) Clustered image maps (CIM) of the two components of sparse partial least squares (sPLS) regression analysis. Pairwise correlations between MOTUs (x-axis) and environmental variables (y-axis). Colour indicates correlation: browns show negative correlations and blues positive, with colour intensity representing strength of correlation. Hierarchical clusters are displayed on the top (clustering method: average linkage, distance method: Pearson's correlation). Cut-offs = -0.4 and 0.4. Environmental variables: Temperature ($^{\circ}\text{C}$), Buoyancy deficiency (BD), depth of buoyancy deficiency (hBD), Latitude (Lat), Longitude (Lon), Sea ice concentration (SIC; %) and distance to ice edge (Dist_SIC; km). (B) Pie plots showing the proportions of reads assigned to each of the sPLS clusters at each ice floe station.

In the CO1 dataset, cluster 1 was characterized by strong positive correlations (>0.4) with sea ice concentration and hBD, as well as with distance from the ice edge. This suggests high sea ice coverage and stations located farther from the ice edge with high hBD, characteristics typical of inner MIZ ice floes. There were also significant relationships with lower temperature and longitude (**Figure 5A**). This cluster consisted of 46 MOTUs and was the most dominant

at F24_1 (**Figure 5B**). Metazoan MOTUs in this cluster included those assigned to the Malacostraca, Anthozoa and Scyphozoa classes. Additionally, the algae species *Bathycoccus prasinos* and *Micromonas polaris* were present in the highest proportions at floe F24_1 and FS_V1 (**Table S9**).

Cluster 2 showed strong positive correlations with BD and hBD, indicating a high concentration of meltwater distributed over a deeper layer. Moreover, this cluster showed negative correlations with temperature, which is also indicative of meltwater, as well as longitude, suggesting the more western stations (**Figure 5A**). The proportion of cluster 2 reads was highest at the westernmost stations F24_1, FM_V3 and FS_V3 (**Figure 5B**). This cluster contained 31 MOTUs, more than half of which were algae, with three belonging to metazoans (phyla Arthropoda, Scyphozoa and Actinopterygii) (**Table S9**).

Cluster 3 showed negative correlations with SIC, hBD, distance to ice edge and salinity. The MOTUs in this cluster were positively correlated with temperature and most were positively correlated with BD (**Figure 5A** and **Table S9**). The low sea ice cover and distance to the ice edge are indicative of the outer MIZ, while the low hBD and high BD show shallow meltwater stratification. The MOTUs in this cluster that correlated with low hBD but high BD are more likely to be found at stations with a stratified meltwater layer. This cluster contained 47 MOTUs, which were present at outer and middle MIZ stations (FS) and at FM_V3 (**Figure 5B**). It was almost absent at F24_1, where the meltwater layer was deeper. The metazoans in this cluster included single MOTUs from classes Hydrozoa and Scyphozoa, as well as one each from Arthropoda and Porifera. Algal representatives included one MOTU assigned to *Pseudonitzschia*, seven MOTUs from the brown algae class Phaeophyceae, and five MOTUs from the Plantae class Mamiellophyceae (**Table S9**).

Cluster 4 showed the strongest negative correlations with BD and positive correlations with salinity, indicating low concentrations of meltwater. Positive correlations with longitude and latitude, although less pronounced, suggest a connection to the north-eastern stations. The highest proportion of cluster 4 reads were found at FN_V1 and FS_V1, located in the north-eastern part of our sampling area (**Figure 5B**). This cluster contained 42 MOTUs, including the sea ice diatom genera *Fragilariopsis* and *Nitzschia*, the dinoflagellate genus *Symbiodinium*, and the green algae genus *Chloroparvula* (**Table S9**).

3.6.2 sPLS analysis of the 18S dataset

18S

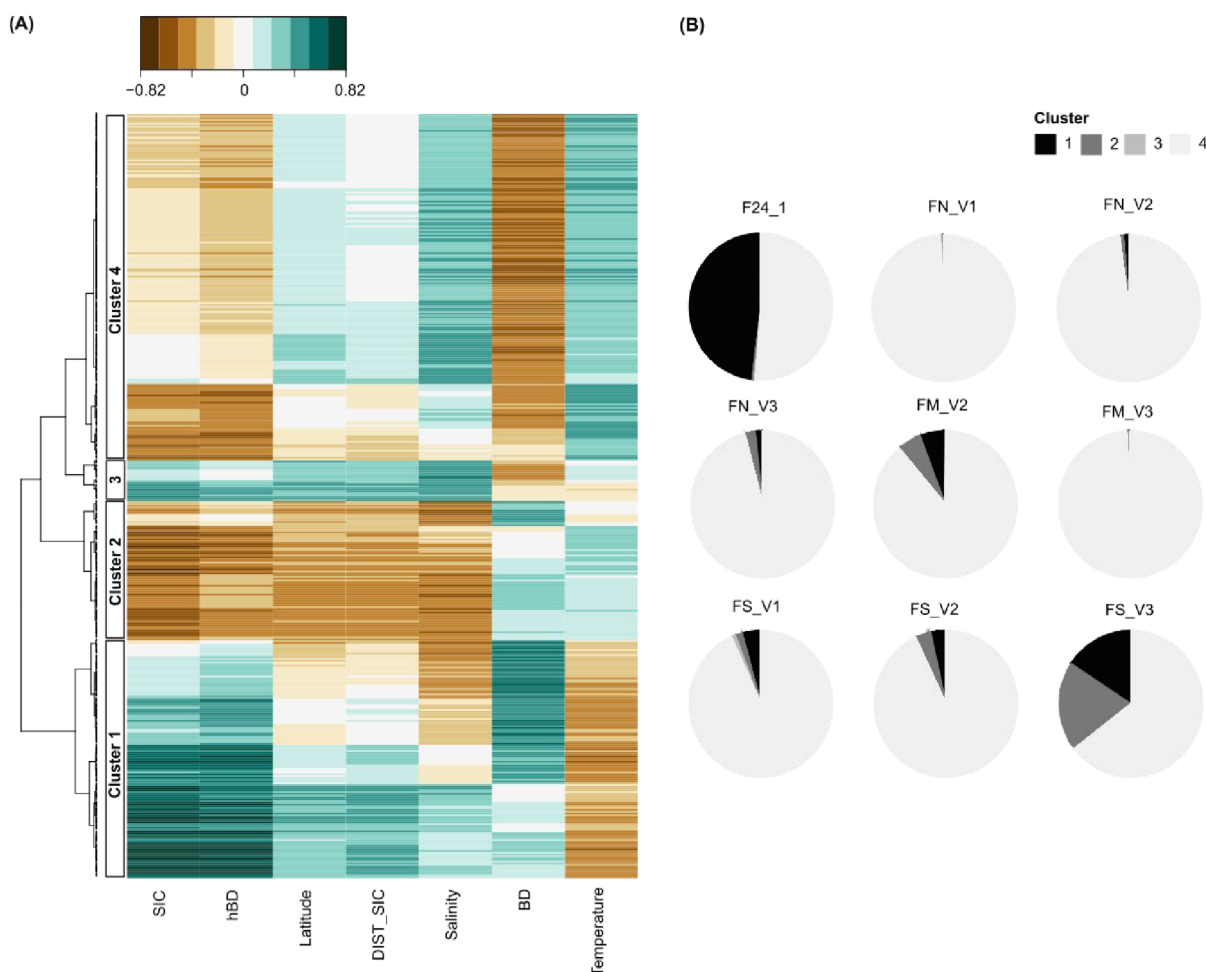


Figure 6. Sparse least square analyses (sPLS) indicating relationships between community composition and environmental variables in the 18S dataset. (A) Clustered image maps (CIM) of the two components of sparse partial least squares (sPLS) regression analysis. Pairwise correlations between ASVs (x-axis) and environmental variables (y-axis). Colour indicates correlation: browns show negative correlations and blues positive, with colour intensity representing strength of correlation. Hierarchical clusters are displayed on the top (clustering method: average linkage, distance method: Pearson's correlation). Cut-offs = -0.4 and 0.4. Environmental variables: Temperature ($^{\circ}\text{C}$), Buoyancy deficiency (BD), depth of buoyancy deficiency (hBD), Latitude (Lat), Longitude (Lon), Sea ice concentration (SIC; %) and distance to ice edge (Dist_SIC; km). (B) Pie plots showing the proportions of 18S reads assigned to each of the sPLS clusters at each ice floe station.

Cluster 1 in the 18S dataset showed the strongest positive correlations with SIC and hBD, followed by BD, and negative correlations with temperature (**Figure 6A**). These patterns are characteristics of the inner MIZ (high ice cover) and a higher concentration of colder meltwater distributed deeper in the upper water column. The cluster also showed weaker correlations (both positive and negative) with distance to the ice edge, latitude and salinity. Comprising 134 ASVs, this cluster was the most dominant at F24_1, where the highest hBD was measured (Table 1; **Figure 6B**). ASVs positively correlated with distance to the ice edge, latitude and salinity were most abundant at F24_1. In contrast, ASVs with negative correlations to salinity and strong positive correlations with other factors were more prevalent at FS_V3. Plantae

ASVs, including those assigned to the picoplankton genera *Bathycoccus* (1 ASV) and *Micromonas* (3 ASVs), were most abundant at F24_1 (**Table S10**).

Cluster 2 showed strong negative correlations with SIC, hBD, salinity, distance to the ice edge and latitude, along with weak positive correlations with BD and temperature. These patterns are characteristic of outer MIZ sites with a meltwater layer beneath thinner ice. This cluster included 78 ASVs, mostly Chromista, as well as four Protozoa, one Plantae and one Metazoa ASV. Reads from this cluster were most abundant at FS_V3, where low sea ice cover and a stratified meltwater layer were observed (Table 1). ASVs from the diatom genera *Gyrodinium* (14), *Pseudo-nitzschia* (3), and *Chaetoceros* (4) were identified in this cluster (**Table S10**).

Cluster 3 was the smallest cluster in the 18S dataset with 23 ASVs, all of which were Chromista, along with a single ASV each from Protozoa and Plantae (**Table S10**). This cluster showed positive correlations with salinity, SIC, distance to the ice edge, as well as weaker positive correlations with latitude and hBD. It also showed negative correlations with BD (**Figure 6A**). These characteristics are indicative of stations with high ice coverage in the inner MIZ and well mixed meltwater in the upper water column. The reads in this cluster were most prevalent at F24_1 and FS_V1 (**Figure 6B**).

Cluster 4 was the largest in terms of ASVs and was mainly characterised by negative correlations with BD and hBD, along with positive correlations with temperature and salinity (**Figure 6A**). These patterns suggest conditions with weak but shallow meltwater layers and less ice cover. This cluster included 195 ASVs and was highly dominant at all stations except F24_1 and FS_V3 (**Figure 6B**). Apart from a single ASV assigned to Metazoa in cluster 2, this cluster was the only cluster containing Metazoans (54 ASVs), including an ASV assigned to the GZP family Rhopalonematidae, mainly abundant at FM_V3 and FN_V3, and an ascidian from the family Perophoridae, which was mostly found at FS_V2. Moreover, 52 ASVs were assigned to the copepod family Calanidae (**Table S10**).

4. Discussion

4.1 Biodiversity detection in the sub-ice water column

We detected high levels of eukaryotic richness from relatively small volumes of water (6 – 18 L in total per ice floe station), with 522 MOTUs (COI) and 1428 ASVs (18S) assigned to 30 phyla and five eukaryotic kingdoms. Although the COI gene generally makes high resolution taxonomic assignment possible, only 11% of MOTUs were identified at the genus and 5% at the species level. In the 18S dataset, 69% of ASVs were identified to family level, with about one-third assigned to lower taxonomic resolutions or left completely unassigned. These high proportions of low-resolution taxonomic assignments highlight a significant gap in our

understanding of eukaryotic diversity in the upper water column of the MIZ, which is often overlooked by morphological studies. This is likely in part explained by a large number of eukaryotes in the MIZ that have yet to be identified with molecular methods, and the limitations of reference databases that remain a major challenge for eDNA metabarcoding studies. The high proportions of unassigned eukaryotes are consistent with findings from previous eDNA studies of pelagic eukaryotic communities, which report considerable unknown diversity in other oceans (Bakker et al., 2019; López-Escardó et al., 2018) as well as in the Arctic Ocean (Questel et al., 2021). A recent COI-based eDNA study in Fram Strait found lower levels of unassigned metazoans throughout the water column compared to our study (Murray et al., 2024), suggesting that this hidden diversity is higher directly under the ice than in open waters in Fram Strait.

4.1.2 Taxonomic composition of primary producers

Primary producers in the MIZ consist of ice algae, which typically live inside and on the lower surface of sea ice, and phytoplankton found in the sub-ice water column. As the Arctic sea ice is declining in both thickness and distribution, primary producers are being exposed to different environmental conditions, with changes in light regimes. This has led shifts in the timing and duration of the ice-algae and phytoplankton blooms each year in the MIZ. Recent evidence shows phytoplankton blooms are increasingly occurring under the sea ice due to thin single year ice and consequentially higher light availability (Ardyna et al., 2020; Assmy et al., 2017), rather than being restricted to patches of open water in the MIZ.

We detected a combination of ice algae and phytoplankton with both eDNA markers, with typical phytoplankton taxa showing greater sequence read abundance and richness. Sympagic blooms are generally dominated by the sea ice specialist diatom genera such as *Nitzschia*, *Navicula* and *Melosira* (Reviewed in: Barber et al., 2015). In our samples, we observed low read abundances of *Nitzschia* and *Navicula*, and we did not detect *Melosira*. This could be due to our sampling occurring after the peak of the spring bloom when these taxa's abundances had significantly declined. Pelagic blooms in the MIZ are typically dominated by the cryo-pelagic diatom genera such as *Thalassiosira*, *Chaetoceros* and *Fragilariopsis*, all of which we found in our samples with high read abundances. Furthermore, we detected a number of dinoflagellates (class: Dinophyceae), the haptophyte family Phaeocystales (genus *Phaeocystis* with 18S), and two prasinophytes (unicellular green algae) genera (*Micromona* and *Bathycoccus*) that are typical of Arctic summer waters (Benner et al., 2020; Freyria et al., 2021; Joli et al., 2017). Interestingly, we also found a number of MOTUs and ASVs belonging to the brown algae class Phaeophyceae. While these are not necessarily part of the primary producer community in the MIZ, they are present in nearby Svalbard fjords.

We hypothesize that these detections are due to gametophytes being advected north from the Svalbard coast towards the Yermak Plateau by the West Spitsbergen Current (**Figure 1A**).

4.1.2 Taxonomic composition of metazoans

Arctic sea ice fauna is typically a combination of pelagic, benthic and sympagic taxa, and are a mix of arctic-endemic, arctic-boreal and boreal species (Bluhm et al., 2010; Kosobokova et al., 2011). Sea ice associated fauna live in the lower centimetres of the sea ice and its brine channels, as well the lower surface or in the water column directly below. We observed both ice-associated and pelagic metazoans typical of the region (Barber et al., 2015; Hop et al., 2021; Weydmann et al., 2014), including meiofauna (e.g., Rotifera, Arthropoda, Annelida), zooplankton (copepods, amphipods and gelatinous zooplankton), potential meroplankton (e.g., polychaetes, gastropods and poriferans) and vertebrates (fish: *Boreogadus saida* and whales: *Balaena mysticetus* and *Monodon monoceros*). Overall, the proportion of metazoan reads was highest at 5 m across all stations, except for FS_V3 (COI dataset only) station in the outer MIZ. However, despite this general trend, several metazoan taxa (i.e., Rotifera, Tunicata and Annelida) were found in higher read abundances at 0 m than 5 m. This suggests a higher abundance or biomass of these taxa closer to the ice surface. For example, larvae from Tunicata and Annelida are known to settle and feed on the lower surface of the ice (Barber et al., 2015; Bluhm et al., 2017, 2010).

Arthropods, particularly copepods, are the most dominant zooplankton in the Arctic in terms of richness, biomass and abundance. More than 50% of the holoplanktonic species in the Arctic are copepods (Barber et al., 2015). This was evident in both of our eDNA datasets, where Arthropoda had the highest relative read abundances and the richness compared to the other phyla. In the summer surface waters, *Calanus glacialis* and *C. finmarchicus* typically have the highest biomass, while smaller species such as *O. similis*, *Triconia borealis* and *Pseudocalanus* spp. have the highest abundances (Hop et al., 2006). We detected these trends to a certain extent in our two eDNA datasets. In the COI dataset, *O. similis* and *P. minutus* were two of the most dominant MOTUs in terms of read abundance. We also detected all three of the *Calanus* species typical of the region, albeit at lower read abundances. In a morphological study, Kaiser et al., (2021) found *Calanus* spp., *Pseudocalanus* spp., and *Oithona* spp. when sampling the water column under an ice filament in the MIZ. *Oithona* spp. was observed in the highest abundances in the upper water column at the centre of the ice filament, where ice concentration was the highest. Another MIZ study, Kiko et al. (2017) also found *Oithona* spp. to be one of the most abundant metazoans in the sub-ice water column. In the 18S dataset, calanoid copepods were by far the most dominant in both read abundance and ASV richness. Oithonidae (the family that includes *Oithona* spp.) and the order Harpacticoida were also present, but in low read abundances. With regards to amphipods, we

detected the sympagic *Apherusa glacialis*, but we did not detect *Onisimus* sp. and *Gammarus wilkitzkii*, both well-known ice-associated amphipod taxa in the region. Indeed, Hop et al. (2011) found that the highest abundances of ice-amphipods such as *G. wilkitzkii* and *A. glacialis* are typically found in multi-year sea ice. The abundant pelagic amphipod genus *Themisto* was also absent from both datasets. The ice floes in this study were second-year ice (i.e., multi-year ice), and a recent COI-based eDNA study also failed to detect *Themisto* in Fram Strait (Murray et al., 2024). Therefore, the absence of *Themisto* in our results is likely due to primer or sequencing biases and/or rapid degradation of extra-cellular DNA, rather than an absence of the organisms. While detections of copepod groups (genus and species for COI and families for 18S) reflect previous findings in the MIZ, these differing patterns in abundance may demonstrate the well-known limitations to interpreting read abundances in eDNA samples as direct representations of organism abundance or biomass (Rourke et al., 2022; Ruppert et al., 2019). While semi-quantitative patterns (i.e., relative read abundances) provide more reliable insights than read counts, they must still be interpreted with some caution.

Gelatinous zooplankton (GZP), especially appendicularians and ctenophores, have been reported to be dominant components of the pelagic community in the MIZ (Bluhm et al., 2010; David et al., 2015; Ehrlich et al., 2020). In our study, we indeed detected these major GZP groups but with relatively low taxonomic resolution and generally low reads. Reads assigned to the appendicularian family Oikopleuridae and the ctenophore families Bolinopsidae, Mertensiidae and Euplokamididae were all recovered. Species in these families have been found in areas with high ice cover in the Arctic (e.g., David et al., 2015). One explanation for the low reads could be the patchy distribution typical of these groups, with a lack of aggregations occurring at or near the ice floe stations around the sampling time. Dense, yet patchily distributed aggregations of both ctenophores and appendicularians have been observed under-ice in the Arctic (e.g., David et al. 2015). However, previous studies have also failed to amplify appendicularians with the COI Leray marker used (Ershova et al., 2021; Murray et al., 2024), suggesting it may not be suitable for this taxonomic group.

We recovered a number of meiofauna taxa with high resolution taxonomy. These included *Pseudocalanus* spp. and members of the order Harpacticoida (e.g., *Tisbe furcata*), which are typical sympagic copepods (Arndt & Swadling, 2006; Kiko et al., 2017). The Arctic ice hydroid *Sympagohydra tuuli*, which inhabits brine channels and has been found in previous sea ice studies (Kiko et al., 2017; Siebert et al., 2009) was not detected. However, we did recover a large number of MOTUs assigned to the class Hydrozoa, some of which could belong to sympagic hydrozoans. However, *S. tuuli* is poorly represented in public reference databases, and further barcoding efforts are necessary to enhance its detectability in eDNA samples. Ice meiofauna remains a largely understudied group (Patrohay et al., 2022), but with further

optimisation, eDNA metabarcoding could become a useful tool furthering our understanding of their diversity and community dynamics within the changing MIZ.

4.2 Spatial patterns of alpha and beta diversity

Sea ice affects both light availability (through its cover and thickness) and stratification in the upper meters of the water column (e.g., from meltwater input), thereby playing a crucial role in shaping the dynamics of primary production and consumers. Despite the high proportions of low-resolution assignments, the alpha and beta diversity analyses in the present study are essentially taxon-free (Berry et al., 2019; Feng et al., 2022), which allowed us to detect aspects of the ecology of many of the MOTUs and ASVs in relation to depth, location and sea ice conditions.

Regarding the vertical patterns, we found significantly higher alpha diversity indices at 0 m, along with distinct variations in community composition between the two sampled depths in both the COI and 18S datasets. The proportion of primary producer sequence reads (Chromista and Plantae) was higher at 0 m than at 5 m (both datasets) across all stations except the F24_1 ice floe, whereas the opposite was true for Chromista. Metazoans as a whole were more abundant at 5 m than 0 m, but distinct depth patterns emerged for individual taxa. The most abundant metazoan ASVs and MOTUs, in particular, showing differences at the two sampling depths. In the COI dataset, some MOTUs (e.g., Annelida, Ascidiacea and Monogononta) were present in larger relative read abundances at 0 m than at 5 m. The reverse was true for the pelagic copepods *O. similis* and *P. minutus*. In the 18S dataset, this was the most obvious in the Calanoida ASV (ASV_1) that made up 99% of the metazoan reads, which was in larger proportions at 5 m depth (**Figure 3**). These small-scale vertical variations in diversity and composition could be due to the input of in-ice or melt-pond communities into the meltwater layer immediately under the ice, either as eDNA or the release of whole organisms with melting. This enrichment of the sub-ice community by taxa from sea ice melt is supported by previous findings in the Arctic (Smith et al., 2023; Xu et al., 2020). Significant differences in metazoan composition between in-ice and sub-ice water were also found by a morphological study in the MIZ on the Russian side of the Arctic (Kiko et al., 2017). Here, they observed meiofauna in the sub-ice water re-colonising the sea ice, both passively as ice re-formed and actively, depending on the taxa. Meiofauna taxa have high osmotic tolerance, allowing them to survive in a range of salinities that occur in brine channels and meltwater, whereas pelagic taxa may be sensitive to lower salinities in the meltwater (Grainger and Mohammed, 1990; Smith et al., 2023). However, the community at 5 m depth is likely influenced by pelagic taxa from deeper waters or by advection from nearby open water areas adjacent to the MIZ.

Location played also a significant role of eukaryotic diversity and distribution, with the F24_1 and FS_V3 floes showing the greatest variability compared to the other ice floe stations. In the COI dataset, the alpha diversity was generally higher towards the outer edge of the MIZ. The same was true for the 18S dataset, with the exception of floe F24_1, which had high richness and Shannon diversity. Furthermore, the ordination analyses and subsequent iris plots showed that F24_1 and FS_V3 formed the most distinct clusters in the ordination analyses (**Figure 4**) for both datasets. These differences in diversity and community composition are likely explained by the distinct location and environmental conditions of the inner and outer MIZ floes. F24_1, the only floe on the slope of the Yermak plateau, had the deepest seafloor depth (1400 m) and was where we measure the highest sea ice concentration and the deepest distribution of meltwater. In contrast, FS_V3, located on the outer edge of the MIZ, was the floe with the lowest sea ice cover and had a shallower meltwater layer depth than the floes towards the inner MIZ. These distinct patterns in diversity and community assemblages over relatively small scales, fit with previous morphology-based findings, which indicate that Arctic sea ice habitats and their associated communities are highly dynamic, even over small spatial gradients (David et al., 2015; Ehrlich et al., 2020; Ribeiro et al., 2024).

4.3 Signature communities across different environmental conditions

When analysing the signature communities linked to different environmental conditions with the sPLS analyses (**Figures 5 and 6**), we identified meltwater dynamics and sea ice concentration as the key environmental variables that strongly influences community composition. Four clusters were found in each dataset, with congruent patterns for both markers. The most dominant conditions were those typical of the inner MIZ (high sea ice coverage and greater distance to the ice edge) and the outer MIZ (low ice coverage and close to ice edge). The clusters indicating different meltwater conditions varied slightly between the markers and were associated with the depth of meltwater distribution and the volume of meltwater. Primary producers made up the majority of the taxa with significant correlations to environmental variables in all of the signature communities, highlighting the crucial role that the environmental conditions play in shaping the diversity and distribution of primary producers. Overall, we found the majority of taxa had strong correlations with the high ice cover and the deeper meltwater layer present at F24_1, or to the outer MIZ conditions of less ice cover and meltwater at FS_V3. In the phytoplankton community for example, the most abundance ASV assigned to the *Phaeocystis* genus was present at all ice floes, with the highest abundance at F24_1, also suggesting an affinity for inner MIZ conditions. This is in line with previous finding by Assmy et al. (2017), who detected under-ice phytoplankton blooms dominated by *Phaeocystis* in the same region in 2015. The sequences assigned to

the *Micromonas* and *Bathycoccus* genera exhibited a strong relationship with low temperature and high sea ice concentration and had the highest read abundance at F24_1 followed by FS_V1 in both datasets. This was further illustrated in the sPLS analyses where both genera were part of the signature communities (cluster 1 in both **Figures 5** and **6**) for high sea ice cover and meltwater content. Different thermo-types have been found in Arctic *Micromonas* species, including cold-water specialists, which may explain their higher abundances at the station with the inner MIZ conditions (Demory et al., 2019). However, sequencing longer gene fragments would be necessary to confirm that the observed organisms are indeed the cold-water specialists mentioned.

We also detected significant relationships between a number of metazoan taxa and environmental variables, although these were in lower proportions compared to the primary producers and were restricted to low resolution assignments (i.e., class-level in COI). They included a range of groups including the Annelida, Arthropoda, Chordata and Cnidaria phyla. In the COI dataset, the highest number of significant MOTUs was found in the phylum Cnidaria, including the classes Anthozoa, Hydrozoa and Scyphozoa. In the 18S dataset, the majority of significant relationships were with ASVs assigned to Arthropoda, with the exception of single hydrozoan (family: Rhopalonematidae) and an ascidian (family: Perophoridae) ASVs. As sea ice conditions change due to warming and as the phenology and composition of ice-algae and phytoplankton blooms shift, metazoans whose life cycles are linked to blooms will also be affected. However, with limited taxonomic resolution of the 18S gene and the high levels of uncharacterised diversity resulting in a low number of species-level detections with COI, we are constrained to conclusion at the genus or family level and cannot yet identify specific indicator species or strains.

4.4 Multi-marker approach to surveying under-ice biodiversity

Marker choice can be a significant source of bias on the biodiversity captured by eDNA metabarcoding (Clarke et al., 2017; Collins et al., 2019). Using multiple markers increases coverage and the chances of detecting a more complete picture of the biodiversity present. Both of the markers employed in this study have benefits and known limitations. The Leray-XT primers (Wangensteen et al., 2018b) were designed for eukaryotes with a focus on metazoans and allow for high taxonomic precision. The fast evolutionary rates of the COI gene allows for species-level identifications (Tang et al., 2012; Wangensteen et al., 2018b). Furthermore, the Leray fragment is useful for detecting levels of intraspecific diversity, allowing us to also investigate haplotype diversity (Antich et al., 2022). It has well-stocked and curated public reference databases available for taxonomic assignment (Andújar et al., 2018), such as the BOLD database (Ratnasingham and Hebert, 2007). The 18S rRNA gene is more conservative than COI, but can amplify a wide taxonomic range of eukaryotes, including those

where COI is limited (Questel et al., 2021). For example, ctenophores and appendicularians are thought to be often missed by COI, but successfully detected by 18S (e.g., Dischereit et al., 2024). In our study, this held true except for a ctenophore family detected by both (Bolinopsidae). The 18S gene is also has high representation of public reference databases for a wide range of eukaryotic taxa. However, a major trade-off is that high levels of universality, due to its slow-evolving nature, hampers the accuracy of high-resolution taxonomic assignment (e.g., genus and species levels in metazoans). The most reliable level of identification is limited to order or family-level for metazoans (Questel et al., 2021; Tang et al., 2012; Wu et al., 2015). So, although we captured families overlooked by COI, we cannot yet say with certainty which species the eDNA belongs to.

Using two different markers can also result in contrasting quantitative patterns detected within the same samples (Bakker et al., 2019), and there remain limitations to interpreting relative read abundances as a proxy for biomass or organism abundances. Here, we detected similar patterns in alpha and beta diversity, which are in principle taxonomy-free analyses. We found the same elevated diversity under the ice compared to 5 m depth, as well as differences in community composition between depths and stations (especially F24_1) in both datasets. However, the relative read abundances of dominant taxa were not always congruent between the two markers. For example, the cyclopoid copepod species *O. similis* was the most dominant MOTU (18.74 %), while the 18S dataset was dominated by a single calanoid copepod ASV (71.49 % of total reads). Although a single ASV assigned to Oithonidae was indeed in the top 15 ASVs for 18S, it had a relative read abundance of less than 1%. Relative read abundances are likely semi-quantitative representations of abundances or biomass of the organisms, but to which degree is both gene and taxon-dependent and currently not easily resolved (Lamb et al., 2019). Correlations between biomass and read abundance has been found for a number of zooplankton taxa when analysing the COI marker and bulk samples (Ershova et al., 2023, 2021). These findings support the assumption that our COI-based patterns for zooplankton can be interpreted with more confidence than in the 18S dataset. Another factor affecting read counts is some taxa having higher numbers of gene copies than others. For instance, dinoflagellates have a high number of 18S copies which can inflate read abundances recovered in metabarcoding (Ribeiro et al., 2022). Furthermore, the strong dominance of a single calanoid ASV (79% of all reads and 99% of metazoan reads) in our 18S reads, suggests that primer or sequencing biases have a significant effect on read abundances in this dataset that needs to be resolved. Overall, there is a need for more taxon- and marker-specific work, including linking extracellular DNA reads (i.e., eDNA) and biomass for specific taxa, and ecological patterns linked to these relative read abundance must still be interpreted with caution.

4.5 Conclusions

This study provides the first high-resolution, multi-marker metabarcoding analysis of eukaryotic biodiversity in the upper five meters of sub-ice water in the Arctic MIZ. The taxonomic composition of sub-ice water observed in this study was largely consistent with previous studies, demonstrating eDNA as an effective tool for assessing biodiversity in the sub-ice water. The use of the two markers increased the taxonomic coverage, resolution and the biodiversity captured. We show that gaps remain in reference databases that require improvement in order to characterise the biodiversity found here to high taxonomic resolution, particularly in the centimetres directly below the ice. We were able to demonstrate that depth, melt water and sea ice properties are dominant drivers of diversity and community composition, with generally congruent patterns detected in two widely used universal metabarcoding markers. Furthermore, we demonstrated the potential of multi-marker surveys to highlight signature communities of specific environmental states within ice-covered environments such as the MIZ. In future studies, increasing the sampling volume of sea-water as well as the temporal and spatial resolution of sampling would likely increase the number of taxa detected by both markers. The use of passive filtration systems has been shown to improve biodiversity capture in tropical and temperate marine systems (Bessey et al., 2021) and in the deep sea (Govindarajan et al., 2022). This approach could significantly enhance the effectiveness of eDNA as a biodiversity tool in the MIZ. For instance, using static filter membranes placed beneath the ice at different depths could increase exposure to larger volumes of water and, consequently higher concentration of eDNA. Additionally, further research is needed in the upper layers of the sub-ice water across seasons and wider parts of the MIZ to track the dynamics of eukaryotic communities over time and across different locations.

Declaration of interests

The authors declare that they have no known competing financial interests or personal relationships that could have appeared to influence the work reported in this paper.

Data availability statement

All MSS measurements are available at: <https://doi.pangaea.de/10.1594/PANGAEA.956086>.

All CTD data is available at: <https://doi.org/10.1594/PANGAEA.971721>

Reference database for COI marker is available at:

<https://github.com/adriantich/NJORDR-MJOLNIR3/tree/main>

Reference database for 18S marker is available at:

https://www.st.nmfs.noaa.gov/copepod/collaboration/metazoogene/atlas/html-src/data_T4000000_o00.html

The raw metabarcoding sequence data are used in this project are publicly available at NCBI on the SRA database under the BioProject ID: PRJNA1135808

Advanced Microwave Scanning Radiometer-2 (AMSR-2) sensor data downloaded from:

OSI SAF Global Sea Ice Concentration (AMSR-2), OSI-408-a, DOI: 10.15770/EUM_SAF_OSI_NRT_2023. EUMETSAT Ocean and Sea Ice Satellite Application Facility. Data extracted from OSI SAF FTP server. The presented work contains primary and altered Sentinel1 data products.

Acknowledgements

This study has been conducted in the framework of the Helmholtz Young Investigator Group “ARJEL – Arctic Jellies” with the project number VH-NG-1400, led by CH and funded by the Helmholtz Society and the Alfred Wegener Institute Helmholtz Centre for Polar and Marine Research. The concept and eDNA data for this manuscript were produced as part of the ICE-Jelly project with the Polarstern grant number AWI_PS131_10. The sea ice physics sampling was part of grant number AWI_PS131_02. The oceanographic sampling was part of grant number AWI_PS131_07. The authors thank all of the scientists, crew and technical support on board PS131 for support with sampling. Especially to Torsten Kanzow as chief scientist and for access to the under-ice CTD data, as well as Ilke Fer for supplying for the MSS data.

References

- Adams, C.I.M., Jeunen, G.-J., Cross, H., Taylor, H.R., Bagnaro, A., Currie, K., Hepburn, C., Gemmill, N.J., Urban, L., Baltar, F., Stat, M., Bunce, M., Knapp, M., 2023. Environmental DNA metabarcoding describes biodiversity across marine gradients. *ICES Journal of Marine Science* 80, 953–971. <https://doi.org/10.1093/icesjms/fsad017>
- Aksenov, Y., Popova, E.E., Yool, A., Nurser, A.J.G., Williams, T.D., Bertino, L., Bergh, J., 2017. On the future navigability of Arctic sea routes: High-resolution projections of the Arctic Ocean and sea ice. *Marine Policy* 75, 300–317. <https://doi.org/10.1016/j.marpol.2015.12.027>
- Alabia, I.D., García Molinos, J., Hirata, T., Mueter, F.J., David, C.L., 2023. Pan-Arctic marine biodiversity and species co-occurrence patterns under recent climate. *Sci Rep* 13, 4076. <https://doi.org/10.1038/s41598-023-30943-y>
- Andújar, C., Arribas, P., Yu, D.W., Vogler, A.P., Emerson, B.C., 2018. Why the COI barcode should be the community DNA metabarcode for the metazoa. *Molecular Ecology* 27, 3968–3975. <https://doi.org/10.1111/mec.14844>
- Antich, A., Palacín, C., Zarceró, J., Wangensteen, O.S., Turon, X., 2022. Metabarcoding reveals high-resolution biogeographical and metaphylogeographical patterns through marine barriers. *Journal of Biogeography*.
- Antich González, A., Palacin, C., Wangensteen, O., Turon, X., 2021. To denoise or to cluster, that is not the question: optimizing pipelines for COI metabarcoding and metaphylogeography. *BMC Bioinformatics* 22. <https://doi.org/10.1186/s12859-021-04115-6>
- Ardyna, M., Mundy, C.J., Mayot, N., Matthes, L.C., Oziel, L., Horvat, C., Leu, E., Assmy, P., Hill, V., Matrai, P.A., Gale, M., Melnikov, I.A., Arrigo, K.R., 2020. Under-Ice Phytoplankton Blooms: Shedding Light on the “Invisible” Part of Arctic Primary Production. *Frontiers in Marine Science* 7.
- Assmy, P., Fernández-Méndez, M., Duarte, P., Meyer, A., Randelhoff, A., Mundy, C.J., Olsen, L.M., Kauko, H.M., Bailey, A., Chierici, M., Cohen, L., Doulgeris, A.P., Ehn, J.K., Fransson, A., Gerland, S., Hop, H., Hudson, S.R., Hughes, N., Itkin, P., Johnsen, G., King, J.A., Koch, B.P., Koenig, Z., Kwasniewski, S., Laney, S.R., Nicolaus, M., Pavlov, A.K., Polashenski, C.M., Provost, C., Rösel, A., Sandbu, M., Spreen, G., Smedsrud, L.H., Sundfjord, A., Taskjelle, T., Tatarek, A., Wiktor, J., Wagner, P.M., Wold, A., Steen, H., Granskog, M.A., 2017. Leads in Arctic pack ice enable early phytoplankton blooms below snow-covered sea ice. *Sci Rep* 7, 40850. <https://doi.org/10.1038/srep40850>
- Bakker, J., Wangensteen, O.S., Baillie, C., Buddo, D., Chapman, D.D., Gallagher, A.J., Guttridge, T.L., Hertler, H., Mariani, S., 2019. Biodiversity assessment of tropical shelf eukaryotic communities via pelagic eDNA metabarcoding. *Ecology and Evolution* 9, 14341–14355. <https://doi.org/10.1002/ece3.5871>
- Barber, D.G., Hop, H., Mundy, C.J., Else, B., Dmitrenko, I.A., Tremblay, J.-E., Ehn, J.K., Assmy, P., Daase, M., Candlish, L.M., Rysgaard, S., 2015. Selected physical, biological and biogeochemical implications of a rapidly changing Arctic Marginal Ice Zone. *Progress in Oceanography, Overarching perspectives of contemporary and future ecosystems in the Arctic Ocean* 139, 122–150. <https://doi.org/10.1016/j.pocean.2015.09.003>
- Benner, I., Irwin, A.J., Finkel, Z.V., 2020. Capacity of the common Arctic picoeukaryote *Micromonas* to adapt to a warming ocean. *Limnology and Oceanography Letters* 5, 221–227. <https://doi.org/10.1002/lol2.10133>
- Bernatchez, L., Ferchaud, A.-L., Berger, C.S., Venney, C.J., Xuereb, A., 2024. Genomics for monitoring and understanding species responses to global climate change. *Nat Rev Genet* 25, 165–183. <https://doi.org/10.1038/s41576-023-00657-y>

- Berry, T.E., Saunders, B.J., Coghlan, M.L., Stat, M., Jarman, S., Richardson, A.J., Davies, C.H., Berry, O., Harvey, E.S., Bunce, M., 2019. Marine environmental DNA biomonitoring reveals seasonal patterns in biodiversity and identifies ecosystem responses to anomalous climatic events. *PLOS Genetics* 15, e1007943. <https://doi.org/10.1371/journal.pgen.1007943>
- Bessey, C., Neil Jarman, S., Simpson, T., Miller, H., Stewart, T., Kenneth Keesing, J., Berry, O., 2021. Passive eDNA collection enhances aquatic biodiversity analysis. *Commun Biol* 4, 1–12. <https://doi.org/10.1038/s42003-021-01760-8>
- Beule, L., Karlovsky, P., 2020. Improved normalization of species count data in ecology by scaling with ranked subsampling (SRS): application to microbial communities. *PeerJ* 8, e9593. <https://doi.org/10.7717/peerj.9593>
- Blaxter, M.L., De Ley, P., Garey, J.R., Liu, L.X., Scheldeman, P., Vierstraete, A., Vanfleteren, J.R., Mackey, L.Y., Dorris, M., Frisse, L.M., Vida, J.T., Thomas, W.K., 1998. A molecular evolutionary framework for the phylum Nematoda. *Nature* 392, 71–75. <https://doi.org/10.1038/32160>
- Bluhm, B.A., Gradinger, R., Schnack-Schiel, S., 2010. Sea Ice Meio- and Macrofauna, in: *Sea Ice*. Wiley, pp. 357–393.
- Bluhm, B.A., Swadling, K.M., Gradinger, R., 2017. Sea ice as a habitat for macrograzers, in: *Sea Ice*. John Wiley & Sons, Ltd, pp. 394–414. <https://doi.org/10.1002/9781118778371.ch16>
- Boetius, A., Albrecht, S., Bakker, K., Bienhold, C., Felden, J., Fernández-Méndez, M., Hendricks, S., Katlein, C., Lalande, C., Krumpfen, T., Nicolaus, M., Peeken, I., Rabe, B., Rogacheva, A., Rybakova, E., Somavilla, R., Wenzhöfer, F., RV POLARSTERN ARK27-3-SHIPBOARD SCIENCE PARTY, 2013. Export of Algal Biomass from the Melting Arctic Sea Ice. *Science* 339, 1430–1432. <https://doi.org/10.1126/science.1231346>
- Boyer, F., Mercier, C., Bonin, A., Le Bras, Y., Taberlet, P., Coissac, E., 2016. obitools: a unix-inspired software package for DNA metabarcoding. *Molecular Ecology Resources* 16, 176–182. <https://doi.org/10.1111/1755-0998.12428>
- Buchner, D., Leese, F., 2020. BOLDigger – a Python package to identify and organise sequences with the Barcode of Life Data systems. *Metabarcoding and Metagenomics* 4, e53535. <https://doi.org/10.3897/mbmg.4.53535>
- Bucklin, A., Peijnenburg, K.T.C.A., Kosobokova, K.N., O'Brien, T.D., Blanco-Bercial, L., Cornils, A., Falkenhaus, T., Hopcroft, R.R., Hosia, A., Laakmann, S., Li, C., Martell, L., Questel, J.M., Wall-Palmer, D., Wang, M., Wiebe, P.H., Weydmann-Zwolicka, A., 2021. Toward a global reference database of COI barcodes for marine zooplankton. *Mar Biol* 168, 78. <https://doi.org/10.1007/s00227-021-03887-y>
- Callahan, B.J., McMurdie, P.J., Rosen, M.J., Han, A.W., Johnson, A.J.A., Holmes, S.P., 2016. DADA2: High-resolution sample inference from Illumina amplicon data. *Nat Methods* 13, 581–583. <https://doi.org/10.1038/nmeth.3869>
- Castro de la Guardia, L., Garcia-Quintana, Y., Claret, M., Hu, X., Galbraith, E.D., Myers, P.G., 2019. Assessing the Role of High-Frequency Winds and Sea Ice Loss on Arctic Phytoplankton Blooms in an Ice-Ocean-Biogeochemical Model. *Journal of Geophysical Research: Biogeosciences* 124, 2728–2750. <https://doi.org/10.1029/2018JG004869>
- Clarke, L.J., Beard, J.M., Swadling, K.M., Deagle, B.E., 2017. Effect of marker choice and thermal cycling protocol on zooplankton DNA metabarcoding studies. *Ecology and Evolution* 7, 873–883. <https://doi.org/10.1002/ece3.2667>
- Collins, R.A., Bakker, J., Wangenstein, O.S., Soto, A.Z., Corrigan, L., Sims, D.W., Genner, M.J., Mariani, S., 2019. Non-specific amplification compromises environmental DNA metabarcoding with COI. *Methods in Ecology and Evolution* 10, 1985–2001. <https://doi.org/10.1111/2041-210X.13276>
- David, C., Lange, B., Rabe, B., Flores, H., 2015. Community structure of under-ice fauna in the Eurasian central Arctic Ocean in relation to environmental properties of sea-ice habitats. *Mar. Ecol. Prog. Ser.* 522, 15–32. <https://doi.org/10.3354/meps11156>

- Demory, D., Baudoux, A.-C., Monier, A., Simon, N., Six, C., Ge, P., Rigaut-Jalabert, F., Marie, D., Sciandra, A., Bernard, O., Rabouille, S., 2019. Picoeukaryotes of the *Micromonas* genus: sentinels of a warming ocean. *The ISME Journal* 13, 132–146. <https://doi.org/10.1038/s41396-018-0248-0>
- Dischereit, A., Throm, J.K., Werner, K.-M., Neuhaus, S., Havermans, C., 2024. A belly full of jelly? DNA metabarcoding shows evidence for gelatinous zooplankton predation by several fish species in Greenland waters. *Royal Society Open Science*. <https://doi.org/10.1098/rsos.240797>
- Dumont, D., 2022. Marginal ice zone dynamics: history, definitions and research perspectives. *Philosophical Transactions of the Royal Society A: Mathematical, Physical and Engineering Sciences* 380, 20210253. <https://doi.org/10.1098/rsta.2021.0253>
- Ehrlich, J., Schaafsma, F.L., Bluhm, B.A., Peeken, I., Castellani, G., Brandt, A., Flores, H., 2020. Sympagic Fauna in and Under Arctic Pack Ice in the Annual Sea-Ice System of the New Arctic. *Front. Mar. Sci.* 7. <https://doi.org/10.3389/fmars.2020.00452>
- Ershova, E.A., Descoteaux, R., Wangensteen, O.S., Iken, K., Hopcroft, R.R., Smoot, C., Grebmeier, J.M., Bluhm, B.A., 2019. Diversity and Distribution of Meroplanktonic Larvae in the Pacific Arctic and Connectivity With Adult Benthic Invertebrate Communities. *Frontiers in Marine Science* 6.
- Ershova, E.A., Wangensteen, O.S., Descoteaux, R., Barth-Jensen, C., Præbel, K., 2021. Metabarcoding as a quantitative tool for estimating biodiversity and relative biomass of marine zooplankton. *ICES Journal of Marine Science* 78, 3342–3355. <https://doi.org/10.1093/icesjms/fsab171>
- Ershova, E.A., Wangensteen, O.S., Falkenhaus, T., 2023. Mock samples resolve biases in diversity estimates and quantitative interpretation of zooplankton metabarcoding data. *Mar. Biodivers.* 53, 66. <https://doi.org/10.1007/s12526-023-01372-x>
- Falk-Petersen, S., Mayzaud, P., Kattner, G., Sargent, J.R., 2009. Lipids and life strategy of Arctic *Calanus*. *Marine Biology Research*. <https://doi.org/10.1080/17451000802512267>
- Feng, Y., Sun, D., Shao, Q., Fang, C., Wang, C., 2022. Mesozooplankton biodiversity, vertical assemblages, and diel migration in the western tropical Pacific Ocean revealed by eDNA metabarcoding and morphological methods. *Frontiers in Marine Science* 9. <https://doi.org/10.3389/fmars.2022.1004410>
- Freyria, N.J., Joli, N., Lovejoy, C., 2021. A decadal perspective on north water microbial eukaryotes as Arctic Ocean sentinels. *Sci Rep* 11, 8413. <https://doi.org/10.1038/s41598-021-87906-4>
- Galí, M., Lizotte, M., Kieber, D.J., Randelhoff, A., Husserr, R., Xue, L., Dinasquet, J., Babin, M., Rehm, E., Levasseur, M., 2021. DMS emissions from the Arctic marginal ice zone. *Elementa: Science of the Anthropocene* 9, 00113. <https://doi.org/10.1525/elementa.2020.00113>
- Geller, J., Meyer, C., Parker, M., Hawk, H., 2013. Redesign of PCR primers for mitochondrial cytochrome c oxidase subunit I for marine invertebrates and application in all-taxa biotic surveys. *Molecular Ecology Resources* 13, 851–861. <https://doi.org/10.1111/1755-0998.12138>
- Geraldi, N.R., Krause-Jensen, D., Ørberg, S.B., Frühe, L., Sejr, M.K., Hansen, J.L.S., Lund-Hansen, L., Duarte, C.M., 2024. Environmental drivers of Arctic communities based on metabarcoding of marine sediment eDNA. *Proceedings of the Royal Society B: Biological Sciences* 291, 20231614. <https://doi.org/10.1098/rspb.2023.1614>
- Giebner, H., Langen, K., Bourlat, S.J., Kukowka, S., Mayer, C., Astrin, J.J., Misof, B., Fonseca, V.G., 2020. Comparing diversity levels in environmental samples: DNA sequence capture and metabarcoding approaches using 18S and COI genes. *Molecular Ecology Resources* 20, 1333–1345. <https://doi.org/10.1111/1755-0998.13201>
- Govindarajan, A.F., McCartin, L., Adams, A., Allan, E., Belani, A., Francolini, R., Fujii, J., Gomez-Ibañez, D., Kukulya, A., Marin, F., Tradd, K., Yoerger, D.R., McDermott, J.M.,

- Herrera, S., 2022. Improved biodiversity detection using a large-volume environmental DNA sampler with in situ filtration and implications for marine eDNA sampling strategies. *Deep Sea Research Part I: Oceanographic Research Papers* 189, 103871. <https://doi.org/10.1016/j.dsr.2022.103871>
- Grainger, E.H., Mohammed, A.A., 1990. High salinity tolerance in sea ice copepods. *Ophelia* 31, 177–185. <https://doi.org/10.1080/00785326.1990.10430860>
- He, X., Gilmore, S.R., Sutherland, T.F., Hajibabaei, M., Miller, K.M., Westfall, K.M., Pawlowski, J., Abbott, C.L., 2021. Biotic signals associated with benthic impacts of salmon farms from eDNA metabarcoding of sediments. *Molecular Ecology* 30, 3158–3174. <https://doi.org/10.1111/mec.15814>
- Heidrich, V., Karlovsky, P., Beule, L., 2021. 'SRS' R Package and 'q2-srs' QIIME 2 Plugin: Normalization of Microbiome Data Using Scaling with Ranked Subsampling (SRS). *Applied Sciences* 11, 11473. <https://doi.org/10.3390/app112311473>
- Hestetun, J.T., Lanzén, A., Dahlgren, T.G., 2021. Grab what you can—an evaluation of spatial replication to decrease heterogeneity in sediment eDNA metabarcoding. *PeerJ* 9, e11619. <https://doi.org/10.7717/peerj.11619>
- Hodapp, D., Roca, I.T., Fiorentino, D., Garilao, C., Kaschner, K., Kesner-Reyes, K., Schneider, B., Segschneider, J., Kocsis, Á.T., Kiessling, W., Brey, T., Froese, R., 2023. Climate change disrupts core habitats of marine species. *Global Change Biology* 29, 3304–3317. <https://doi.org/10.1111/gcb.16612>
- Hop, H., Falk-Petersen, S., Svendsen, H., Kwasniewski, S., Pavlov, V., Pavlova, O., Søreide, J.E., 2006. Physical and biological characteristics of the pelagic system across Fram Strait to Kongsfjorden. *Progress in Oceanography, Structure and function of contemporary food webs on Arctic shelves: a pan-Arctic comparison* 71, 182–231. <https://doi.org/10.1016/j.pocean.2006.09.007>
- Hop, H., Mundy, C.J., Gosselin, M., Rossnagel, A.L., Barber, D.G., 2011. Zooplankton boom and ice amphipod bust below melting sea ice in the Amundsen Gulf, Arctic Canada. *Polar Biol* 34, 1947–1958. <https://doi.org/10.1007/s00300-011-0991-4>
- Hop, H., Vihtakari, M., Bluhm, B.A., Daase, M., Gradinger, R., Melnikov, I.A., 2021. Ice-Associated Amphipods in a Pan-Arctic Scenario of Declining Sea Ice. *Front. Mar. Sci.* 8. <https://doi.org/10.3389/fmars.2021.743152>
- Hosia, A., Falkenhaus, T., Baxter, E.J., Pagès, F., 2017. Abundance, distribution and diversity of gelatinous predators along the northern Mid-Atlantic Ridge: A comparison of different sampling methodologies. *PLoS ONE* 12, e0187491. <https://doi.org/10.1371/journal.pone.0187491>
- Jahn, A., Holland, M.M., Kay, J.E., 2024. Projections of an ice-free Arctic Ocean. *Nat Rev Earth Environ* 5, 164–176. <https://doi.org/10.1038/s43017-023-00515-9>
- Joli, N., Monier, A., Logares, R., Lovejoy, C., 2017. Seasonal patterns in Arctic prasinophytes and inferred ecology of *Bathycoccus* unveiled in an Arctic winter metagenome. *ISME J* 11, 1372–1385. <https://doi.org/10.1038/ismej.2017.7>
- Joy-Warren, H.L., Lewis, K.M., Ardyna, M., Tremblay, J.-É., Babin, M., Arrigo, K.R., 2023. Similarity in phytoplankton photophysiology among under-ice, marginal ice, and open water environments of Baffin Bay (Arctic Ocean). *Elementa: Science of the Anthropocene* 11, 00080. <https://doi.org/10.1525/elementa.2021.00080>
- Kaiser, P., Hagen, W., von Appen, W.-J., Niehoff, B., Hildebrandt, N., Auel, H., 2021. Effects of a Submesoscale Oceanographic Filament on Zooplankton Dynamics in the Arctic Marginal Ice Zone. *Frontiers in Marine Science* 8.
- Kanzow, T., 2023. The Expedition PS131 of the Research Vessel POLARSTERN to the Fram Strait in 2022 [WWW Document]. *Berichte zur Polar- und Meeresforschung = Reports on polar and marine research*. https://doi.org/10.57738/BzPM_0770_2023
- Kassambara, A., 2023. *rstatix: Pipe-Friendly Framework for Basic Statistical Tests*.
- Kiko, R., Kern, S., Kramer, M., Mütze, H., 2017. Colonization of newly forming Arctic sea ice by meiofauna: a case study for the future Arctic? *Polar Biol* 40, 1277–1288. <https://doi.org/10.1007/s00300-016-2052-5>

- Kosobokova, K.N., Hopcroft, R.R., Hirche, H.-J., 2011. Patterns of zooplankton diversity through the depths of the Arctic's central basins. *Mar Biodiv* 41, 29–50. <https://doi.org/10.1007/s12526-010-0057-9>
- Krumpen, T., Belter, H.J., Boetius, A., Damm, E., Haas, C., Hendricks, S., Nicolaus, M., Nöthig, E.-M., Paul, S., Peeken, I., Ricker, R., Stein, R., 2019. Arctic warming interrupts the Transpolar Drift and affects long-range transport of sea ice and ice-rafted matter. *Sci Rep* 9, 5459. <https://doi.org/10.1038/s41598-019-41456-y>
- Lacoursière-Roussel, A., Howland, K., Normandeau, E., Grey, E.K., Archambault, P., Deiner, K., Lodge, D.M., Hernandez, C., Leduc, N., Bernatchez, L., 2018. eDNA metabarcoding as a new surveillance approach for coastal Arctic biodiversity. *Ecology and Evolution* 8, 7763–7777. <https://doi.org/10.1002/ece3.4213>
- Lamb, P.D., Hunter, E., Pinnegar, J.K., Creer, S., Davies, R.G., Taylor, M.I., 2019. How quantitative is metabarcoding: A meta-analytical approach. *Molecular Ecology* 28, 420–430. <https://doi.org/10.1111/mec.14920>
- Lannuzel, D., Tedesco, L., van Leeuwe, M., Campbell, K., Flores, H., Delille, B., Miller, L., Stefels, J., Assmy, P., Bowman, J., Brown, K., Castellani, G., Chierici, M., Crabeck, O., Damm, E., Else, B., Fransson, A., Fripiat, F., Geilfus, N.-X., Jacques, C., Jones, E., Kaartokallio, H., Kotovitch, M., Meiners, K., Moreau, S., Nomura, D., Peeken, I., Rintala, J.-M., Steiner, N., Tison, J.-L., Vancoppenolle, M., Van der Linden, F., Vichi, M., Wongpan, P., 2020. The future of Arctic sea-ice biogeochemistry and ice-associated ecosystems. *Nat. Clim. Chang.* 10, 983–992. <https://doi.org/10.1038/s41558-020-00940-4>
- Leu, E., Mundy, C.J., Assmy, P., Campbell, K., Gabrielsen, T.M., Gosselin, M., Juul-Pedersen, T., Gradinger, R., 2015. Arctic spring awakening – Steering principles behind the phenology of vernal ice algal blooms. *Progress in Oceanography*, Overarching perspectives of contemporary and future ecosystems in the Arctic Ocean 139, 151–170. <https://doi.org/10.1016/j.pocean.2015.07.012>
- Leu, E., Søreide, J.E., Hessen, D.O., Falk-Petersen, S., Berge, J., 2011. Consequences of changing sea-ice cover for primary and secondary producers in the European Arctic shelf seas: Timing, quantity, and quality. *Progress in Oceanography, Arctic Marine Ecosystems in an Era of Rapid Climate Change* 90, 18–32. <https://doi.org/10.1016/j.pocean.2011.02.004>
- López-Escardó, D., Paps, J., de Vargas, C., Massana, R., Ruiz-Trillo, I., del Campo, J., 2018. Metabarcoding analysis on European coastal samples reveals new molecular metazoan diversity. *Sci Rep* 8, 9106. <https://doi.org/10.1038/s41598-018-27509-8>
- McMurdie, P.J., Holmes, S., 2013. phyloseq: An R Package for Reproducible Interactive Analysis and Graphics of Microbiome Census Data. *PLOS ONE* 8, e61217. <https://doi.org/10.1371/journal.pone.0061217>
- Meredith, M., Sommerkorn, M., Cassotta, S., Derksen, C., Ekaykin, A., Hollowed, A., Kofinas, G., Mackintosh, A., Melbourne-Thoma, J., Muelber, M.M.C., Ottersen, G., Pritchard, H., Schuur, E.A.G., 2022. *The Ocean and Cryosphere in a Changing Climate: Special Report of the Intergovernmental Panel on Climate Change*, 1st ed. Cambridge University Press. <https://doi.org/10.1017/9781009157964>
- Merten, V., Puebla, O., Bayer, T., Reusch, T.B.H., Fuss, J., Stefanschitz, J., Metfies, K., Stauffer, J.B., Hoving, H.-J., 2023. Arctic nekton uncovered by eDNA metabarcoding: Diversity, potential range expansions, and pelagic-benthic coupling. *Environmental DNA* n/a. <https://doi.org/10.1002/edn3.403>
- Mueter, F.J., Planque, B., Hunt, G.L., Alabia, I.D., Hirawake, T., Eisner, L., Dalpadado, P., Chierici, M., Drinkwater, K.F., Harada, N., Arneberg, P., Saitoh, S.-I., 2021. Possible future scenarios in the gateways to the Arctic for Subarctic and Arctic marine systems: II. prey resources, food webs, fish, and fisheries. *ICES Journal of Marine Science* 78, 3017–3045. <https://doi.org/10.1093/icesjms/fsab122>
- Murray, A., Priest, T., Antich, A., von Appen, W.-J., Neuhaus, S., Havermans, C., 2024. Investigating pelagic biodiversity and gelatinous zooplankton communities in the

- rapidly changing European Arctic: An eDNA metabarcoding survey. *Environmental DNA* 6, e569. <https://doi.org/10.1002/edn3.569>
- Oksanen, J., F., Blanchet, G., Friendly, M., Kindt, R., Legendre, P., McGlinn, D., Minchin, P.R., O'hara, R.B., Simpson, G.L., Solymos, P., Stevens, M.H.H., 2019. *Vegan: community ecology package (version 2.5-6)*. The Comprehensive R Archive Network.
- Patrohay, E., Gradinger, R., Marquardt, M., Bluhm, B.A., 2022. First trait-based characterization of Arctic ice meiofauna taxa. *Polar Biol* 45, 1673–1688. <https://doi.org/10.1007/s00300-022-03099-0>
- Polyakov, I.V., Pnyushkov, A.V., Alkire, M.B., Ashik, I.M., Baumann, T.M., Carmack, E.C., Goszczko, I., Guthrie, J., Ivanov, V.V., Kanzow, T., Kirshfield, R., 2017. Greater role for Atlantic inflows on sea-ice loss in the Eurasian Basin of the Arctic Ocean. *Science* 356, 285–291.
- Questel, J.M., Hopcroft, R.R., DeHart, H.M., Smoot, C.A., Kosobokova, K.N., Bucklin, A., 2021. Metabarcoding of zooplankton diversity within the Chukchi Borderland, Arctic Ocean: improved resolution from multi-gene markers and region-specific DNA databases. *Mar. Biodivers.* 51, 4. <https://doi.org/10.1007/s12526-020-01136-x>
- Quinn, T.P., Erb, I., Richardson, M.F., Crowley, T.M., 2018. Understanding sequencing data as compositions: an outlook and review. *Bioinformatics* 34, 2870–2878. <https://doi.org/10.1093/bioinformatics/bty175>
- R Core Team, 2023. *R: A Language and Environment for Statistical Computing*.
- Rantanen, M., Karpechko, A.Y., Lipponen, A., Nordling, K., Hyvärinen, O., Ruosteenoja, K., K, V., Laaksonen, A., 2022. The Arctic has warmed nearly four times faster than the globe since 1979. *Communications Earth & Environment* 3, 1–10.
- Ratnasingham, S., Hebert, P.D.N., 2007. *bold: The Barcode of Life Data System* (<http://www.barcodinglife.org>). *Molecular Ecology Notes* 7, 355–364. <https://doi.org/10.1111/j.1471-8286.2007.01678.x>
- Ribeiro, C.G., Dos Santos, A.L., Trefault, N., Marie, D., Lovejoy, C., Vaultot, D., 2022. Arctic phytoplankton spring bloom diversity across the marginal ice zone in Baffin Bay (preprint). *Microbiology*. <https://doi.org/10.1101/2022.03.14.484350>
- Ribeiro, C.G., Lopes dos Santos, A., Trefault, N., Marie, D., Lovejoy, C., Vaultot, D., 2024. Arctic phytoplankton microdiversity across the marginal ice zone: Subspecies vulnerability to sea-ice loss. *Elementa: Science of the Anthropocene* 12, 00109. <https://doi.org/10.1525/elementa.2023.00109>
- Rohart, F., Gautier, B., Singh, A., Lê Cao, K.-A., 2017. *mixOmics: An R package for 'omics feature selection and multiple data integration*. *PLoS Comput Biol* 13, e1005752. <https://doi.org/10.1371/journal.pcbi.1005752>
- Rolph, R.J., Feltham, D.L., Schröder, D., 2020. Changes of the Arctic marginal ice zone during the satellite era. *The Cryosphere* 14, 1971–1984. <https://doi.org/10.5194/tc-14-1971-2020>
- Rourke, M.L., Fowler, A.M., Hughes, J.M., Broadhurst, M.K., DiBattista, J.D., Fielder, S., Wilkes Walburn, J., Furlan, E.M., 2022. Environmental DNA (eDNA) as a tool for assessing fish biomass: A review of approaches and future considerations for resource surveys. *Environmental DNA* 4, 9–33. <https://doi.org/10.1002/edn3.185>
- Ruppert, K.M., Kline, R.J., Rahman, M.S., 2019. Past, present, and future perspectives of environmental DNA (eDNA) metabarcoding: A systematic review in methods, monitoring, and applications of global eDNA. *Global Ecology and Conservation* 17, e00547. <https://doi.org/10.1016/j.gecco.2019.e00547>
- Siebert, S., Anton-Erxleben, F., Kiko, R., Kramer, M., 2009. *Sympagohydra tuuli* (Cnidaria, Hydrozoa): first report from sea ice of the central Arctic Ocean and insights into histology, reproduction and locomotion. *Mar Biol* 156, 541–554. <https://doi.org/10.1007/s00227-008-1106-9>
- Sinniger, F., Pawlowski, J., Harii, S., Gooday, A.J., Yamamoto, H., Chevaldonné, P., Cedhagen, T., Carvalho, G., Creer, S., 2016. Worldwide Analysis of Sedimentary DNA Reveals Major Gaps in Taxonomic Knowledge of Deep-Sea Benthos. *Frontiers in Marine Science* 3.

- Smith, M.M., Angot, H., Chamberlain, E.J., Droste, E.S., Karam, S., Muilwijk, M., Webb, A.L., Archer, S.D., Beck, I., Blomquist, B.W., Bowman, J., Boyer, M., Bozzato, D., Chierici, M., Creamean, J., D'Angelo, A., Delille, B., Fer, I., Fong, A.A., Fransson, A., Fuchs, N., Gardner, J., Granskog, M.A., Hoppe, C.J.M., Hoppema, M., Hoppmann, M., Mock, T., Muller, S., Müller, O., Nicolaus, M., Nomura, D., Petäjä, T., Salganik, E., Schmale, J., Schmidt, K., Schulz, K.M., Shupe, M.D., Stefels, J., Thielke, L., Tippenhauer, S., Ulfso, A., Van Leeuwe, M., Webster, M., Yoshimura, M., Zhan, L., 2023. Thin and transient meltwater layers and false bottoms in the Arctic sea ice pack—Recent insights on these historically overlooked features. *Elem Sci Anth* 11, 00025. <https://doi.org/10.1525/elementa.2023.00025>
- Søreide, J.E., Leu, E., Berge, J., Graeve, M., Falk-Petersen, S., 2010. Timing of blooms, algal food quality and *Calanus glacialis* reproduction and growth in a changing Arctic. *Global Change Biology* 16, 3154–3163. <https://doi.org/10.1111/j.1365-2486.2010.02175.x>
- Strong, C., 2012. Atmospheric influence on Arctic marginal ice zone position and width in the Atlantic sector, February–April 1979–2010. *Clim Dyn* 39, 3091–3102. <https://doi.org/10.1007/s00382-012-1356-6>
- Strong, C., Rigor, I.G., 2013. Arctic marginal ice zone trending wider in summer and narrower in winter. *Geophysical Research Letters* 40, 4864–4868. <https://doi.org/10.1002/grl.50928>
- Suter, L., Polanowski, A.M., Clarke, L.J., Kitchener, J.A., Deagle, B.E., 2021. Capturing open ocean biodiversity: Comparing environmental DNA metabarcoding to the continuous plankton recorder. *Molecular Ecology* 30, 3140–3157. <https://doi.org/10.1111/mec.15587>
- Tang, C.Q., Leasi, F., Obertegger, U., Kieneke, A., Barraclough, T.G., Fontaneto, D., 2012. The widely used small subunit 18S rDNA molecule greatly underestimates true diversity in biodiversity surveys of the meiofauna. *Proceedings of the National Academy of Sciences* 109, 16208–16212. <https://doi.org/10.1073/pnas.1209160109>
- Tsubouchi, T., Appen, W.-J. von, Kanzow, T., Steur, L. de, 2023. Temporal Variability of the Overturning Circulation in the Arctic Ocean and the Associated Heat and Freshwater Transports during 2004–10. *Journal of Physical Oceanography* 54, 81–94. <https://doi.org/10.1175/JPO-D-23-0056.1>
- Vipindas, P.V., Venkatachalam, S., Jabir, T., Yang, E.J., Cho, K.-H., Jung, J., Lee, Y., Krishnan, K.P., 2023. Water Mass Controlled Vertical Stratification of Bacterial and Archaeal Communities in the Western Arctic Ocean During Summer Sea-Ice Melting. *Microb Ecol* 85, 1150–1163. <https://doi.org/10.1007/s00248-022-01992-z>
- Wangensteen, O.S., Cebrian, E., Palacín, C., Turon, X., 2018a. Under the canopy: Community-wide effects of invasive algae in Marine Protected Areas revealed by metabarcoding. *Marine Pollution Bulletin* 127, 54–66. <https://doi.org/10.1016/j.marpolbul.2017.11.033>
- Wangensteen, O.S., Palacín, C., Guardiola, M., Turon, X., 2018b. DNA metabarcoding of littoral hard-bottom communities: high diversity and database gaps revealed by two molecular markers. *PeerJ* 6, e4705. <https://doi.org/10.7717/peerj.4705>
- Weydmann, A., Carstensen, J., Goszczko, I., Dmoch, K., Olszewska, A., Kwasniewski, S., 2014. Shift towards the dominance of boreal species in the Arctic: inter-annual and spatial zooplankton variability in the West Spitsbergen Current. *Marine Ecology Progress Series* 501, 41–52.
- Weydmann-Zwolicka, A., Dąbrowska, A.M., Mioduchowska, M., Zwolicki, A., 2024. Comparison of DNA metabarcoding and microscopy in analysing planktonic protists from the European Arctic. *Mar. Biodivers.* 54, 44. <https://doi.org/10.1007/s12526-024-01436-6>
- Wickham, H., 2016. *ggplot2: Elegant Graphics for Data Analysis*.
- Wu, S., Xiong, J., Yu, Y., 2015. Taxonomic Resolutions Based on 18S rRNA Genes: A Case Study of Subclass Copepoda. *PLOS ONE* 10, e0131498. <https://doi.org/10.1371/journal.pone.0131498>

Xu, D., Kong, H., Yang, E.-J., Li, X., Jiao, N., Warren, A., Wang, Y., Lee, Y., Jung, J., Kang, S.-H., 2020. Contrasting Community Composition of Active Microbial Eukaryotes in Melt Ponds and Sea Water of the Arctic Ocean Revealed by High Throughput Sequencing. *Front. Microbiol.* 11. <https://doi.org/10.3389/fmicb.2020.01170>

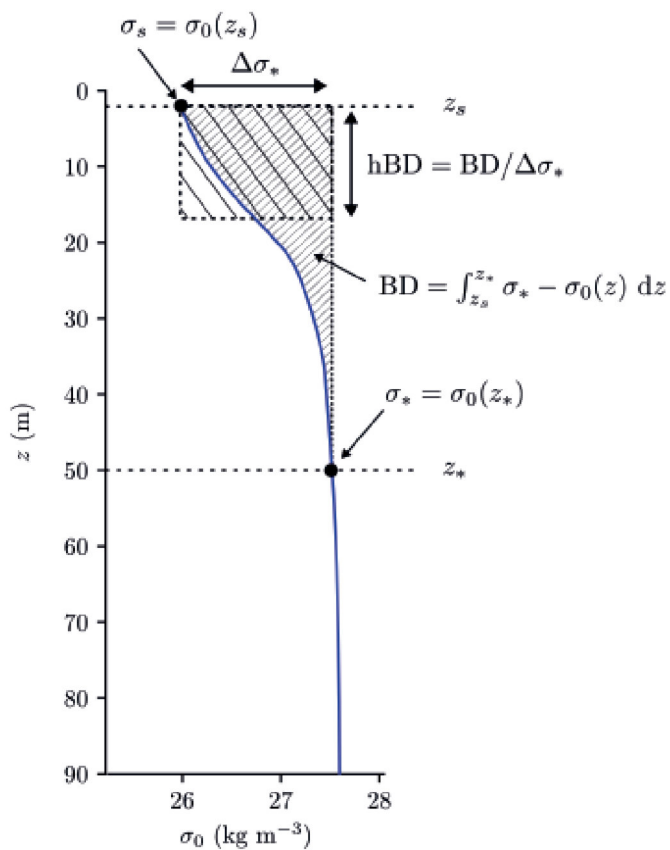


Figure S1. Schematic of parameters used for describing the meltwater stratification in the upper ocean. Diagram is adapted from Randelhoff et al. (2017). The blue line shows a representative density profile. The buoyancy deficit (BD) is given by the integrated density deviation relative to a reference density (σ_*), and the equivalent mixed layer depth h_{BD} is obtained by dividing BD through the density deviation at the surface ($\Delta\sigma_*$). z_s refers to the surface depth (3 M) and z_* refers to the reference depth (50 m).

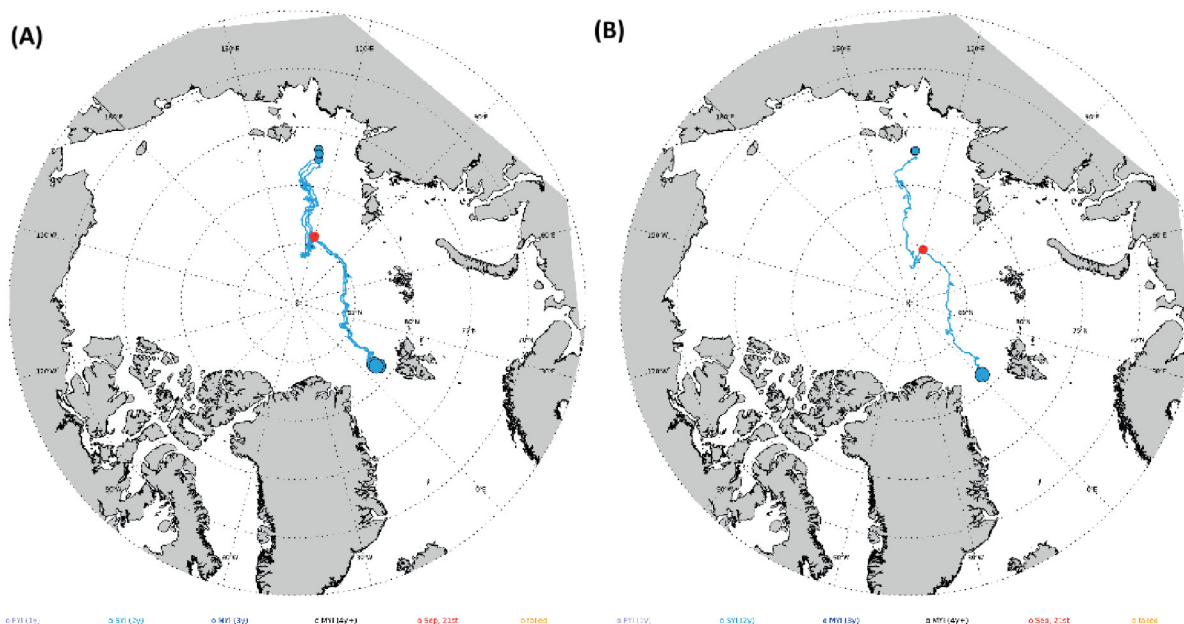


Figure S2. Tracks of ice floe trajectory two years before sampling date. (A) the eight ice floes named FN, FM and FS. (B) Track of ice floe F24_1.

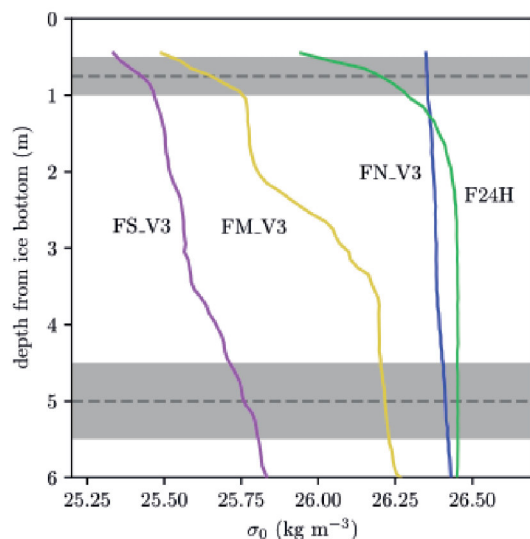
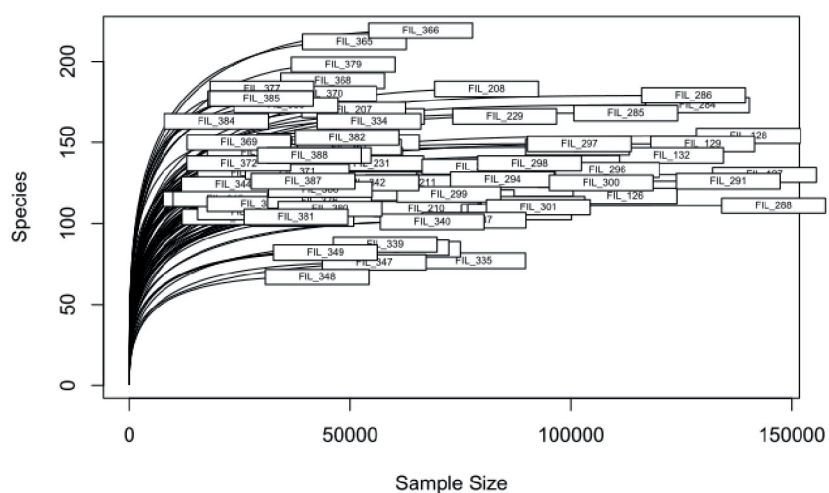


Figure S3. Representative under-ice CTD density profiles for each of the four ice floes sampled. The depth from the bottom of the ice is measure on the y axis and density on the x-axis. Horizontal dashed lines indicate eDNA sampling points. Grey shaded areas indicated the range of sampling points used to calculate mean temperature and salinity at 0 m and 5 m.

(A)



(B)

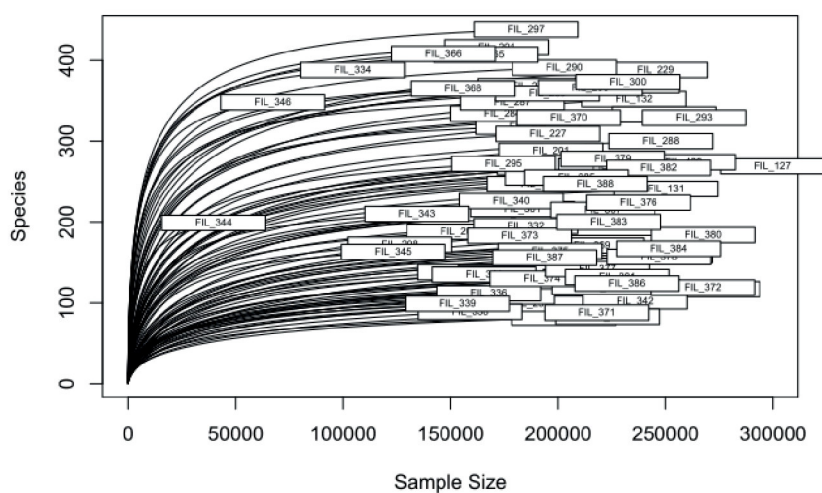


Figure S4. Rarefaction curves based on raw MOTU and ASV datasets. (A) COI samples and (B) 18s samples.

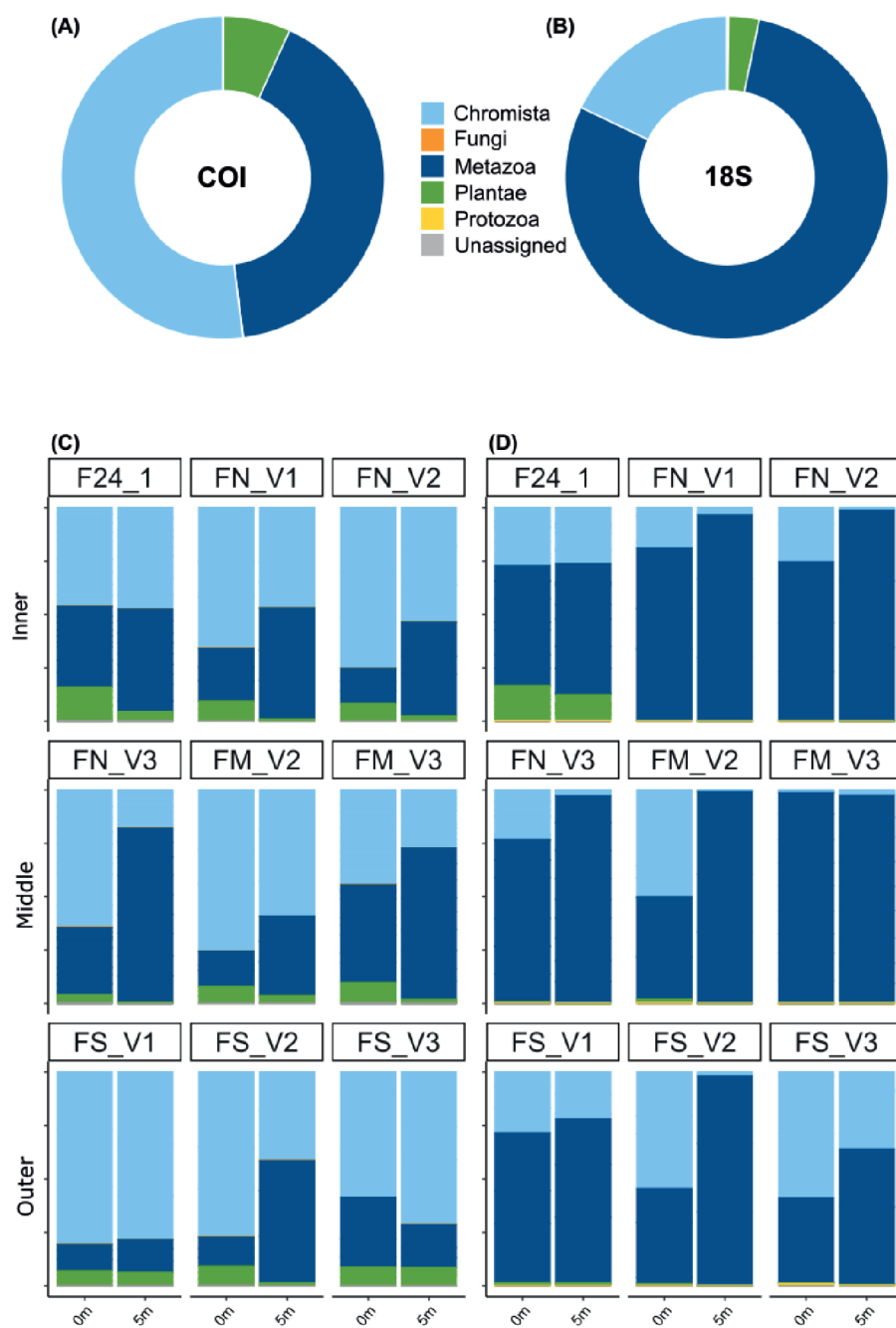


Fig S5. Proportion of reads assigned to Eukaryote kingdoms for each marker. (A) COI gene and (B) 18S gene with all sampling sites and samples combined. (C) RRAs at 0 m and 5 m at each individual ice floe station for COI and (D) for 18S.

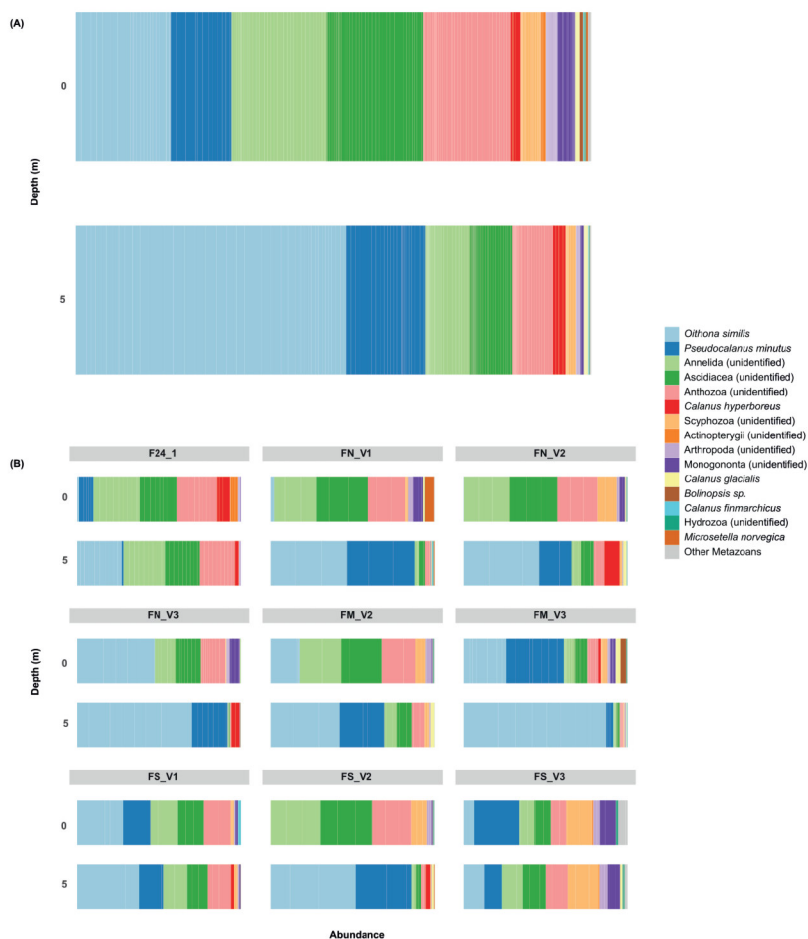


Figure S6. Relative read abundances (%) of the most abundant metazoans in the COI dataset. The MOTUs are collapsed at species level where possible and the highest resolution taxonomic level possible when not.

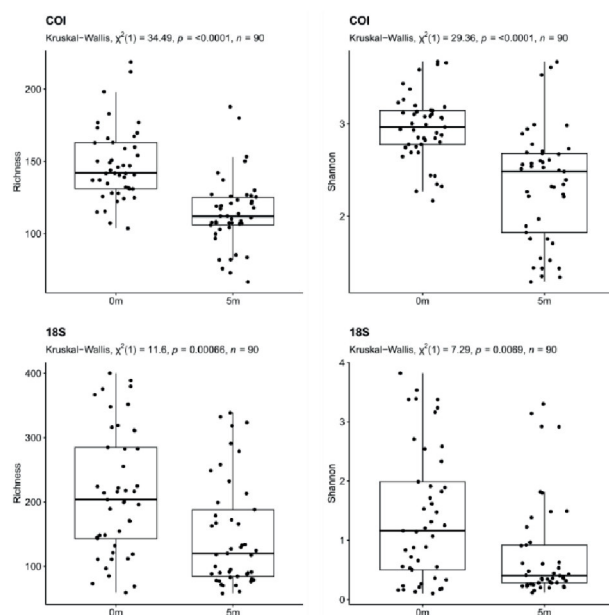


Figure S7. Levels of alpha diversity at the two sampling depths. (A) rarefied MOTU richness and (B) Shannon Diversity in the COI dataset, (C) rarefied ASV richness and (D) Shannon Diversity in the 18S dataset and results of Kruskal-Wallis tests (non-parametric ANOVA). All sampling sites and samples combined per depth.

Table S1. Characteristics of sampling sites where eDNA and corresponding environmental data were collected during the present study.

Sample name	Ice Floe	Depth (m)	Lon (decimal)	Lat (decimal)	SIC %	DIST SIC (km)	Depth seafloor (m)	BD (kg/m ²)	hBD (m)	Ice thickness (modal, m)	Temp (°C)	Salinity (psu)	Density (kg/m ³)
FIL_121	FN_V1	0	6.813	81.596	68.06	129.596	-485	14.566	21.503	2.1	-1.446	33.358	26.713
FIL_122	FN_V1	0	6.813	81.596	68.06	129.596	-485	14.566	21.503	2.1	-1.446	33.358	26.713
FIL_123	FN_V1	0	6.813	81.596	68.06	129.596	-485	14.566	21.503	2.1	-1.446	33.358	26.713
FIL_124	FN_V1	5	6.813	81.596	68.06	129.596	-485	14.566	21.503	2.1	-1.562	33.74	27.024
FIL_125	FN_V1	5	6.813	81.596	68.06	129.596	-485	14.566	21.503	2.1	-1.562	33.74	27.024
FIL_126	FN_V1	5	6.813	81.596	68.06	129.596	-485	14.566	21.503	2.1	-1.562	33.74	27.024
FIL_127	FS_V1	0	7.728	81.183	72.34	84.331	-727	11.616	15.298	1.4	-1.582	33.382	26.736
FIL_128	FS_V1	0	7.728	81.183	72.34	84.331	-727	11.616	15.298	1.4	-1.582	33.382	26.736
FIL_129	FS_V1	0	7.728	81.183	72.34	84.331	-727	11.616	15.298	1.4	-1.582	33.382	26.736
FIL_130	FS_V1	5	7.728	81.183	72.34	84.331	-727	11.616	15.298	1.4	-1.569	33.485	26.819
FIL_131	FS_V1	5	7.728	81.183	72.34	84.331	-727	11.616	15.298	1.4	-1.569	33.485	26.819
FIL_132	FS_V1	5	7.728	81.183	72.34	84.331	-727	11.616	15.298	1.4	-1.569	33.485	26.819
FIL_199	FN_V2	0	4.779	81.501	75.4	81.357	-740	17.217	17.486	1.7	-1.464	32.973	26.402
FIL_200	FN_V2	0	4.779	81.501	75.4	81.357	-740	17.217	17.486	1.7	-1.464	32.973	26.402
FIL_201	FN_V2	0	4.779	81.501	75.4	81.357	-740	17.217	17.486	1.7	-1.464	32.973	26.402
FIL_202	FN_V2	5	4.779	81.501	75.4	81.357	-740	17.217	17.486	1.7	-1.464	33.127	26.527
FIL_203	FN_V2	5	4.779	81.501	75.4	81.357	-740	17.217	17.486	1.7	-1.464	33.127	26.527
FIL_204	FN_V2	5	4.779	81.501	75.4	81.357	-740	17.217	17.486	1.7	-1.464	33.127	26.527
FIL_206	FS_V2	0	5.425	81.189	70.44	39.341	-667	14.112	12.142	1.3	-1.539	32.541	26.056
FIL_207	FS_V2	0	5.425	81.189	70.44	39.341	-667	14.112	12.142	1.3	-1.539	32.541	26.056
FIL_208	FS_V2	0	5.425	81.189	70.44	39.341	-667	14.112	12.142	1.3	-1.539	32.541	26.056
FIL_209	FS_V2	5	5.425	81.189	70.44	39.341	-667	14.112	12.142	1.3	-1.492	33.026	26.446
FIL_210	FS_V2	5	5.425	81.189	70.44	39.341	-667	14.112	12.142	1.3	-1.492	33.026	26.446
FIL_211	FS_V2	5	5.425	81.189	70.44	39.341	-667	14.112	12.142	1.3	-1.492	33.026	26.446
FIL_227	FM_V2	0	5.127	81.351	70.65	67.34	-820	14.478	11.188	1.2	-1.462	32.467	25.994
FIL_228	FM_V2	0	5.127	81.351	70.65	67.34	-820	14.478	11.188	1.2	-1.462	32.467	25.994
FIL_229	FM_V2	0	5.127	81.351	70.65	67.34	-820	14.478	11.188	1.2	-1.462	32.467	25.994
FIL_230	FM_V2	5	5.127	81.351	70.65	67.34	-820	14.478	11.188	1.2	-1.417	32.946	26.379
FIL_231	FM_V2	5	5.127	81.351	70.65	67.34	-820	14.478	11.188	1.2	-1.417	32.946	26.379
FIL_232	FM_V2	5	5.127	81.351	70.65	67.34	-820	14.478	11.188	1.2	-1.417	32.946	26.379
FIL_284	F24_1	0	1.286	81.325	81.33	99.959	-1469	24.386	25.43	1.7	-1.576	32.696	26.182
FIL_285	F24_1	0	1.286	81.325	81.33	99.959	-1469	24.386	25.43	1.7	-1.576	32.696	26.182
FIL_286	F24_1	0	1.286	81.325	81.33	99.959	-1469	24.386	25.43	1.7	-1.576	32.696	26.182
FIL_287	F24_1	5	1.286	81.325	81.33	99.959	-1469	24.386	25.43	1.7	-1.598	33.031	26.453
FIL_288	F24_1	5	1.286	81.325	81.33	99.959	-1469	24.386	25.43	1.7	-1.598	33.031	26.453
FIL_289	F24_1	5	1.286	81.325	81.33	99.959	-1469	24.386	25.43	1.7	-1.598	33.031	26.453
FIL_296	F24_1	0	1.286	81.325	81.33	99.959	-1469	24.386	25.43	1.7	-1.595	32.696	26.182
FIL_297	F24_1	0	1.286	81.325	81.33	99.959	-1469	24.386	25.43	1.7	-1.595	32.696	26.182
FIL_298	F24_1	0	1.286	81.325	81.33	99.959	-1469	24.386	25.43	1.7	-1.595	32.696	26.182
FIL_299	F24_1	5	1.286	81.325	81.33	99.959	-1469	24.386	25.43	1.7	-1.597	33.031	26.453
FIL_300	F24_1	5	1.286	81.325	81.33	99.959	-1469	24.386	25.43	1.7	-1.597	33.031	26.453
FIL_301	F24_1	5	1.286	81.325	81.33	99.959	-1469	24.386	25.43	1.7	-1.597	33.031	26.453
FIL_332	FN_V3	0	2.36	81.179	67.6	86.451	-1031	17.705	16.472	1.5	-1.544	32.917	26.359
FIL_333	FN_V3	0	2.36	81.179	67.6	86.451	-1031	17.705	16.472	1.5	-1.544	32.917	26.359
FIL_334	FN_V3	0	2.36	81.179	67.6	86.451	-1031	17.705	16.472	1.5	-1.544	32.917	26.359
FIL_335	FN_V3	5	2.36	81.179	67.6	86.451	-1031	17.705	16.472	1.5	-1.529	32.97	26.402
FIL_336	FN_V3	5	2.36	81.179	67.6	86.451	-1031	17.705	16.472	1.5	-1.529	32.97	26.402
FIL_337	FN_V3	5	2.36	81.179	67.6	86.451	-1031	17.705	16.472	1.5	-1.529	32.97	26.402
FIL_341	FN_V3	0	2.36	81.179	67.6	86.451	-1031	17.705	16.472	1.5	-1.541	32.914	26.357
FIL_342	FN_V3	0	2.36	81.179	67.6	86.451	-1031	17.705	16.472	1.5	-1.541	32.914	26.357
FIL_343	FN_V3	0	2.36	81.179	67.6	86.451	-1031	17.705	16.472	1.5	-1.541	32.914	26.357
FIL_338	FN_V3	5	2.36	81.179	67.6	86.451	-1031	17.705	16.472	1.5	-1.53	33.002	26.427
FIL_339	FN_V3	5	2.36	81.179	67.6	86.451	-1031	17.705	16.472	1.5	-1.53	33.002	26.427
FIL_340	FN_V3	5	2.36	81.179	67.6	86.451	-1031	17.705	16.472	1.5	-1.53	33.002	26.427
FIL_344	FN_V3	0	2.36	81.179	67.6	86.451	-1031	17.705	16.472	1.5	-1.529	32.91	26.353
FIL_345	FN_V3	0	2.36	81.179	67.6	86.451	-1031	17.705	16.472	1.5	-1.529	32.91	26.353
FIL_346	FN_V3	0	2.36	81.179	67.6	86.451	-1031	17.705	16.472	1.5	-1.529	32.91	26.353
FIL_347	FN_V3	5	2.36	81.179	67.6	86.451	-1031	17.705	16.472	1.5	-1.529	32.984	26.413
FIL_348	FN_V3	5	2.36	81.179	67.6	86.451	-1031	17.705	16.472	1.5	-1.529	32.984	26.413
FIL_349	FN_V3	5	2.36	81.179	67.6	86.451	-1031	17.705	16.472	1.5	-1.529	32.984	26.413
FIL_365	FS_V3	0	3.784	80.927	57.7	50.827	-721	29.098	14.454	1	-1.554	31.753	25.42
FIL_366	FS_V3	0	3.784	80.927	57.7	50.827	-721	29.098	14.454	1	-1.554	31.753	25.42
FIL_367	FS_V3	0	3.784	80.927	57.7	50.827	-721	29.098	14.454	1	-1.554	31.753	25.42
FIL_368	FS_V3	5	3.784	80.927	57.7	50.827	-721	29.098	14.454	1	-1.52	32.182	25.765
FIL_369	FS_V3	5	3.784	80.927	57.7	50.827	-721	29.098	14.454	1	-1.52	32.182	25.765
FIL_370	FS_V3	5	3.784	80.927	57.7	50.827	-721	29.098	14.454	1	-1.52	32.182	25.765
FIL_371	FM_V3	0	2.123	81.069	63.35	80.106	-1136	20.971	15.015	1.1	-1.427	32.228	25.801
FIL_372	FM_V3	0	2.123	81.069	63.35	80.106	-1136	20.971	15.015	1.1	-1.427	32.228	25.801
FIL_373	FM_V3	0	2.123	81.069	63.35	80.106	-1136	20.971	15.015	1.1	-1.427	32.228	25.801
FIL_374	FM_V3	5	2.123	81.069	63.35	80.106	-1136	20.971	15.015	1.1	-1.408	32.769	26.237
FIL_375	FM_V3	5	2.123	81.069	63.35	80.106	-1136	20.971	15.015	1.1	-1.408	32.769	26.237
FIL_376	FM_V3	5	2.123	81.069	63.35	80.106	-1136	20.971	15.015	1.1	-1.408	32.769	26.237
FIL_383	FM_V3	0	2.123	81.069	63.35	80.106	-1136	20.971	15.015	1.1	-1.426	32.032	25.642
FIL_384	FM_V3	0	2.123	81.069	63.35	80.106	-1136	20.971	15.015	1.1	-1.426	32.032	25.642
FIL_385	FM_V3	0	2.123	81.069	63.35	80.106	-1136	20.971	15.015	1.1	-1.426	32.032	25.642
FIL_386	FM_V3	5	2.123	81.069	63.35	80.106	-1136	20.971	15.015	1.1	-1.382	32.746	26.217

FIL_387	FM_V3	5	2.123	81.069	63.35	80.106	-1136	20.971	15.015	1.1	-1.382	32.746	26.217
FIL_388	FM_V3	5	2.123	81.069	63.35	80.106	-1136	20.971	15.015	1.1	-1.382	32.746	26.217

Table S3. Number of unique taxa at each taxonomic level

	Kingdom	Phylum	Class	Order	Family	Genus	Species
COI	4	25	45	40	39	35	21
18s	4	20	40	75	-	-	-

Table S4. Top 15 MOTUs and ASVs by relative abundance

MOTU_name	RRA	Kingdom	Phylum	Class	Order	Family	Genus	Species
Oithona similis_2	18.74%	Metazoa	Arthropoda	Copepoda	Cyclopoida	Oithonidae	<i>Oithona</i>	<i>Oithona similis</i>
Chaetocerotaceae	11.39%	Chromista	Bacillariophyta	Coscinodiscophyceae	Chaetocerotales	Chaetocerotaceae	-	-
Pseudocalanus minutus	7.49%	Metazoa	Arthropoda	Copepoda	Calanoida	Clausocalanidae	<i>Pseudocalanus</i>	<i>Pseudocalanus minutus</i>
Phaeocystales	5.19%	Chromista	Haptophyta	Coccolithophyceae	Phaeocystales	-	-	-
Annelida_4	4.05%	Metazoa	Annelida	-	-	-	-	-
Asciacea_2	4.00%	Metazoa	Chordata	Asciacea	-	-	-	-
Skeletonemataceae	3.87%	Chromista	Heterokontophyta	Mediophyceae	Thalassiosirales	Skeletonemataceae	-	-
Anthozoa_3	3.72%	Metazoa	Cnidaria	Anthozoa	-	-	-	-
Dinophyceae_22	3.62%	Chromista	Myzozoa	Dinophyceae	-	-	-	-
Chlorophyta	3.57%	Plantae	Chlorophyta	-	-	-	-	-
Heterokontophyta_13	3.52%	Chromista	Heterokontophyta	-	-	-	-	-
Heterokontophyta_12	2.75%	Chromista	Heterokontophyta	-	-	-	-	-
Phaeophyceae_74	2.23%	Chromista	Ochrophyta	Phaeophyceae	-	-	-	-
Phaeophyceae_73	2.20%	Chromista	Ochrophyta	Phaeophyceae	-	-	-	-
Heterokontophyta_11	2.07%	Chromista	Heterokontophyta	-	-	-	-	-
ASV Name	RRA	Kingdom	Phylum	Class	Order	Family	Genus	Species
ASV_1	71.49%	Metazoa	Arthropoda	Copepoda	Calanoida	Calanidae	-	-
ASV_3	2.97%	Metazoa	Arthropoda	Copepoda	Calanoida	Calanidae	-	-
ASV_5	2.93%	Chromista	Myzozoa	Dinophyceae	Gymnodiniales	Gymnodiniaceae	Gyrodinium	-
ASV_6	2.50%	Chromista	Myzozoa	Dinophyceae	Gymnodiniales	Gymnodiniaceae	Gyrodinium	-
ASV_4	2.45%	Plantae	Chlorophyta	Mamiellophyceae	Mamiellales	Mamiellaceae	Micromonas	-
ASV_7	1.55%	Chromista	Myzozoa	Dinophyceae	Gymnodiniales	Gymnodiniaceae	Gyrodinium	-
ASV_8	1.27%	Chromista	Heterokontophyta	Bacillariophyceae	Bacillariales	Bacillariaceae	Pseudonitzschia	-
ASV_9	1.26%	Chromista	Myzozoa	Dinophyceae	Gymnodiniales	Gymnodiniaceae	Gyrodinium	-
ASV_10	1.05%	Chromista	Myzozoa	Dinophyceae	-	-	-	-
ASV_11	0.65%	Chromista	Heterokontophyta	Bacillariophyceae	Coscinodiscales	Coscinodiscaceae	Coscinodiscus	-
ASV_14	0.56%	Chromista	Myzozoa	Dinophyceae	Gymnodiniales	Gymnodiniaceae	Gyrodinium	-
ASV_15	0.01%	Chromista	Myzozoa	Dinophyceae	Suessiales	Biecheleriaceae	Biecheleria	-
ASV_13	0.01%	Metazoa	Arthropoda	Copepoda	Calanoida	Calanidae	-	-
ASV_12	0.01%	Chromista	Heterokontophyta	Bacillariophyceae	Thalassiosirales	Thalassiosiraceae	Thalassiosira	-
ASV_16	0.01%	Metazoa	Arthropoda	Copepoda	Cyclopoida	Oithonidae	-	-

Table S5. Taxonomic information of all ASVs recovered with the 18S gene.□

ASV_name	Kingdom	Phylum	Class	Order	Family	Genus
ASV_123	Chromista	Bigyra	Labyrinthulea	Thraustochytrida	NA	NA
ASV_1451	Chromista	Bigyra	Labyrinthulea	Thraustochytrida	Thraustochytriaceae	Schizochytrium
ASV_1485	Chromista	Bigyra	Labyrinthulea	Thraustochytrida	Thraustochytriaceae	Thraustochytrium
ASV_1676	Chromista	Bigyra	Labyrinthulea	Thraustochytrida	NA	NA
ASV_282	Chromista	Bigyra	Labyrinthulea	Thraustochytrida	NA	NA
ASV_649	Chromista	Bigyra	Labyrinthulea	Thraustochytrida	NA	NA
ASV_678	Chromista	Bigyra	Labyrinthulea	Thraustochytrida	Thraustochytriaceae	Oblongichytrium
ASV_873	Chromista	Bigyra	Labyrinthulea	Thraustochytrida	Thraustochytriaceae	Oblongichytrium
ASV_1026	Chromista	Cercozoa	Imbricatea	NA	NA	NA
ASV_1042	Chromista	Cercozoa	Imbricatea	NA	NA	NA
ASV_1129	Chromista	Cercozoa	Imbricatea	Thaumatomonadida	Esquamulidae	Esquamula
ASV_1136	Chromista	Cercozoa	Imbricatea	NA	NA	NA
ASV_1612	Chromista	Cercozoa	Imbricatea	Thaumatomonadida	Thaumatomastigidae	Reckertia
ASV_556	Chromista	Cercozoa	Imbricatea	Thaumatomonadida	Thaumatomastigidae	Reckertia
ASV_617	Chromista	Cercozoa	Imbricatea	Thaumatomonadida	Thaumatomastigidae	Reckertia
ASV_647	Chromista	Cercozoa	Imbricatea	Thaumatomonadida	Esquamulidae	Esquamula
ASV_660	Chromista	Cercozoa	Imbricatea	Thaumatomonadida	Thaumatomastigidae	Reckertia
ASV_693	Chromista	Cercozoa	Imbricatea	Thaumatomonadida	Esquamulidae	Esquamula
ASV_703	Chromista	Cercozoa	Imbricatea	Thaumatomonadida	Esquamulidae	Esquamula
ASV_738	Chromista	Cercozoa	Imbricatea	Thaumatomonadida	Esquamulidae	Esquamula
ASV_744	Chromista	Cercozoa	Imbricatea	NA	NA	NA
ASV_831	Chromista	Cercozoa	Imbricatea	Thaumatomonadida	Esquamulidae	Esquamula
ASV_862	Chromista	Cercozoa	Imbricatea	Thaumatomonadida	Thaumatomastigidae	Reckertia
ASV_895	Chromista	Cercozoa	Imbricatea	Thaumatomonadida	Thaumatomastigidae	Reckertia
ASV_995	Chromista	Cercozoa	Imbricatea	Thaumatomonadida	Esquamulidae	Esquamula
ASV_1509	Chromista	Cercozoa	Monadofilosa_EXT	Monadofilosa_EXT	Monadofilosa_EXT	Quadrifilia
ASV_336	Chromista	Cercozoa	Monadofilosa_EXT	Monadofilosa_EXT	Monadofilosa_EXT	Quadrifilia
ASV_1160	Chromista	Cercozoa	NA	NA	NA	NA
ASV_121	Chromista	Cercozoa	NA	NA	NA	NA
ASV_1314	Chromista	Cercozoa	NA	NA	NA	NA
ASV_1396	Chromista	Cercozoa	NA	NA	NA	NA
ASV_1453	Chromista	Cercozoa	NA	NA	NA	NA
ASV_1511	Chromista	Cercozoa	NA	NA	NA	NA
ASV_198	Chromista	Cercozoa	NA	NA	NA	NA
ASV_531	Chromista	Cercozoa	NA	NA	NA	NA
ASV_544	Chromista	Cercozoa	NA	NA	NA	NA
ASV_613	Chromista	Cercozoa	NA	NA	NA	NA
ASV_743	Chromista	Cercozoa	NA	NA	NA	NA
ASV_861	Chromista	Cercozoa	NA	NA	NA	NA
ASV_893	Chromista	Cercozoa	NA	NA	NA	NA
ASV_908	Chromista	Cercozoa	NA	NA	NA	NA
ASV_972	Chromista	Cercozoa	NA	NA	NA	NA
ASV_1039	Chromista	Cercozoa	Thecofilosea	Cryomonadida	Protaspidae	Protaspis
ASV_1050	Chromista	Cercozoa	Thecofilosea	Cryomonadida	Protaspidae	Protaspis
ASV_1090	Chromista	Cercozoa	Thecofilosea	Cryomonadida	Protaspidae	Protaspis
ASV_1148	Chromista	Cercozoa	Thecofilosea	Cryomonadida	Protaspidae	Protaspis
ASV_1159	Chromista	Cercozoa	Thecofilosea	NA	NA	NA
ASV_1168	Chromista	Cercozoa	Thecofilosea	Cryomonadida	Protaspidae	Protaspis
ASV_1171	Chromista	Cercozoa	Thecofilosea	NA	NA	NA
ASV_1191	Chromista	Cercozoa	Thecofilosea	Cryomonadida	Protaspidae	Protaspis
ASV_1245	Chromista	Cercozoa	Thecofilosea	Cryomonadida	Protaspidae	Protaspis
ASV_1260	Chromista	Cercozoa	Thecofilosea	Cryomonadida	Protaspidae	Protaspis
ASV_1344	Chromista	Cercozoa	Thecofilosea	NA	NA	NA
ASV_1375	Chromista	Cercozoa	Thecofilosea	NA	NA	NA
ASV_1395	Chromista	Cercozoa	Thecofilosea	Thecofilosea_incertae_sedis	Thecofilosea_incertae_sedis	Mataza
ASV_1501	Chromista	Cercozoa	Thecofilosea	Thecofilosea_incertae_sedis	Thecofilosea_incertae_sedis	Mataza
ASV_1514	Chromista	Cercozoa	Thecofilosea	NA	NA	NA
ASV_1530	Chromista	Cercozoa	Thecofilosea	NA	NA	NA
ASV_155	Chromista	Cercozoa	Thecofilosea	NA	NA	NA
ASV_1576	Chromista	Cercozoa	Thecofilosea	Cryomonadida	Protaspidae	Protaspis
ASV_158	Chromista	Cercozoa	Thecofilosea	Cryomonadida	Protaspidae	Protaspis
ASV_1615	Chromista	Cercozoa	Thecofilosea	Cryomonadida	Protaspidae	Protaspis
ASV_186	Chromista	Cercozoa	Thecofilosea	Cryomonadida	Protaspidae	Protaspis
ASV_188	Chromista	Cercozoa	Thecofilosea	Cryomonadida	Protaspidae	Protaspis
ASV_194	Chromista	Cercozoa	Thecofilosea	Cryomonadida	Protaspidae	Protaspis
ASV_234	Chromista	Cercozoa	Thecofilosea	Cryomonadida	Protaspidae	Protaspis
ASV_237	Chromista	Cercozoa	Thecofilosea	NA	NA	NA
ASV_239	Chromista	Cercozoa	Thecofilosea	Cryomonadida	Protaspidae	Protaspis
ASV_243	Chromista	Cercozoa	Thecofilosea	NA	NA	NA
ASV_247	Chromista	Cercozoa	Thecofilosea	Cryomonadida	Protaspidae	Protaspis
ASV_249	Chromista	Cercozoa	Thecofilosea	NA	NA	NA
ASV_25	Chromista	Cercozoa	Thecofilosea	NA	NA	NA
ASV_260	Chromista	Cercozoa	Thecofilosea	Cryomonadida	Protaspidae	Protaspis
ASV_264	Chromista	Cercozoa	Thecofilosea	Cryomonadida	Protaspidae	Protaspis
ASV_305	Chromista	Cercozoa	Thecofilosea	Thecofilosea_incertae_sedis	Thecofilosea_incertae_sedis_EXT	Mataza
ASV_319	Chromista	Cercozoa	Thecofilosea	Cryomonadida	Protaspidae	Protaspis
ASV_32	Chromista	Cercozoa	Thecofilosea	Cryomonadida	Protaspidae	Protaspis
ASV_324	Chromista	Cercozoa	Thecofilosea	Cryomonadida	Protaspidae	Protaspis
ASV_329	Chromista	Cercozoa	Thecofilosea	NA	NA	NA
ASV_337	Chromista	Cercozoa	Thecofilosea	Cryomonadida	Protaspidae	Protaspis
ASV_361	Chromista	Cercozoa	Thecofilosea	Cryomonadida	Protaspidae	Protaspis
ASV_364	Chromista	Cercozoa	Thecofilosea	Cryomonadida	Protaspidae	Protaspis
ASV_422	Chromista	Cercozoa	Thecofilosea	NA	NA	NA
ASV_430	Chromista	Cercozoa	Thecofilosea	NA	NA	NA
ASV_444	Chromista	Cercozoa	Thecofilosea	Cryomonadida	Protaspidae	Protaspis
ASV_452	Chromista	Cercozoa	Thecofilosea	NA	NA	NA

ASV_461	Chromista	Cercozoa	Thecofilosea	Cryomonadida	Protaspidae	Protaspis
ASV_464	Chromista	Cercozoa	Thecofilosea	Cryomonadida	Protaspidae	Protaspis
ASV_47	Chromista	Cercozoa	Thecofilosea	Cryomonadida	Protaspidae	Protaspis
ASV_470	Chromista	Cercozoa	Thecofilosea	Cryomonadida	Protaspidae	Protaspis
ASV_478	Chromista	Cercozoa	Thecofilosea	Cryomonadida	Protaspidae	Protaspis
ASV_502	Chromista	Cercozoa	Thecofilosea	Cryomonadida	Protaspidae	Protaspis
ASV_505	Chromista	Cercozoa	Thecofilosea	Cryomonadida	Protaspidae	Protaspis
ASV_508	Chromista	Cercozoa	Thecofilosea	Cryomonadida	Protaspidae	Protaspis
ASV_526	Chromista	Cercozoa	Thecofilosea	Thecofilosea_incertae_sedis	Thecofilosea_incertae_sedis_EXT	Mataza
ASV_56	Chromista	Cercozoa	Thecofilosea	Cryomonadida	Protaspidae	Protaspis
ASV_585	Chromista	Cercozoa	Thecofilosea	Thecofilosea_incertae_sedis	Thecofilosea_incertae_sedis_EXT	Mataza
ASV_589	Chromista	Cercozoa	Thecofilosea	Thecofilosea_incertae_sedis	Thecofilosea_incertae_sedis_EXT	Mataza
ASV_594	Chromista	Cercozoa	Thecofilosea	NA	NA	NA
ASV_605	Chromista	Cercozoa	Thecofilosea	Cryomonadida	Protaspidae	Protaspis
ASV_621	Chromista	Cercozoa	Thecofilosea	Cryomonadida	Protaspidae	Protaspis
ASV_631	Chromista	Cercozoa	Thecofilosea	Cryomonadida	Protaspidae	Protaspis
ASV_658	Chromista	Cercozoa	Thecofilosea	Cryomonadida	Protaspidae	Protaspis
ASV_661	Chromista	Cercozoa	Thecofilosea	NA	NA	NA
ASV_683	Chromista	Cercozoa	Thecofilosea	Thecofilosea_incertae_sedis	Thecofilosea_incertae_sedis_EXT	Mataza
ASV_701	Chromista	Cercozoa	Thecofilosea	NA	NA	NA
ASV_725	Chromista	Cercozoa	Thecofilosea	Cryomonadida	Protaspidae	Protaspis
ASV_749	Chromista	Cercozoa	Thecofilosea	Cryomonadida	Protaspidae	Protaspis
ASV_789	Chromista	Cercozoa	Thecofilosea	NA	NA	NA
ASV_80	Chromista	Cercozoa	Thecofilosea	Cryomonadida	Protaspidae	Protaspis
ASV_804	Chromista	Cercozoa	Thecofilosea	Cryomonadida	Protaspidae	Protaspis
ASV_812	Chromista	Cercozoa	Thecofilosea	Thecofilosea_incertae_sedis	Thecofilosea_incertae_sedis_EXT	Mataza
ASV_852	Chromista	Cercozoa	Thecofilosea	NA	NA	NA
ASV_909	Chromista	Cercozoa	Thecofilosea	Cryomonadida	Protaspidae	Protaspis
ASV_928	Chromista	Cercozoa	Thecofilosea	NA	NA	NA
ASV_94	Chromista	Cercozoa	Thecofilosea	NA	NA	NA
ASV_958	Chromista	Cercozoa	Thecofilosea	NA	NA	NA
ASV_979	Chromista	Cercozoa	Thecofilosea	Cryomonadida	Protaspidae	Protaspis
ASV_993	Chromista	Cercozoa	Thecofilosea	Cryomonadida	Protaspidae	Protaspis
ASV_752	Chromista	Ciliophora	Heterotrichea	Heterotrichida	Peritromidae	Peritromus
ASV_1481	Chromista	Ciliophora	Litostomatea	Haptorida	Lacrymariidae	NA
ASV_307	Chromista	Ciliophora	Litostomatea	Pleurostomatida	Litonotidae	Loxophyllum
ASV_388	Chromista	Ciliophora	Litostomatea	Haptorida	Lacrymariidae	Phialina
ASV_420	Chromista	Ciliophora	Litostomatea	Haptorida	Didiniidae	Cyclotrichium
ASV_457	Chromista	Ciliophora	Litostomatea	Haptorida	Lacrymariidae	NA
ASV_578	Chromista	Ciliophora	Litostomatea	Haptorida	Lacrymariidae	Phialina
ASV_664	Chromista	Ciliophora	Litostomatea	Haptorida	Lacrymariidae	Phialina
ASV_728	Chromista	Ciliophora	Litostomatea	Haptorida	NA	NA
ASV_811	Chromista	Ciliophora	Litostomatea	Cyclotrichiida	Mesodiniidae	Mesodinium
ASV_92	Chromista	Ciliophora	Litostomatea	Haptorida	NA	NA
ASV_1212	Chromista	Ciliophora	NA	NA	NA	NA
ASV_146	Chromista	Ciliophora	NA	NA	NA	NA
ASV_1589	Chromista	Ciliophora	NA	NA	NA	NA
ASV_1608	Chromista	Ciliophora	NA	NA	NA	NA
ASV_1624	Chromista	Ciliophora	NA	NA	NA	NA
ASV_210	Chromista	Ciliophora	NA	NA	NA	NA
ASV_248	Chromista	Ciliophora	NA	NA	NA	NA
ASV_262	Chromista	Ciliophora	NA	NA	NA	NA
ASV_303	Chromista	Ciliophora	NA	NA	NA	NA
ASV_377	Chromista	Ciliophora	NA	NA	NA	NA
ASV_378	Chromista	Ciliophora	NA	NA	NA	NA
ASV_490	Chromista	Ciliophora	NA	NA	NA	NA
ASV_529	Chromista	Ciliophora	NA	NA	NA	NA
ASV_534	Chromista	Ciliophora	NA	NA	NA	NA
ASV_628	Chromista	Ciliophora	NA	NA	NA	NA
ASV_650	Chromista	Ciliophora	NA	NA	NA	NA
ASV_751	Chromista	Ciliophora	NA	NA	NA	NA
ASV_81	Chromista	Ciliophora	NA	NA	NA	NA
ASV_892	Chromista	Ciliophora	NA	NA	NA	NA
ASV_912	Chromista	Ciliophora	NA	NA	NA	NA
ASV_920	Chromista	Ciliophora	NA	NA	NA	NA
ASV_1650	Chromista	Ciliophora	Oligohymenophorea	Apostomatida	Pseudocolliniidae	Pseudocollinia
ASV_417	Chromista	Ciliophora	Oligohymenophorea	Philasterida	Uronematidae	Homalogastra
ASV_767	Chromista	Ciliophora	Oligohymenophorea	Philasterida	Uronematidae	Homalogastra
ASV_841	Chromista	Ciliophora	Oligohymenophorea	Philasterida	Uronematidae	Homalogastra
ASV_1044	Chromista	Ciliophora	Oligotrichea	Oligotrichida	Strombidiidae	NA
ASV_1089	Chromista	Ciliophora	Oligotrichea	Choreotrichida	Strombidinopsidae	Strombidinopsis
ASV_1138	Chromista	Ciliophora	Oligotrichea	Oligotrichida	Strombidiidae	Strombidium
ASV_1157	Chromista	Ciliophora	Oligotrichea	Oligotrichida	NA	NA
ASV_1207	Chromista	Ciliophora	Oligotrichea	Oligotrichida	Strombidiidae	Strombidium
ASV_130	Chromista	Ciliophora	Oligotrichea	Oligotrichida	Strombidiidae	Strombidium
ASV_136	Chromista	Ciliophora	Oligotrichea	Oligotrichida	Tontoniidae	Pseudotontonia
ASV_142	Chromista	Ciliophora	Oligotrichea	Choreotrichida	Strobiliidiidae	NA
ASV_144	Chromista	Ciliophora	Oligotrichea	Oligotrichida	Strombidiidae	Strombidium
ASV_1610	Chromista	Ciliophora	Oligotrichea	Oligotrichida	Strombidiidae	Strombidium
ASV_1614	Chromista	Ciliophora	Oligotrichea	Oligotrichida	Strombidiidae	Strombidium
ASV_1621	Chromista	Ciliophora	Oligotrichea	Choreotrichida	NA	NA
ASV_1626	Chromista	Ciliophora	Oligotrichea	Oligotrichida	Strombidiidae	Strombidium
ASV_168	Chromista	Ciliophora	Oligotrichea	Choreotrichida	NA	NA
ASV_187	Chromista	Ciliophora	Oligotrichea	Choreotrichida	Xystonellidae	Parafavella
ASV_199	Chromista	Ciliophora	Oligotrichea	Oligotrichida	Strombidiidae	Strombidium
ASV_207	Chromista	Ciliophora	Oligotrichea	Choreotrichida	NA	NA
ASV_222	Chromista	Ciliophora	Oligotrichea	Oligotrichida	NA	NA
ASV_229	Chromista	Ciliophora	Oligotrichea	Choreotrichida	Strobiliidiidae	NA

ASV_23	Chromista	Ciliophora	Oligotrichea	Oligotrichida	Strombidiidae	Strombidium
ASV_233	Chromista	Ciliophora	Oligotrichea	Oligotrichida	NA	NA
ASV_275	Chromista	Ciliophora	Oligotrichea	Choreotrichida	Strombidiopsidae	Parastrombidinoj
ASV_279	Chromista	Ciliophora	Oligotrichea	Oligotrichida	Strombidiidae	Strombidium
ASV_28	Chromista	Ciliophora	Oligotrichea	Oligotrichida	NA	NA
ASV_284	Chromista	Ciliophora	Oligotrichea	Choreotrichida	Strobiliidiidae	Pelagostrombidium
ASV_301	Chromista	Ciliophora	Oligotrichea	Oligotrichida	Strombidiidae	Strombidium
ASV_310	Chromista	Ciliophora	Oligotrichea	Oligotrichida	Strombidiidae	Strombidium
ASV_352	Chromista	Ciliophora	Oligotrichea	Oligotrichida	Strombidiidae	Strombidium
ASV_390	Chromista	Ciliophora	Oligotrichea	Choreotrichida	NA	NA
ASV_407	Chromista	Ciliophora	Oligotrichea	Oligotrichida	Strombidiidae	Strombidium
ASV_427	Chromista	Ciliophora	Oligotrichea	Choreotrichida	Strobiliidiidae	Rimostrombidium
ASV_481	Chromista	Ciliophora	Oligotrichea	Oligotrichida	NA	NA
ASV_483	Chromista	Ciliophora	Oligotrichea	Choreotrichida	Strobiliidiidae	NA
ASV_539	Chromista	Ciliophora	Oligotrichea	Oligotrichida	Strombidiidae	Strombidium
ASV_54	Chromista	Ciliophora	Oligotrichea	Oligotrichida	Strombidiidae	Strombidium
ASV_59	Chromista	Ciliophora	Oligotrichea	NA	NA	NA
ASV_669	Chromista	Ciliophora	Oligotrichea	Choreotrichida	Strobiliidiidae	NA
ASV_689	Chromista	Ciliophora	Oligotrichea	Oligotrichida	NA	NA
ASV_698	Chromista	Ciliophora	Oligotrichea	Oligotrichida	NA	NA
ASV_802	Chromista	Ciliophora	Oligotrichea	Oligotrichida	NA	NA
ASV_864	Chromista	Ciliophora	Oligotrichea	Choreotrichida	Strobiliidiidae	NA
ASV_96	Chromista	Ciliophora	Oligotrichea	Oligotrichida	NA	NA
ASV_977	Chromista	Ciliophora	Oligotrichea	Oligotrichida	Strombidiidae	Strombidium
ASV_1169	Chromista	Ciliophora	Prostomatea	Prorodontida	Balanionidae	Balanion
ASV_1208	Chromista	Ciliophora	Prostomatea	Prorodontida	Balanionidae	Balanion
ASV_1590	Chromista	Ciliophora	Prostomatea	Prorodontida	NA	NA
ASV_479	Chromista	Ciliophora	Prostomatea	Prorodontida	Balanionidae	Balanion
ASV_494	Chromista	Ciliophora	Prostomatea	Prorodontida	NA	NA
ASV_702	Chromista	Ciliophora	Prostomatea	Prorodontida	NA	NA
ASV_786	Chromista	Ciliophora	Prostomatea	Prorodontida	Balanionidae	Balanion
ASV_876	Chromista	Ciliophora	Prostomatea	Prorodontida	NA	NA
ASV_1105	Chromista	Ciliophora	Spirotrichea	Euplotida	Uronychiidae	Diophrys
ASV_415	Chromista	Ciliophora	Spirotrichea	Hypotrichia_EXT	NA	NA
ASV_491	Chromista	Ciliophora	Spirotrichea	Hypotrichia_EXT	Amphisiliidae	Protogastrostyla
ASV_519	Chromista	Ciliophora	Spirotrichea	Hypotrichia_EXT	NA	NA
ASV_646	Chromista	Ciliophora	Spirotrichea	NA	NA	NA
ASV_1622	Chromista	Cryptophyta	Cryptophyceae	Pyrenomonadales	Chroomonadaceae	Falcomonas
ASV_1666	Chromista	Cryptophyta	Cryptophyceae	Pyrenomonadales	Geminigeraceae	Teleaulax
ASV_466	Chromista	Cryptophyta	Cryptophyceae	Pyrenomonadales	Chroomonadaceae	Falcomonas
ASV_484	Chromista	Cryptophyta	Cryptophyceae	Pyrenomonadales	Geminigeraceae	Teleaulax
ASV_563	Chromista	Cryptophyta	Cryptophyceae	Cryptomonadales	Cryptomonadaceae	Goniomonas
ASV_58	Chromista	Cryptophyta	Cryptophyceae	Pyrenomonadales	Chroomonadaceae	Falcomonas
ASV_610	Chromista	Cryptophyta	Cryptophyceae	Cryptomonadales	NA	NA
ASV_95	Chromista	Cryptophyta	Cryptophyceae	Pyrenomonadales	Geminigeraceae	Teleaulax
ASV_997	Chromista	Cryptophyta	Cryptophyceae	Cryptomonadales	Cryptomonadaceae	Goniomonas
ASV_304	Chromista	Cryptophyta	Cryptophyta_incertae	Cryptophyta_incertae_sedis_EXT	Katablepharidaceae	Leucocryptos
ASV_827	Chromista	Cryptophyta	Cryptophyta_incertae	Cryptophyta_incertae_sedis_EXT	Katablepharidaceae	Katablepharis
ASV_1132	Chromista	Haptophyta	NA	NA	NA	NA
ASV_480	Chromista	Haptophyta	NA	NA	NA	NA
ASV_999	Chromista	Haptophyta	Pavlovophyceae	Pavlovales	Pavlovaceae	NA
ASV_1051	Chromista	Haptophyta	Coccolithophyceae	Phaeocystales	Phaeocystaceae	Phaeocystis
ASV_1259	Chromista	Haptophyta	Coccolithophyceae	Prymnesiales	Prymnesiaceae	Pseudohaptolina
ASV_1321	Chromista	Haptophyta	Coccolithophyceae	NA	NA	NA
ASV_1328	Chromista	Haptophyta	Coccolithophyceae	Phaeocystales	Phaeocystaceae	Phaeocystis
ASV_1336	Chromista	Haptophyta	Coccolithophyceae	Phaeocystales	Phaeocystaceae	Phaeocystis
ASV_1337	Chromista	Haptophyta	Coccolithophyceae	Prymnesiales	Chrysochromulinaceae	Chrysochromulin
ASV_1477	Chromista	Haptophyta	Coccolithophyceae	NA	NA	NA
ASV_170	Chromista	Haptophyta	Coccolithophyceae	Prymnesiales	Chrysochromulinaceae	Chrysochromulin
ASV_214	Chromista	Haptophyta	Coccolithophyceae	Prymnesiales	Chrysochromulinaceae	Chrysochromulin
ASV_272	Chromista	Haptophyta	Coccolithophyceae	Prymnesiales	Prymnesiaceae	Haptolina
ASV_298	Chromista	Haptophyta	Coccolithophyceae	NA	NA	NA
ASV_309	Chromista	Haptophyta	Coccolithophyceae	Prymnesiales	Chrysochromulinaceae	Chrysochromulin
ASV_340	Chromista	Haptophyta	Coccolithophyceae	Prymnesiales	Prymnesiaceae	Pseudohaptolina
ASV_37	Chromista	Haptophyta	Coccolithophyceae	Phaeocystales	Phaeocystaceae	Phaeocystis
ASV_440	Chromista	Haptophyta	Coccolithophyceae	Coccolithales	Coccolithaceae	Cruciplacolithus
ASV_538	Chromista	Haptophyta	Coccolithophyceae	Isochrysidales	Isochrysidaceae	NA
ASV_557	Chromista	Haptophyta	Coccolithophyceae	Prymnesiales	Prymnesiaceae	Pseudohaptolina
ASV_575	Chromista	Haptophyta	Coccolithophyceae	NA	NA	NA
ASV_612	Chromista	Haptophyta	Coccolithophyceae	Phaeocystales	Phaeocystaceae	Phaeocystis
ASV_642	Chromista	Haptophyta	Coccolithophyceae	Prymnesiales	Chrysochromulinaceae	Chrysochromulin
ASV_770	Chromista	Haptophyta	Coccolithophyceae	Prymnesiales	Chrysochromulinaceae	Chrysochromulin
ASV_982	Chromista	Haptophyta	Coccolithophyceae	Prymnesiales	NA	NA
ASV_486	Chromista	Heliozoa	Centrohelea	Centrohelida	Heterophryidae	Heterophrys
ASV_823	Chromista	Heliozoa	Centrohelea	Centrohelida	Heterophryidae	Heterophrys
ASV_1072	Chromista	Heterokontopl	Bacillariophyceae	Bacillariales	Bacillariaceae	NA
ASV_11	Chromista	Heterokontopl	Bacillariophyceae	Coscinodiscales	Coscinodisceae	Coscinodiscus
ASV_111	Chromista	Heterokontopl	Bacillariophyceae	NA	NA	NA
ASV_1133	Chromista	Heterokontopl	Bacillariophyceae	Thalassiosirales	Thalassiosiraceae	NA
ASV_1135	Chromista	Heterokontopl	Bacillariophyceae	Coscinodiscales	Coscinodisceae	Coscinodiscus
ASV_1150	Chromista	Heterokontopl	Bacillariophyceae	Melosirales	Stephanopyxidaceae	Stephanopyxis
ASV_12	Chromista	Heterokontopl	Bacillariophyceae	Thalassiosirales	Thalassiosiraceae	Thalassiosira
ASV_1265	Chromista	Heterokontopl	Bacillariophyceae	Chaetocerotanae_incertae_sedis	Chaetocerotaceae	Chaetoceros
ASV_1277	Chromista	Heterokontopl	Bacillariophyceae	Coscinodiscales	Coscinodisceae	Coscinodiscus
ASV_1297	Chromista	Heterokontopl	Bacillariophyceae	Thalassiosirales	Thalassiosiraceae	NA
ASV_1368	Chromista	Heterokontopl	Bacillariophyceae	NA	NA	NA
ASV_1370	Chromista	Heterokontopl	Bacillariophyceae	Coscinodiscales	NA	NA
ASV_1371	Chromista	Heterokontopl	Bacillariophyceae	Coscinodiscales	Coscinodisceae	Coscinodiscus

ASV_1380	Chromista	Heterokontopl Bacillariophyceae	NA	NA	NA
ASV_1382	Chromista	Heterokontopl Bacillariophyceae	NA	NA	NA
ASV_1388	Chromista	Heterokontopl Bacillariophyceae	NA	NA	NA
ASV_1442	Chromista	Heterokontopl Bacillariophyceae	Thalassiosirales	Thalassiosiraceae	Thalassiosira
ASV_1444	Chromista	Heterokontopl Bacillariophyceae	Thalassiosirales	NA	NA
ASV_145	Chromista	Heterokontopl Bacillariophyceae	NA	NA	NA
ASV_147	Chromista	Heterokontopl Bacillariophyceae	NA	NA	NA
ASV_150	Chromista	Heterokontopl Bacillariophyceae	Thalassiosirales	Thalassiosiraceae	Thalassiosira
ASV_1523	Chromista	Heterokontopl Bacillariophyceae	NA	NA	NA
ASV_1553	Chromista	Heterokontopl Bacillariophyceae	Bacillariales	Bacillariaceae	Pseudonitzschia
ASV_156	Chromista	Heterokontopl Bacillariophyceae	Bacillariales	Bacillariaceae	Pseudonitzschia
ASV_1562	Chromista	Heterokontopl Bacillariophyceae	Chaetocerotanae_incertae_sedis	Chaetocerotaceae	Chaetoceros
ASV_1566	Chromista	Heterokontopl Bacillariophyceae	Coscinodiscales	Coscinodisceae	Coscinodiscus
ASV_1572	Chromista	Heterokontopl Bacillariophyceae	Coscinodiscales	NA	NA
ASV_1575	Chromista	Heterokontopl Bacillariophyceae	Coscinodiscales	Hemidiscaceae	Actinocyclus
ASV_1596	Chromista	Heterokontopl Bacillariophyceae	Chaetocerotanae_incertae_sedis	Chaetocerotaceae	Chaetoceros
ASV_1618	Chromista	Heterokontopl Bacillariophyceae	NA	NA	NA
ASV_1627	Chromista	Heterokontopl Bacillariophyceae	Chaetocerotanae_incertae_sedis	Chaetocerotaceae	Chaetoceros
ASV_1658	Chromista	Heterokontopl Bacillariophyceae	Thalassiosirales	Thalassiosiraceae	Thalassiosira
ASV_1665	Chromista	Heterokontopl Bacillariophyceae	Coscinodiscales	Coscinodisceae	Coscinodiscus
ASV_17	Chromista	Heterokontopl Bacillariophyceae	Thalassiosirales	Thalassiosiraceae	Thalassiosira
ASV_173	Chromista	Heterokontopl Bacillariophyceae	Fragilariales	Fragilariaceae	NA
ASV_175	Chromista	Heterokontopl Bacillariophyceae	Chaetocerotanae_incertae_sedis	Chaetocerotaceae	Chaetoceros
ASV_176	Chromista	Heterokontopl Bacillariophyceae	Bacillariales	Bacillariaceae	NA
ASV_184	Chromista	Heterokontopl Bacillariophyceae	Naviculales	Naviculaceae	Navicula
ASV_193	Chromista	Heterokontopl Bacillariophyceae	Bacillariales	Bacillariaceae	Nitzschia
ASV_204	Chromista	Heterokontopl Bacillariophyceae	Bacillariales	Bacillariaceae	Pseudonitzschia
ASV_21	Chromista	Heterokontopl Bacillariophyceae	Chaetocerotanae_incertae_sedis	Chaetocerotaceae	Chaetoceros
ASV_215	Chromista	Heterokontopl Bacillariophyceae	Fragilariales	Fragilariaceae	Fragilaria
ASV_230	Chromista	Heterokontopl Bacillariophyceae	Bacillariophycidae_incertae_sedis_E	Bacillariophycidae_incertae_sedis_E	Syndendrium
ASV_232	Chromista	Heterokontopl Bacillariophyceae	Thalassiosirales	Skeletonemaceae	Skeletonema
ASV_240	Chromista	Heterokontopl Bacillariophyceae	Bacillariales	Bacillariaceae	Nitzschia
ASV_259	Chromista	Heterokontopl Bacillariophyceae	Thalassiosirales	Thalassiosiraceae	Thalassiosira
ASV_266	Chromista	Heterokontopl Bacillariophyceae	Bacillariales	Bacillariaceae	Nitzschia
ASV_270	Chromista	Heterokontopl Bacillariophyceae	Chaetocerotanae_incertae_sedis	Chaetocerotaceae	Chaetoceros
ASV_306	Chromista	Heterokontopl Bacillariophyceae	NA	NA	NA
ASV_311	Chromista	Heterokontopl Bacillariophyceae	Bacillariales	Bacillariaceae	NA
ASV_318	Chromista	Heterokontopl Bacillariophyceae	NA	NA	NA
ASV_328	Chromista	Heterokontopl Bacillariophyceae	Naviculales	Naviculaceae	Navicula
ASV_345	Chromista	Heterokontopl Bacillariophyceae	NA	NA	NA
ASV_354	Chromista	Heterokontopl Bacillariophyceae	Bacillariales	Bacillariaceae	NA
ASV_43	Chromista	Heterokontopl Bacillariophyceae	Thalassiosirales	Thalassiosiraceae	Thalassiosira
ASV_435	Chromista	Heterokontopl Bacillariophyceae	Chaetocerotanae_incertae_sedis	Chaetocerotaceae	Chaetoceros
ASV_44	Chromista	Heterokontopl Bacillariophyceae	Bacillariales	Bacillariaceae	Pseudonitzschia
ASV_442	Chromista	Heterokontopl Bacillariophyceae	NA	NA	NA
ASV_445	Chromista	Heterokontopl Bacillariophyceae	Chaetocerotanae_incertae_sedis	Chaetocerotaceae	Chaetoceros
ASV_45	Chromista	Heterokontopl Bacillariophyceae	Coscinodiscales	Hemidiscaceae	Actinocyclus
ASV_49	Chromista	Heterokontopl Bacillariophyceae	Hemiaulales	Hemiaulaceae	Eucampia
ASV_499	Chromista	Heterokontopl Bacillariophyceae	Chaetocerotanae_incertae_sedis	Chaetocerotaceae	Chaetoceros
ASV_545	Chromista	Heterokontopl Bacillariophyceae	Bacillariales	Bacillariaceae	Pseudonitzschia
ASV_55	Chromista	Heterokontopl Bacillariophyceae	Chaetocerotanae_incertae_sedis	Attheyaceae	Attheya
ASV_562	Chromista	Heterokontopl Bacillariophyceae	Thalassiosirales	Thalassiosiraceae	Thalassiosira
ASV_573	Chromista	Heterokontopl Bacillariophyceae	Chaetocerotanae_incertae_sedis	Chaetocerotaceae	Chaetoceros
ASV_584	Chromista	Heterokontopl Bacillariophyceae	Fragilariales	Fragilariaceae	Fragilaria
ASV_629	Chromista	Heterokontopl Bacillariophyceae	Thalassiosirales	Thalassiosiraceae	Thalassiosira
ASV_659	Chromista	Heterokontopl Bacillariophyceae	Naviculales	NA	NA
ASV_662	Chromista	Heterokontopl Bacillariophyceae	Naviculales	NA	NA
ASV_712	Chromista	Heterokontopl Bacillariophyceae	Chaetocerotanae_incertae_sedis	Chaetocerotaceae	Chaetoceros
ASV_724	Chromista	Heterokontopl Bacillariophyceae	Thalassiosirales	Thalassiosiraceae	Thalassiosira
ASV_735	Chromista	Heterokontopl Bacillariophyceae	Bacillariales	Bacillariaceae	Nitzschia
ASV_742	Chromista	Heterokontopl Bacillariophyceae	Chaetocerotanae_incertae_sedis	Chaetocerotaceae	Chaetoceros
ASV_755	Chromista	Heterokontopl Bacillariophyceae	Chaetocerotanae_incertae_sedis	Chaetocerotaceae	Chaetoceros
ASV_8	Chromista	Heterokontopl Bacillariophyceae	Bacillariales	Bacillariaceae	Pseudonitzschia
ASV_85	Chromista	Heterokontopl Bacillariophyceae	Chaetocerotanae_incertae_sedis	Chaetocerotaceae	Chaetoceros
ASV_868	Chromista	Heterokontopl Bacillariophyceae	Naviculales	Naviculaceae	NA
ASV_889	Chromista	Heterokontopl Bacillariophyceae	Surirellales	Entomoneidaceae	Entomoneis
ASV_922	Chromista	Heterokontopl Bacillariophyceae	Thalassiosirales	Thalassiosiraceae	Thalassiosira
ASV_1023	Chromista	Ochrophyta Chrysophyceae	Chromulinales	Chrysolepidomonadaceae	Chrysolepidomor
ASV_1114	Chromista	Ochrophyta Chrysophyceae	Chromulinales	NA	NA
ASV_1115	Chromista	Ochrophyta Chrysophyceae	Chromulinales	NA	NA
ASV_1151	Chromista	Ochrophyta Chrysophyceae	Chromulinales	NA	NA
ASV_1193	Chromista	Ochrophyta Chrysophyceae	Chromulinales	NA	NA
ASV_1278	Chromista	Ochrophyta Chrysophyceae	Chromulinales	NA	NA
ASV_1327	Chromista	Ochrophyta Chrysophyceae	Chromulinales	NA	NA
ASV_1334	Chromista	Ochrophyta Chrysophyceae	Hibberdiales	Stylococcaceae	Helicopedinella
ASV_1338	Chromista	Ochrophyta Chrysophyceae	Parmales	Triparmaceae	Triparma
ASV_1397	Chromista	Ochrophyta Chrysophyceae	Parmales	Triparmaceae	Triparma
ASV_1412	Chromista	Ochrophyta Chrysophyceae	Chromulinales	Chrysolepidomonadaceae	Chrysolepidomor
ASV_1466	Chromista	Ochrophyta Chrysophyceae	Parmales	Triparmaceae	Triparma
ASV_163	Chromista	Ochrophyta Chrysophyceae	Chromulinales	NA	NA
ASV_1646	Chromista	Ochrophyta Chrysophyceae	Chromulinales	Chrysolepidomonadaceae	Chrysolepidomor
ASV_181	Chromista	Ochrophyta Chrysophyceae	Chromulinales	Chrysolepidomonadaceae	Chrysolepidomor
ASV_20	Chromista	Ochrophyta Chrysophyceae	Chromulinales	NA	NA
ASV_209	Chromista	Ochrophyta Chrysophyceae	Chromulinales	NA	NA
ASV_27	Chromista	Ochrophyta Chrysophyceae	Chromulinales	Chrysolepidomonadaceae	Chrysolepidomor
ASV_29	Chromista	Ochrophyta Chrysophyceae	Chromulinales	Chrysolepidomonadaceae	Chrysolepidomor
ASV_374	Chromista	Ochrophyta Chrysophyceae	Chromulinales	NA	NA
ASV_389	Chromista	Ochrophyta Chrysophyceae	Chromulinales	Chrysolepidomonadaceae	Chrysolepidomor

ASV_391	Chromista	Ochrophyta	Chrysophyceae	Chromulinales	Chrysolepidomonadaceae	Chrysolepidomor
ASV_406	Chromista	Ochrophyta	Chrysophyceae	Chromulinales	NA	NA
ASV_454	Chromista	Ochrophyta	Chrysophyceae	Chromulinales	NA	NA
ASV_467	Chromista	Ochrophyta	Chrysophyceae	Parmales	Triparmaceae	Triparma
ASV_506	Chromista	Ochrophyta	Chrysophyceae	Chromulinales	Chrysolepidomonadaceae	Chrysolepidomor
ASV_507	Chromista	Ochrophyta	Chrysophyceae	Parmales	Triparmaceae	Triparma
ASV_547	Chromista	Ochrophyta	Chrysophyceae	Chromulinales	Paraphysomonadaceae	Paraphysomona
ASV_548	Chromista	Ochrophyta	Chrysophyceae	Chromulinales	Chrysolepidomonadaceae	Chrysolepidomor
ASV_551	Chromista	Ochrophyta	Chrysophyceae	Chromulinales	Chrysolepidomonadaceae	Chrysolepidomor
ASV_598	Chromista	Ochrophyta	Chrysophyceae	Chromulinales	NA	NA
ASV_65	Chromista	Ochrophyta	Chrysophyceae	Chromulinales	Chrysolepidomonadaceae	Chrysolepidomor
ASV_67	Chromista	Ochrophyta	Chrysophyceae	Chromulinales	NA	NA
ASV_707	Chromista	Ochrophyta	Chrysophyceae	Parmales	Triparmaceae	Triparma
ASV_721	Chromista	Ochrophyta	Chrysophyceae	Chromulinales	NA	NA
ASV_739	Chromista	Ochrophyta	Chrysophyceae	Chromulinales	Chrysolepidomonadaceae	Chrysolepidomor
ASV_83	Chromista	Ochrophyta	Chrysophyceae	Hibberdiales	Stylococcaceae	Helicopedinella
ASV_863	Chromista	Ochrophyta	Chrysophyceae	Chromulinales	Chrysolepidomonadaceae	Chrysolepidomor
ASV_978	Chromista	Ochrophyta	Chrysophyceae	Chromulinales	NA	NA
ASV_330	Chromista	Heterokontopl	Bacillariophyceae	Asterolamprales	Asterolampraceae	Asteromphalus
ASV_153	Chromista	Ochrophyta	Dictyochophyceae	Pedinellales	Pedinellaceae	Pseudopedinella
ASV_1587	Chromista	Ochrophyta	Dictyochophyceae	Florenciellales	Florenciellales_incertae_sedis	Florenciella
ASV_191	Chromista	Ochrophyta	Dictyochophyceae	Dictyochales	Dictyochaceae	Octactis
ASV_261	Chromista	Ochrophyta	Dictyochophyceae	Florenciellales	Florenciellales_incertae_sedis	Florenciella
ASV_429	Chromista	Ochrophyta	Dictyochophyceae	Pedinellales	Pedinellaceae	Pteridomonas
ASV_472	Chromista	Ochrophyta	Dictyochophyceae	Florenciellales	Florenciellales_incertae_sedis	Florenciella
ASV_570	Chromista	Ochrophyta	Dictyochophyceae	Florenciellales	Florenciellales_incertae_sedis	Florenciella
ASV_1045	Chromista	Ochrophyta	NA	NA	NA	NA
ASV_1067	Chromista	Ochrophyta	NA	NA	NA	NA
ASV_1231	Chromista	Cryptophyta	NA	NA	NA	NA
ASV_1591	Chromista	Ochrophyta	NA	NA	NA	NA
ASV_1655	Chromista	Ochrophyta	NA	NA	NA	NA
ASV_626	Chromista	Ochrophyta	NA	NA	NA	NA
ASV_76	Chromista	Ochrophyta	NA	NA	NA	NA
ASV_837	Chromista	Ochrophyta	NA	NA	NA	NA
ASV_945	Chromista	Ochrophyta	NA	NA	NA	NA
ASV_1480	Chromista	Ochrophyta	Pelagophyceae	Sarcinochrysidales	Sarcinochrysidaceae	Ankylochrysis
ASV_166	Chromista	Ochrophyta	Pelagophyceae	Sarcinochrysidales	Sarcinochrysidaceae	NA
ASV_179	Chromista	Ochrophyta	Pelagophyceae	Pelagomonadales	Pelagomonadaceae	Aureococcus
ASV_271	Chromista	Ochrophyta	Pelagophyceae	Sarcinochrysidales	Sarcinochrysidaceae	Sarcinochrysis
ASV_451	Chromista	Ochrophyta	Pelagophyceae	Sarcinochrysidales	Sarcinochrysidaceae	NA
ASV_48	Chromista	Ochrophyta	Pelagophyceae	NA	NA	NA
ASV_498	Chromista	Ochrophyta	Pelagophyceae	Sarcinochrysidales	Sarcinochrysidaceae	Ankylochrysis
ASV_518	Chromista	Ochrophyta	Pelagophyceae	Sarcinochrysidales	Sarcinochrysidaceae	Sarcinochrysis
ASV_530	Chromista	Ochrophyta	Pelagophyceae	Sarcinochrysidales	Sarcinochrysidaceae	Ankylochrysis
ASV_608	Chromista	Ochrophyta	Pelagophyceae	Sarcinochrysidales	Sarcinochrysidaceae	NA
ASV_641	Chromista	Ochrophyta	Pelagophyceae	Pelagomonadales	Pelagomonadaceae	Aureococcus
ASV_82	Chromista	Ochrophyta	Pelagophyceae	NA	NA	NA
ASV_981	Chromista	Ochrophyta	Pelagophyceae	NA	NA	NA
ASV_487	Chromista	Ochrophyta	Phaeophyceae	Laminariales	Alariaceae	Undaria
ASV_1268	Chromista	Myzozoa	Dinoflagellata_incertae_sedis_EXT	Dinoflagellata_incertae_sedis_EXT	Dinoflagellata_incertae_sedis_EXT	Duboscquella
ASV_1515	Chromista	Myzozoa	Dinoflagellata_incertae_sedis_EXT	Dinoflagellata_incertae_sedis_EXT	Dinoflagellata_incertae_sedis_EXT	Duboscquella
ASV_174	Chromista	Myzozoa	Dinoflagellata_incertae_sedis_EXT	Dinoflagellata_incertae_sedis_EXT	Dinoflagellata_incertae_sedis_EXT	Stoeckeria
ASV_178	Chromista	Myzozoa	Dinoflagellata_incertae_sedis_EXT	Dinoflagellata_incertae_sedis_EXT	Dinoflagellata_incertae_sedis_EXT	Impagidinium
ASV_280	Chromista	Myzozoa	Dinoflagellata_incertae_sedis_EXT	Dinoflagellata_incertae_sedis_EXT	Dinoflagellata_incertae_sedis_EXT	Stoeckeria
ASV_316	Chromista	Myzozoa	Dinoflagellata_incertae_sedis_EXT	Dinoflagellata_incertae_sedis_EXT	Dinoflagellata_incertae_sedis_EXT	Duboscquella
ASV_398	Chromista	Myzozoa	Dinoflagellata_incertae_sedis_EXT	Dinoflagellata_incertae_sedis_EXT	Dinoflagellata_incertae_sedis_EXT	Duboscquella
ASV_819	Chromista	Myzozoa	Dinoflagellata_incertae_sedis_EXT	Dinoflagellata_incertae_sedis_EXT	Dinoflagellata_incertae_sedis_EXT	Duboscquella
ASV_917	Chromista	Myzozoa	Dinoflagellata_incertae_sedis_EXT	Dinoflagellata_incertae_sedis_EXT	Dinoflagellata_incertae_sedis_EXT	Duboscquella
ASV_976	Chromista	Myzozoa	Dinoflagellata_incertae_sedis_EXT	Dinoflagellata_incertae_sedis_EXT	Dinoflagellata_incertae_sedis_EXT	Stoeckeria
ASV_10	Chromista	Myzozoa	Dinophyceae	NA	NA	NA
ASV_100	Chromista	Myzozoa	Dinophyceae	Gymnodiniales	Gymnodiniaceae	Gyrodinium
ASV_1000	Chromista	Myzozoa	Dinophyceae	Gymnodiniales	Gymnodiniaceae	Gyrodinium
ASV_1001	Chromista	Myzozoa	Dinophyceae	NA	NA	NA
ASV_1008	Chromista	Myzozoa	Dinophyceae	Gymnodiniales	Gymnodiniaceae	Gyrodinium
ASV_101	Chromista	Myzozoa	Dinophyceae	NA	NA	NA
ASV_1022	Chromista	Myzozoa	Dinophyceae	NA	NA	NA
ASV_1024	Chromista	Myzozoa	Dinophyceae	NA	NA	NA
ASV_1025	Chromista	Myzozoa	Dinophyceae	NA	NA	NA
ASV_1027	Chromista	Myzozoa	Dinophyceae	Peridinales	Protoperidiniaceae	Protoperidinium
ASV_1035	Chromista	Myzozoa	Dinophyceae	NA	NA	NA
ASV_1037	Chromista	Myzozoa	Dinophyceae	NA	NA	NA
ASV_1046	Chromista	Myzozoa	Dinophyceae	NA	NA	NA
ASV_1047	Chromista	Myzozoa	Dinophyceae	NA	NA	NA
ASV_1048	Chromista	Myzozoa	Dinophyceae	NA	NA	NA
ASV_1052	Chromista	Myzozoa	Dinophyceae	Suessiales	Biecheleriaceae	Biecheleria
ASV_1056	Chromista	Myzozoa	Dinophyceae	NA	NA	NA
ASV_1068	Chromista	Myzozoa	Dinophyceae	NA	NA	NA
ASV_107	Chromista	Myzozoa	Dinophyceae	Gymnodiniales	Gymnodiniaceae	Gyrodinium
ASV_109	Chromista	Myzozoa	Dinophyceae	NA	NA	NA
ASV_1091	Chromista	Myzozoa	Dinophyceae	NA	NA	NA
ASV_1101	Chromista	Myzozoa	Dinophyceae	Gymnodiniales	Gymnodiniaceae	NA
ASV_1106	Chromista	Myzozoa	Dinophyceae	Syndiniales	Amoebophryaceae	Amoebophrya
ASV_1108	Chromista	Myzozoa	Dinophyceae	Syndiniales	Amoebophryaceae	Amoebophrya
ASV_1113	Chromista	Myzozoa	Dinophyceae	Gymnodiniales	Gymnodiniaceae	Gyrodinium
ASV_1116	Chromista	Myzozoa	Dinophyceae	NA	NA	NA
ASV_1134	Chromista	Myzozoa	Dinophyceae	Gymnodiniales	Gymnodiniaceae	Lepidodinium
ASV_1141	Chromista	Myzozoa	Dinophyceae	Gymnodiniales	Gymnodiniaceae	Gyrodinium
ASV_115	Chromista	Myzozoa	Dinophyceae	Gymnodiniales	NA	NA

ASV_1601	Chromista	Myzozoa	Dinophyceae	Gymnodiniales	NA	NA
ASV_1603	Chromista	Myzozoa	Dinophyceae	Suessiales	Biecheleriaceae	Biecheleria
ASV_1604	Chromista	Myzozoa	Dinophyceae	NA	NA	NA
ASV_1606	Chromista	Myzozoa	Dinophyceae	NA	NA	NA
ASV_1607	Chromista	Myzozoa	Dinophyceae	NA	NA	NA
ASV_1613	Chromista	Myzozoa	Dinophyceae	NA	NA	NA
ASV_1616	Chromista	Myzozoa	Dinophyceae	NA	NA	NA
ASV_162	Chromista	Myzozoa	Dinophyceae	Gymnodiniales	Gymnodiniaceae	Lepidodinium
ASV_1620	Chromista	Myzozoa	Dinophyceae	Gymnodiniales	Gymnodiniaceae	NA
ASV_1625	Chromista	Myzozoa	Dinophyceae	Gymnodiniales	Gymnodiniaceae	NA
ASV_1628	Chromista	Myzozoa	Dinophyceae	NA	NA	NA
ASV_1630	Chromista	Myzozoa	Dinophyceae	Gymnodiniales	Gymnodiniaceae	Gyrodinium
ASV_1633	Chromista	Myzozoa	Dinophyceae	Gymnodiniales	Gymnodiniaceae	Gyrodinium
ASV_1634	Chromista	Myzozoa	Dinophyceae	NA	NA	NA
ASV_1644	Chromista	Myzozoa	Dinophyceae	NA	NA	NA
ASV_1647	Chromista	Myzozoa	Dinophyceae	NA	NA	NA
ASV_1651	Chromista	Myzozoa	Dinophyceae	Peridinales	Protoperidiniaceae	Protoperidinium
ASV_1652	Chromista	Myzozoa	Dinophyceae	Gymnodiniales	Gymnodiniaceae	Gyrodinium
ASV_1654	Chromista	Myzozoa	Dinophyceae	NA	NA	NA
ASV_1657	Chromista	Myzozoa	Dinophyceae	Gymnodiniales	Gymnodiniaceae	Gyrodinium
ASV_1664	Chromista	Myzozoa	Dinophyceae	Peridinales	Protoperidiniaceae	Protoperidinium
ASV_1675	Chromista	Myzozoa	Dinophyceae	NA	NA	NA
ASV_1679	Chromista	Myzozoa	Dinophyceae	NA	NA	NA
ASV_171	Chromista	Myzozoa	Dinophyceae	Gymnodiniales	Gymnodiniaceae	Torodinium
ASV_172	Chromista	Myzozoa	Dinophyceae	NA	NA	NA
ASV_180	Chromista	Myzozoa	Dinophyceae	NA	NA	NA
ASV_189	Chromista	Myzozoa	Dinophyceae	NA	NA	NA
ASV_19	Chromista	Myzozoa	Dinophyceae	NA	NA	NA
ASV_190	Chromista	Myzozoa	Dinophyceae	NA	NA	NA
ASV_201	Chromista	Myzozoa	Dinophyceae	Gymnodiniales	Gymnodiniaceae	Lepidodinium
ASV_202	Chromista	Myzozoa	Dinophyceae	NA	NA	NA
ASV_206	Chromista	Myzozoa	Dinophyceae	Gymnodiniales	Gymnodiniaceae	Margalefidinium
ASV_208	Chromista	Myzozoa	Dinophyceae	Gymnodiniales	Brachidiniaceae	Takayama
ASV_211	Chromista	Myzozoa	Dinophyceae	Gymnodiniales	Gymnodiniaceae	Gyrodinium
ASV_212	Chromista	Myzozoa	Dinophyceae	NA	NA	NA
ASV_216	Chromista	Myzozoa	Dinophyceae	NA	NA	NA
ASV_218	Chromista	Myzozoa	Dinophyceae	Gymnodiniales	Gymnodiniaceae	Lepidodinium
ASV_22	Chromista	Myzozoa	Dinophyceae	Gymnodiniales	Karenaceae	Karlodinium
ASV_220	Chromista	Myzozoa	Dinophyceae	Gymnodiniales	Gymnodiniaceae	Gyrodinium
ASV_223	Chromista	Myzozoa	Dinophyceae	NA	NA	NA
ASV_224	Chromista	Myzozoa	Dinophyceae	NA	NA	NA
ASV_228	Chromista	Myzozoa	Dinophyceae	Gymnodiniales	Gymnodiniaceae	Gyrodinium
ASV_235	Chromista	Myzozoa	Dinophyceae	NA	NA	NA
ASV_242	Chromista	Myzozoa	Dinophyceae	NA	NA	NA
ASV_244	Chromista	Myzozoa	Dinophyceae	Peridinales	Heterocapsaceae	Heterocapsa
ASV_245	Chromista	Myzozoa	Dinophyceae	NA	NA	NA
ASV_246	Chromista	Myzozoa	Dinophyceae	Suessiales	Biecheleriaceae	Biecheleria
ASV_251	Chromista	Myzozoa	Dinophyceae	Gymnodiniales	Gymnodiniaceae	Gyrodinium
ASV_252	Chromista	Myzozoa	Dinophyceae	NA	NA	NA
ASV_253	Chromista	Myzozoa	Dinophyceae	NA	NA	NA
ASV_255	Chromista	Myzozoa	Dinophyceae	NA	NA	NA
ASV_256	Chromista	Myzozoa	Dinophyceae	Peridinales	NA	NA
ASV_26	Chromista	Myzozoa	Dinophyceae	Gymnodiniales	Gymnodiniaceae	Gyrodinium
ASV_263	Chromista	Myzozoa	Dinophyceae	Syndiniales	Amoebophryaceae	Amoebophrya
ASV_267	Chromista	Myzozoa	Dinophyceae	NA	NA	NA
ASV_273	Chromista	Myzozoa	Dinophyceae	Gymnodiniales	Gymnodiniaceae	Gyrodinium
ASV_287	Chromista	Myzozoa	Dinophyceae	NA	NA	NA
ASV_290	Chromista	Myzozoa	Dinophyceae	Gonyaulacales	Ceratiaceae	Tripos
ASV_292	Chromista	Myzozoa	Dinophyceae	Gymnodiniales	Gymnodiniaceae	Lepidodinium
ASV_294	Chromista	Myzozoa	Dinophyceae	Gymnodiniales	Karenaceae	Karlodinium
ASV_300	Chromista	Myzozoa	Dinophyceae	Gymnodiniales	NA	NA
ASV_308	Chromista	Myzozoa	Dinophyceae	Gymnodiniales	Gymnodiniaceae	Nusuttodinium
ASV_312	Chromista	Myzozoa	Dinophyceae	NA	NA	NA
ASV_315	Chromista	Myzozoa	Dinophyceae	NA	NA	NA
ASV_317	Chromista	Myzozoa	Dinophyceae	Gymnodiniales	Gymnodiniaceae	Lepidodinium
ASV_321	Chromista	Myzozoa	Dinophyceae	NA	NA	NA
ASV_322	Chromista	Myzozoa	Dinophyceae	NA	NA	NA
ASV_325	Chromista	Myzozoa	Dinophyceae	Gymnodiniales	NA	NA
ASV_33	Chromista	Myzozoa	Dinophyceae	Gymnodiniales	Gymnodiniaceae	Lepidodinium
ASV_333	Chromista	Myzozoa	Dinophyceae	Gymnodiniales	Gymnodiniaceae	Gyrodinium
ASV_335	Chromista	Myzozoa	Dinophyceae	Peridinales	Protoperidiniaceae	Protoperidinium
ASV_339	Chromista	Myzozoa	Dinophyceae	Gymnodiniales	Karenaceae	Karlodinium
ASV_344	Chromista	Myzozoa	Dinophyceae	Peridinales	Protoperidiniaceae	Protoperidinium
ASV_350	Chromista	Myzozoa	Dinophyceae	Gymnodiniales	Gymnodiniaceae	Gyrodinium
ASV_36	Chromista	Myzozoa	Dinophyceae	Gymnodiniales	Gymnodiniaceae	Gyrodinium
ASV_360	Chromista	Myzozoa	Dinophyceae	Gymnodiniales	Gymnodiniaceae	Gyrodinium
ASV_367	Chromista	Myzozoa	Dinophyceae	Gymnodiniales	Gymnodiniaceae	Gyrodinium
ASV_368	Chromista	Myzozoa	Dinophyceae	NA	NA	NA
ASV_369	Chromista	Myzozoa	Dinophyceae	Peridinales	Protoperidiniaceae	Protoperidinium
ASV_371	Chromista	Myzozoa	Dinophyceae	Gymnodiniales	Gymnodiniaceae	Lepidodinium
ASV_372	Chromista	Myzozoa	Dinophyceae	Gymnodiniales	Gymnodiniaceae	Gyrodinium
ASV_373	Chromista	Myzozoa	Dinophyceae	Gymnodiniales	Gymnodiniaceae	Gyrodinium
ASV_379	Chromista	Myzozoa	Dinophyceae	Syndiniales	Amoebophryaceae	Amoebophrya
ASV_38	Chromista	Myzozoa	Dinophyceae	Gymnodiniales	Gymnodiniaceae	Gyrodinium
ASV_380	Chromista	Myzozoa	Dinophyceae	NA	NA	NA
ASV_381	Chromista	Myzozoa	Dinophyceae	Gymnodiniales	Gymnodiniaceae	Nusuttodinium
ASV_385	Chromista	Myzozoa	Dinophyceae	NA	NA	NA
ASV_39	Chromista	Myzozoa	Dinophyceae	Gymnodiniales	Gymnodiniaceae	Lepidodinium

ASV_393	Chromista	Myzozoa	Dinophyceae	Gymnodiniales	Gymnodiniaceae	Gyrodinium
ASV_394	Chromista	Myzozoa	Dinophyceae	Gymnodiniales	Gymnodiniaceae	Gyrodinium
ASV_396	Chromista	Myzozoa	Dinophyceae	Gymnodiniales	Gymnodiniaceae	Gyrodinium
ASV_40	Chromista	Myzozoa	Dinophyceae	Gymnodiniales	Kareniaceae	Karodinium
ASV_400	Chromista	Myzozoa	Dinophyceae	NA	NA	NA
ASV_401	Chromista	Myzozoa	Dinophyceae	Syndiniales	Amoebophryaceae	Amoebophrya
ASV_404	Chromista	Myzozoa	Dinophyceae	NA	NA	NA
ASV_408	Chromista	Myzozoa	Dinophyceae	Suessiales	Suessiaceae	Polarella
ASV_411	Chromista	Myzozoa	Dinophyceae	NA	NA	NA
ASV_414	Chromista	Myzozoa	Dinophyceae	NA	NA	NA
ASV_419	Chromista	Myzozoa	Dinophyceae	NA	NA	NA
ASV_423	Chromista	Myzozoa	Dinophyceae	Peridinales	Peridiniaceae	Scrippsiella
ASV_432	Chromista	Myzozoa	Dinophyceae	Gymnodiniales	Gymnodiniaceae	Gyrodinium
ASV_433	Chromista	Myzozoa	Dinophyceae	NA	NA	NA
ASV_436	Chromista	Myzozoa	Dinophyceae	NA	NA	NA
ASV_439	Chromista	Myzozoa	Dinophyceae	Peridinales	Protoperidiniaceae	Protoperidinium
ASV_450	Chromista	Myzozoa	Dinophyceae	Gymnodiniales	Gymnodiniaceae	Gyrodinium
ASV_453	Chromista	Myzozoa	Dinophyceae	NA	NA	NA
ASV_46	Chromista	Myzozoa	Dinophyceae	NA	NA	NA
ASV_463	Chromista	Myzozoa	Dinophyceae	Gymnodiniales	Gymnodiniaceae	Gyrodinium
ASV_471	Chromista	Myzozoa	Dinophyceae	NA	NA	NA
ASV_475	Chromista	Myzozoa	Dinophyceae	NA	NA	NA
ASV_476	Chromista	Myzozoa	Dinophyceae	Suessiales	Biecheleriaceae	Biecheleria
ASV_477	Chromista	Myzozoa	Dinophyceae	Gymnodiniales	Gymnodiniaceae	NA
ASV_492	Chromista	Myzozoa	Dinophyceae	Syndiniales	Amoebophryaceae	Amoebophrya
ASV_493	Chromista	Myzozoa	Dinophyceae	NA	NA	NA
ASV_5	Chromista	Myzozoa	Dinophyceae	Gymnodiniales	Gymnodiniaceae	Gyrodinium
ASV_500	Chromista	Myzozoa	Dinophyceae	Gymnodiniales	NA	NA
ASV_503	Chromista	Myzozoa	Dinophyceae	Syndiniales	Amoebophryaceae	Amoebophrya
ASV_51	Chromista	Myzozoa	Dinophyceae	NA	NA	NA
ASV_514	Chromista	Myzozoa	Dinophyceae	Syndiniales	Amoebophryaceae	Amoebophrya
ASV_52	Chromista	Myzozoa	Dinophyceae	Gymnodiniales	Gymnodiniaceae	NA
ASV_521	Chromista	Myzozoa	Dinophyceae	Suessiales	Suessiaceae	NA
ASV_524	Chromista	Myzozoa	Dinophyceae	Gymnodiniales	Gymnodiniaceae	Gyrodinium
ASV_527	Chromista	Myzozoa	Dinophyceae	Gymnodiniales	Gymnodiniaceae	NA
ASV_528	Chromista	Myzozoa	Dinophyceae	NA	NA	NA
ASV_535	Chromista	Myzozoa	Dinophyceae	Syndiniales	Amoebophryaceae	Amoebophrya
ASV_546	Chromista	Myzozoa	Dinophyceae	NA	NA	NA
ASV_550	Chromista	Myzozoa	Dinophyceae	Peridinales	Protoperidiniaceae	Islandinium
ASV_552	Chromista	Myzozoa	Dinophyceae	Suessiales	Suessiaceae	NA
ASV_554	Chromista	Myzozoa	Dinophyceae	Gymnodiniales	NA	NA
ASV_558	Chromista	Myzozoa	Dinophyceae	Peridinales	Protoperidiniaceae	Islandinium
ASV_566	Chromista	Myzozoa	Dinophyceae	Gymnodiniales	Gymnodiniaceae	Gyrodinium
ASV_567	Chromista	Myzozoa	Dinophyceae	Suessiales	Suessiaceae	Polarella
ASV_57	Chromista	Myzozoa	Dinophyceae	Gymnodiniales	Gymnodiniaceae	Lepidodinium
ASV_571	Chromista	Myzozoa	Dinophyceae	Gymnodiniales	Gymnodiniaceae	Lepidodinium
ASV_576	Chromista	Myzozoa	Dinophyceae	Dinophysiales	Oxyphysaceae	Phalacroma
ASV_577	Chromista	Myzozoa	Dinophyceae	Syndiniales	Amoebophryaceae	Amoebophrya
ASV_581	Chromista	Myzozoa	Dinophyceae	Suessiales	Biecheleriaceae	Biecheleria
ASV_586	Chromista	Myzozoa	Dinophyceae	Syndiniales	Amoebophryaceae	Amoebophrya
ASV_597	Chromista	Myzozoa	Dinophyceae	Gymnodiniales	Gymnodiniaceae	Gyrodinium
ASV_6	Chromista	Myzozoa	Dinophyceae	Gymnodiniales	Gymnodiniaceae	Gyrodinium
ASV_60	Chromista	Myzozoa	Dinophyceae	NA	NA	NA
ASV_602	Chromista	Myzozoa	Dinophyceae	NA	NA	NA
ASV_603	Chromista	Myzozoa	Dinophyceae	NA	NA	NA
ASV_606	Chromista	Myzozoa	Dinophyceae	Syndiniales	Amoebophryaceae	Amoebophrya
ASV_611	Chromista	Myzozoa	Dinophyceae	Peridinales	Peridiniaceae	Pentapharsodinit
ASV_614	Chromista	Myzozoa	Dinophyceae	NA	NA	NA
ASV_62	Chromista	Myzozoa	Dinophyceae	Gymnodiniales	Gymnodiniaceae	Gyrodinium
ASV_622	Chromista	Myzozoa	Dinophyceae	Gymnodiniales	Gymnodiniaceae	Gyrodinium
ASV_623	Chromista	Myzozoa	Dinophyceae	Gymnodiniales	Kareniaceae	Karodinium
ASV_63	Chromista	Myzozoa	Dinophyceae	Gymnodiniales	Gymnodiniaceae	Lepidodinium
ASV_632	Chromista	Myzozoa	Dinophyceae	NA	NA	NA
ASV_635	Chromista	Myzozoa	Dinophyceae	NA	NA	NA
ASV_636	Chromista	Myzozoa	Dinophyceae	NA	NA	NA
ASV_637	Chromista	Myzozoa	Dinophyceae	NA	NA	NA
ASV_638	Chromista	Myzozoa	Dinophyceae	NA	NA	NA
ASV_64	Chromista	Myzozoa	Dinophyceae	Peridinales	Peridiniaceae	NA
ASV_640	Chromista	Myzozoa	Dinophyceae	Dinophysiales	Dinophysiaceae	Dinophysis
ASV_643	Chromista	Myzozoa	Dinophyceae	NA	NA	NA
ASV_652	Chromista	Myzozoa	Dinophyceae	Syndiniales	Amoebophryaceae	Amoebophrya
ASV_653	Chromista	Myzozoa	Dinophyceae	NA	NA	NA
ASV_655	Chromista	Myzozoa	Dinophyceae	Gymnodiniales	Kareniaceae	Karodinium
ASV_656	Chromista	Myzozoa	Dinophyceae	Suessiales	Suessiaceae	Polarella
ASV_670	Chromista	Myzozoa	Dinophyceae	NA	NA	NA
ASV_671	Chromista	Myzozoa	Dinophyceae	Syndiniales	Amoebophryaceae	Amoebophrya
ASV_672	Chromista	Myzozoa	Dinophyceae	Dinophysiales	Dinophysiaceae	Dinophysis
ASV_675	Chromista	Myzozoa	Dinophyceae	Gymnodiniales	Gymnodiniaceae	Gyrodinium
ASV_676	Chromista	Myzozoa	Dinophyceae	Gymnodiniales	Gymnodiniaceae	Gyrodinium
ASV_68	Chromista	Myzozoa	Dinophyceae	NA	NA	NA
ASV_685	Chromista	Myzozoa	Dinophyceae	NA	NA	NA
ASV_686	Chromista	Myzozoa	Dinophyceae	NA	NA	NA
ASV_687	Chromista	Myzozoa	Dinophyceae	NA	NA	NA
ASV_7	Chromista	Myzozoa	Dinophyceae	Gymnodiniales	Gymnodiniaceae	Gyrodinium
ASV_705	Chromista	Myzozoa	Dinophyceae	Gymnodiniales	Gymnodiniaceae	Paragymnodinium
ASV_706	Chromista	Myzozoa	Dinophyceae	Gymnodiniales	Gymnodiniaceae	Gyrodinium
ASV_711	Chromista	Myzozoa	Dinophyceae	Suessiales	Suessiaceae	Ansanella
ASV_715	Chromista	Myzozoa	Dinophyceae	Gymnodiniales	Kareniaceae	Karodinium

ASV_717	Chromista	Myzozoa	Dinophyceae	Syndiniales	Amoebophryaceae	Amoebophrya
ASV_719	Chromista	Myzozoa	Dinophyceae	NA	NA	NA
ASV_727	Chromista	Myzozoa	Dinophyceae	Suessiales	Suessiaceae	NA
ASV_73	Chromista	Myzozoa	Dinophyceae	Gymnodiniales	Gymnodiniaceae	Gyrodinium
ASV_732	Chromista	Myzozoa	Dinophyceae	NA	NA	NA
ASV_733	Chromista	Myzozoa	Dinophyceae	Syndiniales	Amoebophryaceae	Amoebophrya
ASV_737	Chromista	Myzozoa	Dinophyceae	Gymnodiniales	Gymnodiniaceae	Gyrodinium
ASV_746	Chromista	Myzozoa	Dinophyceae	Gymnodiniales	Kareniaceae	Karlodinium
ASV_75	Chromista	Myzozoa	Dinophyceae	Gymnodiniales	Gymnodiniaceae	NA
ASV_750	Chromista	Myzozoa	Dinophyceae	Gymnodiniales	Gymnodiniaceae	Gyrodinium
ASV_754	Chromista	Myzozoa	Dinophyceae	NA	NA	NA
ASV_756	Chromista	Myzozoa	Dinophyceae	Gymnodiniales	Kareniaceae	Karlodinium
ASV_762	Chromista	Myzozoa	Dinophyceae	Gymnodiniales	Gymnodiniaceae	Lepidodinium
ASV_766	Chromista	Myzozoa	Dinophyceae	NA	NA	NA
ASV_768	Chromista	Myzozoa	Dinophyceae	Syndiniales	Amoebophryaceae	Amoebophrya
ASV_77	Chromista	Myzozoa	Dinophyceae	Gymnodiniales	NA	NA
ASV_780	Chromista	Myzozoa	Dinophyceae	Suessiales	Biecheleriaceae	Biecheleria
ASV_782	Chromista	Myzozoa	Dinophyceae	Gymnodiniales	Kareniaceae	Karlodinium
ASV_784	Chromista	Myzozoa	Dinophyceae	Syndiniales	Amoebophryaceae	Amoebophrya
ASV_785	Chromista	Myzozoa	Dinophyceae	NA	NA	NA
ASV_79	Chromista	Myzozoa	Dinophyceae	Gymnodiniales	Gymnodiniaceae	Gyrodinium
ASV_790	Chromista	Myzozoa	Dinophyceae	Peridinales	Protoperidiniaceae	Protoperidinium
ASV_796	Chromista	Myzozoa	Dinophyceae	NA	NA	NA
ASV_806	Chromista	Myzozoa	Dinophyceae	Gymnodiniales	Gymnodiniaceae	Gyrodinium
ASV_807	Chromista	Myzozoa	Dinophyceae	Gymnodiniales	Gymnodiniaceae	Gyrodinium
ASV_825	Chromista	Myzozoa	Dinophyceae	NA	NA	NA
ASV_829	Chromista	Myzozoa	Dinophyceae	NA	NA	NA
ASV_830	Chromista	Myzozoa	Dinophyceae	Peridinales	Peridiniaceae	Scrippsiella
ASV_833	Chromista	Myzozoa	Dinophyceae	Syndiniales	Amoebophryaceae	Amoebophrya
ASV_835	Chromista	Myzozoa	Dinophyceae	Peridinales	Protoperidiniaceae	Protoperidinium
ASV_838	Chromista	Myzozoa	Dinophyceae	Gymnodiniales	Gymnodiniaceae	NA
ASV_839	Chromista	Myzozoa	Dinophyceae	NA	NA	NA
ASV_840	Chromista	Myzozoa	Dinophyceae	NA	NA	NA
ASV_842	Chromista	Myzozoa	Dinophyceae	NA	NA	NA
ASV_847	Chromista	Myzozoa	Dinophyceae	Gymnodiniales	Gymnodiniaceae	Gyrodinium
ASV_848	Chromista	Myzozoa	Dinophyceae	Syndiniales	Amoebophryaceae	Amoebophrya
ASV_850	Chromista	Myzozoa	Dinophyceae	Peridinales	Protoperidiniaceae	Protoperidinium
ASV_851	Chromista	Myzozoa	Dinophyceae	Peridinales	Protoperidiniaceae	Protoperidinium
ASV_859	Chromista	Myzozoa	Dinophyceae	NA	NA	NA
ASV_86	Chromista	Myzozoa	Dinophyceae	NA	NA	NA
ASV_87	Chromista	Myzozoa	Dinophyceae	Gymnodiniales	Gymnodiniaceae	Gyrodinium
ASV_875	Chromista	Myzozoa	Dinophyceae	Gymnodiniales	Kareniaceae	Karlodinium
ASV_878	Chromista	Myzozoa	Dinophyceae	NA	NA	NA
ASV_880	Chromista	Myzozoa	Dinophyceae	NA	NA	NA
ASV_882	Chromista	Myzozoa	Dinophyceae	NA	NA	NA
ASV_888	Chromista	Myzozoa	Dinophyceae	Gymnodiniales	Gymnodiniaceae	Gyrodinium
ASV_896	Chromista	Myzozoa	Dinophyceae	NA	NA	NA
ASV_9	Chromista	Myzozoa	Dinophyceae	Gymnodiniales	Gymnodiniaceae	Gyrodinium
ASV_90	Chromista	Myzozoa	Dinophyceae	Gymnodiniales	Gymnodiniaceae	Lepidodinium
ASV_901	Chromista	Myzozoa	Dinophyceae	Gymnodiniales	Gymnodiniaceae	Gyrodinium
ASV_910	Chromista	Myzozoa	Dinophyceae	NA	NA	NA
ASV_918	Chromista	Myzozoa	Dinophyceae	NA	NA	NA
ASV_926	Chromista	Myzozoa	Dinophyceae	NA	NA	NA
ASV_93	Chromista	Myzozoa	Dinophyceae	Gymnodiniales	Gymnodiniaceae	Lepidodinium
ASV_936	Chromista	Myzozoa	Dinophyceae	Suessiales	Biecheleriaceae	Biecheleria
ASV_943	Chromista	Myzozoa	Dinophyceae	NA	NA	NA
ASV_951	Chromista	Myzozoa	Dinophyceae	NA	NA	NA
ASV_956	Chromista	Myzozoa	Dinophyceae	NA	NA	NA
ASV_957	Chromista	Myzozoa	Dinophyceae	NA	NA	NA
ASV_968	Chromista	Myzozoa	Dinophyceae	NA	NA	NA
ASV_969	Chromista	Myzozoa	Dinophyceae	NA	NA	NA
ASV_971	Chromista	Myzozoa	Dinophyceae	NA	NA	NA
ASV_974	Chromista	Myzozoa	Dinophyceae	NA	NA	NA
ASV_99	Chromista	Myzozoa	Dinophyceae	NA	NA	NA
ASV_992	Chromista	Myzozoa	Dinophyceae	Gymnodiniales	Gymnodiniaceae	Gyrodinium
ASV_1081	Chromista	Myzozoa	NA	NA	NA	NA
ASV_1214	Chromista	Myzozoa	NA	NA	NA	NA
ASV_1320	Chromista	Myzozoa	NA	NA	NA	NA
ASV_1408	Chromista	Myzozoa	NA	NA	NA	NA
ASV_1602	Chromista	Myzozoa	NA	NA	NA	NA
ASV_1609	Chromista	Myzozoa	NA	NA	NA	NA
ASV_1662	Chromista	Myzozoa	NA	NA	NA	NA
ASV_375	Chromista	Myzozoa	NA	NA	NA	NA
ASV_583	Chromista	Myzozoa	NA	NA	NA	NA
ASV_745	Chromista	Myzozoa	NA	NA	NA	NA
ASV_853	Chromista	Myzozoa	NA	NA	NA	NA
ASV_942	Chromista	Myzozoa	NA	NA	NA	NA
ASV_959	Chromista	Myzozoa	NA	NA	NA	NA
ASV_996	Chromista	Myzozoa	NA	NA	NA	NA
ASV_1119	Chromista	NA	NA	NA	NA	NA
ASV_1202	Chromista	NA	NA	NA	NA	NA
ASV_1213	Chromista	NA	NA	NA	NA	NA
ASV_126	Chromista	NA	NA	NA	NA	NA
ASV_1267	Chromista	NA	NA	NA	NA	NA
ASV_1312	Chromista	NA	NA	NA	NA	NA
ASV_1329	Chromista	NA	NA	NA	NA	NA
ASV_1479	Chromista	NA	NA	NA	NA	NA
ASV_1489	Chromista	NA	NA	NA	NA	NA

ASV_1498	Chromista	NA	NA	NA	NA	NA
ASV_1503	Chromista	NA	NA	NA	NA	NA
ASV_1546	Chromista	NA	NA	NA	NA	NA
ASV_1592	Chromista	NA	NA	NA	NA	NA
ASV_1599	Chromista	NA	NA	NA	NA	NA
ASV_1635	Chromista	NA	NA	NA	NA	NA
ASV_1648	Chromista	NA	NA	NA	NA	NA
ASV_1649	Chromista	NA	NA	NA	NA	NA
ASV_1653	Chromista	NA	NA	NA	NA	NA
ASV_1659	Chromista	NA	NA	NA	NA	NA
ASV_1663	Chromista	NA	NA	NA	NA	NA
ASV_185	Chromista	NA	NA	NA	NA	NA
ASV_257	Chromista	NA	NA	NA	NA	NA
ASV_31	Chromista	NA	NA	NA	NA	NA
ASV_392	Chromista	NA	NA	NA	NA	NA
ASV_395	Chromista	NA	NA	NA	NA	NA
ASV_399	Chromista	NA	NA	NA	NA	NA
ASV_447	Chromista	NA	NA	NA	NA	NA
ASV_459	Chromista	NA	NA	NA	NA	NA
ASV_462	Chromista	NA	NA	NA	NA	NA
ASV_485	Chromista	NA	NA	NA	NA	NA
ASV_497	Chromista	NA	NA	NA	NA	NA
ASV_517	Chromista	NA	NA	NA	NA	NA
ASV_53	Chromista	NA	NA	NA	NA	NA
ASV_537	Chromista	NA	NA	NA	NA	NA
ASV_542	Chromista	NA	NA	NA	NA	NA
ASV_587	Chromista	NA	NA	NA	NA	NA
ASV_593	Chromista	NA	NA	NA	NA	NA
ASV_600	Chromista	NA	NA	NA	NA	NA
ASV_673	Chromista	NA	NA	NA	NA	NA
ASV_70	Chromista	NA	NA	NA	NA	NA
ASV_716	Chromista	NA	NA	NA	NA	NA
ASV_748	Chromista	NA	NA	NA	NA	NA
ASV_773	Chromista	NA	NA	NA	NA	NA
ASV_788	Chromista	NA	NA	NA	NA	NA
ASV_855	Chromista	NA	NA	NA	NA	NA
ASV_906	Chromista	NA	NA	NA	NA	NA
ASV_921	Chromista	NA	NA	NA	NA	NA
ASV_952	Chromista	NA	NA	NA	NA	NA
ASV_973	Chromista	NA	NA	NA	NA	NA
ASV_980	Chromista	NA	NA	NA	NA	NA
ASV_1306	Chromista	Oomycota	Peronosporae	NA	NA	NA
ASV_1332	Chromista	Oomycota	Peronosporae	NA	NA	NA
ASV_1376	Chromista	Oomycota	Peronosporae	NA	NA	NA
ASV_1441	Chromista	Oomycota	Peronosporae	Peronosporales	Peronosporaceae	Halophytophthor
ASV_1450	Chromista	Oomycota	Peronosporae	NA	NA	NA
ASV_1564	Chromista	Oomycota	Peronosporae	Olpidiopsidales	Olpidiopsidaceae	Olpidiopsis
ASV_1569	Chromista	Oomycota	Peronosporae	NA	NA	NA
ASV_241	Chromista	Oomycota	Peronosporae	Olpidiopsidales	Olpidiopsidaceae	Olpidiopsis
ASV_351	Chromista	Oomycota	Peronosporae	NA	NA	NA
ASV_383	Chromista	Oomycota	Peronosporae	NA	NA	NA
ASV_387	Chromista	Oomycota	Peronosporae	NA	NA	NA
ASV_691	Chromista	Oomycota	Peronosporae	NA	NA	NA
ASV_836	Chromista	Oomycota	Peronosporae	NA	NA	NA
ASV_890	Chromista	Oomycota	Peronosporae	Saprolegniales	Haliphthoraceae	Haliphthoros
ASV_113	Chromista	Radiozoa	Acantharia	Acantharia_incertae_sedis	Acantharia_incertae_sedis_EXT	Heteracon
ASV_362	Chromista	Radiozoa	Acantharia	Acantharia_incertae_sedis	Acantharia_incertae_sedis_EXT	Heteracon
ASV_726	Chromista	Radiozoa	Acantharia	NA	NA	NA
ASV_1010	Chromista	Radiozoa	Polycystina	Nassellaria	Plagiacanthidae	Lithomelissa
ASV_1	Metazoa	Arthropoda	Copepoda	Calanoida	Calanidae	NA
ASV_1002	Metazoa	Arthropoda	Copepoda	Calanoida	Calanidae	NA
ASV_1004	Metazoa	Arthropoda	Copepoda	Calanoida	Calanidae	NA
ASV_1005	Metazoa	Arthropoda	Copepoda	Calanoida	Calanidae	NA
ASV_1006	Metazoa	Arthropoda	Copepoda	Calanoida	Calanidae	NA
ASV_1009	Metazoa	Arthropoda	Copepoda	Calanoida	Calanidae	NA
ASV_1011	Metazoa	Arthropoda	Copepoda	Calanoida	Calanidae	NA
ASV_1012	Metazoa	Arthropoda	Copepoda	Calanoida	Calanidae	NA
ASV_1013	Metazoa	Arthropoda	Copepoda	Calanoida	Calanidae	NA
ASV_1014	Metazoa	Arthropoda	Copepoda	Calanoida	Calanidae	NA
ASV_1016	Metazoa	Arthropoda	Copepoda	Calanoida	NA	NA
ASV_1017	Metazoa	Arthropoda	Copepoda	Calanoida	Calanidae	NA
ASV_1018	Metazoa	Arthropoda	Copepoda	Calanoida	Calanidae	NA
ASV_1019	Metazoa	Arthropoda	Copepoda	Calanoida	Calanidae	NA
ASV_1020	Metazoa	Arthropoda	Copepoda	Calanoida	Calanidae	NA
ASV_1021	Metazoa	Arthropoda	Copepoda	Calanoida	Calanidae	NA
ASV_1028	Metazoa	Arthropoda	Copepoda	Calanoida	Calanidae	NA
ASV_1029	Metazoa	Arthropoda	Copepoda	Calanoida	Calanidae	NA
ASV_103	Metazoa	Arthropoda	Copepoda	Calanoida	Calanidae	NA
ASV_1034	Metazoa	Arthropoda	Copepoda	Calanoida	Calanidae	NA
ASV_1038	Metazoa	Arthropoda	Copepoda	Calanoida	Calanidae	NA
ASV_1040	Metazoa	Arthropoda	Copepoda	Calanoida	Calanidae	NA
ASV_1041	Metazoa	Arthropoda	Copepoda	Calanoida	Calanidae	NA
ASV_1043	Metazoa	Arthropoda	Copepoda	Calanoida	Rhincalanidae	NA
ASV_1049	Metazoa	Arthropoda	Copepoda	Calanoida	Calanidae	NA
ASV_105	Metazoa	Arthropoda	Copepoda	Calanoida	Calanidae	NA
ASV_1053	Metazoa	Arthropoda	Copepoda	Calanoida	Calanidae	NA
ASV_1054	Metazoa	Arthropoda	Copepoda	Calanoida	Calanidae	NA
ASV_1055	Metazoa	Arthropoda	Copepoda	Calanoida	Calanidae	NA

ASV_988	Metazoa	Arthropoda	Copepoda	Calanoida	Calanidae	NA
ASV_989	Metazoa	Arthropoda	Copepoda	Calanoida	Calanidae	NA
ASV_991	Metazoa	Arthropoda	Copepoda	Calanoida	Calanidae	NA
ASV_994	Metazoa	Arthropoda	Copepoda	Calanoida	Calanidae	NA
ASV_998	Metazoa	Arthropoda	Copepoda	Calanoida	Calanidae	NA
ASV_1554	Metazoa	Chaetognatha	Sagittoidea	Phragmophora	Eukrohniidae	NA
ASV_465	Metazoa	Chaetognatha	Sagittoidea	Phragmophora	Eukrohniidae	NA
ASV_763	Metazoa	Chaetognatha	Sagittoidea	Phragmophora	Eukrohniidae	NA
ASV_990	Metazoa	Chaetognatha	Sagittoidea	Phragmophora	Eukrohniidae	NA
ASV_1487	Metazoa	Chordata	Actinopterygii	Gadiformes	Merlucciidae	NA
ASV_1438	Metazoa	Chordata	Appendicularia	Copelata	Oikopleuridae	NA
ASV_604	Metazoa	Chordata	Ascidiacea	Phlebobranchia	Perophoridae	NA
ASV_609	Metazoa	Cnidaria	Hydrozoa	Trachymedusae	Rhopalonematidae	NA
ASV_118	Metazoa	Ctenophora	Tentaculata	Lobata	Bolinopsidae	NA
ASV_342	Metazoa	Ctenophora	Tentaculata	Cydidippa	Mertensiidae	NA
ASV_797	Metazoa	Ctenophora	Tentaculata	Cydidippa	Euplokamididae	NA
ASV_183	Metazoa	NA	NA	NA	NA	NA
ASV_572	Metazoa	Nematoda	NA	NA	NA	NA
ASV_488	Metazoa	Rotifera	Eurotatoria	Ploima	Synchaetidae	NA
ASV_513	Metazoa	Rotifera	Eurotatoria	Ploima	Synchaetidae	NA
ASV_1155	Plantae	Chlorophyta	Chlorophyceae	Chlamydomonadales	Chlamydomonadaceae	Carteria
ASV_1551	Plantae	Chlorophyta	Chlorophyceae	Chlamydomonadales	Chlamydomonadaceae	Carteria
ASV_299	Plantae	Chlorophyta	Chlorophyceae	Chlamydomonadales	Chlamydomonadaceae	Chlamydomonas
ASV_320	Plantae	Chlorophyta	Chlorophyceae	Chlamydomonadales	Chlamydomonadaceae	Chlamydomonas
ASV_42	Plantae	Chlorophyta	Chlorophyceae	Chlamydomonadales	Chlamydomonadaceae	Carteria
ASV_217	Plantae	Chlorophyta	Mamiellophyceae	Mamiellales	Mamiellaceae	NA
ASV_332	Plantae	Chlorophyta	Mamiellophyceae	Mamiellales	Bathycocaceae	Bathycoccus
ASV_355	Plantae	Chlorophyta	Mamiellophyceae	Dolichomastigales	Dolichomastigaceae	Crustomastix
ASV_4	Plantae	Chlorophyta	Mamiellophyceae	Mamiellales	Mamiellaceae	Micromonas
ASV_416	Plantae	Chlorophyta	Mamiellophyceae	Mamiellales	Mamiellaceae	Mantoniella
ASV_437	Plantae	Chlorophyta	Mamiellophyceae	Mamiellales	Mamiellaceae	Micromonas
ASV_591	Plantae	Chlorophyta	Mamiellophyceae	Dolichomastigales	Dolichomastigaceae	Dolichomastix
ASV_654	Plantae	Chlorophyta	Mamiellophyceae	Dolichomastigales	Dolichomastigaceae	Crustomastix
ASV_74	Plantae	Chlorophyta	Mamiellophyceae	Mamiellales	Mamiellaceae	Micromonas
ASV_967	Plantae	Chlorophyta	Mamiellophyceae	Dolichomastigales	Dolichomastigaceae	Dolichomastix
ASV_1394	Plantae	Chlorophyta	NA	NA	NA	NA
ASV_1611	Plantae	Chlorophyta	NA	NA	NA	NA
ASV_341	Plantae	Chlorophyta	NA	NA	NA	NA
ASV_431	Plantae	Chlorophyta	NA	NA	NA	NA
ASV_564	Plantae	Chlorophyta	NA	NA	NA	NA
ASV_713	Plantae	Chlorophyta	NA	NA	NA	NA
ASV_795	Plantae	Chlorophyta	NA	NA	NA	NA
ASV_923	Plantae	Chlorophyta	NA	NA	NA	NA
ASV_940	Plantae	Chlorophyta	NA	NA	NA	NA
ASV_955	Plantae	Chlorophyta	NA	NA	NA	NA
ASV_1082	Plantae	Chlorophyta	Pyramimonadophyceae	Pyramimonadales	Pyramimonadaceae	Pyramimonas
ASV_139	Plantae	Chlorophyta	Pyramimonadophyceae	Pyramimonadales	Pyramimonadaceae	Pyramimonas
ASV_18	Plantae	Chlorophyta	Pyramimonadophyceae	Pyramimonadales	Pyramimonadaceae	Pyramimonas
ASV_30	Plantae	Chlorophyta	Pyramimonadophyceae	Pyramimonadales	Pyramimonadaceae	Pyramimonas
ASV_924	Plantae	Chlorophyta	Pyramimonadophyceae	NA	NA	NA
ASV_927	Plantae	Chlorophyta	Pyramimonadophyceae	Pyramimonadales	Pyramimonadaceae	Pyramimonas
ASV_102	Protozoa	Choanozoa	Choanoflagellata	Acanthoecida	Acanthoecidae	Diaphanoeca
ASV_108	Protozoa	Choanozoa	Choanoflagellata	Acanthoecida	Stephanoecidae	Didymoeca
ASV_135	Protozoa	Choanozoa	Choanoflagellata	Acanthoecida	NA	NA
ASV_137	Protozoa	Choanozoa	Choanoflagellata	Acanthoecida	Acanthoecidae	Calliakantha
ASV_1597	Protozoa	Choanozoa	Choanoflagellata	Acanthoecida	NA	NA
ASV_347	Protozoa	Choanozoa	Choanoflagellata	Acanthoecida	Stephanoecidae	Didymoeca
ASV_522	Protozoa	Choanozoa	Choanoflagellata	Acanthoecida	NA	NA
ASV_708	Protozoa	Choanozoa	Choanoflagellata	Acanthoecida	Acanthoecidae	NA
ASV_774	Protozoa	Choanozoa	Choanoflagellata	Acanthoecida	Acanthoecidae	Calliakantha
ASV_78	Protozoa	Choanozoa	Choanoflagellata	Acanthoecida	Acanthoecidae	Calliakantha
ASV_887	Protozoa	Choanozoa	Choanoflagellata	Acanthoecida	Acanthoecidae	NA
ASV_110	Protozoa	Picozoa	Picomonadea	Picomonadida	Picomonadidae	Picomonas
ASV_1109	Protozoa	Picozoa	Picomonadea	Picomonadida	Picomonadidae	Picomonas
ASV_169	Protozoa	Picozoa	Picomonadea	Picomonadida	Picomonadidae	Picomonas
ASV_250	Protozoa	Picozoa	Picomonadea	Picomonadida	Picomonadidae	Picomonas
ASV_295	Protozoa	Picozoa	Picomonadea	Picomonadida	Picomonadidae	Picomonas
ASV_296	Protozoa	Picozoa	Picomonadea	Picomonadida	Picomonadidae	Picomonas
ASV_323	Protozoa	Picozoa	Picomonadea	Picomonadida	Picomonadidae	Picomonas
ASV_474	Protozoa	Picozoa	Picomonadea	Picomonadida	Picomonadidae	Picomonas
ASV_601	Protozoa	Picozoa	Picomonadea	Picomonadida	Picomonadidae	Picomonas
ASV_677	Protozoa	Picozoa	Picomonadea	Picomonadida	Picomonadidae	Picomonas
ASV_1186	Protozoa	Protozoa_incl	Ebriophyceae	Ebriales	Ebriaceae	Ebria
ASV_1393	Protozoa	Protozoa_incl	Ebriophyceae	Ebriales	Ebriaceae	Ebria
ASV_197	Protozoa	Protozoa_incl	Ebriophyceae	Ebriales	Ebriaceae	Ebria
ASV_489	Protozoa	Protozoa_incl	Ebriophyceae	Ebriales	Ebriaceae	Ebria
ASV_516	Protozoa	Protozoa_incl	Ebriophyceae	Ebriales	Ebriaceae	Ebria
ASV_540	Protozoa	Protozoa_incl	Ebriophyceae	Ebriales	Ebriaceae	Ebria
ASV_615	Protozoa	Protozoa_incl	Ebriophyceae	Ebriales	Ebriaceae	Ebria
ASV_644	Protozoa	Protozoa_incl	Ebriophyceae	Ebriales	Ebriaceae	Ebria
ASV_813	Protozoa	Protozoa_incl	Ebriophyceae	Ebriales	Ebriaceae	Ebria
ASV_817	Protozoa	Protozoa_incl	Ebriophyceae	Ebriales	Ebriaceae	Ebria
ASV_904	Protozoa	Protozoa_incl	Protozoa_incertae_sedis_EXT	Protozoa_incertae_sedis_EXT	Protozoa_incertae_sedis_EXT	Solenicola
ASV_1036	Unassigned_Kingdom	NA	NA	NA	NA	NA
ASV_1163	Unassigned_Kingdom	NA	NA	NA	NA	NA
ASV_1167	Unassigned_Kingdom	NA	NA	NA	NA	NA
ASV_1198	Unassigned_Kingdom	NA	NA	NA	NA	NA
ASV_1219	Unassigned_Kingdom	NA	NA	NA	NA	NA

ASV_1221	Unassigned_Kingdom	NA	NA	NA	NA	NA
ASV_1230	Unassigned_Kingdom	NA	NA	NA	NA	NA
ASV_1251	Unassigned_Kingdom	NA	NA	NA	NA	NA
ASV_1254	Unassigned_Kingdom	NA	NA	NA	NA	NA
ASV_1272	Unassigned_Kingdom	NA	NA	NA	NA	NA
ASV_1307	Unassigned_Kingdom	NA	NA	NA	NA	NA
ASV_1316	Unassigned_Kingdom	NA	NA	NA	NA	NA
ASV_1413	Unassigned_Kingdom	NA	NA	NA	NA	NA
ASV_1416	Unassigned_Kingdom	NA	NA	NA	NA	NA
ASV_1446	Unassigned_Kingdom	NA	NA	NA	NA	NA
ASV_1458	Unassigned_Kingdom	NA	NA	NA	NA	NA
ASV_1504	Unassigned_Kingdom	NA	NA	NA	NA	NA
ASV_1545	Unassigned_Kingdom	NA	NA	NA	NA	NA
ASV_1623	Unassigned_Kingdom	NA	NA	NA	NA	NA
ASV_1656	Unassigned_Kingdom	NA	NA	NA	NA	NA
ASV_1673	Unassigned_Kingdom	NA	NA	NA	NA	NA
ASV_302	Unassigned_Kingdom	NA	NA	NA	NA	NA
ASV_448	Unassigned_Kingdom	NA	NA	NA	NA	NA
ASV_692	Unassigned_Kingdom	NA	NA	NA	NA	NA
ASV_758	Unassigned_Kingdom	NA	NA	NA	NA	NA
ASV_772	Unassigned_Kingdom	NA	NA	NA	NA	NA
ASV_776	Unassigned_Kingdom	NA	NA	NA	NA	NA

Notes: Species-level assignments were not considered for the whole 18S dataset due to the conservative nature of the gene.

Genus level assignments were not considered for Metazoans

Table S6. Taxonomic information for all MOTUs recovered with the COI gene

MOTU Name	Kingdom	Phylum	Class	Order	Family	Genus	Species
Labyrinthulea	Chromista	Bigyra	Labyrinthulea	NA	NA	NA	NA
Cryptophyceae_1	Chromista	Cryptophyta	Cryptophyceae	NA	NA	NA	NA
Cryptophyceae_2	Chromista	Cryptophyta	Cryptophyceae	NA	NA	NA	NA
Cryptophyceae_3	Chromista	Cryptophyta	Cryptophyceae	NA	NA	NA	NA
Cryptophyceae_4	Chromista	Cryptophyta	Cryptophyceae	NA	NA	NA	NA
Coccolithophyceae_1	Chromista	Haptophyta	Coccolithophyceae	NA	NA	NA	NA
Coccolithophyceae_10	Chromista	Haptophyta	Coccolithophyceae	NA	NA	NA	NA
Coccolithophyceae_11	Chromista	Haptophyta	Coccolithophyceae	NA	NA	NA	NA
Coccolithophyceae_12	Chromista	Haptophyta	Coccolithophyceae	NA	NA	NA	NA
Coccolithophyceae_2	Chromista	Haptophyta	Coccolithophyceae	NA	NA	NA	NA
Coccolithophyceae_3	Chromista	Haptophyta	Coccolithophyceae	NA	NA	NA	NA
Coccolithophyceae_4	Chromista	Haptophyta	Coccolithophyceae	NA	NA	NA	NA
Coccolithophyceae_5	Chromista	Haptophyta	Coccolithophyceae	NA	NA	NA	NA
Coccolithophyceae_6	Chromista	Haptophyta	Coccolithophyceae	NA	NA	NA	NA
Coccolithophyceae_7	Chromista	Haptophyta	Coccolithophyceae	NA	NA	NA	NA
Coccolithophyceae_8	Chromista	Haptophyta	Coccolithophyceae	NA	NA	NA	NA
Coccolithophyceae_9	Chromista	Haptophyta	Coccolithophyceae	NA	NA	NA	NA
Phaeocystales	Chromista	Haptophyta	Coccolithophyceae	Phaeocystales	NA	NA	NA
Prymniales	Chromista	Haptophyta	Coccolithophyceae	Prymniales	NA	NA	NA
Haptophyceae_1	Chromista	Haptophyta	Haptophyceae	NA	NA	NA	NA
Haptophyceae_2	Chromista	Haptophyta	Haptophyceae	NA	NA	NA	NA
Haptophyceae_3	Chromista	Haptophyta	Haptophyceae	NA	NA	NA	NA
Haptophyta_1	Chromista	Haptophyta	NA	NA	NA	NA	NA
Haptophyta_2	Chromista	Haptophyta	NA	NA	NA	NA	NA
Haptophyta_3	Chromista	Haptophyta	NA	NA	NA	NA	NA
Haptophyta_4	Chromista	Haptophyta	NA	NA	NA	NA	NA
Haptophyta_5	Chromista	Haptophyta	NA	NA	NA	NA	NA
Prymnesiophyceae_1	Chromista	Haptophyta	Prymnesiophyceae	NA	NA	NA	NA
Prymnesiophyceae_2	Chromista	Haptophyta	Prymnesiophyceae	NA	NA	NA	NA
Prymnesiophyceae_3	Chromista	Haptophyta	Prymnesiophyceae	NA	NA	NA	NA
Bacillariaceae_1	Chromista	Heterokontophyta	Bacillariophyceae	Bacillariales	Bacillariaceae	NA	NA
Bacillariaceae_2	Chromista	Heterokontophyta	Bacillariophyceae	Bacillariales	Bacillariaceae	NA	NA
Bacillariaceae_3	Chromista	Heterokontophyta	Bacillariophyceae	Bacillariales	Bacillariaceae	NA	NA
Bacillariales_1	Chromista	Heterokontophyta	Bacillariophyceae	Bacillariales	NA	NA	NA
Bacillariales_2	Chromista	Heterokontophyta	Bacillariophyceae	Bacillariales	NA	NA	NA
Bacillariales_3	Chromista	Heterokontophyta	Bacillariophyceae	Bacillariales	NA	NA	NA
Bacillariales_4	Chromista	Heterokontophyta	Bacillariophyceae	Bacillariales	NA	NA	NA
Bacillariales_5	Chromista	Heterokontophyta	Bacillariophyceae	Bacillariales	NA	NA	NA
Bacillariales_6	Chromista	Heterokontophyta	Bacillariophyceae	Bacillariales	NA	NA	NA
Bacillariales_7	Chromista	Heterokontophyta	Bacillariophyceae	Bacillariales	NA	NA	NA
Bacillariophyceae_1	Chromista	Heterokontophyta	Bacillariophyceae	NA	NA	NA	NA
Bacillariophyceae_10	Chromista	Heterokontophyta	Bacillariophyceae	NA	NA	NA	NA
Bacillariophyceae_11	Chromista	Heterokontophyta	Bacillariophyceae	NA	NA	NA	NA
Bacillariophyceae_12	Chromista	Heterokontophyta	Bacillariophyceae	NA	NA	NA	NA
Bacillariophyceae_13	Chromista	Heterokontophyta	Bacillariophyceae	NA	NA	NA	NA
Bacillariophyceae_14	Chromista	Heterokontophyta	Bacillariophyceae	NA	NA	NA	NA
Bacillariophyceae_15	Chromista	Heterokontophyta	Bacillariophyceae	NA	NA	NA	NA
Bacillariophyceae_16	Chromista	Heterokontophyta	Bacillariophyceae	NA	NA	NA	NA
Bacillariophyceae_17	Chromista	Heterokontophyta	Bacillariophyceae	NA	NA	NA	NA
Bacillariophyceae_18	Chromista	Heterokontophyta	Bacillariophyceae	NA	NA	NA	NA
Bacillariophyceae_19	Chromista	Heterokontophyta	Bacillariophyceae	NA	NA	NA	NA
Bacillariophyceae_2	Chromista	Heterokontophyta	Bacillariophyceae	NA	NA	NA	NA
Bacillariophyceae_20	Chromista	Heterokontophyta	Bacillariophyceae	NA	NA	NA	NA
Bacillariophyceae_21	Chromista	Heterokontophyta	Bacillariophyceae	NA	NA	NA	NA
Bacillariophyceae_22	Chromista	Heterokontophyta	Bacillariophyceae	NA	NA	NA	NA
Bacillariophyceae_23	Chromista	Heterokontophyta	Bacillariophyceae	NA	NA	NA	NA
Bacillariophyceae_24	Chromista	Heterokontophyta	Bacillariophyceae	NA	NA	NA	NA
Bacillariophyceae_3	Chromista	Heterokontophyta	Bacillariophyceae	Naviculales	NA	NA	NA
Bacillariophyceae_4	Chromista	Heterokontophyta	Bacillariophyceae	NA	NA	NA	NA
Bacillariophyceae_5	Chromista	Heterokontophyta	Bacillariophyceae	NA	NA	NA	NA
Bacillariophyceae_6	Chromista	Heterokontophyta	Bacillariophyceae	NA	NA	NA	NA
Bacillariophyceae_7	Chromista	Heterokontophyta	Bacillariophyceae	NA	NA	NA	NA
Bacillariophyceae_8	Chromista	Heterokontophyta	Bacillariophyceae	NA	NA	NA	NA
Bacillariophyceae_9	Chromista	Heterokontophyta	Bacillariophyceae	NA	NA	NA	NA
Cylindrotheca_1	Chromista	Heterokontophyta	Bacillariophyceae	Bacillariales	Bacillariaceae	Cylindrotheca	NA
Cylindrotheca_2	Chromista	Heterokontophyta	Bacillariophyceae	Bacillariales	Bacillariaceae	Cylindrotheca	NA
Entomoneis_1	Chromista	Heterokontophyta	Bacillariophyceae	Surirellales	Entomoneidaceae	Entomoneis	NA
Entomoneis_2	Chromista	Heterokontophyta	Bacillariophyceae	Surirellales	Entomoneidaceae	Entomoneis	NA
Entomoneis_3	Chromista	Heterokontophyta	Bacillariophyceae	Surirellales	Entomoneidaceae	Entomoneis	NA
Fragilariopsis	Chromista	Heterokontophyta	Bacillariophyceae	Bacillariales	Bacillariaceae	Fragilariopsis	NA
Naviculaceae_1	Chromista	Heterokontophyta	Bacillariophyceae	Naviculales	Naviculaceae	NA	NA
Naviculaceae_2	Chromista	Heterokontophyta	Bacillariophyceae	Naviculales	Naviculaceae	NA	NA
Naviculales_1	Chromista	Heterokontophyta	Bacillariophyceae	Naviculales	NA	NA	NA
Naviculales_2	Chromista	Heterokontophyta	Bacillariophyceae	Naviculales	NA	NA	NA
Naviculales_3	Chromista	Heterokontophyta	Bacillariophyceae	Naviculales	NA	NA	NA
Nitzschia_1	Chromista	Heterokontophyta	Bacillariophyceae	Bacillariales	Bacillariaceae	Nitzschia	NA
Nitzschia_2	Chromista	Heterokontophyta	Bacillariophyceae	Bacillariales	Bacillariaceae	Nitzschia	Nitzschia cf. promare
Pseudo-nitzschia	Chromista	Heterokontophyta	Bacillariophyceae	Bacillariales	Bacillariaceae	Pseudo-nitzschia	NA
Attheya	Chromista	Heterokontophyta	Coccinodiscophyceae	Chaetocerotales	Attheyaceae	Attheya	NA
Attheya longicornis	Chromista	Heterokontophyta	Coccinodiscophyceae	Chaetocerotales	Attheyaceae	Attheya	Attheya longicornis
Chaetocerotaceae	Chromista	Heterokontophyta	Coccinodiscophyceae	Chaetocerotales	Chaetocerotaceae	NA	NA
Coccinodiscophyceae	Chromista	Heterokontophyta	Coccinodiscophyceae	NA	NA	NA	NA
Raphidophyceae_18	Chromista	Heterokontophyta	Coccinodiscophyceae	Rhizosoleniales	Rhizosoleniaceae	NA	NA
Thalassiosirales	Chromista	Heterokontophyta	Coccinodiscophyceae	Thalassiosirales	NA	NA	NA
Ceramiales	Plantae	Rhodophyta	Florideophyceae	Ceramiales	NA	NA	NA
Fragilariaceae	Chromista	Heterokontophyta	Fragilariophyceae	Fragilariiales	Fragilariaceae	NA	NA
Chaetocerotales	Chromista	Heterokontophyta	Mediophyceae	Chaetocerotales	NA	NA	NA
Mediophyceae_1	Chromista	Heterokontophyta	Mediophyceae	NA	NA	NA	NA
Mediophyceae_2	Chromista	Heterokontophyta	Mediophyceae	NA	NA	NA	NA
Skeletonemataceae	Chromista	Heterokontophyta	Mediophyceae	Thalassiosirales	Skeletonemataceae	NA	NA
Bacillariophyta_1	Chromista	Heterokontophyta	NA	NA	NA	NA	NA
Bacillariophyta_10	Chromista	Heterokontophyta	NA	NA	NA	NA	NA
Bacillariophyta_11	Chromista	Heterokontophyta	NA	NA	NA	NA	NA
Bacillariophyta_12	Chromista	Heterokontophyta	NA	NA	NA	NA	NA
Bacillariophyta_13	Chromista	Heterokontophyta	NA	NA	NA	NA	NA
Bacillariophyta_2	Chromista	Heterokontophyta	NA	NA	NA	NA	NA

Raphidophyceae_15	Chromista	Ochrophyta	Raphidophyceae	NA	NA	NA	NA
Raphidophyceae_16	Chromista	Ochrophyta	Raphidophyceae	NA	NA	NA	NA
Raphidophyceae_17	Chromista	Ochrophyta	Raphidophyceae	NA	NA	NA	NA
Raphidophyceae_2	Chromista	Ochrophyta	Raphidophyceae	NA	NA	NA	NA
Raphidophyceae_4	Chromista	Ochrophyta	Raphidophyceae	NA	NA	NA	NA
Raphidophyceae_5	Chromista	Ochrophyta	Raphidophyceae	NA	NA	NA	NA
Raphidophyceae_6	Chromista	Ochrophyta	Raphidophyceae	NA	NA	NA	NA
Raphidophyceae_7	Chromista	Ochrophyta	Raphidophyceae	NA	NA	NA	NA
Raphidophyceae_8	Chromista	Ochrophyta	Raphidophyceae	NA	NA	NA	NA
Raphidophyceae_9	Chromista	Ochrophyta	Raphidophyceae	NA	NA	NA	NA
Oomycota_14	Chromista	Oomycota	NA	NA	NA	NA	NA
Oomycota_3	Chromista	Oomycota	NA	NA	NA	NA	NA
Oomycota_35	Chromista	Oomycota	NA	NA	NA	NA	NA
Oomycota_4	Chromista	Oomycota	NA	NA	NA	NA	NA
Oomycota_43	Chromista	Oomycota	NA	NA	NA	NA	NA
Oomycota_53	Chromista	Oomycota	NA	NA	NA	NA	NA
Oomycota_6	Chromista	Oomycota	NA	NA	NA	NA	NA
Oomycota_9	Chromista	Oomycota	NA	NA	NA	NA	NA
Eurotiomycetes_1	Fungi	Ascomycota	Eurotiomycetes	NA	NA	NA	NA
Eurotiomycetes_2	Fungi	Ascomycota	Eurotiomycetes	NA	NA	NA	NA
Leotiomycetes_1	Fungi	Ascomycota	Leotiomycetes	NA	NA	NA	NA
Leotiomycetes_2	Fungi	Ascomycota	Leotiomycetes	NA	NA	NA	NA
Leotiomycetes_3	Fungi	Ascomycota	Leotiomycetes	NA	NA	NA	NA
Myxotrichaceae	Fungi	Ascomycota	Leotiomycetes	Leotiomycetes_incertae_sedis	Myxotrichaceae	NA	NA
Ascomycota_1	Fungi	Ascomycota	NA	NA	NA	NA	NA
Ascomycota_2	Fungi	Ascomycota	NA	NA	NA	NA	NA
Ascomycota_3	Fungi	Ascomycota	NA	NA	NA	NA	NA
Ascomycota_4	Fungi	Ascomycota	NA	NA	NA	NA	NA
Ascomycota_5	Fungi	Ascomycota	NA	NA	NA	NA	NA
Geotrichum candidum	Fungi	Ascomycota	Saccharomycetes	Saccharomycetales	Dipodascaceae	Geotrichum	Geotrichum candidum
Hypocreales	Fungi	Ascomycota	Sordariomycetes	Hypocreales	NA	NA	NA
Sordariomycetes_1	Fungi	Ascomycota	Sordariomycetes	NA	NA	NA	NA
Sordariomycetes_2	Fungi	Ascomycota	Sordariomycetes	NA	NA	NA	NA
Trichoderma	Fungi	Ascomycota	Sordariomycetes	Hypocreales	Hypocreaceae	Trichoderma	NA
Agaricales_1	Fungi	Basidiomycota	Agaricomycetes	Agaricales	NA	NA	NA
Agaricales_2	Fungi	Basidiomycota	Agaricomycetes	Agaricales	NA	NA	NA
Agaricomycetes_1	Fungi	Basidiomycota	Agaricomycetes	NA	NA	NA	NA
Agaricomycetes_2	Fungi	Basidiomycota	Agaricomycetes	NA	NA	NA	NA
Agaricomycetes_3	Fungi	Basidiomycota	Agaricomycetes	NA	NA	NA	NA
Agaricomycetes_4	Fungi	Basidiomycota	Agaricomycetes	NA	NA	NA	NA
Entoloma_1	Fungi	Basidiomycota	Agaricomycetes	Agaricales	Entolomataceae	Entoloma	NA
Entoloma_2	Fungi	Basidiomycota	Agaricomycetes	Agaricales	Entolomataceae	Entoloma	NA
Entoloma_3	Fungi	Basidiomycota	Agaricomycetes	Agaricales	Entolomataceae	Entoloma	NA
Polyporaceae	Fungi	Basidiomycota	Agaricomycetes	Polyporales	Polyporaceae	NA	NA
Polyporales	Fungi	Basidiomycota	Agaricomycetes	Polyporales	NA	NA	NA
Stropharia	Fungi	Basidiomycota	Agaricomycetes	Agaricales	Strophariaceae	Stropharia	NA
Exobasidiomycetes	Fungi	Basidiomycota	Exobasidiomycetes	NA	NA	NA	NA
Malassezia	Fungi	Basidiomycota	Malasseziomycetes	Malasseziales	Malasseziaceae	Malassezia	NA
Microbotryomycetes_1	Fungi	Basidiomycota	Microbotryomycetes	NA	NA	NA	NA
Microbotryomycetes_2	Fungi	Basidiomycota	Microbotryomycetes	NA	NA	NA	NA
Microbotryomycetes_3	Fungi	Basidiomycota	Microbotryomycetes	NA	NA	NA	NA
Basidiomycota_2	Fungi	Basidiomycota	NA	NA	NA	NA	NA
Basidiomycota_3	Fungi	Basidiomycota	NA	NA	NA	NA	NA
Basidiomycota_4	Fungi	Basidiomycota	NA	NA	NA	NA	NA
Basidiomycota_6	Fungi	Basidiomycota	NA	NA	NA	NA	NA
Basidiomycota_7	Fungi	Basidiomycota	NA	NA	NA	NA	NA
Basidiomycota_8	Fungi	Basidiomycota	NA	NA	NA	NA	NA
Basidiomycota_1	Fungi	Basidiomycota	NA	NA	NA	NA	NA
Basidiomycota_5	Fungi	Basidiomycota	NA	NA	NA	NA	NA
Basidiomycota_9	Fungi	Basidiomycota	NA	NA	NA	NA	NA
Mucorales	Fungi	Mucoromycota	Mucoromycotina	Mucorales	NA	NA	NA
Mucoromycotina_1	Fungi	Mucoromycota	Mucoromycotina	NA	NA	NA	NA
Mucoromycotina_2	Fungi	Mucoromycota	Mucoromycotina	NA	NA	NA	NA
Mucoromycota	Fungi	Mucoromycota	NA	NA	NA	NA	NA
Annelida_1	Metazoa	Annelida	NA	NA	NA	NA	NA
Annelida_2	Metazoa	Annelida	NA	NA	NA	NA	NA
Annelida_3	Metazoa	Annelida	NA	NA	NA	NA	NA
Annelida_4	Metazoa	Annelida	NA	NA	NA	NA	NA
Polychaeta_1	Metazoa	Annelida	Polychaeta	NA	NA	NA	NA
Polychaeta_2	Metazoa	Annelida	Polychaeta	NA	NA	NA	NA
Copepoda	Metazoa	Arthropoda	Copepoda	NA	NA	NA	NA
Microsetella norvegica	Metazoa	Arthropoda	Copepoda	Haracticoida	Ectinosomatidae	Microsetella	Microsetella norvegica
Tisbe furcata	Metazoa	Arthropoda	Copepoda	Haracticoida	Tisbidae	Tisbe	Tisbe furcata
Amphipoda	Metazoa	Arthropoda	Malacostraca	Amphipoda	NA	NA	NA
Apherusa glacialis_1	Metazoa	Arthropoda	Malacostraca	Amphipoda	Calliopidae	Apherusa	Apherusa glacialis
Apherusa glacialis_2	Metazoa	Arthropoda	Malacostraca	Amphipoda	Calliopidae	Apherusa	Apherusa glacialis
Apherusa glacialis_3	Metazoa	Arthropoda	Malacostraca	Amphipoda	Calliopidae	Apherusa	Apherusa glacialis
Apherusa glacialis_4	Metazoa	Arthropoda	Malacostraca	Amphipoda	Calliopidae	Apherusa	Apherusa glacialis
Apherusa_1	Metazoa	Arthropoda	Malacostraca	Amphipoda	Calliopidae	Apherusa	NA
Apherusa_2	Metazoa	Arthropoda	Malacostraca	Amphipoda	Calliopidae	Apherusa	NA
Malacostraca_1	Metazoa	Arthropoda	Malacostraca	NA	NA	NA	NA
Malacostraca_2	Metazoa	Arthropoda	Malacostraca	NA	NA	NA	NA
Malacostraca_3	Metazoa	Arthropoda	Malacostraca	NA	NA	NA	NA
Calanus finmarchicus	Metazoa	Arthropoda	Maxillopoda	Calanoida	Calanidae	Calanus	Calanus finmarchicus
Calanus glacialis	Metazoa	Arthropoda	Maxillopoda	Calanoida	Calanidae	Calanus	Calanus glacialis
Calanus hyperboreus	Metazoa	Arthropoda	Maxillopoda	Calanoida	Calanidae	Calanus	Calanus hyperboreus
Oithona similis_1	Metazoa	Arthropoda	Maxillopoda	Cyclopoida	Oithonidae	Oithona	Oithona similis
Oithona similis_2	Metazoa	Arthropoda	Maxillopoda	Cyclopoida	Oithonidae	Oithona	Oithona similis
Pseudocalanus minutus	Metazoa	Arthropoda	Maxillopoda	Calanoida	Clausocalanidae	Pseudocalanus	Pseudocalanus minutus
Triconia borealis	Metazoa	Arthropoda	Maxillopoda	Poeclostomatoida	Oncaeidae	Triconia	Triconia borealis
Arthropoda_1	Metazoa	Arthropoda	NA	NA	NA	NA	NA
Arthropoda_2	Metazoa	Arthropoda	NA	NA	NA	NA	NA
Arthropoda_3	Metazoa	Arthropoda	NA	NA	NA	NA	NA
Arthropoda_4	Metazoa	Arthropoda	NA	NA	NA	NA	NA
Arthropoda_5	Metazoa	Arthropoda	NA	NA	NA	NA	NA
Arthropoda_6	Metazoa	Arthropoda	NA	NA	NA	NA	NA
Arthropoda_7	Metazoa	Arthropoda	NA	NA	NA	NA	NA
Eukrohnia bathyantartic	Metazoa	Chaetognatha	Sagittoidea	Phragmophora	Eukrohniidae	Eukrohnia	Eukrohnia bathyantartica

Actinopterygii	Metazoa	Chordata	Actinopterygii	NA	NA	NA	NA
Boreogadus saida	Metazoa	Chordata	Actinopterygii	Gadiformes	Gadidae	Boreogadus	Boreogadus saida
Asciidiacea_1	Metazoa	Chordata	Asciidiacea	NA	NA	NA	NA
Asciidiacea_2	Metazoa	Chordata	Asciidiacea	NA	NA	NA	NA
Balaena mysticetus	Metazoa	Chordata	Mammalia	Artiodactyla	Balaenidae	Balaena	Balaena mysticetus
Monodon monoceros	Metazoa	Chordata	Mammalia	Artiodactyla	Monodontidae	Monodon	Monodon monoceros
Anthozoa_1	Metazoa	Cnidaria	Anthozoa	NA	NA	NA	NA
Anthozoa_2	Metazoa	Cnidaria	Anthozoa	NA	NA	NA	NA
Anthozoa_3	Metazoa	Cnidaria	Anthozoa	NA	NA	NA	NA
Hydrozoa_1	Metazoa	Cnidaria	Hydrozoa	NA	NA	NA	NA
Hydrozoa_10	Metazoa	Cnidaria	Hydrozoa	NA	NA	NA	NA
Hydrozoa_11	Metazoa	Cnidaria	Hydrozoa	NA	NA	NA	NA
Hydrozoa_12	Metazoa	Cnidaria	Hydrozoa	NA	NA	NA	NA
Hydrozoa_13	Metazoa	Cnidaria	Hydrozoa	NA	NA	NA	NA
Hydrozoa_14	Metazoa	Cnidaria	Hydrozoa	NA	NA	NA	NA
Hydrozoa_15	Metazoa	Cnidaria	Hydrozoa	NA	NA	NA	NA
Hydrozoa_16	Metazoa	Cnidaria	Hydrozoa	NA	NA	NA	NA
Hydrozoa_2	Metazoa	Cnidaria	Hydrozoa	NA	NA	NA	NA
Hydrozoa_3	Metazoa	Cnidaria	Hydrozoa	NA	NA	NA	NA
Hydrozoa_4	Metazoa	Cnidaria	Hydrozoa	NA	NA	NA	NA
Hydrozoa_5	Metazoa	Cnidaria	Hydrozoa	NA	NA	NA	NA
Hydrozoa_6	Metazoa	Cnidaria	Hydrozoa	NA	NA	NA	NA
Hydrozoa_7	Metazoa	Cnidaria	Hydrozoa	NA	NA	NA	NA
Hydrozoa_9	Metazoa	Cnidaria	Hydrozoa	NA	NA	NA	NA
Obelia bidentata	Metazoa	Cnidaria	Hydrozoa	Leptothecata	Obeliidae	Obelia	Obelia bidentata
Raphidophyceae_3	Metazoa	Cnidaria	Hydrozoa	NA	NA	NA	NA
Cnidaria_1	Metazoa	Cnidaria	NA	NA	NA	NA	NA
Cnidaria_2	Metazoa	Cnidaria	NA	NA	NA	NA	NA
Scyphozoa_1	Metazoa	Cnidaria	Scyphozoa	NA	NA	NA	NA
Scyphozoa_2	Metazoa	Cnidaria	Scyphozoa	NA	NA	NA	NA
Scyphozoa_3	Metazoa	Cnidaria	Scyphozoa	NA	NA	NA	NA
Scyphozoa_4	Metazoa	Cnidaria	Scyphozoa	NA	NA	NA	NA
Scyphozoa_5	Metazoa	Cnidaria	Scyphozoa	NA	NA	NA	NA
Scyphozoa_6	Metazoa	Cnidaria	Scyphozoa	NA	NA	NA	NA
Ctenophora	Metazoa	Ctenophora	NA	NA	NA	NA	NA
Bolinopsis_1	Metazoa	Ctenophora	Tentaculata	Lobata	Bolinopsidae	Bolinopsis	NA
Bolinopsis_2	Metazoa	Ctenophora	Tentaculata	Lobata	Bolinopsidae	Bolinopsis	NA
Tentaculata	Metazoa	Ctenophora	Tentaculata	NA	NA	NA	NA
Gastropoda_1	Metazoa	Mollusca	Gastropoda	NA	NA	NA	NA
Gastropoda_2	Metazoa	Mollusca	Gastropoda	NA	NA	NA	NA
Gastropoda_3	Metazoa	Mollusca	Gastropoda	NA	NA	NA	NA
Mollusca_1	Metazoa	Mollusca	NA	NA	NA	NA	NA
Mollusca_2	Metazoa	Mollusca	NA	NA	NA	NA	NA
Mollusca_3	Metazoa	Mollusca	NA	NA	NA	NA	NA
Metazoa	Metazoa	NA	NA	NA	NA	NA	NA
Chromadorea	Metazoa	Nematoda	Chromadorea	NA	NA	NA	NA
Hoploneurtea	Metazoa	Nemertea	Hoploneurtea	NA	NA	NA	NA
Nemertea	Metazoa	Nemertea	NA	NA	NA	NA	NA
Palaeonemertea	Metazoa	Nemertea	Palaeonemertea	NA	NA	NA	NA
Bubarida	Metazoa	Porifera	Demospongiae	Bubarida	NA	NA	NA
Demospongiae_1	Metazoa	Porifera	Demospongiae	NA	NA	NA	NA
Demospongiae_2	Metazoa	Porifera	Demospongiae	NA	NA	NA	NA
Demospongiae_3	Metazoa	Porifera	Demospongiae	NA	NA	NA	NA
Demospongiae_4	Metazoa	Porifera	Demospongiae	NA	NA	NA	NA
Habrotricha	Metazoa	Rotifera	Bdelloidea	Philodinida	Habrotrichidae	Habrotricha	NA
Monogononta_1	Metazoa	Rotifera	Monogononta	NA	NA	NA	NA
Monogononta_2	Metazoa	Rotifera	Monogononta	NA	NA	NA	NA
Monogononta_3	Metazoa	Rotifera	Monogononta	NA	NA	NA	NA
Monogononta_4	Metazoa	Rotifera	Monogononta	NA	NA	NA	NA
Ploima_1	Metazoa	Rotifera	Monogononta	Ploima	NA	NA	NA
Ploima_2	Metazoa	Rotifera	Monogononta	Ploima	NA	NA	NA
Polyarthra	Metazoa	Rotifera	Monogononta	Ploima	Synchaetidae	Polyarthra	NA
Rotifera	Metazoa	Rotifera	NA	NA	NA	NA	NA
Eukaryota_1	Unassigned_NA	NA	NA	NA	NA	NA	NA
Eukaryota_2	Unassigned_NA	NA	NA	NA	NA	NA	NA
Eukaryota_3	Unassigned_NA	NA	NA	NA	NA	NA	NA
Eukaryota_4	Unassigned_NA	NA	NA	NA	NA	NA	NA
Eukaryota_5	Unassigned_NA	NA	NA	NA	NA	NA	NA
Eukaryota_6	Unassigned_NA	NA	NA	NA	NA	NA	NA
Unassigned_1	Unassigned_NA	NA	NA	NA	NA	NA	NA
Unassigned_10	Unassigned_NA	NA	NA	NA	NA	NA	NA
Unassigned_11	Unassigned_NA	NA	NA	NA	NA	NA	NA
Unassigned_12	Unassigned_NA	NA	NA	NA	NA	NA	NA
Unassigned_13	Unassigned_NA	NA	NA	NA	NA	NA	NA
Unassigned_14	Unassigned_NA	NA	NA	NA	NA	NA	NA
Unassigned_15	Unassigned_NA	NA	NA	NA	NA	NA	NA
Unassigned_16	Unassigned_NA	NA	NA	NA	NA	NA	NA
Unassigned_17	Unassigned_NA	NA	NA	NA	NA	NA	NA
Unassigned_18	Unassigned_NA	NA	NA	NA	NA	NA	NA
Unassigned_19	Unassigned_NA	NA	NA	NA	NA	NA	NA
Unassigned_2	Unassigned_NA	NA	NA	NA	NA	NA	NA
Unassigned_20	Unassigned_NA	NA	NA	NA	NA	NA	NA
Unassigned_3	Unassigned_NA	NA	NA	NA	NA	NA	NA
Unassigned_4	Unassigned_NA	NA	NA	NA	NA	NA	NA
Unassigned_5	Unassigned_NA	NA	NA	NA	NA	NA	NA
Unassigned_6	Unassigned_NA	NA	NA	NA	NA	NA	NA
Unassigned_7	Unassigned_NA	NA	NA	NA	NA	NA	NA
Unassigned_8	Unassigned_NA	NA	NA	NA	NA	NA	NA
Unassigned_9	Unassigned_NA	NA	NA	NA	NA	NA	NA
Chlamydomonas	Plantae	Chlorophyta	Chlorophyceae	Chlamydomonadales	Chlamydomonadaceae	Chlamydomonas	NA
Chloroparvula pacifica	Plantae	Chlorophyta	Chlorocicophyceae	Chloropicales	Chloropicaceae	Chloroparvula	Chloroparvula pacifica
Bathycoccus prasinos	Plantae	Chlorophyta	Mamiellophyceae	Mamiellales	Bathycoccaceae	Bathycoccus	Bathycoccus prasinos
Dolichomastix_1	Plantae	Chlorophyta	Mamiellophyceae	Dolichomastigales	Dolichomastigaceae	Dolichomastix	NA
Dolichomastix_2	Plantae	Chlorophyta	Mamiellophyceae	Dolichomastigales	Dolichomastigaceae	Dolichomastix	NA
Dolichomastix_3	Plantae	Chlorophyta	Mamiellophyceae	Dolichomastigales	Dolichomastigaceae	Dolichomastix	NA
Dolichomastix_4	Plantae	Chlorophyta	Mamiellophyceae	Dolichomastigales	Dolichomastigaceae	Dolichomastix	NA
Mamiellophyceae_1	Plantae	Chlorophyta	Mamiellophyceae	NA	NA	NA	NA
Mamiellophyceae_2	Plantae	Chlorophyta	Mamiellophyceae	NA	NA	NA	NA

Mamiellophyceae_3	Plantae	Chlorophyta	Mamiellophyceae	NA	NA	NA	NA
Mamiellophyceae_4	Plantae	Chlorophyta	Mamiellophyceae	NA	NA	NA	NA
Mamiellophyceae_5	Plantae	Chlorophyta	Mamiellophyceae	NA	NA	NA	NA
Micromonas	Plantae	Chlorophyta	Mamiellophyceae	Mamiellales	Mamiellaceae	Micromonas	NA
Micromonas pusilla	Plantae	Chlorophyta	Mamiellophyceae	Mamiellales	Mamiellaceae	Micromonas	Micromonas pusilla
Chlorophyta	Plantae	Chlorophyta	NA	NA	NA	NA	NA
Plantae	Plantae	NA	NA	NA	NA	NA	NA
Florideophyceae	Plantae	Rhodophyta	Florideophyceae	NA	NA	NA	NA
Rhodophyta_1	Plantae	Rhodophyta	NA	NA	NA	NA	NA
Rhodophyta_10	Plantae	Rhodophyta	NA	NA	NA	NA	NA
Rhodophyta_11	Plantae	Rhodophyta	NA	NA	NA	NA	NA
Rhodophyta_12	Plantae	Rhodophyta	NA	NA	NA	NA	NA
Rhodophyta_13	Plantae	Rhodophyta	NA	NA	NA	NA	NA
Rhodophyta_14	Plantae	Rhodophyta	NA	NA	NA	NA	NA
Rhodophyta_15	Plantae	Rhodophyta	NA	NA	NA	NA	NA
Rhodophyta_16	Plantae	Rhodophyta	NA	NA	NA	NA	NA
Rhodophyta_17	Plantae	Rhodophyta	NA	NA	NA	NA	NA
Rhodophyta_18	Plantae	Rhodophyta	NA	NA	NA	NA	NA
Rhodophyta_19	Plantae	Rhodophyta	NA	NA	NA	NA	NA
Rhodophyta_2	Plantae	Rhodophyta	NA	NA	NA	NA	NA
Rhodophyta_20	Plantae	Rhodophyta	NA	NA	NA	NA	NA
Rhodophyta_21	Plantae	Rhodophyta	NA	NA	NA	NA	NA
Rhodophyta_22	Plantae	Rhodophyta	NA	NA	NA	NA	NA
Rhodophyta_23	Plantae	Rhodophyta	NA	NA	NA	NA	NA
Rhodophyta_24	Plantae	Rhodophyta	NA	NA	NA	NA	NA
Rhodophyta_25	Plantae	Rhodophyta	NA	NA	NA	NA	NA
Rhodophyta_3	Plantae	Rhodophyta	NA	NA	NA	NA	NA
Rhodophyta_4	Plantae	Rhodophyta	NA	NA	NA	NA	NA
Rhodophyta_5	Plantae	Rhodophyta	NA	NA	NA	NA	NA
Rhodophyta_6	Plantae	Rhodophyta	NA	NA	NA	NA	NA
Rhodophyta_7	Plantae	Rhodophyta	NA	NA	NA	NA	NA
Rhodophyta_8	Plantae	Rhodophyta	NA	NA	NA	NA	NA
Rhodophyta_9	Plantae	Rhodophyta	NA	NA	NA	NA	NA
Streptophyta	Plantae	Streptophyta	NA	NA	NA	NA	NA

Table S7. MOTU and ASV richness at Phylum level in COI and 18S datasets

Kingdom		COI			18S		
	Phylum	MOTU Richness	Reads	% of Kingdom reads	ASV Richness	Reads	% of Kingdom reads
Chromista		309	2399006	-	849	3246346	-
	Bigyra	1	53	<0.1%	8	3959	0.10%
	Cercozoa	-	-	-	111	122045	3.80%
	Ciliophora	-	-	-	92	139415	4.30%
	Cryptophyta	4	423	0.10%	12	14976	0.50%
	Haptophyta	25	424442	17.70%	25	22113	0.70%
	Heliozoa	-	-	-	2	219	<0.1%
	Heterokontophyta	72	1022090	42.00%	81	661442	20.40%
	Myozoa	48	282167	11.80%	382	2062705	63.50%
	Ochrophyta	103	534602	22.30%	68	167339	5.20%
	Oomycota	55	135224	5.60%	14	2153	<0.1%
	Radiozoa	-	-	-	4	3922	0.10%
	Unassigned	1	5	<0.1%	50	46058	1.40%
Fungi		42	2225	-			
	Ascomycota	16	459	20.10%	-	-	-
	Basidiomycota	26	1043	46.90%	-	-	-
	Mucoromycota	4	723	32.50%	-	-	-
Metazoa		96	2378355	-	489	14359051	-
	Annelida	6	290197	12.20%	-	-	0.10%
	Arthropoda	27	1477060	62.10%	474	14352768	99.90%
	Chaetognatha	1	126	<0.1%	4	266	<0.1%
	Chordata	6	288140	12.10%	3	96	<0.1%
	Cnidaria	27	288817	12.10%	1	74	<0.1%
	Ctenophora	4	8134	0.30%	3	3765	0.10%
	Mollusca	6	195	<0.1%	-	-	-
	Nematoda	1	29	<0.1%	1	100	<0.1%
	Nemertea	3	20	<0.1%	-	-	-
	Porifera	5	144	0.10%	-	-	-
	Rotifera	9	25488	1.10%	2	339	<0.1%
	Unassigned	1	5	<0.1%	1	1643	<0.1%
Plantae		44	392894	-	31	553924	-
	Chlorophyta	15	326037	83%	31	553924	100%
	Rhodophyta	27	45889	11.70%	-	-	-
	Streptophyta	1	20682	5.30%	-	-	-
	Unassigned	1	286	<0.1%	-	-	-
Protozoa					32	31360	-
	Choanozoa	-	-	-	11	20314	64.80%
	Picozoa	-	-	-	10	8843	28.20%
	Unassigned	-	-	-	11	2203	7.00%
Unassigned Kingdom	Unassigned	25	2627	-	27	1174	-

Table S8. Results from PERMANOVA for the effect of Depth, and Ice floe station on Community composition

COI					
	DF	Sums of Sqs	R2	F	p-value
<i>Depth</i>	1	4297.76	0.087	16.19	0.001
<i>Floe name</i>	8	20638.53	0.42	9.67	0.001
<i>Depth: Floe name</i>	8	5345.08	0.11	2.5	0.001
Residual	72	19209.45	0.39		
Total	89	49490.81	1		
18S					
	DF	Sums of Sqs	R2	F	p-value
<i>Depth</i>	1	8742.71	0.06	8.66	0.001
<i>Floe name</i>	8	53510.07	0.35	6.62	0.001
<i>Depth: Floe name</i>	8	17439.33	0.11	2.16	0.001
Residual	72	72722.25	0.48		
Total	89	152414.35	1		

Table S9. Taxonomic information, cluster information, relative read abundance and correlation details of all MOTUs included in the CIM of the sPLS analysis for COI

MOTU Name	sPLS Cluster	Taxonomic information							Relative read abundance information										Correlation information						
		Kingdom	Phylum	Class	Order	Family	Genus	Species	Total Reads	F24_1	FM_V2	FM_V3	FN_V1	FN_V2	FN_V3	FS_V1	FS_V2	FS_V3	Temp	Lon	BD MSS	DIST MSS	SIC	hBD MSS	Sal
Rhodophyta_23	1	Plantae	Rhodophyta	NA	NA	NA	NA	6607	64.18	6.15	1.38	6.3	2.3	1.44	13.57	3.45	1.24	-0.366	-0.138	-0.004	0.440	0.626	0.583	0.363	0.413
Myzozoa_19	1	Chromista	Myzozoa	NA	NA	NA	NA	276	52.3	4.6	4.18	9.21	1.67	14.23	12.55	1.26	0	-0.380	-0.132	-0.021	0.463	0.655	0.604	0.395	0.441
Anthozoa_2	1	Metazoa	Cnidaria	Anthozoa	NA	NA	NA	732	43.63	3.23	12.73	3.57	3.9	25.13	5.94	1.87	0	-0.300	-0.140	0.038	0.444	0.496	0.479	0.255	0.308
Eukaryota_5	1	NA	NA	NA	NA	NA	NA	581	64.22	8.67	0	6.22	1.11	1.33	14.67	2.22	1.56	-0.404	-0.191	0.055	0.462	0.666	0.645	0.339	0.412
Phaeophyceae_37	1	Chromista	Ochrophyta	Phaeophyceae	NA	NA	NA	99	100	0	0	0	0	0	0	0	0	-0.245	-0.107	0.019	0.286	0.410	0.391	0.221	0.261
Ochrophyta_6	1	Chromista	Ochrophyta	NA	NA	NA	NA	8920	76.68	4.67	0.4	1.7	2.2	0.42	12.01	1.33	0.59	-0.392	-0.173	0.033	0.456	0.655	0.625	0.350	0.415
Annelida_3	1	Metazoa	Annelida	NA	NA	NA	NA	1593	77.97	1.08	1.41	2	1.08	0.75	15.46	0.25	0	-0.458	-0.247	0.108	0.506	0.737	0.732	0.336	0.434
Phaeophyceae_32	1	Chromista	Ochrophyta	Phaeophyceae	NA	NA	NA	46	100	0	0	0	0	0	0	0	0	-0.328	-0.173	0.072	0.364	0.530	0.524	0.246	0.315
Ascidacea_2	1	Metazoa	Chordata	Ascidacea	NA	NA	NA	263830	56.89	6.5	4.09	5.98	5.07	6.55	6.44	5.3	3.17	-0.461	-0.258	0.123	0.503	0.735	0.737	0.322	0.425
Ochrophyta_3	1	Chromista	Ochrophyta	NA	NA	NA	NA	95	88.51	0	0	6.9	4.6	0	0	0	0	-0.342	-0.188	0.086	0.375	0.547	0.546	0.244	0.319
Annelida_4	1	Metazoa	Annelida	NA	NA	NA	NA	287777	63.83	5.91	3.19	4.32	4.25	5.14	6.13	4.55	2.68	-0.467	-0.291	0.170	0.491	0.726	0.748	0.279	0.398
Phaeophyceae_72	1	Chromista	Ochrophyta	Phaeophyceae	NA	NA	NA	49760	71.4	4.05	5.14	2.19	2.15	2.57	9.35	1.78	1.37	-0.421	-0.262	0.153	0.443	0.655	0.674	0.252	0.359
Anthozoa_30	1	Metazoa	Cnidaria	Anthozoa	NA	NA	NA	254761	60.86	5.57	3.77	4.59	4.48	6.46	6.93	4.26	3.08	-0.470	-0.292	0.169	0.495	0.732	0.752	0.283	0.402
Bacillariophyceae_19	1	Chromista	Bacillariophyta	Bacillariophyceae	NA	NA	NA	1585	60.65	0.56	0	1.6	7.24	26.46	2.86	0.35	0.28	-0.384	-0.253	0.161	0.395	0.588	0.615	0.207	0.311
Malacostraca_3	1	Metazoa	Arthropoda	Malacostraca	NA	NA	NA	130	84.78	0	4.35	8.7	2.17	0	0	0	0	-0.375	-0.248	0.158	0.385	0.574	0.600	0.201	0.303
Raphidophyceae_10	1	Chromista	Ochrophyta	Raphidophyceae	NA	NA	NA	70	100	0	0	0	0	0	0	0	0	-0.300	-0.194	0.120	0.312	0.463	0.481	0.168	0.248
Oomycota_36	1	Chromista	Ochrophyta	Oomycota	NA	NA	NA	66	100	0	0	0	0	0	0	0	0	-0.283	-0.185	0.116	0.293	0.435	0.453	0.155	0.232
Bacillariophyceae_18	1	Chromista	Bacillariophyta	Bacillariophyceae	NA	NA	NA	1457	55.9	1.21	2.8	4.84	6.58	7.03	9.68	3.78	8.17	-0.337	-0.237	0.164	0.338	0.508	0.541	0.158	0.257
Dinophyceae_18	1	Chromista	Myzozoa	Dinophyceae	NA	NA	NA	1591	93.26	0.61	0	0.52	0	0	5.25	0	0.35	-0.481	-0.338	0.234	0.483	0.724	0.771	0.225	0.367
Scyphozoa_5	1	Metazoa	Cnidaria	Scyphozoa	NA	NA	NA	285	57.77	14.74	1.59	4.38	1.99	3.59	4.78	4.78	6.37	-0.342	-0.238	0.162	0.345	0.517	0.549	0.165	0.264
Bacillariophyceae_11	1	Chromista	Bacillariophyta	Bacillariophyceae	NA	NA	NA	159	71.71	5.92	0	1.32	4.61	5.26	3.29	4.61	3.29	-0.309	-0.221	0.156	0.308	0.464	0.496	0.139	0.232
Oomycota_44	1	Chromista	Ochrophyta	Oomycota	NA	NA	NA	154	98.67	0	0	0	0	1.33	0	0	0	-0.350	-0.289	0.235	0.326	0.501	0.564	0.096	0.219
Basidiomycota_9	1	Fungi	Basidiomycota	NA	NA	NA	NA	154	96.1	0	0	0	0	0	3.9	0	0	-0.395	-0.326	0.266	0.368	0.565	0.636	0.108	0.247
Karlodinium	1	Chromista	Myzozoa	Dinophyceae	Gymnodiniales	Kareniaceae	Karlodinium	41150	84.61	1.89	2.11	1.03	1.48	1.43	4.73	1.16	1.55	-0.434	-0.356	0.289	0.405	0.622	0.698	0.122	0.274
Myzozoa_21	1	Chromista	Myzozoa	NA	NA	NA	NA	1476	96.89	0.43	0.17	0.35	0.17	0.86	0.61	0.17	0.35	-0.508	-0.423	0.347	0.471	0.725	0.818	0.134	0.315
Chaetocerotales	1	Chromista	Bacillariophyta	Mediophyceae	Chaetocerotales	NA	NA	4052	96.32	0.18	1.22	1.37	0.33	0.2	0.1	0.28	0	-0.417	-0.350	0.290	0.384	0.593	0.671	0.104	0.254
Phaeocystales	1	Chromista	Haptophyta	Coccolithophyceae	Phaeocystales	NA	NA	422830	70.89	3.01	1.8	1.27	1.8	1.39	11.35	4.46	4.02	-0.372	-0.317	0.266	0.339	0.525	0.598	0.085	0.221
Phaeophyceae_46	1	Chromista	Ochrophyta	Phaeophyceae	NA	NA	NA	320	78.45	2.69	3.7	2.02	4.38	1.35	2.69	2.69	2.02	-0.283	-0.220	0.170	0.271	0.413	0.454	0.098	0.192
Rhodophyta_22	1	Plantae	Rhodophyta	NA	NA	NA	NA	1404	64.93	6.1	2.74	3.98	3.71	2.65	7.69	2.39	5.83	-0.382	-0.298	0.231	0.366	0.518	0.614	0.132	0.259
Phaeophyceae_43	1	Chromista	Ochrophyta	Phaeophyceae	NA	NA	NA	215	90	0	2	0	0	1.33	2.67	1.33	2.67	-0.377	-0.374	0.349	0.312	0.500	0.608	0.002	0.165
Raphidophyceae_16	1	Chromista	Ochrophyta	Raphidophyceae	NA	NA	NA	3087	99.84	0	0.06	0	0	0.1	0	0	0	-0.320	-0.309	0.284	0.271	0.430	0.517	0.015	0.150
Dinophyceae_20	1	Chromista	Myzozoa	Dinophyceae	NA	NA	NA	2999	59.46	6.59	8.12	4.16	4.29	5.69	3.65	2	6.03	-0.307	-0.300	0.278	0.257	0.410	0.496	0.008	0.139
Myzozoa_16	1	Chromista	Myzozoa	NA	NA	NA	NA	156	72.57	3.54	7.08	0	1.77	6.19	3.54	1.77	3.54	-0.370	-0.326	0.280	0.332	0.516	0.596	0.068	0.209
Rhodophyta_24	1	Plantae	Rhodophyta	NA	NA	NA	NA	16606	70.98	4.72	3.08	2.08	2.53	5.1	3.19	2.82	5.5	-0.427	-0.402	0.362	0.368	0.581	0.689	0.038	0.213
Mamiellophyceae_4	1	Plantae	Chlorophyta	Mamiellophyceae	NA	NA	NA	1207	97.62	0.22	0.54	0	0.33	0.33	0	0.22	0.76	-0.505	-0.479	0.434	0.432	0.684	0.815	0.038	0.247
Bacillariophyta_13	1	Chromista	Bacillariophyta	NA	NA	NA	NA	242972	53.75	5.7	3.96	0.59	3.02	13.51	12.84	2.99	3.64	-0.369	-0.334	0.293	0.326	0.510	0.596	0.054	0.198
Phaeophyceae_48	1	Chromista	Ochrophyta	Phaeophyceae	NA	NA	NA	330	98.17	0	0	0	0	0	0	0.61	1.22	-0.269	-0.249	0.221	0.235	0.369	0.434	0.031	0.139
Phaeophyceae_53	1	Chromista	Ochrophyta	Phaeophyceae	NA	NA	NA	891	93.64	1.04	1.56	1.43	0	2.08	0	0	0.26	-0.461	-0.426	0.379	0.402	0.633	0.744	0.054	0.239
Micromonas pusilla	1	Plantae	Chlorophyta	Mamiellophyceae	Mamiellales	Mamiellaceae	Micromonas pusilla	43992	49.28	2.45	0.28	4.25	0.83	0.58	41.73	0.56	0.06	-0.385	-0.038	-0.167	0.526	0.723	0.608	0.553	0.553
Unassigned_19	1	NA	NA	NA	NA	NA	NA	504	31.28	4.57	7.31	14.84	5.94	9.13	15.3	7.76	3.88	-0.259	-0.018	-0.124	0.358	0.490	0.408	0.383	0.380
Annelida_2	1	Metazoa	Annelida	NA	NA	NA	NA	776	34.27	14.77	5.02	6.94	8.57	4.14	13.59	8.86	3.84	-0.234	-0.042	-0.072	0.308	0.427	0.370	0.305	0.315
Arthropoda_5	1	Metazoa	Arthropoda	NA	NA	NA	NA	455	47.72	7.67	4.32	6.24	8.39	6.24	9.83	9.11	0.48	-0.344	-0.063	-0.106	0.453	0.629	0.545	0.449	0.463
Bathycoccus prasinus	1	Plantae	Chlorophyta	Mamiellophyceae	Mamiellales	Bathycoccaceae	Bathycoccus prasinus	55313	38.59	8.96	0.92	7.17	5.05	0.85	34.18	3.5	0.79	-0.287	-0.050	-0.092	0.379	0.525	0.454	0.378	0.388
Phaeophyceae_74	1	Chromista	Ochrophyta	Phaeophyceae	NA	NA	NA	115519	29.91	10.02	2.9	5.39	7.94	31.48	8.51	3.72	0.12	-0.273	0.169	-0.418	0.492	0.634	0.424	0.707	0.612
Oomycota_27	1	Chromista	Ochrophyta	Oomycota	NA	NA	NA	37	66.67	0	0	13.33	6.67	0	13.33	0	0	-0.206	0.037	-0.177	0.316	0.422	0.323	0.388	0.360
Haptophyta_5	1	Chromista	Haptophyta	NA	NA	NA	NA	623	29.07	16.29	6.65	4.38	8.76	11.56	13.13	10.16	0	-0.220	0.078	-0.247	0.360	0.474	0.343	0.475	0.427
Phaeophyceae_60	2	Chromista	Ochrophyta	Phaeophyceae	NA	NA	NA	3423	77.44	1.45	10.69	0.93</													

Phaeophyceae_57	2	Chromista	Ochrophyta	Phaeophyceae	NA	NA	NA	NA	1188	59.26	2.94	7.84	5.01	3.05	6.21	2.61	3.7	9.37	-0.352	-0.459	0.494	0.226	0.399	0.573	-0.174	0.032
Prymnesiophyceae_3	2	Chromista	Haptophyta	Prymnesiophyceae	NA	NA	NA	NA	321	92.03	0	1.45	0	0	0	0	0	6.52	-0.371	-0.470	0.498	0.247	0.430	0.604	-0.160	0.050
Phaeophyceae_71	2	Chromista	Ochrophyta	Phaeophyceae	NA	NA	NA	NA	38750	54.83	8.19	10	1.68	3.58	3.73	7	4.49	6.51	-0.278	-0.347	0.366	0.188	0.325	0.452	-0.112	0.043
Ochrophyta_5	2	Chromista	Ochrophyta	NA	NA	NA	NA	NA	2021	34.61	7.4	9.79	5.61	6.03	10.8	8.35	7.58	9.84	-0.250	-0.303	0.314	0.175	0.299	0.407	-0.085	0.050
Bacillariophyceae_14	2	Chromista	Bacillariophyta	Bacillariophyceae	NA	NA	NA	NA	477	67.06	0	1.9	3.79	1.9	6.4	2.13	3.08	13.74	-0.368	-0.435	0.447	0.264	0.447	0.598	-0.109	0.084
Bacillariales_4	2	Chromista	Bacillariophyta	Bacillariophyceae	Bacillariales	NA	NA	NA	805	26.33	5.32	10.64	0.65	6.36	4.8	12.58	3.24	30.09	0.015	-0.254	0.395	-0.176	-0.186	-0.014	-0.431	-0.307
Phaeophyceae_47	2	Chromista	Ochrophyta	Phaeophyceae	NA	NA	NA	NA	322	46.65	5.75	14.06	0	1.28	0	0.64	31.63	0.026	-0.315	0.495	-0.224	-0.244	-0.028	-0.546	-0.392	
Phaeophyceae_69	2	Chromista	Ochrophyta	Phaeophyceae	NA	NA	NA	NA	19814	19.23	10.1	16.92	0.68	4.78	8.28	5.14	9.1	25.78	0.033	-0.295	0.469	-0.224	-0.246	-0.040	-0.525	-0.381
Phaeophyceae_61	2	Chromista	Ochrophyta	Phaeophyceae	NA	NA	NA	NA	3678	8.3	0.67	15.18	0	0	2.06	0.21	0.09	73.48	0.002	-0.455	0.694	-0.276	-0.283	0.016	-0.731	-0.510
Bacillariophyceae_15	2	Chromista	Bacillariophyta	Bacillariophyceae	NA	NA	NA	NA	603	37.35	6.03	12.06	2.72	2.92	1.17	5.25	4.09	28.4	-0.054	-0.313	0.445	-0.111	-0.088	0.098	-0.415	-0.266
Phaeophyceae_38	2	Chromista	Ochrophyta	Phaeophyceae	NA	NA	NA	NA	121	32.76	6.9	12.07	0	3.45	3.45	0	41.38	-0.042	-0.283	0.407	-0.110	-0.093	0.078	-0.386	-0.251	
Bacillariophyceae_13	2	Chromista	Bacillariophyta	Bacillariophyceae	NA	NA	NA	NA	288	22.16	2.06	15.46	0	1.55	41.24	2.06	1.03	14.43	-0.044	-0.285	0.408	-0.108	-0.089	0.081	-0.385	-0.249
Phaeophyceae_52	2	Chromista	Ochrophyta	Phaeophyceae	NA	NA	NA	NA	853	56.77	2.92	20.46	0	0.46	4.31	0	1.23	13.85	-0.148	-0.470	0.630	-0.071	-0.002	0.252	-0.517	-0.296
Bacillariophyta_7	2	Chromista	Bacillariophyta	NA	NA	NA	NA	NA	653	54.74	0	17.02	0	0	2.81	2.11	1.75	21.58	-0.097	-0.446	0.622	-0.129	-0.086	0.171	-0.559	-0.347
Oomycota_55	2	Chromista	Ochrophyta	Oomycota	NA	NA	NA	NA	80216	58.73	2.74	15.55	0.81	0.88	4.05	1.09	0.73	15.41	-0.116	-0.463	0.638	-0.113	-0.060	0.202	-0.556	-0.337
Phaeophyceae_63	2	Chromista	Ochrophyta	Phaeophyceae	NA	NA	NA	NA	4389	39.74	0.9	44.51	1.45	1.04	6.32	0.52	0.52	5.01	-0.108	-0.383	0.520	-0.076	-0.026	0.186	-0.441	-0.260
Attheya	3	Chromista	Bacillariophyta	Coccolodiscophyceae	Chaetocerotales	Attheyaceae	Attheya	NA	72467	0.48	4.24	6.25	7.45	3.41	2.87	35.29	7.14	32.85	0.405	0.314	-0.241	-0.389	-0.592	-0.651	-0.144	-0.277
Pseudo-nitzschia	3	Chromista	Bacillariophyta	Bacillariophyceae	Bacillariales	Bacillariaceae	Pseudo-nitzschia	NA	14546	2.09	14.46	17.13	5.72	10.78	11.41	7.1	10.98	20.32	0.451	0.324	-0.230	-0.448	-0.674	-0.723	-0.200	-0.336
Ceramiales	3	Chromista	Bacillariophyta	Floriidophyceae	Ceramiales	NA	NA	NA	3224	0	9.06	16.39	4.68	7.26	17.99	7.02	7.96	29.63	0.481	0.330	-0.222	-0.488	-0.730	-0.772	-0.239	-0.376
Raphidophyceae_18	3	Chromista	Bacillariophyta	Coccolodiscophyceae	Rhizosoleniales	Rhizosoleniaceae	NA	NA	14145	0.02	12.14	12.93	3.64	11.85	9.43	4.28	19.28	26.44	0.476	0.309	-0.192	-0.493	-0.733	-0.762	-0.265	-0.392
Dolichomastix_3	3	Plantae	Chlorophyta	Mamiellophyceae	Dolichomastigales	Dolichomastigaceae	Dolichomastix	NA	2204	0.87	27.86	9.25	2.81	15.36	8.53	1.7	15.89	17.73	0.369	0.211	-0.106	-0.399	-0.585	-0.589	-0.250	-0.335
Rhodophyta_25	3	Plantae	Rhodophyta	NA	NA	NA	NA	NA	17221	0.52	8.73	23.1	3.67	10.03	13.66	1.76	7.98	30.55	0.503	0.298	-0.159	-0.539	-0.793	-0.805	-0.326	-0.447
Bacillariophyta_9	3	Chromista	Bacillariophyta	NA	NA	NA	NA	NA	4071	0.15	12.33	7.16	10.05	12.58	8.47	10.23	11.94	27.08	0.452	0.409	-0.359	-0.399	-0.625	-0.730	-0.066	-0.243
Bacillariophyceae_22	3	Chromista	Bacillariophyta	Bacillariophyceae	NA	NA	NA	NA	15837	0.88	8.67	10.44	7.01	6.59	4.61	34.95	13.12	13.73	0.414	0.382	-0.339	-0.361	-0.567	-0.667	-0.049	-0.214
Bacillariophyta_11	3	Chromista	Bacillariophyta	NA	NA	NA	NA	NA	130555	0.87	7.07	8.34	5.34	6.49	2.08	51.08	9.08	9.65	0.315	0.275	-0.234	-0.285	-0.442	-0.508	-0.063	-0.181
Bacillariales_5	3	Chromista	Bacillariophyta	Bacillariophyceae	Bacillariales	NA	NA	NA	1712	0.37	13.22	5.24	6.52	0.91	0.3	44.96	8.65	22.84	0.295	0.258	-0.221	-0.266	-0.413	-0.475	-0.057	-0.168
Chattonellales_2	3	Chromista	Ochrophyta	Raphidophyceae	Chattonellales	NA	NA	NA	31741	0.38	25.6	10.04	0.95	11.8	22.44	1.22	23.52	4.05	0.433	0.367	-0.306	-0.397	-0.614	-0.697	-0.103	-0.261
Fragilariaceae	3	Chromista	Bacillariophyta	Fragilariophyceae	Fragilariales	Fragilariaceae	NA	NA	633	0	5.91	7.43	8.45	9.46	5.91	31.59	10.14	21.11	0.319	0.366	-0.325	-0.253	-0.412	-0.516	0.029	-0.119
Ectocarpaceae	3	Chromista	Ochrophyta	Phaeophyceae	Ectocarpaceae	NA	NA	NA	1179	1.02	13.31	8.69	5.36	11.55	4.44	32.16	12.29	11.18	0.300	0.329	-0.325	-0.230	-0.379	-0.485	0.048	-0.097
Chaetocerotaceae	3	Chromista	Bacillariophyta	Coccolodiscophyceae	Chaetocerotales	Chaetocerotaceae	NA	NA	512966	0.09	13.29	8.33	10.81	10.13	26.77	16.31	10.93	3.33	0.464	0.568	-0.594	-0.320	-0.550	-0.754	0.170	-0.084
Cylindrotheca_2	3	Chromista	Bacillariophyta	Bacillariophyceae	Bacillariales	Bacillariaceae	Cylindrotheca	NA	12250	7.02	6.05	10.35	5.4	18.54	26.32	8.82	10.9	6.58	0.263	0.327	-0.345	-0.178	-0.308	-0.427	0.105	-0.041
Oomycota_54	3	Chromista	Ochrophyta	Oomycota	NA	NA	NA	NA	24985	0.52	16.32	2.93	3.34	6.32	2.62	52.87	11.78	3.3	0.319	0.378	-0.389	-0.228	-0.385	-0.517	0.096	-0.072
Raphidophyceae_15	3	Chromista	Ochrophyta	Raphidophyceae	NA	NA	NA	NA	2185	3.44	7.07	17.19	1.03	3.49	2.65	0.15	3.78	61.2	0.178	-0.259	0.499	-0.410	-0.504	-0.270	-0.699	-0.565
Bacillariophyta_10	3	Chromista	Bacillariophyta	NA	NA	NA	NA	NA	27704	7.33	4.92	10.81	2.13	3.16	23.42	10.09	3.27	34.86	0.120	-0.170	0.330	-0.273	-0.337	-0.182	-0.464	-0.376
Raphidophyceae_14	3	Chromista	Ochrophyta	Raphidophyceae	NA	NA	NA	NA	2046	8.71	15.5	18.05	2.09	7.14	6.04	4	8.53	29.95	0.136	-0.141	0.294	-0.278	-0.350	-0.209	-0.442	-0.367
Dolichomastix_4	3	Plantae	Chlorophyta	Mamiellophyceae	Dolichomastigales	Dolichomastigaceae	Dolichomastix	NA	5534	10.93	14.76	19.21	2.58	3.42	12.65	5.39	7.58	23.48	0.167	-0.146	0.320	-0.326	-0.414	-0.257	-0.500	-0.421
Phaeophyceae_67	3	Chromista	Ochrophyta	Phaeophyceae	NA	NA	NA	NA	13975	5.36	2.36	30.93	0.71	3.12	4.88	0.89	2.35	49.4	0.132	-0.334	0.586	-0.390	-0.462	-0.195	-0.746	-0.578
Oomycota_47	3	Chromista	Ochrophyta	Oomycota	NA	NA	NA	NA	310	10.48	2.38	23.33	0	1.43	9.52	1.9	0	50.95	0.136	-0.267	0.486	-0.355	-0.428	-0.204	-0.645	-0.509
Phaeophyceae_55	3	Chromista	Ochrophyta	Phaeophyceae	NA	NA	NA	NA	965	0	0	22.16	0	0.23	0	0	2.27	75.34	0.301	-0.177	0.445	-0.535	-0.692	-0.466	-0.763	-0.662
Rotifera	3	Metazoa	Rotifera	NA	NA	NA	NA	NA	2190	0	8.1	0	0	0	0	0.83	0	90.86	0.166	-0.096	0.243	-0.294	-0.380	-0.257	-0.418	-0.363
Oomycota_46	3	Chromista	Ochrophyta	Oomycota	NA	NA	NA	NA	249	0	0.9	31.22	0	0	1.81	0	0	66.06	0.266	-0.178	0.427	-0.487	-0.626	-0.412	-0.710	-0.611
Dolichomastix_1	3	Plantae	Chlorophyta	Mamiellophyceae	Dolichomastigales	Dolichomastigaceae	Dolichomastix	NA	347	0	0	27.7	0	0	1.35	0	0	70.95	0.268	-0.200	0.462	-0.503	-0.643	-0.415	-0.748	-0.639
Arthropoda_6	3	Metazoa	Arthropoda	NA	NA	NA	NA	NA	471	0	1.95	18.05	0	0	8.29	0	1.71	70	0.287	-0.143	0.386	-0.496	-0.645	-0.446	-0.687	-0.604
Rhodophyta_20	3	Plantae	Rhodophyta	NA	NA	NA	NA	NA	111	0	4.26	20.21	0	0	0	0	6.38	69.15	0.272	-0.120	0.342	-0.460	-0.601	-0.424	-0.626	-0.555
Cryptophyceae_3	3	Chromista	Cryptophyta	Cryptophyceae	NA	NA	NA	NA	107	5.26	0	34.74	0	2.11	11.58	0	3.16	43.16	0.207	-0.096	0.267	-0.353	-0.460	-0.322	-0.484	-0.427
Bacillariophyta_8	3	Chromista	Bacillariophyta	NA	NA	NA																				

Hydrozoa_9	4	Metazoa	Cnidaria	Hydrozoa	NA	NA	NA	NA	32	29.17	0	0	12.5	8.33	12.5	29.17	8.33	0	-0.033	0.233	-0.374	0.187	0.207	0.042	0.425	0.311
Oomycota_53	4	Chromista	Oomycota	NA	NA	NA	NA	NA	13948	3.38	50.33	0.48	4.38	13.81	0.43	4.62	22.34	0.23	-0.041	0.243	-0.394	0.204	0.229	0.055	0.454	0.335
Bacillariophyta_12	4	Chromista	Bacillariophyta	NA	NA	NA	NA	NA	193843	0.96	13.89	3.3	6.7	6.58	7.58	46.91	12.57	1.52	0.278	0.434	-0.499	-0.136	-0.273	-0.456	0.251	0.054
Phaeophyceae_58	4	Chromista	Ochrophyta	Phaeophyceae	NA	NA	NA	NA	1300	0	9	5.42	9.32	12.91	7.57	43.51	9	3.27	0.264	0.467	-0.557	-0.096	-0.224	-0.435	0.327	0.113
Bacillariophyta_6	4	Chromista	Bacillariophyta	NA	NA	NA	NA	NA	407	1.29	4.64	5.93	23.2	15.46	14.69	20.1	9.79	4.9	0.174	0.360	-0.446	-0.032	-0.116	-0.289	0.298	0.132
Myozoa_17	4	Chromista	Myozoa	NA	NA	NA	NA	NA	165	1.9	13.29	8.86	15.19	3.16	2.53	24.68	20.89	9.49	0.183	0.380	-0.471	-0.033	-0.122	-0.304	0.316	0.140
Phaeophyceae_24	4	Chromista	Ochrophyta	Phaeophyceae	NA	NA	NA	NA	32	0	70	0	0	0	6.67	13.33	10	0	0.119	0.310	-0.403	0.017	-0.040	-0.200	0.307	0.162
Skeletonemataceae	4	Chromista	Bacillariophyta	Mediophyceae	Thalassiosirales	Skeletonemataceae	NA	NA	290433	0.29	8.23	1.3	19.5	4.49	0.75	56.83	8.13	0.47	0.221	0.502	-0.635	-0.014	-0.120	-0.369	0.450	0.218
Bacillariophyceae_16	4	Chromista	Bacillariophyta	Bacillariophyceae	NA	NA	NA	NA	613	1.73	6.4	6.4	14.53	12.46	6.57	35.99	11.94	3.98	0.207	0.492	-0.628	0.000	-0.099	-0.346	0.457	0.229
Nitzschia	4	Chromista	Bacillariophyta	Bacillariophyceae	Bacillariales	Bacillariaceae	Nitzschia	NA	17	29.41	0	0	17.65	0	17.65	23.53	11.76	0	0.021	0.274	-0.405	0.135	0.128	-0.044	0.405	0.274
Leotiomyces_3	4	Fungi	Ascomycota	Leotiomyces	NA	NA	NA	NA	22	0	0	0	45	0	10	25	20	0	0.069	0.319	-0.446	0.093	0.062	-0.122	0.401	0.249
Stropharia	4	Fungi	Basidiomycota	Agaricomycetes	Agaricales	Strophariaceae	Stropharia	NA	104	0	1.92	0	50.96	3.85	0	9.62	33.65	0	0.068	0.339	-0.476	0.106	0.076	-0.121	0.434	0.273
Oomycota_17	4	Chromista	Ochrophyta	Oomycota	NA	NA	NA	NA	19	0	0	0	0	0	0	100	0	0	0.068	0.338	-0.475	0.107	0.077	-0.120	0.433	0.272
Fragilariopsis	4	Chromista	Bacillariophyta	Bacillariophyceae	Bacillariales	Bacillariaceae	Fragilariopsis	NA	11	0	0	18.18	63.64	0	18.18	0	0	0	0.063	0.315	-0.444	0.100	0.073	-0.111	0.405	0.255
Ascidiacea_1	4	Metazoa	Chordata	Ascidiacea	NA	NA	NA	NA	16	0	12.5	0	25	18.75	0	43.75	0	0	0.074	0.384	-0.542	0.125	0.093	-0.132	0.497	0.314
Phaeophyceae_20	4	Chromista	Ochrophyta	Phaeophyceae	NA	NA	NA	NA	22	0	0	0	0	0	0	100	0	0	0.071	0.367	-0.517	0.119	0.088	-0.126	0.474	0.300
Ascomycota_5	4	Fungi	Ascomycota	NA	NA	NA	NA	NA	288	1.74	0.69	0	36.46	1.39	7.99	14.58	37.15	0	0.048	0.336	-0.484	0.134	0.114	-0.089	0.462	0.301
Dinophyceae_17	4	Chromista	Myozoa	Dinophyceae	NA	NA	NA	NA	292	9.09	3.5	5.24	20.63	8.74	5.59	42.66	2.8	1.75	0.041	0.352	-0.512	0.153	0.137	-0.079	0.499	0.330
Dinophyceae_16	4	Chromista	Myozoa	Dinophyceae	NA	NA	NA	NA	223	3.62	2.71	0	28.96	7.69	11.76	28.96	16.29	0	0.048	0.379	-0.549	0.160	0.140	-0.091	0.530	0.349
Polychaeta_1	4	Metazoa	Annelida	Polychaeta	NA	NA	NA	NA	8	0	0	0	100	0	0	0	0	0	0.055	0.347	-0.496	0.131	0.108	-0.100	0.468	0.303
Ascomycota_2	4	Fungi	Ascomycota	NA	NA	NA	NA	NA	24	0	0	0	79.17	0	0	0	20.83	0	0.047	0.291	-0.416	0.108	0.088	-0.086	0.391	0.252
Myozoa_7	4	Chromista	Myozoa	NA	NA	NA	NA	NA	20	0	0	0	42.86	0	0	57.14	0	0	0.060	0.352	-0.501	0.126	0.100	-0.108	0.468	0.300
Annelida_1	4	Metazoa	Annelida	NA	NA	NA	NA	NA	23	14.29	9.52	0	0	19.05	14.29	33.33	9.52	0	0.049	0.294	-0.419	0.106	0.085	-0.089	0.392	0.252
Ascomycota_4	4	Fungi	Ascomycota	NA	NA	NA	NA	NA	26	0	15.38	0	15.38	0	11.54	23.08	34.62	0	0.099	0.339	-0.458	0.062	0.016	-0.170	0.384	0.224
Phaeophyceae_73	4	Chromista	Ochrophyta	Phaeophyceae	NA	NA	NA	NA	113430	3.54	26.29	2.12	7.77	25.81	1.96	9.68	20.32	2.51	0.108	0.367	-0.496	0.066	0.016	-0.185	0.415	0.242
Unassigned_17	4	NA	NA	NA	NA	NA	NA	NA	46	0	15.91	11.36	4.55	11.36	0	56.82	0	0	0.106	0.367	-0.497	0.069	0.020	-0.182	0.418	0.245
Rhodophyta_7	4	Plantae	Rhodophyta	NA	NA	NA	NA	NA	12	0	44.44	0	0	33.33	0	0	22.22	0	0.097	0.323	-0.435	0.056	0.011	-0.165	0.362	0.210
Myozoa_3	4	Chromista	Myozoa	NA	NA	NA	NA	NA	8	0	0	50	25	25	0	0	0	0	0.079	0.311	-0.427	0.074	0.038	-0.137	0.372	0.225
Chloroparvula pacifica	4	Plantae	Chlorophyta	Chloropicophyceae	Chloropicales	Chloropicaceae	Chloroparvula	NA	25	0	20	28	36	0	0	16	0	0	0.075	0.294	-0.403	0.069	0.035	-0.130	0.350	0.211
Ascomycota_3	4	Fungi	Ascomycota	NA	NA	NA	NA	NA	24	0	0	0	22.73	0	0	40.91	36.36	0	0.084	0.336	-0.463	0.082	0.043	-0.146	0.404	0.245
Dinophyceae_9	4	Chromista	Myozoa	Dinophyceae	NA	NA	NA	NA	34	0	5.88	0	0	20.59	0	73.53	0	0	0.071	0.290	-0.400	0.073	0.041	-0.123	0.352	0.214
Oomycota_19	4	Chromista	Ochrophyta	Oomycota	NA	NA	NA	NA	22	0	0	16.67	0	0	16.67	66.67	0	0	0.080	0.305	-0.417	0.068	0.032	-0.139	0.360	0.216
Microbotryomycetes_3	4	Fungi	Basidiomycota	Microbotryomycetes	NA	NA	NA	NA	323	1.27	2.86	2.22	26.67	0.63	13.02	19.37	33.33	0.63	0.085	0.314	-0.429	0.067	0.028	-0.147	0.367	0.219
Mucoromycotina_1	4	Fungi	Mucoromycota	Mucoromycotina	NA	NA	NA	NA	16	0	12.5	0	0	0	0	62.5	25	0	0.090	0.332	-0.453	0.071	0.030	-0.155	0.388	0.232
Oomycota_51	4	Chromista	Ochrophyta	Oomycota	NA	NA	NA	NA	2900	0	4.68	1.25	56.17	2.84	0.8	23.8	10.08	0.38	0.171	0.493	-0.651	0.053	-0.028	-0.289	0.517	0.286
Bacillariophyceae_10	4	Chromista	Bacillariophyta	Bacillariophyceae	NA	NA	NA	NA	119	0	12.5	10.58	3.85	14.42	2.88	46.15	9.62	0	0.127	0.354	-0.464	0.031	-0.029	-0.215	0.363	0.198
Unassigned_12	4	NA	NA	NA	NA	NA	NA	NA	17	0	70.59	0	0	11.76	0	17.65	0	0	0.101	0.319	-0.428	0.048	0.001	-0.172	0.351	0.201
Oomycota_16	4	Chromista	Ochrophyta	Oomycota	NA	NA	NA	NA	19	0	31.58	0	0	0	26.32	31.58	0	10.53	0.099	0.303	-0.404	0.041	-0.005	-0.168	0.328	0.186
Unassigned_20	4	NA	NA	NA	NA	NA	NA	NA	1120	1.45	24.68	1.54	3.8	14.29	0.9	14.01	39.15	0.18	0.148	0.448	-0.595	0.058	-0.012	-0.252	0.480	0.270
Phaeophyceae_14	4	Chromista	Ochrophyta	Phaeophyceae	NA	NA	NA	NA	14	0	21.43	21.43	21.43	21.43	0	0	14.29	0	0.101	0.306	-0.407	0.039	-0.008	-0.172	0.329	0.185

Table S10. Taxonomic information, cluster information, relative read abundance and correlation details of all ASVs included in the CIM of the sPLS analysis for 18S.

ASV Name	sPLS Cluster	Taxonomic information							Relative read abundance information													Correlation information					
		Kingdom	Phylum	Class	Order	Family	Genus	Total Reads	F24_1	FM_V2	FM_V3	FN_V1	FN_V2	FN_V3	FS_V1	FS_V2	FS_V3	Temp	BD MSS	Sal	DIST SIC	Lat	hBD MSS	SIC			
ASV_136	1	Chromista	Ciliophora	Oligotrichea	Oligotrichida	Tontoniidae	Pseudotontonia	2129	77.5	0.85	3.95	0.75	0.47	6.34	6.2	2.77	1.17	-0.361	0.156	0.179	0.323	0.266	0.556	0.576			
ASV_10	1	Chromista	Myzozoa	Dinophyceae	NA	NA	NA	150338	89.47	0.85	0.06	0.52	0.4	0.31	6.9	1.38	0.11	-0.396	0.171	0.198	0.355	0.293	0.611	0.633			
ASV_212	1	Chromista	Myzozoa	Dinophyceae	NA	NA	NA	960	90.73	0	0	0.21	0.1	5.1	2.08	1.77	0	-0.440	0.177	0.237	0.406	0.338	0.685	0.714			
ASV_222	1	Chromista	Ciliophora	Oligotrichea	Oligotrichida	NA	NA	930	96.45	0.75	0.22	0	1.72	0.54	0.11	0.22	0	-0.453	0.183	0.244	0.418	0.348	0.706	0.736			
ASV_180	1	Chromista	Myzozoa	Dinophyceae	NA	NA	NA	1196	87.21	4.1	0.75	0.33	0.84	2.93	3.09	0.42	0.33	-0.444	0.178	0.241	0.411	0.342	0.693	0.722			
ASV_81	1	Chromista	Ciliophora	NA	NA	NA	NA	4528	97.22	0	0.33	0	0	0.38	1.37	0.27	0.44	-0.447	0.182	0.238	0.411	0.341	0.696	0.724			
ASV_175	1	Chromista	Ochrophyta	Bacillariophyceae	Chaetocerotanae i.s.	Chaetocerotaceae	Chaetoceros	1675	98.99	0	0.12	0.18	0	0.42	0.18	0.12	0	-0.355	0.135	0.203	0.336	0.282	0.558	0.585			
ASV_245	1	Chromista	Myzozoa	Dinophyceae	NA	NA	NA	697	79.91	0.72	1.58	0.29	0	11.48	5.45	0	0.57	-0.417	0.203	0.175	0.350	0.282	0.629	0.643			
ASV_68	1	Chromista	Myzozoa	Dinophyceae	NA	NA	NA	5630	99.47	0	0.05	0	0	0.12	0.25	0.04	0.07	-0.493	0.239	0.208	0.414	0.334	0.744	0.760			
ASV_272	1	Chromista	Haptophyta	Prymnesiophyceae	Prymnesiales	Prymnesiaceae	Haptolina	543	83.06	7.55	0	0	0	4.97	2.95	1.47	0	-0.465	0.236	0.182	0.381	0.305	0.696	0.708			
ASV_379	1	Chromista	Myzozoa	Dinophyceae	Syndiniales	Amoebophryaceae	Amoebophrya	241	88.8	2.9	0.41	0	0.41	1.66	1.24	0.41	4.15	-0.420	0.197	0.187	0.360	0.293	0.639	0.656			
ASV_142	1	Chromista	Ciliophora	Oligotrichea	Choreotrichida	Strobiliidae	NA	1975	96.15	0.61	0.3	0.05	0.35	0.2	1.97	0	0.35	-0.477	0.223	0.213	0.410	0.333	0.726	0.745			
ASV_223	1	Chromista	Myzozoa	Dinophyceae	NA	NA	NA	826	81.84	5.33	0.24	0.24	0	1.09	5.33	5.45	0.48	-0.440	0.201	0.203	0.382	0.312	0.672	0.691			
ASV_143	1	Chromista	Myzozoa	Dinophyceae	NA	NA	NA	1917	98.7	0.37	0	0.1	0.05	0.26	0.42	0	0.1	-0.495	0.228	0.226	0.428	0.349	0.754	0.775			
ASV_86	1	Chromista	Myzozoa	Dinophyceae	NA	NA	NA	3876	95.87	0.21	0.41	0.15	0.23	0.49	2.01	0.59	0.03	-0.497	0.259	0.185	0.400	0.318	0.740	0.750			
ASV_28	1	Chromista	Ciliophora	Oligotrichea	Oligotrichida	NA	NA	22481	98.44	0.09	0.19	0	0.05	0.07	0.86	0.1	0.2	-0.483	0.323	0.078	0.317	0.232	0.677	0.659			
ASV_401	1	Chromista	Myzozoa	Dinophyceae	Syndiniales	Amoebophryaceae	Amoebophrya	232	81.47	4.31	0.86	0.86	2.16	2.59	0.86	0	6.9	-0.415	0.260	0.092	0.291	0.219	0.593	0.584			
ASV_400	1	Chromista	Myzozoa	Dinophyceae	NA	NA	NA	251	82.87	1.99	0	0	1.99	3.19	1.2	0.8	7.97	-0.430	0.275	0.088	0.296	0.220	0.611	0.600			
ASV_340	1	Chromista	Haptophyta	Prymnesiophyceae	Prymnesiales	Prymnesiaceae	Pseudohaptolina	361	93.63	0	0	0	0	3.32	0.28	0	2.77	-0.423	0.247	0.120	0.314	0.242	0.615	0.613			
ASV_315	1	Chromista	Myzozoa	Dinophyceae	NA	NA	NA	414	92.75	0	0	0	0	7.25	0	0	0	-0.399	0.071	0.343	0.459	0.404	0.676	0.737			
ASV_390	1	Chromista	Ciliophora	Oligotrichea	Choreotrichida	NA	NA	258	86.82	1.55	1.16	0	1.16	1.55	0	3.49	4.26	-0.267	0.040	0.240	0.314	0.279	0.456	0.500			
ASV_335	1	Chromista	Myzozoa	Dinophyceae	Peridiniales	Protoperidiniaceae	Protoperidinium	375	90.93	1.07	0	0	0	2.4	3.47	1.07	1.07	-0.295	0.047	0.261	0.344	0.305	0.502	0.550			
ASV_202	1	Chromista	Myzozoa	Dinophyceae	NA	NA	NA	1391	86.94	2.88	0.79	7.98	0.79	3.38	4.82	20.99	1.44	-0.230	0.026	0.219	0.279	0.249	0.398	0.439			
ASV_248	1	Chromista	Ciliophora	NA	NA	NA	NA	683	93.56	0	0.15	0	0	0.59	5.56	0.15	0	-0.427	0.097	0.337	0.469	0.410	0.710	0.767			
ASV_395	1	Chromista	NA	NA	NA	NA	NA	244	93.03	0	0.41	0.41	0	1.23	3.28	0	1.64	-0.402	0.087	0.323	0.446	0.390	0.671	0.726			
ASV_279	1	Chromista	Ciliophora	Oligotrichea	Oligotrichida	Strombidiidae	Strombidium	456	98.46	0.88	0	0	0	0.66	0	0	0	-0.420	0.125	0.290	0.432	0.371	0.681	0.726			
ASV_481	1	Chromista	Ciliophora	Oligotrichea	Oligotrichida	NA	NA	155	81.94	0.65	0.65	0	0.65	0	1.29	1.94	12.9	-0.303	0.092	0.206	0.310	0.266	0.491	0.522			
ASV_122	1	Chromista	Myzozoa	Dinophyceae	NA	NA	NA	2423	93.11	0.25	0	0	0	5.53	1.11	0	0	-0.420	0.109	0.312	0.448	0.388	0.690	0.741			
ASV_218	1	Chromista	Myzozoa	Dinophyceae	Gymnodiniales	Gymnodiniaceae	Lepidodinium	929	80.28	0.75	3.66	0.86	0.97	1.61	31	0.32	0.54	-0.353	0.097	0.255	0.371	0.321	0.577	0.618			
ASV_207	1	Chromista	Ciliophora	Oligotrichea	Choreotrichida	NA	NA	1166	89.37	0.69	0	0.86	1.2	1.11	4.37	2.4	0	-0.390	0.105	0.284	0.412	0.356	0.639	0.685			
ASV_130	1	Chromista	Ciliophora	Oligotrichea	Oligotrichida	Strombidiidae	Strombidium	638	76.33	2.51	0	12.38	0	7.68	1.1	0	0	-0.312	0.110	0.191	0.305	0.258	0.497	0.523			
ASV_480	1	Chromista	Haptophyta	NA	NA	NA	NA	139	83.45	2.16	0	0	0.72	2.16	1.44	1.44	8.63	-0.328	0.106	0.214	0.329	0.281	0.527	0.559			
ASV_144	1	Chromista	Ciliophora	Oligotrichea	Oligotrichida	Strombidiidae	Strombidium	1751	97.03	0.06	0	0.23	0	0.29	2.28	0.06	0.06	-0.467	0.153	0.302	0.467	0.398	0.749	0.793			
ASV_199	1	Chromista	Ciliophora	Oligotrichea	Oligotrichida	Strombidiidae	Strombidium	1284	98.05	0.39	0.23	0	0.16	0.31	0.31	0.16	0.39	-0.426	0.143	0.270	0.422	0.358	0.681	0.720			
ASV_477	1	Chromista	Myzozoa	Dinophyceae	Gymnodiniales	Gymnodiniaceae	NA	130	83.85	0	3.08	0	0	7.69	2.31	0.77	2.31	-0.227	-0.066	0.347	0.368	0.346	0.448	0.524			
ASV_229	1	Chromista	Ciliophora	Oligotrichea	Choreotrichida	Strobiliidae	NA	921	80.89	0.22	0.98	1.09	0	0	16.83	0	0	-0.271	-0.038	0.356	0.398	0.368	0.510	0.584			
ASV_486	1	Chromista	Heliozoa	Centrohelea	Heterophryidae	Heterophrys	NA	149	65.1	10.07	0	0	1.34	6.71	14.77	2.01	0	-0.248	-0.045	0.341	0.375	0.349	0.474	0.547			
ASV_466	1	Chromista	Cryptophyta	Cryptophyceae	Pyrenomonadales	Chroomonadaceae	Falcomonas	137	100	0	0	0	0	0	0	0	0	-0.286	-0.063	0.409	0.444	0.414	0.552	0.640			
ASV_252	1	Chromista	Myzozoa	Dinophyceae	NA	NA	NA	793	92.69	0	0	0	7.31	0	0	0	0	-0.209	0.012	0.217	0.266	0.240	0.369	0.411			
ASV_484	1	Chromista	Cryptophyta	Cryptophyceae	Pyrenomonadales	Geminigeraceae	Teleaulax	155	90.32	1.29	1.94	0	0	3.23	1.94	0	1.29	-0.342	0.019	0.354	0.435	0.393	0.604	0.673			
ASV_404	1	Chromista	Myzozoa	Dinophyceae	NA	NA	NA	224	94.2	0	0	0	0	5.8	0	0	0	-0.357	0.011	0.383	0.464	0.420	0.637	0.712			
ASV_453	1	Chromista	Myzozoa	Dinophyceae	NA	NA	NA	164	97.56	0	1.22	0	0	1.22	0	0	0	-0.337	-0.006	0.385	0.454	0.414	0.611	0.688			
ASV_492	1	Chromista	Myzozoa	Dinophyceae	Syndiniales	Amoebophryaceae	Amoebophrya	127	81.89	6.3	0.79	0	0	0	0	1.57	9.45	-0.215	-0.007	0.249	0.293	0.267	0.391	0.442			
ASV_162	1	Chromista	Myzozoa	Dinophyceae	Gymnodiniales	Gymnodiniaceae	Lepidodinium	1669	41.04	19.29	0.72	0.84	4.61	4.49	8.39	17.26	3.36	-0.334	0.316	-0.079	0.126	0.059	0.412	0.364			
ASV_77	1	Chromista	Myzozoa	Dinophyceae	Gymnodiniales	NA	NA	4636	72.82	4.29	0.39	0.41	0.6	2.07	6.75	9.86	2.8	-0.426	0.399	-0.095	0.165	0.079	0.529	0.469			
ASV_282	1	Chromista	Bigyra	Labyrinthulea	Thraustochytrida	NA	NA	589	75.72	3.74	0.68	0	1.02	3.06	4.58	2.04	9.17	-0.390	0.360	-0.080	0.156	0.078	0.487	0.434			
ASV_82	1	Chromista	Ochrophyta	Pelagophyceae	NA	NA	NA	4286	86.02	4.13	0.7	0.28	0.16	1.49	2.38	1	3.83	-0.499	0.484	-0.135	0.175	0.074	0.609	0.531			
ASV_255	1	Chromista	Myzozoa	Dinophyceae	NA	NA	NA	635	82.99	2.2	2.68	0	0.31	0.63	0	0	11.18	-0.410	0.395	-0.107	0.147	0.065	0.502	0.440			
ASV_307	1	Chromista	Ciliophora	Litostomatea	Pleurostomatida	Litonotidae	Loxophyllum	438	80.37	1.37	0	0	0.23	5.48	0	0.91	11.64	-0.471	0.451	-0.119	0.171	0.076	0.578	0.507			
ASV_25	1	Chromista	Cercozoa	Thecofilosea	NA	NA	NA	36680	53.68	16.46	0.53	0.58	6.08	3.06	3.81	12.58	3.23	-0.332	0.324	-0.093	0.115	0.047	0.404	0.352			
ASV_306	1	Chromista	Ochrophyta	Bacillariophyceae	NA	NA	NA	543	72.38	0.55	0.55	0.18	2.76	3.68	3.68	3.68	12.52	-0.377	0.369	-0.107	0.129	0.053	0.458	0.399			
ASV_261	1	Chromista	Ochrophyta	Dictyochophyceae	Florenciellales	Florenciellales i.s.	Florenciella	588	72.45	4.08	0	0.85	1.7	6.12	5.1	3.06	6.63	-0.475	0.428	-0.081	0.201	0.108	0.600	0.540			
ASV_95	1	Chromista	Cryptophyta	Cryptophyceae	Pyrenomonadales	Geminigeraceae	Teleaulax	3423	95.79	1.08	0.06	0.09	0.29	0.93	0.53	0.35	0.88	-0.525	0.391	0.028	0.305	0.209	0.712	0.677			
ASV_262	1	Chromista	Ciliophora	NA	NA	NA	NA	665	78.05	5.11	1.05	0	0.45	9.62	2.11	0.9	2.71	-0.443									

ASV_240	1	Chromista	Ochrophyta	Bacillariophyceae	Bacillariales	Bacillariaceae	Nitzschia	817	57.04	3.06	2.2	0	2.94	7.83	1.96	3.43	21.54	-0.380	0.518	-0.316	-0.016	-0.106	0.375	0.259
ASV_20	1	Chromista	Ochrophyta	Chrysophyceae	Chromulinales	NA	NA	9821	88.41	1.03	1.51	0.1	0.27	4.07	0.39	0.24	3.97	-0.365	0.496	-0.302	-0.015	-0.101	0.360	0.248
ASV_211	1	Chromista	Myzozoa	Dinophyceae	Gymnodiniales	Gymnodiniaceae	Gyrodinium	1102	49.27	7.08	2.99	0	3.81	10.89	1	12.52	12.43	-0.342	0.462	-0.278	-0.010	-0.090	0.340	0.237
ASV_158	1	Chromista	Cercozoa	Thecofilosea	Cryomonadida	Protaspidae	Protaspis	1766	85.96	0.4	0.62	0.45	0.57	0.85	0.96	0.96	9.23	-0.313	0.423	-0.255	-0.010	-0.083	0.311	0.217
ASV_65	1	Chromista	Ochrophyta	Chrysophyceae	Chromulinales	Chrysolepidomonadaceae	Chrysolepidomonas	1149	83.38	0.35	2.09	0.26	0	1.48	0.17	0.52	11.75	-0.325	0.432	-0.255	-0.003	-0.079	0.327	0.231
ASV_63	1	Chromista	Myzozoa	Dinophyceae	Gymnodiniales	Gymnodiniaceae	Lepidodinium	6239	64.06	8.56	1.84	0.14	1.33	1.84	2.87	4.81	14.54	-0.418	0.546	-0.314	0.005	-0.091	0.426	0.307
ASV_271	1	Chromista	Ochrophyta	Pelagophyceae	Sarcinochrysidales	Sarcinochrysidaceae	Sarcinochrysis	605	54.55	8.28	2.31	0	1.32	7.27	2.81	2.64	22.81	-0.409	0.570	-0.358	-0.030	-0.128	0.396	0.266
ASV_31	1	Chromista	NA	NA	NA	NA	NA	18206	46.1	2.64	1.83	1.35	2.58	21.54	6.29	1.48	16.19	-0.313	0.431	-0.267	-0.018	-0.092	0.306	0.209
ASV_190	1	Chromista	Myzozoa	Dinophyceae	NA	NA	NA	1336	43.86	6.89	3.07	0.37	1.72	23.28	2.69	3.97	14.15	-0.376	0.531	-0.339	-0.035	-0.125	0.359	0.237
ASV_172	1	Chromista	Myzozoa	Dinophyceae	NA	NA	NA	1513	55.72	18.31	3.57	0.2	2.05	5.75	1.39	4.76	8.26	-0.383	0.495	-0.279	0.012	-0.076	0.395	0.288
ASV_92	1	Chromista	Ciliophora	Litostomatea	Haptorida	NA	NA	4167	64.65	4.15	0.5	0.24	0.65	3.22	3.67	0.65	22.27	-0.398	0.508	-0.282	0.017	-0.074	0.413	0.304
ASV_37	1	Chromista	Haptophyta	Phaeocystaceae	Phaeocystales	Phaeocystaceae	Phaeocystis	12431	68.54	5.98	0.91	0.13	0.56	2.99	4.91	4.88	11.1	-0.430	0.538	-0.290	0.029	-0.068	0.452	0.339
ASV_208	1	Chromista	Myzozoa	Dinophyceae	Gymnodiniales	Brachidiniaeae	Takayama	962	71.21	1.66	0.73	0.1	0.42	11.02	0.94	1.77	12.16	-0.452	0.525	-0.245	0.073	-0.026	0.501	0.398
ASV_224	1	Chromista	Myzozoa	Dinophyceae	NA	NA	NA	908	62.78	6.39	1.76	0.33	1.54	9.25	1.54	8.37	8.04	-0.379	0.448	-0.217	0.053	-0.031	0.414	0.325
ASV_260	1	Chromista	Cercozoa	Thecofilosea	Cryomonadida	Protaspidae	Protaspis	712	61.8	1.83	0.56	0	0.42	0	0	2.39	33.01	-0.389	0.458	-0.220	0.057	-0.029	0.428	0.336
ASV_39	1	Chromista	Myzozoa	Dinophyceae	Gymnodiniales	Gymnodiniaceae	Lepidodinium	12079	79.24	6.25	0.6	0.21	1.65	2.98	1.08	2.25	5.75	-0.457	0.521	-0.235	0.083	-0.017	0.511	0.410
ASV_53	1	Chromista	NA	NA	NA	NA	NA	7680	75.74	7.64	1.08	0.16	2.2	4.28	1.12	4.53	3.24	-0.428	0.491	-0.224	0.075	-0.019	0.477	0.382
ASV_54	1	Chromista	Ciliophora	Oligotrichea	Oligotrichida	Strombidiidae	Strombidium	8067	73.99	7.02	3.77	0.68	0.41	1.44	2.09	2.34	8.26	-0.398	0.445	-0.192	0.081	-0.005	0.451	0.366
ASV_21	1	Chromista	Ochrophyta	Bacillariophyceae	Chaetocerotanae i.s.	Chaetocerotaceae	Chaetoceros	34157	69.42	5.54	0.78	0.07	0.47	10.13	6.45	1.69	5.45	-0.410	0.498	-0.254	0.044	-0.048	0.441	0.339
ASV_126	1	Chromista	NA	NA	NA	NA	NA	1225	88.33	0.33	1.06	0	0	1.63	0.24	0.33	8.08	-0.378	0.461	-0.236	0.039	-0.046	0.406	0.311
ASV_80	1	Chromista	Cercozoa	Thecofilosea	Cryomonadida	Protaspidae	Protaspis	5194	87.89	2.66	0.44	0	0.31	1.46	1.21	0.94	5.08	-0.443	0.529	-0.262	0.056	-0.043	0.481	0.374
ASV_201	1	Chromista	Myzozoa	Dinophyceae	Gymnodiniales	Gymnodiniaceae	Lepidodinium	1158	67.18	6.56	1.47	0.17	0.09	12.44	1.3	0	10.79	-0.420	0.456	-0.183	0.100	0.010	0.484	0.401
ASV_191	1	Chromista	Ochrophyta	Dictyochophyceae	Dictyochaetales	Dictyochaetaeae	Oectactis	1253	81.96	0.32	1.2	0	0	3.03	0.4	0.08	13.01	-0.463	0.494	-0.190	0.117	0.020	0.538	0.449
ASV_93	1	Chromista	Myzozoa	Dinophyceae	Gymnodiniales	Gymnodiniaceae	Lepidodinium	4090	82.71	2.54	1.42	0	0	2.64	1.78	0.44	8.46	-0.451	0.460	-0.153	0.137	0.044	0.538	0.460
ASV_170	1	Chromista	Haptophyta	Prymnesiophyceae	Prymnesiales	Chrysochromulinaeae	Chrysochromulina	1513	48.58	9.32	3.5	0.66	0.93	7.27	1.32	7.6	20.82	-0.385	0.562	-0.373	-0.054	-0.148	0.358	0.225
ASV_115	1	Chromista	Myzozoa	Dinophyceae	Gymnodiniales	NA	NA	2784	49.21	7	1.9	0	1.22	8.76	3.56	1.87	26.47	-0.390	0.568	-0.377	-0.054	-0.149	0.363	0.229
ASV_242	1	Chromista	Myzozoa	Dinophyceae	NA	NA	NA	699	50.5	0	3.86	1.14	0	6.01	3.15	3.72	31.62	-0.332	0.477	-0.311	-0.039	-0.120	0.312	0.201
ASV_153	1	Chromista	Ochrophyta	Dictyochophyceae	Pedinellales	Pedinellaceae	Pseudopedinella	1854	35.6	20.06	0.81	0.32	3.72	8.79	4.42	8.52	17.75	-0.371	0.572	-0.374	-0.062	-0.154	0.338	0.207
ASV_56	1	Chromista	Cercozoa	Thecofilosea	Cryomonadida	Protaspidae	Protaspis	8366	74.95	0.88	1.69	0	0	1.22	0.44	0.31	20.51	-0.345	0.511	-0.345	-0.056	-0.141	0.316	0.194
ASV_48	1	Chromista	Ochrophyta	Pelagophyceae	NA	NA	NA	11015	68.11	0.53	1.06	0.03	0.04	0.84	0.05	0.2	29.15	-0.394	0.592	-0.406	-0.072	-0.170	0.356	0.214
ASV_46	1	Chromista	Myzozoa	Dinophyceae	NA	NA	NA	11802	39.5	17.95	0.42	0.41	7.21	4.54	0.79	3.61	25.58	-0.365	0.553	-0.382	-0.071	-0.162	0.328	0.194
ASV_51	1	Chromista	Myzozoa	Dinophyceae	NA	NA	NA	7876	45.92	8.98	1.43	0.13	1.83	9.4	0.24	2.92	29.15	-0.377	0.592	-0.425	-0.095	-0.190	0.226	0.180
ASV_90	1	Chromista	Myzozoa	Dinophyceae	Gymnodiniales	Gymnodiniaceae	Lepidodinium	4565	34.85	1.2	2.34	0.39	1.45	7.67	3.92	4.58	32.79	-0.323	0.508	-0.365	-0.082	-0.164	0.279	0.153
ASV_23	1	Chromista	Ciliophora	Oligotrichea	Oligotrichida	Strombidiidae	Strombidium	38377	30.07	11.44	1.42	0.51	3.24	6.87	2.23	5.72	38.5	-0.346	0.541	-0.387	-0.084	-0.172	0.300	0.167
ASV_9	1	Chromista	Myzozoa	Dinophyceae	Gymnodiniales	Gymnodiniaceae	Gyrodinium	174621	36.55	12.36	0.61	0.13	1.5	7.1	1.53	5.32	34.9	-0.366	0.569	-0.405	-0.086	-0.179	0.319	0.180
ASV_64	1	Chromista	Myzozoa	Dinophyceae	Peridinales	Peridiniaeae	NA	1192	43.62	14.85	1.17	0.42	1.59	14.51	2.94	4.03	16.86	-0.350	0.462	-0.294	-0.071	-0.136	0.211	0.111
ASV_109	1	Chromista	Myzozoa	Dinophyceae	NA	NA	NA	3403	38.35	12.02	1.26	0.26	1.29	5.05	1.91	1.94	37.91	-0.360	0.571	-0.415	-0.097	-0.189	0.307	0.165
ASV_256	1	Chromista	Myzozoa	Dinophyceae	Peridinales	NA	NA	654	40.21	12.39	7.95	0.31	1.68	14.22	2.45	0.92	19.88	-0.311	0.492	-0.356	-0.082	-0.161	0.267	0.145
ASV_47	1	Chromista	Cercozoa	Thecofilosea	Cryomonadida	Protaspidae	Protaspis	7343	49.54	4.55	2.4	0.11	0.97	2.68	1.78	1.44	36.52	-0.335	0.548	-0.409	-0.107	-0.194	0.275	0.137
ASV_210	1	Chromista	Ciliophora	NA	NA	NA	NA	1126	29.75	25.75	1.87	0	1.69	7.55	1.87	7.9	23.62	-0.322	0.545	-0.419	-0.121	-0.206	0.254	0.114
ASV_179	1	Chromista	Ochrophyta	Pelagophyceae	Pelagomonadales	Pelagomonadaceae	Aureococcus	1558	72.53	1.93	0.71	0.58	0.64	3.98	0.39	0.83	18.42	-0.277	0.465	-0.355	-0.099	-0.172	0.222	0.103
ASV_83	1	Chromista	Ochrophyta	Chrysophyceae	Hibberdiales	Stylococccaceae	Helicopedinella	4744	32.02	10.92	3.08	0.04	1.05	10.05	1.45	3.52	37.86	-0.358	0.601	-0.460	-0.130	-0.224	0.285	0.131
ASV_59	1	Chromista	Ciliophora	Oligotrichea	NA	NA	NA	7635	29.51	12	1.11	0.25	2.58	6.81	3.8	3.58	40.37	-0.333	0.553	-0.419	-0.115	-0.202	0.269	0.128
ASV_100	1	Chromista	Myzozoa	Dinophyceae	Gymnodiniales	Gymnodiniaceae	Gyrodinium	4068	27.83	9.27	1.2	0.05	4.03	7.28	1.16	3.54	45.65	-0.343	0.603	-0.478	-0.151	-0.244	0.257	0.099
ASV_99	1	Chromista	Myzozoa	Dinophyceae	NA	NA	NA	4112	23.57	14.88	0.41	0.97	1.36	6.06	3.67	14.71	34.36	-0.280	0.482	-0.377	-0.114	-0.188	0.216	0.091
ASV_171	1	Chromista	Myzozoa	Dinophyceae	Gymnodiniales	Gymnodiniaceae	Torodinium	1554	35.33	4.89	2.38	0	1.48	14.29	4.31	4.18	33.14	-0.320	0.553	-0.433	-0.131	-0.217	0.246	0.103
ASV_237	1	Chromista	Cercozoa	Thecofilosea	NA	NA	NA	837	26.16	2.03	0.84	0	0	1.79	0.48	2.27	66.43	-0.201	0.455	-0.426	-0.191	-0.254	0.091	-0.041
ASV_70	1	Chromista	NA	NA	NA	NA	NA	6380	15.49	3.76	1.05	0	0.56	16.54	0.09	0.31	62.19	-0.253	0.					

ASV_137	1	Protozoa	Choanozoa	Choanoflagellata	Acanthoecida	Acanthoecidae	Calliacantha	1954	89.82	2.2	0	0.15	0.26	4.81	2.41	0.36	0	-0.484	0.258	0.172	0.385	0.304	0.718	0.726
ASV_78	1	Protozoa	Choanozoa	Choanoflagellata	Acanthoecida	Acanthoecidae	Calliacantha	4416	90.78	2.38	0.32	0.07	0.25	4.26	1.18	0.72	0.05	-0.494	0.313	0.105	0.342	0.256	0.703	0.692
ASV_295	1	Protozoa	Picozoa	Picomonadea	Picomonadida	Picomonadidae	Picomonas	505	93.66	1.98	0	0.2	0	1.39	0.4	0.4	1.98	-0.483	0.285	0.132	0.355	0.273	0.699	0.696
ASV_135	1	Protozoa	Choanozoa	Choanoflagellata	Acanthoecida	NA	NA	1954	87.56	3.99	0.2	0	0.56	3.63	1.84	0.77	1.43	-0.512	0.408	-0.013	0.269	0.173	0.677	0.632
ASV_347	1	Protozoa	Choanozoa	Choanoflagellata	Acanthoecida	Stephanoecidae	Didymoeca	331	58.91	6.65	4.23	0	0.6	6.04	1.51	8.16	13.9	-0.380	0.444	-0.210	0.058	-0.025	0.420	0.332
ASV_296	1	Protozoa	Picozoa	Picomonadea	Picomonadida	Picomonadidae	Picomonas	530	43.4	5.28	2.26	0.19	0	8.49	0.19	2.64	37.55	-0.375	0.560	-0.382	-0.065	-0.158	0.340	0.206
ASV_102	1	Protozoa	Choanozoa	Choanoflagellata	Acanthoecida	Picomonadidae	Diaphanoeca	3872	22.65	24.56	5.4	0.31	1.5	13.58	12.29	10.12	9.58	-0.261	0.436	-0.331	-0.092	-0.160	0.210	0.099
ASV_169	1	Protozoa	Picozoa	Picomonadea	Picomonadida	Picomonadidae	Picomonas	1711	11.1	3.92	3.16	0.06	1.29	9	0.76	2.28	68.44	-0.223	0.579	-0.578	-0.286	-0.362	0.056	-0.119
ASV_267	2	Chromista	Myzozoa	Dinophyceae	NA	NA	NA	735	8.84	0.41	2.04	0	6.53	4.76	0.95	1.77	74.69	0.129	0.198	-0.427	-0.371	-0.372	-0.350	-0.456
ASV_462	2	Chromista	NA	NA	NA	NA	NA	198	10.1	1.01	2.53	0	0	0	0	86.36	0.119	0.187	-0.399	-0.346	-0.347	-0.325	-0.424	
ASV_148	2	Chromista	Myzozoa	Dinophyceae	Gymnodiniales	Gymnodiniaceae	Gyrodinium	2285	0	10.24	3.85	0	2.36	54.49	1.62	3.46	23.98	0.163	0.206	-0.476	-0.424	-0.422	-0.417	-0.533
ASV_301	2	Chromista	Ciliophora	Oligotricha	Oligotrichida	Strombidiidae	Strombidium	569	1.58	3.34	2.46	0.53	0.88	1.58	0.53	7.21	81.9	0.165	0.213	-0.488	-0.433	-0.431	-0.424	-0.543
ASV_60	2	Chromista	Myzozoa	Dinophyceae	NA	NA	NA	8350	0.17	2.67	2.57	1.21	2.14	4.14	1.1	6	79.99	0.172	0.221	-0.508	-0.452	-0.450	-0.442	-0.567
ASV_298	2	Chromista	Haptophyta	Prymnesiophyceae	NA	NA	NA	605	2.15	1.65	5.29	0.83	0	0.33	0.5	0.5	88.76	0.154	0.215	-0.479	-0.421	-0.421	-0.405	-0.523
ASV_440	2	Chromista	Haptophyta	Prymnesiophyceae	Coccolithales	Coccolithaceae	Cruciplacolithus	244	6.56	3.28	0.82	0	0.41	0.82	1.64	0	86.48	0.137	0.190	-0.425	-0.374	-0.374	-0.361	-0.465
ASV_273	2	Chromista	Myzozoa	Dinophyceae	Gymnodiniales	Gymnodiniaceae	Gyrodinium	725	0	36.83	0.28	0	0.69	28.55	1.52	5.79	26.34	0.158	0.178	-0.430	-0.389	-0.385	-0.391	-0.495
ASV_49	2	Chromista	Ochrophyta	Bacillariophyceae	Hemialiales	Hemialaceae	Eucampia	10442	0.51	20.23	4.22	1	2.01	27.38	6.15	7.05	31.46	0.172	0.189	-0.461	-0.419	-0.414	-0.422	-0.533
ASV_333	2	Chromista	Myzozoa	Dinophyceae	Gymnodiniales	Gymnodiniaceae	Gyrodinium	503	0.99	11.13	2.78	0	1.79	53.28	2.19	5.17	22.66	0.171	0.182	-0.451	-0.411	-0.406	-0.417	-0.525
ASV_292	2	Chromista	Myzozoa	Dinophyceae	Gymnodiniales	Gymnodiniaceae	Lepidodinium	638	2.98	5.96	0.63	0	5.17	13.48	0	0	71.79	0.169	0.131	-0.376	-0.357	-0.348	-0.383	-0.471
ASV_111	2	Chromista	Ochrophyta	Bacillariophyceae	NA	NA	NA	3757	0.03	16.66	1.89	0.16	2.5	18.13	17.33	4.29	39.02	0.199	0.156	-0.444	-0.421	-0.411	-0.451	-0.556
ASV_350	2	Chromista	Myzozoa	Dinophyceae	Gymnodiniales	Gymnodiniaceae	Gyrodinium	426	0	8.69	4.46	0	1.88	54.69	0	6.34	23.94	0.198	0.158	-0.446	-0.422	-0.411	-0.450	-0.556
ASV_391	2	Chromista	Ochrophyta	Chrysophyceae	Chromulinales	Chrysolepidomonadaceae	Chrysolepidomonas	294	0	13.61	2.38	0	0	18.03	0	4.08	61.9	0.208	0.179	-0.488	-0.456	-0.447	-0.481	-0.596
ASV_368	2	Chromista	Myzozoa	Dinophyceae	NA	NA	NA	347	0	3.46	3.46	0	2.88	17.87	2.88	3.75	65.71	0.214	0.193	-0.514	-0.479	-0.469	-0.501	-0.623
ASV_329	2	Chromista	Cercozoa	Thecofilosea	NA	NA	NA	498	0.6	1.2	5.02	0.4	1	18.47	0	1.2	72.09	0.232	0.155	-0.479	-0.463	-0.449	-0.509	-0.621
ASV_372	2	Chromista	Myzozoa	Dinophyceae	Gymnodiniales	Gymnodiniaceae	Gyrodinium	355	6.76	10.99	1.69	0.85	0.85	34.08	0.56	1.41	42.82	0.089	0.227	-0.424	-0.347	-0.356	-0.296	-0.404
ASV_38	2	Chromista	Myzozoa	Dinophyceae	Gymnodiniales	Gymnodiniaceae	Gyrodinium	15121	0.71	10.87	3.62	0.12	2.96	50.72	2.02	6.34	22.63	0.097	0.254	-0.471	-0.385	-0.395	-0.327	-0.447
ASV_107	2	Chromista	Myzozoa	Dinophyceae	Gymnodiniales	Gymnodiniaceae	Gyrodinium	4004	0.82	11.16	3.37	0.17	2.07	48.9	1.55	5.27	26.67	0.101	0.284	-0.490	-0.400	-0.410	-0.339	-0.464
ASV_220	2	Chromista	Myzozoa	Dinophyceae	Gymnodiniales	Gymnodiniaceae	Gyrodinium	1108	0.99	14.26	0.309	0	1.26	39.08	0.63	3.16	40.52	0.107	0.267	-0.501	-0.411	-0.421	-0.352	-0.480
ASV_204	2	Chromista	Ochrophyta	Bacillariophyceae	Bacillariales	Bacillariaceae	Pseudonitzschia	1330	2.11	19.1	0.75	1.2	3.23	8.8	3.31	11.73	49.77	0.093	0.261	-0.476	-0.386	-0.397	-0.323	-0.445
ASV_8	2	Chromista	Ochrophyta	Bacillariophyceae	Bacillariales	Bacillariaceae	Pseudonitzschia	194380	1.74	21.25	3.88	1.6	2.99	6.36	7.23	11.2	43.77	0.083	0.260	-0.464	-0.373	-0.385	-0.305	-0.425
ASV_383	2	Chromista	Peronospora	Oomycota	NA	NA	NA	311	7.07	17.36	1.93	0	2.25	3.86	4.5	8.68	54.34	0.092	0.292	-0.521	-0.417	-0.431	-0.341	-0.475
ASV_287	2	Chromista	Myzozoa	Dinophyceae	NA	NA	NA	641	3.28	9.98	2.18	0	0	6.55	0	2.18	75.82	0.099	0.315	-0.560	-0.449	-0.464	-0.367	-0.511
ASV_209	2	Chromista	Ochrophyta	Chrysophyceae	Chromulinales	NA	NA	1264	1.74	38.77	1.9	0.08	4.27	28.8	0.47	12.97	11	0.077	0.235	-0.455	-0.378	-0.386	-0.333	-0.448
ASV_62	2	Chromista	Myzozoa	Dinophyceae	Gymnodiniales	Gymnodiniaceae	Gyrodinium	8320	0.65	9.71	3.68	0.26	3.21	51.83	1.95	5.89	22.82	0.111	0.248	-0.478	-0.397	-0.405	-0.348	-0.469
ASV_79	2	Chromista	Myzozoa	Dinophyceae	Gymnodiniales	Gymnodiniaceae	Gyrodinium	5724	0.68	12.32	2.9	0.12	2.67	48.38	1.66	5.19	26.08	0.112	0.248	-0.480	-0.399	-0.407	-0.350	-0.472
ASV_87	2	Chromista	Myzozoa	Dinophyceae	Gymnodiniales	Gymnodiniaceae	Gyrodinium	5368	0.67	15.33	2.63	0.11	2.65	46.31	1.99	5.35	24.96	0.106	0.251	-0.477	-0.394	-0.402	-0.340	-0.461
ASV_251	2	Chromista	Myzozoa	Dinophyceae	Gymnodiniales	Gymnodiniaceae	Gyrodinium	866	0.81	37.18	0.46	0	2.66	27.94	0.81	5.2	24.94	0.117	0.239	-0.472	-0.396	-0.402	-0.354	-0.472
ASV_317	2	Chromista	Myzozoa	Dinophyceae	Gymnodiniales	Gymnodiniaceae	Lepidodinium	525	4.57	2.29	5.33	0	4.76	1.14	1.9	14.1	65.9	0.104	0.207	-0.412	-0.347	-0.352	-0.311	-0.415
ASV_119	2	Chromista	Myzozoa	Dinophyceae	Gymnodiniales	Gymnodiniaceae	Gyrodinium	3231	0.9	10.71	3.5	0.25	3.31	49.46	1.73	5.66	24.48	0.120	0.238	-0.474	-0.399	-0.405	-0.358	-0.477
ASV_257	2	Chromista	NA	NA	NA	NA	NA	784	3.06	39.03	1.02	0.64	4.97	9.82	3.44	20.79	17.22	0.063	0.242	-0.416	-0.327	-0.340	-0.258	-0.366
ASV_206	2	Chromista	Myzozoa	Dinophyceae	Gymnodiniales	Gymnodiniaceae	Margalefidinium	1334	2.17	6.97	2.55	0	2.17	7.95	0.07	3.15	74.96	0.081	0.346	-0.585	-0.456	-0.476	-0.353	-0.505
ASV_459	2	Chromista	NA	NA	NA	NA	NA	203	0	2.96	5.42	2.96	0	14.78	0.99	2.96	69.95	0.260	0.132	-0.478	-0.478	-0.458	-0.547	-0.656
ASV_570	2	Chromista	Ochrophyta	Dictyochophyceae	Florenciellales	Florenciellales <i>i.s.</i>	Florenciella	92	19.57	4.35	1.09	0	0	7.61	4.35	1.09	61.96	0.176	0.088	-0.322	-0.323	-0.309	-0.370	-0.443
ASV_435	2	Chromista	Ochrophyta	Bacillariophyceae	Chaetocerotanae <i>i.s.</i>	Chaetocerotaceae	Chaetoceros	253	0	12.25	5.93	1.98	0.79	24.11	2.77	8.3	48.87	0.259	0.140	-0.489	-0.485	-0.466	-0.549	-0.661
ASV_445	2	Chromista	Ochrophyta	Bacillariophyceae	Chaetocerotanae <i>i.s.</i>	Chaetocerotaceae	Chaetoceros	242	0	16.12	0.83	0.41	0	8.68	4.13	3.72	66.12	0.245	0.130	-0.459	-0.457	-0.439	-0.519	-0.624
ASV_270	2	Chromista	Ochrophyta	Bacillariophyceae	Chaetocerotanae <i>i.s.</i>	Chaetocerotaceae	Chaetoceros	728	0	3.98	0.96	0	1.51	4.4	5.77	10.44	72.94	0.240	0.111	-0.426	-0.431	-0.411	-0.498	-0.595
ASV_451	2	Chromista	Ochrophyta	Pelagophyceae	Sarcinochrysidales	Sarcinochrysidaceae	NA	225	3.11	11.56	3.11	0	5.33	16.44	8	19.11	33.33	0.184	0.081	-0.321	-0.327	-0.311	-0.380	-0.453
ASV_556	2	Chromista	Cercozoa	Imbriccatea	Thaumatomonadida	Thaumatomastigidae	Reckertia	88	20.45	0	3.41	0	0	11.36	0	4.55	60.23	0.163	0.073	-0.286	-0.290	-0.276	-0.336	-0.401
ASV_479	2	Chromista	Ciliophora	Prostomatea	Prorodontida	Balanionidae	Balanion	193	0	1.55	2.59	2.59	4.66	24.35	3.63	2.59	58.03	0.239	0.075	-0.373	-0.393	-0.370	-0.474	-0.556
ASV_147	2	Chromista	Ochrophyta	Bacillariophyceae	NA	NA	NA	2284	0.22	8.89	4.51	1.44	4.38	7.71	3.24	21.02	48.6	0.248	0.088	-0.402	-0.418	-0.396	-0.499	-0.588
ASV_429	2	Chromista	Ochrophyta	Dictyochophyceae	Pedinellales	Pedinellaceae	Pteridomonas	248	0	0	3.23	0	0	0	0	0	96.77	0.261	0.068	-0.388	-0.415	-0.389	-0.510	-0.594
ASV_75	2	Chromista	Myzozoa	Dinophyceae	Gymnodiniales	Gymnodiniaceae	NA	5605	0.16	14.58	19.09	0.36	1.52	41.89	9.51	6.39	6.51	0.189	0.050	-0.283	-0.302	-0.283	-0.371	-0.432
ASV_452	2	Chromista	Cercozoa	Thecofilosea	NA	NA	NA	233	0	0	0	0	0	5.15	2.58	0	92.27	0.268	0.060	-0.384	-0.416	-0.389	-0.518	-0.601
ASV_535	2	Chromista	Myzozoa	Dinophyceae	Syndiniales	Amoeboophyceae	Amoebo																	

ASV_498	2	Chromista	Ochrophyta	Pelagophyceae	Sarcinochrysidales	Sarcinochrysidaceae	Ankylochrysis	162	0	0	0	0.62	0	9.26	19.75	0	70.37	0.291	-0.077	-0.214	-0.309	-0.267	-0.477	-0.512
ASV_605	2	Chromista	Cercozoa	Thecofilosea	Cryomonadida	Protaspidae	Protaspis	82	8.54	0	0	3.66	0	2.44	0	4.88	80.49	0.294	-0.088	-0.203	-0.303	-0.260	-0.477	-0.509
ASV_321	2	Chromista	Myzozoa	Dinophyceae	NA	NA	NA	483	14.7	10.35	2.9	0	0.41	6.63	3.11	2.48	59.42	-0.050	0.367	-0.468	-0.303	-0.340	-0.129	-0.261
ASV_447	2	Chromista	NA	NA	NA	NA	NA	234	23.08	3.85	2.14	0	1.28	8.55	0	0.43	60.68	-0.070	0.338	-0.404	-0.246	-0.283	-0.075	-0.190
ASV_185	2	Chromista	NA	NA	NA	NA	NA	1542	7.2	20.69	3.96	0.19	2.92	12.32	2.79	12.39	37.55	-0.082	0.451	-0.553	-0.345	-0.394	-0.122	-0.279
ASV_392	2	Chromista	NA	NA	NA	NA	NA	281	22.78	3.91	4.27	0	3.2	8.54	0	3.91	53.38	-0.108	0.429	-0.492	-0.289	-0.338	-0.062	-0.205
ASV_230	2	Chromista	Ochrophyta	Bacillariophyceae	NA	NA	NA	960	9.58	6.15	0.83	0.31	0.1	15	6.25	5.94	55.83	-0.102	0.397	-0.453	-0.264	-0.310	-0.053	-0.184
ASV_145	2	Chromista	Ochrophyta	Bacillariophyceae	NA	NA	NA	2251	12.48	3.02	4.49	0.22	1.6	11.28	11.37	6.53	49	-0.127	0.409	-0.442	-0.243	-0.293	-0.015	-0.145
ASV_123	2	Chromista	Bigyra	Labyrinthulea	Thraustochytrida	NA	NA	2951	7.42	29.45	1.83	0.1	3.12	9.79	1.42	10.64	36.23	-0.149	0.492	-0.537	-0.298	-0.568	-0.026	-0.184
ASV_194	2	Chromista	Cercozoa	Thecofilosea	Cryomonadida	Protaspidae	Protaspis	1492	7.17	1.94	3.62	0	0.94	9.25	0.27	4.76	72.05	0.017	0.374	-0.554	-0.400	-0.430	-0.255	-0.404
ASV_22	2	Chromista	Myzozoa	Dinophyceae	Gymnodiniales	Kareniaceae	Karladinium	40964	6.26	2.91	3.64	0.38	0.91	11.32	0.68	4.37	69.51	0.015	0.341	-0.504	-0.364	-0.391	-0.231	-0.367
ASV_417	2	Chromista	Ciliophora	Oligohymenophorea	Philasterida	Uronematidae	Homalogastra	241	21.16	11.62	1.66	0	1.66	17.43	1.66	6.64	38.17	0.015	0.283	-0.420	-0.304	-0.326	-0.195	-0.308
ASV_140	2	Chromista	Myzozoa	Dinophyceae	Gymnodiniales	Gymnodiniaceae	Gyrodinium	2558	1.68	13.64	0.23	0.12	1.06	36.59	0.35	2.42	43.9	0.035	0.340	-0.525	-0.389	-0.414	-0.267	-0.406
ASV_472	2	Chromista	Ochrophyta	Dictyochophyceae	Florentiellales	Florentiellales	Florentiella	187	17.65	16.58	1.07	0	0	12.3	4.28	4.28	43.85	-0.019	0.336	-0.459	-0.313	-0.444	-0.167	-0.293
ASV_27	2	Chromista	Ochrophyta	Chrysophyceae	Chromulinales	Chrysolepidomonadaceae	Chrysolepidomonas	31738	1.83	13.68	3.68	0.24	1.37	22.99	1.24	7.56	47.41	-0.021	0.384	-0.525	-0.358	-0.394	-0.191	-0.335
ASV_183	2	Metazoa	NA	NA	NA	NA	NA	1593	0	4.27	2.57	0	2.39	11.86	1.63	7.03	70.24	0.214	0.182	-0.500	-0.469	-0.458	-0.495	-0.613
ASV_564	2	Plantae	Chlorophyta	NA	NA	NA	NA	97	2.06	8.25	6.19	0	0	11.34	0	0	72.16	0.321	-0.017	-0.335	-0.410	-0.370	-0.568	-0.633
ASV_250	2	Protozoa	Picozoa	Picomonadea	Picomonadida	Picomonadidae	Picomonas	830	2.05	4.22	4.1	0.24	0	7.95	0	2.41	79.04	0.117	0.301	-0.560	-0.458	-0.469	-0.389	-0.532
ASV_474	2	Protozoa	Picozoa	Picomonadea	Picomonadida	Picomonadidae	Picomonas	197	13.71	6.6	4.06	0	1.02	7.11	0	0	67.51	0.078	0.258	-0.456	-0.364	-0.376	-0.294	-0.412
ASV_108	2	Protozoa	Choanozoa	Choanoflagellata	Acanthoecida	Stephanocididae	Didymoeca	3644	1.51	11.83	7	0.25	1.56	31.26	1.1	3.68	41.82	0.130	0.288	-0.556	-0.462	-0.471	-0.406	-0.546
ASV_110	2	Protozoa	Picozoa	Picomonadea	Picomonadida	Picomonadidae	Picomonas	3680	1.6	10.24	4.24	0.08	2.74	15.95	0.38	5.65	59.1	0.018	0.400	-0.591	-0.426	-0.458	-0.271	-0.430
ASV_362	3	Chromista	Radiozoa	Acantharia	Acantharia i.s.	Acantharia i.s.	Heteracon	326	54.6	1.53	3.99	1.53	1.23	3.07	31.9	2.15	0	-0.172	-0.139	0.390	0.369	0.360	0.393	0.485
ASV_407	3	Chromista	Ciliophora	Oligotrichida	Oligotrichida	Strombididae	Strombidium	216	88.89	0	0	5.09	0	0	6.02	0	0	-0.179	-0.142	0.402	0.381	0.371	0.407	0.502
ASV_534	3	Chromista	Ciliophora	NA	NA	NA	NA	101	97.03	0	0	0	0	0	2.97	0	0	-0.200	-0.156	0.447	0.424	0.413	0.454	0.559
ASV_475	3	Chromista	Myzozoa	Dinophyceae	NA	NA	NA	178	100	0	0	0	0	0	0	0	0	-0.138	-0.134	0.345	0.319	0.313	0.329	0.412
ASV_146	3	Chromista	Ciliophora	NA	NA	NA	NA	2370	24.98	1.65	1.22	3.21	0	0.13	67.64	1.18	0	-0.184	-0.114	0.368	0.360	0.347	0.400	0.485
ASV_233	3	Chromista	Ciliophora	Oligotrichida	Oligotrichida	NA	NA	889	46.01	0.34	3.49	0.9	1.69	3.37	40.83	3.37	0	-0.193	-0.113	0.377	0.370	0.357	0.415	0.502
ASV_433	3	Chromista	Myzozoa	Dinophyceae	NA	NA	NA	204	97.55	0.98	0	0	0	0	1.47	0	0	-0.218	-0.114	0.406	0.405	0.388	0.461	0.553
ASV_612	3	Chromista	Haptophyta	Prymnesiophyceae	Phaeocystales	Phaeocystaceae	Phaeocystis	65	93.85	1.54	0	0	1.54	0	0	0	3.08	-0.146	-0.204	0.453	0.399	0.398	0.384	0.495
ASV_577	3	Chromista	Myzozoa	Dinophyceae	Syndiniales	Amoebophryaceae	Amoebophrya	78	91.03	2.56	1.28	0	0	0	1.28	1.28	3.85	-0.124	-0.168	0.378	0.333	0.333	0.323	0.416
ASV_638	3	Chromista	Myzozoa	Dinophyceae	NA	NA	NA	63	100	0	0	0	0	0	0	0	0	-0.087	-0.260	0.468	0.377	0.388	0.311	0.431
ASV_502	3	Chromista	Cercozoa	Thecofilosea	Cryomonadida	Protaspidae	Protaspis	147	46.94	12.93	0	2.72	6.12	1.36	21.77	8.16	0	-0.045	-0.256	0.417	0.318	0.335	0.235	0.344
ASV_768	3	Chromista	Myzozoa	Dinophyceae	Syndiniales	Amoebophryaceae	Amoebophrya	22	100	0	0	0	0	0	0	0	0	0.148	-0.432	0.452	0.238	0.292	-0.009	0.126
ASV_811	3	Chromista	Ciliophora	Litostomatea	Cyclotrichiida	Mesodiniidae	Mesodinium	20	100	0	0	0	0	0	0	0	0	0.171	-0.498	0.520	0.273	0.336	-0.011	0.144
ASV_689	3	Chromista	Ciliophora	Oligotrichida	Oligotrichida	NA	NA	34	85.29	0	0	0	0	0	14.71	0	0	0.111	-0.372	0.407	0.226	0.271	0.022	0.141
ASV_827	3	Chromista	Cryptophyta	Cryptophyta i.s.	Cryptophyta i.s.	Katablepharidaceae	Katablepharis	27	100	0	0	0	0	0	0	0	0	0.103	-0.381	0.428	0.246	0.290	0.041	0.166
ASV_653	3	Chromista	Myzozoa	Dinophyceae	NA	NA	NA	59	77.97	0	0	0	0	0	22.03	0	0	0.105	-0.413	0.472	0.275	0.323	0.056	0.193
ASV_36	3	Chromista	Myzozoa	Dinophyceae	Gymnodiniales	Gymnodiniaceae	Gyrodinium	16442	17.95	1.76	4.57	11.99	1	5.57	52.24	4.88	0.04	0.081	-0.398	0.478	0.293	0.336	0.092	0.228
ASV_717	3	Chromista	Myzozoa	Dinophyceae	Syndiniales	Amoebophryaceae	Amoebophrya	39	100	0	0	0	0	0	0	0	0	0.036	-0.369	0.487	0.324	0.359	0.156	0.291
ASV_643	3	Chromista	Myzozoa	Dinophyceae	NA	NA	NA	55	98.18	0	0	0	0	1.82	0	0	0	0.024	-0.335	0.451	0.305	0.337	0.157	0.281
ASV_650	3	Chromista	Ciliophora	NA	NA	NA	NA	47	100	0	0	0	0	0	0	0	0	0.013	-0.350	0.486	0.335	0.366	0.185	0.318
ASV_713	3	Plantae	Chlorophyta	NA	NA	NA	NA	36	75	2.78	0	0	0	22.22	0	0	0	0.076	-0.379	0.457	0.281	0.322	0.089	0.220
ASV_522	3	Protozoa	Choanozoa	Choanoflagellata	Acanthoecida	NA	NA	88	87.5	0	0	0	0	0	12.5	0	0	-0.095	-0.231	0.436	0.359	0.367	0.308	0.419
ASV_615	3	Protozoa	Protozoa i.s.	Ebriophyceae	Ebriales	Ebriaceae	Ebria	80	60	0	0	30	2.5	5	2.5	0	0	0.124	-0.385	0.412	0.223	0.270	0.006	0.128
ASV_478	4	Chromista	Cercozoa	Thecofilosea	Cryomonadida	Protaspidae	Protaspis	201	1	5.97	3.48	0.5	0	3.48	31.34	25.37	28.86	0.274	-0.141	-0.105	-0.222	-0.178	-0.409	-0.415
ASV_649	4	Chromista	Bigyra	Labyrinthulea	Thraustochytrida	NA	NA	65	0	9.23	12.31	0	1.54	36.92	6.15	3.08	30.77	0.361	-0.197	-0.122	-0.282	-0.221	-0.532	-0.536
ASV_767	4	Chromista	Ciliophora	Oligohymenophorea	Philasterida	Uronematidae	Homalogastra	33	9.09	0	3.03	0	0	3.03	0	0	84.85	0.375	-0.224	-0.098	-0.273	-0.208	-0.541	-0.537
ASV_567	4	Chromista	Myzozoa	Dinophyceae	Suessiales	Suessiaceae	Polarella	78	3.85	3.85	0	1.28	0	15.38	12.82	19.23	48.59	0.340	-0.202	-0.090	-0.248	-0.190	-0.490	-0.487
ASV_316	4	Chromista	Myzozoa	Dinoflagellata i.s.	Dinoflagellata i.s.	Dinoflagellata i.s.	Duboscquella	550	1.27	2	13.27	5.09	3.82	18	21.09	17.27	18.18	0.295	-0.136	-0.134	-0.254	-0.207	-0.449	-0.462
ASV_585	4	Chromista	Cercozoa	Thecofilosea	Thecofilosea i.s.	Thecofilosea i.s.	Mataza	67	7.46	0	2.99	1.49	0	0	1.49	0	86.57	0.313	-0.129	-0.165	-0.287	-0.238	-0.487	-0.506
ASV_642	4	Chromista	Haptophyta	Prymnesiophyceae	Prymnesiales	Chrysochromulinaceae	Chrysochromulina	66	3.03	24.24	12.12	0	9.09	3.03	0	7.58	40.91	0.338	-0.141	-0.176	-0.308	-0.255	-0.525	-0.545
ASV_773	4	Chromista	NA	NA	NA	NA	NA	32	15.62	6.25	0	0	0	0	0	0	78.12	0.360	-0.247	-0.049	-0.230	-0.166	-0.501	-0.485
ASV_673	4	Chromista	NA	NA	NA	NA	NA	54	9.26	12.96	7.41	3.7	0	20.37	7.41	5.56	33.33	0.333	-0.225	-0.050	-0.216	-0.157	-0.465	-0.452
ASV_716	4	Chromista	NA	NA	NA	NA	NA	29	3.45	3.45	3.45	0	0	10.34	3.45	0	75.86	0.403	-0.298	-0.024	-0.236	-0.162	-0.548	-0.522
ASV_742	4	Chromista	Ochrophyta	Bacillariophyceae	Chaetocerotanaceae	Chaetocerotaceae	Chaetoceros	34	0	5.88	5.88	0	0	23.53	0	5.88	58.82	0.406	-0.287	-0.043	-0.251	-0.178	-0.560	-0.539
ASV_748	4	Chromista	NA	NA	NA	NA	NA	36	8.33	0	5.56	0	0	5.56	5.56	0	75	0.380	-0.294					

ASV_873	4	Chromista	Bigyra	Labyrinthulea	Thraustochytrida	Thraustochytriaceae	Oblongichytrium	20	10	0	15	0	0	10	25	5	35	0.383	-0.459	0.229	-0.047	0.038	-0.415	-0.322
ASV_842	4	Chromista	Myzozoa	Dinophyceae	NA	NA	NA	22	40.91	0	0	0	0	22.73	0	0	36.36	0.338	-0.404	0.200	-0.042	0.033	-0.367	-0.285
ASV_1202	4	Chromista	NA	NA	NA	NA	NA	10	0	10	0	0	0	0	0	0	90	0.406	-0.476	0.227	-0.061	0.029	-0.447	-0.353
ASV_1001	4	Chromista	Myzozoa	Dinophyceae	NA	NA	NA	16	0	0	0	0	0	18.75	0	0	81.25	0.420	-0.413	0.122	-0.142	-0.056	-0.509	-0.442
ASV_698	4	Chromista	Ciliophora	Oligotrichea	Oligotrichida	NA	NA	21	9.52	0	0	0	0	38.1	9.52	0	42.86	0.383	-0.416	0.167	-0.090	-0.009	-0.441	-0.365
ASV_812	4	Chromista	Cercozoa	Thecofilosea	Thecofilosea i.s.	Mataza	NA	13	15.38	0	0	0	0	7.69	0	0	76.92	0.420	-0.453	0.179	-0.102	-0.013	-0.486	-0.403
ASV_770	4	Chromista	Haptophyta	Prymnesiophyceae	Prymnesiales	Chrysochromulinaceae	Chrysochromulina	31	16.13	9.68	3.23	0	6.45	0	9.68	6.45	48.39	0.407	-0.367	0.070	-0.172	-0.091	-0.514	-0.462
ASV_981	4	Chromista	Ochrophyta	Pelagophyceae	NA	NA	NA	16	0	0	0	0	0	0	0	0	100	0.434	-0.387	0.069	-0.187	-0.102	-0.550	-0.497
ASV_906	4	Chromista	NA	NA	NA	NA	NA	21	0	4.76	0	0	0	0	0	0	95.24	0.401	-0.372	0.084	-0.159	-0.079	-0.500	-0.445
ASV_878	4	Chromista	Myzozoa	Dinophyceae	NA	NA	NA	21	0	14.29	0	0	0	23.81	0	0	61.9	0.408	-0.388	0.099	-0.152	-0.070	-0.503	-0.443
ASV_750	4	Chromista	Myzozoa	Dinophyceae	Gymnodiniales	Gymnodiniaceae	Gyrodinium	35	0	11.43	5.71	0	0	42.86	0	14.29	25.71	0.383	-0.361	0.087	-0.147	-0.070	-0.475	-0.420
ASV_711	4	Chromista	Myzozoa	Dinophyceae	Suessiales	Suessiaceae	Ansanella	44	6.82	27.27	0	2.27	2.27	0	0	29.55	31.82	0.367	-0.346	0.085	-0.139	-0.065	-0.454	-0.401
ASV_840	4	Chromista	Myzozoa	Dinophyceae	NA	NA	NA	21	100	0	0	0	0	0	0	0	0	0.201	-0.486	0.470	0.222	0.288	-0.071	0.073
ASV_726	4	Chromista	Radiozoa	Acantharia	NA	NA	NA	32	87.5	0	3.12	0	0	3.12	0	6.25	0	0.169	-0.448	0.451	0.226	0.285	-0.037	0.099
ASV_754	4	Chromista	Myzozoa	Dinophyceae	NA	NA	NA	33	51.52	0	0	12.12	0	15.15	21.21	0	0	0.207	-0.479	0.454	0.208	0.273	-0.086	0.054
ASV_802	4	Chromista	Ciliophora	Oligotrichea	Oligotrichida	NA	NA	26	73.08	0	0	0	0	26.92	0	0	0	0.216	-0.489	0.458	0.205	0.273	-0.096	0.045
ASV_583	4	Chromista	Myzozoa	NA	NA	NA	NA	92	68.48	0	1.09	4.35	0	0	26.09	0	0	0.199	-0.452	0.424	0.191	0.253	-0.088	0.044
ASV_890	4	Chromista	Oomycota	Peronosporae	Saprolegniales	Haliphthoraceae	Haliphthoros	22	72.73	4.55	0	0	9.09	0	0	13.64	0	0.253	-0.485	0.410	0.152	0.223	-0.166	-0.034
ASV_823	4	Chromista	Heliozoa	Centrohelea	Centrohelida	Heterophryidae	Heterophrys	23	60.87	0	4.35	0	0	17.39	17.39	0	0	0.261	-0.501	0.425	0.158	0.232	-0.170	-0.034
ASV_852	4	Chromista	Cercozoa	Thecofilosea	NA	NA	NA	23	69.57	17.39	0	0	0	4.35	0	8.7	0	0.232	-0.437	0.365	0.132	0.197	-0.156	-0.038
ASV_656	4	Chromista	Myzozoa	Dinophyceae	Suessiales	Suessiaceae	Polarella	65	20	0	49.23	10.77	13.85	0	6.15	0	0	0.221	-0.401	0.326	0.110	0.171	-0.159	-0.052
ASV_524	4	Chromista	Myzozoa	Dinophyceae	Gymnodiniales	Gymnodiniaceae	Gyrodinium	139	7.19	1.44	0	6.47	0	2.16	48.2	34.53	0	0.222	-0.411	0.340	0.119	0.181	-0.153	-0.043
ASV_628	4	Chromista	Ciliophora	NA	NA	NA	NA	69	14.49	2.9	4.35	1.45	0	72.46	0	0	0	0.253	-0.468	0.387	0.135	0.206	-0.175	-0.050
ASV_825	4	Chromista	Myzozoa	Dinophyceae	NA	NA	NA	27	81.48	0	0	0	0	0	0	3.7	14.81	0.259	-0.476	0.390	0.134	0.206	-0.182	-0.055
ASV_1132	4	Chromista	Haptophyta	NA	NA	NA	NA	11	72.73	0	0	0	0	9.09	18.18	0	0	0.306	-0.563	0.463	0.160	0.245	-0.125	-0.064
ASV_780	4	Chromista	Myzozoa	Dinophyceae	Suessiales	Biecheleriaceae	Biecheleria	31	41.94	3.23	0	45.16	0	0	3.23	6.45	0	0.232	-0.492	0.444	0.187	0.257	-0.124	0.015
ASV_796	4	Chromista	Myzozoa	Dinophyceae	NA	NA	NA	20	75	0	5	0	0	5	0	15	0	0.221	-0.479	0.438	0.189	0.256	-0.112	0.025
ASV_841	4	Chromista	Ciliophora	Oligohymenophorea	Phylasterida	Uronematidae	Homalogastra	23	100	0	0	0	0	0	0	0	0	0.199	-0.430	0.392	0.168	0.228	-0.102	0.021
ASV_920	4	Chromista	Ciliophora	NA	NA	NA	NA	16	93.75	0	0	0	0	0	6.25	0	0	0.249	-0.536	0.487	0.208	0.283	-0.129	0.023
ASV_864	4	Chromista	Ciliophora	Oligotrichea	Choreotrichida	Strobilidiidae	NA	12	100	0	0	0	0	0	0	0	0	0.268	-0.533	0.462	0.180	0.257	-0.165	-0.017
ASV_788	4	Chromista	NA	NA	NA	NA	NA	16	93.75	0	0	0	0	6.25	0	0	0	0.251	-0.507	0.444	0.176	0.250	-0.150	-0.009
ASV_926	4	Chromista	Myzozoa	Dinophyceae	NA	NA	NA	15	93.33	0	0	0	0	0	0	0	6.67	0.261	-0.528	0.463	0.185	0.261	-0.155	-0.008
ASV_855	4	Chromista	NA	NA	NA	NA	NA	17	100	0	0	0	0	0	0	0	0	0.221	-0.455	0.403	0.164	0.230	-0.127	0.001
ASV_784	4	Chromista	Myzozoa	Dinophyceae	Syndiniales	Amoebophryaceae	Amoebophrya	26	80.77	3.85	0	0	0	3.85	0	0	11.54	0.214	-0.441	0.392	0.160	0.223	-0.121	0.003
ASV_859	4	Chromista	Myzozoa	Dinophyceae	NA	NA	NA	23	86.96	0	0	0	0	0	13.04	0	0	0.237	-0.491	0.437	0.180	0.250	-0.133	0.005
ASV_917	4	Chromista	Myzozoa	Dinoflagellata i.s.	Dinoflagellata i.s.	Duboscquella	NA	18	77.78	5.56	0	0	0	0	16.67	0	0	0.256	-0.534	0.476	0.196	0.273	-0.143	0.007
ASV_724	4	Chromista	Ochrophyta	Bacillariophyceae	Thalassiosirales	Thalassiosiraceae	Thalassiosira	41	0	0	0	0	0	2.44	97.56	0	0	0.321	-0.530	0.398	0.106	0.190	-0.262	-0.128
ASV_1134	4	Chromista	Myzozoa	Dinophyceae	Gymnodiniales	Gymnodiniaceae	Lepidodinium	10	70	0	0	0	0	20	10	0	0	0.341	-0.562	0.421	0.111	0.200	-0.279	-0.137
ASV_1108	4	Chromista	Myzozoa	Dinophyceae	Syndiniales	Amoebophryaceae	Amoebophrya	12	75	0	0	0	0	0	0	25	0	0.318	-0.521	0.389	0.102	0.184	-0.261	-0.129
ASV_672	4	Chromista	Myzozoa	Dinophyceae	Dinophysiales	Dinophysiacae	Dinophysis	54	3.7	1.85	0	5.56	0	0	74.07	14.81	0	0.307	-0.516	0.395	0.112	0.192	-0.244	-0.112
ASV_835	4	Chromista	Myzozoa	Dinophyceae	Peridiniales	Protoperidiniaceae	Protoperidinium	20	65	0	10	0	5	0	10	0	10	0.267	-0.446	0.339	0.094	0.164	-0.214	-0.101
ASV_1039	4	Chromista	Cercozoa	Thecofilosea	Cryomonadida	Protaspidae	Protaspis	14	57.14	0	14.29	0	0	14.29	14.29	0	0	0.324	-0.538	0.407	0.111	0.196	-0.263	-0.126
ASV_922	4	Chromista	Ochrophyta	Bacillariophyceae	Thalassiosirales	Thalassiosiraceae	Thalassiosira	20	55	25	0	0	0	0	0	20	0	0.293	-0.502	0.390	0.116	0.194	-0.227	-0.097
ASV_971	4	Chromista	Myzozoa	Dinophyceae	NA	NA	NA	12	75	8.33	0	0	0	16.67	0	0	0	0.305	-0.530	0.417	0.128	0.210	-0.233	-0.095
ASV_789	4	Chromista	Cercozoa	Thecofilosea	NA	NA	NA	25	40	0	0	0	0	60	0	0	0	0.251	-0.438	0.345	0.107	0.174	-0.191	-0.077
ASV_557	4	Chromista	Haptophyta	Prymnesiophyceae	Prymnesiales	Prymnesiaceae	Pseudohaptolina	8	87.5	0	0	0	0	12.5	0	0	0	0.320	-0.553	0.433	0.131	0.217	-0.246	-0.103
ASV_901	4	Chromista	Myzozoa	Dinophyceae	Gymnodiniales	Gymnodiniaceae	Gyrodinium	20	0	5	5	15	15	40	0	20	0	0.379	-0.554	0.369	0.054	0.147	-0.352	-0.221
ASV_1245	4	Chromista	Cercozoa	Thecofilosea	Cryomonadida	Protaspidae	Protaspis	4	50	0	0	0	0	25	25	0	0	0.405	-0.597	0.401	0.063	0.163	-0.372	-0.230
ASV_1010	4	Chromista	Radiozoa	Polycystina	Nassellarida	Plagiocanthidae	Lithomelissa	8	0	0	25	25	0	12.5	37.5	0	0	0.401	-0.595	0.403	0.066	0.165	-0.366	-0.224
ASV_851	4	Chromista	Myzozoa	Dinophyceae	Peridiniales	Protoperidiniaceae	Protoperidinium	25	0	12	0	0	0	28	60	0	0	0.348	-0.516	0.350	0.058	0.143	-0.318	-0.194
ASV_691	4	Chromista	Oomycota	Peronosporae	NA	NA	NA	52	0	13.46	7.69	13.46	0	9.62	34.62	21.15	0	0.349	-0.519	0.352	0.058	0.144	-0.319	-0.195
ASV_833	4	Chromista	Myzozoa	Dinophyceae	Syndiniales	Amoebophryaceae	Amoebophrya	23	0	0	0	30.43	17.39	26.09	26.09	0	0	0.357	-0.532	0.362	0.061	0.149	-0.325	-0.198
ASV_766	4	Chromista	Myzozoa	Dinophyceae	NA	NA	NA	22	54.55	0	0	0	0	31.82	0	13.64	0	0.275	-0.410	0.279	0.047	0.115	-0.250	-0.152
ASV_629	4	Chromista	Ochrophyta	Bacillariophyceae	Thalassiosirales	Thalassiosiraceae	Thalassiosira	71	1.41	12.68	2.82	1.41	1.41	66.2	11.27	0	0	0.329	-0.491	0.334	0.057	0.138	-0.299	-0.181
ASV_562	4	Chromista	Ochrophyta	Bacillariophyceae	Thalassiosirales	Thalassiosiraceae	Thalassiosira	109	0	9.17	0.92	0	1.83	5.5	73.89	8.26	0.92	0.287	-0.430	0.294	0.051	0.122	-0.260	-0.157
ASV_972	4	Chromista	Cercozoa	NA	NA	NA	NA	14	50	21.43	0	0	0	0	0	28.57	0	0.347	-0.519	0.354	0.061	0.147	-0.315	-0.190
ASV_1362	4	Chromista	Myzozoa	Dinophyceae	Suessiales	Biecheleriaceae	Biecheleria	7	57.14	0	0	14.29	0	0	0	28.57	0	0.360	-0.574	0.419	0.100	0.192	-0.305	-0.162
ASV_848	4	Chromista	Myzozoa	Dinophyceae	Syndiniales	Amoebophryaceae	Amoebophrya	25	12	8	0	4	4	0	72	0	0	0.363	-0.578	0.420	0.099			

ASV_850	4	Chromista	Myzozoa	Dinophyceae	Peridinales	Protooperidiniaceae	Protooperidinium	25	0	0	0	4	0	4	92	0	0	0.347	-0.549	0.398	0.092	0.180	-0.296	-0.160
ASV_351	4	Chromista	Oomycota	Peronosporae	NA	NA	NA	417	0	4.32	0	18.94	2.16	0	48.92	24.7	0.96	0.254	-0.401	0.289	0.066	0.131	-0.218	-0.119
ASV_611	4	Chromista	Myzozoa	Dinophyceae	Peridinales	Peridiniaceae	Pentaparsodium	71	0	0	0	2.82	0	0	97.18	0	0	0.316	-0.498	0.359	0.082	0.162	-0.271	-0.148
ASV_1191	4	Chromista	Cercozoa	Thecofilosea	Cryomonadida	Protaspidae	Protaspis	8	50	0	0	12.5	0	0	25	0	12.5	0.368	-0.579	0.417	0.094	0.188	-0.316	-0.173
ASV_892	4	Chromista	Ciliophora	NA	NA	NA	NA	22	68.18	9.09	0	0	0	0	22.73	0	0	0.288	-0.447	0.317	0.067	0.140	-0.252	-0.142
ASV_1468	4	Chromista	Myzozoa	Dinophyceae	NA	NA	NA	6	33.33	0	0	0	0	66.67	0	0	0.376	-0.575	0.402	0.080	0.174	-0.333	-0.193	
ASV_1035	4	Chromista	Myzozoa	Dinophyceae	NA	NA	NA	14	0	14.29	0	0	0	0	85.71	0	0	0.382	-0.587	0.412	0.083	0.179	-0.337	-0.194
ASV_861	4	Chromista	Cercozoa	NA	NA	NA	NA	24	16.67	4.17	12.5	0	0	25	4.17	4.17	0.365	-0.452	0.238	-0.031	0.052	-0.388	-0.294	
ASV_921	4	Chromista	NA	NA	NA	NA	NA	16	0	62.5	0	0	0	0	12.5	25	0.386	-0.483	0.259	-0.027	0.061	-0.407	-0.305	
ASV_908	4	Chromista	Cercozoa	NA	NA	NA	NA	20	40	0	10	0	0	15	0	35	0.343	-0.438	0.244	-0.014	0.064	-0.355	-0.261	
ASV_952	4	Chromista	NA	NA	NA	NA	NA	18	0	5.56	11.11	0	5.56	66.67	0	11.11	0.400	-0.521	0.298	-0.007	0.085	-0.409	-0.295	
ASV_1008	4	Chromista	Myzozoa	Dinophyceae	Gymnodiniales	Gymnodiniaceae	Gyrodinium	15	13.33	13.33	0	26.67	0	0	6.67	0	40	0.406	-0.532	0.307	-0.004	0.090	-0.414	-0.298
ASV_670	4	Chromista	Myzozoa	Dinophyceae	NA	NA	NA	40	0	0	20	0	0	17.5	57.5	0	5	0.329	-0.455	0.283	0.021	0.099	-0.321	-0.217
ASV_853	4	Chromista	Myzozoa	NA	NA	NA	NA	25	48	0	0	0	0	0	8	44	0.312	-0.431	0.269	0.020	0.094	-0.304	-0.205	
ASV_819	4	Chromista	Myzozoa	Dinoflagellata <i>i.s.</i>	Dinoflagellata <i>i.s.</i>	Dinoflagellata <i>i.s.</i>	Duboscquella	27	7.41	25.93	0	14.81	0	14.81	14.81	11.11	11.11	0.362	-0.503	0.314	0.025	0.111	-0.351	-0.237
ASV_725	4	Chromista	Cercozoa	Thecofilosea	Cryomonadida	Protaspidae	Protaspis	28	17.86	17.86	32.14	0	3.57	14.29	0	3.57	10.71	0.350	-0.486	0.304	0.024	0.107	-0.340	-0.229
ASV_1129	4	Chromista	Cercozoa	Imbricatea	Thaumatomonadida	Esquamulidae	Esquamula	11	18.18	18.18	0	9.09	0	36.36	0	18.18	0	0.389	-0.533	0.327	0.019	0.111	-0.382	-0.262
ASV_993	4	Chromista	Cercozoa	Thecofilosea	Cryomonadida	Protaspidae	Protaspis	9	33.33	0	33.33	0	0	0	0	33.33	0.404	-0.555	0.342	0.021	0.117	-0.396	-0.271	
ASV_719	4	Chromista	Myzozoa	Dinophyceae	NA	NA	NA	40	20	0	0	25	0	27.5	2.5	12.5	12.5	0.321	-0.440	0.270	0.016	0.092	-0.315	-0.216
ASV_1068	4	Chromista	Myzozoa	Dinophyceae	NA	NA	NA	13	0	0	30.77	0	46.15	7.69	0	15.38	0	0.398	-0.544	0.332	0.018	0.112	-0.392	-0.270
ASV_889	4	Chromista	Ochrophyta	Bacillariophyceae	Surirellales	Entomoneidaceae	Entomoneis	20	35	5	0	0	0	5	25	0	30	0.327	-0.445	0.271	0.013	0.091	-0.323	-0.223
ASV_973	4	Chromista	NA	NA	NA	NA	NA	17	52.94	17.65	0	0	0	0	0	29.41	0.331	-0.451	0.275	0.014	0.092	-0.327	-0.226	
ASV_671	4	Chromista	Myzozoa	Dinophyceae	Syndiniales	Amoebophryaceae	Amoebophrya	59	0	3.39	15.25	1.69	0	45.76	11.86	16.95	5.08	0.330	-0.441	0.263	0.006	0.083	-0.330	-0.232
ASV_875	4	Chromista	Myzozoa	Dinophyceae	Gymnodiniales	Kareniaceae	Karlodinium	19	5.26	15.79	21.05	0	5.26	21.05	0	10.53	21.05	0.394	-0.526	0.312	0.006	0.098	-0.396	-0.279
ASV_836	4	Chromista	Oomycota	Peronosporae	NA	NA	NA	26	0	15.38	11.54	0	19.23	53.85	0	0	0	0.360	-0.484	0.291	0.009	0.094	-0.358	-0.250
ASV_1259	4	Chromista	Haptophyta	Prymnesiophyceae	Prymnesiales	Prymnesiaceae	Pseudohaptolina	9	44.44	0	0	0	0	0	0	55.56	0.373	-0.503	0.302	0.010	0.098	-0.372	-0.259	
ASV_641	4	Chromista	Ochrophyta	Pelagophyceae	Pelagomonadales	Pelagomonadaceae	Aureococcus	69	0	21.74	0	0	7.25	4.35	47.83	18.84	0	0.311	-0.420	0.253	0.009	0.083	-0.309	-0.215
ASV_623	4	Chromista	Myzozoa	Dinophyceae	Gymnodiniales	Kareniaceae	Karlodinium	74	0	0	0	6.76	0	4.05	60.81	13.51	14.86	0.335	-0.450	0.269	0.007	0.086	-0.335	-0.235
ASV_1067	4	Chromista	Ochrophyta	NA	NA	NA	NA	13	0	0	0	15.38	0	23.08	15.38	46.15	0	0.405	-0.575	0.369	0.040	0.138	-0.387	-0.254
ASV_969	4	Chromista	Myzozoa	Dinophyceae	NA	NA	NA	17	11.76	29.41	17.65	0	17.65	0	0	23.53	0	0.361	-0.515	0.333	0.039	0.126	-0.342	-0.222
ASV_847	4	Chromista	Myzozoa	Dinophyceae	Gymnodiniales	Gymnodiniaceae	Gyrodinium	25	4	0	8	8	0	44	0	28	8	0.371	-0.522	0.332	0.032	0.121	-0.357	-0.236
ASV_1042	4	Chromista	Cercozoa	Imbricatea	NA	NA	NA	13	38.46	0	0	0	0	0	30.77	30.77	0.380	-0.533	0.338	0.032	0.123	-0.365	-0.243	
ASV_1329	4	Chromista	NA	NA	NA	NA	NA	8	0	0	0	0	0	100	0	0	0	0.390	-0.550	0.351	0.035	0.129	-0.374	-0.247
ASV_645	4	Metazoa	Arthropoda	Copepoda	Calanoida	Calanidae	NA	61	13.11	0	6.56	8.2	0	44.26	27.87	0	0	0.278	-0.458	0.344	0.091	0.164	-0.227	-0.111
ASV_468	4	Metazoa	Arthropoda	Copepoda	Calanoida	Calanidae	NA	182	10.99	7.69	27.47	12.64	5.49	14.84	10.44	7.14	3.3	0.265	-0.434	0.324	0.085	0.153	-0.218	-0.109
ASV_822	4	Metazoa	Arthropoda	Copepoda	Calanoida	Calanidae	NA	27	44.44	3.7	0	0	0	33.33	18.52	0	0	0.279	-0.469	0.358	0.100	0.174	-0.223	-0.103
ASV_639	4	Metazoa	Arthropoda	Copepoda	Calanoida	Calanidae	NA	49	28.57	6.12	28.57	8.16	8.16	16.33	4.08	0	0	0.270	-0.452	0.344	0.096	0.167	-0.217	-0.101
ASV_849	4	Metazoa	Arthropoda	Copepoda	Calanoida	Calanidae	NA	25	60	0	8	20	0	0	0	12	0	0.291	-0.484	0.367	0.101	0.177	-0.234	-0.111
ASV_35	4	Metazoa	Arthropoda	Copepoda	Calanoida	Calanidae	NA	13369	13.92	3.81	17.56	7.86	0.57	47.16	5.7	2.72	0.69	0.281	-0.467	0.353	0.096	0.170	-0.227	-0.109
ASV_288	4	Metazoa	Arthropoda	Copepoda	Calanoida	Calanidae	NA	566	8.45	5.76	25.54	9.35	1.8	21.76	14.03	12.05	1.26	0.237	-0.401	0.309	0.089	0.152	-0.187	-0.084
ASV_525	4	Metazoa	Arthropoda	Copepoda	Calanoida	Calanidae	NA	123	2.44	2.44	24.39	23.58	9.76	12.2	5.69	12.2	7.32	0.306	-0.447	0.297	0.043	0.118	-0.284	-0.178
ASV_473	4	Metazoa	Arthropoda	Copepoda	Calanoida	Calanidae	NA	164	4.27	6.1	20.73	11.59	6.71	20.12	18.9	4.88	6.71	0.318	-0.465	0.309	0.045	0.123	-0.295	-0.185
ASV_690	4	Metazoa	Arthropoda	Copepoda	Calanoida	Calanidae	NA	48	0	0	14.58	20.83	14.58	12.5	25	6.25	6.25	0.329	-0.482	0.321	0.047	0.128	-0.305	-0.191
ASV_820	4	Metazoa	Arthropoda	Copepoda	Calanoida	Calanidae	NA	25	16	0	24	8	0	16	0	8	28	0.332	-0.486	0.324	0.048	0.129	-0.307	-0.192
ASV_810	4	Metazoa	Arthropoda	Copepoda	Calanoida	Calanidae	NA	24	4.17	0	20	0	37.5	8.33	0	0	0	0.344	-0.502	0.332	0.047	0.131	-0.320	-0.202
ASV_801	4	Metazoa	Arthropoda	Copepoda	Calanoida	Calanidae	NA	25	0	8	58	40	0	24	0	0	0	0.337	-0.496	0.332	0.051	0.133	-0.311	-0.194
ASV_358	4	Metazoa	Arthropoda	Copepoda	Calanoida	Calanidae	NA	359	3.9	9.19	15.32	8.08	8.36	44.85	4.74	3.62	1.95	0.299	-0.439	0.294	0.045	0.118	-0.276	-0.172
ASV_634	4	Metazoa	Arthropoda	Copepoda	Calanoida	Calanidae	NA	57	0	0	14.04	21.05	14.04	35.09	5.26	10.53	0	0.310	-0.457	0.306	0.047	0.123	-0.286	-0.178
ASV_297	4	Metazoa	Arthropoda	Copepoda	Calanoida	Calanidae	NA	559	5.55	7.51	24.87	10.38	5.55	18.78	10.55	13.06	3.76	0.311	-0.458	0.307	0.048	0.124	-0.286	-0.178
ASV_914	4	Metazoa	Arthropoda	Copepoda	Calanoida	Calanidae	NA	16	0	0	62.5	12.5	12.5	6.25	0	0	6.25	0.366	-0.538	0.361	0.056	0.146	-0.337	-0.209
ASV_874	4	Metazoa	Arthropoda	Copepoda	Calanoida	Calanidae	NA	12	0	0	0	0	0	91.67	8.33	0	0	0.359	-0.529	0.355	0.055	0.143	-0.331	-0.205
ASV_939	4	Metazoa	Arthropoda	Copepoda	Calanoida	Calanidae	NA	14	0	0	7.14	0	0	71.43	0	21.43	0	0.365	-0.539	0.363	0.057	0.147	-0.336	-0.208
ASV_872	4	Metazoa	Arthropoda	Copepoda	Calanoida	Calanidae	NA	22	0	0	18.18	4.55	45.45	31.82	0	0	0	0.351	-0.517	0.348	0.055	0.141	-0.322	-0.200
ASV_413	4	Metazoa	Arthropoda	Copepoda	Calanoida	Calanidae	NA	249	6.02	6.43	27.31	7.63	14.06	16.47	11.65	6.43	4.02	0.316	-0.467	0.315	0.051	0.128	-0.289	-0.178
ASV_103	4	Metazoa	Arthropoda	Copepoda	Calanoida	Calanidae	NA	3695	6.66	8.12	23.25	10.37	9.07	21.08	9.99	7.01	4.47	0.372	-0.552	0.374	0.061	0.153	-0.341	-0.209
ASV_449	4	Metazoa	Arthropoda	Copepoda	Calanoida	Calanidae	NA	219	8.22	14.61	16.89	7.31	7.31	21.92	5.48	12.79	5.48	0.287	-0.426	0.288	0.047	0.118	-0.262	-0.161
ASV_834	4	Metazoa	Arthropoda	Copepoda	Calanoida	Calanidae	NA	20	0	20	0	10	25	45	0	0	0	0.355	-0.529	0.360	0.061	0.148	-0.	

ASV_684	4	Metazoa	Arthropoda	Copepoda	Calanoida	Calanidae	NA	36	13.89	0	22.22	30.56	0	16.67	0	13.89	2.78	0.306	-0.484	0.350	0.080	0.158	-0.262	-0.143	
ASV_1197	4	Metazoa	Arthropoda	Copepoda	Calanoida	Calanidae	NA	10	40	0	10	0	50	0	0	0	0	0.351	-0.533	0.370	0.070	0.158	-0.313	-0.184	
ASV_133	4	Metazoa	Arthropoda	Copepoda	Calanoida	Calanidae	NA	2336	6.76	9.72	24.74	9.29	7.83	21.06	8.05	7.62	4.92	0.340	-0.516	0.358	0.068	0.153	-0.304	-0.179	
ASV_496	4	Metazoa	Arthropoda	Copepoda	Calanoida	Calanidae	NA	138	5.8	13.04	13.77	1.45	1.45	41.3	17.39	4.35	1.45	0.290	-0.436	0.299	0.053	0.125	-0.262	-0.157	
ASV_949	4	Metazoa	Arthropoda	Copepoda	Calanoida	Calanidae	NA	10	0	0	10	60	0	30	0	0	0	0.370	-0.558	0.384	0.069	0.161	-0.333	-0.199	
ASV_286	4	Metazoa	Arthropoda	Copepoda	Calanoida	Calanidae	NA	543	8.47	9.02	19.52	9.94	8.29	21.36	7.73	11.23	4.42	0.317	-0.493	0.351	0.075	0.155	-0.276	-0.155	
ASV_800	4	Metazoa	Arthropoda	Copepoda	Calanoida	Calanidae	NA	29	17.24	0	0	6.9	0	37.93	24.14	3.45	10.34	0.308	-0.478	0.339	0.071	0.149	-0.269	-0.152	
ASV_269	4	Metazoa	Arthropoda	Copepoda	Calanoida	Calanidae	NA	607	5.27	7.25	30.64	10.05	7.25	20.59	10.87	5.44	2.64	0.296	-0.453	0.316	0.062	0.136	-0.263	-0.153	
ASV_704	4	Metazoa	Arthropoda	Copepoda	Calanoida	Calanidae	NA	46	6.52	0	28.26	4.35	0	0	60.87	0	0	0.301	-0.465	0.328	0.068	0.144	-0.265	-0.151	
ASV_1	4	Metazoa	Arthropoda	Copepoda	Calanoida	Calanidae	NA	1E+07	7.58	8.64	22.2	9.5	9.04	21.19	9.25	7.65	4.96	0.350	-0.538	0.378	0.077	0.164	-0.309	-0.178	
ASV_456	4	Metazoa	Arthropoda	Copepoda	Calanoida	Calanidae	NA	189	2.12	13.23	26.46	15.34	5.29	14.81	7.41	11.64	3.7	0.315	-0.435	0.270	0.019	0.094	-0.308	-0.209	
ASV_553	4	Metazoa	Arthropoda	Copepoda	Calanoida	Calanidae	NA	77	0	15.58	29.87	0	11.69	14.29	10.39	18.18	0	0.290	-0.401	0.249	0.018	0.087	-0.283	-0.192	
ASV_681	4	Metazoa	Arthropoda	Copepoda	Calanoida	Calanidae	NA	38	0	21.05	15.79	10.53	0	26.32	0	0	26.32	0.322	-0.441	0.271	0.017	0.093	-0.315	-0.216	
ASV_366	4	Metazoa	Arthropoda	Copepoda	Calanoida	Calanidae	NA	280	0	7.5	36.79	6.43	6.07	18.93	3.21	11.43	9.64	0.329	-0.437	0.258	0.003	0.080	-0.330	-0.234	
ASV_203	4	Metazoa	Arthropoda	Copepoda	Calanoida	Calanidae	NA	1253	3.91	6.23	34.56	9.5	5.51	18.2	6.94	7.98	7.18	0.320	-0.432	0.260	0.010	0.085	-0.318	-0.221	
ASV_460	4	Metazoa	Arthropoda	Copepoda	Calanoida	NA	NA	204	1.96	9.8	12.25	20.59	7.35	10.29	13.24	15.2	9.31	0.314	-0.422	0.252	0.007	0.081	-0.314	-0.220	
ASV_651	4	Metazoa	Arthropoda	Copepoda	Calanoida	Calanidae	NA	54	0	7.41	51.85	14.81	5.56	7.41	7.41	0	5.56	0.313	-0.451	0.294	0.037	0.113	-0.295	-0.190	
ASV_818	4	Metazoa	Arthropoda	Copepoda	Calanoida	Calanidae	NA	25	0	16	0	36	16	4	0	8	20	0.356	-0.511	0.332	0.041	0.127	-0.336	-0.217	
ASV_682	4	Metazoa	Arthropoda	Copepoda	Calanoida	Calanidae	NA	55	0	0	30.91	0	16.36	5.45	20	27.27	0	0.311	-0.440	0.281	0.030	0.104	-0.297	-0.195	
ASV_794	4	Metazoa	Arthropoda	Copepoda	Calanoida	Calanidae	NA	30	0	0	0	0	6.67	36.67	20	36.67	0	0.340	-0.483	0.311	0.035	0.117	-0.323	-0.211	
ASV_568	4	Metazoa	Arthropoda	Copepoda	Calanoida	Calanidae	NA	101	0	1.98	48.51	4.95	8.91	29.7	0	5.94	0	0.292	-0.408	0.257	0.022	0.092	-0.282	-0.189	
ASV_609	4	Metazoa	Cnidaria	Hydrozoa	Trachymedusae	Rhopalonematidae	NA	33	0	0	63.64	0	0	33.33	3.03	0	0	0.327	-0.460	0.293	0.029	0.107	-0.314	-0.207	
ASV_302	4	NA	NA	NA	NA	NA	NA	589	0	2.89	10.19	2.04	4.24	59.76	0	15.11	5.77	0.288	-0.182	-0.061	-0.200	-0.150	-0.410	-0.404	
ASV_692	4	NA	NA	NA	NA	NA	NA	52	0	3.85	3.85	3.85	0	67.31	0	7.69	13.46	0.355	-0.358	0.115	-0.112	-0.039	-0.426	-0.366	
ASV_758	4	NA	NA	NA	NA	NA	NA	32	78.12	0	3.12	0	0	18.75	0	0	0	0.223	-0.458	0.406	0.165	0.231	-0.127	0.001	
ASV_772	4	NA	NA	NA	NA	NA	NA	32	34.38	6.25	0	0	0	6.25	0	53.12	0	0.266	-0.470	0.375	0.120	0.192	-0.198	-0.074	
ASV_1307	4	NA	NA	NA	NA	NA	NA	8	25	12.5	0	0	0	0	0	50	12.5	0.389	-0.576	0.390	0.063	0.159	-0.356	-0.219	
ASV_1221	4	NA	NA	NA	NA	NA	NA	10	0	0	0	0	0	100	0	0	0	0.375	-0.542	0.356	0.048	0.139	-0.351	-0.224	
ASV_1316	4	NA	NA	NA	NA	NA	NA	8	25	0	0	0	0	12.5	0	62.5	0	0.394	-0.551	0.348	0.032	0.126	-0.380	-0.253	
ASV_1163	4	NA	NA	NA	NA	NA	NA	11	0	0	0	0	0	100	0	0	0	0.377	-0.526	0.330	0.028	0.118	-0.365	-0.245	
ASV_654	4	Plantae	Chlorophyta	Mamiellophyceae	Dolichomastigales	Dolichomastigaceae	Crustomastix	60	8.33	36.67	1.67	0	3.33	15	0	0	35	0.307	-0.176	-0.090	-0.230	-0.178	-0.447	-0.446	
ASV_955	4	Plantae	Chlorophyta	NA	NA	NA	NA	13	23.08	0	15.38	0	0	15.38	0	0	46.15	0.421	-0.507	0.254	-0.050	0.044	-0.456	-0.353	
ASV_795	4	Plantae	Chlorophyta	NA	NA	NA	NA	16	0	0	0	0	0	0	0	25	75	0.422	-0.446	0.166	-0.112	-0.024	-0.493	-0.414	
ASV_924	4	Plantae	Chlorophyta	Pyramimonadophyceae	NA	NA	NA	20	0	10	5	0	0	5	0	0	80	0.434	-0.375	0.052	-0.199	-0.115	-0.557	-0.508	
ASV_923	4	Plantae	Chlorophyta	NA	NA	NA	NA	19	73.68	0	0	0	0	10.53	0	15.79	0	0.244	-0.500	0.443	0.180	0.251	-0.140	0.000	
ASV_967	4	Plantae	Chlorophyta	Mamiellophyceae	Dolichomastigales	Dolichomastigaceae	Dolichomastix	13	46.15	15.38	0	0	0	0	0	7.69	30.77	0	0.339	-0.531	0.380	0.083	0.169	-0.294	-0.163
ASV_940	4	Plantae	Chlorophyta	NA	NA	NA	NA	19	0	5.26	36.84	0	0	36.84	0	0	21.05	0.399	-0.507	0.280	-0.019	0.072	-0.415	-0.307	
ASV_540	4	Protozoa	Protozoa i.s.	Ebriophyceae	Ebriales	Ebriaceae	Ebria	111	1.8	10.81	25.23	0	0	11.71	0.9	18.92	30.63	0.340	-0.225	-0.058	-0.226	-0.165	-0.478	-0.466	
ASV_904	4	Protozoa	Protozoa	NA	NA	NA	NA	18	27.78	11.11	0	0	0	0	0	5.56	55.56	0.377	-0.428	0.191	-0.070	0.012	-0.423	-0.340	
ASV_887	4	Protozoa	Choanozoa	Choanoflagellata	Acanthoecida	Acanthoecidae	NA	19	5.26	0	0	15.79	0	0	0	0	78.95	0.403	-0.408	0.133	-0.125	-0.042	-0.481	-0.413	
ASV_644	4	Protozoa	Protozoa i.s.	Ebriophyceae	Ebriales	Ebriaceae	Ebria	68	1.47	7.35	0	4.41	16.18	7.35	23.53	16.18	23.53	0.352	-0.346	0.102	-0.119	-0.047	-0.426	-0.370	
ASV_708	4	Protozoa	Choanozoa	Choanoflagellata	Acanthoecida	Acanthoecidae	NA	19	100	0	0	0	0	0	0	0	0	0.188	-0.469	0.461	0.223	0.285	-0.058	0.082	
ASV_774	4	Protozoa	Choanozoa	Choanoflagellata	Acanthoecida	Acanthoecidae	Calliacantha	24	83.33	0	4.17	0	0	12.5	0	0	0	0.224	-0.449	0.392	0.155	0.220	-0.135	-0.010	
ASV_817	4	Protozoa	Protozoa i.s.	Ebriophyceae	Ebriales	Ebriaceae	Ebria	27	0	0	0	74.07	25.93	0	0	0	0	0.343	-0.532	0.377	0.079	0.166	-0.300	-0.170	

Notes: Relative read abundance across the different ice floes is indicated with yellow bars. Negative correlations are indicated in blue and positive correlations indicated in red.

Species-level assignments are not considered for the entire 18S dataset due to the conservative nature of the gene. Genus-level assignments are not considered for metazoans.

i.s. = *Incertae sedis*

Chapter 4

Surveying marine biodiversity using eDNA metabarcoding of seawater and sediment in a high Arctic fjord during the polar night (Kongsfjorden, Svalbard)

Ayla Murray^{1,2}, Adria Antich³, Annkathrin Dischereit^{1,2}, Luisa Düsedau¹, Clara J.M. Hoppe¹, Charlotte Havermans^{1,2}

1. Alfred Wegener Institute Helmholtz Centre for Polar and Marine Research, Am Handelshafen 12, 27570 Bremerhaven, Germany
2. Marine Zoologie, Fachbereich 2, University of Bremen, Bremen, Germany
3. NORCE Climate and Environment, NORCE Norwegian Research Centre AS and Bjerknes Centre for Climate Research, Bergen, Norway

Manuscript submitted in Marine Environmental Research (November 2024)

Abstract

Arctic fjords are highly productive components of marine ecosystems, hosting a high biodiversity of taxa, but are threatened by ongoing climate change. Kongsfjorden, a fjord in northwest Svalbard, is shifting from Arctic to Atlantic conditions with warming. This is directly impacting the marine community in the fjord, with changes in species composition and distribution already underway. The polar night is a period of challenging conditions and is historically understudied, and thus our understanding of the community composition and distributions of major eukaryotic groups is particularly limited at this time of year. Here we provide a comprehensive snapshot of eukaryotic biodiversity present in Kongsfjorden during the polar night through the use of environmental DNA (eDNA) metabarcoding of the mitochondrial cytochrome c oxidase subunit 1 gene (COI). Furthermore, we aimed to establish a baseline dataset for gelatinous zooplankton (GZP) during this period by combining eDNA with net sampling. Lastly, we tested for the impact of PCR-inhibition on the recovery of eDNA from turbid fjord waters. We successfully detected a large component of the pelagic community known to inhabit Kongsfjorden, as well as benthic and hyperbenthic species typical for the area. We detected taxa from major functional groups including macroalgae, phytoplankton, zooplankton, large vertebrates and benthic taxa. Furthermore, we recovered a richer community than previously detected with traditional methods alone. Our study provides a baseline for future polar night eDNA-based biodiversity monitoring in Kongsfjorden, a time of year that remains understudied in this highly-studied area of the Arctic.

Key words

Gelatinous zooplankton, environmental DNA, primary producers, metazoans, COI, PCR-inhibitors, vertebrates

1. Introduction

Effective biodiversity monitoring is crucial to understanding ecosystem health and detecting the impacts of climate change on sensitive marine ecosystems. Detailed data on species distribution and abundance in relation to their environment is necessary for detecting shifts in biodiversity and therefore making informed management and mitigation decisions. Biodiversity assessments are often highly dependent on morphological identification and while this remains a valuable tool, it comes with drawbacks and limitations that mean sample collection can outpace sample processing (Porter and Hajibabaei, 2018). For example, taxonomic identification requires expert knowledge which can be scarce and difficult to access (Paknia et al., 2015). Additionally, it is crucial that specimens are well-preserved after sampling and have visually identifiable characteristics. However, collecting organisms for such identification is often invasive, impacting fragile organisms, and can overlook difficult to detect life stages such as larvae. All of these factors can reduce the cost and time-effectiveness (Pawlowski et al., 2022), and in turn limit their usefulness for early detection of the biological impacts of rapidly changing environmental conditions in areas such as the Arctic. Advances in molecular (meta)barcoding can complement information gained through morphological work by circumventing some of these limitations, as well as providing the opportunity to increase sampling coverage over space and time while reducing costs per sample (Porter and Hajibabaei, 2018). One such tool that has become a popular tool in biodiversity monitoring in the last decade is environmental DNA (eDNA) metabarcoding, which relies on the isolation of DNA from environmental samples such as water or sediment. It is composed of DNA shed by organisms (e.g., metabolic waste products, shed cells, gametes and mucus) as well as whole organisms themselves in the case of small taxa (e.g., diatoms and microscopic meiofauna). After isolation, eDNA can be sequenced using Next Generation Sequencing (NGS) technology and subsequently compared to reference databases, producing taxon data. It is increasingly being implemented in remote systems such as the Arctic, including in coastal waters (Lacoursière-Roussel et al., 2018; Leduc et al., 2019), surveying pelagic and deep-sea metazoans in the open ocean (Murray et al., 2024) and benthic communities in fjords (van den Heuvel-Greve et al., 2021; Willassen et al., 2022).

Fjord systems are highly productive and diverse components of the Arctic marine realm and thus are important habitats to a diverse and unique spectrum of species. As transition zones between land, glaciers and ocean, Arctic Fjords are particularly vulnerable to the impacts of anthropogenic climate change (reviewed in Bianchi et al., 2020). The Arctic is a hotspot for climate change, with warming occurring up to four times faster than the global average caused by a phenomenon known as Arctic Amplification (Cohen et al., 2020; Isaksen et al., 2022; Rantanen et al., 2022).

The Svalbard Archipelago is situated on the eastern side of Fram Strait in the European Arctic and its western fjords are particularly vulnerable to Atlantification, which describes the process of physical conditions, as well as biological communities, becoming more like those in the North Atlantic (Ingvaldsen et al., 2023; Polyakov et al., 2023, 2020). One of the major drivers is the influence of the West Spitsbergen Current (WSC)(Cottier et al., 2005). The WSC, which transports warm and saline waters of Atlantic origin northward through Fram Strait and into the Arctic basin, has continuously warmed over the last decades, resulting in Fram Strait and western Svalbard becoming increasingly Atlantified (Ingvaldsen et al., 2023; Polyakov et al., 2023). Kongsfjorden is an open fjord located on the north-west coast of Svalbard, and is at the interface between high-Arctic and sub-Arctic marine biogeographic regions (Bischof et al., 2019). Furthermore, the deep Kongsfjordrenna channel and the lack of a sill at the mouth of the fjord allow the advection of coastal currents (i.e., the WSC) on the adjacent shelf (Svendsen et al., 2002). Here, Arctic and Atlantic water masses converge to form transformed Atlantic water (TAW), which is regularly transported into the fjord (Cottier et al., 2005). These advection events predominantly occur in the summer but can also happen in the winter (De Rovere et al., 2022). The impacts of warming are evident year-round in the region, but are particularly strong in the winter period (Francis and Vavrus, 2012; Pithan and Mauritsen, 2014). Higher temperatures during the polar night and winter prevent water from cooling to freezing temperature, resulting in less sea ice formation in the coldest months. Indeed, land-fast ice has rarely occurred in Kongsfjorden since the abnormally warm winter of 2005/06 (Cottier et al., 2019, 2007; Gerland et al., 2020).

The hydrographic conditions in Kongsfjorden have significant impacts on the local ecosystem, influencing the biomass and community composition of zooplankton (Basedow et al., 2004; Gluchowska et al., 2016), primary production (Dragańska-Deja et al., 2024; Hegseth et al., 2019), and larger vertebrates such as fish and marine mammals (de Vincenzi et al., 2019; Marques et al., 2023). The influence of both Atlantic and Arctic water masses, means that Kongsfjorden harbours communities that are a combination of arctic, arctic-boreal and boreal taxa. In years when higher levels of Atlantic water masses are advected into the fjord, for example, the zooplankton community is likely to be dominated by species of Atlantic-origin, and the opposite is true in years where Arctic water masses prevail (Dalpadado et al., 2016; Gluchowska et al., 2016). Major changes in abundance and community composition have been already observed or are predicted to occur in many key functional groups including macroalgae (Düsedau et al., 2024), crustaceans (Hop et al., 2019; Węśławski et al., 2018), and fish (Gorska et al., 2023). Another group posited to undergo major shifts due to changing conditions in the Arctic is gelatinous zooplankton (GZP), defined here as the pelagic life stages of cnidarians, tunicates and ctenophores. They have remained understudied until recent

years, despite having major roles throughout pelagic food-webs as filter feeders (e.g., Stukel et al., 2024), predators (e.g., Hansson et al., 2005; J. E. Purcell et al., 2010) or as prey (Dischereit et al., 2024a, 2024b). Furthermore, species distribution models have predicted that the distribution of many GZP species is likely to increase significantly poleward as a consequence of climate change, while some others will experience range contractions (Pantiukhin et al., 2024). There remain large gaps in baseline data regarding the distribution and community composition of these groups during the polar night, however, the extreme low light and temperature conditions may represent a bottleneck for range expansions of temperate species.

One of the most characteristic features of high-latitude systems such as Kongsfjorden is their strong seasonality. The Arctic “polar night” occurs during the winter season and is typically characterised by the sun remaining below the horizon for 24 hours per day and consequentially low (although not devoid of) incoming light levels. Thus, the polar night has traditionally been considered as a period of dormancy in the Arctic due to low light and food availability. It was assumed that biological activity dropped to negligible levels and thus not considered as important to research compared to other, highly productive periods (Berge et al., 2020b). Nevertheless, other physical processes occur during this period including increased vertical mixing in the water column and cooling of the surface layers. The coldest surface temperatures typically occur after the polar night in March and April, where freezing and sea-ice formation is the most likely to occur (Cottier and Porter, 2020). Due to these aforementioned physical properties, sampling during the polar night is also constrained by technical and logistical challenges and this season therefore remains a relatively understudied aspect of the Arctic ecosystem (Berge et al., 2020b). As a result, our understanding of marine Arctic biodiversity and community composition is biased towards the polar day period. A growing body of research in the last decade has found that the polar night is not only highly productive across trophic levels, but also crucial to our understanding of Arctic ecology and understanding the ongoing impacts of climate change (Berge et al., 2015a, 2015b; Grenvald et al., 2016; Last et al., 2016).

Another key feature of Kongsfjorden and other Arctic fjords is that they can have high levels of suspended organic and inorganic particles present in the water column as a result of glacier discharge, river runoff and snow and permafrost melt. Discharge from the tidal glaciers at the head of the Kongsfjorden increases water turbidity and sedimentation, impacting composition and biomass of benthic and pelagic communities (Hop et al., 2023; Włodarska-Kowalczyk et al., 2019). These suspended particles can also impact the efficacy of eDNA capture. Fragments of eDNA can bind to suspended particulate matter and result in increased levels of DNA in a sample and even help reduce DNA degradation (Alvarez et al., 1998). However,

turbid waters typical contain higher levels of PCR-inhibitors such as humic acids, which are extracted from filters along with the target DNA. The presence of these inhibitors can significantly hamper PCR amplification success and therefore eDNA sequencing results from water samples (Albers et al., 2013). The highest rates of melting are during the summer months, but particulate matter is also present during the polar night and the overall input is increasing in Arctic fjords with winter warming.

Kongsfjorden is the location of multiple long-term observation systems (Berge et al., 2020b) with the research station based in Ny-Ålesund and as a result, it is one of the best studied fjords in the Arctic. Despite intensive monitoring in the fjord over the last decades, however, studies on polar night biology are still low in number. Thus, our main objectives were to implement eDNA metabarcoding to (i) conduct a survey of the eukaryotic community present during the polar night, (ii) combine eDNA with net-caught specimens to determine the gelatinous zooplankton community in detail and (iii) test for the impact if PCR-inhibitors on eDNA diversity recovered from turbid water of an Arctic glacial fjord.

2. Materials and Methods

2.1 Sampling Area

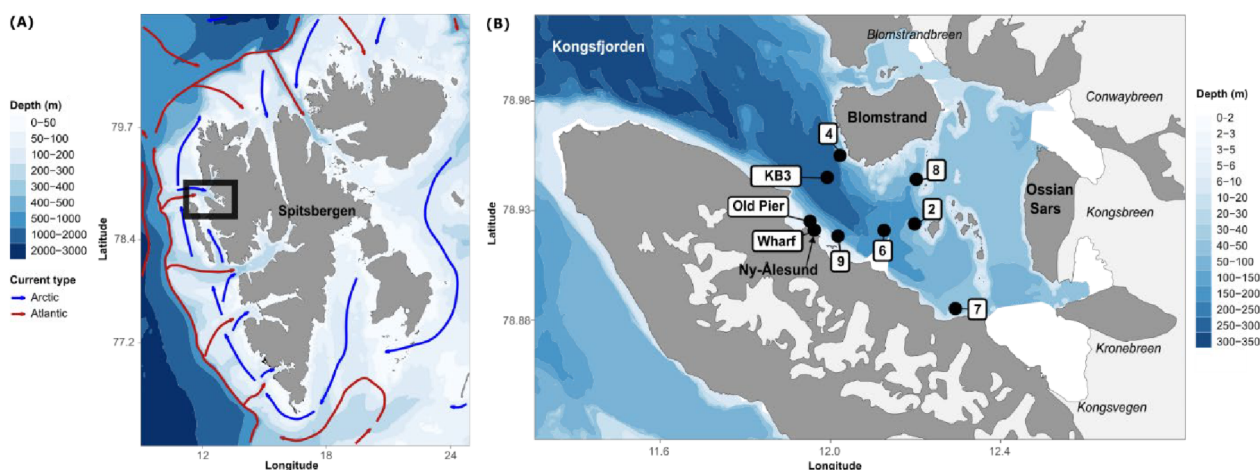


Figure 1. Sampling Location. (A) Map of the Svalbard archipelago with the major Arctic and Atlantic currents. Sampling area is indicated by black polygon. (B) Map of sampling stations in Kongsfjorden. Black dots indicate the approximate location of the individual stations. Glacier names are indicated in italic text. Maps were produced using PlotSvalbard package in R: <https://github.com/MikkoVihtakari/PlotSvalbard>.

Sampling occurred in vicinity of the German-French Research station AWIPEV, located in Ny-Ålesund in Kongsfjorden, Svalbard, between January 20th – February 4th 2022. Kongsfjorden is on the western side of the island of Spitsbergen and is approximately 20 km long, 4 - 10 km wide and is located at approximately 79°N. There are five major tidal glaciers which terminate in the inner part of the fjord (Fig. 1). The polar night in Kongsfjorden takes place between 25th October and 17th of February (Berge et al., 2015b).

2.2. Sampling

All samples were collected aboard the working vessel *Teisten* or from the pontoon attached to the wharf inside the harbour of Ny -Ålesund. All stations are located in the middle part of the fjord as sampling the outer and inner parts were limited by weather and ice conditions (Table 1 and Figure 1).

Table 1. Location and physical properties of sampling stations.

Station	Latitude	Longitude	Date Sampled	Distance from Land (km)	Water sample depths (m)	Sediment sample depth (m)
St. 2	78.93365	12.173167	20.01.2022	0.57	1, 10, 20, 30, 50, 70, AB	79
St. Old Pier	78.932433	11.924717	27.01.2022	0.37	1, 10, 20, AB	36
St. 4	78.963183	11.9878	27.01.2022	0.44	1, 10, 20, 30, 50, AB	65
St. KB3	78.952833	11.960017	28.01.2022	1.56	1, 10, 20, 30, 50, 70, 100, 150, 200, 250, AB	NA
St. 6	78.929983	12.10135	31.01.2022	1.74	1, 10, 20, 30, 50, 70, 100, AB	112
St. 7	78.895783	12.279233	31.01.2022	0.45	1, 10, AB	20
St. 8	78.954	12.172233	01.02.2022	0.50	1, 10, 20, 30, 50, AB	72
St 9	78.9263	11.992967	01.02.2022	0.50	1, 10, 20, 30, AB	70
St. Wharf_1	78.928533	11.936272	29.01.2022	0.03	1	NA
St. Wharf_2			02.02.2022			
St. Wharf_3			04.02.2022			

Notes: AB refers to "Above Bottom". This sample was taken within approximately 5 – 10 m of the sea floor. Longitude and latitude are measured in decimal degrees. NA = no sample available.

2.2.1 Environmental data

Hydrographic profiles were conducted at each station (except the wharf) immediately before collecting water samples. Salinity and temperature data were measured using a MiniSTD conductivity-temperature-depth (CTD, SD-204, SAIV A/S, Bergen, Norway) sensor mounted in on a winch cable from the ship. Density plots were produced using the R package PlotSvalbard (Vihtakari, 2020) and the command *ts_plot*. The dominant water masses affecting KF are defined here as: Atlantic Water (AW, $>3.0^{\circ}$ and > 34.65 psu), Arctic Water (ArW $-1.5^{\circ}\text{C} - 1.0^{\circ}\text{C}$, $34.30 - 34.80$ psu), Intermediate Water (IW, $>1.0^{\circ}$ and $> 34.0 - 34.65$ psu) and Transformed Atlantic Water (TAW, $>1.0^{\circ}\text{C} - 3.0^{\circ}\text{C}$ and > 34.65 psu) (Cottier et al., 2005). The distance of each station from land was calculated based on geodesic distances using the *dist2land()* function.

2.2.2 Gelatinous zooplankton net sampling

A WP3 net with a mesh size of 500µm was deployed vertically from the working vessel at each station following completion of water eDNA sampling. The hand-net specimens were all caught in the inner harbour at from the wharf. All specimens were identified to the highest possible taxonomic level in the onsite lab using identification guides (e.g., Bouillon et al., 2006; Licandro et al., 2017; Licandro & Lindsay, 2017). Tissue for DNA extraction was aliquoted and either extracted immediately at the on-site lab or frozen at -80°C for extraction at a later date in the home lab.

2.2.3 Environmental DNA sampling

Seawater for eDNA metabarcoding was collected using Niskin bottles (Hydrobios, Kiel), which were either handheld (Wharf station) or deployed on a winch cable aboard the research vessel R/V Tiesten (all other stations). A total of 6L of water per sample was collected at each depth before being decanted into sterilized Kautex cannisters and stored below 0°C until filtration (within a maximum of 6 hours). Water was filtered across 0.22 µm Sterivex-GP filters (Merck Millipore) using a peristaltic pump and Masterflex tubing following Murray et al., (2024). Each 6L sample was split across three filters (up to 2L on each filter) and the tubing was changed in between each sample. All sampling equipment and laboratory benches were sterilized with a solution of 1:10 bleach and milliQ wash, followed by a milliQ wash and dried using 70% ethanol. A field blank was collected for each station by filtering 1L of milliQ water across a filter and was subsequently treated identically to all other samples. Filters were then stored at -80°C for downstream processing.

Sediment for eDNA metabarcoding was collected using a Van Veen grab (KC Denmark, Silkeborg, Denmark) after seawater eDNA sampling at each station. The grab was opened at the top and the undisturbed upper layer of sediment (maximum 1 cm in thickness) was collected using a sterile spatula and stored in sterile 50mL falcon tubes. The sediment was preserved at -20°C for downstream processing. Disposable gloves were also used when processing all eDNA samples to avoid cross contamination between sampling sites.

2. 3. Molecular work

2.3.1 Tissue extraction and sanger sequencing of GZP specimens

DNA was extracted from a total of 16 GZP individuals of 8 species, in order to confirm morphological identifications. The DNA of tissue from these individuals was extracted using the Qiagen Blood and Tissue kit (QIAGEN), following the manufacturer's protocol. DNA was eluted on 100uL of elution buffer and stored at -20°C until Polymerase chain reaction (PCR) processing. PCR amplification was conducted following the conditions in (Murray et al., 2023). The 'Folmer' fragment of the mitochondrial cytochrome c oxidase subunit 1 gene (COI) using

the primer pair HCO 2198 (5'-TAAACTTCAGGGTGACCAAAAAATCA-3') and LCO 1490 (5'-GGTCAACAAAT-CTAAAGATATTGG-3')(Folmer et al., 1994). PCR product was sequenced bidirectionally by EUROFINS Germany. The resulting sequences were manually checked for spurious base calls and stop codons, primer sequences removed. The sequences and specimen data were submitted to BOLD. Accession numbers are detailed in **Table S1**.

2.3.2 Environmental DNA extraction

A total of 174 eDNA filters (165 samples and 9 field blanks) and 8 eDNA sediment samples were collected. Environmental DNA of the water samples was isolated from the filters using the Qiagen Blood and Tissue kit (QIAGEN) following (Murray et al., 2024). Extraction controls were made using a new Sterivex filter for each extraction event and processing it alongside the samples (9 in total). Sediment eDNA was extracted from a 10g subsample of vortex-homogenized sediment from each individual station. This was done using the Qiagen DNeasy PowerMax Soil kit according to the manufacturer's protocol. A total of 8 sediment samples and 1 extraction control were processed. DNA extractions and library preparation were conducted in separate, dedicated laboratory rooms and on different days to PCR and post-PCR steps. All equipment and benches were sterilized using a 10% bleach solution followed by a milliQ wash and 70% ethanol for drying, before being radiated with UV light for a minimum of 1 hour before each extraction. During the extraction DNA-ExitusPlus™ (ITW Reagents) was used for sterilizing gloves and pipettes.

2.3.3 PCR inhibitors-removal treatment on water samples

Sediment was visible on the filter membranes after filtration of seawater for eDNA. In order to check for the significant negative effect of potential PCR inhibitors on sequencing, we processed and sequenced a small subset of the water eDNA samples (6 surface and 2 above bottom filters) with a post-extraction inhibitor removal kit. To do so, we treated 50uL of the DNA extract with the OneStep™ PCR Inhibitor Removal Kit from Zymo Research. The treated extracts were sequenced alongside the untreated extracts, resulting in 16 samples in total (8 treated and 8 with no treatment).

2.3.4. Metabarcoding primers

We used the universal eukaryote barcode of the mitochondrial DNA fragment known as the “Leray” fragment (Leray et al., 2013). It is an approximately 313-base pair region of the COI fragment that has been optimised to amplify eukaryotes. It has been successfully implemented in Arctic studies to investigate pelagic metazoan communities (Murray et al., 2024), coastal biodiversity (Lacoursière-Roussel et al., 2018; Leduc et al., 2019) and fjord benthic biodiversity (Mazurkiewicz et al., 2024). We used the highly degenerated Leray-XT primers pair: mICOLintF-XT:(5 'GGWACWRGWTGRACWITITAYCCYCC3') (Wangenstein et al., 2018) and the reverse jgHCO2198: (5'TAIACYTCIGGRTGICCRAARAAYCA3') (Geller et al., 2013).

2.3.5 Metabarcoding library preparation and sequencing

For the inhibitor test, library preparation and sequencing were done by AllGenetics (Spain) following the same 2 step-PCR protocol as described in Murray et al., (2024). This dataset was also sequenced on the Illumina Novaseq 6000 platform and had four PCR controls.

For the main water eDNA dataset, PCR was performed in triplicate. Sample-specific tags and a variable number of leading Ns (2-4) were attached to both the forward and reverse primers (tagged). The PCR master mix contained 10 μ L of Amplitaq Gold Master Mix (Applied Biosystems), 0.16 μ L of 20 μ g/ μ L BSA, 5.84 μ L molecular grade water, 1 μ L each of 5 μ M forward and reverse primers and 2 μ L of DNA template. The PCR conditions were: denaturing for 10 mins at 95°C, followed by 35 cycles of 1 min at 94°C, 1 min at 45°C, 1 min at 72°C, and a final extension for 5 mins at 72°C. PCR product was checked for successful amplification on 1.5% agarose gel. PCR triplicates were then pooled at equal volumes before being purified with Min-Elute columns (Qiagen) and following the manufacturer's protocol before being pooled into a single library. The library pool was sent to Novogene (Cambridge, UK) for ligation of Illumina adaptors and sequencing on the Illumina Novaseq 6000 platform in a paired-end sequencing run.

2.4 Bioinformatic analysis and curation of metabarcoding data

The bioinformatic workflow was based on OBITOOLS 3 (Boyer et al., 2016) , following Antich et al., (2022) with some modifications (<https://github.com/adriantich/MJOLNIR3>). Briefly, libraries and samples of the main dataset were demultiplexed and the tags and primers removed using *ngsfilter*. The inhibitor dataset was demultiplexed by the sequencing company using *cutadapt* (Martin, 2011). OBITools 3 was used to merge paired-end reads, length filter and dereplicate sequences per sample. Chimaeric sequences were removed with the *uchime denovo* algorithm in VSEARCH v2.28.1. Sequences were denoised using *DnoisE v1.4* (Antich González et al., 2022) (alpha = 4) and a blank correction of 10% was applied following Antich et al., 2021. Singletons were removed and a relative threshold abundance of 0.002% for in each sample was applied to filter out sequencing artefacts. Next, denoised sequences were clustered into molecular operational taxonomic units (MOTUs) (d=13) with SWARM v3.1.5 (Mahé et al., 2021). Any remaining MOTUs with a total read count of <5 were removed. The *ecotaq* algorithm was used for taxonomic assignment against a custom reference database (<https://github.com/adriantich/NJORDR-MJOLNIR3>), which is comprised of reference sequences from GenBank, BOLD and in-house sequences. The post-clustering filter LULU v1.0 (Frøslev et al., 2017) was used to remove potentially further erroneous sequences. Finally, bacteria were removed and NUMTs filtered out. Taxonomic assignments were further checked using the BOLDigger2 software v2.2.1 (Buchner and Leese, 2020) and the Barcode of Life Data System (BOLD)(Ratnasingham and Hebert, 2007). Taxonomic assignments were improved

and extra taxonomic information added where possible. The following identity thresholds were used: species (97%), genus (95%), family (90%), class (85%), phylum (80%) following Murray et al., 2024. All MOTUs with taxonomic assignments <75% were removed from the metabarcoding datasets completely.

The species-level detection lists were compiled from detections in all of the eDNA datasets combined. Detections in Kongsfjorden and Svalbard were based on Global Biodiversity Information Facility (GBIF) species occurrence data accessed via: <https://www.gbif.org/species>. When occurrences were not recorded on GBIF for Kongsfjorden or Svalbard, further literature searches were conducted and citations included in species tables where necessary.

2.5 Statistical analysis

Data visualisations and analyses were all done using R 4.3.0 using several R packages. Plots were made using *phyloseq* v 1.46.0 (McMurdie and Holmes, 2013), *Fantaxtic* v 0.2.0 (Teunisse, 2022), *microViz* v 0.12.1 (Barnett et al., 2021) and *ggplot2* v 3.5.0 (Wickham, 2016) packages, and statistical analyses conducted with *vegan* v 2.6.4 (Oksanen et al., 2019).

The main dataset was used for all community composition and beta diversity visualisations and analyses. Filter triplicates were pooled into single samples (one for each sampling depth at each station) by summing reads. The net-caught specimen data was only used for gelatinous zooplankton detections (presence-only). Due to different library preparation methods, number of PCR replicates and sequencing companies, the inhibitor test dataset was not combined with or compared to the main dataset. It was used only for testing the effect of a PCR inhibitor removal treatment on the DNA extract as well as in the presence-only list of genus and species detections. Relative read abundances were used to visualize the taxonomic composition. Alpha diversity indices (observed richness and Shannon-Wiener index) were used in the inhibitor treatment dataset. These were calculated based on read counts normalised using the Scaled Ranked Sums (SRS) method (Beule and Karlovsky, 2020) following Murray et al., (2024). ANOVA tests and subsequent pairwise comparisons were conducted to test for the effect of station, depth and inhibitor treatment on alpha diversity.

Spatial variance in community composition at the species level (main dataset only) were analysed through NMDS based on Aitchison's distances (CLR transformation and Euclidian distance) to account for the compositional nature of metabarcoding data (Quinn et al., 2018). This was done to test for the effect of station, depth, inhibitor treatment and eDNA sample type (water or sediment) on beta diversity. PERMANOVA tests were used to check for significance between grouping factors using the *adonis2()* function, and beta dispersion was tested for using the *betadisper()* functions in *vegan*.

3. Results

3.1 Environmental conditions

Station KB3 was the deepest station sampled, with a bottom depth of approximately 300 m and the shallowest was the Wharf station with a bottom depth of 4 m (Table 1). Distance of stations from land ranged from 0.03 km (Wharf) to 1.74 km (Station 6). Station KB3 was the closest to the fjord mouth and Station 7 closest to the glaciers (**Figure 1 and Table 1**). The oceanographic conditions in winter 2022 did not vary greatly between sampling sites, with gradients occurring mostly with depth. Seawater temperatures ranged from -0.9 to 1.5 °C and salinity from 34.4 to 34.8. Surface water temperatures were all below 0.5°C and the warmest temperatures were measured below 50 m at Station 2 and KB3 (**Figure S1**). Arctic water masses (ArW) were by far the most dominant with some Transformed Atlantic Water (TAW) measured at Station KB3 and Station 2, as a small amount of Intermediate Water (IW) measured at Station 2 (**Figure S2**).

3.2 Sequencing results of main dataset

We sequenced a total of 164 samples, as well as 23 field blanks and laboratory controls. Two samples (one water and one sediment) and one extraction control (sediment) failed in sequencing and were removed from the dataset. The failed extraction control was checked for DNA concentration using a Qubit and contained no detectable DNA. A further three water filters were excluded from the dataset as outliers based on MOTU composition and relative read abundances. After data curation and blank correction, 161 samples remained (154 water filters and 7 sediment samples), with a total of 1,452,732 reads assigned to 1387 MOTUs. The sequencing depth per sample ranged from 8325 to 101768 and the mean number of reads was 24, 622 reads per sample. Rarefaction curves plateaued or were approaching plateau for the majority of samples (**Figure S3**), suggesting sequencing depth was sufficient to capture most of the diversity present. Separate MOTU accumulation curves for water and sediment samples plateaued for water samples, but not for all of the sediment samples. This suggests that more samples are needed to capture all of the diversity in the sediment. Approximately one third of the MOTUs assigned to domain only (Eukaryota). This was followed by assignments to kingdom level (64%), phylum (54%), class (34%), order (23%), family (17%), genus (14%) and species (12%).

3.2.1 Community composition in water versus sediment eDNA

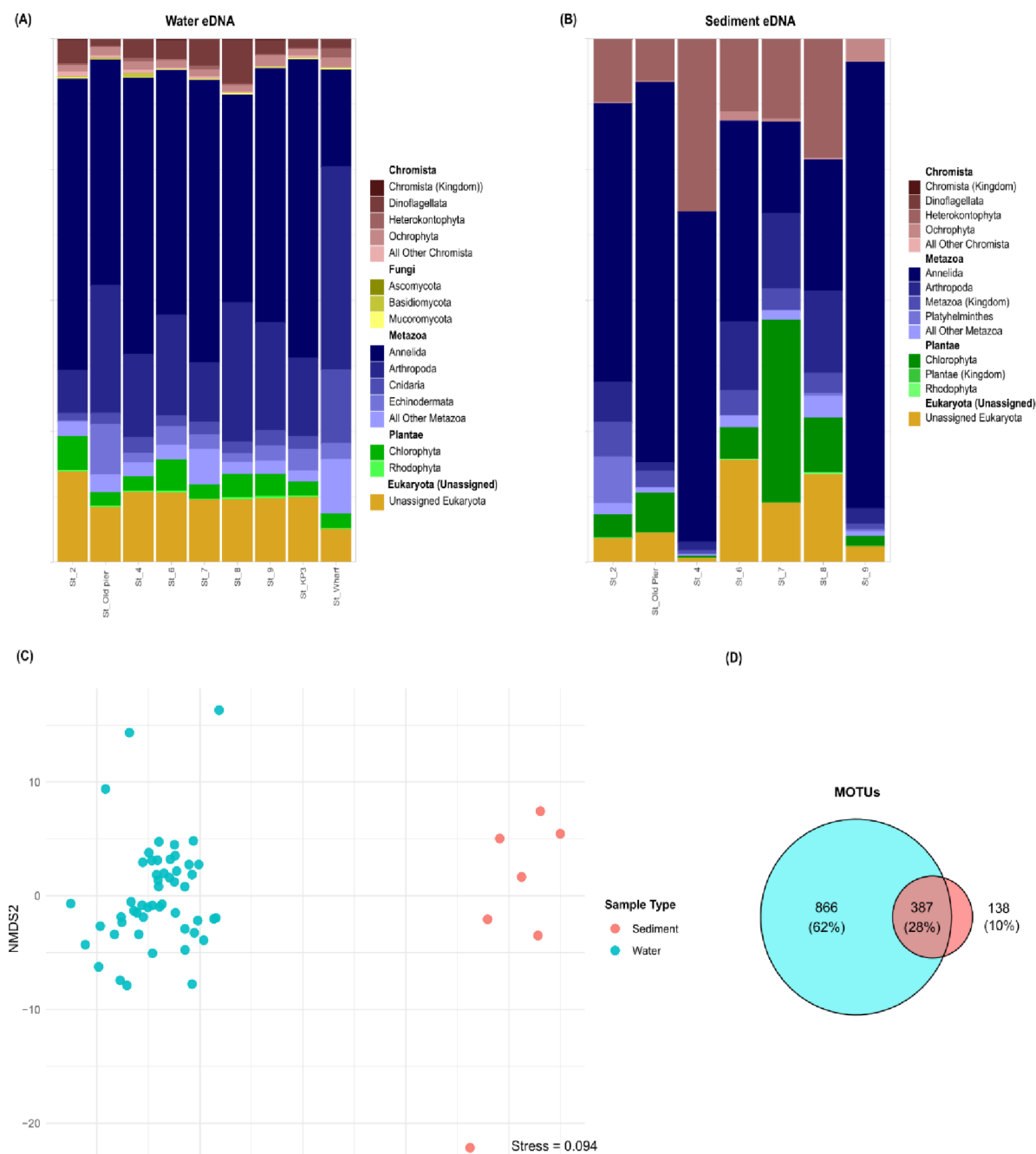


Figure 2. Eukaryotic community composition in water and sediment eDNA samples. (A) Relative abundances of the top 4 phyla in each eukaryotic kingdom in water eDNA. (B) Relative abundances in sediment eDNA. (C) NMDS calculated using MOTUs agglomerated at species level assignments and Aitchison's distance. (D) Venn diagrams showing shared MOTUs and shared species between the sampling types. Venn diagrams are based on presence absence data only.

Relative read abundances of the eukaryotic groups varied between stations and sample types (Figures 2A and B). The kingdom metazoan was more dominant in the water than the sediment samples. The kingdom Fungi was only detected in water, and the kingdoms Chromista and Plantae were more dominant in sediment samples compared to water. The

variation between relative read abundance at the sampling stations, and the variation in the proportion of unassigned sequences, was higher in the sediment than the water samples.

A PERMANOVA revealed that community composition varied significantly between eDNA sample types of water and sediment (Sample Type: $F_1=10.6$, $p=0.001$). This was further supported in the NMDS ordination plot (**Figure 2C**). When comparing the shared MOTUs (presence-only), 62% were detected only in the water samples and 10% in the sediment. A total of 28% of the MOTUs in the main dataset were detected in both water and sediment eDNA (**Figure 2D**).

3.2.2 Water eDNA

The final water eDNA dataset (main dataset only) consisted of 1,222,037 reads assigned to 1250 MOTUs from 52 samples (filters triplicates combined). The primary producer component of the water samples was made up 119,993 reads assigned to 216 MOTUs. A total of 57% these reads were assigned to Chromista and 43% to Plantae. The most dominant primary producer phylum was Chlorophyta (40% of primary producer reads in water and 13 MOTUs), followed by Dinoflagellata (31% and 19 MOTUs), Ochrophyta (16% and 66 MOTUs) and the remaining phyla (<5%). We were able to detect a number of species in Chlorophyta, Ochrophyta and Rhodophyta, but the assignments were restricted to mostly class or order level in the other phyla (**Figure 3A**). MOTUs assigned to the prasinophyte *Bathycoccus prasinos* made up 33% of the primary producer reads, followed by MOTUs assigned to the dinoflagellate class Dinophyceae (15%) and then MOTUs assigned only as Phaeophyceae (Phylum: Ochrophyta) with 12%. The most dominant group at all stations were Chlorophytes, except for stations 7 and 8 where dinoflagellates were more dominant (**Figure 3A**). MOTUs assigned to Heterokontophyta and Rhodophyta were present in low abundances at all stations, with the exception of station wharf, where there were significantly more reads assigned to Heterokontophyta.

A total of 947,392 reads were assigned to 559 metazoan MOTUs in the water samples. The most dominant metazoan phyla in both reads and MOTU richness were Annelida with 66% of reads in the water and 145 MOTUs, followed by Arthropoda (22% and 131 MOTUs). The next most abundant in reads were Echinodermata (4% of reads and 15 MOTUs), Cnidaria (4 % of reads and 77 MOTUs) and then Chordata (1% of reads and 31 MOTUs). The most abundant metazoan taxa were MOTUs assigned only to Annelida (63%), followed by the copepod species *Microcalanus pusillus* (15%) and the sea urchin *Strongylocentrotus droebachiensis* (4%) (**Figure 3B**). MOTUs assigned only to Annelida were the most dominant group at all stations, except for the Wharf station, where the copepod *M. pusillus* made up the highest proportion of reads.

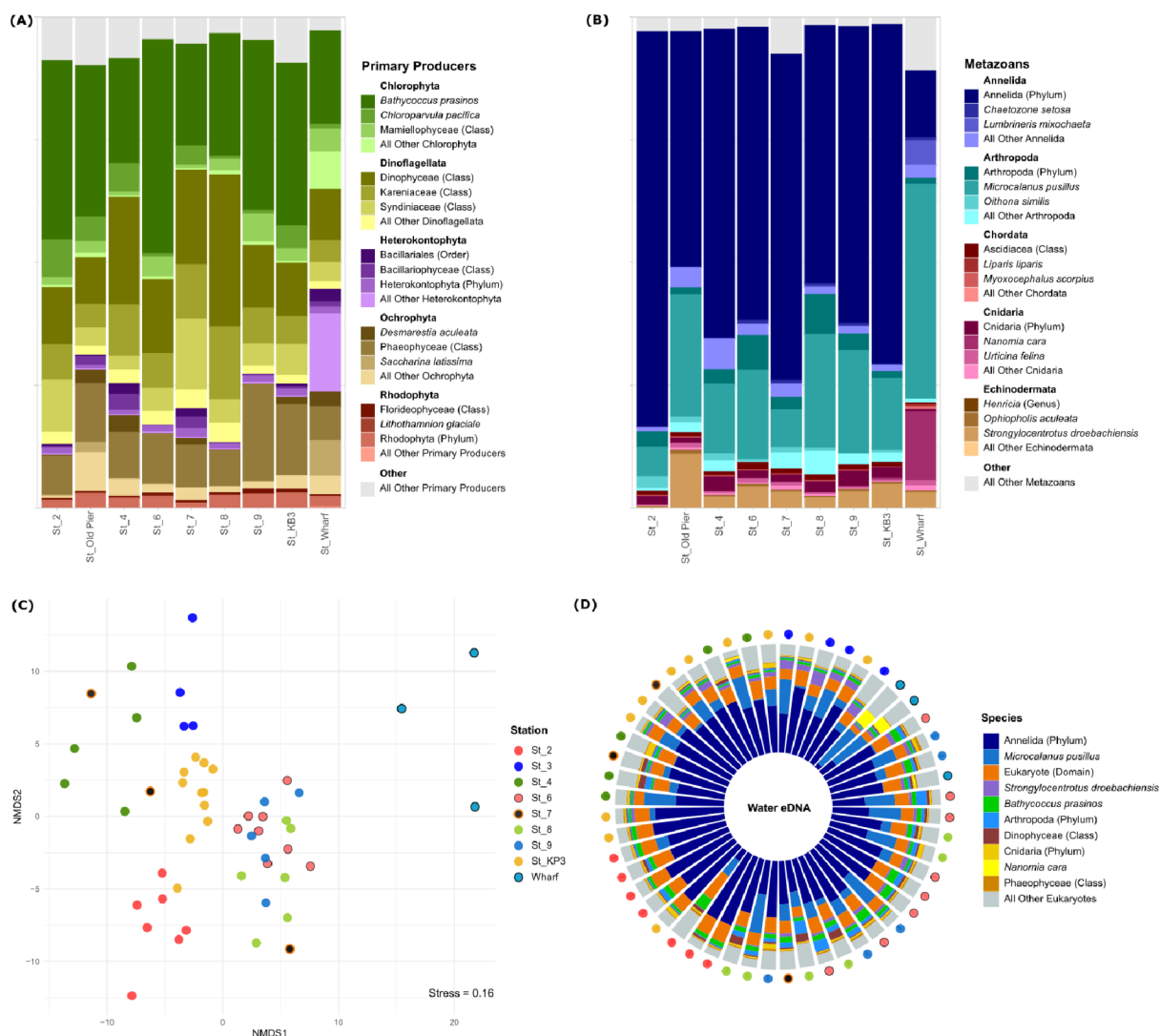


Figure 3. Eukaryotic community composition in water eDNA. MOTUs are aggregated at species-level or the next highest taxonomic level possible. (A) Primary producers and (B) Metazoans. The five most abundant phyla and the three most abundant species in those phyla are shown. All other MOTUs are pooled together as “Other”. (C) NMDS plot of species composition based on CLR transformed and Euclidian (Aitchison’s distance) matrix of community composition. Colours indicate different stations (D) Iris plot of the RRA’s of the top 15 taxa at each sampling point. MOTUs are aggregated at species level where possible, and lower taxonomic levels when not. Each bar represents a sampling point. Bars are arranged in order according to the NMDS and the coloured circles next to each bar correspond to the stations on the NMDS plot.

We tested for station and sampling depth as drivers of community composition in the water eDNA. Only station had a significant effect on community composition (Station: $F = 3.48$, $p = 0.001$, $R^2 = 0.42$), and explained 42% of the variation. This was supported by the clusters on the NMDS plot, where the majority of the stations form distinct clusters from one another, with the wharf being the most dissimilar to the other stations (Figure 3C). This was further evidenced in the relative read abundances of the top 10 most abundant MOTUs at each sampling point (Figure 3D). The wharf samples in particular were the most dissimilar to the other clusters (Figure 3C), which is driven by higher proportions of *M. pusillus* reads than the other stations and relatively high proportions of reads assigned of the siphonophore *Nanomia*

cara (Figure 3D). However, significant differences in beta dispersion for the grouping factor “station” were found. This is likely due to the uneven sampling sizes at the different stations due to different maximum depth profiles at each station (4 m – 300 m). As a result, the clustering of the stations in the NDMS must be interpreted with some caution.

3.2.3 Sediment eDNA

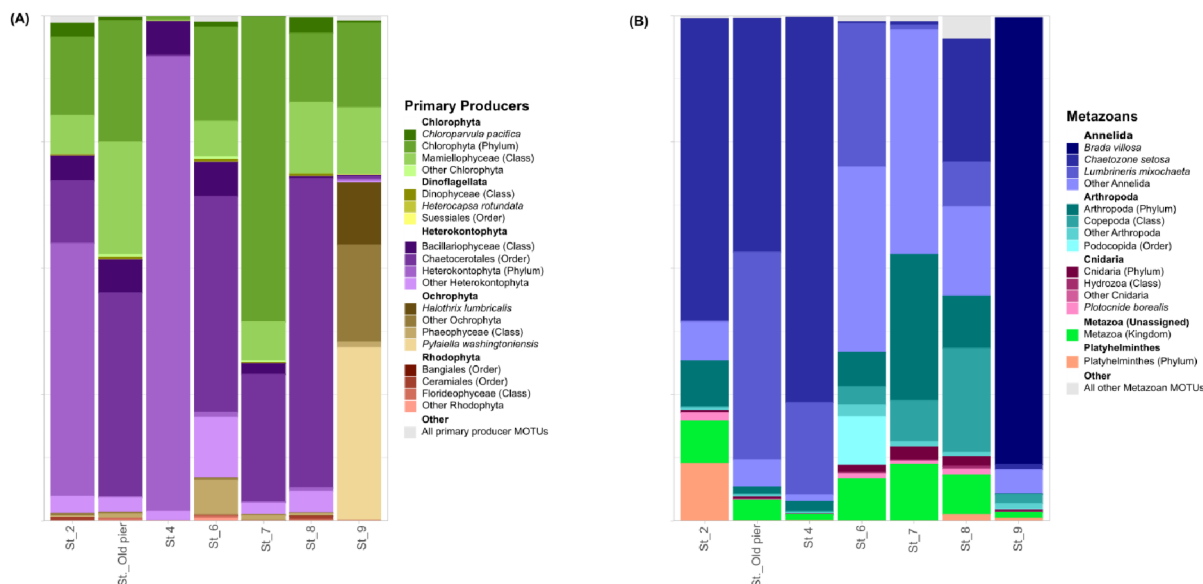


Figure 4. Relative read abundances of most abundant primary producers and metazoans in the sediment eDNA. MOTUs are aggregated at species-level or the next highest taxonomic level possible. The five most abundant phyla and the three most abundant species in those phyla are shown. All other MOTUs are pooled together as “Other”. (A) Primary producers and (B) Metazoans.

The sediment dataset consisted of 230,695 sequenced reads assigned to 523 eukaryotic MOTUs across 7 samples. After data curation, 135 MOTUs were assigned to the primary producer kingdoms Chromista (66%) and Plantae (35%), totalling 58,956 reads. The most dominant primary producer phyla were Heterokontophyta (54% of primary producer in sediment and 58 MOTUs), Chlorophyta (33% and 14 MOTUs) and Ochrophyta (11% and 32 MOTUs). The majority of MOTUs in the phylum Heterokontophyta could only be assigned to class or order level and MOTUs assigned to the order Chaetocerotales was the most dominant group, making up 26% of the primary producer reads in the sediment. MOTUs assigned to Chlorophyta (phylum level) made up 21% of primary producer reads, followed by those assigned only to Mamiellophyceae (10%). In Ochrophyta, reads assigned to the species *Pylaiella washingtoniensis* were the most dominant (5% of primary producer reads), followed by *Halothrix lumbricalis* (2%). Phylum Heterokontophyta dominated in read abundance at all stations except St. 7, where Chlorophyta were more abundant, and St. 9 where Ochrophyta dominated the reads. Dinoflagellata were present in low abundances at all stations and Rhodophyta at all stations except St. 4 (Figure 4A).

A total of 225 MOTUs were assigned as metazoans in the sediment. The most dominant metazoan phylum in both reads and MOTU richness was Annelida, which made up 73% of metazoan reads in the sediment and was represented by 51 MOTUs. MOTUs assigned as the species *Chaetozone setosa* were the most abundant Annelida taxa (30% of sediment reads), followed by *Lumbrineris mixochaeta* (14%) and *Brada villosa* (13%). The next most abundance metazoan phylum was Arthropoda (16% of sediment metazoan reads and 59 MOTUs) and then Cnidaria (2% and 32 MOTUs). In terms of reads number, Annelida were dominant phyla at all stations, but Arthropoda also made up a significant proportion of reads at stations 6, 7 and 8 (**Figure 4B**).

3.3 PCR-inhibitor treatment dataset

Particulate matter was visible on the water filters after filtration due to suspended matter in the water, so a subset of 8 samples were treated and sequenced before the main data set to investigate the potential presence of PCR inhibitors (Kumar et al., 2022). After bioinformatic filtering and data curation, all samples were retained (8 treated and 8 untreated) with a total of 1,411,255 reads (>75% identity match) assigned to 1275 MOTUs. Rarefaction curves plateaued for all samples, indicating that the sequencing depth was sufficient to capture the biodiversity in the samples.

We tested for the effect of inhibitor removal treatment on MOTU richness, Shannon diversity and total read counts. Richness and Shannon diversity were calculated based on SRS transformed values, and raw data was used for the read counts (**Table S2**). One-way ANOVA tests found that treatment did not have a significant effect on any of the values (**Table S3**). Analysis of community composition between the treated and non-treated samples showed no significant difference (PERMANOVA, $F_1 = 0.270$, $p = 0.885$). This indicates that inhibitor removal treatment did not have a significant effect on the beta diversity captured in sequencing. This was further supported by an NMDS ordination, which showed no obvious clustering between the treated and non-treated samples (**Figure S4**).

3.4 List of species-level detections using eDNA metabarcoding

We were able to detect a total of 225 individual species using DNA metabarcoding of water and sediment samples. The highest number of metazoan species-level detections were in the phylum Annelida, with 65 assignments. This was followed by Arthropoda (30), Chordata (29) and Cnidaria (23) and then the remaining metazoan phyla. In the primary producers, the most species-level detections were found in the Chromista phylum Ochrophyta (22). This was followed by the Plantae phyla Rhodophyta (7) and Chlorophyta (4). The full list of species detections can be found in **Table S4**.

3.4.1 Macroalgae

We detected 29 species of macroalgae in the eDNA sampling. These included kelps (e.g., *Laminaria digitata* and *Saccharina latissima*), filamentous brown (e.g., *Desmarestia aculeata*) and red algae (e.g., *Savoiea arctica*), as well as crusting red algae (*Lithothamnion glaciale* and *Boreolithothamnion lemoineae*). All of the species were found in water, and approximately half were found in both water and sediment. In total, five species were not previously reported in Kongsfjorden, four were new records in Svalbard and four were first molecular detections (Table 2).

Table 2. Species-level detections of macroalgae from eDNA samples.

Phylum	Class	Species	eDNA type	Previously detected in KF	Previously detected in SV		
Ochrophyta	Phaeophyceae	<i>Alaria esculenta</i>	W+S	Y	Y		
		<i>Chaetopterus plumosa</i>	W	Y	Y		
		<i>Chorda filum</i>	W	Y	Y		
		<i>Chordaria</i>	W	Y	Y		
		<i>chordaeformis</i>					
		<i>Chordaria flagelliformis</i>	W+S	Y	Y		
		<i>Desmarestia aculeata</i>	W+S	Y	Y		
		<i>Dictyosiphon ekmanii</i>	W+S	N	N		
		<i>Dictyosiphon foeniculaceus</i>	W+S	Y (Fredriksen et al., 2019)	Y		
		<i>Dictyosiphon sinicola</i>	W+S	Y (Düsedau et al., unpublished results)	Y (Düsedau et al., unpublished results)		
		<i>Eudesme borealis</i>	W	Y (Düsedau et al., unpublished results)	Y (Düsedau et al., unpublished results)		
		<i>Fucus distichus</i>	W	Y	Y		
		<i>Halothrix lumbricalis</i>	W+S	Y (Düsedau et al., unpublished results)	Y (Düsedau et al., unpublished results)		
		<i>Haplospora globosa</i>	W+S	Y	Y		
		<i>Hedophyllum nigripes</i>	W+S	Y (Dankworth et al., 2020)	Y (Dankworth et al., 2020)		
		<i>Laminaria digitata</i>	W	Y	Y		
		<i>Laminariocolax aecidioides</i>	W+S	Y* (Fredriksen et al., 2019)	Y (Fredriksen et al., 2019)		
		<i>Phaeosaccion collinsii</i>	W+S	N	Y		
		<i>Pogotrichum filiforme</i>	W	Y	Y		
		<i>Pylaiella washingtoniensis</i>	W+S	Y (Düsedau et al., unpublished results)	Y (Düsedau et al., unpublished results)		
		<i>Saccharina latissima</i>	W+S	Y	Y		
		<i>Saundersella doloresiae</i>	W+S	N	N		
		<i>Stictyosiphon tortilis</i>	W+S	Y*	Y		
		Rhodophyta	Phaeothamniophyceae	<i>Grania efflorescens</i>	W	Y* (Fredriksen et al., 2019)	Y (Fredriksen et al., 2019)
			Florideophyceae	<i>Ahnfeltia borealis</i>	W	N	N
				<i>Boreolithothamnion lemoineae</i>	W	N	N
				<i>Devaleraea ramentacea</i>	W+S	Y	Y

<i>Lithothamnion glaciale</i>	W	Y*	Y
<i>Rhodomela</i>	W	Y	Y
<i>lycopodioides</i>			
<i>Savoiea arctica</i>	W	Y	Y

Notes: W = water eDNA, W+S = water and Sediment eDNA, S = Sediment. Previous detections based on observations listed in GBIF https://www.gbif.org/occurrence/search?occurrence_status=present&q=. * present study is first molecular detection. Bold text indicates that the present study is the first record

3.4.2 Cnidaria

A total of 23 species-level assignments were recovered in the phylum Cnidaria, across three classes (Anthozoa, Hydrozoa and Scyphozoa). We detected sea anemones (e.g., *Urticina felina*), soft corals (e.g., *Gersemia rubiformis*), hydroids (e.g., *Calycella syringa*), siphonophores (e.g., *Nanomia cara*) hydromedusae (e.g., *Ptychogena lactea*) and large scyphomedusae (e.g., *Periphylla Periphylla*). All of the cnidarians were found in water eDNA, except for one (*Catablema vesicarium*) which was only found in the sediment. Three were found in both water and sediment samples. All of the anthozoans have been previously detected in Svalbard, and one of them in Kongsfjorden. A total of 6 of the hydrozoans have previously been found in Kongsfjorden, 11 in Svalbard and two more further south in Bear Island waters. A total 11 of the hydrozoan sequences we recovered were new detections for Kongsfjorden. Both of the scyphozoans have been observed previously in Kongsfjorden (Table 3).

Table 3. Species-level detections in the Phylum Cnidaria from eDNA samples

Phylum	Class	Species	eDNA type	Previously detected in Kongsfjorden	Previously detected in Svalbard		
Cnidaria	Anthozoa	<i>Gersemia rubiformis</i>	W	Y	Y		
		<i>Hormathia nodosa</i>	W	N	Y		
		<i>Stomphia coccinea</i>	W	N	Y		
		<i>Urticina felina</i>	W+S	N	Y		
Hydrozoa		<i>Bougainvillia principis</i>	W	N	N		
		<i>Bougainvillia superciliaris</i>	W	Y	Y		
		<i>Calycella syringa</i>	W	N	Y		
		<i>Catablema vesicarium</i>	S	N	N		
		<i>Lafoea dumosa</i>	W	Y	Y		
		<i>Nanomia cara</i>	W	Y	Y		
		<i>Obelia longissima</i>	W	N	Y		
		<i>Opercularella lacerata</i>	W	N	Y (Ronowicz et al., 2013)		
		<i>Orthopyxis integra</i>	W	Y	Y		
		<i>Plotocnide borealis</i>	W+S	Y	Y		
		<i>Ptychogena lactea</i>	W	Y	Y		
		<i>Rathkea octopunctata</i>	W	N	Y		
		<i>Sarsia lovenii</i>	W+S	N	Y		
		<i>Sarsia princeps</i>	W	N	Y		
		<i>Sarsia tubulosa</i>	W	N	N (Bear Island)		
		<i>Stauridiosarsia producta</i>	W	N	N		
		<i>Tiaropsis multicirrata</i>	W	N	N (Bear Island)		
		Scyphozoa		<i>Cyanea capillata</i>	W	Y	Y
				<i>Periphylla periphylla</i>	W	Y	Y

Notes: W = water eDNA, W+S = water and Sediment eDNA, S = Sediment. Previous detections based on observations listed in GBIF https://www.gbif.org/occurrence/search?occurrence_status=present&q=. Bold indicates new detections.

3.4.3 Arthropoda

We recovered 29 species-level assignments in the Phylum Arthropoda. These included five classes, with Malacostraca having the highest species richness. We detected species belonging to several crustacean groups including krill (e.g., *Thysanoessa longicaudata*), pelagic copepods (e.g., *Calanus finmarchicus*), decapods including shrimps (e.g., *Lebbeus polaris*) and crabs (e.g., *Hyas araneus*), amphipods (e.g., *Caprella septentrionalis*) and barnacles (e.g., *Semibalanus balanoides*). All of the Arthropoda species were found in water samples, and two were also found in sediment. All of the species have been found in Svalbard waters before except for two (the amphipod *Lembos websteri* and the euphausiid *Hansarsia megalops*). A further five have no previous detections in Kongsfjorden according to GBIF (Table 4).

Table 4. Species-level detections in the Phylum Arthropoda from eDNA samples

Phylum	Class	Species	eDNA type	Previously detected in Kongsfjorden	Previously detected in Svalbard	
Arthropoda	Copepoda	<i>Tisbe furcata</i>	W	N	Y	
		<i>Lembos websteri</i>	W	N	N	
	Malacostraca	<i>Calliopius laeviusculus</i>	W+S	N	Y	
		<i>Caprella septentrionalis</i>	W	Y	Y	
		<i>Gammarus locusta</i>	W	N	Y	
		<i>Gammarus setosus</i>	W	Y	Y	
		<i>Ischyrocerus anguipes</i>	W	Y	Y	
		<i>Orchomenella minuta</i>	W	Y	Y	
		<i>Pleustes glaber</i>	W	Y	Y	
		<i>Anonyx sarsi</i>	W	Y	Y	
		<i>Eualus gaimardii</i>	W	Y	Y	
		<i>Lebbeus polaris</i>	W	Y	Y	
		<i>Hyas araneus</i>	W	Y	Y	
		<i>Pandalus borealis</i>	W	Y	Y	
		<i>Hansarsia megalops</i>	W	N	N	
		<i>Thysanoessa longicaudata</i>	W	Y	Y	
		Maxillopoda	<i>Calanus finmarchicus</i>	W	Y	Y
			<i>Calanus hyperboreus</i>	W	Y	Y
			<i>Microcalanus pusillus</i>	W+S	Y	Y
			<i>Pseudocalanus acuspes</i>	W	Y	Y
			<i>Pseudocalanus minutus</i>	W	Y	Y
			<i>Pseudocalanus moultoni</i>	W	N	Y
	<i>Metridia longa</i>		W	Y	Y	
	<i>Metridia lucens</i>		W	Y	Y	
	<i>Oithona atlantica</i>		W	Y	Y	
	<i>Oithona similis</i>		W	Y	Y	
	<i>Triconia borealis</i>		W	Y	Y	
	Thecostraca		<i>Balanus balanus</i>	W	Y	Y
		<i>Semibalanus balanoides</i>	W	N	Y	

Notes: W = water eDNA, W+S = water and Sediment eDNA, S = Sediment. Previous detections based on observations listed in GBIF https://www.gbif.org/occurrence/search?occurrence_status=present&q=. Bold indicates new detections

3.4.4 Chordata

We recovered 23 species of vertebrates in the eDNA dataset, across three classes (*Aves*, *Mammalia* and *Teleostei*). These species included sea birds (e.g., *Cephus grille*), sperm whale (*Physeter macrocephalus*), walrus (*Odobenus rosmarus*), seals (e.g., *Pagophilus groenlandicus*) and fish (e.g., *Mallotus villosus*). All vertebrate species-level detections were in water samples and none were found in sediment samples. All of these species have previously been recorded in Svalbard, and all but five in Kongsfjorden (**Table 5**).

Table 5. Species-level detections of Chordata from eDNA samples

Phylum	Class	Species	eDNA type	Previously detected in Kongsfjorden	Previously detected in Svalbard
Chordata	Aves	<i>Cephus grille</i> (Black Guillemot)	W	Y	Y
		<i>Fulmarus glacialis</i> (Fulmar)	W	Y	Y
	Mammalia	<i>Physeter macrocephalus</i> (Sperm Whale)	W	Y (Pöyhönen et al., 2024)	Y
		<i>Odobenus rosmarus</i> (Walrus)	W	Y	Y
		<i>Erignathus barbatus</i> (Atlantic Bearded Seal)	W	Y	Y
		<i>Pagophilus groenlandicus</i> (Harp Seal)	W	Y	Y
		<i>Phoca vitulina</i> (Harbour Seal)	W	Y	Y
	Teleostei	<i>Boreogadus saida</i> (Polar cod)	W	Y	Y
		<i>Mallotus villosus</i> (Capelin)	W	Y	Y
		<i>Anarhichas lupus</i> (Atlantic Wolffish)	W	Y	Y
		<i>Gymnocanthus tricuspis</i> (Arctic Staghorn Sculpin)	W	Y	Y
		<i>Myoxocephalus Scorpius</i> (Arctic Sculpin)	W	Y	Y
		<i>Cyclopterus lumpus</i> (Hen Fish)	W	Y	Y
		<i>Liparis bathyarticus</i> (Nebulous Snailfish)	W	Y	Y
		<i>Liparis fabricii</i> (Gelatinous Snailfish)	W	Y	Y
		<i>Liparis liparis</i> (Sea Snail)	W	Y	Y
		<i>Leptoclinus maculatus</i> (Daubed Shanny)	W	Y	Y
		<i>Lumpenus lampraeformis</i> (Serpent Blenny)	W	Y	Y
		<i>Lycodes squamiventer</i> (Scalebelly Eelpout)	W	N	Y
		<i>Hippoglossoides platessoides</i> (American Plaice)	W	Y	Y
		<i>Hippoglossus hippoglossus</i> (Atlantic Halibut)	W	N	Y
		<i>Salvelinus alpinus</i> (Arctic Char)	W	N	Y
		<i>Ammodytes marinus</i> (Launce)	W	N	Y

Notes: W = water eDNA, W+S = water and Sediment eDNA, S = Sediment. Previous detections based on observations listed in GBIF https://www.gbif.org/occurrence/search?occurrence_status=present&q=. Bold text indicates new detections

3.5 Gelatinous Zooplankton

We detected 19 gelatinous zooplankton to species-level and a further three to genus-level, with both net and eDNA sampling methods combined (**Figure 5**). Of these, 16 were detected in water eDNA, three in sediment and 11 with nets. Of the net specimens, eight were confirmed with barcoding of the COI Folmer fragment. A total of 8 detections were unique to water eDNA, 1 to sediment eDNA and 6 to the nets. There were 5 species detected by both eDNA and water, but no overlaps between sediment and nets nor all three methods. The dominant Arctic cnidarian (Hydrozoa and Scyphozoa) and ctenophore classes (Nuda and Tentaculata) were all detected. *Cyanea capillata* and *Nanomia cara* were ubiquitous across the water eDNA stations, while *Plotocnide borealis* was the most widespread in the sediment. In the nets, *Aglantha digitale*, *Sminthea arctica* and *Beroe* spp. were the most widespread (**Figure 5**).

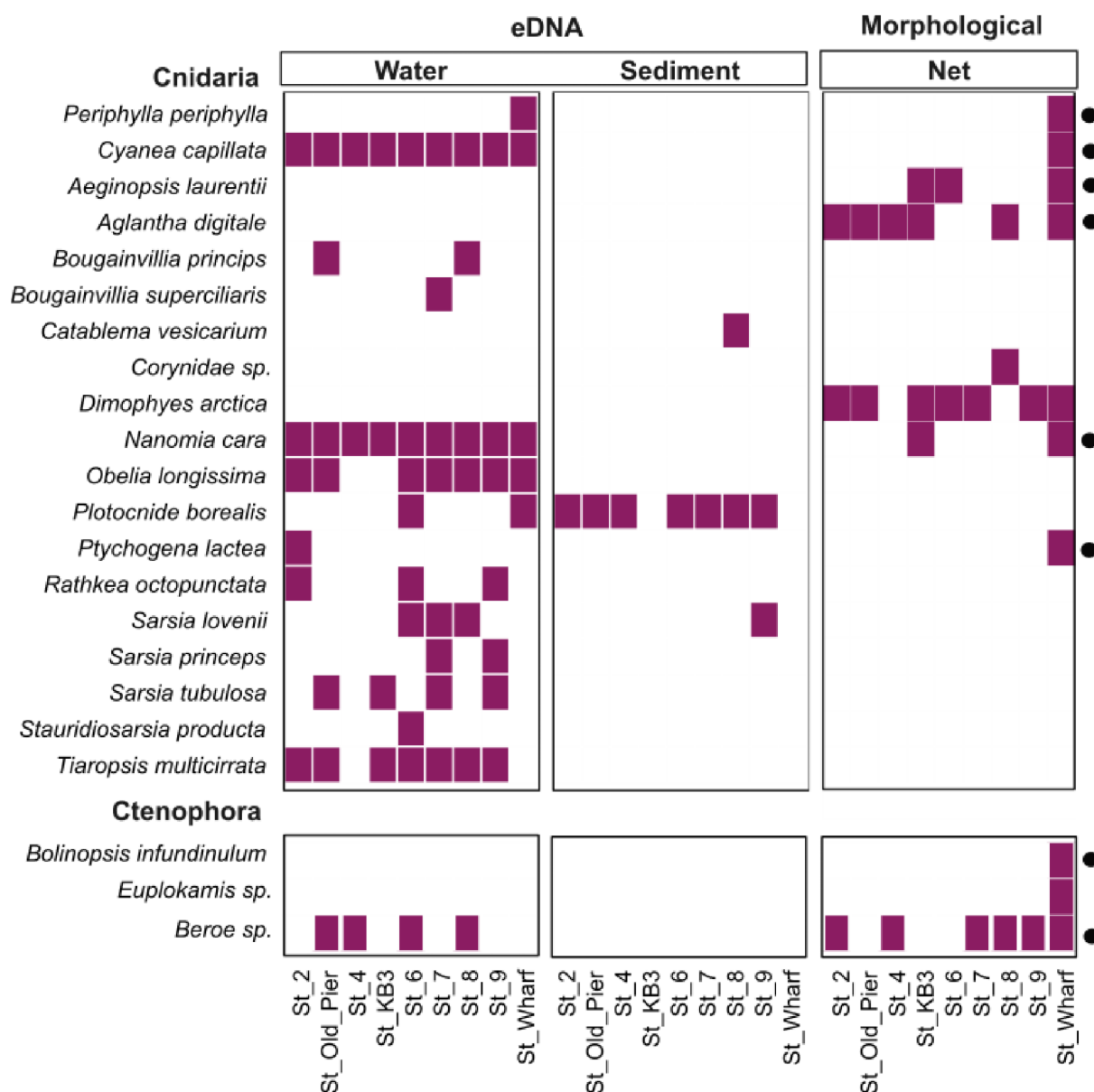


Figure 5. Gelatinous zooplankton genus and species level detections in eDNA samples and nets. Presence of GZP at the different stations detected by the different sampling methods. Species detected in the main water eDNA and inhibitor test datasets are combined here under “water”. Hand net and WP3 net caught specimens are combined under “Nets”. Black circle indicates species of which net-caught specimens been barcoded.

4. Discussion

This study, to our knowledge, represents the first COI-based eDNA metabarcoding survey targeting eukaryotic biodiversity during the polar night in Kongsfjorden, Svalbard. We successfully recovered a wide range of taxa belonging to the pelagic community, seabird, fish and mammals, as well as benthic and hyperbenthic taxa known to the area. Additionally, we detected species that were, based on existing literature and published datasets, previously

not known to occur in the fjord or in the Svalbard area. Furthermore, by implementing a comprehensive sampling program targeting gelatinous zooplankton (GZP), we were able to provide a baseline dataset for a hitherto overlooked component of the winter pelagic community. Our study provides a baseline for future polar night eDNA-based biodiversity monitoring in Kongsfjorden, a time of year that remains underrepresented in a highly-studied area of the Arctic.

4.1 Different eDNA assemblages recovered from water and sediment

Sample type-dependent eDNA assemblages have been well documented in marine systems (Cordier et al., 2022; Holman et al., 2019). Based on presence data alone, more than two thirds of the MOTUs detected here in the sediment were also present in the water samples (**Figure 2D**). Yet multivariate analysis (**Figure 2C**), which was based on transformed read abundance data, showed a significant difference in community composition between the two. This incongruence can be explained by many of the shared MOTUs being low in abundance in one of the two sample types, and the fact that more than double the amount of MOTUs were found in water versus sediment. Many benthic organisms release eDNA into the water column (e.g., gametes or excretion products), which could explain the presence of many of the sediment MOTUs in the water column. Indeed, previous research has found that benthic taxa left traces of eDNA in adjacent waters (Antich et al., 2021). Sediment also harbours eDNA of pelagic origin, but its persistence depends on many factors including but not limited to: microbial activity, taxon-specific decay-rates, DNA hydrolysis and temperature (reviewed in Torti et al., 2015). Hence, we would expect traces of the pelagic community in the sediment, and vice versa, but our findings further highlight the necessity of including multiple sample types when investigating both pelagic and benthic communities.

It must be noted that high levels of heterogeneity were observed between the sediment samples compared to the water samples (**Figure 2**). In a previous Arctic coastal eDNA study Leduc et al., (2019) also found higher variation in benthic samples compared to pelagic samples. Sediment is a heterogeneous habitat that and can have significantly different assemblages from centimetres to kilometres (Angulo-Preckler et al., 2023; Hewitt et al., 2005; Nascimento et al., 2018). Indeed, Kongsfjorden has a range of benthic substrates (e.g., soft sediments and rocky shore), as well as ice-scouring and high glacier run-off, all of which are important drivers of benthic assemblages across relatively small spatial scales (Molis et al., 2019; Renaud et al., 2020). However, low sample numbers prevented statistical analysis of community composition between the sediment samples. The sediment also had lower total MOTU richness (523 MOTUs) than the water samples (main dataset: 1250 MOTUs, and inhibitor test dataset: 1275 MOTUs). This is contradictory to many other eDNA studies where sediment has typically higher richness than water-based eDNA (e.g., Cordier et al., 2022;

Holman et al., 2019), but similar patterns have been detected before in aquatic studies (e.g., Sakata et al., 2020). The different levels of richness and between sample variation here may be explained in part by the differences in sampling strategies employed. The number of sediment samples was significantly lower than water samples (7 sediment and 52 water) and their sampling volumes differed (10g sediment vs 6L water per sample). Furthermore, the MOTU accumulation curves did not all reach asymptote for all of the sediment samples, indicating that increasing the sequencing depth is necessary to capture all MOTUs present in the samples. We used the extraction kit with the highest sample input volume (10g)(Pearman et al., 2020), which has been shown to more accurately reflect the community assemblages than other extraction kits with lower input volumes (Brinkmann et al., 2023). Thus, based on the rarefaction curves, low MOTU richness and the high between-site variation, we hypothesize that increasing the spatial resolution and number of sediment samples and sequencing depth rather than sample volume would be key to increasing the number of MOTUs, and therefore biodiversity recovered.

4.2 Spatial patterns of community structure

Contrary to other Arctic eDNA studies (Lacoursière-Roussel et al., 2018; Murray et al., 2024), we did not find a significant influence of depth on community composition in the water column. The polar night is the period with the highest levels of vertical mixing, as a result of wind and similar temperatures throughout the water column for example, compared to the coldest months of the year (Cottier and Porter, 2020; Tverberg et al., 2019). Thus, there is less stratification, which is also a general characteristic of the fjord in other seasons (except summer), resulting in a reduced vertical structuring. Further, the lack of sunlight prevents the accumulation of primary producers and associated higher trophic levels feeding on their production in surface waters. These factors likely result in high levels of localised dispersion of pelagic organisms and their eDNA signals throughout the water column, but to which extent cannot be determined based on the present study.

Multivariate analysis did, however, reveal that sampling location had a significant effect on pelagic community composition. The wharf, which was the shallowest station and experiences the most human disturbance (e.g., artificial light and vessel activity), showed the most dissimilar community composition compared to the other locations. However, the remainder of the stations were further out in the fjord and showed more similarity to one another (**Figure 3**). Horizontal community structuring has been found before in coastal systems using water-derived eDNA (Jeunen et al., 2019; Lacoursière-Roussel et al., 2018), showing its potential to detect small-scale patterns despite possible dispersion. The relatively low levels of horizontal community structuring in the present study are likely influenced by the hydrological dynamics specific to the polar night, as well as tidal currents, eddies and advection events from the

adjacent shelf via the West Spitsbergen Current (WSC) (Cottier et al., 2005; Tverberg et al., 2019), causing high connectivity between stations. Sampling location explained approximately 40% of the variance in community composition here, suggesting further parameters should be measured to uncover other significant environmental factors. Furthermore, the extent of the sampling area was restricted to the central part of the fjord, omitting the inner fjord for example, where the influence of meltwater and sediment plumes from the tidal glaciers is stronger. Expanding the spatial range of sampling to encompass more of the fjord would likely increase the chance of uncovering distribution patterns and community structuring potentially overlooked in the present study.

4.3 Primary producers

The phytoplankton community during the polar night in Kongsfjorden is characterised by low biomass during the winter months, but with a species occurrences similar to other seasons (Hegseth et al., 2019; Z. Smola pers. comm). In the present study, eDNA metabarcoding recovered a community composition largely congruent with the few studies that have targeted phytoplankton in the fjord. For example, the typical spring bloom genera *Micromonas* and *Phaeocystis* were found to be widespread in the water column of a neighbouring fjord during the polar night with eRNA (Vader et al., 2015). In the present study, we recovered *Phaeocystis* in low read abundances in the water column at every station. We also found *Micromonas* to genus-level in very low read abundances, as well as MOTUs assigned to the class Mamiellophyceae (e.g., *Bathycoccus prasinos*) which were widespread and in relatively high read abundances. Furthermore, we detected other genera typical of the spring bloom such as *Nitzschia*, *Entomoneis*, *Attheya*, *Chaetoceros* and *Skeletonema* (von Quillfeldt, 2000).

Many phytoplankton species have adaptations for winter survival that include some form of dormancy. For example, many diatoms form highly silicified resting stages that settle on surface sediment, while other species maintain active cells that persist in the water column in low abundances throughout the winter. These individuals then seed the spring bloom when the light returns at the end of the polar night (Hegseth et al., 2019; Hoppe, 2022). In the present study, we were able to detect evidence of these different overwintering strategies by using both water and sediment-derived eDNA. The most abundant (by reads) primary producer group in the water column, however, were assigned to the phylum Chlorophyta, which includes species that do not form resting stages at all, and thus overwinter as active cells in the water column. Similar observations have been made in another Svalbard fjord (Isfjorden) during the same time of year (Marquardt et al., 2016; Vader et al., 2015). Additionally, the fraction of diatom (Bacillariophyceae) reads in the sediment was significant, where they are traditionally considered to overwinter. Congruently, the high read abundance of the order Chaetocerotales in the sediment is indicative of a pelagic bloom forming species *Chaetoceros gelidus*, which

is known to form particularly many resting stages (Booth et al., 2002; Chamnansinp et al., 2013). However, diatoms also made up a noteworthy proportion of the Heterokontophyta reads in the water column, adding to building evidence that indicates some cells stay present in the water column throughout the winter (Hoppe, 2022; Kvernvik et al., 2018; Vader et al., 2015). Dinoflagellates are considered to be the dominant component of the winter protist community, partially due to their mixotrophic characteristics. Interestingly, in the present study they were less dominant (in reads) than previously reported compared to Chlorophyta for example, hinting to a possible sampling bias of traditional (light microscopy-based) studies that underestimate the relevance of the picoplanktonic component of the pelagic community (MacKeigan et al., 2022).

The red and brown macroalgae composition was largely in agreement with published data from Kongsfjorden (Düsedau et al., 2024; Fredriksen et al., 2019, 2014), and four previously unrecorded species were detected as well. Macroalgae MOTUs made up a significant proportion of the sequence reads and species richness recovered by eDNA metabarcoding of both the water and sediment. In total, 29 macroalgae were detected to species level, including kelps, filamentous red and browns, and encrusting red algae. Many of these are well known in the fjord (e.g., *Saccharina latissima* and *Laminaria digitata*), while others have only been found at genus level (e.g., *Saundersella doloresiae*), or have no previous distribution data recorded in the fjord (e.g., *Ahnfeltia borealis* and *Boreolithothamnion lemoineae*). Recent research on macroalgae in the Arctic and North-Atlantic using eDNA metabarcoding of the 18S gene demonstrated eDNA as a useful tool for not only identify species but also determine the fate of macroalgae matter in sediments (Ørberg et al., 2023). Here, we show that the COI gene can also recover many brown and red macroalgae Arctic species from water and sediments and could be used in conjunction with other markers (e.g., Ortega et al., 2019), to detect similar patterns in Kongsfjorden. It is worth noting, that the identification of macroalgae using molecular approaches is generally challenging, because of their complex evolutionary history no universal protocol can be applied and they are highly underrepresented in the reference databases (Ortega et al., 2019; Saunders and McDevit, 2013, 2012). Most biodiversity assessments of this group in Kongsfjorden were therefore purely based on morphology (Fredriksen et al., 2019, 2014; Hop et al., 2012) but a recent DNA barcode survey revealed many overlooked and wrongly identified species (Düsedau et al., unpublished results). Significant regime and distribution shifts of macroalgal communities in Kongsfjorden were documented over the last three decades as a result of the rapidly changing environmental conditions in the fjord (Düsedau et al., 2024). For example, the Arctic endemic kelp *Laminaria solidungula*. It used to be rare at the sampling site 'Hansneset' (Bartsch et al., 2016; Hop et al., 2012), but was neither detected in the latest biomass sampling (Düsedau et

al., 2024) nor in our metabarcoding analysis. Both polar night and eDNA-based studies targeting Arctic macroalgae are scarce, and filling polar night data gaps on macroalgae is essential in understand these changes on a seasonal scale.

4.4 Marine metazoans

Kongsfjorden hosts a diverse metazoan community, for which many important biological processes occur during the polar night. Previous research have shown activities such as feeding in benthic-pelagic amphipods (Dischereit et al., 2024a) and fish (Berge et al., 2015a), spawning of benthic taxa and Arctic fish species (Geoffroy and Priou, 2020), as well as high growth rates in bivalves (Berge et al., 2015a) all occur during these dark months. In the present study, we were able to detect pelagic and benthic metazoan taxa across a wide range of phyla, functional groups and sizes including, zooplankton, benthic fauna, marine mammals and fish.

Earlier polar night studies have found that zooplankton communities are dominated in species richness by crustaceans, and in number and biomass by copepods in particular (Berge et al., 2020a). Small copepod species tend to be the most abundant (Berge et al., 2015a) as they do not migrate to deeper layers but stay active in surface water (Barth-Jensen et al., 2022), which was a pattern reflected in the relative read abundances in our study. *Microcalanus pusillus* was the second most abundant MOTU and the most abundant arthropod species in the water samples, followed by another small copepod species, *Oithona similis*. Both species were ubiquitous across the stations sampled (**Figure 4**). Interestingly, reads assigned to Annelida (e.g., polychaete species *Chaetozone setosa* and *Lumbrineris mixochaeta*) were the most dominant at almost every depth and station in the water eDNA. They are typically dominant in benthic fjord communities on Svalbard (Pawłowska et al., 2011; Włodarska-Kowalczyk and Pearson, 2004), as well as in the polar night in Kongsfjorden (Kędra et al., 2011). Many arctic polychaete species reproduce via pelagic larvae (Fetzer and Arntz, 2008), and the dominance of Annelida reads observed here in the water column could indicate a large reproductive event during the polar night and therefore the presence of their pelagic phases.

Benthic fauna communities are disproportionally less studied during the polar night than their pelagic counterparts (Berge et al., 2015b; Renaud et al., 2020). While some studies have indeed been conducted at this time of year, which include benthic metazoans (Berge et al., 2015a, 2015b; Pawłowska et al., 2011), many ecological knowledge gaps remain. We found that polychaetes were the most dominant in terms of reads and richness in our sediment samples (**Figure 4**). This is in line with a previous morphological study in Kongsfjorden, where they found that polychaetes dominated the shallow water benthic communities at the end of winter (Kędra et al., 2011). We also detected other key groups including anthozoans (e.g., *Urticina felina*), the abundant sea urchin *Strongylocentrotus droebachiensis* and benthic and

benthic-pelagic amphipods (*Anonyx sarsi*, *Gammarus* spp., *Orchominella minuta*). Additionally, we recovered many hyperbenthic species, which are predominantly crustaceans that inhabit the water just above the seafloor and perform migration to feed in pelagic parts of the water column (McGovern et al., 2018). These included the shrimp *Pandalous borealis* and *Lebbus polaris*, as well as the amphipod (or skeleton shrimp) *Caprella septentrionalis* which have previously been observed in January (McGovern et al., 2018; Renaud et al., 2020). Although we cannot distinguish between different life stages of these invertebrates using eDNA metabarcoding, this dataset provides important information on the diversity, distribution and community composition in a previously overlooked period.

Another salient find was the high number of vertebrate species that we were able to detect using the COI marker, rather than 12S which is commonly used in eDNA studies targeting these groups (e.g., Jensen et al., 2023; Marques et al., 2023; Westgaard et al., 2024). We recovered 16 species of fish, five marine mammals and two sea birds in the water samples, but no vertebrate MOTUs in the sediment. All of these species have previously been found in Svalbard waters and many in Kongsfjorden itself. Detection of marine mammals and seabirds is largely reliant of visual observations, while fish monitoring is reliant on trawls, all of which are hindered by the logistical challenges of sampling at this time of year (e.g., ice conditions and lack of daylight). Moreover, trawling can damage the benthos and be detrimental to the health of benthic communities (Jennings et al., 2001; Jørgensen et al., 2019). We demonstrate that eDNA has the potential to extend at least one method of monitoring of vertebrates to a year-round timeframe, and could be a non-invasive addition to summer monitoring programs that are already in place in Kongsfjorden. Indeed, eDNA has already been successfully combined with traditional sampling methods and human observations in other parts of the Arctic to increase the detection of both fish and marine mammals (Schjøtt et al., 2023; Westgaard et al., 2024). Furthermore, sequencing vertebrate-specific markers using the same eDNA extracts would no doubt increase the species missed by COI and allow for stronger conclusions to be drawn regarding their diversity and distribution.

4.5 Gelatinous Zooplankton in the polar night

Understanding of gelatinous zooplankton ecology in the Arctic is limited, including in Svalbard fjords and especially during the polar night. Evidence of overwintering by large scyphozoans and ctenophores has been found in the Chukchi Sea (Purcell et al., 2018), yet studies on the European side of the Arctic are lacking. In the present study, we recovered a high richness of GZP species present in Kongsfjorden during this period, with 19 species-level detections and a further three to genus-level recovered by eDNA and plankton nets combined. Additionally, we detected many more cnidarian MOTUs, which could only be assigned with low taxonomic resolution due to gaps in reference databases, hence potentially including further GZP taxa.

This is more than has been recovered previously in morphological zooplankton studies that included GZP in the summer. In a 20-year summer zooplankton monitoring study (1996 – 2016), using Multi-Net, Tucker Trawl and MIK net sampling, Hop et al., (2019) found 10 genera and species to be regular inhabitants of Kongsfjorden. In a polar night zooplankton study, Grenvald et al., (2016), reported six species as well as unidentified appendicularians, but in low abundances compared to crustaceans. The hydrozoan *Aglantha digitale*, and the ctenophores *Mertensia ovum* and *Beroe cucumis* were reported to be the most abundant GZP in the summer surveys, and the polar night survey did not report abundance data for individual species but GZP as a group. We detected many of the same taxa in the present study, with the notable exceptions of the small hydrozoan *Sminthea arctica* and appendicularians. Juvenile ctenophores were caught in the nets, likely including *M. ovum*, but we were unable to identify to a high resolution morphologically or confirm with COI barcoding. One explanation for the lower species richness in previous studies in Kongsfjorden is the sampling biases associated with using traditional plankton nets and trawls to sample GZP (Hosia et al., 2017). The fragility of their gelatinous bodies means that they are often destroyed, discarded or identified with low taxonomic resolution and grouped as “GZP” or “other”. Many species also have life stages such as planula larvae or benthic polyps which are easily missed and lead to underestimates of richness and distribution. Overall, we recovered a GZP community richer than was previously found with morphological surveys during daylight months, with many of the summertime GZP present during the polar night. Furthermore, the presence of juvenile ctenophores, which has also been observed in previous years (Berge et al., 2020a), suggests that reproduction regularly occurs during these dark months. However, without year-round monitoring that targets GZP, it is not possible to determine significant differences between the community present in the polar night and other periods. Nor is it currently possible to elucidate whether there has been a recent increase in GZP richness with ongoing Atlantification or whether the GZP diversity uncovered in the present study is typical of the fjord.

As expected, we recovered different GZP communities depending on the method used (**Figure 6**), with only five genera/species recovered by both methods. This is in line with a previous GZP study in Fram Strait, which found that eDNA, nets and optical surveys had some overlaps but also many unique detections, depending on the sampling equipment used (Murray et al., 2024). Morphological studies still provide many benefits, including abundance estimates for less-easily destroyed species and providing tissue for barcoding. However, we demonstrate here that the use of eDNA metabarcoding increased the number of GZP species detected by morphological methods alone. Furthermore, using eDNA to supplement morphological methods enabled us to detect cnidarians, such as hydroids, that have medusae stages representing an otherwise overlooked component of the Arctic GZP community. In

addition, by barcoding specimens caught in nets, we were able to confirm species identifications and provide regional-specific sequences to public reference databases, which can improve the accuracy of future eDNA detections. Overall, by combining both molecular and morphological sampling strategies, our understanding of the polar night GZP community in Kongsfjorden has increased significantly.

4.6 eDNA detection in turbid fjord waters

Biodiversity recovered from sampling eDNA in turbid waters can be negatively impacted by the presence of particulate organic matter and associated PCR-inhibitors. When filtering water-eDNA samples in the present study, we found visible sediment deposits on the filter membranes. Common strategies for reducing the impact of PCR-inhibitors in environmental samples is to either remove them from the DNA extract using specific DNA extraction kits, use a post-extraction inhibitor removal kit (Kumar et al., 2022) or including bovine albumin serum (BSA) in the PCR master mix (Albers et al., 2013). Based on the statistical comparison between sequencing outputs of treated and non-treated samples in the present study, we found that using a post-extraction PCR-inhibitor removal kit had no significant impact on the alpha diversity indices nor beta diversity. Our findings indicate that the inclusion of BSA was sufficient to reduce the impacts of potential PCR inhibitors associated with water turbidity, and the extra removal step was not necessary. Previous studies have found that extracting eDNA from the particles themselves results in high DNA yields can be a successful method for biodiversity surveys (Díaz et al., 2020). Furthermore, due to the binding of eDNA to suspended particulate matter, some studies have found significantly higher DNA yields in turbid marine waters than clear waters that smaller volumes of water are necessary to sample biodiversity in the region than in clear waters (Kumar et al., 2022).

4.7 eDNA as a tool for polar night surveys

With a relatively low number of environmental samples, we were able to detect many of the common eukaryotic groups and species that are known to inhabit Kongsfjorden and the surrounding area and detect new species for the fjord or even the entire archipelago. Morphological studies in the fjord typically involve specialized sampling methods targeting specific groups (e.g., benthic-pelagic trawls for fish, pelagic net sampling for zooplankton, and benthic grabs for benthos), that can be difficult to deploy in the polar night due to low visibility, and dangerous weather and ice conditions. As highlighted in our integrated survey targeting GZP, eDNA is a valuable tool for complementing morphological methods, but it has its own drawbacks and biases that lead to false negatives for example. One such issue is primer-related biases that mean even “universal” barcodes such as COI are unable to amplify some species (Wangensteen et al., 2018), and well-known gaps in public reference databases that

prevent high-resolution taxonomic identification in some taxa (Hestetun et al., 2020). Despite these limitations, eDNA-based surveys remain a highly valuable tool in the challenging conditions of the polar night, where light, wind and ice conditions often restrict other sampling possibilities.

5. Conclusion

Our findings highlight the potential of eDNA metabarcoding to produce a large amount of high-quality biodiversity data that encompasses different taxonomic and functional groups, from unicellular phytoplankton to large marine mammals, all from the same small volumes of water or sediment. The present study relied on a relatively limited sampling effort, but recovered many taxa known to inhabit the fjord and we were able to produce species lists for major functional groups that contribute to baseline data for the polar night. Understanding the patterns of diversity, community composition and distribution of marine organisms in the polar night is essential for monitoring the impacts of global climate change on sensitive Arctic marine ecosystems. Future eDNA monitoring in Kongsfjorden during the polar night could serve as a powerful tool for detecting more taxa as well as small-scale patterns with increased spatial coverage and frequency. Finally, including further environmental parameters and data such as weather events and fluorescence would allow for exploration into the drivers of diversity and community composition uncovered by eDNA metabarcoding.

Data availability statement

Net dataset is publicly available at: <https://doi.org/10.1594/PANGAEA.955899>

NCBI SRA archive of metabarcoding dataset: SUB14844940 (Data will be made public upon publication)

Acknowledgements

This study has been conducted in the framework of the Helmholtz Young Investigator Group “ARJEL – Arctic Jellies” with the project number VH-NG-1400, led by CH and funded by the Helmholtz Society and the Alfred Wegener Institute Helmholtz Centre for Polar and Marine Research. The sampling was conducted during the AWIPEV KOP-183 winter campaign entitled “Arctic gelatinous zooplankton in the Polar night”. A permit for this project was obtained and registered under Research in Svalbard RIS-11789. We thank the ARJEL team present during the campaign for all the sample collection in such challenging conditions. We are very grateful to the AWIPEV coordination for organizing our campaign, and to AWIPEV station leader Gregory Tran and logistics engineer Yohann Dulong for their skilful support on site. We are also thankful for the support of Kings Bay Marine Lab, in particular the engineer Marine Ilg and the captain Erlend Havenstrøm, for their assistance during sampling with the MS Teisten.

Declaration of interests

The authors declare that they have no known competing financial interests or personal relationships that could have appeared to influence the work reported in this paper.

References

- Albers, C.N., Jensen, A., Bælum, J., Jacobsen, C.S., 2013. Inhibition of DNA Polymerases Used in Q-PCR by Structurally Different Soil-Derived Humic Substances. *Geomicrobiology Journal* 30, 675–681. <https://doi.org/10.1080/01490451.2012.758193>
- Alvarez, A.J., Khanna, M., Toranzos, G.A., Stotzky, G., 1998. Amplification of DNA bound on clay minerals. *Molecular Ecology* 7, 775–778. <https://doi.org/10.1046/j.1365-294x.1998.00339.x>
- Angulo-Preckler, C., Turon, M., Præbel, K., Avila, C., Wangensteen, O.S., 2023. Spatio-temporal patterns of eukaryotic biodiversity in shallow hard-bottom communities from the West Antarctic Peninsula revealed by DNA metabarcoding. *Diversity and Distributions* n/a. <https://doi.org/10.1111/ddi.13703>
- Antich, A., Palacín, C., Cebrian, E., Golo, R., Wangensteen, O.S., Turon, X., 2021. Marine biomonitoring with eDNA: Can metabarcoding of water samples cut it as a tool for surveying benthic communities? *Molecular Ecology* 30, 3175–3188. <https://doi.org/10.1111/mec.15641>
- Antich González, A., Palacín, C., Xavier, T., Wangensteen, O.S., 2022. DnoisE: distance denoising by entropy. An open-source parallelizable alternative for denoising sequence datasets [PeerJ].
- Barnett, D., Arts, I., Penders, J., 2021. microViz: an R package for microbiome data visualization and statistics. *JOSS* 6, 3201. <https://doi.org/10.21105/joss.03201>
- Barth-Jensen, C., Daase, M., Ormańczyk, M.R., Varpe, Ø., Kwaśniewski, S., Svensen, C., 2022. High abundances of small copepods early developmental stages and nauplii strengthen the perception of a non-dormant Arctic winter. *Polar Biol* 45, 675–690. <https://doi.org/10.1007/s00300-022-03025-4>
- Bartsch, I., Paar, M., Fredriksen, S., Schwanitz, M., Daniel, C., Hop, H., Wiencke, C., 2016. Changes in kelp forest biomass and depth distribution in Kongsfjorden, Svalbard, between 1996–1998 and 2012–2014 reflect Arctic warming. *Polar Biol* 39, 2021–2036. <https://doi.org/10.1007/s00300-015-1870-1>
- Basedow, S.L., Eiane, K., Tverberg, V., Spindler, M., 2004. Advection of zooplankton in an Arctic fjord (Kongsfjorden, Svalbard). *Estuarine, Coastal and Shelf Science* 60, 113–124. <https://doi.org/10.1016/j.ecss.2003.12.004>
- Berge, J., Daase, M., Hobbs, L., Falk-Petersen, S., Darnis, G., Søreide, J.E., 2020a. Zooplankton in the Polar Night, in: Berge, J., Johnsen, G., Cohen, J.H. (Eds.), *POLAR NIGHT Marine Ecology: Life and Light in the Dead of Night*. Springer International Publishing, Cham, pp. 113–159. https://doi.org/10.1007/978-3-030-33208-2_5
- Berge, J., Daase, M., Renaud, P.E., Ambrose, W.G., Darnis, G., Last, K.S., Leu, E., Cohen, J.H., Johnsen, G., Moline, M.A., Cottier, F., Varpe, Ø., Shunatova, N., Bałazy, P., Morata, N., Massabuau, J.-C., Falk-Petersen, S., Kosobokova, K., Hoppe, C.J.M., Węśławski, J.M., Kukliński, P., Legeżyńska, J., Nikishina, D., Cusa, M., Kędra, M., Włodarska-Kowalczyk, M., Vogedes, D., Camus, L., Tran, D., Michaud, E., Gabrielsen, T.M., Granovitch, A., Gonchar, A., Krapp, R., Callesen, T.A., 2015a. Unexpected Levels of Biological Activity during the Polar Night Offer New Perspectives on a Warming Arctic. *Current Biology* 25, 2555–2561. <https://doi.org/10.1016/j.cub.2015.08.024>
- Berge, J., Johnsen, G., Cohen, J.H., 2020b. Introduction, in: Berge, J., Johnsen, G., Cohen, J.H. (Eds.), *POLAR NIGHT Marine Ecology: Life and Light in the Dead of Night*. Springer International Publishing, Cham, pp. 1–15. https://doi.org/10.1007/978-3-030-33208-2_1
- Berge, J., Renaud, P.E., Darnis, G., Cottier, F., Last, K., Gabrielsen, T.M., Johnsen, G., Seuthe, L., Wesławski, J.M., Leu, E., Moline, M., Nahrgang, J., Søreide, J.E., Varpe, Ø., Lønne, O.J., Daase, M., Falk-Petersen, S., 2015b. In the dark: A review of ecosystem processes during the Arctic polar night. *Progress in Oceanography*,

- Overarching perspectives of contemporary and future ecosystems in the Arctic Ocean 139, 258–271. <https://doi.org/10.1016/j.pocean.2015.08.005>
- Beule, L., Karlovsky, P., 2020. Improved normalization of species count data in ecology by scaling with ranked subsampling (SRS): application to microbial communities. *PeerJ* 8, e9593. <https://doi.org/10.7717/peerj.9593>
- Bianchi, T.S., Arndt, S., Austin, W.E.N., Benn, D.I., Bertrand, S., Cui, X., Faust, J.C., Kozirowska-Makuch, K., Moy, C.M., Savage, C., Smeaton, C., Smith, R.W., Syvitski, J., 2020. Fjords as Aquatic Critical Zones (ACZs). *Earth-Science Reviews* 203, 103145. <https://doi.org/10.1016/j.earscirev.2020.103145>
- Bischof, K., Convey, P., Duarte, P., Gattuso, J.-P., Granberg, M., Hop, H., Hoppe, C., Jiménez, C., Lisitsyn, L., Martinez, B., Roleda, M.Y., Thor, P., Wiktor, J.M., Gabrielsen, G.W., 2019. Kongsfjorden as Harbinger of the Future Arctic: Knowns, Unknowns and Research Priorities, in: Hop, H., Wiencke, C. (Eds.), *The Ecosystem of Kongsfjorden, Svalbard*. Springer International Publishing, Cham, pp. 537–562. https://doi.org/10.1007/978-3-319-46425-1_14
- Booth, B.C., Larouche, P., Bélanger, S., Klein, B., Amiel, D., Mei, Z.-P., 2002. Dynamics of *Chaetoceros socialis* blooms in the North Water. *Deep Sea Research Part II: Topical Studies in Oceanography, The International North Water Polynya Study* 49, 5003–5025. [https://doi.org/10.1016/S0967-0645\(02\)00175-3](https://doi.org/10.1016/S0967-0645(02)00175-3)
- Bouillon, J., Gravili, C., Pagès, F., Gili, J.-M., Boero, F., 2006. *An introduction to Hydrozoa*. Muséum national d'Histoire naturelle, Paris.
- Boyer, F., Mercier, C., Bonin, A., Le Bras, Y., Taberlet, P., Coissac, E., 2016. obitools: a unix-inspired software package for DNA metabarcoding. *Molecular Ecology Resources* 16, 176–182. <https://doi.org/10.1111/1755-0998.12428>
- Brinkmann, I., Schweizer, M., Singer, D., Quinchard, S., Barras, C., Bernhard, J.M., Filipsson, H.L., 2023. Through the eDNA looking glass: Responses of fjord benthic foraminiferal communities to contrasting environmental conditions. *Journal of Eukaryotic Microbiology* 70, e12975. <https://doi.org/10.1111/jeu.12975>
- Buchner, D., Leese, F., 2020. BOLDigger – a Python package to identify and organise sequences with the Barcode of Life Data systems. *Metabarcoding and Metagenomics* 4, e53535. <https://doi.org/10.3897/mbmg.4.53535>
- Chamnansinp, A., Li, Y., Lundholm, N., Moestrup, Ø., 2013. Global diversity of two widespread, colony-forming diatoms of the marine plankton, *haetoceros socialis* (syn. *radians*) and *haetoceros gelidus* sp. nov. *Journal of Phycology* 49, 1128–1141. <https://doi.org/10.1111/jpy.12121>
- Cohen, J., Zhang, X., Francis, J., Jung, T., Kwok, R., Overland, J., Ballinger, T.J., Bhatt, U.S., Chen, H.W., Coumou, D., Feldstein, S., Gu, H., Handorf, D., Henderson, G., Ionita, M., Kretschmer, M., Laliberte, F., Lee, S., Linderholm, H.W., Maslowski, W., Peings, Y., Pfeiffer, K., Rigor, I., Semmler, T., Stroeve, J., Taylor, P.C., Vavrus, S., Vihma, T., Wang, S., Wendisch, M., Wu, Y., Yoon, J., 2020. Divergent consensus on Arctic amplification influence on midlatitude severe winter weather. *Nat. Clim. Chang.* 10, 20–29. <https://doi.org/10.1038/s41558-019-0662-y>
- Cordier, T., Angeles, I.B., Henry, N., Lejzerowicz, F., Berney, C., Morard, R., Brandt, A., Cambon-Bonavita, M.-A., Guidi, L., Lombard, F., Arbizu, P.M., Massana, R., Orejas, C., Poulain, J., Smith, C.R., Wincker, P., Arnaud-Haond, S., Gooday, A.J., de Vargas, C., Pawlowski, J., 2022. Patterns of eukaryotic diversity from the surface to the deep-ocean sediment. *Science Advances* 8, eabj9309. <https://doi.org/10.1126/sciadv.abj9309>
- Cottier, F., Porter, M., 2020. The Marine Physical Environment During the Polar Night, in: Berge, J., Johnsen, G., Cohen, J.H. (Eds.), *POLAR NIGHT Marine Ecology: Life and Light in the Dead of Night*. Springer International Publishing, Cham, pp. 17–36. https://doi.org/10.1007/978-3-030-33208-2_2
- Cottier, F., Skogseth, R., David, D., Berge, J., 2019. Temperature time-series in Svalbard fjords. A contribution from the “Integrated Marine Observatory Partnership.” Svalbard

- Integrated Arctic Earth Observing System, Longyearbyen.
<https://doi.org/10.5281/zenodo.4778378>
- Cottier, F., Tverberg, V., Inall, M., Svendsen, H., Nilsen, F., Griffiths, C., 2005. Water mass modification in an Arctic fjord through cross-shelf exchange: The seasonal hydrography of Kongsfjorden, Svalbard. *Journal of Geophysical Research: Oceans* 110. <https://doi.org/10.1029/2004JC002757>
- Cottier, F.R., Nilsen, F., Inall, M.E., Gerland, S., Tverberg, V., Svendsen, H., 2007. Wintertime warming of an Arctic shelf in response to large-scale atmospheric circulation. *Geophysical Research Letters* 34. <https://doi.org/10.1029/2007GL029948>
- Dalpadado, P., Hop, H., Rønning, J., Pavlov, V., Sperfeld, E., Buchholz, F., Rey, A., Wold, A., 2016. Distribution and abundance of euphausiids and pelagic amphipods in Kongsfjorden, Isfjorden and Rijpfjorden (Svalbard) and changes in their relative importance as key prey in a warming marine ecosystem. *Polar Biol* 39, 1765–1784. <https://doi.org/10.1007/s00300-015-1874-x>
- Dankworth, M., Heinrich, S., Fredriksen, S., Bartsch, I., 2020. DNA barcoding and mucilage ducts in the stipe reveal the presence of *Hedophyllum nigripes* (Laminariales, Phaeophyceae) in Kongsfjorden (Spitsbergen). *Journal of Phycology*. <https://doi.org/10.1111/jpy.13012>
- De Rovere, F., Langone, L., Schroeder, K., Miserocchi, S., Giglio, F., Aliani, S., Chiggiato, J., 2022. Water Masses Variability in Inner Kongsfjorden (Svalbard) During 2010–2020. *Front. Mar. Sci.* 9. <https://doi.org/10.3389/fmars.2022.741075>
- de Vincenzi, G., Parisi, I., Torri, M., Papale, E., Mazzola, S., Nuth, C., Buscaino, G., 2019. Influence of environmental parameters on the use and spatiotemporal distribution of the vocalizations of bearded seals (*Erignathus barbatus*) in Kongsfjorden, Spitsbergen. *Polar Biol* 42, 1241–1254. <https://doi.org/10.1007/s00300-019-02514-3>
- Díaz, C., Wege, F.-F., Tang, C.Q., Crampton-Platt, A., Rüdell, H., Eilebrecht, E., Koschorreck, J., 2020. Aquatic suspended particulate matter as source of eDNA for fish metabarcoding. *Sci Rep* 10, 14352. <https://doi.org/10.1038/s41598-020-71238-w>
- Dischereit, A., Beermann, J., Lebreton, B., Wangensteen, O.S., Neuhaus, S., Havermans, C., 2024a. DNA metabarcoding reveals a diverse, omnivorous diet of Arctic amphipods during the polar night, with jellyfish and fish as major prey. *Front. Mar. Sci.* 11. <https://doi.org/10.3389/fmars.2024.1327650>
- Dischereit, A., Throm, J.K., Werner, K.-M., Neuhaus, S., Havermans, C., 2024b. A belly full of jelly? DNA metabarcoding shows evidence for gelatinous zooplankton predation by several fish species in Greenland waters. *Royal Society Open Science*. <https://doi.org/10.1098/rsos.240797>
- Dragańska-Deja, K., Stoń-Egiert, J., Wiktor, J., Ostrowska, M., 2024. Productivity of Spitsbergen fjords ecosystems in summer—Spatial changes of in situ primary production in Kongsfjorden and Hornsund in the period 1994–2019. *Ecology and Evolution* 14, e11607. <https://doi.org/10.1002/ece3.11607>
- Düsedau, L., Bartsch, I., Weinberger, F., Fredriksen, S., Bull, R., Künzel, S., Savoie, A., unpublished results. Novel molecular biodiversity assessment reveals high cryptic biodiversity in marine macroalgae from Kongsfjorden (Svalbard).
- Düsedau, L., Fredriksen, S., Brand, M., Fischer, P., Karsten, U., Bischof, K., Savoie, A., Bartsch, I., 2024. Kelp forest community structure and demography in Kongsfjorden (Svalbard) across 25 years of Arctic warming. *Ecology and Evolution* 14, e11606. <https://doi.org/10.1002/ece3.11606>
- Fetzer, I., Arntz, W., 2008. Reproductive strategies of benthic invertebrates in the Kara Sea (Russian Arctic): adaptation of reproduction modes to cold water. *Mar. Ecol. Prog. Ser.* 356, 189–202. <https://doi.org/10.3354/meps07271>
- Folmer, O., Black, M., Hoeh, W., Lutz, R., Vrijenhoek, R., 1994. DNA primers for amplification of mitochondrial cytochrome c oxidase subunit I from diverse metazoan invertebrates. *Molecular Marine Biology and Biotechnology* 3, 294–299.

- Francis, J.A., Vavrus, S.J., 2012. Evidence linking Arctic amplification to extreme weather in mid-latitudes. *Geophysical Research Letters* 39. <https://doi.org/10.1029/2012GL051000>
- Fredriksen, S., Bartsch, I., Wiencke, C., 2014. New additions to the benthic marine flora of Kongsfjorden, western Svalbard, and comparison between 1996/1998 and 2012/2013. *Botanica Marina* 57, 203–216. <https://doi.org/10.1515/bot-2013-0119>
- Fredriksen, S., Karsten, U., Bartsch, I., Woelfel, J., Koblowsky, M., Schumann, R., Moy, S.R., Steneck, R.S., Wiktor, J.M., Hop, H., Wiencke, C., 2019. Biodiversity of Benthic Macro- and Microalgae from Svalbard with Special Focus on Kongsfjorden, in: Hop, H., Wiencke, C. (Eds.), *The Ecosystem of Kongsfjorden, Svalbard*. Springer International Publishing, Cham, pp. 331–371. https://doi.org/10.1007/978-3-319-46425-1_9
- Frøslev, T.G., Kjølner, R., Bruun, H.H., Ejrnæs, R., Brunbjerg, A.K., Pietroni, C., Hansen, A.J., 2017. Algorithm for post-clustering curation of DNA amplicon data yields reliable biodiversity estimates. *Nat Commun* 8, 1188. <https://doi.org/10.1038/s41467-017-01312-x>
- Geller, J., Meyer, C., Parker, M., Hawk, H., 2013. Redesign of PCR primers for mitochondrial cytochrome c oxidase subunit I for marine invertebrates and application in all-taxa biotic surveys. *Molecular Ecology Resources* 13, 851–861. <https://doi.org/10.1111/1755-0998.12138>
- Geoffroy, M., Priou, P., 2020. Fish Ecology During the Polar Night, in: Berge, J., Johnsen, G., Cohen, J.H. (Eds.), *POLAR NIGHT Marine Ecology: Life and Light in the Dead of Night*. Springer International Publishing, Cham, pp. 181–216. https://doi.org/10.1007/978-3-030-33208-2_7
- Gerland, S., Pavlova, O., Divine, D., Negrel, J., Dahlke, S., Johansson, A.M., Maturilli, M., Semmling, M., 2020. Long-term monitoring of landfast sea ice extent and thickness in Kongsfjorden, and related applications (FastIce) [WWW Document]. SESS report 2019. URL https://sios-svalbard.org/sites/sios-svalbard.org/files/common/SESS_2019_06_FastIce.pdf (accessed 9.25.24).
- Gluchowska, M., Kwasniewski, S., Prominska, A., Ōlszewska, A., Goszczko, I., Falk-Petersen, S., Hop, H., Weslawski, J.M., 2016. Zooplankton in Svalbard fjords on the Atlantic–Arctic boundary. *Polar Biol* 39, 1785–1802. <https://doi.org/10.1007/s00300-016-1991-1>
- Gorska, N., Schmidt, B., Węslawski, J.M., Grabowski, M., Dragan-Górska, A., Szczucka, J., Beszczynska-Möller, A., 2023. Fish in Kongsfjorden under the influence of climate warming. *Front. Mar. Sci.* 10. <https://doi.org/10.3389/fmars.2023.1213081>
- Grenvald, J.C., Callesen, T.A., Daase, M., Hobbs, L., Darnis, G., Renaud, P.E., Cottier, F., Nielsen, T.G., Berge, J., 2016. Plankton community composition and vertical migration during polar night in Kongsfjorden. *Polar Biol* 39, 1879–1895. <https://doi.org/10.1007/s00300-016-2015-x>
- Hansson, L., Moeslund, O., Kiørboe, T., Riisgård, H., 2005. Clearance rates of jellyfish and their potential predation impact on zooplankton and fish larvae in a neritic ecosystem (Limfjorden, Denmark). *Mar. Ecol. Prog. Ser.* 304, 117–131. <https://doi.org/10.3354/meps304117>
- Hegseth, E.N., Assmy, P., Wiktor, J.M., Wiktor, J., Kristiansen, S., Leu, E., Tverberg, V., Gabrielsen, T.M., Skogseth, R., Cottier, F., 2019. Phytoplankton Seasonal Dynamics in Kongsfjorden, Svalbard and the Adjacent Shelf, in: Hop, H., Wiencke, C. (Eds.), *The Ecosystem of Kongsfjorden, Svalbard*. Springer International Publishing, Cham, pp. 173–227. https://doi.org/10.1007/978-3-319-46425-1_6
- Hestetun, J.T., Bye-Ingebrigtsen, E., Nilsson, R.H., Glover, A.G., Johansen, P.-O., Dahlgren, T.G., 2020. Significant taxon sampling gaps in DNA databases limit the operational use of marine macrofauna metabarcoding. *Mar. Biodivers.* 50, 70. <https://doi.org/10.1007/s12526-020-01093-5>

- Hewitt, J.E., Thrush, S.F., Halliday, J., Duffy, C., 2005. The Importance of Small-Scale Habitat Structure for Maintaining Beta Diversity. *Ecology* 86, 1619–1626. <https://doi.org/10.1890/04-1099>
- Holman, L.E., de Bruyn, M., Creer, S., Carvalho, G., Robidart, J., Rius, M., 2019. Detection of introduced and resident marine species using environmental DNA metabarcoding of sediment and water. *Sci Rep* 9, 11559. <https://doi.org/10.1038/s41598-019-47899-7>
- Hop, H., Falk-Petersen, S., Svendsen, H., Kwasniewski, S., Pavlov, V., Pavlova, O., Søreide, J.E., 2006. Physical and biological characteristics of the pelagic system across Fram Strait to Kongsfjorden. *Progress in Oceanography, Structure and function of contemporary food webs on Arctic shelves: a pan-Arctic comparison* 71, 182–231. <https://doi.org/10.1016/j.pocean.2006.09.007>
- Hop, H., Wiencke, C., Vögele, B., Kovaltchouk, N.A., 2012. Species composition, zonation, and biomass of marine benthic macroalgae in Kongsfjorden, Svalbard. *Botanica Marina* 55, 399–414. <https://doi.org/10.1515/bot-2012-0097>
- Hop, H., Wold, A., Vihtakari, M., Assmy, P., Kuklinski, P., Kwasniewski, S., Griffith, G.P., Pavlova, O., Duarte, P., Steen, H., 2023. Tidewater glaciers as “climate refugia” for zooplankton-dependent food web in Kongsfjorden, Svalbard. *Front. Mar. Sci.* 10. <https://doi.org/10.3389/fmars.2023.1161912>
- Hop, H., Wold, A., Vihtakari, M., Daase, M., Kwasniewski, S., Gluchowska, M., Lischka, S., Buchholz, F., Falk-Petersen, S., 2019. Zooplankton in Kongsfjorden (1996–2016) in Relation to Climate Change, in: Hop, H., Wiencke, C. (Eds.), *The Ecosystem of Kongsfjorden, Svalbard*. Springer International Publishing, Cham, pp. 229–300. https://doi.org/10.1007/978-3-319-46425-1_7
- Hoppe, C.J.M., 2022. Always ready? Primary production of Arctic phytoplankton at the end of the polar night. *Limnology and Oceanography Letters* 7, 167–174. <https://doi.org/10.1002/lol2.10222>
- Hosia, A., Falkenhaus, T., Baxter, E.J., Pagès, F., 2017. Abundance, distribution and diversity of gelatinous predators along the northern Mid-Atlantic Ridge: A comparison of different sampling methodologies. *PLoS ONE* 12, e0187491. <https://doi.org/10.1371/journal.pone.0187491>
- Ingvaldsen, R.B., Eriksen, E., Gjørseter, H., Engås, A., Schuppe, B.K., Assmann, K.M., Cannaby, H., Dalpadado, P., Bluhm, B.A., 2023. Under-ice observations by trawls and multi-frequency acoustics in the Central Arctic Ocean reveals abundance and composition of pelagic fauna. *Sci Rep* 13, 1000. <https://doi.org/10.1038/s41598-023-27957-x>
- Isaksen, K., Nordli, Ø., Ivanov, B., Køltzow, M.A.Ø., Aaboe, S., Gjeltén, H.M., Mezghani, A., Eastwood, S., Førland, E., Benestad, R.E., Hanssen-Bauer, I., Brækkan, R., Sviashchennikov, P., Demin, V., Revina, A., Karandasheva, T., 2022. Exceptional warming over the Barents area. *Sci Rep* 12, 9371. <https://doi.org/10.1038/s41598-022-13568-5>
- Jennings, S., Pinnegar, J.K., Polunin, N.V.C., Warr, K.J., 2001. Impacts of trawling disturbance on the trophic structure of benthic invertebrate communities. *Marine Ecology Progress Series* 213, 127–142. <https://doi.org/10.3354/meps213127>
- Jensen, M.R., Høgslund, S., Knudsen, S.W., Nielsen, J., Møller, P.R., Rysgaard, S., Thomsen, P.F., 2023. Distinct latitudinal community patterns of Arctic marine vertebrates along the East Greenlandic coast detected by environmental DNA. *Diversity and Distributions* 29, 316–334. <https://doi.org/10.1111/ddi.13665>
- Jeunen, G.-J., Knapp, M., Spencer, H.G., Lamare, M.D., Taylor, H.R., Stat, M., Bunce, M., Gemmell, N.J., 2019. Environmental DNA (eDNA) metabarcoding reveals strong discrimination among diverse marine habitats connected by water movement. *Molecular Ecology Resources* 19, 426–438. <https://doi.org/10.1111/1755-0998.12982>
- Jørgensen, L.L., Primicerio, R., Ingvaldsen, R.B., Fossheim, M., Strelkova, N., Thangstad, T.H., Manushin, I., Zakharov, D., 2019. Impact of multiple stressors on sea bed fauna

- in a warming Arctic. *Marine Ecology Progress Series* 608, 1–12.
<https://doi.org/10.3354/meps12803>
- Kędra, M., Legeżyńska, J., Walkusz, W., 2011. Shallow winter and summer macrofauna in a high Arctic fjord (79° N, Spitsbergen). *Mar Biodiv* 41, 425–439.
<https://doi.org/10.1007/s12526-010-0066-8>
- Kumar, G., Farrell, E., Reaume, A.M., Eble, J.A., Gaither, M.R., 2022. One size does not fit all: Tuning eDNA protocols for high- and low-turbidity water sampling. *Environmental DNA* 4, 167–180. <https://doi.org/10.1002/edn3.235>
- Kvernvik, A.C., Hoppe, C.J.M., Lawrenz, E., Prášil, O., Greenacre, M., Wiktor, J.M., Leu, E., 2018. Fast reactivation of photosynthesis in arctic phytoplankton during the polar night1. *Journal of Phycology* 54, 461–470. <https://doi.org/10.1111/jpy.12750>
- Lacoursière-Roussel, A., Howland, K., Normandeau, E., Grey, E.K., Archambault, P., Deiner, K., Lodge, D.M., Hernandez, C., Leduc, N., Bernatchez, L., 2018. eDNA metabarcoding as a new surveillance approach for coastal Arctic biodiversity. *Ecology and Evolution* 8, 7763–7777. <https://doi.org/10.1002/ece3.4213>
- Last, K.S., Hobbs, L., Berge, J., Brierley, A.S., Cottier, F., 2016. Moonlight Drives Ocean-Scale Mass Vertical Migration of Zooplankton during the Arctic Winter. *Current Biology* 26, 244–251. <https://doi.org/10.1016/j.cub.2015.11.038>
- Leduc, N., Lacoursière-Roussel, A., Howland, K.L., Archambault, P., Sevellec, M., Normandeau, E., Dispas, A., Winkler, G., McKindsey, C.W., Simard, N., Bernatchez, L., 2019. Comparing eDNA metabarcoding and species collection for documenting Arctic metazoan biodiversity. *Environmental DNA* 1, 342–358.
<https://doi.org/10.1002/edn3.35>
- Leray, M., Yang, J.Y., Meyer, C.P., Mills, S.C., Agudelo, N., Ranwez, V., Boehm, J.T., Machida, R.J., 2013. A new versatile primer set targeting a short fragment of the mitochondrial COI region for metabarcoding metazoan diversity: application for characterizing coral reef fish gut contents. *Frontiers in Zoology* 10, 34.
<https://doi.org/10.1186/1742-9994-10-34>
- Licandro, P., Carré, C., Lindsay, D.J., 2017. Cnidaria: Colonial Hydrozoa (Siphonophorae), in: Castellani, C., Edwards, M. (Eds.), *Marine Plankton: A Practical Guide to Ecology, Methodology, and Taxonomy*. Oxford University Press, p. 0.
<https://doi.org/10.1093/oso/9780199233267.003.0019>
- Licandro, P., Lindsay, D.J., 2017. Ctenophora, in: *Marine Plankton: A Practical Guide to Ecology, Methodology, and Taxonomy*. Oxford University Press.
- MacKeigan, P.W., Garner, R.E., Monchamp, M.-È., Walsh, D.A., Onana, V.E., Kraemer, S.A., Pick, F.R., Beisner, B.E., Agbeti, M.D., da Costa, N.B., Shapiro, B.J., Gregory-Eaves, I., 2022. Comparing microscopy and DNA metabarcoding techniques for identifying cyanobacteria assemblages across hundreds of lakes. *Harmful Algae* 113, 102187. <https://doi.org/10.1016/j.hal.2022.102187>
- Mahé, F., Czech, L., Stamatakis, A., Quince, C., de Vargas, C., Dunthorn, M., Rognes, T., 2021. Swarm v3: towards tera-scale amplicon clustering. *Bioinformatics* 38, 267–269.
<https://doi.org/10.1093/bioinformatics/btab493>
- Marquardt, M., Vader, A., Stübner, E.I., Reigstad, M., Gabrielsen, T.M., 2016. Strong Seasonality of Marine Microbial Eukaryotes in a High-Arctic Fjord (Isfjorden, in West Spitsbergen, Norway) [WWW Document]. <https://doi.org/10.1128/AEM.03208-15>
- Marques, V., Hassler, C., Deiner, K., Meier, E., Valentini, A., Albouy, C., Pellissier, L., 2023. Environmental drivers of eukaryotic plankton and fish biodiversity in an Arctic fjord. *Polar Biol* 46, 1083–1096. <https://doi.org/10.1007/s00300-023-03187-9>
- Martin, M., 2011. Cutadapt removes adapter sequences from high-throughput sequencing reads. *EMBnet.journal* 17, 10–12. <https://doi.org/10.14806/ej.17.1.200>
- Mazurkiewicz, M., Pawłowska, J., Barrenechea Angeles, I.A., Grzelak, K., Deja, K., Zaborska, A., Pawłowski, J., Włodarska-Kowalczyk, M., 2024. Sediment DNA metabarcoding and morphology provide complementary insight into macrofauna and meiobenthos response to environmental gradients in an Arctic glacial fjord. *Marine Environmental Research* 106552. <https://doi.org/10.1016/j.marenvres.2024.106552>

- McGovern, M., Berge, J., Szymczycha, B., Weęsławski, J., Renaud, P., 2018. Hyperbenthic food-web structure in an Arctic fjord. *Mar. Ecol. Prog. Ser.* 603, 29–46. <https://doi.org/10.3354/meps12713>
- McMurdie, P.J., Holmes, S., 2013. phyloseq: An R Package for Reproducible Interactive Analysis and Graphics of Microbiome Census Data. *PLOS ONE* 8, e61217. <https://doi.org/10.1371/journal.pone.0061217>
- Molis, M., Beuchel, F., Laudien, J., Włodarska-Kowalczyk, M., Buschbaum, C., 2019. Ecological Drivers of and Responses by Arctic Benthic Communities, with an Emphasis on Kongsfjorden, Svalbard, in: Hop, H., Wiencke, C. (Eds.), *The Ecosystem of Kongsfjorden, Svalbard*. Springer International Publishing, Cham, pp. 423–481. https://doi.org/10.1007/978-3-319-46425-1_11
- Murray, A., Præbel, K., Desiderato, A., Auel, H., Havermans, C., 2023. Phylogeography and molecular diversity of two highly abundant *Themisto* amphipod species in a rapidly changing Arctic Ocean. *Ecology and Evolution* 13, e10359. <https://doi.org/10.1002/ece3.10359>
- Murray, A., Priest, T., Antich, A., von Appen, W.-J., Neuhaus, S., Havermans, C., 2024. Investigating pelagic biodiversity and gelatinous zooplankton communities in the rapidly changing European Arctic: An eDNA metabarcoding survey. *Environmental DNA* 6, e569. <https://doi.org/10.1002/edn3.569>
- Nascimento, F.J.A., Lallias, D., Bik, H.M., Creer, S., 2018. Sample size effects on the assessment of eukaryotic diversity and community structure in aquatic sediments using high-throughput sequencing. *Sci Rep* 8, 11737. <https://doi.org/10.1038/s41598-018-30179-1>
- Oksanen, J., F., Blanchet, G., Friendly, M., Kindt, R., Legendre, P., McGlinn, D., Minchin, P.R., O'hara, R.B., Simpson, G.L., Solymos, P., Stevens, M.H.H., 2019. *Vegan: community ecology package (version 2.5-6)*. The Comprehensive R Archive Network.
- Ørberg, S.B., Duarte, C.M., Geraldi, N.R., Sejr, M.K., Wegeberg, S., Hansen, J.L.S., Krause-Jensen, D., 2023. Prevalent fingerprint of marine macroalgae in arctic surface sediments. *Science of The Total Environment* 898, 165507. <https://doi.org/10.1016/j.scitotenv.2023.165507>
- Ortega, A., Geraldi, N.R., Alam, I., Kamau, A.A., Acinas, S.G., Logares, R., Gasol, J.M., Massana, R., Krause-Jensen, D., Duarte, C.M., 2019. Important contribution of macroalgae to oceanic carbon sequestration. *Nat. Geosci.* 12, 748–754. <https://doi.org/10.1038/s41561-019-0421-8>
- Paknia, O., Rajaei Sh., H., Koch, A., 2015. Lack of well-maintained natural history collections and taxonomists in megadiverse developing countries hampers global biodiversity exploration. *Org Divers Evol* 15, 619–629. <https://doi.org/10.1007/s13127-015-0202-1>
- Pantiukhin, D., Verhaegen, G., Havermans, C., 2024. Pan-Arctic distribution modeling reveals climate-change-driven poleward shifts of major gelatinous zooplankton species. *Limnology and Oceanography* 69, 1316–1334. <https://doi.org/10.1002/lno.12568>
- Pawłowska, J., Włodarska-Kowalczyk, M., Zajączkowski, M., Nygård, H., Berge, J., 2011. Seasonal variability of meio- and macrobenthic standing stocks and diversity in an Arctic fjord (Adventfjorden, Spitsbergen). *Polar Biol* 34, 833–845. <https://doi.org/10.1007/s00300-010-0940-7>
- Pawlowski, J., Bruce, K., Panksep, K., Aguirre, F.I., Amalfitano, S., Apothéoz-Perret-Gentil, L., Baussant, T., Bouchez, A., Carugati, L., Cermakova, K., Cordier, T., Corinaldesi, C., Costa, F.O., Danovaro, R., Dell'Anno, A., Duarte, S., Eisendle, U., Ferrari, B.J.D., Frontalini, F., Frühe, L., Haegerbaeumer, A., Kisand, V., Krolicka, A., Lanzén, A., Leese, F., Lejzerowicz, F., Lyautey, E., Maček, I., Sagova-Marečková, M., Pearman, J.K., Pochon, X., Stoeck, T., Vivien, R., Weigand, A., Fazi, S., 2022. Environmental DNA metabarcoding for benthic monitoring: A review of sediment sampling and DNA extraction methods. *Science of The Total Environment* 818, 151783. <https://doi.org/10.1016/j.scitotenv.2021.151783>

- Pearman, J.K., Keeley, N.B., Wood, S.A., Laroche, O., Zaiko, A., Thomson-Laing, G., Biessy, L., Atalah, J., Pochon, X., 2020. Comparing sediment DNA extraction methods for assessing organic enrichment associated with marine aquaculture. *PeerJ* 8, e10231. <https://doi.org/10.7717/peerj.10231>
- Pithan, F., Mauritsen, T., 2014. Arctic amplification dominated by temperature feedbacks in contemporary climate models. *Nature Geosci* 7, 181–184. <https://doi.org/10.1038/ngeo2071>
- Polyakov, I.V., Alkire, M.B., Bluhm, B.A., Brown, K.A., Carmack, E.C., Chierici, M., Danielson, S.L., Ellingsen, I., Ershova, E.A., Gårdfeldt, K., Ingvaldsen, R.B., Pnyushkov, A.V., Slagstad, D., Wassmann, P., 2020. Borealization of the Arctic Ocean in Response to Anomalous Advection From Sub-Arctic Seas. *Frontiers in Marine Science* 7.
- Polyakov, I.V., Ingvaldsen, R.B., Pnyushkov, A.V., Bhatt, U.S., Francis, J.A., Janout, M., Kwok, R., Skagseth, Ø., 2023. Fluctuating Atlantic inflows modulate Arctic atlantification. *Science* 381, 972–979. <https://doi.org/10.1126/science.adh5158>
- Porter, T.M., Hajibabaei, M., 2018. Scaling up: A guide to high-throughput genomic approaches for biodiversity analysis. *Molecular Ecology* 27, 313–338. <https://doi.org/10.1111/mec.14478>
- Pöyhönen, V., Thomisch, K., Kovacs, K.M., Lydersen, C., Ahonen, H., 2024. High Arctic “hotspots” for sperm whales (*Physeter macrocephalus*) off western and northern Svalbard, Norway, revealed by multi-year Passive Acoustic Monitoring (PAM). *Sci Rep* 14, 5825. <https://doi.org/10.1038/s41598-024-56287-9>
- Purcell, J., Juhl, A., Mańko, M.K., Aumack, C., 2018. Overwintering of gelatinous zooplankton in the coastal Arctic Ocean. *Mar. Ecol. Prog. Ser.* 591, 281–286. <https://doi.org/10.3354/meps12289>
- Purcell, J.E., Hopcroft, R.R., Kosobokova, K.N., Whitley, T.E., 2010. Distribution, abundance, and predation effects of epipelagic ctenophores and jellyfish in the western Arctic Ocean. *Deep Sea Research Part II: Topical Studies in Oceanography, Observations and Exploration of the Arctic's Canada Basin and the Chukchi Sea: the Hidden Ocean and RUSALCA Expeditions* 57, 127–135. <https://doi.org/10.1016/j.dsr2.2009.08.011>
- Quinn, T.P., Erb, I., Richardson, M.F., Crowley, T.M., 2018. Understanding sequencing data as compositions: an outlook and review. *Bioinformatics* 34, 2870–2878. <https://doi.org/10.1093/bioinformatics/bty175>
- Rantanen, M., Karpechko, A.Y., Lipponen, A., Nordling, K., Hyvärinen, O., Ruosteenoja, K., Vihma, T., Laaksonen, A., 2022. The Arctic has warmed nearly four times faster than the globe since 1979. *Commun Earth Environ* 3, 1–10. <https://doi.org/10.1038/s43247-022-00498-3>
- Ratnasingham, S., Hebert, P.D.N., 2007. bold: The Barcode of Life Data System (<http://www.barcodinglife.org>). *Molecular Ecology Notes* 7, 355–364. <https://doi.org/10.1111/j.1471-8286.2007.01678.x>
- Renaud, P.E., Ambrose, W.G., Węśławski, J.M., 2020. Benthic Communities in the Polar Night, in: Berge, J., Johnsen, G., Cohen, J.H. (Eds.), *POLAR NIGHT Marine Ecology: Life and Light in the Dead of Night*. Springer International Publishing, Cham, pp. 161–179. https://doi.org/10.1007/978-3-030-33208-2_6
- Ronowicz, M., Włodarska-Kowalczyk, M., Kukliński, P., 2013. Hydroid epifaunal communities in Arctic coastal waters (Svalbard): effects of substrate characteristics. *Polar Biol* 36, 705–718. <https://doi.org/10.1007/s00300-013-1297-5>
- Sakata, M.K., Yamamoto, S., Gotoh, R.O., Miya, M., Yamanaka, H., Minamoto, T., 2020. Sedimentary eDNA provides different information on timescale and fish species composition compared with aqueous eDNA. *Environmental DNA* 2, 505–518. <https://doi.org/10.1002/edn3.75>
- Saunders, G.W., McDevit, D.C., 2013. DNA barcoding unmasks overlooked diversity improving knowledge on the composition and origins of the Churchill algal flora. *BMC Ecology* 13, 9. <https://doi.org/10.1186/1472-6785-13-9>

- Saunders, G.W., McDevit, D.C., 2012. Methods for DNA Barcoding Photosynthetic Protists Emphasizing the Macroalgae and Diatoms, in: Kress, W.J., Erickson, D.L. (Eds.), *DNA Barcodes: Methods and Protocols*. Humana Press, Totowa, NJ, pp. 207–222. https://doi.org/10.1007/978-1-61779-591-6_10
- Schiøtt, S., Jensen, M., Sigsgaard, E., Møller, P., Avila, M., Thomsen, P., Rysgaard, S., 2023. Environmental DNA metabarcoding reveals seasonal and spatial variation in the vertebrate fauna of Ilulissat Icefjord, Greenland. *Mar. Ecol. Prog. Ser.* 706, 91–108. <https://doi.org/10.3354/meps14250>
- Stukel, M.R., Décima, M., Fender, C.K., Gutierrez-Rodriguez, A., Selph, K.E., 2024. Gelatinous filter feeders increase ecosystem efficiency. *Commun Biol* 7, 1–11. <https://doi.org/10.1038/s42003-024-06717-1>
- Svendsen, H., Beszczynska-Møller, A., Hagen, J.O., Lefauconnier, B., Tverberg, V., Gerland, S., Børre Ørbæk, J., Bischof, K., Papucci, C., Zajaczkowski, M., Azzolini, R., Bruland, O., Wiencke, C., 2002. The physical environment of Kongsfjorden–Krossfjorden, an Arctic fjord system in Svalbard. *Polar Research* 21, 133–166. <https://doi.org/10.3402/polar.v21i1.6479>
- Teunisse, G.M., 2022. *Fantaxtic - Nested Bar Plots for Phyloseq Data*.
- Torti, A., Lever, M.A., Jørgensen, B.B., 2015. Origin, dynamics, and implications of extracellular DNA pools in marine sediments. *Marine Genomics* 24, 185–196. <https://doi.org/10.1016/j.margen.2015.08.007>
- Tverberg, V., Skogseth, R., Cottier, F., Sundfjord, A., Walczowski, W., Inall, M.E., Falck, E., Pavlova, O., Nilsen, F., 2019. The Kongsfjorden Transect: Seasonal and Inter-annual Variability in Hydrography, in: Hop, H., Wiencke, C. (Eds.), *The Ecosystem of Kongsfjorden, Svalbard*. Springer International Publishing, Cham, pp. 49–104. https://doi.org/10.1007/978-3-319-46425-1_3
- Vader, A., Marquardt, M., Meshram, A.R., Gabrielsen, T.M., 2015. Key Arctic phototrophs are widespread in the polar night. *Polar Biol* 38, 13–21. <https://doi.org/10.1007/s00300-014-1570-2>
- van den Heuvel-Greve, M.J., van den Brink, A.M., Glorius, S.T., de Groot, G.A., Laros, I., Renaud, P.E., Pettersen, R., Węśławski, J.M., Kuklinski, P., Murk, A.J., 2021. Early detection of marine non-indigenous species on Svalbard by DNA metabarcoding of sediment. *Polar Biol* 44, 653–665. <https://doi.org/10.1007/s00300-021-02822-7>
- Vihtakari, M., 2020. *PlotSvalbard: PlotSvalbard - Plot research data from Svalbard on maps*.
- von Quillfeldt, C.H., 2000. Common Diatom Species in Arctic Spring Blooms: Their Distribution and Abundance 43, 499–516. <https://doi.org/10.1515/BOT.2000.050>
- Wangensteen, O.S., Palacín, C., Guardiola, M., Turon, X., 2018. DNA metabarcoding of littoral hard-bottom communities: high diversity and database gaps revealed by two molecular markers. *PeerJ* 6, e4705. <https://doi.org/10.7717/peerj.4705>
- Węśławski, J.M., Dragańska-Deja, K., Legeżyńska, J., Walczowski, W., 2018. Range extension of a boreal amphipod *Gammarus oceanicus* in the warming Arctic. *Ecology and Evolution* 8, 7624–7632. <https://doi.org/10.1002/ece3.4281>
- Westgaard, J.-I., Præbel, K., Arneberg, P., Ulaski, B.P., Ingvaldsen, R., Wangensteen, O.S., Johansen, T., 2024. Towards eDNA informed biodiversity studies – Comparing water derived molecular taxa with traditional survey methods. *Progress in Oceanography* 222, 103230. <https://doi.org/10.1016/j.pocean.2024.103230>
- Wickham, H., 2016. *ggplot2: Elegant Graphics for Data Analysis*.
- Willassen, E., Westgaard, J.-I., Kongsrud, J.A., Hanebrikke, T., Buhl-Mortensen, P., Holte, B., 2022. Benthic invertebrates in Svalbard fjords—when metabarcoding does not outperform traditional biodiversity assessment. *PeerJ* 10, e14321. <https://doi.org/10.7717/peerj.14321>
- Włodarska-Kowalczyk, M., Aune, M., Michel, L.N., Zaborska, A., Legeżyńska, J., 2019. Is the trophic diversity of marine benthic consumers decoupled from taxonomic and functional trait diversity? Isotopic niches of Arctic communities. *Limnology and Oceanography* 64, 2140–2151. <https://doi.org/10.1002/lno.11174>

Wlodarska-Kowalczyk, M., Pearson, T.H., 2004. Soft-bottom macrobenthic faunal associations and factors affecting species distributions in an Arctic glacial fjord (Kongsfjord, Spitsbergen). *Polar Biol* 27, 155–167. <https://doi.org/10.1007/s00300-003-0568-y>

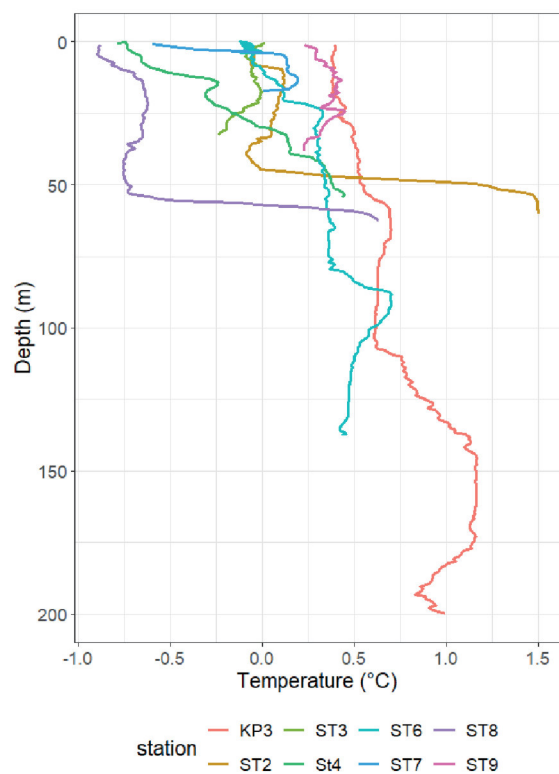


Figure S1. Temperature profiles from CTD deployments at each station.

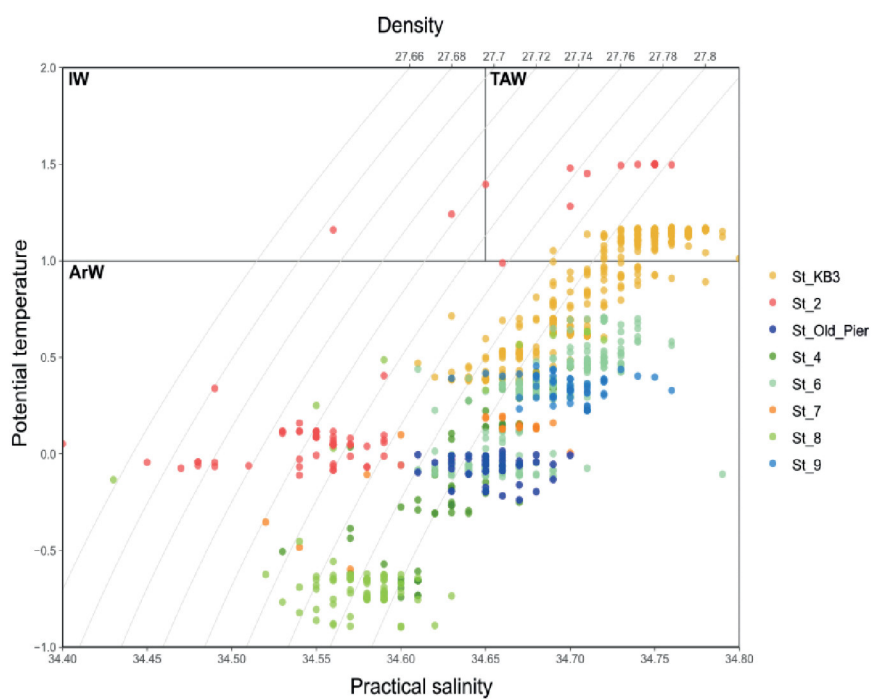


Figure S2. Water masses measured sampling stations. Temperature salinity plot based on CTD data. Different water masses boundaries indicated by lines. IW = Intermediate water; TAW = transformed atlantic water; ArW = Arctic water. Produce using PlotSvalbard package in RStudio.

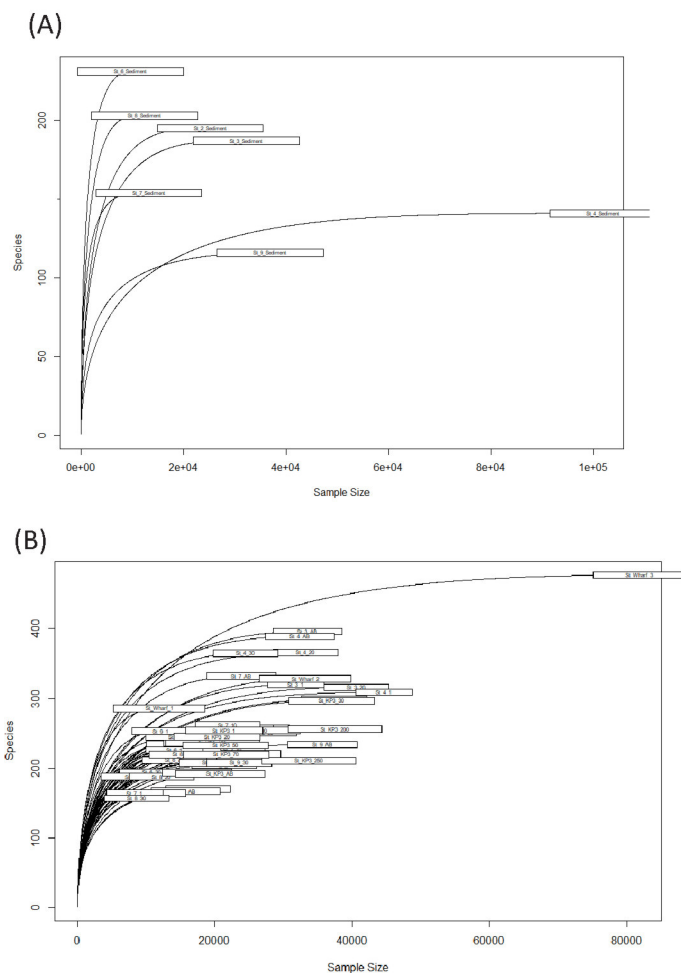


Figure S3. Rarefaction curves of raw sequences per samples. (A) Sediment samples (B) Water samples from main dataset.

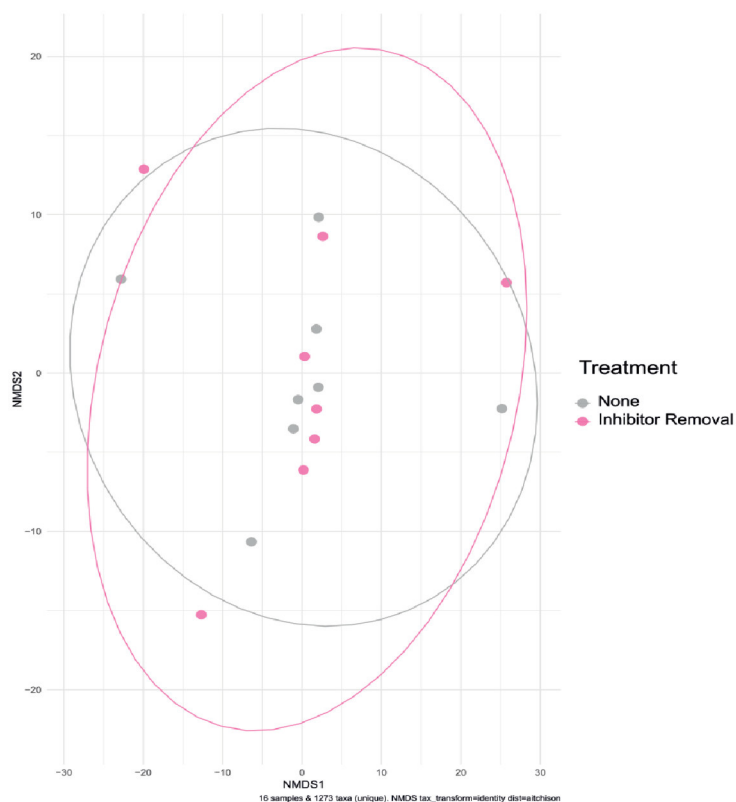


Figure S4. Non-metric multidimensional scaling (NMDS) ordination plot of the community composition in treated and untreated samples for PCR-inhibition testing.

Table S1. Gelatinous zooplankton specimen tissue barcoding sequence details

Species name	BOLD sequence identification number
<u>Phylum: Cnidaria</u>	
<i>Aeginopsis laurentii</i>	ARGZP001-23
<i>Aglantha digitale</i>	AGLAN125-22, AGLAN124-22, AGLAN123-22
<i>Cyanea capillata</i>	ARGZP007-23, ARGZP010-23
<i>Nanomia cara</i>	ARGZP002-23, ARGZP003-23
<i>Periphylla periphylla</i>	SCYPH152-22, SCYPH151-22
<i>Ptychogena lactea</i>	ARGZP004-23, ARGZP005-23, ARGZP006-23
<u>Phylum: Ctenophora</u>	
<i>Beroe cucumis</i>	Not yet submitted to BOLD
<i>Beroe abyssicola</i>	Not yet submitted to BOLD
<i>Bolinopsis infundinulum</i>	Not yet submitted to BOLD

Table S2. PCR inhibitor removal treatment alpha diversity measurements.

Sample	Treatment	Shannon	Richness	Total Reads
St_2_1_S	None	3.63427647	248	93713
St_3_1_S	None	3.96829868	408	73329
St_KP3_AB_S	None	3.6361347	348	86623
St_7_AB_S	None	3.88263073	394	81880
St_7_1_S	None	3.53429651	295	93131
St_6_1_S	None	3.57362083	348	101345
St_8_1_S	None	3.63591406	324	82746
St_9_1_S	None	3.54406989	303	67144
St_2_1_R	Removal	3.59250074	233	87598
St_3_1_R	Removal	3.94247893	371	78012
St_KP3_AB_R	Removal	3.63626884	307	91473
St_7_AB_R	Removal	3.89507704	381	85585
St_7_1_R	Removal	3.54310559	312	106134
St_6_1_R	Removal	3.57374336	315	91114
St_8_1_R	Removal	3.60478777	296	102036
St_9_1_R	Removal	3.5554454	305	89584

Notes: Indices are calculated based on SRS normalised reads.

Table S3. Results of type II ANOVA tests for the effect of PCR inhibition treatment on alpha diversity.

	DF	F-statistic	<i>p value</i>	ges
Shannon Index	1, 14	0.011	0.919	0.000761
Richness	1, 14	0.56	0.466	0.038
Total reads	1, 14	1.616	0.224	0.104

Notes: DF = degrees of freedom, ges = generalized eta squared (estimate of effect size).

Chapter 5

On the effectiveness of two universal metabarcoding primer pairs in amplifying gelatinous zooplankton DNA from tissue and environmental samples

Ayla Murray^{1,2}, Annkathrin Dischereit^{1,2}, Charlotte Havermans^{1,2}

1. Alfred Wegener Institute Helmholtz Centre for Polar and Marine Research, Am Handelshafen 12, 27570 Bremerhaven, Germany

2. Marine Zoologie, Fachbereich 2, University of Bremen, Bremen, Germany

Manuscript in preparation for submission to Journal of Plankton Research

Abstract

Gelatinous zooplankton (GZP) is a highly diverse group of taxa that play important roles throughout the world's oceans. However, they are often difficult to study as their delicate bodies make them susceptible to damage from traditional zooplankton and fish survey methods. DNA metabarcoding is an increasingly valuable tool in GZP research, as it allows for detection without the need to capture whole organisms. Metabarcoding projects targeting zooplankton often use universal primers to target the mitochondrial cytochrome *c* oxidase subunit 1 gene (COI) and (ii) the small sub-unit Ribosomal RNA gene (18S) fragments. However, there has not yet been a study analysing their performance on GZP taxa specifically. Here we aimed to test the efficacy of two universal primer pairs on amplifying species of GZP that occur in the Arctic Ocean. To achieve this, we assembled a mock community and conducted *in silico* Polymerase Chain Reaction (PCR) testing on primer binding efficiency of two primer pairs. Next, we extracted DNA from the tissue of the specimens in the mock community for barcoding with the longer barcode fragments (Folmer for COI and full 18S fragment) as well as the metabarcoding fragments (Leray and 18S V-V2). Finally, we used metabarcoding of DNA from water samples from the mock community experiment to test the primer pairs. We found that the COI primer pairs (Leray-XT) had good coverage and taxonomic resolution to species level, but failed to amplify two hydrozoans, *Aglantha digitale* and *Sminthea arctica*, as well as cypidid ctenophores. In contrast, the 18S primers had a higher coverage, but both the full gene and the metabarcoding had limited resolution and did not allow for the discrimination between genera or species. Moreover, we highlight the gaps in public reference databases for species that occur in the Arctic, as well as specimens caught specifically in the region, as a limiting factor for successful amplification of Arctic GZP species.

Key Words

Jellyfish, Arctic Ocean, eDNA, *in silico* PCR, reference library, COI, 18S

1. Introduction

Gelatinous zooplankton (GZP) is a highly diverse and polyphyletic group which includes pelagic tunicates (Phylum: Chordata), comb-jellies (Phylum: Ctenophora) and medusae (Phylum: Cnidaria). Despite being historically excluded from zooplankton surveys, recent research has demonstrated that they play major roles throughout marine ecosystems and food webs (reviewed in: Hays et al., 2018). Their gelatinous bodies and polymorphic lifecycles, of which the life stages can include, amongst others; pelagic medusae, benthic polyps, small-sized larvae, make them susceptible to damage or being missed completely by invasive sampling techniques such as plankton nets or fishing trawls (Haddock, 2004; Hosia et al., 2017; Nogueira Júnior et al., 2015). Optical surveys represent a non-invasive sampling method that have proven valuable for estimating distribution and abundances of GZP (Pantiukhin et al., 2023, 2024a; Raskoff et al., 2010), yet rely on the presence of easily recognisable morphological features which can hinder high-resolution identifications (Haddock, 2004; Hosia et al., 2017). As a consequence, knowledge of GZP ecology, including community composition, distribution and abundance, remains limited. This is particularly true in remote regions with challenging environmental conditions such as the Arctic Ocean. Here, multiple GZP species are expected to undergo significant shifts in range distribution (Pantiukhin et al., 2024b), as a result of the region being globally one of the most affected by climate change (Rantanen et al., 2022).

Molecular barcoding of tissue as well as metabarcoding of environmental DNA (eDNA) and diet samples have become valuable tools for surveying and identifying delicate taxa like GZP (Ames et al., 2021; Bolte et al., 2021; Günther et al., 2021; Minamoto et al., 2017; Ogata et al., 2021; Rantanen et al., 2022). A number of studies based on metabarcoding of eDNA and stomach contents in the Arctic has revealed previously unknown importance of GZP as prey items for fish (Dischereit et al., 2024b), amphipods (Dischereit et al., 2024a, 2022) and a keystone Arctic shrimp (Urban et al., 2022). Additionally, eDNA-based studies in the region have successfully recovered GZP taxa in pelagic and deep-sea habitats (Murray et al., 2024), in the Bering Strait (Verhaegen et al., in review), sub-ice water of the marginal ice zone (Murray et al., under review) and in an Arctic fjord during the polar night (Murray et al., *submitted*). When comparing to morphological sampling from the same sites, eDNA recovered taxa overlooked by nets and/or optical surveys and was able to detect more GZP taxa in total (Murray et al., 2024). Similar results were also found in other oceans (Feng et al., 2022; Govindarajan et al., 2021).

One of the most important factors in affecting the findings of metabarcoding studies is the choice of gene fragment and primer pairs used to amplify it (Clarke et al., 2017; Taberlet et

al., 2018). Mismatches between the primers and the DNA of the target species and other PCR biases as well as gaps in reference databases can lead to false negatives and underestimation of species richness (Taberlet et al., 2018). When targeting a polyphyletic group such as zooplankton, “universal” markers are usually employed in order to ensure as much diversity is captured as possible. Two such gene fragments commonly employed are the nuclear small-subunit ribosomal RNA gene (18S) and the aforementioned COI gene. In earlier zooplankton metabarcoding studies, different regions of the 18S gene were the most frequently used (reviewed in Bucklin et al., 2016). This gene generally is slow evolving and therefore has conserved sites that result in many eukaryotic taxa sharing the same primer binding sequences. As a result, it can amplify a wide range of eukaryotic groups and is well represented on public reference databases. However, its conservative nature also limits its discriminatory power between species and restricts taxonomic identification to only order and family level for many metazoans, including zooplankton (Bucklin et al., 2016; Questel et al., 2021; Tang et al., 2012; Wu et al., 2015). In recent years, the Leray fragment of the COI gene (within the Folmer region) has become a popular choice for species discrimination in marine metazoans (Bucklin et al., 2016; P. D. Hebert et al., 2003). It has a rapid rate of evolution, meaning it has a high accuracy for fine-resolution discrimination (i.e., species-level) and has also emerged as a tool for detecting levels of intraspecific diversity (Adams et al., 2019; Antich et al., 2022). There are a number of primer pairs used to amplify this fragment, with the highly degenerated Leray-XT pair as a recent yet popular addition (Albaina et al., 2024; Geller et al., 2013; Wangensteen et al., 2018). Similar to 18S, well-stocked and curated public databases for this barcode exist (Andújar et al., 2018), such as the Barcode of Life Data System (BOLD) (Ratnasingham and Hebert, 2007) and the zooplankton-specialized MetaZooGene (O’Brien et al., 2024).

Both of these markers have been employed in multi-marker diet metabarcoding (Dischereit et al., 2024b; Ruiz et al., 2024) and eDNA metabarcoding (e.g., Murray et al., *under review*) studies with the aim to increase coverage of GZP taxa in particular. In a study on Greenland fish species, Dischereit and colleagues recovered more hydrozoan and scyphozoan species with COI, but found that 18S recovered more ctenophores. In the Southern Ocean, 18S recovered salps in the diets of demersal fish, which were not recovered with COI (Ruiz et al., 2024). In the Arctic, more GZP taxa overall were found with COI in the sub-ice water column in the Arctic marginal ice zone, but appendicularians detected only with 18S (Murray et al., *under review*). However, it remains unclear whether the reason these GZP taxa are overlooked by COI is due to primer biases or gaps in reference databases. Given the importance of GZP in Arctic marine ecosystems and the increased costs of multi-marker studies compared to single-marker ones, it is important to determine whether the inclusion of

a ribosomal marker such as 18S is justified as a solution for increasing GZP detection in the region.

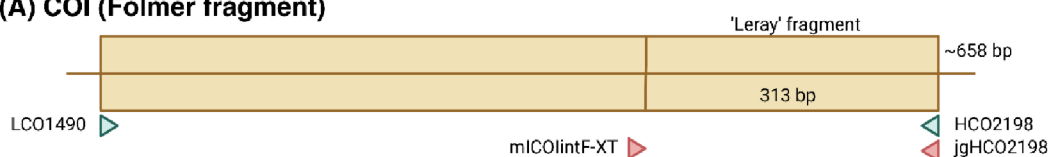
Here, we aim to address these knowledge gaps by investigating the performance of two primer pairs used for amplifying COI and 18S metabarcoding fragments on subset of Arctic GZP species. We approached this by assembling a mock community of Arctic GZP species regularly detected in the region with net and optical sampling, based on morphological identification. We (i) assessed the coverage of the target species on two curated public reference databases, (ii) evaluated primer binding efficiency *in silico* on sequences from these databases, (iii) tested the primers on DNA derived from the tissue of net-caught specimens and finally (iv) tested the primers on a mock community with metabarcoding.

2. Methods

2.1 Primer selection

All primers set selected for analysis target widely used (meta)barcoding fragments of the 18S and COI genes. Molecular barcodes, or DNA barcodes, are gene regions that are used for the purpose of taxonomic identification of single-species samples. The most widely used barcode region for marine metazoans is the ~658 bp region of the mitochondrial cytochrome oxidase I (COI) gene (Bucklin et al., 2011). Whereas a 'metabarcoding' is applied to multi-species samples and is a shorter segment of a barcode (**Figure 1**). Here, in order to contribute barcodes to reference databases, we first barcoded tissue extract using the longer fragments using the whole 18S gene (~1800 bp) and the ~658bp Folmer fragment of the COI gene. A primer set targeting the V1 – V2 fragment was used for the 18S metabarcoding and the highly

(A) COI (Folmer fragment)



(B) 18S rRNA (Full gene)

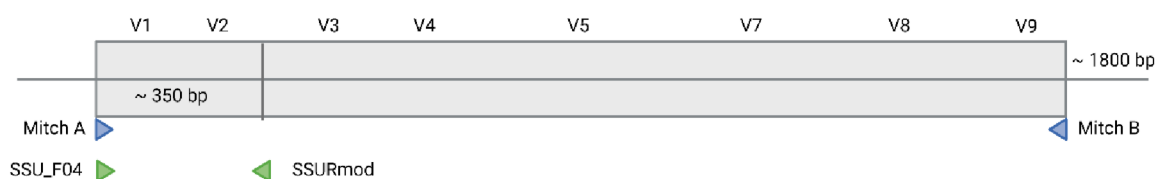


Figure 1. Representative binding locations of primer pairs tested for the 18S and COI genes. Note that the fragment length of the two different genes is not to scale. Figure produced using BioRender.

degenerated Leray-XT primer pair was used to target the Leray fragment of the COI gene. The location of the primer binding sites can be found in **Figure 1** and the sequence details of each primer pair can be found in **Table S1**.

2.2 Reference database coverage

We used two curated databases to estimate the coverage of Arctic GZP in species in publicly available reference databases. First, we used the coverage and completeness summary function in the MetaZooGene (MZG) database (O'Brien et al., 2024) accessed in October 2024. As the current version of MetaZooGene is from 2023, we checked a second database (BOLD) to assure the latest publicly available sequences were included. Both databases have strict curation protocols, meaning they have less sequences than GenBank for example, but have higher accuracy in the taxonomic assignments. MZG contains a combination of sequences from GenBank and BOLD, while BOLD contains sequences from GenBank as well as those directly submitted by registered users. The sequence counts were based on publicly available sequences only.

2.3 *In Silico* PCR assessment of primers

Primer binding success was assessed *in silico* using the “Test Primers” function in Geneious Prime v 2024.0.5 software (www.geneious.com). This function is based on the software Primer3 2.3.7 (Rozen and Skaletsky, 1999). A local sequence database was created by downloading sequences from the MetaZooGene database. When none were available on MZG, further sequences were downloaded from the BOLD database where possible. The primers were tested on each individual sequence using the settings: (a) minimum amplicon length of 250bp (excluding primers) and (b) a maximum of five mismatches for COI and two for 18S. Congeneric sequences were included when the target taxa (mock community species) were identified with a lower than species-level resolution (e.g., *Botrynema sp* and *Atolla sp*). For the unidentified ctenophore juveniles, we included sequences from the most commonly occurring Tentaculata in the region (genera *Pleurobrachia*, *Mertensia*, and *Euplokamis*).

2.4 Field collection of GZP specimens

Gelatinous zooplankton specimens used in the mock community were collected during the oceanographic expedition PS126 aboard the R/V Polarstern (Soltwedel, 2021). The samples were collected at the station called HG-IX (79°07.967'N 002°45.607'E) in the area of the HAUSGARTEN observatory in Fram Strait, between Svalbard and Greenland. The individuals were collected using a Maxi-Multinet (Hydrobios, Kiel) with a 330µm net size. The specimens

were morphologically identified to the highest possible taxonomic resolution using taxonomy keys (Bouillon et al., 2006; Licandro et al., 2017a, 2017b; Licandro and Lindsay, 2017).

2.5 Mock community preparation

A mock community of 18 specimens comprised of individuals of five cnidarian families and the ctenophore class Tentaculata was assembled from net-caught specimens (**Table 1**). These individuals were placed in a non-circulating tank with 14L of filtered seawater for the duration of the experiment. The seawater was collected from the CTD rosette water sampler and filtered through polycarbonate filters to remove as much DNA as possible. The filtration was performed sequentially through a 3 μ M filter and a 0.22 μ M using a peristaltic pump. Before adding the individuals to the tank, a control sample of 500 ml of the filtered seawater was collected before the addition of the GZP specimens and filtered over a 0.22 μ M Sterivex-GP filter (Merck Millipore). The assemblage was kept in the tank for ca. 40h, after which triplicates of approximately 2L were filtered over Sterivex filters. Filters were preserved at -80°C until further processing in the home lab. After retrieval, the specimens were stored at -80°C for DNA extraction in the home lab.

Table 1. Details of specimens included in the mock community.

Phylum	Class	Order	Family	Genus	Species	Specimen name
Cnidaria	Scyphozoa	Coronatae	Atollidae	<i>Atolla</i>	-	IND1329, IND1330
	Hydrozoa	Trachymedusae	Rhopalonematidae	<i>Aglantha</i>	<i>digitale</i>	IND1327, IND1328
				<i>Sminthea</i>	<i>arctica</i>	IND1338, IND1339, IND1340
			Halicreatidae	<i>Botrynema</i>	-	IND1331, IND1332
		Narcomedusae	-	-	-	IND1333
		Siphonophorae	Diphyidae	<i>Dimophyes</i>	<i>arctica</i>	IND1341, IND1342, IND1343, IND1344
Ctenophora	Tentaculata	-	-	-	-	IND1334, IND1335, IND1336, IND1337

2.6 DNA extraction, amplification and sequencing of tissue

Intra-organismal DNA was isolated from the tissue of all individuals used in the mock community experiment. Tissue DNA was extracted using the QIAGEN DNeasy Blood & Tissue kit following (Murray et al., 2023), with a final DNA elution volume in AE buffer of 100uL. The DNA concentration was then checked using a NanoDrop One (Thermo Scientific) and subsequently diluted to a concentration of 50ng where necessary. Four different primer pairs were used to amplify tissue DNA. The primer sequences, PCR reaction master mixes and conditions for each primer pair can be found in **Table S1**. After amplification, PCR products were verified on 2% agarose gel and then bidirectionally sequenced on a Sanger Sequencing platform at EUROFINIS (Germany).

After sequencing, primer sequences were subsequently removed and sequences trimmed using Geneious Prime v 2024.0.5. Consensus sequences were assembled using the forward and reverse reads for each sample. Then they were manually checked for ambiguous base calls and stop codons, before being assigned using a the MegaBlast function in Genious Prime. The COI sequences were further checked with the BOLD “Identification” function.

2.7 Mock community eDNA extraction, library preparation and sequencing

Environmental DNA was isolated from the filter membranes using the DNeasy Blood and Tissue kit (QIAGEN) following the protocol detailed in Murray et al., (2024). All laboratory surfaces and extraction equipment were sterilised between extractions using a 1:10 bleach solution diluted with MilliQ water, followed by a MilliQ rinse and dried using 70% ethanol. Finally, all benches and equipment were treated with a minimum of 1 hour of UV light. RNA/DNA Exitus-plus (Applichem) was used for sterilisation of gloves and pipettes. The DNA extract was stored at -20°C for downstream processing.

The PCR amplification, metabarcoding library preparation and sequencing were all carried out by AllGenetics & Biology SL, Spain. A 2-step PCR protocol was used, with the metabarcoding primers attached in the first PCR and the oligonucleotide indices attached in the second PCR (see **Table S1** for PCR details). PCR products were verified on 2% agarose gel before purification with Mag-Bind RXNPure Plus magnetic beads (Omega Bio-tek), following the manufacturer protocol. Finally, libraries were measured using Qubit dsDNA HS Assay (Thermo Fisher Scientific) before being pooled with equimolar amounts. The pool was sequenced using a NovaSeq PE250 flow cell (Illumina).

2.8 Bioinformatic processing and data curation of mock community eDNA

The raw sequence reads were demultiplexed by the sequencing company using *cutadapt* (Martin, 2011). The bioinformatic pipeline used to process the raw COI sequences was based

on OBITOOLS 3 (Boyer et al., 2016) , following (Murray et al., submitted). Briefly, paired-end reads were merged, length filtered and sequences dereplicated. Chimeric sequences were removed with the *uchime denovo* algorithm in VSEARCH (Rognes et al., 2016). Sequences were denoised using *DnoisE* (Antich González et al., 2022) ($\alpha = 4$) and singletons removed. A relative threshold abundance of 0.002% for in each sample was applied to filter out sequencing artefacts. A blank correction of was applied following Antich et al., 2021. Next, clustering denoised sequences into molecular operational taxonomic units (MOTUs) ($d=13$) with SWARM (Mahé et al., 2021). Any remaining MOTUs with a total read count of <5 were removed. The *ecotaq* algorithm was used for taxonomic assignment against a custom reference database (https://github.com/adriantich/NJORDR-MJOLNIR3/tree/main/DUFA_scripts). The post-clustering filter LULU (Frøslev et al., 2017) was used to remove potentially erroneous sequences. Finally, bacteria and NUMTs were filtered out. Taxonomic assignments were further checked and improved where possible using the BOLDigger2 software (Buchner and Leese, 2020) and the BOLD database (Ratnasingham and Hebert, 2007). The following identity thresholds were used: species (97%), genus (95%), family (90%), class (85%), phylum (80%) following Murray et al., (2024). All MOTUs with taxonomic assignments $<70\%$ were removed from the metabarcoding datasets completely.

The 18S raw sequence reads were processed using DADA2 v1.18 (Callahan et al., 2016) following (Murray et al., under review). Briefly, forward reads were trimmed at 220 bp and reverse reads at 210 bp and filtered with a maximum expected error threshold of 2.2 and 2.1, for forward and reverse reads respectively. Sequences were denoised and paired ends were merged using a minimum overlap of 25bp and zero mismatches when aligning. Singletons were discarded and chimeras filtered out and the same blank correction used in the COI dataset was applied here. Taxonomic assignment of the resulting ASVs was done using the MetaZooGene database (O'Brien et al., 2024). The version "MZGdb 3.0" containing 68,484 18S rRNA sequences containing genus and species data from any ocean was used (Mode C). A minimum identification bootstrap support value of $>75\%$ was set for taxonomic assignment, and lower values were set as unassigned.

For both datasets, reads assigned to bacteria, non-eukaryotes and obvious terrestrial taxa were removed. Finally, reads present in the control sample (the mock community water before the addition of the GZP individuals) were removed from the main samples. We did this on a read by read basis (i.e., if 50 reads of a MOTU/ASV were present in the control then 50 reads of this MOTU/ASV were removed from the samples). In the case of a MOTU/ASV having less reads in the sample than in the control, the number of reads was set to zero.

2.9 Data analysis

The program R version 4.1.0 was used to visualize and conduct all analysis unless otherwise stated. The *phyloseq* (McMurdie and Holmes, 2013) package was used for initial metabarcoding data exploration. Relative read abundances (%) of the target GZP species were visualised using *ggplot2* (Wickham, 2016) and *Fantaxtic* (Teunisse, 2022) packages.

3. Results

3.1 Coverage of Arctic GZP on public databases

According to MetaZooGene (v2023-m07-15, last updated in July 2023), there are 122 species of Hydrozoa, 10 species of Scyphozoa and 7 species of Ctenophora that are commonly found in the Arctic Ocean. Of these, the lowest sequence coverage was for Hydrozoa (COI: 50% and 18S: 40%), followed by Ctenophora (COI: 71%, and 18S: 85%) and Scyphozoa (COI: 100% and 18S: 80%). On the BOLD database, a search (conducted on October 23, 2024) including the four Arctic GZP groups “Ctenophora”, “Hydrozoa”, “Scyphozoa” and “Appendicularia” and as the location “Arctic Ocean”, a total of 167 barcodes of four genes from 15 species were publicly available. The highest number of barcodes was for 18S (44), then 16S (43), 28S (42) and COI (35).

For the species included in the mock community, the highest number of publicly available COI reference sequences were for *A. digitale*, while *S. arctica* had a single sequence that is marked as “unverified” on GenBank. However, this sequence was not considered in further analysis. There were no publicly available sequences for the ctenophore species *Mertensia ovum* nor *Euplokamis dunlapae*. For 18S, every targeted species had at least one reference sequence available. *Botrynema* was the best represented with 12 sequences and the ctenophore *E. dunlapae* the least with a single 18S barcode (**Table S2**).

3.2 Assessment of metabarcoding primers using *in silico* PCR

3.2.1 COI

A total of 73 reference sequences of eight species from the MetaZooGene database were included in the *in silico* testing of the Leray-XT primer pair (COI gene). The binding of the forward primer (mICOLintF-XT) was successful for all species with available reference sequences (**Table S3**). The reverse primer (jgHCO2198) had successful primer binding for at least one sequence of every species, except for *Solmundella bitentaculata*. The highest number of mismatches was 5 on the forward primer and 1 on the reverse primer. The majority of the mismatches occurred in the binding site of the forward primer for the hydrozoan *A. digitale* and ctenophore *Pleurobrachia pileus* (**Table S3**). There were no reference sequences available for the ctenophores *M. ovum*, and *E. dunlapae* nor the hydrozoan *S. arctica*, making their inclusion in the analysis impossible.

3.2.2 18S

A total of 28 sequences from 12 species were used for *in silico* testing of the 18S V1-V2 primers. Primer binding failed in both directions for *S. arctica*. The binding of the forward primer (SSU_F04) was successful for at least one sequence of all species except for *Atolla tenella* (**Table S4**). However, this sequence was shorter than the majority of other *Atolla* sequences (<1800 bp), and an alignment with the conspecific *Atolla wyvillei* confirmed that the primer binding site was excluded from the sequence. No primer mismatches occurred for either of the primers. There were no reference sequences available for *E. dunlapae* and it was thus excluded from this analysis.

3.3 Tissue-derived DNA extract sequencing

3.3.1 COI

When sequencing the Folmer fragment (~658 bp), successful sequences were acquired for only three out of 16 specimens (**Table 2**). Of these, only *A. digitale* DNA was assigned to species level. The narcomedusae specimen was assigned to the family Aeginidae and the ctenophore juvenile did not have any matches on BOLD or when using the Megablast function in Geneious Prime. More successful sequences were produced from the shorter Leray fragment (~313 bp), with 11 out of 16 individuals resulting in successful sequences. Of these, three were identified to species level, one to family and two to class level. The remaining five did not match any sequences.

3.3.2 18S

Successful sequences were produced for all 16 individuals for both the full 18S gene and the V1-V2 fragment (**Table 2**). The only 100% match for the full longer fragment at species level with a match to a single species was for *A. digitale*, followed by a 99.6 % match for *Aegina critea*. All other assignments showed very high matches (>99.5%) with multiple species or genera.

Table 2. Results of Sanger sequencing of DNA extracted from tissue samples from individuals in the mock community.

Sample ID	Morphological ID	COI (BOLD/Megablast)		18S (NCBI)	
		Folmer	Leray-XT	Full 18S	V1-V2
IND1330	<i>Atolla</i> spp.	-	<i>Atolla tenella</i> (99.8%)	<i>Atolla</i> spp. (100%)	<i>Atolla</i> spp. (100%)
IND1327	<i>Aglantha digitale</i>	-	-	<i>Aglantha digitale</i> (100%)	<i>Aglantha digitale</i> (100%) *
IND1328	<i>Aglantha digitale</i>	<i>Aglantha digitale</i> (99.7%)	-	<i>Aglantha digitale</i> (100%)	<i>Aglantha digitale</i> (100%) *
IND1331	<i>Botrynema</i> spp.	-	<i>Botrynema brucei</i> (99.8%)	<i>Botrynema</i> spp. / <i>Halicsera</i> sp. (99.9%)	<i>Botrynema</i> spp. / <i>Halicreas</i> sp. (100%)
IND1332	<i>Botrynema</i> spp.	-	<i>Botrynema brucei</i> (100%)	<i>Botrynema</i> spp. / <i>Halicsera</i> sp. (99.9%)	<i>Botrynema</i> spp. / <i>Halicreas</i> sp. (100%)
IND1341	<i>Dimophyes arctica</i>	-	-	<i>Dimophyes</i> sp. / <i>Crystallophyes</i> sp. (100%)	<i>Dimophyes</i> sp. / <i>Crystallophyes</i> sp. (100%) *
IND1342	<i>Dimophyes arctica</i>	-	-	<i>Dimophyes</i> sp. (99.9%) / <i>Crystallophyes</i> sp. (99.8%)	<i>Dimophyes</i> sp. (99.9%) / <i>Crystallophyes</i> sp. (99.8%)
IND1343	<i>Dimophyes arctica</i>	-	No Match	<i>Gilia</i> sp / <i>Diphyes</i> sp. / <i>Chelophyes</i> sp. / (99.9%)	<i>Diphyes</i> sp. / <i>Chelophyes</i> sp. / (99.9%)
IND1338	<i>Sminthea arctica</i>	-	Hydrozoa (84%)	<i>Pantachogon</i> sp. / <i>Colobonema</i> sp. / <i>Rhoplonema</i> sp. (99.8%)	<i>Pantachogon</i> sp. / <i>Colobonema</i> sp. (100%)
IND1339	<i>Sminthea arctica</i>	-	-	<i>Pantachogon</i> sp. / <i>Colobonema</i> sp. / <i>Rhoplonema</i> sp. (99.9%)	<i>Pantachogon</i> sp. / <i>Colobonema</i> sp. (100%) *
IND1340	<i>Sminthea arctica</i>	-	Hydrozoa (84%)	<i>Pantachogon</i> sp. / <i>Colobonema</i> sp. / <i>Rhoplonema</i> sp. (99.6%)	<i>Pantachogon</i> sp. / <i>Colobonema</i> sp. (100%)
IND1333	Narcomedusae	Aeginidae (90.9%)	Aeginidae (90%)	<i>Solmundella</i> sp. / <i>Aegina</i> sp. (99.4%)	<i>Solmundella</i> sp. / <i>Aegina</i> sp. (99.4%)
IND1334	Ctenophore juvenile	No Match	No Match	Ctenophora (99.98%) / Mertensiidae (99.97%)	Ctenophora / Mertensiidae (100%)
IND1335	Ctenophore juvenile	-	No Match	Ctenophora (99.98%) / Mertensiidae (99.97%)	Ctenophora / Mertensiidae (100%)
IND1336	Ctenophore juvenile	-	No Match	Ctenophora / Mertensiidae (99.6%)	Ctenophora / Mertensiidae (100%)
IND1337	Ctenophore juvenile	-	No Match	Ctenophora (99.99%) / Mertensiidae (99.97%)	Ctenophora / Mertensiidae (100%)
IND1329	<i>Atolla</i> spp.	No tissue extracted			
IND1344	<i>Dimophyes arctica</i>	No tissue extracted			

Notes: (*) = only one sequencing direction was successful, (-) = failed sequencing or bacteria contamination. % = identity match on reference database. Specimens highlighted in grey were not processed for tissue extraction. Identifications highlighted in green are species-level matches, yellow = genus-level, blue = family-level, orange = higher than family and grey = no match.

3.4 Metabarcoding of the mock community

3.4.1 Sequencing summary

A total of three samples, one seawater control, one extraction blank and one PCR blank were sequenced. After bioinformatic filtering and data curation, we obtained 153,885 reads assigned to 89 MOTUs with the COI fragment and 1,193,934 reads assigned to 483 ASVs with the 18S fragment. In the COI dataset, 115,999 reads were assigned to 12 GZP MOTUs of the phyla Cnidaria and Ctenophora (**Table S5**). In the 18S dataset, a total of 54 ASVs were assigned as GZP totalling 804,142 reads (**Table S6**).

3.4.1 Leray-XT primers

In the COI dataset, MOTUs assigned to the three of the four known cnidarian families in the mock community (Atollidae, Halicreatidae, Rhopalonematidae), as well as a MOTU assigned to the family narcomedusae had the highest relative read abundances (**Figure 2A**). Ctenophore and siphonophore MOTUs were present but in low read abundances (<0.1 %) (**Table S5**). The most abundance MOTU was assigned to the species *Atolla tenella*, followed by a MOTU assigned to Narcomedusae (order). A total of seven MOTUs were assigned to genus and species level.

3.4.2 V1-V2 primers

We successfully detected ASVs assigned to all four of the families included in the mock community, as well as to the order Narcomedusae and the phylum Ctenophora in high relative read abundances (**Figure 2B**). The family Diphyidae was the most abundant, followed by Rhopalonematidae and the ctenophore family Mertensiidae. A total of 20 ASVs were assigned to genus level with high bootstrap support, and species-level assignments were not considered due to the high likelihood of assignment errors for this marker (**Table S6**).

3.4.3 Non-target taxa

Both markers amplified sequences from non-target taxa (i.e., families not included in the mock community). The large scyphozoan *Cyanea capillata* (species in COI and family in 18S) was found in low abundances in both datasets. Additionally, the COI dataset recovered the siphonophores *Rudjakovia plicata* and *Crystallophyces amygdalina* (**Table S5**) and the 18S dataset an ASV assigned to the ctenophore family Beroidae (**Table S6**).

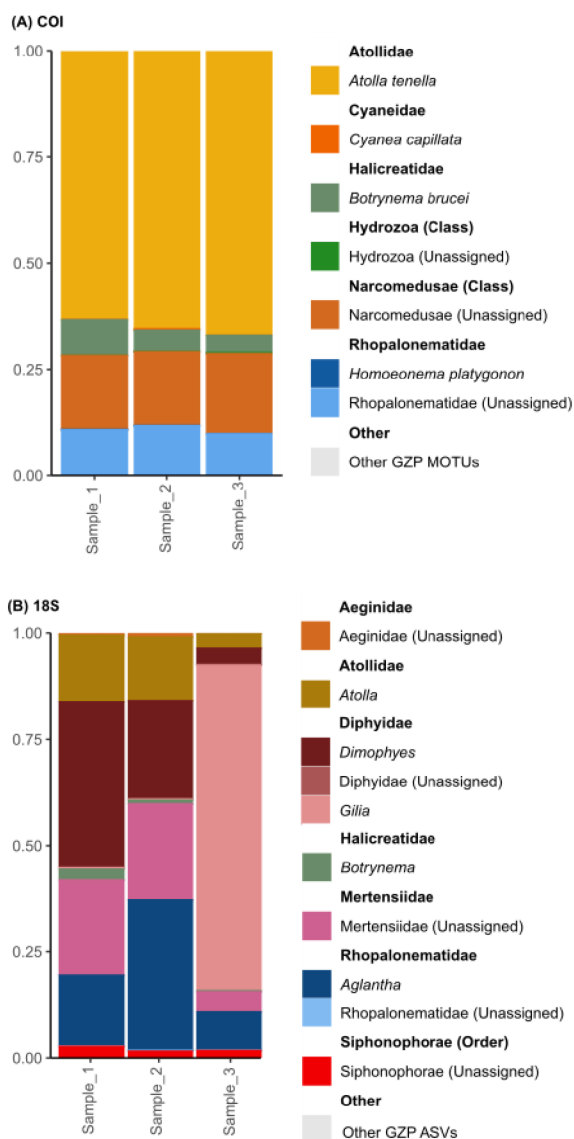


Figure 2. Relative read abundances >0.01 % in metabarcoding of the mock community samples. (A) MOTUs assigned to gelatinous zooplankton taxa with the COI gene and **(B)** ASVs assigned to GZP taxa with the 18S gene.

4. Discussion

Recent advances in molecular techniques have provided opportunities to effectively implement (meta)barcoding for biodiversity surveys across many marine environments (Bucklin et al., 2016; Leray and Knowlton, 2016). This is especially advantageous for targeting delicate taxa such as GZP, and remote areas such as the Arctic Ocean. However, species recovery can be impeded and downstream data interpretation biased by a number of factors. Two of the most significant factors are primer mismatches and gaps in reference databases. Although previous studies have revealed these complexities when targeting GZP (Dischereit et al., 2024b; Murray et al., 2024; Ruiz et al., 2024), there has been a lack of evaluation of the mechanisms behind them and why some species or groups are consistently overlooked in

eDNA surveys in the Arctic. In the present study, we aimed to address these knowledge gaps by evaluating commonly used primer pairs of the COI and 18S genes on a mock community comprised of species commonly found in the Arctic Ocean.

4.1 Database coverage and *in silico* evaluation of metabarcoding primers

The coverage, accuracy and availability of reference databases plays a fundamental role in the effectiveness of metabarcoding studies (Porter and Hajibabaei, 2018a; Taberlet et al., 2018). Curated databases specifically targeting metazoans have been developed and successfully implemented in marine (meta)barcoding studies, including BOLD and MetaZooGene. The use of these curated databases can improve the accuracy of taxonomic assignments over other larger ones such as GenBank and PR2, as they emphasize the quality and taxonomy of the sequences and their associated metadata. However, despite a rapid increase in barcoding effort world-wide (Porter and Hajibabaei, 2018b), some groups still remain under-represented on even the best databases. This continues to impede the accuracy of taxonomic assignments these groups in metabarcoding studies. Overall, we found that database coverage for GZP species known to inhabit the Arctic remains low for both COI and 18S barcodes. This was particularly evident for the class Hydrozoa, where only 40% of the species known to occur in the Arctic had 18S barcodes available on MetaZooGene, and only 50% had COI barcodes. Moreover, our results highlight the fact that not only are there species and genera lacking in reference sequences in general, but there is a paucity of specimens caught and barcoded in the Arctic Ocean. Relying on reference sequences from other oceans and regions could result in endemic conspecifics and cryptic species being overlooked (Porter and Hajibabaei, 2018b). Moreover, although 18S reference barcodes exist for the majority of the groups or species included in the mock community, alignments showed that many were missing bases in the end where the targeted V1-V2 fragment is located. This can be a result of low-quality sequencing at the beginning of the fragments, which is typical of Sanger sequencing (Crossley et al., 2020). Hence it is possible that targeting another commonly used fragment in the middle of the gene such as V4 or V7 would circumvent this issue.

Overall, *in silico* analysis showed that both of the metabarcoding primers pairs investigated had high binding rates for the target GZP. The Leray-XT primer pair successfully amplified at least one of the primers for every species included in the reference dataset, with the exception of the reverse primer on the narcomedusae species *Solmundella bidenticulata*. However, notable omissions in the databases included the cydippid ctenophores and *S. arctica*, which prevented us from testing the primers on them *in silico*. The 18S primers showed successful bindings for all species tested, in both directions. However, while *in silico* assessments of primer coverage can give a good indication of how appropriate a primer pair is for targeting specific groups, some species may show successful amplification *in silico* but not *in vitro* and

vice versa (Ficetola et al., 2010). Such assessments are also affected by the quality of sequences available, and the inclusion of more reference sequences per species, including from the Arctic Ocean, would with no doubt improve the effectiveness of these analyses. Nevertheless, our findings are in-line with the expectation that both primer sets are “universal” and that 18S has a higher coverage for ctenophores of the class Tentaculata (Dischereit et al., 2024b).

4.2 Primer performance: taxonomic coverage

When testing the primers on DNA extract from tissue samples, the 18S primer pairs had a higher coverage than the COI primer pairs. For COI, the Folmer primers (658bp fragment) had the least success at amplifying tissue DNA, with only two out of 16 specimens successfully sequenced. These primers lack degeneracy, which makes them less “universal” than the Leray-XT primers, and is likely one of the reasons behind these low amplification rates (Geller et al., 2013). However, it must be noted that we did not conduct any PCR optimisation nor replicates for the Folmer primers in the present experiment. Doing so could improve the amplification success on the target species and reduce the impact of PCR stochasticity on the number of successful sequences. Optimisation could include decreasing annealing temperature to increase primer binding, the use of different Taq polymerases or the inclusion of bovine albumin serum to reduce the impact of potential PCR inhibitors (Albers et al., 2013; Taberlet et al., 2018). Amplifications using the metabarcoding primers (Leray-XT) were more effective, producing 12 out of 16 successful sequences from the tissue extracts. Amplifications using the Leray-XT primers successfully detected all of the families of the specimens included in the mock community experiment except for the Diphyidae siphonophores (morphologically identified as *D. arctica*) and the ctenophore class Tentaculata. Although MOTUs were assigned to both siphonophores and ctenophore taxa in the metabarcoding output, these were in very low read abundances (<0.01%) and are therefore likely false positives or non-target taxa. In previous Arctic studies targeting GZP in Fram Strait (Murray et al., 2024), a high number of GZP MOTUs were recovered in open water (53 MOTUs assigned as GZP). Furthermore, 27 GZP MOTUs were detected in the surface waters of the marginal ice zone, which indicates that these primers have a wide coverage *in vitro* (Murray et al., under review).

In contrast, the 18S primer pairs generated successful sequences from the tissue of all of the specimens, for both fragment lengths. In the mock community experiment, all of the families included were found to have significant relative read abundances in the metabarcoding output. The highest read abundances were assigned to ASVs of the Diphyidae family, followed by the hydrozoan family Rhopalonematidae. The families with the lowest relative abundances were the narcomedusae family Aeginidae and the hydrozoan family Halicreatidae. The 18S metabarcoding primers were the only ones to amplify ctenophore taxa included in the

experiment (family Tentaculata). This incongruency between the two markers may be due to a number of factors including the degradation rates of mitochondrial DNA and 18S nucleic DNA, primer suitability and biases associated with the PCR protocol. However, given the high number of read copies of mitochondrial DNA present in even degraded tissue (Foran, 2006), it is more likely due to primer and/or PCR-associated biases.

4.3 Primer performance: taxonomic resolution

The ability to detect a high number of genera and species is an important consideration when choosing which gene fragment for community metabarcoding studies. In the present study, the COI markers showed a higher specificity than the 18S primers as they allowed for identification of taxa to species level with high accuracy (>97% match), and congeneric species have enough base differences to confidently distinguish between them. This was especially true for the Leray fragment, which allowed to detect *Atolla tenella* and *Botrynema brucei* to species level with very high accuracy (>99 %) in the tissue samples. The four ctenophore specimens of which sequences were produced had variable Leray sequences, but were categorised as “no match”. This is not surprising considering that cydippids (especially *M. ovum*) were some of the most poorly represented taxa in the databases for the COI gene. In the metabarcoding samples, seven out of the 12 GZP MOTUs were identified to species level. The target groups that were not identified to genus or species were the least represented in the reference databases (e.g., Rhopalonematidae), with the exception of the hydrozoan *A. digitale* (discussed below).

In contrast, 18S primer pairs did not show high levels of specificity. For every specimen except *Aglantha digitale*, at least one other genus or higher taxonomic level also was listed with a 100% match and 100% coverage, and there were multiple specimens that had high matches (>99%) with sister genera, limiting the taxonomic resolution to family level. As *A. digitale* is the only species currently identified in its genus and has only one publicly available reference sequence, we cannot yet conclude if the two 18S fragments can discriminate it to species level. These findings are in line with the assumption that accurate assignments with 18S (both long and short fragments) are restricted to family level for zooplankton in particular (Tang et al., 2012; Wu et al., 2015).

4.4 False negatives in environmental samples

In the Arctic, two species that are regularly caught in nets or detected with optical surveys in high numbers are the Arctic hydrozoan species *Aglantha digitale* and *Sminthea arctica* (family: Rhopalonematidae). Moreover, they are two species that are poised to undergo significant shifts in distribution with climate change, with *S. arctica* predicted to show a poleward range contraction and *A. digitale* poleward range expansion (Pantiukhin et al., 2024b). In the present

study, we found that *A. digitale* was well represented on COI databases and successfully amplified with the primers for the 658 bp Folmer fragment. However, *in silico* analysis revealed that every sequence had at least one mismatch on the forward primer and most had four mismatches. Moreover, it was not successfully amplified with the Leray-XT primer pair (metabarcoding fragment) from tissue DNA nor in the mock community eDNA. In an earlier survey of GZP diversity in the Fram Strait, these two species were successfully detected by both optical and net surveys, yet not by eDNA metabarcoding of the COI gene (Murray et al., 2024) and again in a Svalbard fjord *A. digitale* was caught in high abundances in nets but not detected with eDNA (Murray et al., submitted). Considering that it was the best represented of all the species in the COI databases and the longer barcode (Folmer) fragment was amplified, we conclude that these failures can be attributed to primer mismatch with the forward primer of the Leray-XT pair. The tissue DNA of the second species, *S. arctica*, was successfully amplified with the Leray-XT primers but it was only assigned as hydrozoan (class). A significant proportion of the GZP reads in the mock community metabarcoding dataset were assigned to the same family (Rhopalonematidae), but taxonomic assignment was too low-resolution to identify which genus they belonged to. This is not surprising considering there are no COI reference sequences publicly available for *S. arctica* to date. Reads assigned to Rhopalonematidae also accounted for a significant proportion of the 18S dataset, but the majority of these were assigned to *A. digitale* but not *S. arctica*, despite the availability of 18S reference sequences. This suggests including 18S metabarcoding may not improve the detection rate of *S. arctica* in metabarcoding. Moreover, the fact that we were able to amplify tissue sequences yet only identify them to class level suggests that the paucity of sequences rather than primer mismatch could be the reason. However, more PCR replicates and further barcoding effort would be necessary to confirm this. The development of species-specific primers for these two abundant hydrozoans could be particularly useful in monitoring their predicted distribution shifts (Pantiukhin et al., 2024b), or, due to their particular affinities, as indicators of prevalent water masses.

4.5 Relative read abundances in the mock community

Although linking read abundance to biomass was not the focus of the mock community experiment, some interesting trends were observed nevertheless. In the COI data, the largest proportion was assigned to *Atolla*, which were the largest specimens included in the experiment. However, it is not possible to determine whether this was due to higher biomass or species-specific eDNA shedding rates. For example, the species *Periphylla periphylla*, also in the order Coronatae, has been shown to significantly increase rates of mucus shedding under stress (Stenvers et al., 2023). Another salient finding from the metabarcoding data was the differing levels of variation in relative read abundances between COI and 18S genes. The

18S dataset showed high variation between replicates for GZP whereas the COI replicates were relatively similar. Differences in read abundances between the two markers for the same species are to be expected as mitochondrial genes generally have more read copies than nucleic genes. However, the high variation between the replicates for 18S hint at it being more susceptible to misleading quantitative interpretations compared to COI. This was also evident in the marginal ice zone study targeting GZP with both of these primer sets (Murray et al., *under review*), where the 18S metazoan reads were dominated by calanoid copepods and the COI reads were more balanced between groups. While there may be benefits regarding the number of species recovered, using multiple markers (i.e., mitochondrial and nucleic) can complicate the interpretation of read abundances in relation to biomass. Trends between read abundances and biomass have been identified for zooplankton groups in the Arctic COI in bulk samples (Ershova et al., 2023, 2021), however the lack of experiments on GZP species in particular prevents further conclusions being drawn here.

4.6 Non-target GZP assignments

Gelatinous zooplankton taxa that were not part of the mock community were recovered in both metabarcoding datasets, with the scyphozoan *Cyanea capillata* being the most notable in both datasets. The seawater used for the experiment was filtered several times and as part of the bioinformatic processing, an adjustment was made to remove the taxa detected in the water control sample from the main samples. Furthermore, the extraction and PCR controls used to track cross-contamination during the laboratory processing and sequencing showed very low or no reads, and none assigned to GZP. Therefore, we conclude that the source of DNA of the non-target taxa amplified here was highly likely the GZP individuals themselves. They were caught in plankton nets alongside other GZP species and the specimens were not cleaned in any way before being placed in the aquarium, and hence were likely carrying DNA from other species they were in contact with or traces from the nets.

4.7 Which primers to use for metabarcoding studies on Arctic GZP?

Some studies have suggested the use another mitochondrial marker, 16S RNA, as a more suitable alternative to COI for GZP in general (Lindsay et al., 2015), and for hydrozoans in particular (Zheng et al., 2014). Indeed, some of the species in the mock community that have few or no COI barcodes, do have 16S barcodes in the reference databases (e.g., *Sminthea arctica*). However, according to our MetaZooGene search, there are significantly fewer barcodes for 16S than COI at present despite a marginally higher species coverage. The number of publicly available COI sequences is also significantly higher than for 16S on the BOLD database. Moreover, the prevalence of indels on the 16S gene can significantly affect sequences alignments (Hebert et al., 2003) and as a result of less developed bioinformatic

pipelines being available (compared to COI), it can be difficult to identify their presence as well as the occurrence of pseudogenes (Braukmann et al., 2019). Additionally, 16S is more conservative than COI and has a higher chance of closely related species sharing exactly the same sequence (Andújar et al., 2018), which has been observed for the hydrozoan family Pandeidae (Schuchert, 2018). Finally, while there are well established primer sets available for its longer barcode fragment, widely used 16S metabarcoding primer sets (designed for metazoans) and associated bioinformatic pipelines are still lacking. Using 16S barcoding to target species-specific questions may be an effective tactic if these issues were addressed, but considering the higher amounts publicly available resources that already exist for COI and 18S (meta)barcoding (e.g., reference databases, bioinformatic pipelines and primer options), we argue that further optimisation of the COI marker is a more efficient use of resources for multi-species studies.

5. Conclusions

Our findings show that amplifying the COI Leray fragment with the Leray-XT primers allows for accurate and high-resolution assignments of Arctic GZP species. However, its use may overlook some species as a result of primer mismatches and a lack of reference sequences. Secondly, the V1-V2 fragment and primers had excellent coverage for the target GZP groups. But, as expected, there is not enough variation on the full nor the V1-V2 18S fragments to distinguish between closely related genera and most species of the GZP. While multi-marker metabarcoding can increase the number of target taxa recovered, which is what we saw at the family level in the present study, it is not always economically viable and does not necessarily increase the ecologically meaningful information (e.g., species-level detections). It can also introduce further complications in interpreting the differing read abundances of the same species, which were obtained from the same DNA extract. Furthermore, the difference in taxonomic resolution can make direct comparisons between the markers impossible. In conclusion, the choice of primer pairs and target fragments for metabarcoding of GZP in the Arctic used should be determined by the study goal and take the targeted taxonomic resolution and reference database coverage into consideration (Elbrecht et al., 2019; Porter and Hajibabaei, 2018a). Finally, we highlight the urgent need for improving public reference databases by increasing barcoding effort that targets GZP species and specifically from specimens caught in the Arctic Ocean.

References

- Adams, C.I.M., Knapp, M., Gemmell, N.J., Jeunen, G.-J., Bunce, M., Lamare, M.D., Taylor, H.R., 2019. Beyond Biodiversity: Can Environmental DNA (eDNA) Cut It as a Population Genetics Tool? *Genes* 10, 192. <https://doi.org/10.3390/genes10030192>
- Albaina, A., Garić, R., Yebra, L., 2024. Know your limits; miniCOI metabarcoding fails with key marine zooplankton taxa. *Journal of Plankton Research* fbae057. <https://doi.org/10.1093/plankt/fbae057>
- Albers, C.N., Jensen, A., Bælum, J., Jacobsen, C.S., 2013. Inhibition of DNA Polymerases Used in Q-PCR by Structurally Different Soil-Derived Humic Substances. *Geomicrobiology Journal* 30, 675–681. <https://doi.org/10.1080/01490451.2012.758193>
- Ames, C.L., Ohdera, A.H., Colston, S.M., Collins, A.G., Fitt, W.K., Morandini, A.C., Erickson, J.S., Vora, G.J., 2021. Fieldable Environmental DNA Sequencing to Assess Jellyfish Biodiversity in Nearshore Waters of the Florida Keys, United States. *Frontiers in Marine Science* 8.
- Andújar, C., Arribas, P., Yu, D.W., Vogler, A.P., Emerson, B.C., 2018. Why the COI barcode should be the community DNA metabarcode for the metazoa. *Molecular Ecology* 27, 3968–3975. <https://doi.org/10.1111/mec.14844>
- Antich, A., Palacín, C., Zarceró, J., Wangensteen, O.S., Turon, X., 2022. Metabarcoding reveals high-resolution biogeographical and metaphylogeographical patterns through marine barriers. *Journal of Biogeography*.
- Antich González, A., Palacín, C., Xavier, T., Wangensteen, O.S., 2022. DnoisE: distance denoising by entropy. An open-source parallelizable alternative for denoising sequence datasets [PeerJ].
- Blaxter, M.L., De Ley, P., Garey, J.R., Liu, L.X., Scheldeman, P., Vierstraete, A., Vanfleteren, J.R., Mackey, L.Y., Dorris, M., Frisse, L.M., Vida, J.T., Thomas, W.K., 1998. A molecular evolutionary framework for the phylum Nematoda. *Nature* 392, 71–75. <https://doi.org/10.1038/32160>
- Bolte, B., Goldsbury, J., Huerlimann, R., Jerry, D., Kingsford, M., 2021. Validation of eDNA as a viable method of detection for dangerous cubozoan jellyfish. *Environmental DNA* 3, 769–779. <https://doi.org/10.1002/edn3.181>
- Bouillon, J., Gravili, C., Pagès, F., Gili, J.-M., Boero, F., 2006. An introduction to Hydrozoa. *Muséum national d'Histoire naturelle, Paris*.
- Boyer, F., Mercier, C., Bonin, A., Le Bras, Y., Taberlet, P., Coissac, E., 2016. obitools: a unix-inspired software package for DNA metabarcoding. *Molecular Ecology Resources* 16, 176–182. <https://doi.org/10.1111/1755-0998.12428>
- Braukmann, T.W.A., Ivanova, N.V., Prosser, S.W.J., Elbrecht, V., Steinke, D., Ratnasingham, S., de Waard, J.R., Sones, J.E., Zakharov, E.V., Hebert, P.D.N., 2019. Metabarcoding a diverse arthropod mock community. *Molecular Ecology Resources* 19, 711–727. <https://doi.org/10.1111/1755-0998.13008>
- Buchner, D., Leese, F., 2020. BOLDigger – a Python package to identify and organise sequences with the Barcode of Life Data systems. *Metabarcoding and Metagenomics* 4, e53535. <https://doi.org/10.3897/mbmg.4.53535>
- Bucklin, A., Lindeque, P.K., Rodriguez-Ezpeleta, N., Albaina, A., Lehtiniemi, M., 2016. Metabarcoding of marine zooplankton: prospects, progress and pitfalls. *Journal of Plankton Research* 38, 393–400. <https://doi.org/10.1093/plankt/fbw023>
- Bucklin, A., Steinke, D., Blanco-Bercial, L., 2011. DNA Barcoding of Marine Metazoa. *Annual Review of Marine Science* 3, 471–508. <https://doi.org/10.1146/annurev-marine-120308-080950>
- Callahan, B.J., McMurdie, P.J., Rosen, M.J., Han, A.W., Johnson, A.J.A., Holmes, S.P., 2016. DADA2: High-resolution sample inference from Illumina amplicon data. *Nat Methods* 13, 581–583. <https://doi.org/10.1038/nmeth.3869>

- Clarke, L.J., Beard, J.M., Swadling, K.M., Deagle, B.E., 2017. Effect of marker choice and thermal cycling protocol on zooplankton DNA metabarcoding studies. *Ecology and Evolution* 7, 873–883. <https://doi.org/10.1002/ece3.2667>
- Crossley, B.M., Bai, J., Glaser, A., Maes, R., Porter, E., Killian, M.L., Clement, T., Toohey-Kurth, K., 2020. Guidelines for Sanger sequencing and molecular assay monitoring. *J VET Diagn Invest* 32, 767–775. <https://doi.org/10.1177/1040638720905833>
- Dischereit, A., Beermann, J., Lebreton, B., Wangensteen, O.S., Neuhaus, S., Havermans, C., 2024a. DNA metabarcoding reveals a diverse, omnivorous diet of Arctic amphipods during the polar night, with jellyfish and fish as major prey. *Front. Mar. Sci.* 11. <https://doi.org/10.3389/fmars.2024.1327650>
- Dischereit, A., Throm, J.K., Werner, K.-M., Neuhaus, S., Havermans, C., 2024b. A belly full of jelly? DNA metabarcoding shows evidence for gelatinous zooplankton predation by several fish species in Greenland waters. *Royal Society Open Science*. <https://doi.org/10.1098/rsos.240797>
- Dischereit, A., Wangensteen, O.S., Præbel, K., Auel, H., Havermans, C., 2022. Using DNA Metabarcoding to Characterize the Prey Spectrum of Two Co-Occurring Themisto Amphipods in the Rapidly Changing Atlantic-Arctic Gateway Fram Strait. *Genes* 13, 2035. <https://doi.org/10.3390/genes13112035>
- Elbrecht, V., Braukmann, T.W.A., Ivanova, N.V., Prosser, S.W.J., Hajibabaei, M., Wright, M., Zakharov, E.V., Hebert, P.D.N., Steinke, D., 2019. Validation of COI metabarcoding primers for terrestrial arthropods. *PeerJ* 7, e7745. <https://doi.org/10.7717/peerj.7745>
- Ershova, E.A., Wangensteen, O.S., Descoteaux, R., Barth-Jensen, C., Præbel, K., 2021. Metabarcoding as a quantitative tool for estimating biodiversity and relative biomass of marine zooplankton. *ICES Journal of Marine Science* 78, 3342–3355. <https://doi.org/10.1093/icesjms/fsab171>
- Ershova, E.A., Wangensteen, O.S., Falkenhaug, T., 2023. Mock samples resolve biases in diversity estimates and quantitative interpretation of zooplankton metabarcoding data. *Mar. Biodivers.* 53, 66. <https://doi.org/10.1007/s12526-023-01372-x>
- Feng, Y., Sun, D., Shao, Q., Fang, C., Wang, C., 2022. Mesozooplankton biodiversity, vertical assemblages, and diel migration in the western tropical Pacific Ocean revealed by eDNA metabarcoding and morphological methods. *Frontiers in Marine Science* 9.
- Ficetola, G.F., Coissac, E., Zundel, S., Riaz, T., Shehzad, W., Bessi re, J., Taberlet, P., Pompanon, F., 2010. An In silico approach for the evaluation of DNA barcodes. *BMC Genomics* 11, 434. <https://doi.org/10.1186/1471-2164-11-434>
- Folmer, O., Black, M., Hoeh, W., Lutz, R., Vrijenhoek, R., 1994. DNA primers for amplification of mitochondrial cytochrome c oxidase subunit I from diverse metazoan invertebrates. *Molecular Marine Biology and Biotechnology* 3, 294–299.
- Foran, D.R., 2006. Relative Degradation of Nuclear and Mitochondrial DNA: An Experimental Approach. *Journal of Forensic Sciences* 51, 766–770. <https://doi.org/10.1111/j.1556-4029.2006.00176.x>
- Fr slev, T.G., Kj ller, R., Bruun, H.H., Ejrn es, R., Brunbjerg, A.K., Pietroni, C., Hansen, A.J., 2017. Algorithm for post-clustering curation of DNA amplicon data yields reliable biodiversity estimates. *Nat Commun* 8, 1188. <https://doi.org/10.1038/s41467-017-01312-x>
- Geller, J., Meyer, C., Parker, M., Hawk, H., 2013. Redesign of PCR primers for mitochondrial cytochrome c oxidase subunit I for marine invertebrates and application in all-taxa biotic surveys. *Molecular Ecology Resources* 13, 851–861. <https://doi.org/10.1111/1755-0998.12138>
- Govindarajan, A.F., Francolini, R.D., Jech, J.M., Lavery, A.C., Llopiz, J.K., Wiebe, P.H., Zhang, W. (Gordon), 2021. Exploring the Use of Environmental DNA (eDNA) to Detect Animal Taxa in the Mesopelagic Zone. *Frontiers in Ecology and Evolution* 9.
- G nther, B., Fromentin, J.-M., Metral, L., Arnaud-Haond, S., 2021. Metabarcoding confirms the opportunistic foraging behaviour of Atlantic bluefin tuna and reveals the importance of gelatinous prey. *PeerJ* 9, e11757. <https://doi.org/10.7717/peerj.11757>

- Haddock, S.H.D., 2004. A golden age of gelata: past and future research on planktonic ctenophores and cnidarians. *Hydrobiologia* 530, 549–556.
<https://doi.org/10.1007/s10750-004-2653-9>
- Hays, G.C., Doyle, T.K., Houghton, J.D.R., 2018. A Paradigm Shift in the Trophic Importance of Jellyfish? *Trends in Ecology & Evolution* 33, 874–884.
<https://doi.org/10.1016/j.tree.2018.09.001>
- Hebert, P., Cywinska, A., Ball, S.L., deWaard, J.R., 2003. Biological identifications through DNA barcodes. *Proceedings of the Royal Society London. Series B: Biological Sciences* 1512, 313–321.
- Hebert, P.D., Ratnasingham, S., Waard, J.R., 2003. Barcoding animal life: cytochrome c oxidase subunit 1 divergences among closely related species, in: *Proceedings of the Royal Society of London*. <https://doi.org/10.1098/rsbl.2003.0025>
- Hosia, A., Falkenhaus, T., Baxter, E.J., Pagès, F., 2017. Abundance, distribution and diversity of gelatinous predators along the northern Mid-Atlantic Ridge: A comparison of different sampling methodologies. *PLoS ONE* 12, e0187491.
<https://doi.org/10.1371/journal.pone.0187491>
- Leray, M., Knowlton, N., 2016. Censusing marine eukaryotic diversity in the twenty-first century. *Philosophical Transactions of the Royal Society B: Biological Sciences* 371, 20150331. <https://doi.org/10.1098/rstb.2015.0331>
- Licandro, P., Carré, C., Lindsay, D.J., 2017a. Cnidaria: Colonial Hydrozoa (Siphonophorae), in: Castellani, C., Edwards, M. (Eds.), *Marine Plankton: A Practical Guide to Ecology, Methodology, and Taxonomy*. Oxford University Press, p. 0.
<https://doi.org/10.1093/oso/9780199233267.003.0019>
- Licandro, P., Fischer, A., Lindsay, D.J., 2017b. Cnidaria: Scyphozoa and non-colonial Hydrozoa, in: *Marine Plankton: A Practical Guide to Ecology, Methodology, and Taxonomy*. Oxford University Press.
- Licandro, P., Lindsay, D.J., 2017. Ctenophora, in: *Marine Plankton: A Practical Guide to Ecology, Methodology, and Taxonomy*. Oxford University Press.
- Lindsay, D.J., Grossmann, M.M., Nishikawa, J., Bentlage, B., Collins, A.G., 2015. DNA barcoding of pelagic cnidarians: current status and future prospects. *日本プランクトン学会報* 62, 39–43. https://doi.org/10.24763/bpsj.62.1_39
- Mahé, F., Czech, L., Stamatakis, A., Quince, C., de Vargas, C., Dunthorn, M., Rognes, T., 2021. Swarm v3: towards tera-scale amplicon clustering. *Bioinformatics* 38, 267–269.
<https://doi.org/10.1093/bioinformatics/btab493>
- Martin, M., 2011. Cutadapt removes adapter sequences from high-throughput sequencing reads. *EMBnet.journal* 17, 10–12. <https://doi.org/10.14806/ej.17.1.200>
- McMurdie, P.J., Holmes, S., 2013. phyloseq: An R Package for Reproducible Interactive Analysis and Graphics of Microbiome Census Data. *PLOS ONE* 8, e61217.
<https://doi.org/10.1371/journal.pone.0061217>
- Medlin, L., Elwood, H.J., Stickel, S., Sogin, M.L., 1988. The characterization of enzymatically amplified eukaryotic 16S-like rRNA-coding regions. *Gene* 71, 491–499.
[https://doi.org/10.1016/0378-1119\(88\)90066-2](https://doi.org/10.1016/0378-1119(88)90066-2)
- Minamoto, T., Fukuda, M., Katsuhara, K.R., Fujiwara, A., Hidaka, S., Yamamoto, S., Takahashi, K., Masuda, R., 2017. Environmental DNA reflects spatial and temporal jellyfish distribution. *PLOS ONE* 12, e0173073.
<https://doi.org/10.1371/journal.pone.0173073>
- Murray, A., Hoppe, C.J.M., Düsedau, L., Antich, A., Havermans, C., *submitted*. Surveying marine biodiversity using eDNA metabarcoding of seawater and sediment in a high Arctic fjord during the polar night (Kongsfjorden, Svalbard). *Marine Environmental Research*.
- Murray, A., Præbel, K., Desiderato, A., Auel, H., Havermans, C., 2023. Phylogeography and molecular diversity of two highly abundant *Themisto* amphipod species in a rapidly changing Arctic Ocean. *Ecology and Evolution* 13, e10359.
<https://doi.org/10.1002/ece3.10359>

- Murray, A., Priest, T., Antich, A., von Appen, W.-J., Neuhaus, S., Havermans, C., 2024. Investigating pelagic biodiversity and gelatinous zooplankton communities in the rapidly changing European Arctic: An eDNA metabarcoding survey. *Environmental DNA* 6, e569. <https://doi.org/10.1002/edn3.569>
- Murray, A., Ramondenc, S., Reifenberg, S., Jucker, M., Neudert, M., McPherson, R., von Appen, W.-J., Havermans, C., under review. Eukaryotic biodiversity of sub-ice water in the Marginal Ice Zone of the European Arctic: A multi-marker eDNA metabarcoding survey. *Science of The Total Environment*.
- Nogueira Júnior, M., Pukanski, L.E. de M., Souza-Conceição, J.M., 2015. Mesh size effects on assessments of planktonic hydrozoan abundance and assemblage structure. *Journal of Marine Systems* 144, 117–126. <https://doi.org/10.1016/j.jmarsys.2014.11.014>
- O'Brien, T.D., Blanco-Bercial, L., Questel, J.M., Batta-Lona, P.G., Bucklin, A., 2024. MetaZooGene Atlas and Database: Reference Sequences for Marine Ecosystems, in: DeSalle, R. (Ed.), *DNA Barcoding: Methods and Protocols*. Springer US, New York, NY, pp. 475–489. https://doi.org/10.1007/978-1-0716-3581-0_28
- Ogata, M., Masuda, R., Harino, H., Sakata, M.K., Hatakeyama, M., Yokoyama, K., Yamashita, Y., Minamoto, T., 2021. Environmental DNA preserved in marine sediment for detecting jellyfish blooms after a tsunami. *Sci Rep* 11, 16830. <https://doi.org/10.1038/s41598-021-94286-2>
- Pantiukhin, D., Soto-Angel, J.J., Hosia, A., Hoving, H.-J., Havermans, C., 2024a. In-situ observations of gelatinous zooplankton aggregations in inshore and offshore Arctic waters. *Polar Biol.* <https://doi.org/10.1007/s00300-024-03306-0>
- Pantiukhin, D., Verhaegen, G., Havermans, C., 2024b. Pan-Arctic distribution modeling reveals climate-change-driven poleward shifts of major gelatinous zooplankton species. *Limnology and Oceanography* 69, 1316–1334. <https://doi.org/10.1002/lno.12568>
- Pantiukhin, D., Verhaegen, G., Kraan, C., Jerosch, K., Neitzel, P., Hoving, H., Havermans, C., 2023. Optical observations and spatio-temporal projections of gelatinous zooplankton in the Fram Strait, a gateway to a changing Arctic Ocean. *Frontiers in Marine Science* Volume 10. <https://doi.org/10.3389/fmars.2023.987700>
- Porter, T.M., Hajibabaei, M., 2018a. Scaling up: A guide to high-throughput genomic approaches for biodiversity analysis. *Molecular Ecology* 27, 313–338. <https://doi.org/10.1111/mec.14478>
- Porter, T.M., Hajibabaei, M., 2018b. Over 2.5 million COI sequences in GenBank and growing. *PLOS ONE* 13, e0200177. <https://doi.org/10.1371/journal.pone.0200177>
- Questel, J.M., Hopcroft, R.R., DeHart, H.M., Smoot, C.A., Kosobokova, K.N., Bucklin, A., 2021. Metabarcoding of zooplankton diversity within the Chukchi Borderland, Arctic Ocean: improved resolution from multi-gene markers and region-specific DNA databases. *Mar. Biodivers.* 51, 4. <https://doi.org/10.1007/s12526-020-01136-x>
- Rantanen, M., Karpechko, A.Y., Lipponen, A., Nordling, K., Hyvärinen, O., Ruosteenoja, K., K., V., Laaksonen, A., 2022. The Arctic has warmed nearly four times faster than the globe since 1979. *Communications Earth & Environment* 3, 1–10.
- Raskoff, K.A., Hopcroft, R.R., Kosobokova, K.N., Purcell, J.E., Youngbluth, M., 2010. Jellies under ice: ROV observations from the Arctic 2005 hidden ocean expedition. *Deep Sea Research Part II: Topical Studies in Oceanography, Observations and Exploration of the Arctic's Canada Basin and the Chukchi Sea: the Hidden Ocean and RUSALCA Expeditions* 57, 111–126. <https://doi.org/10.1016/j.dsr2.2009.08.010>
- Ratnasingham, S., Hebert, P.D.N., 2007. bold: The Barcode of Life Data System (<http://www.barcodinglife.org>). *Molecular Ecology Notes* 7, 355–364. <https://doi.org/10.1111/j.1471-8286.2007.01678.x>
- Rognes, T., Flouri, T., Nichols, B., Quince, C., Mahé, F., 2016. VSEARCH: a versatile open source tool for metagenomics. *PeerJ* 4, e2584. <https://doi.org/10.7717/peerj.2584>
- Rozen, S., Skaletsky, H., 1999. Primer3 on the WWW for General Users and for Biologist Programmers, in: Misener, S., Krawetz, S.A. (Eds.), *Bioinformatics Methods and*

- Protocols. Humana Press, Totowa, NJ, pp. 365–386. <https://doi.org/10.1385/1-59259-192-2:365>
- Ruiz, M.B., Moreira, E., Novillo, M., Neuhaus, S., Leese, F., Havermans, C., 2024. Detecting the invisible through DNA metabarcoding: The role of gelatinous taxa in the diet of two demersal Antarctic key stone fish species (Notothenioidei). *Environmental DNA* 6, e561. <https://doi.org/10.1002/edn3.561>
- Schuchert, P., 2018. DNA barcoding of some Pandeidae species (Cnidaria, Hydrozoa, Anthoathecata). *Revue suisse de Zoologie* 125, 101–127. <https://doi.org/10.5281/zenodo.1196029>
- Sinniger, F., Pawlowski, J., Harii, S., Gooday, A.J., Yamamoto, H., Chevaldonné, P., Cedhagen, T., Carvalho, G., Creer, S., 2016. Worldwide Analysis of Sedimentary DNA Reveals Major Gaps in Taxonomic Knowledge of Deep-Sea Benthos. *Frontiers in Marine Science* 3.
- Soltwedel, T., 2021. The Expedition PS126 of the Research Vessel POLARSTERN to the Fram Strait in 2021 [WWW Document]. *Berichte zur Polar- und Meeresforschung = Reports on polar and marine research*. https://doi.org/10.48433/BzPM_0757_2021
- Stenvers, V.I., Hauss, H., Bayer, T., Havermans, C., Hentschel, U., Schmittmann, L., Sweetman, A.K., Hoving, H.-J.T., 2023. Experimental mining plumes and ocean warming trigger stress in a deep pelagic jellyfish. *Nat Commun* 14, 7352. <https://doi.org/10.1038/s41467-023-43023-6>
- Taberlet, P., Bonin, A., Zinger, L., Coissac, E., 2018. *Environmental DNA: For Biodiversity Research and Monitoring*. Oxford University Press.
- Tang, C.Q., Leasi, F., Obertegger, U., Kieneke, A., Barraclough, T.G., Fontaneto, D., 2012. The widely used small subunit 18S rDNA molecule greatly underestimates true diversity in biodiversity surveys of the meiofauna. *Proceedings of the National Academy of Sciences* 109, 16208–16212. <https://doi.org/10.1073/pnas.1209160109>
- Teunisse, G.M., 2022. *Fantaxtic - Nested Bar Plots for Phyloseq Data*.
- Urban, P., Præbel, K., Bhat, S., Dierking, J., Wangensteen, O.S., 2022. DNA metabarcoding reveals the importance of gelatinous zooplankton in the diet of *Pandalus borealis*, a keystone species in the Arctic. *Molecular Ecology* 31, 1562–1576. <https://doi.org/10.1111/mec.16332>
- Verhaegen, G., Kawakami, T., Murray, A., Kasai, A., Havermans, C., in review. Metazoan diversity and its drivers: an eDNA survey in the Pacific Gateway of a changing Arctic Ocean. *Environmental DNA*.
- Wangensteen, O.S., Palacín, C., Guardiola, M., Turon, X., 2018. DNA metabarcoding of littoral hard-bottom communities: high diversity and database gaps revealed by two molecular markers. *PeerJ* 6, e4705. <https://doi.org/10.7717/peerj.4705>
- Wickham, H., 2016. *ggplot2: Elegant Graphics for Data Analysis*.
- Wu, S., Xiong, J., Yu, Y., 2015. Taxonomic Resolutions Based on 18S rRNA Genes: A Case Study of Subclass Copepoda. *PLOS ONE* 10, e0131498. <https://doi.org/10.1371/journal.pone.0131498>
- Zheng, L., He, J., Lin, Y., Cao, W., Zhang, W., 2014. 16S rRNA is a better choice than COI for DNA barcoding hydrozoans in the coastal waters of China. *Acta Oceanol. Sin.* 33, 55–76. <https://doi.org/10.1007/s13131-014-0415-8>

Table S1. Primer pair details and PCR conditions.

Target	Primer name	Primer sequence	Target sequence length	Reference	Tissue Extractions		Metabarcoding		
					Master mix	PCR Conditions	Master mix	PCR Conditions	
COI	Leray	mICOLintF-XT	5'-GGWACWR GWTGRAC WITITAYCC YCC-3'	313	(Wangenstein et al., 2018)	Final volume of 25 µL, containing 2.5 µL of template DNA, 0.5 µM of the primers, 12.5 µL of Supreme NZYtaq 2x Colourless Master Mix (NZYTech), and ultrapure water up to 12.5 µL	Initial denaturation step at 95°C for 5 min, followed by 35 cycles of 95 °C for 30 s, 54.7 °C for 45 s, 72 °C for 45 s, and a final extension step at 72 °C for 7 min	First PCR: Same as tissue except half of all volumes used for a 12.5µL final volume and Supreme NZYtaq 2x Green Master Mix (NZYTech)	First PCR: Same as tissue
		jpgHCO2198	5'-TAIACYTCI GGRTGICC RAARAAAYC A-3'	313	(Geller et al., 2013)				
	Folmer	LCO1490	5'-GGTCAACA AATCTAAA GATATTGG -3'	658	(Folmer et al., 1994)	Final volume of 25 µL, containing 3 µL of template DNA, 0.5 µM of the primers, 0.1 µL of Accu Start II polymerase Taq (Quantabio), 0.5 mM dNTP, 1.5 mM MgCl and ultrapure water up to 25 µL.	Initial denaturation step at 94°C for 5 min, followed by 4 cycles of 94 °C for 30 s, 45 °C for 30 s, 72 °C for 1 min. Followed by 30 cycles of 94°C for 45 s, 50°C for 30 s, 72°C for 1 min and final extension step of 72°C for 10 min	-	-
		HCO2198	5'-TAAACTTC AGGGTGA CCAAAAA TCA- 3'	658	(Folmer et al., 1994)				
18S	V1-V2	SSU_F04	5'-GCTTGCT CAAAGATT AAGCC 3'	~350	(Blaxter et al., 1998)	Final volume of 25 µL, containing 2.5 µL of template DNA, 0.5 µM of the primers, 12.5 µL of Supreme NZYtaq 2x Colourless Master Mix (NZYTech), and ultrapure water up to 25 µL.	Initial denaturation step at 95°C for 5 min, followed by 35 cycles of 95 °C for 30 s, 54.7 °C for 45 s, 72 °C for 45 s, and a final extension step at 72 °C for 7 min	First PCR: Same as tissue except half of all volumes used for a 12.5µL final volume and Supreme NZYtaq 2x Green Master Mix (NZYTech)	First PCR: Same as tissue except annealing temperature of 49.7 °C used.

	SSURmod	5' CCTGCTGC CTTCCTTR GA 3'	~350	(Sinniger et al., 2016)			Second PCR: Final volume of 25 μL, containing 2.5 μL of PCR product, 1 μM of the dual-index primers, 6.5 μL of Supreme NZYTaq 2x Green Master Mix (NZYTech), ultrapure water up to 25 μL	Second PCR: Same as first PCR but with 60 °C denaturation step
Full 18S	Mitch A	5'- AACCTGGT TGATCCTG CCAGT-3'	~1800	(Medlin et al., 1988)	Final volume of 25 μL, containing 3 μL of template DNA, 0.2 μM of the primers, 0.15 μL of TaKaRa polymerase Taq (Takara), 0.25 mM dNTP, 1.5 mM MgCl and ultrapure water up to 25 μL.	Initial denaturation step at 98°C for 1 min, followed by 35 cycles of 98 °C for 30 s, 56 °C for 1 min, 72 °C for 1 min, and a final extension step at 72 °C for 10 min	-	-
	Mitch B	5'- TGATCCTT CTGCAGGT TCACCTAC -3'	~1800					

Table S2. Summary of reference sequences available for each target species on the public databases BOLD and MetaZooGene.

Species	COI		18S	
	MetaZooGene	BOLD	MetaZooGene	BOLD
<i>Aglantha digitale</i>	34	41	1	5
<i>Atolla spp*</i>	7	8	3	6
<i>Botrynema spp*</i>	2	2	1	12
<i>Dimophyes arctica</i>	3	3	2	4
<i>Sminthea arctica</i>	0	0	0	8
<i>Solmundella bidenticulata</i>	12	14	1	3
<i>Aegina citrea</i>	7	9	1	4
<i>Euplokamis dunlapae</i>	0	0	1	0
<i>Mertensia ovum</i>	0	3	3	20

Notes: (*)= only species found in Arctic included. (+) = sequence originated on GenBank where it is marked as "unverified".

Table S3. *In silico* PCR results for Leray-XT primers

Species	Sequence Name	Sequence_length	Primer	Direction	Minimum	Maximum	Mismatches	Mismatch Positions
<i>Aegina_citrea</i>	KY040285	642	Leray 5'	forward	318	343	0	
<i>Aegina_citrea</i>	KY040286	655	Leray 5'	forward	317	342	0	
<i>Aegina_citrea</i>	KY040291	649	Leray 5'	forward	311	336	0	
<i>Aegina_citrea</i>	KY040292	845	Leray 3'	reverse	642	667	0	
<i>Aegina_citrea</i>	KY040292	845	Leray 5'	forward	303	328	0	
<i>Aegina_citrea</i>	KY040293	886	Leray 3'	reverse	664	689	1	=====T=====
<i>Aegina_citrea</i>	KY040293	886	Leray 5'	forward	325	350	0	
<i>Aegina_citrea</i>	KY040294	656	Leray 5'	forward	315	340	0	
<i>Aegina_citrea</i>	QHAK892-21	658	Leray 5'	forward	320	345	0	
<i>Aglantha_digitale</i>	CAISN1013-13	657	Leray 5'	forward	319	344	4	==T====T====T=====T==
<i>Aglantha_digitale</i>	CAISN1015-13	657	Leray 5'	forward	319	344	4	==T====T====T=====T==
<i>Aglantha_digitale</i>	CAISN1277-13	483	Leray 5'	forward	241	266	3	==T====T====T=====
<i>Aglantha_digitale</i>	CAISN185-12	657	Leray 5'	forward	319	344	4	==T====T====T=====T==
<i>Aglantha_digitale</i>	ECHAR083-19	658	Leray 5'	forward	320	345	4	==T====T====T=====T==
<i>Aglantha_digitale</i>	ECHAR084-19	658	Leray 5'	forward	320	345	4	==T====T====T=====T==
<i>Aglantha_digitale</i>	ECHAR085-19	658	Leray 5'	forward	320	345	4	==T====T====T=====T==
<i>Aglantha_digitale</i>	ECHAR086-19	658	Leray 5'	forward	320	345	4	==T====T====T=====T==
<i>Aglantha_digitale</i>	ECHAR087-19	658	Leray 5'	forward	320	345	4	==T====T====T=====T==
<i>Aglantha_digitale</i>	ECHAR088-19	658	Leray 5'	forward	320	345	4	==T====T====T=====T==
<i>Aglantha_digitale</i>	FJ602534	515	Leray 5'	forward	316	341	4	==T====T====T=====T==
<i>Aglantha_digitale</i>	FJ602535	536	Leray 5'	forward	316	341	4	==T====T====T=====T==
<i>Aglantha_digitale</i>	GQ120073	812	Leray 3'	reverse	578	603	1	=====T=====
<i>Aglantha_digitale</i>	GQ120073	812	Leray 5'	forward	239	264	4	==T====T====T=====T==
<i>Aglantha_digitale</i>	HQ970923	658	Leray 5'	forward	320	345	4	==T====T====T=====T==
<i>Aglantha_digitale</i>	HQ970924	658	Leray 5'	forward	320	345	4	==T====T====T=====T==
<i>Aglantha_digitale</i>	HQ970926	658	Leray 5'	forward	320	345	4	==T====T====T=====T==
<i>Aglantha_digitale</i>	HQ970927	658	Leray 5'	forward	320	345	4	==T====T====T=====T==
<i>Aglantha_digitale</i>	HYPNO049-15	574	Leray 5'	forward	277	302	4	==T====T====T=====T==
<i>Aglantha_digitale</i>	HYPNO257-17	658	Leray 5'	forward	320	345	4	==T====T====T=====T==

<i>Aglantha_digitale</i>	JN314229	636	Leray 5'	forward	298	323	4	==T====T====T====T==
<i>Aglantha_digitale</i>	KBCSM529-14	646	Leray 5'	forward	318	343	4	==T====T====T====T==
<i>Aglantha_digitale</i>	KBCSM792-14	648	Leray 5'	forward	320	345	4	==T====T====T====T==
<i>Aglantha_digitale</i>	KC440117	657	Leray 5'	forward	320	345	4	==T====T====T====T==
<i>Aglantha_digitale</i>	KC440118	657	Leray 5'	forward	320	345	4	==T====T====T====T==
<i>Aglantha_digitale</i>	KC440119	650	Leray 5'	forward	313	338	4	==T====T====T====T==
<i>Aglantha_digitale</i>	KC440120	650	Leray 5'	forward	313	338	3	==T====T====T====T==
<i>Aglantha_digitale</i>	KC440121	629	Leray 5'	forward	313	338	3	==T====T====T====T==
<i>Aglantha_digitale</i>	KC440122	624	Leray 5'	forward	320	345	3	==T====T====T====T==
<i>Aglantha_digitale</i>	KC440123	624	Leray 5'	forward	320	345	4	==T====T====T====T==
<i>Aglantha_digitale</i>	KC440124	658	Leray 5'	forward	320	345	4	==T====T====T====T==
<i>Aglantha_digitale</i>	KC440125	658	Leray 5'	forward	320	345	4	==T====T====T====T==
<i>Aglantha_digitale</i>	KC440126	658	Leray 5'	forward	320	345	4	==T====T====T====T==
<i>Aglantha_digitale</i>	KY040280	625	Leray 5'	forward	307	332	4	==T====T====T====T==
<i>Aglantha_digitale</i>	MH242648	633	Leray 5'	forward	320	345	4	==T====T====T====T==
<i>Atolla_tenella</i>	OM214510	665	Leray 3'	reverse	555	580	0	
<i>Atolla_tenella</i>	OM214510	665	Leray 5'	forward	216	241	1	==T====T====T====T==
<i>Atolla_tenella</i>	OM214511	665	Leray 3'	reverse	555	580	0	
<i>Atolla_tenella</i>	OM214511	665	Leray 5'	forward	216	241	1	==T====T====T====T==
<i>Atolla_tenella</i>	OM214512	665	Leray 3'	reverse	555	580	0	
<i>Atolla_tenella</i>	OM214512	665	Leray 5'	forward	216	241	1	==T====T====T====T==
<i>Atolla_wyvillei</i>	EKDFO107-07	658	Leray 5'	forward	320	345	1	====T====T====T====
<i>Atolla_wyvillei</i>	GQ120086	637	Leray 3'	reverse	534	559	0	
<i>Atolla_wyvillei</i>	GQ120086	637	Leray 5'	forward	195	220	1	====T====T====T====
<i>Atolla_wyvillei</i>	GQ120087	684	Leray 3'	reverse	566	591	0	
<i>Atolla_wyvillei</i>	GQ120087	684	Leray 5'	forward	227	252	1	====T====T====T====
<i>Atolla_wyvillei</i>	GQ120088	831	Leray 3'	reverse	641	666	0	
<i>Atolla_wyvillei</i>	GQ120088	831	Leray 5'	forward	302	327	1	====T====T====T====
<i>Botrynuma_brucei</i>	FJ602530	410	Leray 5'	forward	171	196	1	====T====T====T====
<i>Botrynuma_brucei</i>	GQ120075	824	Leray 3'	reverse	643	668	0	
<i>Botrynuma_brucei</i>	GQ120075	824	Leray 5'	forward	304	329	1	====T====T====T====

<i>Dimophyes_arctica</i>	MZ292875		Leray 3'	reverse	643	668	0	
<i>Dimophyes_arctica</i>	ON539931		Leray 3'	reverse	632	657	0	
<i>Dimophyes_arctica</i>	GQ119966		Leray 3'	reverse	621	646	0	
<i>Dimophyes_arctica</i>	MZ292875		Leray 5'	forward	304	329	2	=====T=====
<i>Dimophyes_arctica</i>	ON539931		Leray 5'	forward	302	327	2	=====T=====
<i>Dimophyes_arctica</i>	GQ119966		Leray 5'	forward	282	307	3	=====T=====
<i>Pleurobrachia_pileus</i>	JF760211	1533	Leray 3'	reverse	703	728	0	
<i>Pleurobrachia_pileus</i>	JF760211	1533	Leray 5'	forward	361	386	4	G==A=====T=====
<i>Pleurobrachia_pileus</i>	MH688176	683	Leray 3'	reverse	170	195	0	
<i>Pleurobrachia_pileus</i>	MH688177	683	Leray 3'	reverse	170	195	0	
<i>Pleurobrachia_pileus</i>	MH688178	683	Leray 3'	reverse	170	195	0	
<i>Pleurobrachia_pileus</i>	MH688179	683	Leray 3'	reverse	170	195	0	
<i>Pleurobrachia_pileus</i>	MH688180	683	Leray 3'	reverse	170	195	0	
<i>Pleurobrachia_pileus</i>	MW735823	750	Leray 3'	reverse	421	446	0	
<i>Pleurobrachia_pileus</i>	MW735823	750	Leray 5'	forward	79	104	4	G==A=====T=====
<i>Pleurobrachia_pileus</i>	MW735824	750	Leray 3'	reverse	421	446	0	
<i>Pleurobrachia_pileus</i>	MW735824	750	Leray 5'	forward	79	104	4	G==A=====T=====
<i>Solmundella_bitentaculata</i>	JQ353759	681	Leray 5'	forward	330	355	0	
<i>Solmundella_bitentaculata</i>	JQ716088	614	Leray 5'	forward	328	353	0	
<i>Solmundella_bitentaculata</i>	KF977336	686	Leray 5'	forward	332	357	0	
<i>Solmundella_bitentaculata</i>	KF977337	686	Leray 5'	forward	332	357	0	
<i>Solmundella_bitentaculata</i>	KF977338	686	Leray 5'	forward	332	357	0	
<i>Solmundella_bitentaculata</i>	KF977339	687	Leray 5'	forward	333	358	0	
<i>Solmundella_bitentaculata</i>	KF977340	687	Leray 5'	forward	333	358	0	
<i>Solmundella_bitentaculata</i>	KF977341	687	Leray 5'	forward	333	358	0	
<i>Solmundella_bitentaculata</i>	KF977342	687	Leray 5'	forward	332	357	0	
<i>Solmundella_bitentaculata</i>	KF977343	687	Leray 5'	forward	332	357	0	
<i>Solmundella_bitentaculata</i>	KF977344	687	Leray 5'	forward	332	357	0	
<i>Solmundella_bitentaculata</i>	KY040296	683	Leray 5'	forward	331	356	2	==T=====

Table S4. *In silico* PCR results for 18S V1-V2 primers.

Species	Sequence Name	Sequence_length	Primer	Direction	Minimum	Maximum	Mismatches
<i>Aegina_citrea</i>	EU247813	1739	SSURmod (R)	reverse	404	421	0
<i>Aegina_citrea</i>	EU247813	1739	SSU_F04 (F)	forward	16	36	0
<i>Aglantha_digitale</i>	EU247821	1738	SSURmod (R)	reverse	403	420	0
<i>Aglantha_digitale</i>	EU247821	1738	SSU_F04 (F)	forward	16	36	0
<i>Atolla_tenella</i>	HM194799	1674	SSURmod (R)	reverse	311	328	0
<i>Atolla_wyvillei</i>	HM194788	1763	SSURmod (R)	reverse	400	417	0
<i>Atolla_wyvillei</i>	HM194788	1763	SSU_F04 (F)	forward	9	29	0
<i>Atolla_wyvillei</i>	JX393274	1701	SSURmod (R)	reverse	370	387	0
<i>Botrynema_ellinorae</i>	OP921264	1729	SSURmod (R)	reverse	399	416	0
<i>Botrynema_ellinorae</i>	OP921264	1729	SSU_F04 (F)	forward	15	35	0
<i>Botrynema_ellinorae</i>	OP921265	1729	SSURmod (R)	reverse	399	416	0
<i>Botrynema_ellinorae</i>	OP921265	1729	SSU_F04 (F)	forward	15	35	0
<i>Botrynema_brucei</i>	EU247822	1734	SSURmod (R)	reverse	400	417	0
<i>Botrynema_brucei</i>	EU247822	1734	SSU_F04 (F)	forward	16	36	0
<i>Botrynema_brucei</i>	OP921260	1729	SSURmod (R)	reverse	399	416	0
<i>Botrynema_brucei</i>	OP921260	1729	SSU_F04 (F)	forward	15	35	0
<i>Botrynema_brucei</i>	OP921261	1729	SSU_F04 (F)	forward	15	35	0
<i>Botryneman_brucei</i>	OP921261	1729	SSURmod (R)	reverse	399	416	0
<i>Gilia_reticulata</i>	DQ080013	1024	SSURmod (R)	reverse	397	414	0
<i>Gilia_reticulata</i>	DQ080013	1024	SSU_F04 (F)	forward	9	29	0
<i>Mertensia_ovum</i>	AF293679	1803	SSURmod (R)	reverse	420	437	0
<i>Mertensia_ovum</i>	AF293679	1803	SSU_F04 (F)	forward	31	51	0
<i>Mertensia_ovum</i>	FJ668937	2219	SSURmod (R)	reverse	420	437	0
<i>Mertensia_ovum</i>	FJ668937	2219	SSU_F04 (F)	forward	31	51	0
<i>Pleurobrachia_pileus</i>	AF293678	1802	SSURmod (R)	reverse	414	431	0
<i>Pleurobrachia_pileus</i>	AF293678	1802	SSU_F04 (F)	forward	31	51	0
<i>Pleurobrachia_pileus</i>	KJ193811	580	SSURmod (R)	reverse	363	380	0
<i>Pleurobrachia_pileus</i>	KJ754153	1740	SSURmod (R)	reverse	352	369	0
<i>Pleurobrachia_pileus</i>	MF599313	1798	SSURmod (R)	reverse	410	427	0
<i>Pleurobrachia_pileus</i>	MF599313	1798	SSU_F04 (F)	forward	27	47	0
<i>Solmundella_bitentaculata</i>	EU247812	1737	SSURmod (R)	reverse	401	418	0
<i>Solmundella_bitentaculata</i>	EU247812	1737	SSU_F04 (F)	forward	16	36	0

Table S5. Relative read abundances of Gelatinous Zooplankton MOTUs in the COI data set

MOTU Name	Relative read abundance (%)	Kingdom	Phylum	Class	Order	Family	Genus	Species
Hydrozoa_1	0.1	Metazoa	Cnidaria	Hydrozoa	NA	NA	NA	NA
Hydrozoa_2	< 0.1	Metazoa	Cnidaria	Hydrozoa	NA	NA	NA	NA
Bathykoros bouilloni	< 0.1	Metazoa	Cnidaria	Hydrozoa	Narcomedusae	Aeginidae	Bathykoros	<i>Bathykoros bouilloni</i>
Narcomedusae	17.9	Metazoa	Cnidaria	Hydrozoa	Narcomedusae	NA	NA	NA
Rudjakovia plicata	< 0.1	Metazoa	Cnidaria	Hydrozoa	Siphonophorae	Agalmatidae	Rudjakovia	<i>Rudjakovia plicata</i>
Crystallophyes amygdalina	< 0.1	Metazoa	Cnidaria	Hydrozoa	Siphonophorae	Clausophyidae	Crystallophyes	<i>Crystallophyes amygdalina</i>
Botrynuma brucei	5.8	Metazoa	Cnidaria	Hydrozoa	Trachymedusae	Halicreatidae	Botrynuma	<i>Botrynuma brucei</i>
Homoeonema platygonon	< 0.1	Metazoa	Cnidaria	Hydrozoa	Trachymedusae	Rhopalonematidae	Homoeonema	<i>Homoeonema platygonon</i>
Rhopalonematidae	10.8	Metazoa	Cnidaria	Hydrozoa	Trachymedusae	Rhopalonematidae	NA	NA
Atolla tenella	65.2	Metazoa	Cnidaria	Scyphozoa	Coronatae	Atollidae	Atolla	<i>Atolla tenella</i>
Cyanea capillata	0.1	Metazoa	Cnidaria	Scyphozoa	Semaeostomeae	Cyaneidae	Cyanea	<i>Cyanea capillata</i>
Ctenophora	< 0.1	Metazoa	Ctenophora	NA	NA	NA	NA	NA

Table S6. Relative read abundances of Gelatinous Zooplankton ASVs in the 18S data set.

ASV_Name	Abundance (%)	Kingdom	Phylum	Class	Order	Family	Genus	Species
ASV_193	< 0.1	Metazoa	Cnidaria	Hydrozoa	Anthoathecata	NA	NA	NA
ASV_203	< 0.1	Metazoa	Cnidaria	Hydrozoa	NA	NA	NA	NA
ASV_112	< 0.1	Metazoa	Cnidaria	Hydrozoa	NA	NA	NA	NA
ASV_14	0.5	Metazoa	Cnidaria	Hydrozoa	Narcomedusae	Aeginidae	NA	NA
ASV_2	22	Metazoa	Cnidaria	Hydrozoa	Siphonophorae	Diphyidae	Dimophyes	NA
ASV_108	< 0.1	Metazoa	Cnidaria	Hydrozoa	Siphonophorae	Diphyidae	Gilia	NA
ASV_36	0.1	Metazoa	Cnidaria	Hydrozoa	Siphonophorae	Diphyidae	Gilia	NA
ASV_83	< 0.1	Metazoa	Cnidaria	Hydrozoa	Siphonophorae	Diphyidae	Gilia	NA
ASV_52	< 0.1	Metazoa	Cnidaria	Hydrozoa	Siphonophorae	Diphyidae	Gilia	NA
ASV_115	< 0.1	Metazoa	Cnidaria	Hydrozoa	Siphonophorae	Diphyidae	Gilia	NA
ASV_1	25.5	Metazoa	Cnidaria	Hydrozoa	Siphonophorae	Diphyidae	Gilia	NA
ASV_79	< 0.1	Metazoa	Cnidaria	Hydrozoa	Siphonophorae	Diphyidae	Gilia	NA
ASV_99	< 0.1	Metazoa	Cnidaria	Hydrozoa	Siphonophorae	Diphyidae	Gilia	NA
ASV_107	< 0.1	Metazoa	Cnidaria	Hydrozoa	Siphonophorae	Diphyidae	Gilia	NA
ASV_104	< 0.1	Metazoa	Cnidaria	Hydrozoa	Siphonophorae	Diphyidae	Gilia	NA
ASV_29	0.1	Metazoa	Cnidaria	Hydrozoa	Siphonophorae	Diphyidae	NA	NA
ASV_417	< 0.1	Metazoa	Cnidaria	Hydrozoa	Siphonophorae	NA	NA	NA
ASV_13	0.8	Metazoa	Cnidaria	Hydrozoa	Siphonophorae	NA	NA	NA
ASV_86	< 0.1	Metazoa	Cnidaria	Hydrozoa	Siphonophorae	NA	NA	NA
ASV_470	< 0.1	Metazoa	Cnidaria	Hydrozoa	Siphonophorae	NA	NA	NA
ASV_206	< 0.1	Metazoa	Cnidaria	Hydrozoa	Siphonophorae	NA	NA	NA
ASV_116	< 0.1	Metazoa	Cnidaria	Hydrozoa	Siphonophorae	NA	NA	NA
ASV_77	< 0.1	Metazoa	Cnidaria	Hydrozoa	Siphonophorae	NA	NA	NA
ASV_119	< 0.1	Metazoa	Cnidaria	Hydrozoa	Siphonophorae	NA	NA	NA
ASV_131	< 0.1	Metazoa	Cnidaria	Hydrozoa	Siphonophorae	NA	NA	NA
ASV_57	< 0.1	Metazoa	Cnidaria	Hydrozoa	Siphonophorae	NA	NA	NA
ASV_12	0.9	Metazoa	Cnidaria	Hydrozoa	Siphonophorae	NA	NA	NA
ASV_39	0.1	Metazoa	Cnidaria	Hydrozoa	Siphonophorae	NA	NA	NA
ASV_139	< 0.1	Metazoa	Cnidaria	Hydrozoa	Siphonophorae	NA	NA	NA
ASV_268	< 0.1	Metazoa	Cnidaria	Hydrozoa	Siphonophorae	NA	NA	NA
ASV_255	< 0.1	Metazoa	Cnidaria	Hydrozoa	Siphonophorae	NA	NA	NA

ASV_138	< 0.1	Metazoa	Cnidaria	Hydrozoa	Siphonophorae	NA	NA	NA	
ASV_320	< 0.1	Metazoa	Cnidaria	Hydrozoa	Siphonophorae	NA	NA	NA	
ASV_162	< 0.1	Metazoa	Cnidaria	Hydrozoa	Siphonophorae	NA	NA	NA	
ASV_352	< 0.1	Metazoa	Cnidaria	Hydrozoa	Siphonophorae	NA	NA	NA	
ASV_11		1.2	Metazoa	Cnidaria	Hydrozoa	Trachymedusae	Halicreatidae	Botrynema	NA
ASV_85	< 0.1		Metazoa	Cnidaria	Hydrozoa	Trachymedusae	Rhopalonematidae	Aglantha	NA
ASV_448	< 0.1		Metazoa	Cnidaria	Hydrozoa	Trachymedusae	Rhopalonematidae	Aglantha	NA
ASV_3		20.4	Metazoa	Cnidaria	Hydrozoa	Trachymedusae	Rhopalonematidae	Aglantha	NA
ASV_41		0.1	Metazoa	Cnidaria	Hydrozoa	Trachymedusae	Rhopalonematidae	NA	NA
ASV_428	< 0.1		Metazoa	Cnidaria	Hydrozoa	Trachymedusae	Rhopalonematidae	Crossota	NA
ASV_71	< 0.1		Metazoa	Cnidaria	Hydrozoa	Trachymedusae	Rhopalonematidae	NA	NA
ASV_135	< 0.1		Metazoa	Cnidaria	Hydrozoa	Trachymedusae	Rhopalonematidae	NA	NA
ASV_158	< 0.1		Metazoa	Cnidaria	Hydrozoa	Trachymedusae	Rhopalonematidae	NA	NA
ASV_293	< 0.1		Metazoa	Cnidaria	Scyphozoa	Coronatae	Atollidae	Atolla	NA
ASV_6		11.3	Metazoa	Cnidaria	Scyphozoa	Coronatae	Atollidae	Atolla	NA
ASV_449	< 0.1		Metazoa	Cnidaria	Scyphozoa	Coronatae	Atollidae	NA	NA
ASV_228	< 0.1		Metazoa	Cnidaria	Scyphozoa	Coronatae	NA	NA	NA
ASV_292	< 0.1		Metazoa	Cnidaria	Scyphozoa	Coronatae	NA	NA	NA
ASV_371	< 0.1		Metazoa	Cnidaria	Scyphozoa	Semaeostomeae	Cyaneidae	Cyanea	NA
ASV_353	< 0.1		Metazoa	Ctenophora	Nuda	Beroida	Beroidae	Beroe	NA
ASV_114	< 0.1		Metazoa	Ctenophora	Tentaculata	Cydippida	Mertensiidae	NA	NA
ASV_404	< 0.1		Metazoa	Ctenophora	Tentaculata	NA	NA	NA	NA
ASV_5		16.5	Metazoa	Ctenophora	Tentaculata	Cydippida	Mertensiidae	NA	NA

Chapter 6: Overview

6.1 Overview

This thesis presents research based on environmental DNA (eDNA) metabarcoding surveys of biodiversity in three different marine environments and two different seasons in the Atlantic sector of the Arctic (**Table 1**). It provides new insights on eukaryotic diversity in the Fram Strait region of the Arctic, with a focus on gelatinous zooplankton (GZP) as case study group.

Table 1. Brief overview of sampling locations, communities, sample types and genes targeting in the different chapters of this thesis.

	Chapter Two	Chapter Three	Chapter Four	Chapter Five
Location and system	Fram Strait, open ocean	Fram Strait, marginal ice zone	Kongsfjorden (Svalbard), semi-enclosed fjord	Experiment, mock community
Scale	Regional (100's km)	Local (10's km)	Local (100's m - 1000's m)	-
Sampling depths	0 m – 2500 m	1 m – 5 m	0 m – 250 m	-
Season and year	Summer 2021	Summer 2022	Winter 2022	-
Target community	Pelagic metazoans, GZP	Under-ice eukaryotes	Pelagic and benthic eukaryotes, GZP	GZP
Sample types	eDNA water, plankton nets, towed camera	eDNA water	eDNA water, eDNA sediment, plankton nets	Specimen tissue, eDNA water
Target gene	COI	COI, 18S	COI	COI, 18S
Thesis objective	1, 2, 3	1,2,3,4	2,3	4

In **Chapter Two**, water samples from Fram Strait region were subjected to eDNA metabarcoding and a wide range of marine metazoans and GZP typical to the region were recovered. Vertically structured diversity was detected, with the bathypelagic being the most diverse depth zone. Multivariate analysis showed distinct community compositions between depth zones as well as significant relationships with water mass indicators including temperature, salinity and depth. Comparisons between eDNA metabarcoding and morphological sampling (nets and towed camera) indicated that eDNA metabarcoding recovered covered a higher number of GZP species. Moreover, the GZP community recovered depended on the sampling equipment used, with few overlaps between nets, video observations and eDNA. Overall, this study showed that eDNA metabarcoding of the COI gene was able to detect well-known patterns of diversity and established that this method successfully detects GZP for further chapters.

In **Chapter Three**, water samples were collected from the upper meters of the sub-ice water column in the marginal ice zone (MIZ), and sequenced using a multi-marker metabarcoding approach. Both sympagic and pelagic taxa typical to the region were recovered as well as high levels of uncharacterised diversity. The water immediately under the ice was more diverse in richness and evenness than at depth. Significantly different communities were found at the two sampled depths as well as between different ice floes. Sea ice conditions and fine-scale meltwater dynamics were found to be the strongest drivers of sub-ice community assemblages. Using two markers improved taxonomic coverage, however low resolution in the 18S marker and reference database gaps hindered species-level taxonomic assignments in many cases. Overall, this chapter demonstrates that eDNA metabarcoding is a useful survey tool in the rapidly changing, yet grossly understudied MIZ.

In **Chapter Four** water and sediment samples were analysed to characterize eukaryotic diversity during the polar night in Kongsfjorden, Svalbard. Much of the pelagic community known to inhabit the fjord during this period was recovered, as well as many benthic and hyperbenthic taxa. The COI marker was able to provide high taxonomic resolution detections and species lists for major functional groups were produced, including macroalgae, cnidarians, arthropods and vertebrates. Horizontally structured community composition was observed between sampling stations, but not vertically in the water column. Distinctly different assemblages were recovered from water and sediment-derived eDNA, highlighting the need to use the appropriate sample type depending on the community targeted (i.e., pelagic or benthic). Finally, comparisons between eDNA metabarcoding and plankton net catches recovered a rich GZP assemblage inhabiting the fjord during the polar night. The eDNA outperformed nets for the number of species-level detections, while little overlap was found between the methods. This chapter provides valuable baseline data for polar night biodiversity, and highlights the potential of combining eDNA surveys with established monitoring during this period.

In **Chapter Five**, two metabarcoding primer sets were applied to a mock community in order to assess their effectiveness for amplifying species of gelatinous zooplankton known to the Atlantic sector of the Arctic. This was done to specifically address a number of taxa overlooked by eDNA metabarcoding in the previous chapters. Large gaps in public reference databases were found for the target species and *in silico* PCR analysis showed that the 18S primers had higher coverage than COI. However, COI had much higher accuracy for taxonomic assignments, allowing species-level identifications where 18S did not. It was established that primer mismatches explained false negatives for *Aglantha digitale*, while a lack of reference sequences for *Sminthea arctica* and cydippid ctenophores prevented assignments and restricted further *in silico* analysis. Overall, this paper highlights the need for barcoding effort

targeting GZP species caught in the Arctic and the need for developing species-specific primers for those species overlooked by universal primers.

Chapter 7: Synthesis

7.1 Synthesis

The Arctic Ocean is one of the most remote areas in the world and it encompasses a variety of complex ecosystems, habitats and biomes than can be logistically difficult to access. Due to extreme seasonal weather, temperature and light regimes, sampling is typically biased towards the summer months. Consequentially, our understanding of the present state of biodiversity in the Arctic Ocean is still limited across different areas and time periods (CAFF, 2017). This is particularly true in the deep-sea (Ramirez-Llodra et al., 2024), sea-ice habitats (Bluhm et al., 2018, 2017; CAFF, 2017) and during the polar night (Berge et al., 2020b). Improved baseline data on the diversity and distribution of marine taxa in the Arctic Ocean is fundamental to accurately measuring ecosystem responses to the rapid climate change affecting the region. Reliable observational data provides a base for future comparisons and ecological research as well as formulating and implementing successful monitoring, protection and management strategies. Therefore, increasing rapid and accurate assessment of marine biodiversity in the Arctic is imperative. The development of eDNA metabarcoding has proven to be a valuable addition to marine biodiversity surveys and can help to fill data gaps for remote and difficult to sample areas and taxa. This thesis addresses the application of eDNA metabarcoding as a survey tool for marine biodiversity in the Arctic Ocean, with the aim of increasing our baseline knowledge of gelatinous zooplankton (GZP) ecology in particular. It contains some of the first applications of eDNA metabarcoding to specifically target Arctic GZP, as well as the first applications of metabarcoding of the Cytochrome c oxidase subunit I (COI) gene in the Fram Strait region. The main aspects are discussed below according to each of the four thesis objectives, followed by future perspectives.

7.2. Environmental DNA metabarcoding and drivers of pelagic diversity in Fram Strait

Differences in community assemblages across environmental gradients occur throughout marine systems, on both vertical and horizontal planes (Barry and Dayton, 1991). In the Arctic, the presence of a strong halocline is a defining characteristic, which is largely driven by the presence of sea ice, substantial freshwater input from rivers, ice and glacier melt and prevailing water masses (Farmer et al., 2021; Timmermans and Marshall, 2020). Hence, depth-associated variables are among the strongest drivers of pelagic diversity in the region (Bluhm et al., 2011; Kosobokova et al., 2011). Current warming trends are significantly altering hydrographic dynamics, particularly in Fram Strait, as well as facilitating shifts in habitat availability and species distribution (Csapó et al., 2021; Timmermans and Marshall, 2020). Yet, our ability to detect and track the consequences of these disturbances is limited across multiple eukaryotic groups because of persistent data gaps (CAFF, 2017, 2013; Ramirez-

Llodra et al., 2024). Thus, a major aim of this thesis was to use metabarcoding to not only conduct biodiversity surveys in the region but also to link eDNA signals to major environmental variables driving pelagic diversity.

7.2.1 Spatial patterns of diversity

Vertical structuring of diversity has been well documented for pelagic communities in the Arctic, with metazoan abundance typically declining with depth while species richness and evenness increase (Auel and Hagen, 2002; Gluchowska et al., 2017b; Kosobokova and Hirche, 2009; Kosobokova et al., 2011). The same has been found for Arctic GZP, for which richness peaks have been observed in the mesopelagic (Mańko et al., 2020a; Pantiukhin et al., 2023; Raskoff et al., 2010). In the present thesis, eDNA signals in the open ocean of Fram Strait, showed that the epipelagic was characterised by the lowest species richness, with arthropods being the most dominant metazoan taxon (Chapter Two). In contrast, species richness and evenness increased with depth with highest values reported in the bathypelagic, as expected. This was true for the wider metazoan community as well as for GZP. Moreover, distinct community assemblages were recovered across the different depth zones, with the bathypelagic and the epipelagic being the most dissimilar. In upper meters of the sub-ice water column in the MIZ, inverse vertical gradients were detected with eDNA (Chapter Three). Significantly higher alpha diversity values and different community composition was found immediately under the sea ice compared to 5 m depth. This elevated alpha diversity immediately below the ice is supported by an earlier study showing the ice-water interface is enriched with in-ice fauna as melting occurs (Kiko et al., 2017; Smith et al., 2023; Xu et al., 2020). Bathymetry (e.g., shelf, slope or deep-sea) and major currents (e.g., West Spitsbergen Current and the East Greenland Current) are also influential factors across horizontal gradients in Fram Strait and Western Svalbard (e.g., Hop et al., 2006; Käß et al., 2019; Mazanowski et al., 2023). Horizontal structuring in community assemblages were prevalent in the MIZ (Chapter Three), and in Kongsfjorden (Chapter Four). Distinct communities across a horizontal gradient were not identified in Fram Strait, however, increasing the spatial extent of sampling on the slope and shelf areas would likely increase the likelihood of detecting such patterns in pelagic eDNA signals.

7.2.2 Further abiotic drivers

Prevailing water masses, sea ice conditions and meltwater dynamics have been well-established with morphological methods as important determinants of Arctic pelagic assemblages in the upper water column (e.g., Basedow et al., 2018; Gluchowska et al., 2017b; Hop et al., 2019a). Here we were able to observe such patterns in eDNA signals and extend these findings to the less-studied eukaryotic community in the sub-ice water in the MIZ. In Fram Strait (Chapter Two), significant correlations were clustered according to characteristics

of the major water masses of the region: Atlantic Water (higher temperature and salinity), Polar Water (lower salinity, high oxygen saturation) and Deep Water (greater depth, low oxygen saturation). Many of these significant associations were in line with well-investigated relationships of keystone Arctic species to hydrographic parameters (e.g., the abundant copepods *Calanus* spp., *Pseudocalanus* spp., and *Oithona similis*). In contrast, high levels of uncharacterized diversity in the MIZ resulted in coarse taxonomic resolution in much of the data. Community assemblages associated to different sea ice and meltwater conditions were largely composed of primary producers and metazoans assigned to only phylum and class level (Chapter Three). However, the accurate detection of well-established relationships using eDNA supports its utility in elucidating drivers of pelagic diversity and characterizing signature communities associated with specific environmental conditions. Incorporating unassigned sequences in these kinds of analyses allows us to detect ecologically important associations which may be simplified or overlooked otherwise. In the future, incorporating community network analysis combined with higher sampling effort could provide further information on species-interactions across different trophic levels (e.g., Djurhuus et al., 2020).

It is crucial to include temporal aspects in future sampling efforts in order to accurately track shifts in biodiversity over time, as opposed to single snapshots. Each of the studies included in this thesis were based on single sampling campaigns in different regions, years and seasons. Thus, our ability to draw comparisons between them is limited at present. Therefore, future sampling in the same areas would better allow us to track diversity and community composition over time and allow for stronger conclusions in the context of Atlantification. Moreover, the metabarcoding of surface sediment samples in addition to seawater could complement pelagic data and provide more accurate information on benthic and hyper-benthic diversity (Chapter Four). Analysing deeper layers, with temporal calibration, could shed light on historic changes in diversity. If linked to historic environmental changes, this could help improve the accuracy of predicting ecosystem response to future changes (reviewed in Nguyen et al., 2023).

7.3 Environmental DNA for investigating biodiversity across different, spatial scales, habitats and seasons in the Arctic Ocean

Tracking shifts in biodiversity across different spatial scales and habitats is important in understanding the impacts of climate change on specific taxa as well as identifying larger patterns occurring in the ecosystem in which they exist. Furthermore, uniformity in sampling and subsequent processing is crucial for comparisons across datasets, which can be difficult for methods which rely on the taxonomic expertise of the individual conducting the study (Thomsen and Willerslev, 2015). Thus, one of the main objectives of this thesis is to

investigate the potential of applying eDNA metabarcoding across different spatial scales, habitats and seasons in the Arctic.

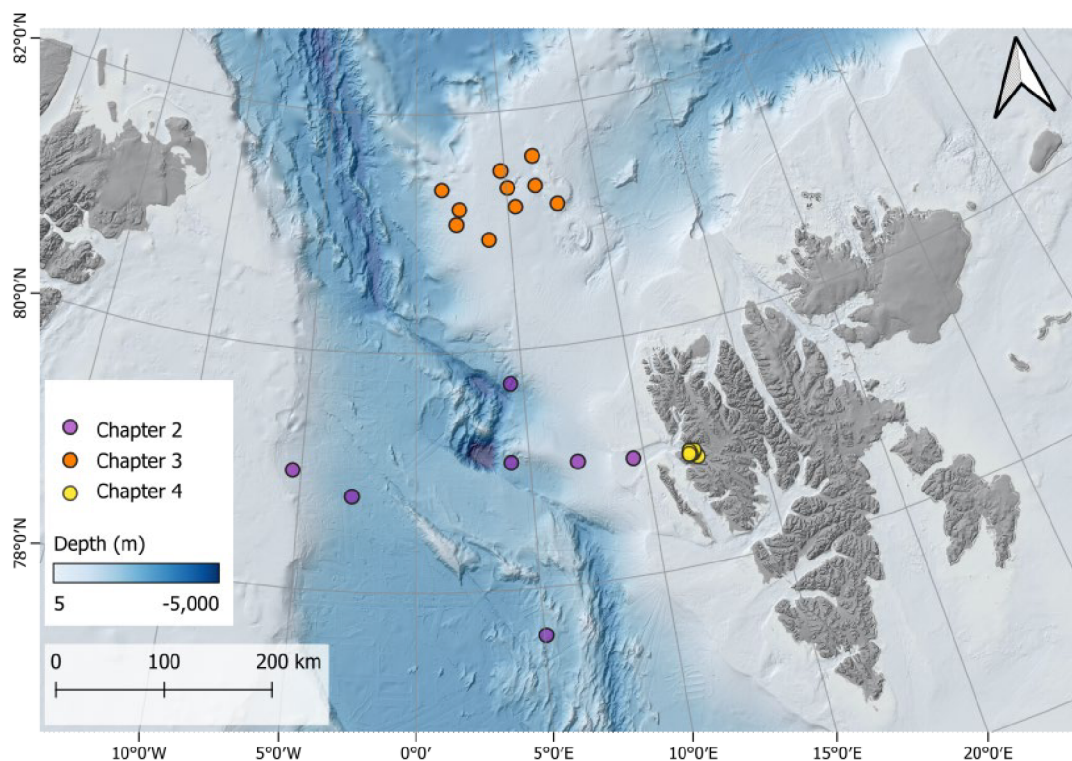


Figure 1. Map of the study area: Fram Strait. Circles indicate the approximate location of sampling stations and colour indicates the thesis chapter the samples were analysed in. Chapter Five was based on a mock community experiment and thus not included in the map. Map produced using QGIS based on bathymetry data downloaded from IBCAO (https://www.gebco.net/data_and_products/gridded_bathymetry_data/arctic_ocean/).

A broad sampling protocol for collecting seawater-derived eDNA was employed throughout this thesis. It included the use of enclosed filters, technical triplicates (two litres each), coupled with PCR-inhibitor precaution (Chapter Four) and a sequencing strategy that prioritized high sequencing depth for targeting rare and elusive taxa. The largest spatial scales were covered in Fram Strait (Chapter Two), during the early summer. Here, samples were collected from the surface to the seafloor with a maximum depth of 2,500 m, at sampling stations located across hundreds of kilometres of open ocean (**Figure 1**). Broad-scale sampling of this nature is particularly important in Fram Strait where water masses can be distributed over many kilometres, and we see communities change significantly in composition over large depth gradients and horizontal scales. Next, the protocol was applied in the upper five meters of the sub-ice water column of the MIZ, during the late summer (Chapter Three). Sampling stations were representative of different ice regimes and were spaced over an area approximately 50 km by 100 km in size. Here, sea ice and meltwater dynamics can have strong influences on biological communities in the upper centimetres and meters of the water column as well as

across the MIZ depending on the ice cover and proximity to the ice edge (reviewed in Barber et al., 2015). It is a highly dynamic environment and thus a sampling scheme with scalability is necessary to capture under-ice communities and their fluxes in relation to environmental parameters. Kongsfjorden was sampled on an even more localized scale with stations distributed across the central section of the fjord, during the polar night (Chapter Four). Here, hydrographic gradients can occur within different areas of the fjord due to the influence of glacier run-off and warm water masses advected from the adjacent shelf (Cottier et al., 2005). Interestingly, despite the influence of tide and advection events likely connecting the sampling stations, we were able to detect distinct communities in both the water and sediment eDNA across the sampling area. This contributes to mounting evidence that eDNA can be highly localized in marine systems and therefore can accurately detect spatial patterns on small scales, even when sampling points are in close proximity to each other (e.g., Jeunen et al., 2019). Moreover, despite air temperatures well below zero and higher water turbidity compared to the sampling in the previous chapters, we were able to implement the same sampling protocol successfully (Chapter Four).

It is important to highlight that some general developments to this protocol should be explored, including the benefits of an increased number of replicates (Smith et al., 2024), higher sampling volumes in deep water (McClenaghan et al., 2020) and increased spatial and temporal coverage (Chapter Two). With targeted improvements, it could be implemented to supplement already established monitoring programs in the Arctic. One example could be supplementing the summer zooplankton time-series (net sampling) in Kongsfjorden (Hop et al., 2019b) and extending the eDNA component into the winter season, when warm water anomalies can also occur and induce major ecosystem changes (e.g., Cottier et al., 2007). Moreover, the remaining DNA extract from such a broad sampling protocol can be stored or 'bio-banked' and used in future studies (e.g., single species detection or genome sequencing) as sequencing methods are improved and new techniques developed (Jarman et al., 2018). The ability to compare patterns of diversity across different Arctic habitats, collected with the same sampling strategies would help us better identify areas or regions of particular concern for further investigation or for targeting with mitigation and protection policies.

7.4 Environmental DNA metabarcoding and surveying of gelatinous zooplankton in the Arctic

Anthropogenic climate change is unequivocally altering the distributions, phenology and food web structure of Arctic pelagic communities (Eriksen et al., 2017; Gluchowska et al., 2017a; Weydmann et al., 2014). As important components of the Arctic marine food web (Dischereit et al., 2024a, 2024b; Purcell et al., 2010; Urban et al., 2022), GZP will undoubtedly be affected too (e.g., Pantiukhin et al., 2024). However, the paucity of basic ecological data for this group

makes assessing such changes and formulating accurate future predictions difficult. There is a small number of recent, morphology-based studies that have set out to survey GZP, providing important baseline data on species assemblages and distribution in the Fram Strait area (Mańko et al., 2020; Mazanowski et al., 2023; Pantiukhin et al., 2023). However, there is a lack of eDNA metabarcoding studies targeting GZP. It is also yet to be determined whether eDNA metabarcoding techniques can be effectively employed to supplement previously-established methods, or even outperform them. Hence, comparing the performance of eDNA metabarcoding to net and optical observations for detecting GZP was a major objective of this thesis.

The benefits of including eDNA metabarcoding was evident in the diverse GZP communities detected using it in combination with morphological methods (Chapter Two and Four). The richest communities were recovered in Kongsfjorden during the polar night, with a total of 19 species and a further three genera captured with eDNA metabarcoding and nets combined. Previous morphological work has found evidence of large scyphozoan and ctenophores overwintering in the Chukchi Sea, suggesting this may be an important life-history strategy for GZP species (Purcell et al., 2018). In Kongsfjorden, polar night data is limited for GZP in particular, but the ctenophores *Mertensia ovum* and *Beroe cucumis* have been reported in zooplankton sampling during this period (Berge et al., 2020a; Havermans et al., 2023). Wintertime distribution data on GZP is disproportionately low compared to the summer months. Thus, the species list produced in Chapter Four greatly expands on the number of species reported previously and is a valuable contribution to our understanding of GZP ecology during the polar night.

Overall, eDNA metabarcoding outperformed morphological methods in detecting Arctic GZP species. Environmental DNA recovered equal or higher numbers of species from only six litres of water per sampling point, compared to morphological sampling methods which covered many thousands of cubic meters of the water column (Chapters Two and Four). Indeed, a total of 27 different GZP species were detected with metabarcoding of the COI gene alone. Two further genera and many additional molecular operational taxonomic units (MOTUs) were recovered, albeit with limited taxonomic assignments (e.g., phylum and class). The number of unassigned MOTUS were predominantly of the class Hydrozoa (e.g., Chapters Two and Three), which has the lowest of coverage (by proportion) in public databases (Chapter Five), yet is the most diverse and abundant GZP group in the region (Majaneva et al., 2024; Ronowicz et al., 2015). It was evident that distinct GZP communities were recovered depending on the method used, with very little overlap between them (Chapters Two and Four). Many of the species recovered with eDNA were either overlooked completely by the morphological methods, or could only be confidently identified to a lower resolution than genus

or species. However, it must be noted that the reverse was also true with multiple false-negatives occurring in the eDNA data (Chapters Two, Four and Five). There are a number of factors possibly contributing to this, including gaps in reference databases and primer choice (Chapter Five), sampling volume, and the dilution and persistence of eDNA in the water column (Collins et al., 2018). Overall, eDNA metabarcoding allows for species-level identifications (Chapters Two, Four and Five) in a group of taxa where taxonomic expertise is limited and morphological identification is hindered by the delicate nature of their gelatinous bodies. However, morphological methods can still provide more reliable abundance estimates for those species that they do successfully detect, as well as information on population structure (i.e., life-stage and age). Hence, it is advisable that multiple sampling strategies, with an emphasis on eDNA-based methods, should be employed where possible in order to gain a more comprehensive view of the GZP community present.

Environmental DNA also provides opportunities to detect patterns in GZP distribution at discrete points in the water column. The standard way to collect seawater for eDNA in marine studies, including the chapters in this thesis, is via Niskin bottles mounted on a conductivity temperature depth (CTD) rosette, or deployed on a line in combination with a CTD (Govindarajan et al., 2022). In contrast, plankton nets used to sample GZP are typically either open trawls (integrating large layers of the water column) or depth stratified over of tens to hundreds of meters. One of the advantages of using Niskin bottles and a CTD set up is the potential for *ad hoc* sampling to target distinct points of interest in the water column which can be determined from the real-time temperature and salinity data produced during the cast. Although standardized, predefined depths were used in the each of the studies herein, future sampling in this manner could be particularly interesting in Fram Strait. Here, hydrographic features such as water mass boundaries and meltwater layers can result in hotspots of biological activity or represent barriers for dispersion of planktonic organisms. Such patterns have been detected in epipelagic waters for zooplankton in a sub-mesoscale ice filament (Kaiser et al., 2021) and for GZP across oceanic fronts near Svalbard (Mańko et al., 2022). However, as demonstrated in the sub-ice eukaryotic community of the MIZ (Chapter Three), these patterns can also occur over small spatial scales that would be better resolved with discrete sampling points as opposed to integrating portions of the water column.

7.5 Marker and primer choice for amplifying Arctic gelatinous zooplankton DNA

Marker and associated primer choice are widely recognised to have significant impacts on metabarcoding output (Clarke et al., 2017; Collins et al., 2019; Taberlet et al., 2018; Wangensteen et al., 2018). Primer mismatches are a major source of amplification biases in community studies, resulting in false negatives of certain taxa and species (Albaina et al.,

2024; Elbrecht et al., 2017; Piñol et al., 2015). The majority of marine eDNA metabarcoding studies are conducted using the Leray fragment of the COI gene, followed by fragments of the nuclear small subunit ribosomal RNA gene (18S) (Bucklin et al., 2016; Lear et al., 2018). However, both have associated limitations including the tendency of COI to overlook certain GZP groups (Albaina et al., 2024; Laakmann et al., 2020) and the inability of 18S to make accurate genus and species-level identifications for metazoans (Bucklin et al., 2021; Questel et al., 2021; Tang et al., 2012; Wu et al., 2015). While research exploring which markers and primer pairs are optimal for assessing marine communities with metabarcoding is increasing (Macheriotou et al., 2019; Tanabe et al., 2016; Yip et al., 2023; Zimmermann et al., 2024), the GZP community has yet to be the focus of such a study. Thus, a major objective of this thesis was to assess the effectiveness of these two commonly used metabarcoding markers and associated primer pairs for recovering Arctic GZP species specifically.

When comparing sampling methods (Chapters Two and Four), the presence of a number of species was confirmed with net and camera deployments, yet repeatedly missing from the eDNA datasets. Two notable examples were the hydrozoan species of the Rhopalonematidae family; *Aglantha digitale* and *Sminthea arctica*. Through *in silico* PCR analysis and sequencing of a mock community experiment (Chapter Five), it could be established that primer mismatches on the forward primer is the most likely explanation for *A. digitale* false negatives. Such mismatches for primers targeting COI are often attributed the primer binding sites not being as well conserved as in other fragments (Deagle et al., 2014; Leray et al., 2013). However, it was not possible to establish whether false negatives for *S. arctica* were due the complete lack of reference sequences alone, or whether other factors such as primer mismatches play a role. For example, a recent study showed that the oversight of appendicularians in COI studies is due to a combination of primer mismatches, the presence of poly-T inserts on the COI gene and an underrepresentation on databases (Albaina et al., 2024). In the context of the Arctic, even genus-level detections can overlook crucial ecological differences between conspecifics. An example is the zooplanktivorous ctenophore genus *Beroe*, which contains at least 25 species worldwide. At least two of these species occur in the Arctic in high abundances (*B. cucumis* and *B. abyssicola*), yet are thought to occupy different depth distributions (Mańko et al., 2020; Purcell et al., 2010; Shiganova and Abyzova, 2022). Multiple species are invasive to European waters and can impose significant top-down impacts on local ecosystems (Johansson et al., 2018). High taxonomic resolution is necessary to track the dynamics of the species already resident in the Arctic, as well as the potential establishment of newcomers as a result of Atlantification or introduction via increased vessel traffic.

The presence of major gaps in publicly available reference databases remains a significant challenge to eDNA metabarcoding projects worldwide (Keck et al., 2023; Taberlet et al., 2018). This was evident in the present thesis for GZP species that occur in the Arctic, and specifically for specimens actually caught in the Arctic Ocean and its adjacent seas (Chapter Five). These gaps hinder the accuracy of taxonomic assignments and targeted barcoding effort should be prioritized to remedy this issue. Going forward, the development of species-specific primers should also be prioritised rather than continuing to use only universal primers to track species of interest. Species-specific primers allow for increased accuracy of biomass data, as well as the detection of species overlooked by universal primers (Collins et al., 2019; Kelly et al., 2019). The targeted sequencing of whole mitochondrial genomes could be used to develop primers for gelatinous groups such as appendicularians and ctenophores for which universal primers do not appear to be suitable (Albaina et al., 2024; Coissac et al., 2016; Collins et al., 2019; Collins and Cruickshank, 2014, Chapter Five). Moreover, genome skimming techniques have been shown to work on specimens stored in ethanol, which provides opportunity to harvest sequences from museum-stored specimens in addition to newly caught ones (Coissac et al., 2016). However, in habitats where there are still high levels of uncharacterised diversity, implementing a multi-marker approach can improve the completeness of the biodiversity captured, albeit with limited taxonomic resolution in cases where 18S is the second marker (Suter et al., 2021, Chapter Three). Moreover, the DNA extract from the samples collected in this thesis (and other projects) could be re-analysed with the goal of detecting previously overlooked species, quantifying abundant species, or detecting rare species that fell below detection limits in the initial sequencing efforts.

7.6 Perspectives for eDNA-based research in the Arctic Ocean

In the context of a rapidly changing Arctic Ocean, the recent development of eDNA metabarcoding techniques represents a valuable and cost-effective tool for biodiversity research in a remote region of the world. However, there remain important limitations that must be acknowledged and addressed, especially those related to how eDNA is transported and degraded, as well as its ability to track biomass and abundance. These are discussed below, followed by opportunities and future outlooks for improving and increasing the application of eDNA techniques in the Arctic Ocean.

7.6.1 Open questions and limitations

A major challenge of working with eDNA is the heterogeneous nature of its persistence and transport in marine ecosystems. Differing levels of microbial activity, temperature, acidity and dilution, as well as currents and tides can affect how eDNA is dispersed and degraded (Collins et al., 2018; Scriver et al., 2023; Wood et al., 2020). A growing body of research has demonstrated that eDNA signals can be highly localised, making it an accurate tool for

detecting distinct communities across small spatial scales (Jeunen et al., 2019; Chapter Three; Chapter Four), and time-frames (e.g., detecting diurnal vertical migration in zooplankton; Suter et al., 2021). These findings suggest that eDNA either degrades, or is dispersed and diluted in the water column, quicker than previously thought. However, these assumptions should be tested in Arctic ecosystems as environmental conditions unique to the region (e.g., elevated UV levels polar day, minimal light in the polar night and low temperatures) may have differential effects on the ecology of eDNA compared to other systems (e.g., Lacoursière-Roussel et al., 2018). Once eDNA is isolated, other workflow choices can influence data including primer-related biases (Chapter Five), the stochastic nature of PCR amplification and the suitability of bioinformatic processing strategies (Hakimzadeh et al., 2023; Kelly et al., 2019; Chapter Five). Taking these factors into account when designing future eDNA metabarcoding studies in the Arctic is paramount to producing ecologically meaningful and reproducible results.

Being able to track biomass and abundance is keystone of biodiversity research and forms the basis of many ecological questions (Preston, 1948). An increasing number of studies, and the chapters herein, demonstrate eDNA metabarcoding can be an accurate tool for analysing the presence of taxa throughout the Arctic food web in marine systems. However, it can only be confidently considered semi-quantitative at best (e.g., relative read abundances) and findings related to biomass or individual abundance must still be interpreted with caution. This is largely attributed to species-specific shedding rates, target gene copy number and PCR-related biases (Fonseca, 2018; Nichols et al., 2018). Promising progress in this regard is underway with evidence that metabarcoding of bulk samples of zooplankton (Ershova et al., 2023, 2021) and arthropods (Krehenwinkel et al., 2017) using the COI gene, show positive correlations between read abundance and biomass. The development of digital droplet PCR (ddPCR) has also greatly improved our ability to exactly quantify DNA read copies, which have the potential to then be linked to biomass (reviewed in Duarte et al., 2023). For example, the combination of eDNA, ddPCR and modelling was used to accurately predict fish biomass in trawls in a Norwegian fjord (Guri et al., 2024). As eDNA shedding and decay rates can be taxon-specific (Andruszkiewicz Allan et al., 2021; Guri et al., 2024) however, future work should target individual species of interest in order to be able to further implement these techniques in the Arctic Ocean.

7.6.2 Future opportunities

An advantage to of eDNA metabarcoding is its ability to recover 'hidden' or unknown diversity, which was evident in the present thesis where many MOTUs could be identified only with coarse taxonomic resolution (Chapters Two, Three and Four). This is particularly advantageous in the ocean, where it is assumed that vast numbers of marine eukaryotic

species remain undescribed globally (Bakker et al., 2019; López-Escardó et al., 2018; Mora et al., 2011). Nevertheless, valuable ecological inferences are possible with unassigned sequences. This holds true for alpha and beta diversity analyses, which are calculated independent of taxonomic information. Furthermore, the use of completely taxonomy-free analysis in eDNA metabarcoding has been demonstrated as an accurate biomonitoring tool for assessing ecosystem health (Cordier et al., 2018; Wilkinson et al., 2024). Similar techniques could be employed to analyse diversity patterns in the Arctic deep-sea habitats for example, where there are many unidentified benthic invertebrates (Ramirez-Llodra et al., 2024). As reference databases improve, our understanding of these unassigned taxa and sequences will also increase.

An exciting advancement in the field of eDNA is the development of automated sampling and filtration systems. These systems have the potential to increase standardization, while reducing the required hands-on time and allowing for regular temporal sampling. This could be particularly useful in remote locations when incorporated into pre-existing long-term monitoring infrastructure, for example the long term ecological research observatory (LTER HAUSGARTEN) in Fram Strait (Soltwedel et al., 2005). Mooring sediment traps (i.e., bulk DNA from marine snow) equipped with automatic samplers are already deployed and have successfully detected fluxes in microbial communities in relation to Atlantic inflow and sea ice cover (Priest et al., 2023; Wietz et al., 2021). However, these collect weekly or fortnightly samples and so could overlook shorter-term fluxes in biological communities caused by temperature or water mass anomalies. Supplementing these with the deployment of automated eDNA sampling systems (Govindarajan et al., 2022; Truelove et al., 2022), with higher resolution temporal sampling to target the wider eukaryotic community, could extend these findings to higher trophic levels and shorter time frames. Such systems would be particularly valuable in the mesopelagic and bathypelagic where it is unclear how ongoing Atlantification is affecting deep-sea species diversity and distribution (Ramirez-Llodra et al., 2024).

Another valuable advancement in eDNA sampling methodology is the increasing availability of commercial field sampling kits and freezer-free preservation methods (e.g., buffer). These give rise to the opportunity for training non-scientists in eDNA collection, particularly in areas where access to scientific infrastructure is limited (e.g., -80°C freezers and UV lights) (Kondoh et al., 2024; Kvalheim et al., 2024). Environmental DNA is emerging as an excellent tool for citizen science initiatives as it produces rapid and accurate biodiversity data, and the per-sample costs are continuously decreasing (Thomsen et al., 2024). Providing training and standardized protocols has already proved successful for characterising coastal fish assemblages in Denmark and Norway (Agersnap et al., 2022; Kvalheim et al., 2024) and

metazoan diversity in ports in the Canadian Arctic (Lacoursière-Roussel et al., 2018). Such programs are beneficial in the sense that they afford incredible opportunities to involve local communities, the potential to integrate traditional knowledge with western science, as well as to increase data coverage in areas and seasons where research vessels may not typically sample. This could be particularly useful in Arctic ports, where commercial vessel activity increases the risk of invasive species establishment (Lacoursière-Roussel et al., 2018; Larson et al., 2020). Another example could be remote coastal areas (e.g., traditional hunting grounds) where ecosystem degradation and shifts in marine biodiversity can severely impact the livelihood, food security and cultural heritage of indigenous peoples (Pearson et al., 2023).

In a time of anthropogenic climate change, rapid environmental degradation, significant biodiversity loss and declining taxonomic expertise (Engel et al., 2021; Thomsen and Willerslev, 2015), we are at risk of losing species before we discover them. The need to rapidly expand our capacity for biodiversity sampling is more urgent than ever, especially in climate change hotspots like the Arctic. Environmental DNA methods have the potential to integrate and build on decades of morphological sampling and taxonomic analysis (Laakmann et al., 2020) as well as incorporating the huge global barcoding effort of the last two decades (e.g., Bucklin et al., 2011). The works in this thesis show that, although there are still limitations, eDNA metabarcoding greatly improves our capabilities to study pelagic diversity in Arctic marine ecosystems, and GZP in particular. Finally, the findings in this thesis significantly contribute valuable baseline data for a number of eukaryotic groups, including GZP, in a region where biodiversity data is still limited.

7.7 References

- Agersnap, S., Sigsgaard, E.E., Jensen, M.R., Avila, M.D.P., Carl, H., Møller, P.R., Krøs, S.L., Knudsen, S.W., Wisz, M.S., Thomsen, P.F., 2022. A National Scale “BioBlitz” Using Citizen Science and eDNA Metabarcoding for Monitoring Coastal Marine Fish. *Front. Mar. Sci.* 9. <https://doi.org/10.3389/fmars.2022.824100>
- Albaina, A., Garić, R., Yebra, L., 2024. Know your limits; miniCOI metabarcoding fails with key marine zooplankton taxa. *Journal of Plankton Research* fbae057. <https://doi.org/10.1093/plankt/fbae057>
- Andruszkiewicz Allan, E., Zhang, W.G., C. Lavery, A., F. Govindarajan, A., 2021. Environmental DNA shedding and decay rates from diverse animal forms and thermal regimes. *Environmental DNA* 3, 492–514. <https://doi.org/10.1002/edn3.141>
- Auel, H., Hagen, W., 2002. Mesozooplankton community structure, abundance and biomass in the central Arctic Ocean. *Marine Biology* 140, 1013–1021. <https://doi.org/10.1007/s00227-001-0775-4>
- Bakker, J., Wangensteen, O.S., Baillie, C., Buddo, D., Chapman, D.D., Gallagher, A.J., Guttridge, T.L., Hertler, H., Mariani, S., 2019. Biodiversity assessment of tropical shelf eukaryotic communities via pelagic eDNA metabarcoding. *Ecology and Evolution* 9, 14341–14355. <https://doi.org/10.1002/ece3.5871>
- Barber, D.G., Hop, H., Mundy, C.J., Else, B., Dmitrenko, I.A., Tremblay, J.-E., Ehn, J.K., Assmy, P., Daase, M., Candlish, L.M., Rysgaard, S., 2015. Selected physical, biological and biogeochemical implications of a rapidly changing Arctic Marginal Ice Zone. *Progress in Oceanography, Overarching perspectives of contemporary and future ecosystems in the Arctic Ocean* 139, 122–150. <https://doi.org/10.1016/j.pocean.2015.09.003>
- Barry, J.P., Dayton, P.K., 1991. Physical Heterogeneity and the Organization of Marine Communities, in: Kolasa, J., Pickett, S.T.A. (Eds.), *Ecological Heterogeneity*. Springer, New York, NY, pp. 270–320. https://doi.org/10.1007/978-1-4612-3062-5_14
- Basedow, S.L., Sundfjord, A., Appen, W.-J., Halvorsen, E., Kwasniewski, S., Reigstad, M., 2018. Seasonal variation in transport of zooplankton into the Arctic basin through the Atlantic gateway, Fram Strait. *Frontiers in Marine Science* 5, 194.
- Berge, J., Daase, M., Hobbs, L., Falk-Petersen, S., Darnis, G., Søreide, J.E., 2020a. Zooplankton in the Polar Night, in: Berge, J., Johnsen, G., Cohen, J.H. (Eds.), *POLAR NIGHT Marine Ecology: Life and Light in the Dead of Night*. Springer International Publishing, Cham, pp. 113–159. https://doi.org/10.1007/978-3-030-33208-2_5
- Berge, J., Johnsen, G., Cohen, J.H., 2020b. Introduction, in: Berge, J., Johnsen, G., Cohen, J.H. (Eds.), *POLAR NIGHT Marine Ecology: Life and Light in the Dead of Night*. Springer International Publishing, Cham, pp. 1–15. https://doi.org/10.1007/978-3-030-33208-2_1
- Bluhm, B., Gebruk, A., Gradinger, R., Hopcroft, R., Huettmann, F., Kosobokova, K., Sirenko, B., Weslawski, M., 2011. Arctic Marine Biodiversity: An Update of Species Richness and Examples of Biodiversity Change. *Oceanog.* 24, 232–248. <https://doi.org/10.5670/oceanog.2011.75>
- Bluhm, B.A., Hop, H., Vihtakari, M., Gradinger, R., Iken, K., Melnikov, I.A., Søreide, J.E., 2018. Sea ice meiofauna distribution on local to pan-Arctic scales. *Ecology and Evolution* 8, 2350–2364. <https://doi.org/10.1002/ece3.3797>
- Bluhm, B.A., Swadling, K.M., Gradinger, R., 2017. *Sea ice as a habitat for macrograzers*, in: *Sea Ice*. John Wiley & Sons, Ltd, pp. 394–414. <https://doi.org/10.1002/9781118778371.ch16>
- Bucklin, A., Lindeque, P.K., Rodriguez-Ezpeleta, N., Albaina, A., Lehtiniemi, M., 2016. Metabarcoding of marine zooplankton: prospects, progress and pitfalls. *Journal of Plankton Research* 38, 393–400. <https://doi.org/10.1093/plankt/fbw023>
- Bucklin, A., Peijnenburg, K.T.C.A., Kosobokova, K.N., O'Brien, T.D., Blanco-Bercial, L., Cornils, A., Falkenhaus, T., Hopcroft, R.R., Hosia, A., Laakmann, S., Li, C., Martell, L.,

- Questel, J.M., Wall-Palmer, D., Wang, M., Wiebe, P.H., Weydmann-Zwolicka, A., 2021. Toward a global reference database of COI barcodes for marine zooplankton. *Mar Biol* 168, 78. <https://doi.org/10.1007/s00227-021-03887-y>
- Bucklin, A., Steinke, D., Blanco-Bercial, L., 2011. DNA Barcoding of Marine Metazoa. *Annual Review of Marine Science* 3, 471–508. <https://doi.org/10.1146/annurev-marine-120308-080950>
- CAFF, 2017. State of the Arctic Marine Biodiversity: Key Findings and Advice for Monitoring. Conservation of Arctic Flora and Fauna International Secretariat, Akureyri, Iceland.
- CAFF, 2013. Arctic Biodiversity Assessment 2013: Status and trends in Arctic biodiversity. Conservation of Arctic Flora and Fauna, Akureyri, Iceland.
- Clarke, L.J., Beard, J.M., Swadling, K.M., Deagle, B.E., 2017. Effect of marker choice and thermal cycling protocol on zooplankton DNA metabarcoding studies. *Ecology and Evolution* 7, 873–883. <https://doi.org/10.1002/ece3.2667>
- Coissac, E., Hollingsworth, P.M., Lavergne, S., Taberlet, P., 2016. From barcodes to genomes: extending the concept of DNA barcoding. *Molecular Ecology* 25, 1423–1428. <https://doi.org/10.1111/mec.13549>
- Collins, R.A., Bakker, J., Wangensteen, O.S., Soto, A.Z., Corrigan, L., Sims, D.W., Genner, M.J., Mariani, S., 2019. Non-specific amplification compromises environmental DNA metabarcoding with COI. *Methods in Ecology and Evolution* 10, 1985–2001. <https://doi.org/10.1111/2041-210X.13276>
- Collins, R.A., Cruickshank, R.H., 2014. Known Knowns, Known Unknowns, Unknown Unknowns and Unknown Knowns in DNA Barcoding: A Comment on Dowton et al. *Systematic Biology* 63, 1005–1009. <https://doi.org/10.1093/sysbio/syu060>
- Collins, R.A., Wangensteen, O.S., O’Gorman, E.J., Mariani, S., Sims, D.W., Genner, M.J., 2018. Persistence of environmental DNA in marine systems. *Commun Biol* 1, 1–11. <https://doi.org/10.1038/s42003-018-0192-6>
- Cordier, T., Forster, D., Dufresne, Y., Martins, C.I.M., Stoeck, T., Pawlowski, J., 2018. Supervised machine learning outperforms taxonomy-based environmental DNA metabarcoding applied to biomonitoring. *Molecular Ecology Resources* 18, 1381–1391. <https://doi.org/10.1111/1755-0998.12926>
- Cottier, F., Tverberg, V., Inall, M., Svendsen, H., Nilsen, F., Griffiths, C., 2005. Water mass modification in an Arctic fjord through cross-shelf exchange: The seasonal hydrography of Kongsfjorden, Svalbard. *Journal of Geophysical Research: Oceans* 110. <https://doi.org/10.1029/2004JC002757>
- Cottier, F.R., Nilsen, F., Inall, M.E., Gerland, S., Tverberg, V., Svendsen, H., 2007. Wintertime warming of an Arctic shelf in response to large-scale atmospheric circulation. *Geophysical Research Letters* 34. <https://doi.org/10.1029/2007GL029948>
- Csapó, H.K., Grabowski, M., Węśławski, J.M., 2021. Coming home - Boreal ecosystem claims Atlantic sector of the Arctic. *Science of The Total Environment* 771, 144817. <https://doi.org/10.1016/j.scitotenv.2020.144817>
- Deagle, B.E., Jarman, S.N., Coissac, E., Pompanon, F., Taberlet, P., 2014. DNA metabarcoding and the cytochrome c oxidase subunit I marker: not a perfect match | *Biology Letters*. <https://doi.org/10.1098/rsbl.2014.0562>
- Dischereit, A., Beermann, J., Lebreton, B., Wangensteen, O.S., Neuhaus, S., Havermans, C., 2024a. DNA metabarcoding reveals a diverse, omnivorous diet of Arctic amphipods during the polar night, with jellyfish and fish as major prey. *Front. Mar. Sci.* 11. <https://doi.org/10.3389/fmars.2024.1327650>
- Dischereit, A., Beermann, J., Lebreton, B., Wangensteen, O.S., Neuhaus, S., Havermans, C., 2024b. DNA metabarcoding reveals a diverse, omnivorous diet of Arctic amphipods during the polar night, with jellyfish and fish as major prey. *Front. Mar. Sci.* 11. <https://doi.org/10.3389/fmars.2024.1327650>
- Djurhuus, A., Closek, C.J., Kelly, R.P., Pitz, K.J., Michisaki, R.P., Starks, H.A., Walz, K.R., Andruszkiewicz, E.A., Olesin, E., Hubbard, K., Montes, E., Otis, D., Muller-Karger, F.E., Chavez, F.P., Boehm, A.B., Breitbart, M., 2020. Environmental DNA reveals

- seasonal shifts and potential interactions in a marine community. *Nat Commun* 11, 254. <https://doi.org/10.1038/s41467-019-14105-1>
- Duarte, S., Simões, L., Costa, F.O., 2023. Current status and topical issues on the use of eDNA-based targeted detection of rare animal species. *Science of The Total Environment* 904, 166675. <https://doi.org/10.1016/j.scitotenv.2023.166675>
- Elbrecht, V., Vamos, E.E., Meissner, K., Aroviita, J., Leese, F., 2017. Assessing strengths and weaknesses of DNA metabarcoding-based macroinvertebrate identification for routine stream monitoring. *Methods in Ecology and Evolution* 8, 1265–1275. <https://doi.org/10.1111/2041-210X.12789>
- Engel, M.S., Ceríaco, L.M.P., Daniel, G.M., Dellapé, P.M., Löbl, I., Marinov, M., Reis, R.E., Young, M.T., Dubois, A., Agarwal, I., Lehmann A., P., Alvarado, M., Alvarez, N., Andreone, F., Araujo-Vieira, K., Ascher, J.S., Baêta, D., Baldo, D., Bandeira, S.A., Barden, P., Barrasso, D.A., Bendifallah, L., Bockmann, F.A., Böhme, W., Borkent, A., Brandão, C.R.F., Busack, S.D., Bybee, S.M., Channing, A., Chatzimanolis, S., Christenhusz, M.J.M., Crisci, J.V., D'elía, G., Da Costa, L.M., Davis, S.R., De Lucena, C.A.S., Deuve, T., Fernandes Elizalde, S., Faivovich, J., Farooq, H., Ferguson, A.W., Gippoliti, S., Gonçalves, F.M.P., Gonzalez, V.H., Greenbaum, E., Hinojosa-Díaz, I.A., Ineich, I., Jiang, J., Kahono, S., Kury, A.B., Lucinda, P.H.F., Lynch, J.D., Malécot, V., Marques, M.P., Marris, J.W.M., Mckellar, R.C., Mendes, L.F., Nihei, S.S., Nishikawa, K., Ohler, A., Orrico, V.G.D., Ota, H., Paiva, J., Parrinha, D., Pauwels, O.S.G., Pereyra, M.O., Pestana, L.B., Pinheiro, P.D.P., Prendini, L., Prokop, J., Rasmussen, C., Rödel, M.-O., Rodrigues, M.T., Rodríguez, S.M., Salatnaya, H., Sampaio, Í., Sánchez-García, A., Shebl, M.A., Santos, B.S., Solórzano-Kraemer, M.M., Sousa, A.C.A., Stoev, P., Teta, P., Trape, J.-F., Dos Santos, C.V.-D., Vasudevan, K., Vink, C.J., Vogel, G., Wagner, P., Wappler, T., Ware, J.L., Wedmann, S., Zacharie, C.K., 2021. The taxonomic impediment: a shortage of taxonomists, not the lack of technical approaches. *Zoological Journal of the Linnean Society* 193, 381–387. <https://doi.org/10.1093/zoolinnean/zlab072>
- Eriksen, E., Skjoldal, H.R., Gjørseter, H., Primicerio, R., 2017. Spatial and temporal changes in the Barents Sea pelagic compartment during the recent warming. *Progress in Oceanography* 151, 206–226. <https://doi.org/10.1016/j.pocean.2016.12.009>
- Ershova, E.A., Wangensteen, O.S., Descoteaux, R., Barth-Jensen, C., Præbel, K., 2021. Metabarcoding as a quantitative tool for estimating biodiversity and relative biomass of marine zooplankton. *ICES Journal of Marine Science* 78, 3342–3355. <https://doi.org/10.1093/icesjms/fsab171>
- Ershova, E.A., Wangensteen, O.S., Falkenhaus, T., 2023. Mock samples resolve biases in diversity estimates and quantitative interpretation of zooplankton metabarcoding data. *Mar. Biodivers.* 53, 66. <https://doi.org/10.1007/s12526-023-01372-x>
- Farmer, J.R., Sigman, D.M., Granger, J., Underwood, O.M., Fripiat, F., Cronin, T.M., Martínez-García, A., Haug, G.H., 2021. Arctic Ocean stratification set by sea level and freshwater inputs since the last ice age. *Nat. Geosci.* 14, 684–689. <https://doi.org/10.1038/s41561-021-00789-y>
- Fonseca, V.G., 2018. “Pitfalls in relative abundance estimation using eDNA metabarcoding.” *Molecular Ecology Resources* 18, 923–926. <https://doi.org/10.1111/1755-0998.12902>
- Gluchowska, M., Dalpadado, P., Beszczynska-Möller, A., Olszewska, A., Ingvaldsen, R.B., Kwasniewski, S., 2017a. Interannual zooplankton variability in the main pathways of the Atlantic water flow into the Arctic Ocean (Fram Strait and Barents Sea branches). *ICES Journal of Marine Science* 74, 1921–1936. <https://doi.org/10.1093/icesjms/fsx033>
- Gluchowska, M., Trudnowska, E., Goszczko, I., Kubiszyn, A.M., Blachowiak-Samolyk, K., Walczowski, W., Kwasniewski, S., 2017b. Variations in the structural and functional diversity of zooplankton over vertical and horizontal environmental gradients en route to the Arctic Ocean through the Fram Strait. *PLOS ONE* 12, e0171715. <https://doi.org/10.1371/journal.pone.0171715>

- Govindarajan, A.F., McCartin, L., Adams, A., Allan, E., Belani, A., Francolini, R., Fujii, J., Gomez-Ibañez, D., Kukulya, A., Marin, F., Tradd, K., Yoerger, D.R., McDermott, J.M., Herrera, S., 2022. Improved biodiversity detection using a large-volume environmental DNA sampler with in situ filtration and implications for marine eDNA sampling strategies. *Deep Sea Research Part I: Oceanographic Research Papers* 189, 103871. <https://doi.org/10.1016/j.dsr.2022.103871>
- Guri, G., Shelton, A.O., Kelly, R.P., Yoccoz, N., Johansen, T., Præbel, K., Hanebrekke, T., Ray, J.L., Fall, J., Westgaard, J.-I., 2024. Predicting trawl catches using environmental DNA. *ICES Journal of Marine Science* 81, 1536–1548. <https://doi.org/10.1093/icesjms/fsae097>
- Hakimzadeh, A., Abdala Asbun, A., Albanese, D., Bernard, M., Buchner, D., Callahan, B., Caporaso, J.G., Curd, E., Djemiel, C., Brandström Durling, M., Elbrecht, V., Gold, Z., Gweon, H.S., Hajibabaei, M., Hildebrand, F., Mikryukov, V., Normandeau, E., Özkurt, E., M. Palmer, J., Pascal, G., Porter, T.M., Straub, D., Vasar, M., Větrovský, T., Zafeiropoulos, H., Anslan, S., 2023. A pile of pipelines: An overview of the bioinformatics software for metabarcoding data analyses. *Molecular Ecology Resources* n/a. <https://doi.org/10.1111/1755-0998.13847>
- Havermans, C., Murray, A., Dischereit, A., 2023. Presence data of gelatinous zooplankton in the Polar Night in Kongsfjorden, Svalbard, in 2022. <https://doi.org/10.1594/PANGAEA.955899>
- Hop, H., Assmy, P., Wold, A., Sundfjord, A., Daase, M., Duarte, P., Kwasniewski, S., Gluchowska, M., Wiktor, J.M., Tatarek, A., Wiktor, J., Kristiansen, S., Fransson, A., Chierici, M., Vihtakari, M., 2019a. Pelagic Ecosystem Characteristics Across the Atlantic Water Boundary Current From Rijpfjorden, Svalbard, to the Arctic Ocean During Summer (2010–2014). *Frontiers in Marine Science* 6.
- Hop, H., Falk-Petersen, S., Svendsen, H., Kwasniewski, S., Pavlov, V., Pavlova, O., Søreide, J.E., 2006. Physical and biological characteristics of the pelagic system across Fram Strait to Kongsfjorden. *Progress in Oceanography, Structure and function of contemporary food webs on Arctic shelves: a pan-Arctic comparison* 71, 182–231. <https://doi.org/10.1016/j.pocean.2006.09.007>
- Hop, H., Wold, A., Vihtakari, M., Daase, M., Kwasniewski, S., Gluchowska, M., Lischka, S., Buchholz, F., Falk-Petersen, S., 2019b. Zooplankton in Kongsfjorden (1996–2016) in Relation to Climate Change, in: Hop, H., Wiencke, C. (Eds.), *The Ecosystem of Kongsfjorden, Svalbard*. Springer International Publishing, Cham, pp. 229–300. https://doi.org/10.1007/978-3-319-46425-1_7
- Jarman, S.N., Berry, O., Bunce, M., 2018. The value of environmental DNA biobanking for long-term biomonitoring. *Nat Ecol Evol* 2, 1192–1193. <https://doi.org/10.1038/s41559-018-0614-3>
- Jeunen, G.-J., Knapp, M., Spencer, H.G., Lamare, M.D., Taylor, H.R., Stat, M., Bunce, M., Gemmell, N.J., 2019. Environmental DNA (eDNA) metabarcoding reveals strong discrimination among diverse marine habitats connected by water movement. *Molecular Ecology Resources* 19, 426–438. <https://doi.org/10.1111/1755-0998.12982>
- Johansson, M.L., Shiganova, T.A., Ringvold, H., Stupnikova, A.N., Heath, D.D., MacIsaac, H.J., 2018. Molecular Insights Into the Ctenophore Genus *Beroe* in Europe: New Species, Spreading Invaders. *Journal of Heredity* 109, 520–529. <https://doi.org/10.1093/jhered/esy026>
- Kaiser, P., Hagen, W., von Appen, W.-J., Niehoff, B., Hildebrandt, N., Auel, H., 2021. Effects of a Submesoscale Oceanographic Filament on Zooplankton Dynamics in the Arctic Marginal Ice Zone. *Frontiers in Marine Science* 8.
- Käb, M., Vedenin, A., Hasemann, C., Brandt, A., Soltwedel, T., 2019. Community structure of macrofauna in the deep Fram Strait: A comparison between two bathymetric gradients in ice-covered and ice-free areas. *Deep Sea Research Part I: Oceanographic Research Papers* 152, 103102. <https://doi.org/10.1016/j.dsr.2019.103102>

- Keck, F., Couton, M., Altermatt, F., 2023. Navigating the seven challenges of taxonomic reference databases in metabarcoding analyses. *Molecular Ecology Resources* 23, 742–755. <https://doi.org/10.1111/1755-0998.13746>
- Kelly, R.P., Shelton, A.O., Gallego, R., 2019. Understanding PCR Processes to Draw Meaningful Conclusions from Environmental DNA Studies. *Sci Rep* 9, 12133. <https://doi.org/10.1038/s41598-019-48546-x>
- Kiko, R., Kern, S., Kramer, M., Mütze, H., 2017. Colonization of newly forming Arctic sea ice by meiofauna: a case study for the future Arctic? *Polar Biol* 40, 1277–1288. <https://doi.org/10.1007/s00300-016-2052-5>
- Kondoh, M., Kasada, M., Abe, T., Kasai, A., Dazai, A., Masuda, R., Seino, S., Suzuki, S., Suzuki-Ohno, Y., Tanabe, A.S., 2024. Community Science Initiatives Utilizing Environmental DNA, in: Suzuki-Ohno, Y. (Ed.), *Community Science in Ecology: Case Studies of Public Participation in Ecological Research in Japan*. Springer Nature, Singapore, pp. 83–99. https://doi.org/10.1007/978-981-97-0304-3_6
- Kosobokova, K., Hirche, H.-J., 2009. Biomass of zooplankton in the eastern Arctic Ocean – A base line study. *Progress in Oceanography* 82, 265–280. <https://doi.org/10.1016/j.pocean.2009.07.006>
- Kosobokova, K.N., Hopcroft, R.R., Hirche, H.-J., 2011. Patterns of zooplankton diversity through the depths of the Arctic's central basins. *Mar Biodiv* 41, 29–50. <https://doi.org/10.1007/s12526-010-0057-9>
- Krehenwinkel, H., Wolf, M., Lim, J.Y., Rominger, A.J., Simison, W.B., Gillespie, R.G., 2017. Estimating and mitigating amplification bias in qualitative and quantitative arthropod metabarcoding. *Sci Rep* 7, 17668. <https://doi.org/10.1038/s41598-017-17333-x>
- Kvalheim, L., Stensrud, E., Knutsen, H., Hyvärinen, O., Eiler, A., 2024. Integration of citizen science and eDNA reveals novel ecological insights for marine fish conservation. *Environmental DNA* 6, e584. <https://doi.org/10.1002/edn3.584>
- Laakmann, S., Blanco-Bercial, L., Cornils, A., 2020. The crossover from microscopy to genes in marine diversity: from species to assemblages in marine pelagic copepods. *Philosophical Transactions of the Royal Society B: Biological Sciences* 375, 20190446. <https://doi.org/10.1098/rstb.2019.0446>
- Lacoursière-Roussel, A., Howland, K., Normandeau, E., Grey, E.K., Archambault, P., Deiner, K., Lodge, D.M., Hernandez, C., Leduc, N., Bernatchez, L., 2018. eDNA metabarcoding as a new surveillance approach for coastal Arctic biodiversity. *Ecology and Evolution* 8, 7763–7777. <https://doi.org/10.1002/ece3.4213>
- Larson, E.R., Graham, B.M., Achury, R., Coon, J.J., Daniels, M.K., Gambrell, D.K., Jonassen, K.L., King, G.D., LaRacuente, N., Perrin-Stowe, T.I., Reed, E.M., Rice, C.J., Ruzi, S.A., Thairu, M.W., Wilson, J.C., Suarez, A.V., 2020. From eDNA to citizen science: emerging tools for the early detection of invasive species. *Frontiers in Ecology and the Environment* 18, 194–202. <https://doi.org/10.1002/fee.2162>
- Lear, G., Dickie, I., Banks, J., Boyer, S., Buckley, H.L., Buckley, T.R., Cruickshank, R., Dopheide, A., Handley, K.M., Hermans, S., Kamke, J., Lee, C.K., MacDiarmid, R., Morales, S.E., Orlovich, D.A., Smissen, R., Wood, J., Holdaway, R., 2018. Methods for the extraction, storage, amplification and sequencing of DNA from environmental samples. *New Zealand Journal of Ecology* 42, 10-50A.
- Leray, M., Yang, J.Y., Meyer, C.P., Mills, S.C., Agudelo, N., Ranwez, V., Boehm, J.T., Machida, R.J., 2013. A new versatile primer set targeting a short fragment of the mitochondrial COI region for metabarcoding metazoan diversity: application for characterizing coral reef fish gut contents. *Frontiers in Zoology* 10, 34. <https://doi.org/10.1186/1742-9994-10-34>
- López-Escardó, D., Paps, J., de Vargas, C., Massana, R., Ruiz-Trillo, I., del Campo, J., 2018. Metabarcoding analysis on European coastal samples reveals new molecular metazoan diversity. *Sci Rep* 8, 9106. <https://doi.org/10.1038/s41598-018-27509-8>
- Macheriotou, L., Guilini, K., Bezerra, T.N., Tytgat, B., Nguyen, D.T., Phuong Nguyen, T.X., Noppe, F., Armenteros, M., Boufahja, F., Rigaux, A., Vanreusel, A., Derycke, S., 2019. Metabarcoding free-living marine nematodes using curated 18S and CO1 reference

- sequence databases for species-level taxonomic assignments. *Ecology and Evolution* 9, 1211–1226. <https://doi.org/10.1002/ece3.4814>
- Majaneva, S., Havermans, C., Hopcroft, R., Kosobokova, K., Verhaegen, G., Hosia, A., 2024. Gelatinous zooplankton - delicate drifters of the Arctic Ocean, in: *Elements of a Pan-Arctic Ocean Ecology*. Orkana Forlag, pp. 234–247.
- Mańko, M.K., Gluchowska, M., Weydmann-Zwolicka, A., 2020. Footprints of Atlantification in the vertical distribution and diversity of gelatinous zooplankton in the Fram Strait (Arctic Ocean). *Progress in Oceanography* 189, 102414. <https://doi.org/10.1016/j.pocean.2020.102414>
- Mańko, M.K., Merchel, M., Kwasniewski, S., Weydmann-Zwolicka, A., 2022. Oceanic Fronts Shape Biodiversity of Gelatinous Zooplankton in the European Arctic. *Front. Mar. Sci.* 9. <https://doi.org/10.3389/fmars.2022.941025>
- Mazanowski, K., Mańko, M.K., Møller, E.F., Weydmann-Zwolicka, A., 2023. Gelatinous zooplankton off the Northeast Greenland coast. *Progress in Oceanography* 219, 103173. <https://doi.org/10.1016/j.pocean.2023.103173>
- McClenaghan, B., Fahner, N., Cote, D., Chawarski, J., McCarthy, A., Rajabi, H., Singer, G., Hajibabaei, M., 2020. Harnessing the power of eDNA metabarcoding for the detection of deep-sea fishes. *PLOS ONE* 15, e0236540. <https://doi.org/10.1371/journal.pone.0236540>
- Mora, C., Tittensor, D.P., Adl, S., Simpson, A.G.B., Worm, B., 2011. How Many Species Are There on Earth and in the Ocean? *PLoS Biology* 9, e1001127. <https://doi.org/10.1371/journal.pbio.1001127>
- Nguyen, N.-L., Devendra, D., Szymańska, N., Greco, M., Angeles, I.B., Weiner, A.K.M., Ray, J.L., Cordier, T., De Schepper, S., Pawłowski, J., Pawłowska, J., 2023. Sedimentary ancient DNA: a new paleogenomic tool for reconstructing the history of marine ecosystems. *Front. Mar. Sci.* 10. <https://doi.org/10.3389/fmars.2023.1185435>
- Nichols, R.V., Vollmers, C., Newsom, L.A., Wang, Y., Heintzman, P.D., Leighton, M., Green, R.E., Shapiro, B., 2018. Minimizing polymerase biases in metabarcoding. *Molecular Ecology Resources* 18, 927–939. <https://doi.org/10.1111/1755-0998.12895>
- Pantiukhin, D., Verhaegen, G., Havermans, C., 2024. Pan-Arctic distribution modeling reveals climate-change-driven poleward shifts of major gelatinous zooplankton species. *Limnology and Oceanography* 69, 1316–1334. <https://doi.org/10.1002/lno.12568>
- Pantiukhin, D., Verhaegen, G., Kraan, C., Jerosch, K., Neitzel, P., Hoving, H.-J.T., Havermans, C., 2023. Optical observations and spatio-temporal projections of gelatinous zooplankton in the Fram Strait, a gateway to a changing Arctic Ocean. *Frontiers in Marine Science* 10.
- Pearson, J., Jackson, G., McNamara, K.E., 2023. Climate-driven losses to knowledge systems and cultural heritage: A literature review exploring the impacts on Indigenous and local cultures. *The Anthropocene Review* 10, 343–366. <https://doi.org/10.1177/20530196211005482>
- Piñol, J., Mir, G., Gomez-Polo, P., Agustí, N., 2015. Universal and blocking primer mismatches limit the use of high-throughput DNA sequencing for the quantitative metabarcoding of arthropods. *Molecular Ecology Resources* 15, 819–830. <https://doi.org/10.1111/1755-0998.12355>
- Preston, F.W., 1948. The Commonness, And Rarity, of Species. *Ecology* 29, 254–283. <https://doi.org/10.2307/1930989>
- Priest, T., von Appen, W.-J., Oldenburg, E., Popa, O., Torres-Valdés, S., Bienhold, C., Metfies, K., Boulton, W., Mock, T., Fuchs, B.M., Amann, R., Boetius, A., Wietz, M., 2023. Atlantic water influx and sea-ice cover drive taxonomic and functional shifts in Arctic marine bacterial communities. *ISME J* 1–14. <https://doi.org/10.1038/s41396-023-01461-6>
- Purcell, J., Juhl, A., Mańko, M.K., Aumack, C., 2018. Overwintering of gelatinous zooplankton in the coastal Arctic Ocean. *Mar. Ecol. Prog. Ser.* 591, 281–286. <https://doi.org/10.3354/meps12289>

- Purcell, J.E., Hopcroft, R.R., Kosobokova, K.N., Whitley, T.E., 2010. Distribution, abundance, and predation effects of epipelagic ctenophores and jellyfish in the western Arctic Ocean. *Deep Sea Research Part II: Topical Studies in Oceanography, Observations and Exploration of the Arctic's Canada Basin and the Chukchi Sea: the Hidden Ocean and RUSALCA Expeditions* 57, 127–135. <https://doi.org/10.1016/j.dsr2.2009.08.011>
- Questel, J.M., Hopcroft, R.R., DeHart, H.M., Smoot, C.A., Kosobokova, K.N., Bucklin, A., 2021. Metabarcoding of zooplankton diversity within the Chukchi Borderland, Arctic Ocean: improved resolution from multi-gene markers and region-specific DNA databases. *Mar. Biodivers.* 51, 4. <https://doi.org/10.1007/s12526-020-01136-x>
- Ramirez-Llodra, E., Meyer, H.K., Bluhm, B.A., Brix, S., Brandt, A., Dannheim, J., Downey, R.V., Egilsdóttir, H., Eilertsen, M.H., Gaudron, S.M., Gebruk, A., Golikov, A., Hasemann, C., Hilario, A., Jørgensen, L.L., Kaiser, S., Korfhage, S.A., Kürzel, K., Lörz, A.-N., Buhl-Mortensen, P., Olafsdóttir, S.H., Piepenburg, D., Purser, A., Ribeiro, P.A., Sen, A., Soltwedel, T., Stratmann, T., Steger, J., Svavarsson, J., Tandberg, A.H.S., Taylor, J., Theising, F.I., Uhlir, C., Waller, R.G., Xavier, J.R., Zhulay, I., Saaedi, H., 2024. The emerging picture of a diverse deep Arctic Ocean seafloor: From habitats to ecosystems. *Elementa: Science of the Anthropocene* 12, 00140. <https://doi.org/10.1525/elementa.2023.00140>
- Raskoff, K.A., Hopcroft, R.R., Kosobokova, K.N., Purcell, J.E., Youngbluth, M., 2010. Jellies under ice: ROV observations from the Arctic 2005 hidden ocean expedition. *Deep Sea Research Part II: Topical Studies in Oceanography, Observations and Exploration of the Arctic's Canada Basin and the Chukchi Sea: the Hidden Ocean and RUSALCA Expeditions* 57, 111–126. <https://doi.org/10.1016/j.dsr2.2009.08.010>
- Ronowicz, M., Kukliński, P., Mapstone, G.M., 2015. Trends in the Diversity, Distribution and Life History Strategy of Arctic Hydrozoa (Cnidaria). *PLOS ONE* 10, e0120204. <https://doi.org/10.1371/journal.pone.0120204>
- Scriver, M., Zaiko, A., Pochon, X., von Ammon, U., 2023. Harnessing decay rates for coastal marine biosecurity applications: A review of environmental DNA and RNA fate. *Environmental DNA* 5, 960–972. <https://doi.org/10.1002/edn3.405>
- Shiganova, T.A., Abyzova, G.A., 2022. Revision of Beroidae (Ctenophora) in the southern seas of Europe: systematics and distribution based on genetics and morphology. *Zoological Journal of the Linnean Society* 194, 297–322. <https://doi.org/10.1093/zoolinnean/zlab021>
- Smith, J., David, B., Hicks, A., Wilkinson, S., Ling, N., Fake, D., Suren, A., Gault, A., 2024. Optimizing eDNA Replication for Standardized Application in Lotic Systems in Aotearoa, New Zealand. *Environmental DNA* 6, e70017. <https://doi.org/10.1002/edn3.70017>
- Smith, M.M., Angot, H., Chamberlain, E.J., Droste, E.S., Karam, S., Muilwijk, M., Webb, A.L., Archer, S.D., Beck, I., Blomquist, B.W., Bowman, J., Boyer, M., Bozzato, D., Chierici, M., Creamean, J., D'Angelo, A., Delille, B., Fer, I., Fong, A.A., Fransson, A., Fuchs, N., Gardner, J., Granskog, M.A., Hoppe, C.J.M., Hoppema, M., Hoppmann, M., Mock, T., Muller, S., Müller, O., Nicolaus, M., Nomura, D., Petäjä, T., Salganik, E., Schmale, J., Schmidt, K., Schulz, K.M., Shupe, M.D., Stefels, J., Thielke, L., Tippenhauer, S., Ulfsbo, A., van Leeuwe, M., Webster, M., Yoshimura, M., Zhan, L., 2023. Thin and transient meltwater layers and false bottoms in the Arctic sea ice pack—Recent insights on these historically overlooked features. *Elementa: Science of the Anthropocene* 11, 00025. <https://doi.org/10.1525/elementa.2023.00025>
- Soltwedel, T., Bauerfeind, E., Bergmann, M., Budaeva, N., Hoste, E., Jaeckisch, N., Juterzenka, K. v., Matthießen, J., Mokievsky, V., Nöthig, E.-M., Quéric, N., Sablotny, B., Sauter, E., Schewe, I., Urban-Malinga, B., Wegner, J., Wlodarska-Kowalczyk, M., Klages, M., 2005. HAUSGARTEN: multidisciplinary investigations at a deep-sea, long-term observatory in the Arctic Ocean. *Oceanography* 18, 46–61.
- Suter, L., Polanowski, A.M., Clarke, L.J., Kitchener, J.A., Deagle, B.E., 2021. Capturing open ocean biodiversity: Comparing environmental DNA metabarcoding to the continuous

- plankton recorder. *Molecular Ecology* 30, 3140–3157. <https://doi.org/10.1111/mec.15587>
- Taberlet, P., Bonin, A., Zinger, L., Coissac, E., 2018. *Environmental DNA: For Biodiversity Research and Monitoring*. Oxford University Press.
- Tanabe, A.S., Nagai, S., Hida, K., Yasuike, M., Fujiwara, A., Nakamura, Y., Takano, Y., Katakura, S., 2016. Comparative study of the validity of three regions of the 18S-rRNA gene for massively parallel sequencing-based monitoring of the planktonic eukaryote community. *Molecular Ecology Resources* 16, 402–414. <https://doi.org/10.1111/1755-0998.12459>
- Tang, C.Q., Leasi, F., Obertegger, U., Kieneke, A., Barraclough, T.G., Fontaneto, D., 2012. The widely used small subunit 18S rDNA molecule greatly underestimates true diversity in biodiversity surveys of the meiofauna. *Proceedings of the National Academy of Sciences* 109, 16208–16212. <https://doi.org/10.1073/pnas.1209160109>
- Thomsen, P.F., Jensen, M.R., Sigsgaard, E.E., 2024. A vision for global eDNA-based monitoring in a changing world. *Cell* 187, 4444–4448. <https://doi.org/10.1016/j.cell.2024.04.019>
- Thomsen, P.F., Willerslev, E., 2015. Environmental DNA – An emerging tool in conservation for monitoring past and present biodiversity. *Biological Conservation, Special Issue: Environmental DNA: A powerful new tool for biological conservation* 183, 4–18. <https://doi.org/10.1016/j.biocon.2014.11.019>
- Timmermans, M.-L., Marshall, J., 2020. Understanding Arctic Ocean Circulation: A Review of Ocean Dynamics in a Changing Climate. *Journal of Geophysical Research: Oceans* 125, e2018JC014378. <https://doi.org/10.1029/2018JC014378>
- Truelove, N.K., Patin, N.V., Min, M., Pitz, K.J., Preston, C.M., Yamahara, K.M., Zhang, Y., Raanan, B.Y., Kieft, B., Hobson, B., Thompson, L.R., Goodwin, K.D., Chavez, F.P., 2022. Expanding the temporal and spatial scales of environmental DNA research with autonomous sampling. *Environmental DNA* 4, 972–984. <https://doi.org/10.1002/edn3.299>
- Urban, P., Præbel, K., Bhat, S., Dierking, J., Wangensteen, O.S., 2022. DNA metabarcoding reveals the importance of gelatinous zooplankton in the diet of *Pandalus borealis*, a keystone species in the Arctic. *Molecular Ecology* 31, 1562–1576. <https://doi.org/10.1111/mec.16332>
- Wangensteen, O.S., Palacín, C., Guardiola, M., Turon, X., 2018. DNA metabarcoding of littoral hard-bottom communities: high diversity and database gaps revealed by two molecular markers. *PeerJ* 6, e4705. <https://doi.org/10.7717/peerj.4705>
- Weydmann, A., Carstensen, J., Goszczko, I., Dmoch, K., Olszewska, A., Kwasniewski, S., 2014. Shift towards the dominance of boreal species in the Arctic: inter-annual and spatial zooplankton variability in the West Spitsbergen Current. *Marine Ecology Progress Series* 501, 41–52.
- Wietz, M., Bienhold, C., Metfies, K., Torres-Valdés, S., von Appen, W.-J., Salter, I., Boetius, A., 2021. The polar night shift: seasonal dynamics and drivers of Arctic Ocean microbiomes revealed by autonomous sampling. *ISME Communications* 1, 76. <https://doi.org/10.1038/s43705-021-00074-4>
- Wilkinson, S.P., Gault, A.A., Welsh, S.A., Smith, J.P., David, B.O., Hicks, A.S., Fake, D.R., Suren, A.M., Shaffer, M.R., Jarman, S.N., Bunce, M., 2024. TICl: a taxon-independent community index for eDNA-based ecological health assessment. *PeerJ* 12, e16963. <https://doi.org/10.7717/peerj.16963>
- Wood, S.A., Biessy, L., Latchford, J.L., Zaiko, A., von Ammon, U., Audrezet, F., Cristescu, M.E., Pochon, X., 2020. Release and degradation of environmental DNA and RNA in a marine system. *Science of The Total Environment* 704, 135314. <https://doi.org/10.1016/j.scitotenv.2019.135314>
- Wu, S., Xiong, J., Yu, Y., 2015. Taxonomic Resolutions Based on 18S rRNA Genes: A Case Study of Subclass Copepoda. *PLOS ONE* 10, e0131498. <https://doi.org/10.1371/journal.pone.0131498>

- Xu, D., Kong, H., Yang, E.-J., Li, X., Jiao, N., Warren, A., Wang, Y., Lee, Y., Jung, J., Kang, S.-H., 2020. Contrasting Community Composition of Active Microbial Eukaryotes in Melt Ponds and Sea Water of the Arctic Ocean Revealed by High Throughput Sequencing. *Front. Microbiol.* 11. <https://doi.org/10.3389/fmicb.2020.01170>
- Yip, Z.T., Quek, Z.B.R., Huang, D., 2023. Complementary broad-range mitochondrial markers improve eDNA characterization of marine metazoan diversity. *Mar. Biodivers.* 53, 76. <https://doi.org/10.1007/s12526-023-01385-6>
- Zimmermann, H.H., Harðardóttir, S., Ribeiro, S., 2024. Assessing the performance of short 18S rDNA markers for environmental DNA metabarcoding of marine protists. *Environmental DNA* 6, e580. <https://doi.org/10.1002/edn3.580>

8. Appendix

8.1 Acknowledgments

First, I sincerely thank all the past and present members of the ARJEL working group for being a great team, building a kind and inclusive atmosphere. An extra special thanks to my expedition partner in crime, Meret. I look forward to many more fruitful discussions on the delights of studying ctenophores and I hope we can go on expedition together again one day.

To my supervisor Charlotte Havermans, thank you for always believing in me and encouraging my independence. You have always led with kindness and positivity with a healthy dash of humour. It has been a delight. And of course, a huge thank you for sending me on all those expeditions. I gained so many wonderful experiences and memories that I would never have been able to fathom without the opportunities you were able to open up.

I would also like to thank the members of my thesis advisory committee: Prof. Dr. Charlotte Havermans, Prof. Dr. Kim Præbel, Dr. Sanna Majaneva, Dr. Gerlien Verhaegen and Dr. Silke Laakman. Thank you for your advice and guidance over the course of my PhD.

A huge thank you to my brother in arms, Annkathrin Dischereit. We went through many exciting, challenging and sometimes frustrating moments during our PhDs together. You were always supportive and were up for tackling many a lab- or bioinformatic-related adventure together. I am grateful to have made a science-buddy and more importantly a life-long friend (even if we have established that sharing a cabin on expedition is a terrible idea - for the sake of sleep).

A big thank you to Stefan Neuhaus and Andria Antich for supporting me through my sometimes slow and painful journey into the world of bioinformatics. Your patience and kindness meant the world to my sanity and I never would have gotten through all of this thesis without your support and time. None of this would have been possible without all of my supportive and constructive co-authors, thank you and I hope to work with many of you again in the near future.

I thank my family and friends who have buoyed me along on this adventure. To my family back home in New Zealand who have supported me through some tough times, especially when I was unable to go home during the first years of my PhD thanks to the pandemic. Especially to my Mum, who still doesn't entirely know what I do, but is always immensely proud and ready to provide much needed unconditional love and empathy. Thanks to my friends back home who are always encouraging me to jump into the next adventure. And for not teasing me too

much about accent I have developed since being away. A special thanks to Eleanor for agreeing to some last minute, but very valuable proof-reading. I am immensely grateful to my friends here in Bremen: Eilish, Jasmin, Lili, Marie, Luisa, Marrit and everyone at the lunch table and on the daily commute. There is nothing like the support of friends who are going through the same rollercoaster experiences of PhD life.

Lastly, but certainly no least, my partner Micha. You have been a constant source of calm and you were always there to love, listen and support me throughout this whole process. And most importantly, thank you for agreeing to adopt our cat, Leni. She has been a constant source of warm fuzzy feelings through some tough times, even if she doesn't necessarily agree.

8.3 Own contribution to manuscripts

Declaration on the contribution of the candidate to a multi-author article/manuscript. Contribution of the candidate in % of the total workload (up to 100% for each of the following categories).

Manuscript 1: Investigating pelagic biodiversity and gelatinous zooplankton communities in the rapidly changing European Arctic: An eDNA metabarcoding survey

Concept and design: 70%

Acquisition of data: 70%

Processing of samples: 100%

Data analysis: 95%

Preparation of figures and tables: 100%

Drafting of manuscript: 100%

Manuscript 2: Eukaryotic biodiversity of sub-ice water in the Marginal Ice Zone of the European Arctic: A multi-marker eDNA metabarcoding survey

Concept and design: 90 %

Acquisition of data: 100 %

Processing of samples: 100 %

Data analysis: 95 %

Preparation of figures and tables: 95 %

Drafting of manuscript: 95 %

Manuscript 3: Surveying marine biodiversity using eDNA metabarcoding of seawater and sediment in a high Arctic fjord during the polar night (Kongsfjorden, Svalbard)

Concept and design: 90 %

Acquisition of data: 100 %

Processing of samples: 100 %

Data analysis: 100 %

Preparation of figures and tables: 100 %

Drafting of manuscript: 95 %

Manuscript 4: On the effectiveness of two universal metabarcoding primer pairs in amplifying gelatinous zooplankton DNA from tissue and environmental samples

Concept and design: 90 %

Acquisition of data: 90 %

Processing of samples: 100 %

Data analysis: 100 %

Preparation of figures and tables: 100 %

Drafting of manuscript: 100 %

Date and place:

Signature:

Universität Bremen | Fachbereich 02 | Postfach 33 04 40, 28334 Bremen

Universität Bremen
 Fachbereich 2
 Prüfungsamt Chemie
 z. Hd. Frau Frauke Ernst
 Leobener Straße

28359 Bremen
 Deutschland

Prüfungsamt
 Chemie

Frauke Ernst
 Geschäftsstelle
 Fachbereich 02
 Leobener Str. / NW2
 D-28359 Bremen

Verwaltungspavillon 06
Tel. 0421 218-62802
Fax 0421 218-9862802
 frauke.ernst@uni-bremen.de
 www.fb2.uni-bremen.de

Versicherung an Eides Statt

Name, Vorname	Murray, Ayla Rosina Cherrington Sealey
Matrikel-Nr.	3166993
Straße	
Ort, PLZ	

Ich, _____ (Vorname, Name)

versichere an Eides Statt durch meine Unterschrift, dass ich die vorstehende Arbeit selbständig und ohne fremde Hilfe angefertigt und alle Stellen, die ich wörtlich dem Sinne nach aus Veröffentlichungen entnommen habe, als solche kenntlich gemacht habe, mich auch keiner anderen als der angegebenen Literatur oder sonstiger Hilfsmittel bedient habe.

Ich versichere an Eides Statt, dass ich die vorgenannten Angaben nach bestem Wissen und Gewissen gemacht habe und dass die Angaben der Wahrheit entsprechen und ich nichts verschwiegen habe.

Die Strafbarkeit einer falschen eidesstattlichen Versicherung ist mir bekannt, namentlich die Strafandrohung gemäß § 156 StGB bis zu drei Jahren Freiheitsstrafe oder Geldstrafe bei vorsätzlicher Begehung der Tat bzw. gemäß § 161 Abs. 1 StGB bis zu einem Jahr Freiheitsstrafe oder Geldstrafe bei fahrlässiger Begehung.

 Ort, Datum / Unterschrift

Ort, Datum: _____

Erklärungen zur elektronischen Version und zur Überprüfung einer Dissertation

Hiermit betätige ich gemäß §7, Abs. 7, Punkt 4, dass die zu Prüfungszwecken beigelegte elektronische Version meiner Dissertation identisch ist mit der abgegebenen gedruckten Version.

Ich bin mit der Überprüfung meiner Dissertation gemäß §6 Abs. 2, Punkt 5 mit qualifizierter Software im Rahmen der Untersuchung von Plagiatsvorwürfen einverstanden.

Unterschrift